AON

Impact Forecasting Florida Flood Model (FCHLPM) Version 3.0 ELEMENTS Version 18.0

Submitted in Compliance with the 2021 Flood Standards of the Florida Commission on Hurricane Loss Projection Methodology

October 24, 2024

Copyright and Disclaimer

©2024 Impact Forecasting LLC (and its parent Aon UK Limited. and affiliates) reserve all rights to the content of this document. No part of this document may be made available to any third party without Impact Forecasting LLC's prior written consent, and the recipient by accepting this document agrees to hold Impact Forecasting LLC harmless for any claim by any third party as a result of the recipient's unauthorized dissemination of all or any portion of this document. While Impact Forecasting LLC has used due care in the preparation of this document, it is being provided on an "as is" basis, without warranty of any kind, express or implied. Impact Forecasting LLC disclaims any liability to any person or organization for loss or damage caused by or resulting from any reliance placed on the contents of this document. This document does not constitute any form of legal, accounting, tax, regulatory or actuarial advice.

January 28, 2024

Chair, Florida Commission on Hurricane Loss Projection Methodology

Florida State Board of Administration

1801 Hermitage Boulevard, Suite 100

Tallahassee, FL 32308

Re: Certification of the Impact Forecasting Florida Flood Model (FCHLPM) Version 3.0

Dear Commission Chair,

We are pleased to inform you that Impact Forecasting is ready for the Commission's review and certification of the Impact Forecasting Florida Flood Model (FCHLPM) Version 3.0 as implemented in the ELEMENTS Version 18.0 software.

As required by the Commission, enclosed are the disclosures, data, and analyses to reflect compliance with the General, Meteorological, Hydrological and Hydraulics, Vulnerability, Actuarial, Statistical, and Computer/Information Standards set forth in the Flood Standards Report of Activities as of November 1, 2021. The Impact Forecasting Florida Flood Model (FCHLPM) Version 3.0 has been reviewed by professionals having credentials and/or experience in the areas of meteorology, hydrology and hydraulics, statistics, structural engineering, actuarial science, and computer/information science, as documented in the signed Expert Certification Forms (GF-1 to GF-7). We have also completed the Editorial Review Expert Certification (Form GF-8).

Impact Forecasting is confident that its Florida Flood Model (FCHLPM) Version 3.0 is in compliance with the Commission's Standards and is ready to be reviewed by the Professional Team.

Seven bound copies of the Impact Forecasting submission are provided herein. Please contact us with any questions on the enclosed.

Sincerely,

Daniel Rees, M.A.

Director of US Flood Model Development

Impact Forecasting

Description of Trade Secret Information

Trade secret information that Impact Forecasting will make available to the Professional Team for review during the on-site visit and to the Commission during the closed portion of the Acceptability Meeting is described below and noted at the appropriate places throughout the submission:

- Form HHF-3: Coastal Flood Characteristics by Annual Exceedance Probabilities (Trade Secret Item)
- Form HHF-5: Inland Flood Characteristics by Annual Exceedance Probabilities (Trade Secret Item)
- Form AF-6: Logical Relationship to Flood Risk (Trade Secret Item)

Florida Commission on Hurricane Loss Projection Methodology Flood Model Identification

Name of Flood Model:	Florida Flood Model (FCHLPM)
Flood Model Version Identification:	Version 3.0
Flood Model Platform Names and Identifications with Primary Flood Model Platform and Identification Listed First:	Elements 18.0
Interim Flood Model Update Version Identification:	
Interim Data Update Designation:	
Name of Modeling Organization:	Impact Forecasting
Street Address:	200 East Randolph Street
City, State, ZIP Code:	Chicago, IL 60601
Mailing Address, if different from above:	Same as Above
Contact Person:	David Colbus
Phone Number:	1-978-305-1995
E-mail Address:	David.Colbus@aon.com
Date:	October 24, 2024

Contents

Copyright and Disclaimer **2**

Description of Trade Secret Information **4**

Florida Commission on Hurricane Loss Projection Methodology Flood Model Identification **5**

GENERAL FLOOD STANDARDS **20**

GF-1 Scope of the Flood Model and Its Implementation 20

GF-2 Qualifications of Modeling Organization Personnel and Consultants Engaged in Development of the Flood Model 49

GF-3 Insured Exposure Location 57

GF-4 Independence of Flood Model Components 61

GF-5 Editorial Compliance 62

METEOROLOGICAL FLOOD STANDARDS **64**

MF-1 Flood Event Data Sources 64

MF-2 Flood Parameters (Inputs) 69

MF-3 Wind and Pressure Fields for Storm Surge 89

MF-4 Flood Characteristics (Outputs) 95

MF-5 Flood Probability Distributions 112

HYDROLOGICAL AND HYDRAULIC FLOOD STANDARDS **118**

HHF-1 Flood Parameters (Inputs) 118

HHF-2 Flood Characteristics (Outputs) 135

HHF-3 Modeling of Major Flood Control Measures 152

HHF-4 Logical Relationships Among Flood Parameters and Characteristics 158

STATISTICAL FLOOD STANDARDS **177**

SF-1 Modeled Results and Goodness-of-Fit 177

SF-2 Sensitivity Analysis for Flood Model Output 194

SF-3 Uncertainty Analysis for Flood Model Output 202

SF-4 Flood Model Loss Cost Convergence by Geographic Zone 205

SF-5 Replication of Known Flood Losses 207

VULNERABILITY FLOOD STANDARDS **210**

VF-1 Derivation of Building Flood Vulnerability Functions 210

VF-2 Derivation of Contents Flood Vulnerability Functions 228

VF-3 Derivation of Time Element Flood Vulnerability Functions 233

VF-4 Flood Mitigation Measures 237

ACTUARIAL FLOOD STANDARDS **242**

AF-1 Flood Model Input Data and Output Reports 242

AF-2 Flood Events Resulting in Modeled Flood Losses 250

AF-3 Flood Coverages 252

AF-4 Modeled Flood Loss Cost and Flood Probable Maximum Loss Level Considerations 254

AF-5 Flood Policy Conditions 258

AF-6 Flood Loss Outputs and Logical Relationships to Risk 260

COMPUTER/INFORMATION FLOOD STANDARDS **265**

CIF-1 Flood Model Documentation 265

CIF-2 Flood Model Requirements 267

CIF-3 Flood Model Organization and Component Design 268

CIF-4 Flood Model Implementation 270

CIF-5 Flood Model Verification 273

CIF-6 Human-Computer Interaction 278

CIF-7 Flood Model Maintenance and Revision 279

CIF-8 Flood Model Security 282

Appendix A: FCHLPM Forms **285**

Form GF-1: General Flood Standards Expert Certification 286

Form GF-2: Meteorological Flood Standards Expert Certification 288

Form GF-3: Hydrological and Hydraulic Flood Standards Expert Certification 290

Form GF-4: Statistical Flood Standards Expert Certification 292

Form GF-5: Vulnerability Flood Standards Expert Certification 294

Form GF-6: Actuarial Flood Standards Expert Certification 296

Form GF-7: Computer/Information Flood Standards Expert Certification 298

Form GF-8: Editorial Review Expert Certification 300

Form HHF-1: Historical Coastal and Inland Event Flood Extent and Elevation or Depth Validation Maps 302

Form HHF-2: Coastal Flood Characteristics by Annual Exceedance Probability 326

Form HHF-3: Coastal Flood Characteristics by Annual Exceedance Probabilities (Trade Secret Item) 333

Form HHF-4: Inland Flood Characteristics by Annual Exceedance Probability 334

Form HHF-5: Inland Flood Characteristics by Annual Exceedance Probabilities (Trade Secret Item) 340

Form SF-1: Distributions of Stochastic Flood Parameters (Coastal, Inland) 341

Form SF-2: Examples of Flood Loss Exceedance Estimates (Coastal and Inland Combined) 347

Form VF-1: Coastal Flood with Damaging Wave Action 349

Form VF-2: Inland Flood by Flood Depth 352

Form VF-3: Flood Mitigation Measures, Range of Changes in Flood Damage 355

Form VF-4: Differences in Flood Mitigation Measures 358

Form AF-1: Zero Deductible Personal Residential Standard Flood Loss Costs 359

Form AF-2: Total Flood Statewide Loss Costs 365

Form AF-3: Personal Residential Standard Flood Losses by ZIP Code 369

Form AF-4: Flood Output Ranges 381

Form AF-5: Percentage Change in Flood Output Ranges 415

Form AF-6: Logical Relationships to Flood Risk (Trade Secret Item) 426

Form AF-7: Percentage Change in Logical Relationships to Flood Risk 427

Form AF-8: Flood Probable Maximum Loss for Florida 428

Appendix B: Individuals Involved in the Impact Forecasting Florida Flood Model (FCHLPM) Model Acceptability Process 430

Appendix C: External Expert Review of Vulnerability Modules 438

Appendix D: External Expert Review of Meteorology and Vulnerability Modules 442

Appendix E: Flood Model Input Form 448

Appendix F: Flood Model Output Form 458

Appendix G: Glossary of Acronyms 462

List of Tables

Table 1: Credentials of individuals involved in the acceptability process and each aspect of the flood model 51
Table 2: Summary of spatially varying Manning's friction coefficients. 72
Table 3: Spatially varying Manning's friction coefficients in the presence of buildings. 72
Table 4: Adjustable Model Parameters in FUSE model. 73
Table 5: NLCD classification and subsequent drainage defense standard. 79
Table 6: Predictor variables is given in Hawker et al. (Hawker, et al., 2022). 83
Table 7: SLOSH Basins for the Florida Region. 87
Table 8: Peak water levels (m, relative to NAVD88) at the location shown in Figure 22. 110
Table 9: Annual rates of unique event impacts across Florida. Bracket values represent Wald confidence bounds obtained from a bootstrapping analysis of the historical dataTC– Tropical Cyclone, NTC – non-Tropical cyclone. 117
Table 10: Summary of validation Test Performance Metrics reported in (Bates, et al., 2021). 117
Table 11: Summary of spatially varying Manning's friction coefficients. 126
Table 12: Spatially varying Manning's friction coefficients in the presence of buildings. 127
Table 13: NLCD classification and subsequent drainage defense standard 127
Table 14: Information for selected assessment locations 159
Table 15: Testing the effect of water-level and depth increments on fluvial simulation when hydraulic roughness is increased by 20% 175
Table 16: Testing the effect of depth change on fluvial simulation when topography is increased by 20% 175
Table 17: Testing the effect of water-level and depth increment on pluvial simulation when soil permeability is switched off. 176
Table 18: Testing the effect of water-level and depth increments on fluvial simulation when input discharge is increased by 20% 176
Table 19: Annual rates of unique event impacts across Florida. Bracket values represent Wald confidence bounds obtained from a bootstrapping analysis of the historical data. 187
Table 20 Calculated SRCs for expected storm surge loss costs for all input variables for all hurricane categories. 195
Table 21: Testing the effect of water-level and depth increments on fluvial simulation when hydraulic roughness is increased by 20% 196

Table 22: Testing the effect of depth change on fluvial simulation when topography is increased by 20% 197
Table 23: Testing the effect of water-level and depth increment on pluvial simulation when soil permeability is switched off. 198
Table 24: Testing the effect of water-level and depth increments on fluvial simulation when input discharge is increased by 20% 199
Table 25: Sensitivity testing parameter choices 201
Table 26: Sensitivity assessment result metrics 201
Table 27: Calculated EPRs for expected storm surge loss costs for all input variables for all hurricane categories. 203
Table 28: Modeled historical losses (Industry and NFIP) and trended observed NFIP losses 208
Table 29: Number of building policies and exposure value by construction type. 214
Table 30: Primary construction materials. 220
Table 31: Modeled number of stories. 220
Table 32: The code enforcement and construction practice for non-MH buildings. 221
Table 33: The code enforcement and construction practice for MH. 221
Table 34: Primary modifiers used in personal residential buildings, condo unit owners and apartment renters vulnerability functions. 224
Table 35: Primary modifiers used in MH vulnerability functions. 225
Table 36: Number of content policies and exposure value by construction type. 230
Table 37: Secondary characteristics included in the present model. 238
Table 38: Mitigation measures included in the present model. 239
Table 39: Required Impact Forecasting Florida Flood Model (FCHLPM) Model v3.0 analysis settings for Florida ratemaking (common settings) 245
Table 40: Required Impact Forecasting Florida Flood Model (FCHLPM) Model v3.0 analysis settings for Florida ratemaking (Tropical Cyclone Induced Flooding (FCHLPM) peril settings) 247
Table 41: Required Impact Forecasting Florida Flood Model (FCHLPM) Model v3.0 analysis settings for Florida ratemaking (Non-Tropical Induced Flooding (FCHLPM) peril settings) 247
Table 42: Hardware and software requirements for the Impact Forecasting Florida Flood Model on the ELEMENTS Version 18.0 platform 271
Table 43: Impact Forecasting verification approaches for externally-acquired data and software 275
Table 44: Distributions of stochastic flood parameters (Coastal, Inland) 342
Table 45: Examples of flood loss exceedance estimates 347
Table 46: Average annual loss for the flood loss exceedance distribution 348
Table 47: Coastal Flood with Damaging Wave Action 350
Table 48: Inland Flood by Flood Depth 353
Table 49: Flood Mitigation Measures, Range of Changes in Flood Damage 357
Table 50: Total Flood Statewide Loss Costs 366
Table 51: Standard Flood loss costs per $1,000 of exposure for 0% deductibles 382
Table 52:Standard Flood loss costs per $1,000 of exposure for specified deductibles 389
Table 53: Standard Flood Time Element loss costs per $1,000 of exposure for 0% deductibles 397
Table 54 Standard Flood Time Element loss costs per $1,000 of exposure for specified deductibles . 404
Table 55: Percentage Change in $0 Deductible Flood Output Ranges 416
Table 56: Percentage Change in $0 Deductible, Time Element Flood Output Ranges 416
Table 57: Percentage Change in Specified Deductible Flood Output Ranges 416

Table 58: Percentage Change in Specified Deductible, Time Element Flood Output Ranges 417
Table 59: Personal Residential Flood Probable Maximum Loss for Florida – Annual Aggregate 429
Table 60: Personal Residential Flood Probable Maximum Loss for Florida – Annual Occurrence 429
Table 61: Impact Forecasting Florida Flood Model (FCHLPM) input fields for location information 448
Table 62: Impact Forecasting Florida Flood Model (FCHLPM) input fields for policy information 451
Table 63: Impact Forecasting Florida Flood Model (FCHLPM) Model input fields for treaty information 454
Table 64: Impact Forecasting Florida Flood Model (FCHLPM) input fields for secondary modifier information 455

List of Figures

Figure 1: Interactions among major flood model components for TC 29
Figure 2: Interactions among major flood model components for non-TC.....30
Figure 3: The network organization within which the Impact Forecasting Florida Flood Model (FCHLPM) Model is designed and operates. 31
Figure 4: Business workflow diagram illustrating the connections between Impact Forecasting personnel 54
Figure 5: Comparisons between modeled and measured annual landfall occurrence rates for Florida coastal segments. 79
Figure 6: Coastal segments of Florida used for calculating annual occurrence rates.....80
Figure 7: FABDEM methodology. 81. Processing predictor data and training data (LiDAR DEMs). 2. Applying these to a machine learning model to correct forests and building artifacts. 3. Merging and post-processing elevations from machine learning model. 84
Figure 8: Comparison of FABDEM with MERIT DEM, and a high-quality local LiDAR DEM. Upper panels show Rockhampton, Australia, and Lower panels show St Louis, USA. 85
Figure 9: Histograms comparing FABDEM with COPDEM30 and MERIT DEM against reference data (reproduced from (Hawker, et al., 2022)). 85
Figure 10: Geometry of the Florida Bay (eke2) SLOSH basin. 87
Figure 11: Non-dimensional wind field profile. 91
Figure 12: The non-dimensional pressure field profile. 92
Figure 13: Storm surge Footprint compared with high water mark observation data for hurricane Opal (1995). 96
Figure 14: Scatter plot comparison of IF modeled storm surge footprint and high water mark observation data for Hurricane Opal (1995). (horizontal datum: NAD83, vertical datum: NAVD88) 97
Figure 15: Storm surge Footprint compared with high water mark observation data for hurricane Charley (2004). 98
Figure 16: Scatter plot comparison of IF modeled storm surge footprint and high water mark observation data for Hurricane Charley (2004). (horizontal datum: NAD83, vertical datum: NAVD88).....99
Figure 17: Storm surge Footprint compared with high water mark observation data for Hurricane Dorian (2019). There are many pixels, all with the same maximum value, located very close to each other. These pixels have been grouped into three clusters, as shown in the figure, represented by the triangles. 99
Figure 18: Scatter plot comparison of IF modeled storm surge footprint and high water mark observation data for Hurricane Dorian (2019). (horizontal datum: NAD83, vertical datum: NAVD88) 100
Figure 19: Storm surge Footprint compared with high water mark observation data for Hurricane Sally (2020). 101
Figure 20: Scatter plot comparison of IF modeled storm surge footprint and high water mark observation data for Hurricane Sally (2020). (horizontal datum: NAD83, vertical datum: NAVD88) 102
Figure 21: Flow chart illustrating the Impact Forecasting Florida Flood Model – Storm Surge components. 106

Figure 22: Flow chart illustrating the Impact Forecasting Florida Flood Model – Inland Flood components. 106
Figure 23: Surface map of maximum modeled water levels (m, relative to NAVD88). 109
Figure 24: Validation of RFFA methods applied by Wing et al. (2017), v1, and the updated version, v2, used in this study. The figure displays the errors in estimated discharge, computed using benchmark data from USGS StreamStats data, for the 1 in 5 (a), 10 (b), 50 (c), 100 (d), 200 (e), and 500 years (f) events. RFFA, Regionalized Flood Frequency Analyses; USGS, United States Geological Survey. 115
Figure 25: Comparison of simulated flood elevation at different frequencies (orange line and markers) with historic frequencies from NOAA (blue line and markers). The upper and low bounds of the 95 percent confidence interval of the measured flood elevation frequencies are also included with dashed blue lines and markers. The comparison was conducted for Vaca Key (top), Cedar Key (middle) and Clearwater Beach (bottom). 116
Figure 26: Fluvial (left) and pluvial (right) discretization of the region. 120
Figure 27: An example demonstrating the process of extracting flood maps for a catchment unit. 121
Figure 28: An example of the overlapping fluvial catchments in three river reaches, with RP100 masks shown in orange and green. 122
Figure 29: Conceptual diagram of (a) LISFLOOD-FP base model, (b) sub-grid channels model and (c) sub-grid section. 131
Figure 30: Evaluation of the flow simulation for tropical cyclone Frances (2004): A) Observed peak flow, the total number of gauges with available data is indicated in the title, gauges with no data are indicated by a cross, the TC track is shown in purple; B) Simulated peak flow at all 291 gauges, the TC track is shown in purple; C) and D) example hydrographs, observed and simulated flow. Gauge locations are marked with a square (for the location in example C), and a triangle (for the location in example D). 138
Figure 31: Evaluation of the flow simulation for cyclone Eta (2020): A) Observed peak flow, the total number of gauges with available data is indicated in the title, gauges with no data are indicated by a cross, the TC track is shown in purple; B) Simulated peak flow at all 291 gauges, the TC track is shown in purple; C) and D) example hydrographs, observed and simulated flow. Gauge locations are marked with a square (for the location in example C), and a triangle (for the location in example D). 139
Figure 32: Evaluation of the flow simulation for cyclone Andrew (1992): A) Observed peak flow, the total number of gauges with available data is indicated in the title, gauges with no data are indicated by a cross, the TC track is shown in purple; B) Simulated peak flow at all 291 gauges, the TC track is shown in purple; C) and D) example hydrographs, observed and simulated flow. Gauge locations are marked with a square (for the location in example C), and a triangle (for the location in example D). 140
Figure 33: Evaluation of the flow simulation for cyclone Michael (2018): A) Observed peak flow, the total number of gauges with available data is indicated in the title, gauges with no data are indicated by a cross, the TC track is shown in purple; B) Simulated peak flow at all 291 gauges, the TC track is shown in purple; C) and D) example hydrographs, observed and simulated flow. Gauge locations are marked with a square (for the location in example C), and a triangle (for the location in example D). 141
Figure 34: Evaluation of the flow simulation for cyclone Wilma (2005): A) Observed peak flow, the total number of gauges with available data is indicated in the title, gauges with no data are indicated by a cross, the TC track is shown in purple; B) Simulated peak flow at all 291 gauges, the TC track is shown in purple; C) and D) example hydrographs, observed and simulated flow. Gauge locations are marked with a square (for the location in example C), and a triangle (for the location in example D). 142
Figure 35: Evaluation of the flow simulation for cyclone Matthew (2016): A) Observed peak flow, the total number of gauges with available data is indicated in the title, gauges with no data are indicated by

a cross, the TC track is shown in purple; B) Simulated peak flow at all 291 gauges, the TC track is shown in purple; C) and D) example hydrographs, observed and simulated flow. Gauge locations are marked with a square (for the location in example C), and a triangle (for the location in example D). 143
Figure 36: Evaluation of the flow simulation for cyclone Irma (2017): A) Observed peak flow, the total number of gauges with available data is indicated in the title, gauges with no data are indicated by a cross, the TC track is shown in purple; B) Simulated peak flow at all 291 gauges, the TC track is shown in purple; C) and D) example hydrographs, observed and simulated flow. Gauge locations are marked with a square (for the location in example C), and a triangle (for the location in example D). 144
Figure 37: Evaluation of the flow simulation for cyclone Hermine (2016): A) Observed peak flow, the total number of gauges with available data is indicated in the title, gauges with no data are indicated by a cross, the TC track is shown in purple; B) Simulated peak flow at all 291 gauges, the TC track is shown in purple; C) and D) example hydrographs, observed and simulated flow. Gauge locations are marked with a square (for the location in example C), and a triangle (for the location in example D). 145
Figure 38: Evaluation of the flow simulation for cyclone Ivan (2004): A) Observed peak flow, the total number of gauges with available data is indicated in the title, gauges with no data are indicated by a cross, the TC track is shown in purple; B) Simulated peak flow at all 291 gauges, the TC track is shown in purple; C) and D) example hydrographs, observed and simulated flow. Gauge locations are marked with a square (for the location in example C), and a triangle (for the location in example D). 146
Figure 39: Spearman rank correlation computed for each gauge across all 9 tropical cyclones and shown as A) a map and B) a histogram. 147
Figure 40: Location of the two levee systems in Florida: (left) Fort Pickens Seawall; and (right) L-31 East levee system. 153
Figure 41: S-67 Tieback Levee: Levee over satellite imagery(left), levee with defended 350-year flood map (center) & levee with undefended 350-year flood map(right).....156
Figure 42: Abruckle Creek Levee: Levee over satellite imagery(left), levee with defended 40-year flood map (center) & levee with undefended 40-year flood map(right).....156
Figure 43: S-84 Tieback North Levee: Levee over satellite imagery(left), levee with defended 750-year flood map (center) & levee with undefended 750-year flood map(right).....156
Figure 44: S-84 L-31 East Levee: Levee over satellite imagery(left), surge footprint without levee failure (center) & surge footprint with levee failure (right). 157
Figure 45: Location of points selected for HHF-4 160
Figure 46: Situation of locations selected for HHF-4 analysis, with modeled 1 in 100 years (base-model) hazard illustrating the on-site flood flow conditions. 162
Figure 47: Demonstration of increased water surface elevation (in feet above the mean sea level) with increased roughness in each of the 5 assessment locations during 100yr fluvial event.....164
Figure 48: Demonstration of increased discharge with increased steepness in each of the 5 assessment locations during 100yr fluvial event.....166
Figure 49: Demonstration of increased discharge with increased imperviousness in each of the 5 assessment locations during 100yr pluvial event 168
Figure 50: Flood hazard comparison (1 in 100 years) and inundation depth for HHF-4 location #1.....169
Figure 51: Flood hazard comparison (1 in 100 years) and inundation depth for HHF-4 location #2.....170
Figure 52: Flood hazard comparison (1 in 100 years) and inundation depth for HHF-4 location #3.....171
Figure 53: Flood hazard comparison (1 in 100 years) and inundation depth for HHF-4 location #4.....172
Figure 54: Flood hazard comparison (1 in 100 years) and inundation depth for HHF-4 location #5.....173

Figure 55: Comparison of modeled and observed frequencies of Florida landfalling tropical cyclones per category. 180
Figure 56: 20yr and 100yr return period comparisons between the non-TC synthetic event set and the historical training data 181
Figure 57: Historical training data and non-TC synthetic event set event size distributions from 2 example data locations representing the best (left) and worst (right) performance. 181
Figure 58: Historical training data and synthetic event set event size distributions. 182
Figure 59: Site example co-occurrence plots; top (Miami), middle (best scoring), bottom (worst scoring) examples 183
Figure 60: The histogram of co-occurrence r2 scores across all Florida data locations 184
Figure 61: Chi statistics (Coles, et al., 2001) over 5,000 data site pairs in the historical training data and the synthetic data. 185
Figure 62: Example fluvial likelihood maps (SiteID = 1398). 186
Figure 63: Example fluvial likelihood maps (SiteID = 5679). 186
Figure 64: The synthetic event set and historic agnostic empirical distributions of events per year (left), an ensemble of CDFs from 5000 iterations of 40yrs of data from the synthetic event set with historical (red) overlain (right). For clarity, the CDFs are linearly interpolated within these figures. 187
Figure 65: The monthly event occurrence rate for TC events affecting Florida. 188
Figure 66: The seasonality of threshold exceedances in the historical training data and synthetic data event sets. 188
Figure 67: The historic (left) and synthetic event set (right) proportional month event rates. 189
Figure 68: The target event metric scores (orange) and the 12 'similar' events from the statistical model non-TC synthetic event set (blue). 190
Figure 69: The fluvial and pluvial footprints associated with the target event chosen from the historical training data. 190
Figure 70: Example events (EventID = 296732 -top and Event ID = 935658 -bottom) from the non-TC synthetic event set that met the specified criteria to be 'similar' to the target event. Magnitudes given in terms of return period. 191
Figure 71: Storm Surge Building Damage Functions Statistical Significance Test 192
Figure 72: Box Plot Of Storm Surge Depth/Damage Ratios with NFIP Claims 192
Figure 73: Inland Flood Building Damage Function Statistical Significance Test 192
Figure 74: Box Plot Of Inland Flood Depth/Damage Ratios with NFIP Claims 193
Figure 75 SRCs for expected storm surge loss costs for all input variables for all hurricane categories. 195
Figure 76 Example of water-level increment after hydraulic roughness was increased by 20% (Alafia River in Hillsborough County) 196
Figure 77 Example of discharge increment after DTM elevation was increased by 20% (Alafia River in Hillsborough County) 197
Figure 78 Example of water-level increment after surface permeability is switched off (Alafia River in Hillsborough County) 198
Figure 79 Example of water-level increment after input discharge was increased by 20% (Alafia River in Hillsborough County) 199
Figure 80 Difference in KGE between the hindcasts using Manning's coefficient of 0.03 versus 0.01. Values greater than 0 indicate a higher KGE with n=0.03, while values smaller than 0 indicate a better performance with n=0.01. 200

Figure 81: Sensitivity analysis empirical CDFs of event duration (left) and event size (right)..... 201
Figure 82: EPRs for expected storm surge loss costs for all input variables for all hurricane categories. 203
Figure 83 Historical Event Loss Comparison..... 209
Figure 84. Development and implementation of building flood vulnerability functions. 212
Figure 85. Hydrostatic and hydrodynamic forces action: a) on an unelevated building for enclosed dry space behind wall; b) on an unelevated building after envelope breach; c) on an elevated building for enclosed dry space behind wall; d) on an elevated building after envelope breach. Legend: Fstat – hydrostatic force; Fdyn – drag (hydrodynamic) force; Cd – drag coefficient (this coefficient differs for piles and walls); ds – still water level; D – pile diameter; Np – number of piles in one row; hf – floor elevation; w – width of wall; ρ – mass density of water; γw – specific weight of water. Intruded water and corresponding hydrostatic forces are not shown to ensure figure simplicity..... 216
Figure 86. Breaking wave force action (for enclosed dry space behind wall): a) on piles; b) on piles and wave slam; c) on piles and reflecting wave; d) reflecting wave crest overtops the building wall. Legend: Fbrkp – drag force on pile; Fbrkw – breaking wave force on wall; Fs – wave slam force; Cdb – breaking wave drag coefficient; Cp – dynamic pressure coefficient; Cs – slam coefficient; ds – still water level; Hb – breaking wave height; D – pile diameter; hf – floor elevation; w – width of wall; hs = (1.55ds-hf) – height of wall affected by slam ; γw – specific weight of water. 217
Figure 87. Development and implementation of content vulnerability functions. 229
Figure 88. Development and implementation of time element vulnerability functions. 234
Figure 89: User workflow to create flood model output 244
Figure 90: Screenshot of the Florida Flood TC/Non-TC Loss Compiler tool that can be used to combine Tropical Cyclone and Non Tropical Cyclone results to create a compiled analysis appropriate for rate filing. 245
Figure 91: Sample Portfolio Import Summary 249
Figure 92:Sample Portfolio Import Log 249
Figure 93: Example of a modeling process flowchart..... 269
Figure 94: Model implementation in ELEMENTS software and deployment process 280
Figure 95: Example of models hosted on the ELEMENTS platform 281
Figure 96: Storm surge validation footprint for Hurricane Andrew (1992). 303
Figure 97: Storm surge validation footprint for Hurricane Ivan (2004). 304
Figure 98: Storm surge validation footprint for Hurricane Frances (2004). 304
Figure 99: Storm surge validation footprint for Hurricane Wilma (2005). 305
Figure 100: Storm surge validation footprint for Hurricane Matthew (2016). There are 25 pixels, all with the same maximum value, located very close to each other. These pixels have been grouped into two clusters, as shown in the figure, represented by the triangles. 306
Figure 101: Inland flood validation footprint for Hurricane Matthew (2016). 307
Figure 102: Storm Surge validation footprint for Hurricane Hermine (2016). 307
Figure 103: Inland flood validation footprint for Hurricane Hermine (2016). 308
Figure 104: Storm surge validation footprint for Hurricane Irma (2017). 309
Figure 105: Inland flood validation footprint for Hurricane Irma (2017). 310
Figure 106: Storm surge validation footprint for Hurricane Michael (2018). 311
Figure 107: Inland flood validation footprint for Hurricane Michael (2018). 311
Figure 108: Storm surge validation footprint for Hurricane Eta (2020). 312
Figure 109: Inland Flood validation footprint for Hurricane Eta (2020). 312

Figure 110: Storm surge validation footprint for Hurricane Ian (2022). 313
Figure 111: Inland flood validation footprint for Hurricane Ian (2022). 314
Figure 112: Storm surge validation scatter plots for Hurricane Andrew (1992). (horizontal datum: NAD83, vertical datum: NAVD88)..... 315
Figure 113: Storm surge validation scatter plots for Hurricane Ivan (2004). (horizontal datum: NAD83, vertical datum: NAVD88)..... 316
Figure 114: Storm surge validation scatter plots for Hurricane Frances (2004). (horizontal datum: NAD83, vertical datum: NAVD88) 316
Figure 115: Inland validation scatter plots for Hurricane Frances (2004). (Vertical datum: EGM 08) 317
Figure 116: Storm surge validation scatter plots for Hurricane Wilma (2005). (horizontal datum: NAD83, vertical datum: NAVD88)..... 318
Figure 117: Storm surge validation scatter plots for Hurricane Matthew (2016). (horizontal datum: NAD83, vertical datum: NAVD88) 318
Figure 118: Inland Flood validation scatter plots for Hurricane Matthew (2016). (Vertical datum: EGM 08) 319
Figure 119: Storm surge validation scatter plots for Hurricane Hermine (2016). (horizontal datum: NAD83, vertical datum: NAVD88) 320
Figure 120: Inland Flood validation scatter plots for Hurricane Hermine (2016). (Vertical datum: EGM 08) 320
Figure 121: Storm surge validation scatter plots for Hurricane Irma (2017). (horizontal datum: NAD83, vertical datum: NAVD88)..... 321
Figure 122: Inland Flood validation scatter plots for Hurricane Irma (2017). (Vertical datum: EGM 08). 321
Figure 123: Storm surge validation scatter plots for Hurricane Michael (2018). (horizontal datum: NAD83, vertical datum: NAVD88)..... 322
Figure 124: Inland Flood validation scatter plots for Hurricane Michael (2018). (Vertical datum: EGM 08) 322
Figure 125: Storm surge validation scatter plots for Hurricane Eta (2020). (horizontal datum: NAD83, vertical datum: NAVD88)..... 323
Figure 126: Inland flood validation scatter plots for Hurricane Eta (2020). (Vertical datum: EGM 08).. 323
Figure 127: Storm surge validation scatter plots for Hurricane Ian (2022). (horizontal datum: NAD83, vertical datum: NAVD88)..... 324
Figure 128: Inland Flood validation scatter plots for Hurricane Ian (2022). (Vertical datum: EGM 08) . 324
Figure 129: Modeled storm surge extent and depth corresponding to the 0.01 annual exceedance probability for Broward County. There are 306 pixels, all with the same maximum value, located very close to each other. These pixels have been grouped into two clusters, as shown in the figure, represented by the triangles. (horizontal datum: WGS84, vertical datum: EGM08) 327
Figure 130: Modeled storm surge extent and depth corresponding to the 0.01 annual exceedance probability for Levy County. (horizontal datum: WGS84, vertical datum: EGM08) 328
Figure 131: Modeled storm surge extent and depth corresponding to the 0.01 annual exceedance probability for Pinellas County. (horizontal datum: WGS84, vertical datum: EGM08) 329
Figure 132: Modeled storm surge extent and depth corresponding to the 0.01 annual exceedance probability for Wakulla County. There are 56 pixels, all with the same maximum value. These pixels have been grouped into two clusters, represented by the triangles. (horizontal datum: WGS84, vertical datum: EGM08) 330

Figure 133: Modeled storm surge extent and depth corresponding to the 0.01 annual exceedance probability for Brevard County. (horizontal datum: WGS84, vertical datum: EGM08)..... 331
Figure 134: Modeled inland flood extent and depth corresponding to the 0.01 annual exceedance probability for Washington County in Panhandle region. 335
Figure 135: Modeled inland flood extent and depth corresponding to the 0.01 annual exceedance probability for Clay County in North Florida region. 336
Figure 136: Modeled inland flood extent and depth corresponding to the 0.01 annual exceedance probability for Hardee County in Southwest Florida region. 337
Figure 137: Modeled inland flood extent and depth corresponding to the 0.01 annual exceedance probability for Broward County in Southeast Florida region. 337
Figure 138: Modeled inland flood extent and depth corresponding to the 0.01 annual exceedance probability for Indian River County in East Florida region. 338
Figure 139: Estimated structure damage ratios by ranges of flood depths for Coastal Flood. 350
Figure 140: Estimated structure damage ratios by ranges of flood depths for Inland Flood. 353
Figure 141: Zero deductible standard flood loss costs by county for frame owners. 360
Figure 142: Zero deductible standard flood loss costs by county for masonry owners. 361
Figure 143: Zero deductible standard flood loss costs by county for manufactured owners. 362
Figure 144: Percentage of total residential flood losses for Hurricane Andrew (1992) by Zip Code..... 371
Figure 145: Percentage of total residential flood losses for Hurricane Ivan (2004) by Zip Code 372
Figure 146: Percentage of total residential flood losses for Hurricane Jeanne (2004) by Zip Code 373
Figure 147: Percentage of total residential flood losses for Hurricane Wilma (2005) by Zip Code..... 374
Figure 148: Percentage of total residential flood losses for Tropical Storm Fay (2008) by Zip Code ... 375
Figure 149: Percentage of total residential flood losses for Unnamed Storm in East Florida (May 2009) by Zip Code 376
Figure 150: Percentage of total residential flood losses for Unnamed Storm in Panhandle (July 2013) by Zip Code 377
Figure 151: Percentage of total residential flood losses for Hurricane Matthew (2016) by Zip Code..... 378
Figure 152: Percentage of total residential flood losses for Hurricane Irma (2017) by Zip Code 379
Figure 153: Percentage of total residential flood losses for Hurricane Michael (2018) by Zip Code 380
Figure 154: Percentage Change in Specified Deductible Flood Loss Costs by County for Frame Owners 418
Figure 155: Percentage Change in Specified Deductible Flood Loss Costs by County for Masonry Owners..... 419
Figure 156: Percentage Change in Specified Deductible Flood Loss Costs by County for Frame Renters 420
Figure 157: Percentage Change in Specified Deductible Flood Loss Costs by County for Masonry Renters 421
Figure 158: Percentage Change in Specified Deductible Flood Loss Costs by County for Frame Condo Unit Owners..... 422
Figure 159: Percentage Change in Specified Deductible Flood Loss Costs by County for Masonry Condo Unit Owners..... 423
Figure 160: Percentage Change in Specified Deductible Flood Loss Costs by County for Manufactured Homes..... 424
Figure 161: Screenshot of sample hurricane model input file (parts 1 through 9). 456
Figure 162: Screenshots of ELEMENTS input file import options (Server Details, part 1 of 3). 456

Figure 163: Screenshots of ELEMENTS input file import options (Input File Details, part 2 of 3)..... 456
Figure 164: Screenshots of ELEMENTS input file import options (Peril / Geocoding Details, part 3 of 3). 457
Figure 165: Screenshot of flood model analysis settings required for Tropical Cyclone Induced Flooding (FCHLPM) (part 1 of 2)..... 458
Figure 166: Screenshot of flood model analysis settings required for Tropical Cyclone Induced Flooding (FCHLPM) (part 2 of 2). 458
Figure 167: Screenshot of flood model analysis settings required for Non-Tropical Cyclone Induced Flooding (FCHLPM) (part 1 of 2). 459
Figure 168: Screenshot of flood model analysis settings required for Non-Tropical Cyclone Induced Flooding (FCHLPM) (part 2 of 2)..... 459
Figure 169: Screenshot of flood model output report (part 1 of 2)..... 460
Figure 170: Screenshot of flood model output report (occurrence exceedance probability, left, and aggregate exceedance probability, right) (part 2 of 2) 460
Figure 171: Screenshot of flood model output report from FCHLPM Florida Flood TC/Non-TC Loss Compiler tool 461

GENERAL FLOOD STANDARDS

GF-1 Scope of the Flood Model and Its Implementation

A. *The flood model shall project loss costs and probable maximum loss levels for primary damage to insured personal residential property from flood events.*

The flood model developed by Impact Forecasting (IF) estimates loss costs and probable maximum losses to insured residential property caused by damage from flood events. Loss outputs are modeled for primary structure, appurtenant structure, contents, and time element coverages and are validated extensively using historical claims data. The methods used by Impact Forecasting in flood loss cost and probable maximum loss estimation are actuarially sound as demonstrated in Standard AF-4.

B. *A documented process shall be maintained to assure continual agreement and correct correspondence of databases, data files, and computer source code to presentation materials, scientific and technical literature, and modeling organization documents.*

Impact Forecasting employs standard methods and procedures to ensure agreement and correct correspondence of databases, data files, and computer source code. Source control software and error tracking systems are used to maintain accuracy.

C. *All software, data, and flowcharts (1) located within the flood model, (2) used to validate the flood model, (3) used to project modeled flood loss costs and flood probable maximum loss levels, and (4) used to create forms required by the Commission in the Flood Standards Report of Activities shall fall within the scope of the Computer/Information Flood Standards and shall be located in centralized, model-level file areas.*

All software, data, and flowcharts used to develop and validate the Impact Forecasting model, project loss outputs, and create forms comply with the Computer/Information Standards and are kept in centralized, model-level file areas.

D. *Differences between historical and modeled flood losses shall be reasonable, given available flood loss data.*

The Impact Forecasting model's simulated event sets are developed and validating using historical data sets, and the model's loss outputs are validated extensively using historical claims data. Individual components of the model are tested and observed to be consistent with historical flood events. Good agreement is observed between modeled flood losses and historical flood losses. Differences between historical and modeled flood losses are reasonable and are due to different sample sizes of historical and stochastic storm sets and various uncertainties within.

E. *Vintage of data, code, and scientific and technical literature used shall be justifiable.*

Impact Forecasting rigorously evaluates data, code, and scientific and technical literature on a continuous basis. When new data, code, and literature are made available, Impact Forecasting incorporates the most recent vintage of data or information when it is a sufficiently defensible

improvement on older sources, and when it is demonstrably fit for use within the model's framework and development cycle.

Disclosures

GF-1.1 ***Specify the flood model version identification. If the flood model submitted for review is implemented on more than one platform, specify each flood model platform identifying the primary platform and the distinguishing aspects of each platform.***

The flood model submitted for review is the Impact Forecasting Florida Flood (FCHLPM) Model Version 3.0. The Impact Forecasting loss modeling platform associated with the model submission is ELEMENTS Version 18.0.

GF-1.2 ***Provide a comprehensive summary of the flood model. This summary should include a technical description of the flood model, including each major component of the flood model used to project loss costs and probable maximum loss levels for insured primary damage to personal residential property from flood events causing damage in Florida. Describe the theoretical basis of the flood model and include a description of the methodology, particularly the meteorology components, the hydrology and hydraulic components, the vulnerability components, and the insured flood loss components used in the flood model. The description should be complete and is not to reference unpublished work.***

The Impact Forecasting Florida Flood model is designed to estimate insured losses from multiple sources of flooding, including fluvial and pluvial flooding arising from both tropical and non-tropical systems along with coastal storm surge flooding caused by tropical systems, including hurricanes. The flood hazard was developed in partnership with Fathom, making use of their flood hazard maps for multiple return periods. The model consists of the following four components: hazard, exposure and geocoding, vulnerability, and financial. These components are discussed in the following sections:

Hazard Component

Event Set

The probabilistic Impact Forecasting Florida Flood model contains two event sets: one that addresses Tropical Cyclone Induced Flooding (fluvial, pluvial, and storm surge), and one that addresses the non-tropical system induced pluvial (precipitation) and fluvial (riverine) flooding. To begin with the Tropical Cyclone event set, the frequency of flooding proceeds from the wind event frequencies. This ensures that the Tropical Cyclone portion of the Flood model is consistent with the Tropical Cyclone Wind model. This event set produces an Event Loss Table (ELT) as a default output.

In order to model the causes of inland flooding apart from Tropical Cyclones, the non-TC event set (Non-Tropical System Induced Flooding) was developed with a separate methodology. The non-TC event set was developed by Fathom and is based on the temporal and spatial extrapolation of flood characteristics derived from MSWEP (Multi-Source Weighted-Ensemble Precipitation) precipitation reanalysis (Beck, et al., 2022) and corresponding discharge estimates from in-house hydrological modeling frameworks using the FUSE (Framework for Understanding Structural Errors) (Clark, et al., 2008) and

mizuRoute (Mizukami, et al., 2016) hydrological and routing software, respectively. The non-TC component of the synthetic event set is fundamentally centered on a derivative of the multivariate extreme value model first introduced by (Heffernan & Tawn, 2004), which aims to characterize tail dependence between a series of datasets (both discharge and precipitation time series), then use those characteristics to inform the creation of synthetic event footprints. All event frequencies in the resulting event set are equal, at a rate of 0.0001 (=1/10,000). To ensure that only precipitation and flows from non-tropical systems were used to generate this event set, the reanalysis hydro-meteorological data, which serves as the basis for calibrating the statistical models, was cleansed of the tropical cyclones data set using records from the IBTrACs (The International Best Track Archive for Climate Stewardship) database (Knapp, et al., 2010; 2018). In the modeling framework, including semi-empirical and Laplace distribution choices are standard in environmental applications within the literature; see for instance (Quinn, et al., 2019; Diederen, et al., 2019; Li, et al., 2023). This event set produces a Year Loss Table (YLT) by default.

As it is important to connect the TC and non-TC view of flooding risk, Impact Forecasting connects the two event sets (TC and non-TC) into a unified table of 200,000 years. The TC event set was created by beginning with 200,000 years of stochastic simulation. Then, in order to improve computational efficiency, events with very similar characteristics are aggregated into a single representative event, whose rate is then adjusted corresponding to the number of stochastically simulated events that were part of the initial aggregation in order to preserve the original events' frequencies of 1/200,000. The result of that aggregation process is a TC event set with a reduced total number of events, but with event rates consistent with the 200,000 years of stochastic simulation. The non-TC event set, provided by Fathom and which originally comprised 10,000 years, is replicated 20 times to produce a matching catalog size. This table and the associated link is accessible in the ELEMENTS Query Explorer or by query (in SQL).

Inundation Modeling

The model contains three flood hazard sub-perils: fluvial (riverine) flood, pluvial (rainfall) flood, and storm surge. The fluvial and pluvial hazard development was done by Fathom, while the storm surge hazard was developed internally by Impact Forecasting.

The fluvial and pluvial hazard are dynamically simulated using the two-dimensional hydrodynamic model LISFLOOD–FP (Bates, et al., 2010), which is a numerical solver of partial differential equations, specifically the Saint-Venant equations. The fluvial model simulates flooding originating from river channels by simulating a range of river discharges through the hydrodynamic model, whilst the pluvial model simulates a range of rainfall intensities and durations through the hydrodynamic model using a rain-on-grid approach. Both approaches are outlined in more detail below.

Fluvial Simulation

Fluvial simulations were performed at a 1 arc second (approximately 30 m) spatial resolution. These simulations were split into a series of 1° x 1° tiles (approximately 100 km x 100 km), plus an additional 0.25° buffer region (so in total covering an area of 1.5° x 1.5°). These included the watercourses coming from the NHD+ dataset and its associated flow direction grid (Buto, 2020). Rivers with an upstream catchment area >193.051 sq mi (500 sq km) are simulated within the fluvial model with boundary conditions distributed along the river network. The NHD+ dataset was used to establish the location of river channels, whilst the underlying terrain is provided by a 1 arc second (approximately 30m) spatial resolution

digital terrain model (DTM) comprised of a combination of LiDAR (Light Detection and Ranging) and FABDEM (Hawker, et al., 2022). The model resolution was determined by Fathom to be an appropriate balance between computational runtime and representation of the landscape's morphology.

In order to address the inability of a 30m terrain model to represent channel geometry below its native resolution, Fathom uses a coupled 1D/2D approach (Neal, et al., 2012) in combination with a bathymetry estimation solver (Neal, et al., 2021) to accurately capture bankfull discharge and simulate inundation caused by discharge in excess of bankfull. The simulation uses an adaptive timestep scheme to calculate the fluxes in the x and y Cartesian directions using an inertial form of shallow water equations.

The hydrologic inputs used in the fluvial simulation process were informed by regional flood frequency analysis (Smith, et al., 2015; Bates, et al., 2021) using long-term observations from USGS (United States Geological Survey) river gauge data.

Pluvial Simulation

Pluvial simulations were performed at a 1 arc second (approximately 30 m) spatial resolution. These simulations were split into the same series tiles as the fluvial model. These included the watercourses coming from the NHD+ dataset and its associated flow direction grid (Buto, 2020) with an upstream catchment area >19.3051 sq miles (50 sq km). The underlying DTM is the same as the fluvial model. The model resolution was determined by Fathom to be an appropriate balance between computational runtime and representation of the landscape's morphology.

The initial forcing for the pluvial simulation are the one-, six-, and 24-hour precipitation intensities associated with several return periods of extreme precipitation. Precipitation intensities for each model simulation are taken from the National Oceanic and Atmospheric Administration (NOAA) National Oceanic and Atmospheric Administration Atlas 14 Intensity Duration Frequency (IDF) estimates (available at https://hdsc.nws.noaa.gov/hdsc/pfds/), which define the intensity and duration of event rainfall, and are explicitly simulated by the hydraulic model using a rain-on-grid approach. The simulation uses an adaptive timestep scheme to calculate the fluxes in the x and y Cartesian directions using an inertial form of shallow water equations. During model runtime, rainfall is simulated directly onto the DTM grid. Sub-grid channels are included in the model and are present for river channels with an upstream catchment area of 19.03 sq mi (50 sq km) or greater to allow rainfall to be routed through the river network. Rainfall intensity is applied uniformly in time. However, rainfall intensity is spatially variable and is further varied depending on assumptions on infiltration and urban drainage, the effects of which are applied to the pluvial boundary conditions rather than modeled explicitly within the hydraulic model (Bates, et al., 2021).

Tropical Cyclone Rainfall

Precipitation is explicitly modeled, utilizing a physics-based Tropical Cyclone Rainfall (TCR) model developed by (Lu, et al., 2018) and (Feldmann, et al., 2019). Detailed information about the model can be found in the studies by (Lu, et al., 2018) and (Feldmann, et al., 2019). This model computes rain rates and accumulated rainfall at specified Points of Interest (POI), defined as any 0.1°×0.1° grid point in the continental United States.

The TCR model estimates rainfall by multiplying the saturation specific humidity and vertical velocity, derived from the time-evolving storm wind field and environmental winds. The TCR encompasses five physical mechanisms including topographic forcing, frictional convergence, vortex stretching, baroclinic effects, and radiative cooling to generate rainfall. The total vertical velocity is computed as the sum of the vertical velocities from these components, and the vertical vapor flux is determined by multiplying the total vertical velocity with the specific humidity.

A rain rate is then calculated by multiplying the vertical vapor flux by the assumed precipitation efficiency of 0.9. Consequently, the hourly rain rate is computed for each point of interest throughout the entire lifetime of the track.

Lacustrine Modeling

As lakes have some slightly different modeling challenges than rivers and streams, the lacustrine modeling was performed separately before being linked with the fluvial and pluvial flood hazard. As Florida's topography is extremely flat, the lacustrine modeling can be very sensitive. Simulation was performed for lake systems with available observational data, such as those with water level gauge stations. For lakes with available data, frequency analyses were carried out on the observed time series, and the water levels for modeled hydrological return periods were identified. These underlying DTM was then subtracted from the water levels, post-processed, and merged with the fluvial hazard. Hazard masks providing a link to the event set were adjusted to reflect the extent of lacustrine inundation. For the remaining lakes without available data, two-dimensional modeling was used, treating the lake as a wide river with excess water accumulation potential being accounted for by the DTM.

Linking Flood Hazard Maps and Event Set

As the hazard data described above are effectively seamless flood hazard maps covering the contiguous United States, it is necessary to generate both stochastic and historical events for the model. To do this, the hazard maps are broken into segments that are linked with the event set. For the pluvial hazard, the HUC10 (hydraulic unit codes) units from the NHD+ dataset are used. Each HUC10 unit is applied a constant Return Period of pluvial hazard during each synthetic event. The pluvial hazard values are taken from the seamless hazard map, and the events in the event set inundation footprints are comprised of combinations of these HUC10 unit areas.

The fluvial hazard requires a more nuanced approach, as the model must account for areas that can be flooded from multiple segments (areas in close proximity to river junctions). As a result, the segments linked to the event set must realistically overlap with each other. Fathom created polygons representing specific river reach inundation zones. These river reaches were generated and defined by a combination of the river network Strahler order and a concentration time threshold of six hours. Hydrodynamic simulations were performed for each river reach. The outputs of these simulations are essentially polygonal rasters, outlining the hazard for different return periods for each river reach and an additional buffer to capture potential overlap with downstream reaches. As multiple river reaches may overlap at confluences, any location receiving hazard from multiple reaches is assigned the higher flood depth.

Storm Surge

The hazard footprint of the Impact Forecasting US Flood Model – Storm Surge is developed based on the Sea, Lake and Overland Surges from Hurricanes (SLOSH) model. It was developed by the National Weather Service (NWS) of the National Oceanic and Atmospheric Administration (NOAA) in the early 1980s to delineate evacuation zones with high computational efficiency. It is still the operational storm surge model of the National Hurricane Center (NHC). Over the years, it was selected as a benchmark model for the evaluation of many other storm surge models because it is the only model in the United States that has been verified extensively against field observations for overland flooding along the East and Gulf coasts (Zhang, et al., 2008).

Storm Tracks

The SLOSH model is a computerized numerical model to estimate storm surge heights resulting from historical, hypothetical, or predicted hurricanes by taking into account their atmospheric pressure, size, forward speed, and track data. The storm surge component of the flood model uses tropical cyclone track data developed in-house to provide an event set that matches the Impact Forecasting Atlantic Tropical Cyclone - Wind (FCHLPM) V2.0 model. These track parameters (e.g. track location, central pressure, Rmax (radius of maximum winds)) are inputs to the SLOSH wind field model, which drives the modeled storm surge.

Wind Field Model

SLOSH uses a parametric wind field model based on the balance of forces along and normal to the surface wind trajectory (Myers, et al., 1961; Jelesnianski, et al., 1992):

$$\frac{1}{\rho_a}\frac{dp}{dr} = \frac{k_s v^2}{\sin\phi} - v\frac{dv}{dr} \tag{1}$$

$$\frac{1}{\rho_a}\frac{dp}{dr}\cos\phi = fv + \frac{v^2}{r}\cos\phi - v^2\frac{d\phi}{dr}\sin\phi + k_n v^2 \tag{2}$$

where $p(r)$ is the pressure field; $\phi(r)$ is the inflow angle field across circular isobars towards the storm center; k_s and k_n are the wind friction coefficients in the tangential direction and radial direction, respectively; f is the Coriolis parameter; ρ_a is density of air; and $v(r)$ is the wind speed field described as follows:

$$v(r) = v_{max}\frac{2R_{max}r}{R_{max}^2 + r^2} \tag{3}$$

where v_{max} is the maximum 1-minute sustained wind speed within the field. The aforementioned friction coefficients, k_s and k_n, are estimated using the following empirical equation:

$$k_s = 1.15k_n = \alpha\sqrt{\frac{10^{-4}R_{max}}{0.3v_{max}+60}} \tag{4}$$

where α is the location parameter ($\alpha = 1$ for ocean winds; $\alpha = 4\sqrt{22/R_{max}}$ for lake winds).

To solve these equations, an iteration procedure is used. v_{max} is approximated (using a table look-up procedure from pre-computations) and Eqs. (1) ~ (2) are then solved for $p(r)$

and $\phi(r)$. The discrepancy between computed and required pressure is then obviated by changing v_{max} until the pressure discrepancy is less than a preassigned value.

Governing Equations for the Surge Model

To compute surge heights, SLOSH uses the following equations of motion to balance the surface forces, including surface friction:

$$\frac{\partial U}{\partial t} = -g(D+h)\left[B_r \frac{\partial(h-h_0)}{\partial x} - B_i \frac{\partial(h-h_0)}{\partial y}\right] + f(A_r V + A_i U) + C_r x_\tau - C_i y_\tau \quad (5)$$

$$\frac{\partial V}{\partial t} = -g(D+h)\left[B_r \frac{\partial(h-h_0)}{\partial y} - B_i \frac{\partial(h-h_0)}{\partial x}\right] + f(A_r U + A_i V) + C_r y_\tau - C_i x_\tau \quad (6)$$

where U and V are the components of transport, g is the gravitational constant, D is the depth of quiescent water relative to a common datum, Ar, ... Ci are the bottom stress terms, h is the height of water above datum, h0 is the hydrostatic water height, f is the Coriolis parameter, and xτ and yτ are components of surface stress.

SLOSH Basin

SLOSH models the propagation of storm surge through wetting and drying of grid cells. Surge is computed at the center of each grid-square, and transport is computed on each momentum point. Factors affecting inland propagation of the storm surge include the ground elevation, trees, levees, and other barriers. All these geographic features used to control, route, and impede the flow of water are considered in SLOSH basins.

There are 28 basins covering the US Atlantic and Gulf of Mexico coasts; of them, 14 are in Florida. The basins are centered upon particularly susceptible features like inlets, large coastal population centers, low-lying topography, and ports. Each of the basins contains information on topography/bathymetry and terrain descriptions (heights referenced to the vertical datum, NAVD88 (North American Vertical Datum of 1988)) for each of the cells in the basin grid. The spatial coverage for each SLOSH basin varies from areas the size of a few counties to areas that cover a few states, the latter of which is not applicable to Florida. The grid is set up to have finer resolution in key areas for storm surge and coarse resolution in deep-water or boundary regions. SLOSH basins are updated at an average rate of 3-6 basins per year, and are governed by the Interagency Coordinating Committee on Hurricanes (ICCOH), a tri-agency supported by the U.S. Army Corps of Engineers (USACE), the Federal Emergency Management Agency (FEMA), and the National Oceanic and Atmospheric Administration (NOAA). Updates include finer grid size resolution to improve surge representation, increasing area covered by hypothetical tracks for improved accuracy, and the latest topography or bathymetric data for better representation of barriers, gaps, passes, and other local features (NOAA, 2023c).

The modeled water heights from SLOSH are mapped to the pre-defined grid system with 0.0025-degree resolution (equivalent to about 250m). The 250m resolution was determined based on the smallest SLOSH basin grid size for the majority of the basins. This predefined grid methodology allows for easy data retrieval.

Storm Surge Footprint Validation

The historical storm surge extents and depths in the model were validated against ADCIRC footprints and observation data obtained from the United States Geological Survey (USGS), the National Oceanic and Atmospheric Administration (NOAA), the Federal Emergency Management Agency (FEMA), the World's Storm Surge Data Center (SURGEDAT), and published literatures. The comparison of flood extent and elevation/depth with observation

data and FEMA return period maps can be found in Disclosure MF-4.1, Disclosure MF-5.3, and Forms HHF-1~HHF-5.

For stochastic events, the modeled return period surge maps are validated against NFIP (National Flood Insurance Program) extents. Detailed comparison maps are shown in Form HHF-3. The modeled stochastic storm surge elevation exceedance probabilities at several NOAA tidal station locations were compared with the observed frequencies (NOAA, 2023a). The validation of the return period storm surge elevation at several NOAA tidal stations is shown in Disclosure MF-5.3.

Exposure and Geocoding Component

The model is designed to process exposure on a location level, consuming either address information or Latitude/Longitude coordinates and assigning coordinates to each location. When address information is available for a location, the Precisely geocoding service is triggered during portfolio import and converts the given information to latitude and longitude coordinates in the WGS 84 coordinate standard. Locations with provided coordinates pass directly to the model, which consumes the coordinates in the WGS 84 coordinate standard. After creating these coordinates, the location is assigned an ID that corresponds to the appropriate 30m x 30m cell in the model.

Vulnerability Component

The vulnerability component of the Impact Forecasting Florida Flood Model (FCHLPM) relies on many years of building vulnerability assessment and structural engineering experience to produce thousands of vulnerability functions for different combinations of exposure variables (e.g., construction type, occupancy, year built, region, number of stories, foundation type, first floor height, and other property-specific characteristics), as well as for different flood sub-perils (e.g., fluvial, pluvial, and storm surge). The vulnerability component has been validated using claims data for different areas in Florida considering building code requirements and compliance practices, as well as using publicly available damage functions (Hazus Flood Model).

The vulnerability component is an integration of a suite of programs developed by Impact Forecasting. The most important program among them is a building component-based flood damage simulator, developed and maintained by Impact Forecasting's vulnerability team. The flood damage simulator uses engineering principles and reliability methods to estimate load and capacity characteristics of various components of a building susceptible to flood damage.

The simulator is based on a Monte Carlo framework which performs statistical sampling for various flood loading conditions (water depth, flow velocity, and wave height) and resistance values on different structural components in order to estimate damage outcomes for each component. These component-based results are aggregated into overall building outcomes, by evaluation of the dependencies between the components failure and the envelope breach or failure condition of the overall structure. Component damage estimates are then combined with a restoration cost model to determine repair cost and time estimates. Finally, these estimates are represented as the proportion of the overall combined component replacement values of the buildings, also known as damage ratios.

For use in the Impact Forecasting ELEMENTS catastrophe modeling platform, damage ratio estimates from the flood damage simulator are sorted by discrete water depth ranges. For each range, the uncertainty associated to the damage ratio is addressed by using the

OASIS format to probabilistically represent damage to assets subject to flooding. This distribution is determined from the simulations and is intended to reflect the damage uncertainty. Furthermore, different loss probability distributions are implemented for building, appurtenant structure, contents, and time element coverages for different combinations of exposure variables. Damage functions consider the impact of the Florida building codes, the NFIP post-FIRM building code, and regional vulnerability differences across Florida.

Impact Forecasting's structural and civil engineers have conducted numerous on-site damage surveys for past hurricane events to assist with the validation of damage modeling. This includes both recent hurricanes, such as Hurricane Matthew (2016), Hurricane Harvey (2017), Hurricane Irma (2017), Hurricane Michael (2018) and Hurricane Ian (2022), and hurricanes that occurred longer ago, like Hurricane Wilma (2005), Hurricane Katrina (2005) and Hurricane Sandy (2012). Complementary to learnings from on-site damage surveys, Impact Forecasting vulnerability engineers have reviewed numerous flood claims data sets and publicly available damage functions to further validate the vulnerability components.

Financial Component

The flood model's financial component applies the appropriate damage ratios to exposure replacement values to determine a risk's ground up loss. During the loss analysis, a Monte Carlo simulation is used to sample the damage distributions for a given level of flood depth (from each sub-peril: fluvial flooding, pluvial flooding, and storm surge) to account for damage uncertainty. Building, appurtenant structure, contents, and time element losses are determined using sampling from a vulnerability damage ratio histogram that is available for each damage function and respective hazard intensity. The appropriate number of damage samples required to ensure loss stability is determined by Impact Forecasting model developers for different analysis types.

Individual coverage-level samples are propagated through the financial component for the application of policy deductibles and limits. In the final step, ground up loss samples, net of policy conditions, are assembled into gross loss statistics including average annual losses and annual return period probable maximum loss levels (PMLs).

The financial component also incorporates a demand surge function to account for the increase in the cost of materials, services, and labor due to spikes in demand following a catastrophe (Olson & Porter, 2011a). The demand surge function exists individually for both TC and non-TC components of the model, capturing the difference in the type of damage and subsequent recovery caused by individual perils. The TC portion of the model function is developed based on analysis of the pricing information for the construction sector from Xactimate and XactContents. For the Non-TC portions of the model, demand surge is represented by a separate function developed using historical loss data and fluctuations in the labor and material costs specific to the construction sector following a major event.

GF-1.3 Provide a flowchart that illustrates interactions among major flood model components.

A flowchart is provided below in Figure 1 and Figure 2.

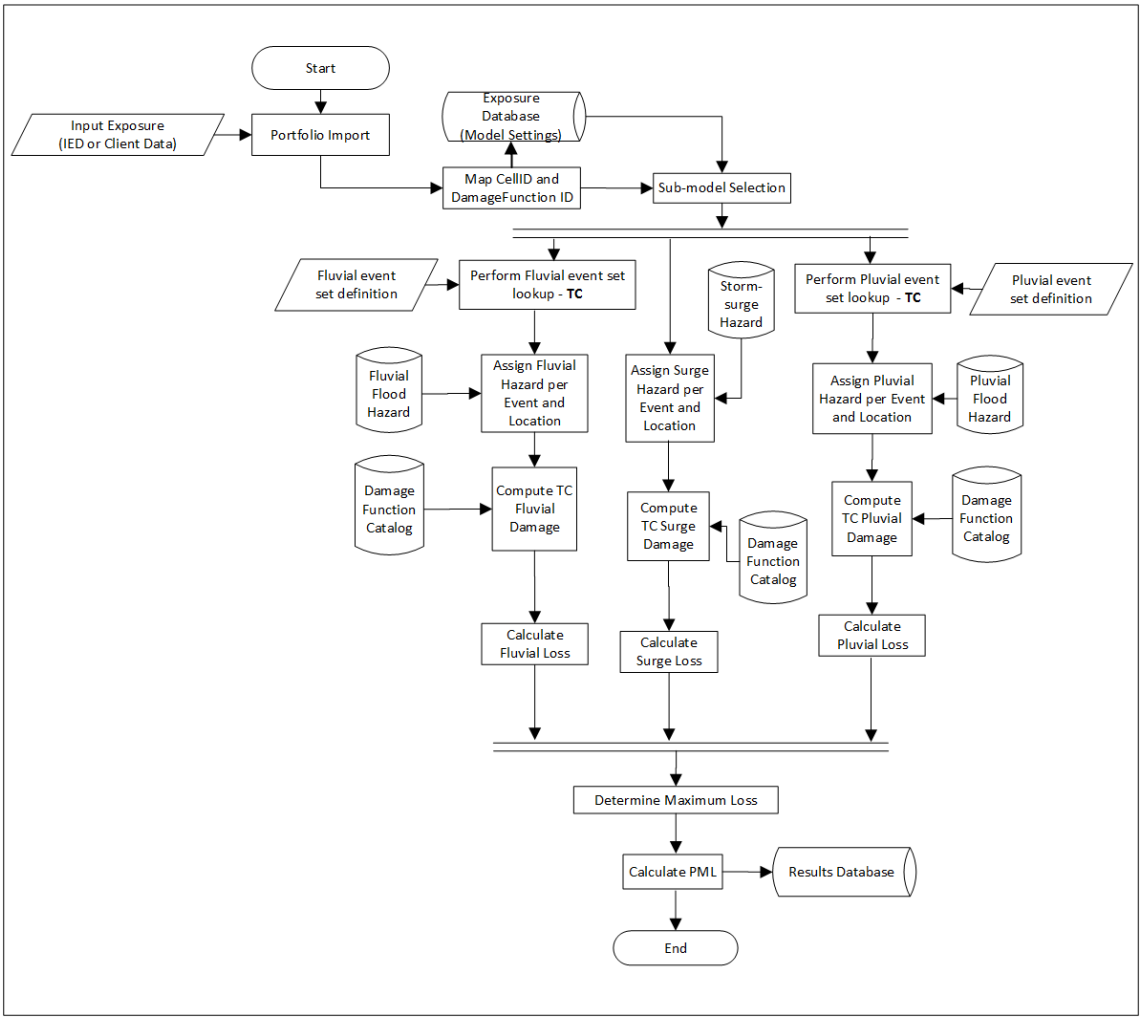

Figure 1: Interactions among major flood model components for TC

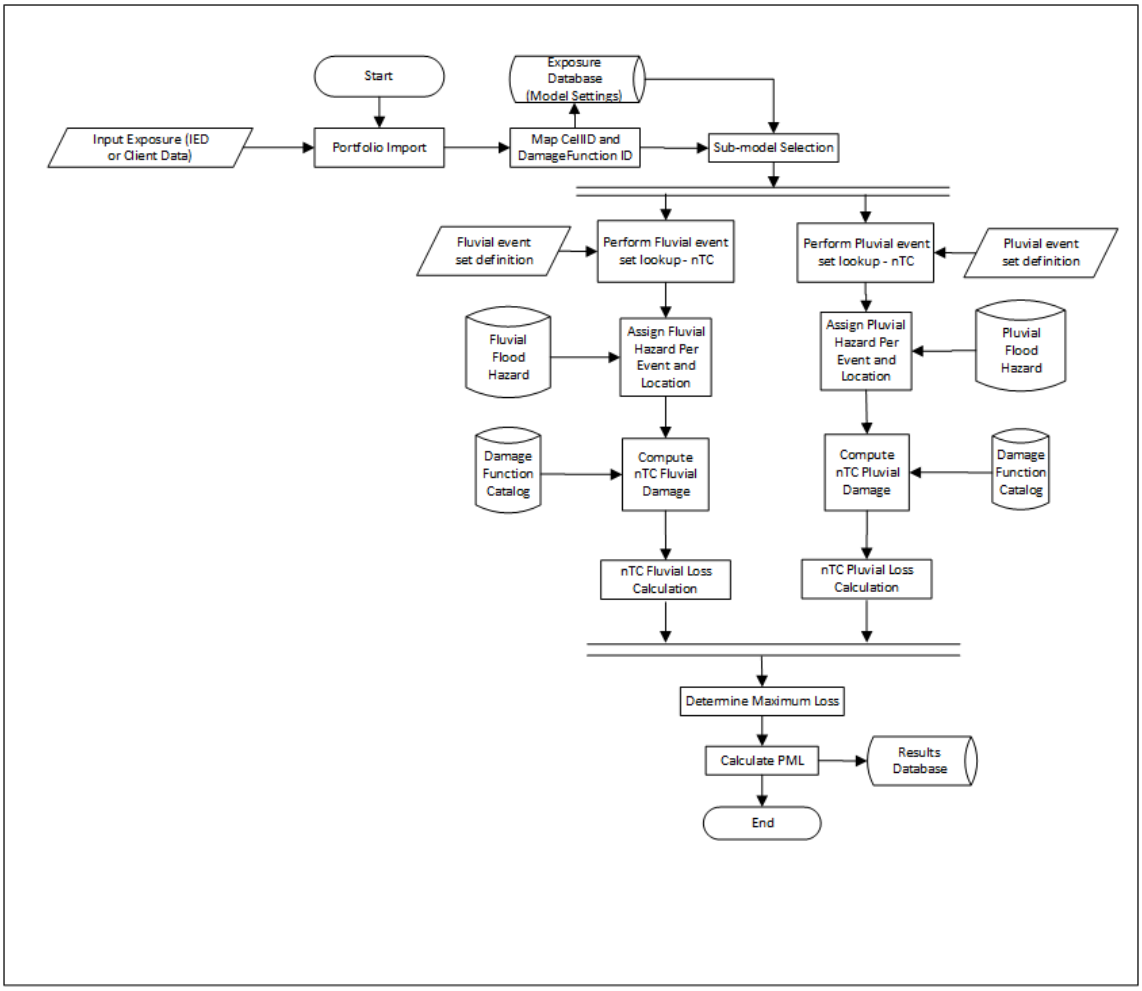

Figure 2: Interactions among major flood model components for non-TC

GF-1.4 Provide a diagram defining the network organization in which the flood model is designed and operates.

A diagram is provided below in Figure 3

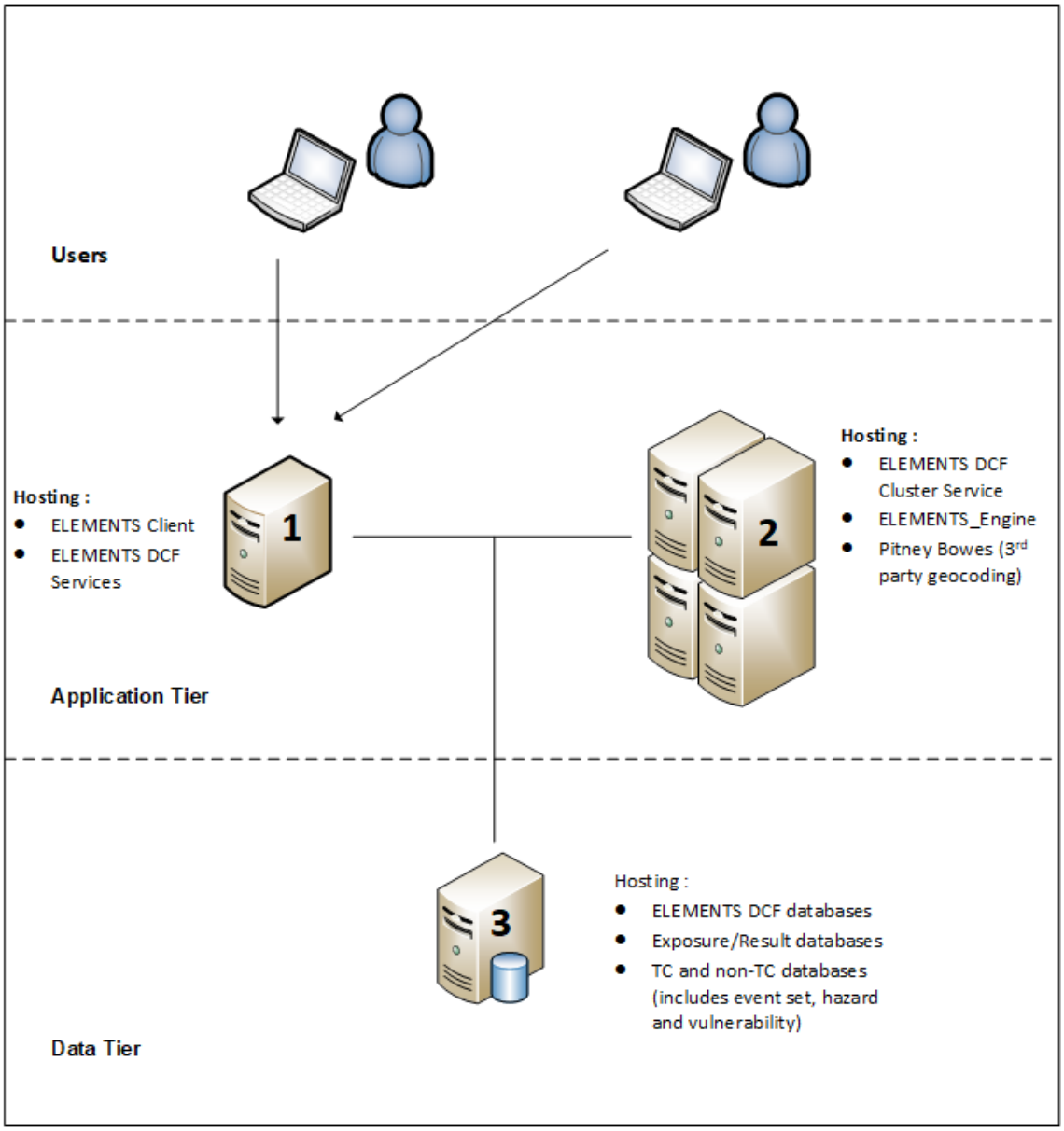

Figure 3: The network organization within which the Impact Forecasting Florida Flood Model (FCHLPM) Model is designed and operates.

GF-1.5 ***Provide detailed information on the flood model implementation on more than one platform, if applicable. In particular, submit Forms VF-3, Flood Mitigation Measures, Range of Changes in Flood Damage; AF-1, Zero Deductible Personal Residential Standard Flood Loss Costs; AF-4, Flood Output Ranges; and AF-8, Flood Probable Maximum Loss for Florida, from each platform including additional calculations showing no differences.***

The Impact Forecasting Florida Flood (FCHLPM) Model is implemented only on the Impact Forecasting ELEMENTS Version 18.0 catastrophe modeling platform.

GF-1.6 ***Provide a comprehensive list of complete references pertinent to the submission by flood standard grouping using professional citation standards.***

General Standards

Bates, P. D. et al., 2021. Combined Modeling of US Fluvial, Pluvial, and Coastal Flood Hazard Under Current and Future Climates. Water Resources Research, Volume 57, p. e2020WR028673.

Beck, H. E. et al., 2022. MSWX: Global 3-Hourly 0.1° Bias-Corrected Meteorological Data Including Near-Real-Time Updates and Forecast Ensembles. Bulletin of the American Meteorological Society, November, Volume 103, pp. E710 - E732.

Buto, S. a. A. R., 2020. NHDPlus High Resolution (NHDPlus HR) - A hydrography framework for the Nation, s.l.: s.n.

Clark, M. P. et al., 2008. Framework for Understanding Structural Errors (FUSE): A modular framework to diagnose differences between hydrological models. Water Resources Research, Volume 44.

Conver, A., Sepanik, J., Louangsaysongkham, B. & Miller, S., 2008. Sea, lake, and overland surges from hurricanes (SLOSH) basin development handbook v2. 0. Silver Springs, MD: NOAA/NWS/Meteorological Development Laboratory.

Diederen, D. et al., 2019. Stochastic generation of spatially coherent river discharge peaks for continental event-based flood risk assessment. Natural Hazards and Earth System Sciences, Volume 19, p. 1041–1053.

Hawker, L. et al., 2022. A 30m global map of elevation with forests and buildings removed. Environmental Research Letters, February.Volume 17.

Heffernan, J. E. & Tawn, J. A., 2004. A conditional approach for multivariate extreme values (with discussion). Journal of the Royal Statistical Society: Series B (Statistical Methodology), Volume 66, pp. 497-546.

Jelesnianski, C. P. et al., 1992. SLOSH: Sea, Lake, and Overland Surges from Hurricanes. s.l.:U.S. Department of Commerce, National Oceanic and Atmospheric Administration, National Weather Service.

Knapp, K. R. et al., 2018. International Best Track Archive for Climate Stewardship (IBTrACS) Project, Version 4. s.l.:NOAA National Centers for Environmental Information. doi:https://doi.org/10.25921/82ty-9e16.

Knapp, K. R. et al., 2010. The International Best Track Archive for Climate Stewardship (IBTrACS): Unifying tropical cyclone best track data. Bulletin of the American Meteorological Society, 91, pp. 363-376. https://doi.org/10.1175/2009BAMS2755.1.

Li, H. et al., 2023. A spatially-dependent synthetic global dataset of extreme sea level events. Weather and Climate Extremes, Volume 41, p. 100596.

Mizukami, N. et al., 2016. mizuRoute version 1: a river network routing tool for a continental domain water resources applications. Geoscientific Model Development, Volume 9, p. 2223–2238.

Myers, V. A., Malkin, W. & (U.S.), N. H. R. P., 1961. Some Properties of Hurricane Wind Fields as Deduced from Trajectories. s.l.:U.S. Department of Commerce, Weather Bureau.

Neal, J. et al., 2021. Estimating River Channel Bathymetry in Large Scale Flood Inundation Models. Water Resources Research, Volume 57, p. e2020WR028301.

Neal, J., Schumann, G. & Bates, P., 2012. A subgrid channel model for simulating river hydraulics and floodplain inundation over large and data sparse areas. Water Resources Research, Volume 48.

NOAA, 2023a. NOAA Extreme Water Levels for Stations in Florida. [Online]

Available at: https://tidesandcurrents.noaa.gov/est/est_states.shtml?region=fl

[Accessed 2023].

NOAA, 2023c. NOAA SLOSH model introduction. [Online]

Available at: https://www.nhc.noaa.gov/surge/slosh.php#:~:text=SLOSH%20model%20coverage-,Basin%20Updates,Committee%20on%20Hurricanes%20(ICCOH)

[Accessed 2023].

Quinn, N. et al., 2019. The Spatial Dependence of Flood Hazard and Risk in the United States. Water Resources Research, Volume 55, pp. 1890-1911.

Smith, A., Sampson, C. & Bates, P., 2015. Regional flood frequency analysis at the global scale. Water Resources. Research, Volume 51, p. 539–553.

Zhang, K., Xiao, C. & Shen, J., 2008. Comparison of the CEST and SLOSH models for storm surge flooding. Journal of Coastal Research, Volume 24, p. 489–499.

Meteorological Standards

Allen, G. H. & Pavelsky, T. M., 2018. Global extent of rivers and streams. Science, Volume 361, pp. 585-588.

Andreadis, K. M., Schumann, G. J.-P. & Pavelsky, T., 2013. A simple global river bankfull width and depth database. Water Resources Research, Volume 49, pp. 7164-7168.

Anthes, R. A., 1982. Hurricanes: Tropical Cyclones. Their Evolution, Structure and Effects.. s.l.:American Meteorological Society Boston, MA.

Arcement, G., Schneider & V., R., 1989. Guide for selecting Manning's roughness coefficients for natural channels and flood plains, s.l.: U.S. G.P.O. ; For sale by the Books and Open-File Reports Section, U.S. Geological Survey.

Bates, P. D., Horritt, M. S. & Fewtrell, T. J., 2010. A simple inertial formulation of the shallow water equations for efficient two-dimensional flood inundation modelling. Journal of Hydrology, Volume 387, pp. 33-45.

Bates, P. D. et al., 2021. Combined Modeling of US Fluvial, Pluvial, and Coastal Flood Hazard Under Current and Future Climates. Water Resources Research, Volume 57, p. e2020WR028673.

Bates, P. D. et al., 2023. A climate-conditioned catastrophe risk model for UK flooding. Natural Hazards and Earth System Sciences, Volume 23, p. 891–908.

Beck, H. E. et al., 2022. MSWX: Global 3-Hourly 0.1° Bias-Corrected Meteorological Data Including Near-Real-Time Updates and Forecast Ensembles. Bulletin of the American Meteorological Society, November, Volume 103, pp. E710 - E732.

Beck, H. E. et al., 2019. MSWEP V2 Global 3-Hourly 0.1° Precipitation: Methodology and Quantitative Assessment. Bulletin of the American Meteorological Society, 100, pp. 473-500, doi:https://doi.org/10.1175/BAMS-D-17-0138.1.

Benson, M. A., 1958. Characteristics of frequency curves based on a theoretical 1,000-year record. s.l., s.n.

Blain, C. A., Westerink, J. J. & Luettich Jr., R. A., 1994. The influence of domain size on the response characteristics of a hurricane storm surge model. Journal of Geophysical Research: Oceans, Volume 99, pp. 18467-18479.

Coastal Emergency Risks Assessment (2023). CERA Historical Storm Surge Archive, 2023. Retrieved from https://cera.coastalrisk.live/.

Chow, V. T., 1959. Open Channel Hydraulics. New York: McGraw-Hill.

Clark, M. P. et al., 2008. Framework for Understanding Structural Errors (FUSE): A modular framework to diagnose differences between hydrological models. Water Resources Research, Volume 44.

Compo, G. P. et al., 2009. The Twentieth Century Reanalysis Project. Quart. J. Roy. Meteor. Soc., submitted.

Conver, A., Sepanik, J., Louangsaysongkham, B. & Miller, S., 2008. Sea, lake, and overland surges from hurricanes (SLOSH) basin development handbook v2. 0. Silver Springs, MD: NOAA/NWS/Meteorological Development Laboratory.

Dangendorf, S. et al., 2023. Acceleration of US Southeast and Gulf coast sea-level rise amplified by internal climate variability. Nature Communications, Volume 14, p. 1935.

Darling, R. W. R., 1991. Estimating Probabilities of Hurricane Wind Speeds Using a Large-Scale Empirical Model. Journal of Climate, Volume 4, pp. 1035-1046.

Delgado, S., Landsea, C. W. & Willoughby, H., 2018. Reanalysis of the 1954–63 Atlantic Hurricane Seasons. Journal of Climate, Volume 31, pp. 4177-4192.

Demuth, J. L., DeMaria, M. & Knaff, J. A., 2006. Improvement of Advanced Microwave Sounding Unit Tropical Cyclone Intensity and Size Estimation Algorithms. Journal of Applied Meteorology and Climatology, Volume 45, pp. 1573-1581.

Dewitz, J., 2021. National Land Cover Database (NLCD) 2019 Products, s.l.: s.n.

Diederen, D. & Liu, Y., 2020. Dynamic spatio-temporal generation of large-scale synthetic gridded precipitation: with improved spatial coherence of extremes. Stochastic Environmental Research and Risk Assessment, Volume 34, p. 1369–1383.

Diederen, D. et al., 2019. Stochastic generation of spatially coherent river discharge peaks for continental event-based flood risk assessment. Natural Hazards and Earth System Sciences, Volume 19, p. 1041–1053.

Emanuel, K. & Rotunno, R., 2012. Self-stratification of tropical cyclone outflow. Part I: Implications for storm structure (vol 68, pg 2236, 2011). Journal of the Atmospheric Sciences, January, Volume 69, pp. 416-416.

England, J. et al., 2018. Bulletin 17C (ver. 1.1, May 2019): U.S. GeologicalSurvey Techniques and Methods. In: s.l.:s.n., p. 148.

Feldmann, M., Emanuel, K., Zhu, L. & Lohmann, U., 2019. Estimation of Atlantic Tropical Cyclone Rainfall Frequency in the United States. Journal of Applied Meteorology and Climatology, Volume 58, pp. 1853-1866.

Fewtrell, T. J. et al., 2011. Benchmarking urban flood models of varying complexity and scale using high resolution terrestrial LiDAR data. Physics and Chemistry of the Earth, Parts A/B/C, Volume 36, p. 281–291.

Forbes, C., Rhome, J., Mattocks, C. & Taylor, A., 2014. Predicting the Storm Surge Threat of Hurricane Sandy with the National Weather Service SLOSH Model. Journal of Marine Science and Engineering, Volume 2, p. 437–476.

Gesch, D., Oimoen, M. & Evans, G., 2014. Accuracy Assessment of the U.S. Geological Survey National Elevation Dataset, and Comparison with Other Large-Area Elevation Datasets—SRTM and ASTER, s.l.: s.n.

Hagen, A. B. & Landsea, C. W., 2012. On the Classification of Extreme Atlantic Hurricanes Utilizing Mid-Twentieth-Century Monitoring Capabilities. Journal of Climate, Volume 25, pp. 4461-4475.

Harman, C., Stewardson, M. & DeRose, R., 2008. Variability and uncertainty in reach bankfull hydraulic geometry. Journal of hydrology, Volume 351, p. 13–25.

Hawker, L. & Neal, J., 2021. FABDEM V1-0. s.l.:s.n.

Hawker, L. et al., 2022. A 30m global map of elevation with forests and buildings removed. Environmental Research Letters, February.Volume 17.

Heffernan, J. E. & Tawn, J. A., 2004. A conditional approach for multivariate extreme values (with discussion). Journal of the Royal Statistical Society: Series B (Statistical Methodology), Volume 66, pp. 497-546.

Ho, F. P. et al., 1987. Hurricane Climatology for the Atlantic and Gulf Coasts of the United States. NOAA Technical Report NWS 38.

Jelesnianski, C., 1970. “BOTTOM STRESS TIME-HISTORY” IN LINEARIZED EQUATIONS OF MOTION FOR STORM SURGES. Monthly Weather Review, Volume 98, pp. 462-478.

Jelesnianski, C. P., 1966. NUMERICAL COMPUTATIONS OF STORM SURGES WITHOUT BOTTOM STRESS. Monthly Weather Review, Volume 95, pp. 740-756.

Jelesnianski, C. P., 1972. SPLASH:(Special Program to List Amplitudes of Surges from Hurricanes). I, Landfall storms, s.l.: s.n.

Jelesnianski, C. P. et al., 1992. SLOSH: Sea, Lake, and Overland Surges from Hurricanes. s.l.:U.S. Department of Commerce, National Oceanic and Atmospheric Administration, National Weather Service.

Jelesnianski, C. P., Taylor, A. D., Office, E. R. L. (. S. W. M. P. & Administration, U. S. N. O. A., 1973. A Preliminary View of Storm Surges Before and After Storm Modifications. s.l.:Environmental Research Laboratories, Weather Modification Program Office.

Kalnay, E. et al., 2018. The NCEP/NCAR 40-year reanalysis project. In: Renewable energy. s.l.:Routledge, p. Vol1_{1}{4}{6}–Vol1_{1}{9}{4}.

Keef, C., Tawn, J. A. & Lamb, R., 2013. Estimating the probability of widespread flood events. Environmetrics, Volume 24, pp. 13-21.

Kim, S.-C. & Chen, J., 1999. Bottom Stress of Wind-Driven Currents Over an Inner Shelf Determined from Depth-Integrated Storm Surge Model. Journal of Coastal Research, Volume 15, pp. 766-773.

Landsea, A. C. et al., 2004a. The Atlantic hurricane database re-analysis project: Documentation for the 1851-1910 alterations and additions to the HURDAT database.. s.l., Columbia University Press,, pp. 177-221.

Landsea, C. et al., 2012. A Reanalysis of the 1921-30 Atlantic Hurricane Database*. Journal of Climate, February, Volume 25, pp. 865-885.

Landsea, C. et al., 2004b. A Reanalysis of Hurricane Andrew's Intensity. Bulletin of The American Meteorological Society - BULL AMER METEOROL SOC, November.Volume 85.

Landsea, C. et al., 2014. A Reanalysis of the 1931–43 Atlantic Hurricane Database*. Journal of Climate, August, Volume 27, pp. 6093-6118.

Landsea, C. W. & Franklin, J. L., 2013. Atlantic Hurricane Database Uncertainty and Presentation of a New Database Format. Monthly Weather Review, Volume 141, pp. 3576-3592.

Landsea, C. W. et al., 2008. A Reanalysis of the 1911–20 Atlantic Hurricane Database. Journal of Climate, Volume 21, pp. 2138-2168.

Leopold, L. B., 1994. A View of the River. s.l.:Harvard University Press.

Li, H. et al., 2023. A spatially-dependent synthetic global dataset of extreme sea level events. Weather and Climate Extremes, Volume 41, p. 100596.

Liu, H., Taylor, A. & Spring, M. D., 2018. Development of the nws' probabilistic extra-tropical storm surge model and post processing methodology. s.l., s.n., p. 7–11.

Lu, P. et al., 2018. Assessing Hurricane Rainfall Mechanisms Using a Physics-Based Model: Hurricanes Isabel (2003) and Irene (2011). Journal of the Atmospheric Sciences, Volume 75, pp. 2337-2358.

Mayo, T. & Lin, N., 2019. The Effect of the Surface Wind Field Representation in the Operational Storm Surge Model of the National Hurricane Center. Atmosphere, Volume 10.

Mizukami, N. et al., 2016. mizuRoute version 1: a river network routing tool for a continental domain water resources applications. Geoscientific Model Development, Volume 9, p. 2223–2238.

Morin, J. & Benyamini, Y., 1977. Rainfall infiltration into bare soils. Water Resources Research, Volume 13, pp. 813-817.

Myers, V. A., Malkin, W. & (U.S.), N. H. R. P., 1961. Some Properties of Hurricane Wind Fields as Deduced from Trajectories. s.l.:U.S. Department of Commerce, Weather Bureau.

Neal, J. et al., 2021. Estimating River Channel Bathymetry in Large Scale Flood Inundation Models. Water Resources Research, Volume 57, p. e2020WR028301.

NOAA; Tides & Currents, 2023a. Extreme Water Levels for Stations in Florida. [Online]

Available at: https://tidesandcurrents.noaa.gov/est/est_states.shtml?region=fl

[Accessed 2023].

NOAA, 2023a. NOAA Extreme Water Levels for Stations in Florida. [Online]

Available at: https://tidesandcurrents.noaa.gov/est/est_states.shtml?region=fl

[Accessed 2023].

NOAA, 2023b. NOAA Introduction to Storm Surge. [Online]

Available at: https://www.weather.gov/media/owlie/surge_intro.pdf

[Accessed 2023].

NOAA, 2023c. NOAA SLOSH model introduction. [Online]

Available at: https://www.nhc.noaa.gov/surge/slosh.php#:~:text=SLOSH%20model%20coverage-,Basin%20Updates,Committee%20on%20Hurricanes%20(ICCOH)

[Accessed 2023].

Platzman, G. W., 1963. The Dynamical Prediction of Wind Tides on Lake Erie. In: The Dynamical Prediction of Wind Tides on Lake Erie. Boston(MA): American Meteorological Society, p. 1–44.

Quinn, N. et al., 2019. The Spatial Dependence of Flood Hazard and Risk in the United States. Water Resources Research, Volume 55, pp. 1890-1911.

Rayner, N. A. et al., 2003. Global analyses of sea surface temperature, sea ice, and night marine air temperature since the late nineteenth century. Journal of Geophysical Research: Atmospheres, Volume 108.

Schloemer, R. W. & Section, U. S. H. S. D. H., 1954. Analysis and Synthesis of Hurricane Wind Patterns Over Lake Okeechobee, Florida. s.l.:U.S. Department of Commerce, Weather Bureau.

Schureman, P., 1958. Manual of Harmonic Analysis and Prediction of Tides. [Revised 1940 edition reprinted 1958 with corrections, reprinted 2001], s.l.: s.n.

Shin, D., Cocke, S. & Kim, B. M., 2022. A Systematic Revision of the NFIP Claims Hazard Data in Florida for Flood Risk Assessment. Applied Sciences, March, Volume 12, p. 3537.

Soil Survey Staff, 2021. Soil Survey Geographic (SSURGO) Database for US, Available online at: https://websoilsurvey.nrcs.usda.gov/: s.n.

Southworth, H. et Al, 2022. Statistical Modelling of Extreme Values: Package 'texmex', s.l.: s.n.

Sweet, W. et al., 2022. 2022: Global and Regional Sea Level Rise Scenarios for the United States: Updated Mean Projections and Extreme Water Level Probabilities Along U.S. Coastlines., National Oceanic and Atmospheric Administration, National Ocean Service, Silver Spring, MD,: NOAA Technical Report NOS 01.

Varty, Z., Tawn, J., Atkinson, P. & Bierman, S., 2021. Inference for extreme earthquake magnitudes accounting for a time-varying measurement process, s.l.: s.n.

Vickery, P., Skerlj, P. & Twisdale, L., 2000. Simulation of Hurricane Risk in the U.S. Using Empirical Track Model. Journal of Structural Engineering-asce - J STRUCT ENG-ASCE, October.Volume 126.

Vickery, P. & Wadhera, D., 2008. Statistical Models of Holland Pressure Profile Parameter and Radius to Maximum Winds of Hurricanes from Flight-Level Pressure and H*Wind Data. Journal of Applied Meteorology and Climatology - J APPL METEOROL CLIMATOL, October, Volume 47, pp. 2497-2517.

Vickery, P., Wadhera, D., Powell, M. & Chen, Y., 2009a. A Hurricane Boundary Layer and Wind Field Model for Use in Engineering Applications. Journal of Applied Meteorology and Climatology - J APPL METEOROL CLIMATOL, February, Volume 48, pp. 381-405.

Vickery, P., Wadhera, D., Twisdale Jr., L. & Lavelle, F., 2009c. US hurricane wind speed risk and uncertainty.. Journal of Structural Engineering, Volume 135, pp. 301-320.

Wdowinski, S., 2019. Coherent saptio-temporal variations in the rate of sea level rise along the US Atlantic and Gulf coasts. s.l., s.n., pp. OS21A-07.

Wing, O. E. J. et al., 2017. Validation of a 30 m resolution flood hazard model of the conterminous United States. Water Resources Research, Volume 53, pp. 7968-7986.

Wing, O. E. J. et al., 2018. Estimates of present and future flood risk in the conterminous United States. Environmental Research Letters, February, Volume 13, p. 034023.

Wing, O. E. J., Pinter, N., Bates, P. D. & Kousky, C., 2020. New insights into US flood vulnerability revealed from flood insurance big data. Nature Communication, Volume vol. 11(1), pp. 1-10.

Wing, O. E. J. et al., 2020. Toward Global Stochastic River Flood Modeling. Water Resources Research, Volume 56, p. e2020WR027692.

Yamazaki, D. et al., 2019. MERIT Hydro: A High-Resolution Global Hydrography Map Based on Latest Topography Dataset. Water Resources Research, Volume 55, pp. 5053-5073.

Yamazaki, D. et al., 2017. A high-accuracy map of global terrain elevations. Geophysical Research Letters, Volume 44, pp. 5844-5853.

Zhang, K., Xiao, C. & Shen, J., 2008. Comparison of the CEST and SLOSH models for storm surge flooding. Journal of Coastal Research, Volume 24, p. 489–499.

Hydrological and Hydraulic Standards

Arcement, G. J., Schneider & V., R., 1989. Guide for selecting Manning's roughness coefficients for natural channels and flood plains, s.l.: U.S. G.P.O. ; For sale by the Books and Open-File Reports Section, U.S. Geological Survey.

Bates, P. D., Horritt, M. S. & Fewtrell, T. J., 2010. A simple inertial formulation of the shallow water equations for efficient two-dimensional flood inundation modelling. Journal of Hydrology, Volume 387, pp. 33-45.

Bates, P. D. et al., 2021. Combined Modeling of US Fluvial, Pluvial, and Coastal Flood Hazard Under Current and Future Climates. Water Resources Research, Volume 57, p. e2020WR028673.

Beck, H. E. et al., 2022. MSWX: Global 3-Hourly 0.1° Bias-Corrected Meteorological Data Including Near-Real-Time Updates and Forecast Ensembles. Bulletin of the American Meteorological Society, November, Volume 103, pp. E710 - E732.

Beck, H. E. et al., 2019. MSWEP V2 Global 3-Hourly 0.1° Precipitation: Methodology and Quantitative Assessment. Bulletin of the American Meteorological Society, 100, pp. 473-500, doi:https://doi.org/10.1175/BAMS-D-17-0138.1.

Brunner, M. I. et al., 2021. An extremeness threshold determines the regional response of floods to changes in rainfall extremes. Communications Earth & Environment, Volume 2, p. 173.

Buto, S. a. A. R., 2020. NHDPlus High Resolution (NHDPlus HR) - A hydrography framework for the Nation, s.l.: s.n.

Chow, V. T., 1959. Open Channel Hydraulics. New York: McGraw-Hill.

Clark, M. P. et al., 2008. Framework for Understanding Structural Errors (FUSE): A modular framework to diagnose differences between hydrological models. Water Resources Research, Volume 44.

Conver, A., Sepanik, J., Louangsaysongkham, B. & Miller, S., 2008. Sea, lake, and overland surges from hurricanes (SLOSH) basin development handbook v2. 0. Silver Springs, MD: NOAA/NWS/Meteorological Development Laboratory.

de Almeida, G. A. M. & Bates, P., 2013. Applicability of the local inertial approximation of the shallow water equations to flood modeling. Water Resources Research, Volume 49, pp. 4833-4844.

Dewitz, J., 2021. National Land Cover Database (NLCD) 2019 Products, s.l.: s.n.

Hawker, L. et al., 2022. A 30m global map of elevation with forests and buildings removed. Environmental Research Letters, February.Volume 17.

Heffernan, J. E. & Tawn, J. A., 2004. A conditional approach for multivariate extreme values (with discussion). Journal of the Royal Statistical Society: Series B (Statistical Methodology), Volume 66, pp. 497-546.

Henn, B., Clark, M. P., Kavetski, D. & Lundquist, J. D., 2015. Estimating mountain basin-mean precipitation from streamflow using Bayesian inference. Water Resources Research, Volume 51, pp. 8012-8033.

Hersbach, H. &. N. C. f. A. R. S., 2023. The Climate Data Guide: ERA5 atmospheric reanalysis., https://climatedataguide.ucar.edu/climate-data/era5-atmospheric-reanalysis: s.n.

Hillel, D., 1982. Introduction to Soil Physics. s.l.:Academic Press.

Hillel, D., 2013. Introduction to Soil Physics. Introduction to Soil Physics, January.pp. 1-364.

Hunter, N. M. et al., 2005. Utility of different data types for calibrating flood inundation models within a GLUE framework. Hydrology and Earth System Sciences, Volume 9, p. 412–430.

Jelesnianski, C. P. et al., 1992. SLOSH: Sea, Lake, and Overland Surges from Hurricanes. s.l.:U.S. Department of Commerce, National Oceanic and Atmospheric Administration, National Weather Service.

Keef, C., Tawn, J. A. & Lamb, R., 2013. Estimating the probability of widespread flood events. Environmetrics, Volume 24, pp. 13-21.

Liang, X., Lettenmaier, D. P., Wood, E. F. & Burges, S. J., 1994. A simple hydrologically based model of land surface water and energy fluxes for general circulation models. Journal of Geophysical Research: Atmospheres, Volume 99, pp. 14415-14428.

Li, H. et al., 2023. A spatially-dependent synthetic global dataset of extreme sea level events. Weather and Climate Extremes, Volume 41, p. 100596.

Luettich, R. & Westerink, J., 2004. Formulation and Numerical Implementation of the 2D/3D ADCIRC Finite Element Model Version 44.XX. January.

Massey, T. C. et al., 2022. Coastal Storm (CSTORM) Modeling SystemStorm Surge and Waves Feasibility Study forNew York & New Jersey Harbor and TributariesFocus Area Study. s.l.:s.n.

Meyer, V., Scheuer, S. & Haase, D., 2009. A multicriteria approach for flood risk mapping exemplified at the Mulde river, Germany. Natural Hazards, Volume 48, pp. 17-39.

Microsoft, 2018. Microsoft Building Footprints. s.l.:s.n.

Millones, R. G. P. J. &. M., 2011. Death to Kappa: birth of quantity disagreement and allocation disagreement for accuracy assessment. International Journal of Remote Sensing, 32(15), pp. 4407-4429.

Mitchell-Wallace, K., Jones, M., Hillier, J. & Foote, M., 2017. Natural Catastrophe Risk Management and Modelling: A Practitioner's Guide. s.l.:Wiley-Blackwell.

Mizukami, N. et al., 2021. A Vector-Based River Routing Model for Earth System Models: Parallelization and Global Applications. Journal of Advances in Modeling Earth Systems, Volume 13, p. e2020MS002434.

Mizukami, N. et al., 2016. mizuRoute version 1: a river network routing tool for a continental domain water resources applications. Geoscientific Model Development, Volume 9, p. 2223–2238.

Morin, J. & Benyamini, Y., 1977. Rainfall infiltration into bare soils. Water Resources Research, Volume 13, pp. 813-817.

Neal, J. et al., 2018. Optimisation of the two-dimensional hydraulic model LISFOOD-FP for CPU architecture. Environmental Modelling & Software, Volume 107, pp. 148-157.

Neal, J., Schumann, G. & Bates, P., 2012. A subgrid channel model for simulating river hydraulics and floodplain inundation over large and data sparse areas. Water Resources Research, Volume 48.

Newman, A. J. et al., 2021. Identifying sensitivities in flood frequency analyses using a stochastic hydrologic modeling system. Hydrology and Earth System Sciences, Volume 25, p. 5603–5621.

NOAA; Tides & Currents, 2023a. Extreme Water Levels for Stations in Florida. [Online]

Available at: https://tidesandcurrents.noaa.gov/est/est_states.shtml?region=fl

[Accessed 2023].

Quinn, N. et al., 2019. The Spatial Dependence of Flood Hazard and Risk in the United States. Water Resources Research, Volume 55, pp. 1890-1911.

Sampson, C. C. et al., 2015. A high-resolution global flood hazard model. Water Resources Research, Volume 51, pp. 7358-7381.

Savage, J. et al., 2016. Quantifying the importance of spatial resolution and other factors through global sensitivity analysis of a flood inundation model. Water Resources Research, 11 November, pp. 9146-9163.

Smith, A., Sampson, C. & Bates, P., 2015. Regional flood frequency analysis at the global scale. Water Resources. Research, Volume 51, p. 539–553.

Soil Survey Staff, 2021. Soil Survey Geographic (SSURGO) Database for US, Available online at: https://websoilsurvey.nrcs.usda.gov/: s.n.

Southworth, H. et al, 2022. Statistical Modelling of Extreme Values: Package ‘texmex’, s.l.: s.n.

U.S. Interagency Advisory Committee on Water Data, 1982. Guidelines for determining flood flow frequency, Bulletin 17-B of the Hydrology Subcommittee: Reston, Virginia, Springfield: s.n.

US Army Corps of Engineers, 2007. The National Levee Database (NLD). s.l.:s.n.

USGS, 2021. Watershed Boundary Dataset, Data Model v 2.3.1, s.l.: s.n.

Vijayan, N. R. L. et al., 2021. Evaluation of parametric wind models for more accurate modeling of storm surge: a case study of Hurricane Michael. Natural Hazards, April.Volume 106.

Wasko, C. & Nathan, R., 2019. Influence of changes in rainfall and soil moisture on trends in flooding. Journal of Hydrology, Volume 575, pp. 432-441.

Westerink, J. J. et al., 2008. A Basin- to Channel-Scale Unstructured Grid Hurricane Storm Surge Model Applied to Southern Louisiana. Monthly Weather Review, Volume 136, pp. 833-864.

Wing, O. E. J. et al., 2017. Validation of a 30 m resolution flood hazard model of the conterminous United States. Water Resources Research, Volume 53, pp. 7968-7986.

Wing, O. E. J. et al., 2018. Estimates of present and future flood risk in the conterminous United States. Environmental Research Letters, February, Volume 13, p. 034023.

Wing, O. E. J., Pinter, N., Bates, P. D. & Kousky, C., 2020. New insights into US flood vulnerability revealed from flood insurance big data. Nature Communication, Volume vol. 11(1), pp. 1-10.

Yamazaki, D. et al., 2019. MERIT Hydro: A High-Resolution Global Hydrography Map Based on Latest Topography Dataset. Water Resources Research, Volume 55, pp. 5053-5073.

Zhu, Z., Wright, D. B. & Yu, G., 2018. The Impact of Rainfall Space-Time Structure in Flood Frequency Analysis. Water Resources Research, Volume 54, pp. 8983-8998.

Statistical Standards

Bates, P. D. et al., 2023. A climate-conditioned catastrophe risk model for UK flooding. Natural Hazards and Earth System Sciences, 23(2), pp. 891-908.

Beck, H. E. et al., 2019. MSWEP V2 Global 3-Hourly 0.1° Precipitation: Methodology and Quantitative Assessment. Bulletin of the American Meteorological Society, 100, pp. 473-500, doi:https://doi.org/10.1175/BAMS-D-17-0138.1.

Coles, S., L., B., T. J. & Dorazio, P., 2001. An Introduction to Statistical Modeling of Extreme Values. s.l.:Springer.

Collins, D. J. a. L. S. P., 2001. A macro validation dataset for U.S. hurricane models. Casualty Actuarial Society, Arlington, Va..

Diederen, D. et al., 2019. Stochastic generation of spatially coherent river discharge peaks for continental event-based flood risk assessment. Natural Hazards and Earth System Sciences, Volume 19, p. 1041–1053.

Heffernan, J. E. & Tawn, J. A., 2004. A conditional approach for multivariate extreme values (with discussion). Journal of the Royal Statistical Society: Series B (Statistical Methodology), Volume 66, pp. 497-546.

Iman, R. L., Johnson, M. & Schroeder, T. A., 2001. Professional Team Demonstration Uncertainty/Sensitivity Analysis, s.l.: Southwest Technology Consultants.

Knapp, K. R. et al., 2018. International Best Track Archive for Climate Stewardship (IBTrACS) Project, Version 4. s.l.:NOAA National Centers for Environmental Information. doi:https://doi.org/10.25921/82ty-9e16.

Knapp, K. R. et al., 2010. The International Best Track Archive for Climate Stewardship (IBTrACS): Unifying tropical cyclone best track data. Bulletin of the American Meteorological Society, 91, pp. 363-376. https://doi.org/10.1175/2009BAMS2755.1.

Kousky, C., Kunreuther, H., Lingle, B. & Shabman, L., 2018. The Emerging Private Residential Flood Insurance Market in the United States, s.l.: Wharton Risk Management and Decision Processes Center.

Li, H. et al., 2023. A spatially-dependent synthetic global dataset of extreme sea level events. Weather and Climate Extremes, Volume 41, p. 100596.

Quinn, N. et al., 2019. The Spatial Dependence of Flood Hazard and Risk in the United States. Water Resources Research, Volume 55, pp. 1890-1911.

Wing, O. E. J. et al., 2020. Toward Global Stochastic River Flood Modeling. Water Resources Research, Volume 56, p. e2020WR027692.

Vulnerability Standards

ACI Committee, 2008. Building code requirements for structural concrete (ACI 318-08) and commentary, s.l.: s.n.

ASCE, 1988. Minimum Design Loads for Buildings and Other Structures, ASCE 7-88, New York: American Society of Civil Engineers.

ASCE, 1998. Flood Resistant Design and Construction. ASCE 24-98, Reston, Virginia: American Society of Civil Engineers.

ASCE, 2014. Flood Resistant Design and Construction. ASCE 24-14, Reston, Virginia: American Society of Civil Engineers.

ASCE, 2016. Minimum Design Loads for Buildings and Other Structures, ASCE 7-16, Reston: American Society of Civil Engineers.

ASCE, 2022. Minimum design loads and associated criteria for buildings and other structures, ASCE/SEI 7-22, s.l.: s.n.

Baradaranshoraka, M., 2017. Vulnerability model of residential structures subject to hurricane induced wind, surge and inundation. Ph.D. dissertation, Dept. of Civil Engineering, Florida Institute of Technology.

Baradaranshoraka, M. et al., 2017. Hurricane Wind versus Storm Surge Damage in the Context of a Risk Prediction Model. Journal of Structural Engineering, Volume 143, p. 04017103.

Baradaranshoraka, M. et al., 2019. Characterization of Coastal Flood Damage States for Residential Buildings. ASCE-ASME Journal of Risk and Uncertainty in Engineering Systems, Part A: Civil Engineering, Volume 5, p. 04019001.

Becker, A. B., Johnstone, W. M. & Lence, B. J., 2011. Wood Frame Building Response to Rapid-Onset Flooding. Natural Hazards Review, Volume 12, pp. 85-95.

Cantelmo, C. & Cuomo, G., 2021. Hydrodynamic loads on buildings in floods. Journal of Hydraulic Research, Volume 59, pp. 61-74.

Carol J. Friedland, M. L. L., 2009. Loss-consistent categorization of hurricane wind and storm surge damage for residential structures. San Juan, Puerto Rico, Proceedings of the 11th Americas Conference on Wind Engineering.

Chidambarathanu, N. & Retnan, R., 2013. Vulnerability of Reinforced Concrete Structures Subjected to Flood. In: O. Petrucci, ed. Natural Disasters. Rijeka: IntechOpen.

Custer, R. & Nishijima, K., 2015. Flood vulnerability assessment of residential buildings by explicit damage process modelling. Natural Hazards, Volume 78, pp. 461-496.

Davis, S. A. & Skaggs, L. L., 1992. Catalog of residential depth-damage functions used by the Army Corps of Engineers in flood damage estimations, s.l.: US Army Corps of Engineers, Water Resources Support Center, Institute for Water Resources.

Endendijk, T. et al., 2023. Flood vulnerability models and household flood damage mitigation measures: An econometric analysis of survey data. Water Resources Research, 59(8).

FBC, 2001. 2001 Florida Building Code, 1st Edition , Birmingham, AL: International Code Council.

FBC, 2004. 2004 Florida Building Code, 2nd Edition, s.l.: Florida Building Commission.

FBC, 2007. 2007 Florida Building Code, 3rd Edition, s.l.: Florida Building Commission.

FBC, 2010. 2010 Florida Building Code, 4th Edition, s.l.: Florida Building Commission.

FBC, 2014. 2014 Florida Building Code, 5th Edition, s.l.: Florida Building Commission.

FBC, 2017. 2017 Florida Building Code, 6th Edition, s.l.: Florida Building Commission.

FBC, 2020. 2020 Florida Building Code, 7th Edition, s.l.: Florida Building Commission.

FEMA, 2009. Protecting Manufactured Homes from Floods and Other Hazards. A Multi-Hazard Foundation and Installation Guide, s.l.: FEMA P-85, Second Edition.

FEMA, 2010. Home Builder's Guide to Coastal Construction. Technical Fact Sheet Series, s.l.: FEMA P-499.

FEMA, 2011. Coastal Construction Manual - Principles and Practices of Planning, Siting, Designing, Constructing, and Maintaining Residential Buildings in Coastal Areas (Fourth Edition), Washington D.C.: s.n.

FEMA, 2013. Multi-hazard loss estimation methodology, flood model, HAZUS, technical manual, s.l.: s.n.

FEMA, 2017. National Flood Insurance Program: Community Rating System, Coordinator's Manual, FIA-15/2017 , s.l.: s.n.

FEMA, 2020a. Lowest floor guide, s.l.: s.n.

FEMA, 2020b. Requirements for Flood Openings in Foundation Walls and Walls of Enclosures, s.l.: NFIP Technical Bulletin 1.

FEMA, 2021a. Design and Construction Guidance for Breakaway Walls, s.l.: NFIP Technical Bulletin 9.

FEMA, 2021b. National Flood Insurance Program: Flood Insurance Manual, s.l.: s.n.

FEMA, 2022a. Hazus Inventory Technical Manual. Washington, D.C.: s.n.

FEMA, 2022b. Wet Floodproofing Requirements and Limitations, s.l.: NFIP Technical Bulletin 7.

Florida Division of Emergency Management, 2017. Floodplain management in Florida: Quick Guide, Tallahassee: Bureau of Mitigation State Floodplain Management Office.

Friedland, C. & Levitan, M., 2009. Loss-consistent categorization of hurricane wind and storm surge damage for residential structures. January.

Frimpong, E., Petrolia, D. R., Harri, A. & Cartwright, J. H., 2020. Flood Insurance and Claims: The Impact of the Community Rating System. Applied Economic Perspectives and Policy, Volume 42, pp. 245-262.

Fritz, H. M. et al., 2007. Hurricane Katrina storm surge distribution and field observations on the Mississippi Barrier Islands. Estuarine, Coastal and Shelf Science, Volume 74, pp. 12-20.

Genovese, E., Hallegatte, S. & Dumas, P., 2011. Damage Assessment from Storm Surge to Coastal Cities: Lessons from the Miami Area. In: Advancing Geoinformation Science of a Changing World. Utrecht, Netherlands: Springer-Verlag Berlin Heidelberg, pp. 21-43.

Gerl, T. et al., 2016. A Review of Flood Loss Models as Basis for Harmonization and Benchmarking. PLOS ONE, July, Volume 11, pp. 1-22.

Gordian, 2024. RSMeans Data Online. [Online]

Available at: https://www.rsmeansonline.com/

[Accessed 15 January 2024].

Gulf Engineers & Consultants (GEC), 1997. Depth-Damage Relationships for Structures, Contents, and Vehicles and Content-to-Structure Value Ratios (CSVR) in Support of the lower Atchafalaya reevaluation and Morganza to the Gulf, Luisiana, Feasibility Study, s.l.: Gulf Engineers & Consultants (GEC) New Orleans, LA, USA.

Gulf Engineers & Consultants (GEC), 2006. Depth-Damage Relationships for Structures, Contents, and Vehicles and Content-to-Structure Value Ratios (CSVR) in Support of the Donaldsonville to the Gulf, Luisiana, Feasibility Study, s.l.: Gulf Engineers & Consultants (GEC) New Orleans, LA, USA.

Gurley, K. R. et al., 2017. Survey and Investigation of Buildings Damaged by Category III Hurricanes in FY 2016-17–Hurricane Matthew 2016, Gainesville: University of Florida.

Hatzikyriakou, A. & Lin, N., 2017. Simulating storm surge waves for structural vulnerability estimation and flood hazard mapping. Natural Hazards, Volume 89, pp. 939-962.

Herbert, D. M., Gardner, D., Harbottle, M. & T.G.Hughes, 2012. The strength of masonry walls when subject to flood loading. s.l., s.n.

HUD, 2007. Part II: Department of housing and urban development. 24 CFR Parts 3280 and 3285. Model manufactured home installation standards; final rule, s.l.: Department of Housing and Urban Development. Published in Federal Register/Vol.72, No. 202/Friday, October 19, 2007/Rules and Regulations.

HUD-MHCSS, 1994. Manufactured Home Construction and Safety Standards, Part 3280, s.l.: U.S. Department of Housing and Urban Development.

Jones, C. P. & Krecic, M. R., 2011. Coastal Flood and Erosion Damage Functions for Mid- and High-Rise Buildings. In: Solutions to Coastal Disasters 2011. s.l.:s.n., pp. 678-689.

Kelman, I. & Spence, R., 2003. A limit analysis of unreinforced masonry failing under flood water pressures. Masonry International, January, Volume 16, pp. 51-61.

Kousky, C. & Michel-Kerjan, E., 2017. Examining Flood Insurance Claims in the United States: Six Key Findings. Journal of Risk and Insurance, Volume 84, pp. 819-850.

Lamond, J., Proverbs, D., Escarameia, M. & Tagg, A., 2013. Towards improved guidelines for drying flood-damaged buildings. Journal of Flood Risk Management, May.Volume 7.

Li, Y. & Ellingwood, B. R., 2006. Hurricane damage to residential construction in the US: Importance of uncertainty modeling in risk assessment. Engineering Structures, Volume 28, pp. 1009-1018.

Li, Y. et al., 2012. Loss Analysis for Combined Wind and Surge in Hurricanes. Natural Hazards Review, Volume 13, pp. 1-10.

Marshall, T. & Haag, P., 2014. Storm surge damage to buildings. s.l., s.n.

Masoomi, H. et al., 2019. Combined Wind-Wave-Surge Hurricane-Induced Damage Prediction for Buildings. Journal of Structural Engineering, Volume 145, p. 04018227.

MLIT, 2005. Manual for Economic Evaluation of Flood Control Investment (Draft), Tokyo: MLIT.

Mosimann, M. et al., 2018. A Robust and Transferable Model for the Prediction of Flood Losses on Household Contents. Water, Volume 10.

Nadal, C. N. C., Zapata-Lopez, R. & Pagán-Trinidad, I., 2006. Building Damage Estimation due to Riverine Floods, Storm Surges and Tsunamis: A Proposed Methodology, s.l.: s.n.

Nadal, N. C. et al., 2010. Building damage due to riverine and coastal floods. Journal of Water Resources Planning and Management, 136(3), pp. 327-336.

Nasiri, H., Mohd Yusof, M. J. & Ali, T., 2016. An overview to flood vulnerability assessment methods. Sustainable Water Resources Management, September.Volume 2.

National Flood Insurance Program, 2023. OpenFEMA Dataset: FIMA NFIP Redacted Claims - v2. [Online]

Available at: https://www.fema.gov/api/open/v2/FimaNfipClaims

Natural Resources Canada (NRCan), 2021. Federal Flood Damage Estimation Guidelines for Buildings and Infrastructure, s.l.: Government of Canada.

NDS, 2018. National design specification for wood construction, s.l.: Americal wood council.

Oasis LMF, 2023. Oasis LMF Documentation. [Online]

Available at: https://oasislmf.github.io/sections/Oasis-model-data-formats.html

[Accessed 15 January 2024].

Paleo-Torres, A. S., 2020. Modeling Residential Infrastructure Vulnerability to Hurricane Induced Coastal Flood, s.l.: s.n.

Park, S., Lindt, J. & Li, Y., 2014. ABV Procedure Combined with Mechanistic Response Modeling for Roof- and Surge-Loss Estimation in Hurricanes. Journal of Performance of Constructed Facilities, April, Volume 28, pp. 206-215.

Porter, K., Kiremidjian, A. & LeGrue, J., 2001. Assembly-Based Vulnerability of Buildings and Its Use in Performance Evaluation. Earthquake Spectra, May.Volume 17.

Prevatt, D. O., Gurley, K. R., Roueche, D. B. & Wong-Parodi, G., 2018. Survey and Investigation of Buildings Damaged by Category II, III, IV and V Hurricanes in FY 2017-18 – Hurricane Irma 2017, Gainesville: University of Florida.

Prevatt, D. O. et al., 2019. Survey and investigation of buildings damaged by category-III, IV & V Hurricanes in FY 2018-2019–Hurricane Michael, Gainesville: University of Florida.

Shin, D., Cocke, S. & Kim, B. M., 2022. A Systematic Revision of the NFIP Claims Hazard Data in Florida for Flood Risk Assessment. Applied Sciences, March, Volume 12, p. 3537.

Smith, C. S. & Scyphers, S., 2019. Past hurricane damage and flood zone outweigh shoreline hardening for predicting residential-scale impacts of Hurricane Matthew. Environmental Science & Policy, Volume 101, pp. 46-53.

Suppasri, A. et al., 2019. Load-resistance analysis: an alternative approach to tsunami damage assessment applied to the 2011 Great East Japan tsunami. Natural Hazards and Earth System Sciences, August, Volume 19, pp. 1807-1822.

Tomiczek, T., Kennedy, A. & Rogers, S., 2014. Collapse Limit State Fragilities of Wood-Framed Residences from Storm Surge and Waves during Hurricane Ike. Journal of Waterway, Port, Coastal, and Ocean Engineering, January, Volume 140, pp. 43-55.

Vishnu, N., Wojtkiewicz, R. & Ramanathan, K., 2021. Understanding flood vulnerability of buildings in US: A perspective through claims data. s.l., s.n.

Wagenaar, D., De Bruijn, K., Bouwer, L. & Moel, H., 2015. Uncertainty in flood damage estimates and its potential effect on investment decisions. Natural Hazards and Earth System Sciences Discussions, January, Volume 3, pp. 607-640.

Weekes, J., 2014. Predicting the vulnerability of typical commercial and single family residential buildings to hurricane damage. s.l., s.n.

Wing, O. E. J., Pinter, N., Bates, P. D. & Kousky, C., 2020. New insights into US flood vulnerability revealed from flood insurance big data. Nature Communication, Volume vol. 11(1), pp. 1-10.

Yokel, F., Yancey, C. W. & Mullen, C. L., 1981. A Study of reaction forces on mobile home foundations caused by wind and flood loads. s.l.:Building Science Series, National Institute of Standards and Technology, Gaithersburg, MD.

Actuarial Standards

Ahmadi, N., & Shahandashti, S. M. (2018). Role of predisaster construction market conditions in influencing postdisaster demand surge. Natural Hazards Review, 19(3), 04018010.

Waszink, H. E. (2006, March). The report of the research working party on correlations and dependencies among all risk sources. Part 4: Serial correlations of interest and inflation rates. The Casualty Actuarial Society Forum, Winter 2006 Edition (p. 255-276).

Döhrmann, D., Gürtler, M., & Hibbeln, M. (2017). Insured loss inflation: How natural catastrophes affect reconstruction costs. Journal of Risk and Insurance, 84(3), 851-879.

EM-DAT Database (2020). Retrieved from https://www.emdat.be/

Meyers, G. (2006, March). The report of the research working party on correlations and dependencies among all risk sources. Part 3: The common shock model for correlated insurance. The Casualty Actuarial Society Forum, Winter 2006 Edition (p. 231-254).

Hallegatte, S. (2008). An adaptive regional input-output model and its application to the assessment of the economic cost of Katrina. Risk Analysis: An International Journal, 28(3), 779-799.

Hallegatte, S., Boissonnade, A., Schlumberger, M. E., & Muir-Wood, R. (2008). Demand surge and worker migrations in disaster aftermaths: application to Florida in 2004 and 2005. Journal of Regional Science. Retrieved from http://www2.centre-cired.fr/IMG/pdf/Migration_Final.pdf

Heckman, P. E., & Meyers, G. G. (1983). The calculation of aggregate loss distributions from claim severity and claim count distributions. In Proceedings of the Casualty Actuarial Society (Vol. 70, No. 133-134, pp. 49-66). Casualty Actuarial Society.

Homer, D., & Li, M. (2017, June). Notes on using property catastrophe model results. In Casualty Actuarial Society E-Forum (Vol. 2). Retrieved from https://www.casact.org/community/affiliates/camar

/0517/CatNotes.pdf

Impact Forecasting (2020). ELEMENTS Computational & Financial Model. (Internal documentation).

Kuzak, D., & Larsen, T. (2005). Use of catastrophe models in insurance rate making. Catastrophe modeling: A new approach to managing risk, Chap. 5 (Springer, New York), 97–118.

Olsen, A. H., & Porter, K. A. (2011a). What we know about demand surge: Brief summary. Natural Hazards Review, 12(2), 62-71.

Olsen, A. H., & Porter, K. A. (2011b). On the contribution of reconstruction labor wages and material prices to demand surge. Report No. SESM-11-1, Dept. of Civil, Environmental, and Architectural Engineering, Univ. of Colorado at Boulder, Boulder, CO.

Property Claim Services (2020). Catastrophe bulletins. Retrieved from https://pcs.iso.com/pcs/app/start.do

Rachel Personius (2020). Construction cost: The impacts of hurricanes Harvey and Irma. Retrieved from https://www.fgould.com/americas/articles/construction-cost-the-impacts-of-hurricanes/

Rick Lloyd (2020). The cost impact of hurricane Harvey on the Texas construction market. Retrieved from https://www.mgac.com/blog/the-cost-impact-of-hurricane-harvey-on-the-texas-construction-market

Significant Flood Events (2020). Retrieved from https://www.fema.gov/significant-flood-events

Smith, A. B., & Katz, R. W. (2013). US billion-dollar weather and climate disasters: Data sources, trends, accuracy and biases. Natural Hazards, 67(2), 387-410.

Trish Hopkinson (2017, November). Hurricanes drive demand surge in reconstruction costs. Retrieved from https://www.verisk.com/insurance/visualize/hurricanes-drive-demand-surge-in-reconstruction-costs

Xactware (2020). Xactware's pricing data. Retrieved from https://www.xactware.com/en-us/resources/pricing-data-services/overview/

Computer/Information Standards

Flannery, B. P., Press, W. H., Teukolsky, S. A., Vetterling, W. T. (1992). Numerical Recipes in C: The Art of Scientific Computing, (2nd ed.). Cambridge, UK: Cambridge University Press.

Fowler, M. (2003). Patterns of enterprise application architecture (1st ed.). Boston, MA: Addison Wesley Professional.

Fowler, M., Scott, K. (1997). UML distilled: Applying the standard object modelling language (Object technology series). Boston, MA: Addison Wesley.

Gamma, E., Helm, R., Johnson, R., Vlissides, J. (1994). Design patterns: Elements of reusable object-oriented software (1st ed.). Boston, MA: Addison-Wesley Professional.

International Organization for Standardization. (2013). Information technology — Object Management Group Business Process Model and Notation (ISO/IEC 19510:2013 (E). Retrieved from https://www.iso.org/standard/62652.html

International Organization for Standardization. (2019). Information processing - Documentation symbols and conventions for data, program and system flowcharts, program network charts and system resources charts (ISO 5807:1985 (E). Retrieved from https://www.iso.org/standard/11955.html

LISA – Localization Industry Standard Association (https://www.gala-global.org/translation-and-localization-industry-standards)

Microsoft Corporation (2002). Developing international software: Developer reference (2nd ed.). Richmond, WA: Microsoft Press.

Object Management Group, Unified Modified Language. (version 2.5.1, published date: December 2017). Documentation symbols and conventions for class, sequence and use case diagrams retrieved from https://www.omg.org/spec/UML/

Unicode (http://www.unicode.org)

GF-1.7 ***Identify and describe the modeling-organization-specified, predetermined, and comprehensive exposure dataset used for projecting personal residential flood loss costs and flood probable maximum loss levels.***

Impact Forecasting developed a Florida residential properties database at a location level, which is used for projecting personal residential flood loss costs and flood probable maximum loss levels. This dataset was developed using a variety of sources including data from third-party vendors, the Federal Emergency Management Agency (FEMA) Hazus program, National Flood Insurance Program (NFIP) exposure, and Aon client exposures. NFIP insurance limits are applied to the database to confine the maximum coverage and minimum deductibles.

GF-1.8 ***Provide the following information related to changes in the flood model from the currently accepted flood model to the initial submission this year.***

This is the first submission of Impact Forecasting Florida Flood Model.

GF-1.9 ***Provide a list and description of any potential interim updates to underlying data relied upon by the flood model. State whether the time interval for the update has a possibility of occurring during the period of time the flood model could be found acceptable by the Commission under the review cycle in this Flood Standards Report of Activities.***

No interim updates to underlying data relied upon by the model are anticipated.

GF-2 Qualifications of Modeling Organization Personnel and Consultants Engaged in Development of the Flood Model

A. Flood model construction, testing, and evaluation shall be performed by modeling organization personnel or consultants who possess the necessary skills, formal education, and experience to develop the relevant components for flood loss projection methodologies.

Impact Forecasting staff and consultants involved in the development of the flood model possess a wide range of multi-disciplinary skills in hydrology, hydraulics, meteorology, structural engineering, actuarial science, statistics, computer science, and risk analysis. Model developers have advanced degrees and the majority hold PhDs in their fields of expertise. They are suitably qualified to develop, test, and evaluate flood loss projection methodologies.

Further information about the qualifications of individuals can be found in Disclosure GF-2.2.

B. The flood model and flood model submission documentation shall be reviewed by modeling organization personnel or consultants in the following professional disciplines with requisite experience: hydrology and hydraulics (advanced degree or currently licensed Professional Engineer, with experience in coastal and inland flooding), meteorology (advanced degree), statistics (advanced degree or equivalent experience), structural engineering (currently licensed Professional Engineer, with experience in the effects of coastal and inland flooding on buildings), actuarial science (Associate or Fellow of Casualty Actuarial Society or Society of Actuaries), and computer/information science (advanced degree or equivalent experience and certifications). These individuals shall certify Expert Certification Forms GF-1 through GF-7 as applicable.

The flood model and flood submission document submitted by Impact Forecasting was reviewed by employees of Aon and Fathom who meet the educational and professional criteria set forth in the ROA for each of the sections within the ROA. Further details on the professional qualifications of each individual and the sections they participated in the review and, where applicable, signatory approval of, can be found in Disclosure GF-2.2.

Disclosures

GF-2.1 Modeling Organization Background

A. Describe the ownership structure of the modeling organization engaged in the development of the flood model. Describe affiliations with other companies and the nature of the relationship, if any. Indicate if the modeling organization has changed its name and explain the circumstances.

Impact Forecasting LLC is a wholly owned subsidiary of Aon Benfield Inc. Aon Benfield Inc. is the reinsurance broking subsidiary of Aon plc, a publicly held global professional services firm providing risk, retirement, and health solutions. Impact Forecasting provides

catastrophe modeling services to Aon Benfield Inc. and directly to insurers, reinsurers, and regulatory organizations.

B. If the flood model is developed by an entity other than the modeling organization, describe its organizational structure and indicate how proprietary rights and control over the flood model and its components are exercised. If more than one entity is involved in the development of the flood model, describe all involved.

Impact Forecasting holds the proprietary rights and controls to the model.

Flood inundation modeling of the inland sub-perils (fluvial and pluvial) and a large proportion of the flood model event set were developed by Fathom – a United Kingdom-based consultant founded in 2013 as SSBN by Bristol University post-graduate abiturients and Professor Paul Bates. In 2017, SSBN was rebranded to Fathom solely for marketing reasons. In 2023, Fathom was acquired by Swiss Re. Impact Forecasting partnered with Fathom mainly due to the quality and openness of their methodologies and their flexibility in cooperation.

Flood inundation modelling of the coastal sub-peril (storm surge) uses the Sea, Lake and Overland Surges from Hurricanes (SLOSH) model, which is a computerized numerical model developed by the National Weather Service (NWS) in National Oceanic and Atmospheric Administration (NOAA) to estimate storm surge heights resulting from historical, hypothetical, or predicted hurricanes by taking into account the atmospheric pressure, size, forward speed, and track data. The source code of the SLOSH model and basin files are freely available upon request.

C. If the flood model is developed by an entity other than the modeling organization, describe the funding source for the development of the flood model.

Fathom provided all inland flood hazard data (hazard maps and event set component) in exchange for a royalty share from future model client-use or external licensing.

NWS from NOAA provided the SLOSH model for storm surge inundation modelling. The SLOSH model is freely available upon request.

D. Describe any services other than flood modeling provided by the modeling organization.

Impact Forecasting develops and maintains a global suite of catastrophe models and software tools to empower insurers, reinsurers, and regulatory organizations to quantify and manage the financial impact of natural catastrophes including hurricanes, earthquakes, and floods.

E. Indicate if the modeling organization has ever been involved directly in litigation or challenged by a governmental authority where the credibility of one of its U.S. flood model versions for projection of flood loss costs or flood probable maximum loss levels was disputed. Describe the nature of each case and its conclusion.

Impact Forecasting LLC has never been directly involved any legal process questioning the quality of any of its flood model versions or output types.

GF-2.2 Professional Credentials

A. Provide in a tabular format (a) the highest degree obtained (discipline and university; b) employment or consultant status and tenure in years, and (c) relevant experience and responsibilities of individuals currently involved in the acceptability process or in any of the following aspects of the flood model:

1. Meteorology

2. Hydrology and Hydraulics

3. Statistics

4. Vulnerability

5. Actuarial Science

6. Computer/Information Science

The credentials of individuals who contributed to development of the Impact Forecasting Florida Flood (FCHLPM) Model are listed below in Table 1. Contributors are either Impact Forecasting employees, Fathom employees who collaborated on the model development, or Aon Benfield Inc. employees acting as consultants on the project. The table identifies the years of professional experience of each contributor as well as their tenure at either Impact Forecasting, Fathom, or Aon Benfield Inc. Further details are provided for each contributor inAppendix B: Individuals Involved in the Impact Forecasting Florida Flood Model (FCHLPM) Model Acceptability Process.

Table 1: Credentials of individuals involved in the acceptability process and each aspect of the flood model

Standard	Name	Degree	Discipline	University	Status	Prof Exp. (Yrs)	Tenure (Yrs)
General	Alec Killoran	B.A.	English	University of California, Santa Barbara	E	7	1
Vulnerability	Andres Paleo	Ph.D.	Structural Engineering	University of Florida	E	5	2
Meteorology, Hydrological and Hydraulics	Ankit Prashnani	M.S.	Geomatics	CEPT University	E	6	3
Meteorology, Hydrological and Hydraulics, Statistics	Anthony Cooper	M.Eng	Engineering	University of Cambridge	F	6	1
Actuarial	Chad Xu	M.S.	Actuarial Science	Temple University	C	2	2
Vulnerability, Actuarial	Christopher Long	M.A.	Economics	Tufts University	E	25	19

Meteorology, Hydrological and Hydraulics, Statistics	Christopher Sampson	Ph.D.	Geographical Sciences	Univerity of Bristol (U.K.)	F	10	10
Vulnerability, Actuarial	Corbin Tucker	M.S.	Actuarial Science	University of Illinois at Urbana Champaign	E	5	2
General, Meteorology, Hydrological and Hydraulics, Statistics	Dan Rees	M.A.	Geographic Information Science	Clark University	E	13	1
General	David Colbus	M.A.	Climate and Society	Columbia University	E	6	1
Meteorology	David Byrne	Ph.D.	Oceanography	University of Liverpool (U.K.)	E	5.5	1
Meteorology, Hydrological and Hydraulics, Statistics	Elham Sharifineyestani	Ph.D.	Civil Engineering	Old Dominion University	E	6	3
Meteorology, Hydrological and Hydraulics, Statistics	James Savage	Ph.D.	Geographical Sciences	University of Bristol (U.K.)	F	7	4
Actuarial	Minchong Mao	M.S., FCAS, MAAA, CCRMP	Computer Science	University of Missouri-Columbia	C	22	5
Meteorology, Hydrological and Hydraulics, Statistics	Nans Addor	Ph.D.	Geography	University of Zurich, Switzerland	F	8	1
Meteorology, Hydrological and Hydraulics, Statistics	Niall Quinn	Ph.D.	Geographical Sciences	University of Southampton	F	6	5
General, Meteorology, Hydrological	Petr Puncochar	Ph.D.	Hydrology and Open-Channel Hydraulics	Czech Technical University in	E	13	13

and Hydraulics, Statistics				Prague (Czechia)			
Computer Information	Purvish Patel	B.S.	Computer Science	South Gujarat University (India)	E	24	10
Statistics	Radek Solnicky	M.S.	Mathematical Statistics	Charles University	E	13	13
Meteorology	Radovan Drinka	M.A.	Physics (with focus on Meteorology and Climatology)	Comenius University in Bratislava (Slovakia)	E	15	12
Vulnerability	Ricardo Wong Montoya	B.S.	Civil Engineering	Pontifical Catholic University of Peru	E	3	2
Computer Information	Sushma Bhat	B.S.	Computer Science	University of Bombay (India)	E	25	16
Computer Information	Venkatesh Ramaiah	M.S.	Computer Science	Birla Institute of Technology and Science, Pilani (India)	E	19	13
Vulnerability	Vipin Unnikrishnan	Ph.D.	Structural Engineering	Louisiana State University	E	9	7
Computer Information	William Dong	Ph.D.	Civil Engineering	University of Nebraska-Lincoln	E	11	6
General, Meteorology, Hydrological and Hydraulics, Statistics, Actuarial	Xian He	Ph.D.	Civil Engineering	University of Illinois at Urbana-Champaign	E	6	5
Vulnerability	Yujin Liang	Ph.D.	Structural Engineering	University of Illinois at Chicago	E	31	18
Vulnerability	Yuliia Khmurovska	Ph.D.	Civil Engineering	Czech Technical University in Prague (Czechia)	E	10	1

Computer Information	Shruthi Srikantegowda	PGDIPL	Information Technology	Symbiosis International, Pune (India)	E	18	14

B. Provide visual business workflow documentation connecting all personnel related to flood model design, testing, execution, maintenance, and decision-making.

A diagram to illustrate connections between all personnel related to flood model design, testing, execution, maintenance, and decision-making is provided below in Figure 4.

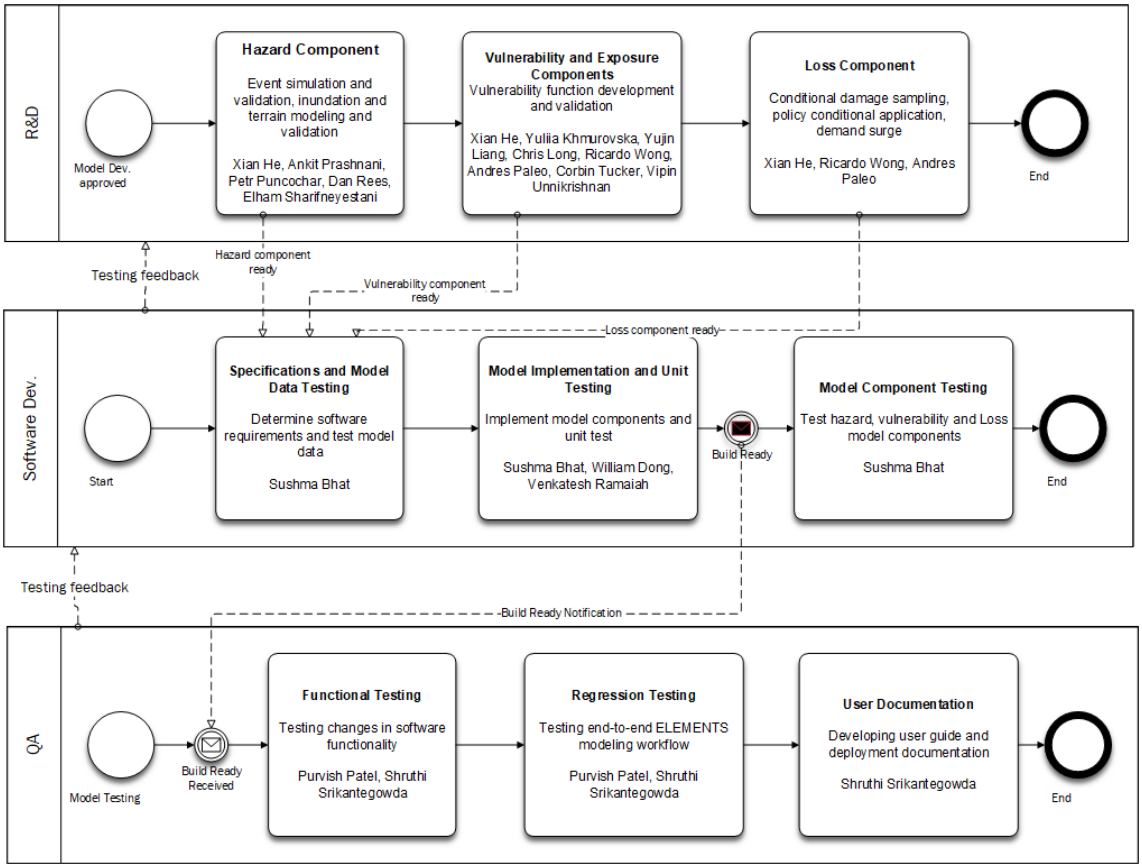

Figure 4: Business workflow diagram illustrating the connections between Impact Forecasting personnel

.

GF-2.3 Independent Peer Review

A. Provide reviewer names and dates of external independent peer reviews that have been performed on the following components as currently functioning in the flood model:

1. Meteorology

2. Hydrology and Hydraulics

3. Statistics

4. Vulnerability

5. Actuarial Science

6. Computer/Information Science

The Meteorology and Vulnerability components were reviewed in January 2024 by Holly Widen, Ph.D.

Dr. Widen leads Americas flood model evaluations for Aon Reinsurance Solutions. Dr. Widen is an expert at evaluating the science and engineering implemented within flood models licensed by Aon Benfield Inc. and has more than 7 years of professional experience in catastrophe risk management, natural hazards, and insurance. Prior to joining Aon, Dr. Widen worked at Risk Management Solutions, Inc. (now Moody's RMS) in Newark, California as the Product Manager of the RMS U.S. Inland Flood HD Model.

Dr. Widen has a Bachelor of Science degree in Atmospheric Science from Indiana University, a Master of Science degree in Geography from Ball State University, and a Doctorate degree in Geography from Florida State University.

The Vulnerability component was reviewed in November 2023 by ERN (Evaluación de Riesgos Naturales), led by Dr. Eduardo Reinoso, the founder of ERN. ERN is a Mexico-based leader in risk assessment modeling in Latin America.

B. Provide documentation of independent peer reviews directly relevant to the modeling organization responses to the flood standards, disclosures, or forms. Identify any unresolved or outstanding issues as a result of these reviews.

There are no unresolved or outstanding issues as a result of these reviews. The review letters provided by ERN and by Dr. Widen are included in Appendix C: External Expert Review of Vulnerability Modules and Appendix D: External Expert Review of Meteorology and Vulnerability Modules, respectively.

C. Describe the nature of any on-going or functional relationship the modeling organization has with any of the persons performing the independent peer reviews.

Dr. Widen is an employee of Aon Benfield Inc., the parent entity of Impact Forecasting. Aon Benfield Inc. is the reinsurance broking subsidiary of Aon plc. Aon Benfield Inc. uses hurricane models from multiple modeling vendor companies, including Impact Forecasting, ensuring that their clients have access to a range of loss perspectives.

ERN was acquired by Aon, the parent entity of Impact Forecasting, in November 2022. ERN is a part of Aon Reinsurance Solutions and collaborates with Impact Forecasting. There was no collaboration between Impact Forecasting and ERN on the Impact Forecasting Florida Flood Model development, as ERN remained an external and un-biased reviewer.

GF-2.4 ***Provide a list of rating agencies and insurance regulators that have reviewed the flood model. Include the dates and purpose of the reviews.***

The Impact Forecasting Florida Flood Model (FCHLPM) has not been reviewed by any rating agencies or insurance regulators.

GF-2.5 ***Provide a completed Form GF-1, General Flood Standards Expert Certification. Provide a link to the location of the form [Form GF-1: General Flood Standards Expert Certification].***

GF-2.6 ***Provide a completed Form GF-2, Meteorological Flood Standards Expert Certification. Provide a link to the location of the form [Form GF-2: Meteorological Flood Standards Expert Certification].***

GF-2.7 ***Provide a completed Form GF-3, Hydrological and Hydraulic Flood Standards Expert Certification. Provide a link to the location of the form [Form GF-3: Hydrological and Hydraulic Flood Standards Expert Certification].***

GF-2.8 ***Provide a completed Form GF-4, Statistical Flood Standards Expert Certification. Provide a link to the location of the form [Form GF-4: Statistical Flood Standards Expert Certification].***

GF-2.9 ***Provide a completed Form GF-5, Vulnerability Flood Standards Expert Certification. Provide a link to the location of the form [Form GF-5: Vulnerability Flood Standards Expert Certification].***

GF-2.10 ***Provide a completed Form GF-6, Actuarial Flood Standards Expert Certification. Provide a link to the location of the form [Form GF-6: Actuarial Flood Standards Expert Certification].***

GF-2.11 ***Provide a completed Form GF-7, Computer/Information Flood Standards Expert Certification. Provide a link to the location of the form [Form GF-7: Computer/Information Flood Standards Expert Certification].***

GF-3 Insured Exposure Location

A. *ZIP Codes used in the flood model shall not differ from the United States Postal Service publication date by more than 48 months at the date of submission of the flood model. ZIP Code information shall originate from the United States Postal Service.*

The Impact Forecasting Florida Flood (FCHLPM) Model uses United States Postal Service ZIP Code data that is post processed by the third-party vendor Zip-Codes.com. The issue date of the current iteration is November 2021, which was within 24 months of the date of the original submission deadline, November 1st, 2023, and is within the 48 months of the actual submission date, January 31st, 2024, as specified by the standard.

B. *Horizontal location information used by the modeling organization shall be verified by the modeling organization for accuracy and timeliness and linked to the personal residential structure where available. The publication date of the horizontal location data shall be no more than 48 months prior to the date of submission of the flood model. The horizontal location information data source shall be documented and updated.*

Impact Forecasting's Industry Exposure Database (IED) uses lat/long locational data, which has been validated for accuracy. The IED relies on exposure from Aethenium, the vintage of the data used is 2022.

C. *If any flood model components are dependent on databases pertaining to location, a logical process shall be maintained for ensuring these components are consistent with the horizontal location database updates.*

Three polygon layers are used in the model serving as a basis for risk aggregation and additional breakouts.

- Zip-code polygon shapefile (provided by zip-codes.com) introduced more in depth in section A above. This is the same layer as was used for the Impact Forecasting Atlantic Tropical Cyclone – Wind (FCHLPM) Model Version 2.0 submission.

- Florida county shapefile (provided by GfK) holding all information about individual counties

- Florida state shapefile (provided by GfK) holding information about states, for Florida is however one polygon only.

In model 'ReferenceData' database the table Geodata holds the hierarchical structure of which zip-codes are covered by respective higher units (counties) and subsequently for states. Small number of polygons where counties and zip-codes boundaries are inconsistent were thoroughly manually checked and proportion with larger area/ and IED sums insured was assigned to.

Any subsequent changes are done and verified in the GIS environment and in this table is updated.

D. *Geocoding methodology shall be justified.*

Impact Forecasting uses industry-proven toolset for geo addressing from Precisely (former Pitney Bowes). ELEMENTS platform is using their GeoAdressing API's (Application programming interface) service to convert street address strings into location coordinates (in WGS 84 coordinate system).

E. *Use and conversion of horizontal and vertical projections and datum references shall be consistent and justified.*

The modeled storm surge elevation is based on the vertical datum of NAVD88 and the horizontal datum of NAD83 (Conver, et al., 2008). During the surge elevation validation process, if the

observation data is not based on NAD83 or NAVD88 datum, the observed water elevations were converted to NAD83 and NAVD88 using NOAA's VDATUM tool (https://vdatum.noaa.gov/). After the validation, the final surge elevation of the surge footprint is converted to EGM08 vertical datum and WGS84 horizontal datum using NOAA's VDATUM tool.

The inland flood model consistently uses the Earth Gravitational Model (EGM) 2008 (EGM 08) vertical datum and the World Geodetic System (WGS) 1984 (WGS 84) horizontal datum.

Disclosures

GF-3.1 List the current location databases used by the flood model and the flood model components to which they relate. Provide the effective dates corresponding to the location databases.

The Impact Forecasting Florida Flood (FCHLPM) Model uses United States Postal Service ZIP Code data that is post-processed by the third-party vendor Zip-Codes.com. The issue date of the current iteration is November 2021, which was within 24 months of the date of the original submission deadline, November 1st, 2023, and is within the 48 months of the actual submission date, January 31st, 2024, as specified by the standard.

GF-3.2 Describe in detail how invalid ZIP Codes, parcels, addresses, and other location information are handled.

After importing a portfolio into ELEMENTS as described in Disclosure GF-3.3, the status of the quality of the data can be found in a summary result which indicates how many exposures were mapped to the street address level, mapped to the ZIP Code level, or were found to be invalid. If a ZIP Code is found to be invalid and cannot be found in the Impact Forecasting ZIP Code database, it will not be modeled. Users have the option to correct the data by changing the address/ZIP Code or setting coordinates and re-importing the portfolio.

.

GF-3.3 Describe any methods used for subdividing or disaggregating the location input data and the treatment of any variations for populated versus unpopulated areas.

For exposure input on zip-code level, the calculation process is done on the cumulative inundation depth exceedance distribution calculated for individual zip-code and modeled event.

GF-3.4 Describe the data, methods, and process used in the flood model to convert between street addresses and geocode locations (latitude-longitude).

There are four geocoding options when importing exposure data into ELEMENTS:

1. Use Most Precise Information Available

If both coordinate and address information are provided by the user, this option outputs the higher precision geographic information. For example, if ZIP Code centroid coordinates are provided but address data is available and can be geocoded to street level, then the address data is used. If the coordinates provide more precise information, reverse geocoding is performed to find related administrative information (i.e., ZIP Code, state, etc.) which is used for reporting.

2. Use Address Information, Ignore Coordinates

This option uses the user-supplied address information (excluding coordinates) for geocoding with the internal geocoding engine. Locations where geocoding cannot be achieved with address information are excluded from analyses even if coordinates were provided.

3. Use Coordinates and only if not available use Address Information

This option uses the user-supplied coordinates regardless of precision. If coordinates are not present, the address data provided is used (as in option 2).

4. Use Coordinates for Hazard and Address Information for Reporting

The coordinates are used to find the appropriate hazard location, and the supplied address information is used for reporting. Generally, administrative information is retained (e.g., ZIP Code, state) when an exact match is available. ZIP Codes entered by the user that do not match exactly to a known ZIP Code may be re-mapped to known ZIP Codes. This avoids the reverse geocoding process performed when attempting to use the Use Most Precise Information Available option (option 1 above), and administrative information is generally retained. If coordinates are not present for a given location, the address information is used (as in option 2). If address information is not present for a given location, the coordinate information is used (as in option 3).

ELEMENTS has the option to validate the address information provided by the user using a third-party geocoder (Precisely, formerly Pitney Bowes) if available.

GF-3.5 Describe the use of geographic information systems (GIS) in the process of converting among street address and geocode locations, and the generation of insured exposure locations.

No use of GIS software or associated libraries are directly used.

The information about the precise risk location is specified by model users with latitude/longitude coordinates (available in WGS 84) or provided by 3rd party geocoder from Precisely's Spectrum Global Geocoding, discussed in Disclosure GF-3.4.

The zip-code ID assignment for risk coordinates is done in ELEMENTS portfolio import process by a spatial query in SQL over the zip-code layer (reference) stored in SQL as an SQL geometry object.

GF-3.6 List and provide a brief description of each database used in the flood model for determining geocode location.

A list of ZIP Code-based databases used in the Impact Forecasting Flood (FCHLPM) Model, along with a brief description of each, is given below.

ZIP Code

ZIP Code boundaries and point ZIP Codes used in the Impact Forecasting model are acquired from Zip-Codes.com. Zip-Codes.com uses algorithms that strictly interpret monthly data feeds from the U.S. Postal Service to construct polygons for postal ZIP Codes. All maps displayed in this submission are created based on this ZIP Code boundary product.

ZIP Code Events

Population-weighted inundated depth profiles are calculated for ZIP Codes affected by events. Using the 2020 U.S. Census population data released in 2022, population is assigned to each model grid cell, and the average population-weighted flood inundation depth is calculated for each event and ZIP Code. Those ZIP Codes that have a population-weighted centroid outside of the event footprint will not be included for that event.

GF-3.7 Describe the process for updating flood model geocode locations as location databases are updated.

Impact Forecasting updates its ZIP Code databases at least every 24 months. The update process is as follows:

1. Acquire the ZIP Code boundary and point ZIP Code data from ZIP-Codes.com.
2. ZIP Code boundary data are compared with previous vintages for accuracy and appropriateness.
3. If the data pass the above inspection, the new version is deployed into the Impact Forecasting flood model.
4. Additional ZIP Code databases described in Disclosure GF-3.4 (ZIP Code Events) are prepared using the new ZIP Code data and U.S. Census data.

GF-3.8 Describe in detail the methods by which ground elevation data at the insured exposure location (e.g., building) is associated with the location databases and how this associated data is used in the flood model.

The altitude of each insured location is extracted from the digital terrain model in Hydrogrid dataset, as is described in Disclosure HHF-1.5. This is subsequently used to reflect first-floor-height in the loss calculation process.

GF-3.9 For each parameter used in the flood model, provide the horizontal and vertical projections and datum references, if applicable. If any horizontal or vertical datum conversions are required, provide conversion factors and describe the conversion methodology used.

For the storm surge portion of the model, the vertical datum employed in the SLOSH basins is NAVD88 and the horizontal datum is NAD83 (Conver, et al., 2008). During the surge elevation validation process, if the observation data is not based on NAD83 or NAVD88 datum, the observed water elevations were converted to NAD83 and NAVD88 using NOAA's VDATUM tool (https://vdatum.noaa.gov/). After the validation, the final surge elevation of the surge footprint is converted to EGM08 vertical datum and WGS84 horizontal datum using NOAA's VDATUM tool to be consistent with other model components.

The parameters used in the Inland Flood Model are based on World Geodetic System (WGS) 1984 (WGS 84) horizontal datum, while the vertical values are based on elevation dataset employing the Earth Gravitational Model (EGM) 2008 (EGM 08) vertical datum.

GF-4 Independence of Flood Model Components

The meteorology, hydrology and hydraulics, vulnerability, and actuarial components of the flood model shall each be theoretically sound without compensation for potential bias from other components.

The meteorological, hydrology and hydraulics, vulnerability, and actuarial components of the Impact Forecasting Florida Flood (FCHLPM) Model are theoretically sound and developed independently. Each component is validated individually without consideration of possible biases in other components.

GF-5 Editorial Compliance

The flood model submission and any revisions provided to the Commission throughout the review process shall be reviewed and edited by a person or persons with experience in reviewing technical documents who shall certify on Form GF-8, Editorial Review Expert Certification, that the flood model submission has been personally reviewed and is editorially correct.

The Impact Forecasting submission has been compiled, edited, and reviewed by a person with experience in authoring and reviewing technical documents for consistency, grammar, and editorial accuracy. The signatory for Form GF-8: Editorial Review Expert Certification (also referred to here as the Editor), David Colbus, has experience in authoring, reviewing, and editing technical documentation, as well as experience understanding the FCHLPM Hurricane Standards and Acceptability Process. Further details on the qualifications and experience of the Editor may be found in Appendix B: Individuals Involved in the Impact Forecasting Florida Flood Model (FCHLPM) Model Acceptability Process .

Disclosures

GF-5.1 Describe the process used for document control of the flood model submission. Describe the process used to ensure that the paper and electronic versions of specific files are identical in content.

Impact Forecasting used the web-based collaboration platform, Microsoft SharePoint, to manage document control of the submission. In addition to facilitating clear version histories, SharePoint has a “check out” feature which is used by the Editor to ensure that (1) only authorized changes are made to the submission document, (2) all required formatting and links are maintained, and (3) ultimately, the paper and electronic versions of the submission document and all associated files are identical in content.

To compile the initial version of the submission document, submission authors and contributors first produced a separate draft of each Standards section within an organized folder structure on SharePoint. Track Changes and Comments were used to facilitate collaboration and discussion among Standard collaborators. Once the draft of each Standards section was completed and reviewed by the section owner (signatory who certifies the corresponding Expert Certification form), the Editor locked each draft document for editing and incorporated its content into a master document template.

From this point forward, in order to maintain a clear and consistent version history and ensure that no changes that weren’t expressly authorized by the section owners would be made to the final document, only the Editor was permitted to make changes to the draft submission. At this stage, the Editor performed a comprehensive editorial review of the draft document using Track Changes and made notes using Comments of any areas that appeared to need clarification or additional information from the section owners.

Further edits were completed on a rolling basis while the Editor maintained a comprehensive version history of each subsequent draft version. To request a change to any submission content (Standards, Disclosures, or Forms), the section owner or

collaborator downloaded the most recent version of the master document, made edits using Track Changes, clearly labeled the file name of their version, and submitted it to the Editor for inclusion. The Editor incorporated the requested changes to the master document (while noting in the version history what changes were made) and requested review from the section owner. A final deadline was established for content changes by section owners, after which point the Editor made a final review of the completed submission document for consistency, grammar, and editorial accuracy.

Finally, to prepare for printing, the submission document was converted to PDF (Portable Document Format). The PDF was reviewed by the Editor for proper bookmark functionality. Upon receipt of the printed copies, the document was personally reviewed by the Editor to ensure print quality and readability.

GF-5.2 ***Describe the process used by the signatories on the Expert Certification Forms GF-1 through GF-7 to ensure that the information contained under each set of flood standards is accurate and complete.***

Each signatory on Expert Certification Form GF-1 through Form GF-7 was responsible for the final review of their section, in addition to preliminary reviews throughout the submission production process. Additional key contributors may submit requested changes to the master document (see Disclosure GF-5.1), but the section owner must ultimately approve them. Upon inclusion of any changes to the working submission draft, the signatory must re-approve the updated version. Prior to submission of the final document, each signatory gives a final review and communicates to the Editor that they have signed off.

GF-5.3 ***Provide a completed Form GF-8, Editorial Review Expert Certification. Provide a link to the location of the form [Form GF-8: Editorial Review Expert Certification].***

METEOROLOGICAL FLOOD STANDARDS

MF-1 Flood Event Data Sources

A. *The modeling of floods in Florida shall involve meteorological, hydrological, hydraulic, and other relevant data sources required to model coastal and inland flooding.*

The Impact Forecasting Florida Flood Model uses current scientific and technical literature involving meteorological, hydrological, hydraulic, and other relevant data sources required to model coastal and inland flooding. A comprehensive list of pertinent references can be found in Disclosure GF-1.6.

B. *The flood model shall incorporate relevant data sources in order to account for meteorological, hydrological, and hydraulic events and circumstances occurring either inside or outside of Florida that result in, or contribute to, flooding in Florida.*

The Impact Forecasting Florida Flood Model incorporates relevant data sources accounting for meteorological, hydrological, and hydraulic events and circumstances occurring either inside or outside Florida that result in or contribute to flooding in Florida. A comprehensive list of pertinent references can be found in Disclosure GF-1.6.

C. *Coastal and inland flood model calibration and validation shall be justified based upon historical data consistent with peer reviewed or publicly developed data sources.*

Coastal and inland flood model calibration and validation are justified and based upon historical data consistent with peer reviewed or publicly developed data sources. The validation data sources and plots can be found in the Form HHF-1 ~ Form HHF-5.

D. *Any trends, weighting, or partitioning shall be justified and consistent with current scientific and technical literature.*

There was no trending, weighting, or partitioning when developing the Impact Forecasting Florida Flood Model.

Disclosures

MF-1.1 Specify relevant data sources, their release dates, and the time periods used to develop and implement flood frequencies for coastal and inland flooding into the flood model.

The Base Hurricane Storm Set from the official HURDAT2 database (Landsea, et al., 2008) and the Hadley Centre Sea Ice and Sea Surface Temperature Dataset (HadISST) (Rayner, et al., 2003) as of August 2, 2021, covering the period from 1900 to 2020, are used to develop and implement flood frequencies and intensities for TC-induced coastal and inland flooding.

The key datasets used in the non-TC synthetic event set model, corresponding hydrological model, and the construction of inland event inundation footprints include:

- MSWEP: reanalysis precipitation fields (Beck, et al., 2019), version 2.8 (Feb 14, 2021) covering the period of 1980 to 2020 were used in the training of the non-TC event set model.
- IBTrACS version v04r00: Storm track and associated dates for historical events (Knapp et al., 2010; 2018), released 2019, using data covering the period of 1980 to 2020, was used to remove historical TC events from our dataset used to train the non-TC model
- USGS watershed units: Polygonal hydrological units, obtained 2020, was used within the event clustering stage of the non-TC synthetic event set model training data creation and as discretization units for the pluvial event footprints.
- Multi-Source Weather (MSWX): bias-corrected and interpolated reanalysis multivariate fields (including temperature) on the same grid as MSWEP (Beck, et al., 2022), version 1.0 (Dec 12 2020), covering the period of 1980 to 2020, was used in the generation of the hydrological hindcast.
- Multi-Error-Removed Improved-Terrain Hydrography (MERIT hydro): Global river hydrography (network) at 3 arcsecond resolution (Yamazaki, et al., 2019), version 1.0.1 (10 June 2019) was used to derive river reach locations and connectivity.
- Multi-Error-Removed Improved-Terrain Digital Elevation Model (MERIT DEM): Global terrain dataset at 3 arcsecond resolution (Yamazaki, et al., 2017), version v1.0.3 (15 oct 2018) was used in the hydrological model.
- Fathom Hazard catalog: Pre-computed flood inundation layers across 15 Return Periods for fluvial and pluvial perils (Bates et al., 2021), version US V2.F are sampled from within each synthetic event to construct a flood inundation footprint. Further datasets are used within this product include river gauge data from the USGS National Water Information System (NWIS) (gauges records cover various dates but last updated in 2021) and extreme rainfall data taken from the National Oceanic and Atmospheric Administration (NOAA) Precipitation Frequency Data Server (PFDS) Atlas 14 - accessed January 2023

MF-1.2 ***Where the flood model incorporates modification, partitioning, or adjustment of the historical data leading to differences between modeled climatological and historical data, justify each modification and describe how it is incorporated.***

The historical data was not modified, partitioned, or adjusted when developing the TC-induced events in the Impact Forecasting Florida Flood Model.

- Within the non-TC synthetic event set training data creation, reanalysis data was modified prior to the characterisation of marginal distributions and subsequent synthetic event set generation by removing the historical Tropical Cyclone and Tropical Storm data points from the records. This data was then used to derive event-max tables that would be used to characterize the non-TC synthetic event set model. This was done to ensure the model did not represent TC and TS (tropical storm) processes, to avoid later double counting in the final event set.

MF-1.3 ***Describe how historical sea-level rise is treated in the flood model validation. If sea-level rise is not used in flood model validation, justify its omission.***

In the coastal flood model validation for historic events, modeled maximum storm tides are validated against observations of peak water levels from sources like NOS (National Ocean Service), USGS, etc. These observations include the effects of sea-level rise. The modeled results do not include sea-level rise due to its small effects. When averaged over all the world's oceans, the global mean sea level has risen by about 0.17m over the last 100 years

(1920-2020), with noted acceleration since about 1970. Relative sea level averaged along the contiguous United States has risen about 0.28m over the same period, which is equivalent to about 0.0028m per year (Sweet, et al., 2022). Studies showed a sea level rise rate in various tide stations along Florida coastline of around 0.0014m per year ~ 0.0037m per year in the 1930s and 0.0024m per year in the 1970s. Since early 2000s, the mean sea level rise rate has increased to about 0.008m per year by the end of 2021 (Wdowinski, 2019; Dangendorf, et al., 2023; NOAA; Tides & Currents, 2023a). Most of the validation data used for the storm surge portion of the Impact Forecasting Florida Flood Model is for events after 1990. So, for the 30 years or so after 1990, the maximum sea level rise could only be around 0.24m, which is not significant enough to alter the loss estimates a lot. Thus, the sea-level rise is not considered in developing the storm surge portion of the Impact Forecasting Florida Flood Model.

The sea level rise is not used in inland flood model validation due to its minimal impact on the study area, leading to a negligible influence on the overall results.

MF-1.4 Describe if and how future projected sea-level rise is treated in the flood model.

The Impact Forecasting Florida Flood Model does not consider projected sea-level rise.

MF-1.5 Describe any assumptions or calculations used in the flood model relating to future conditions (e.g., changes in precipitation patterns, changes in storm frequency or severity).

No assumptions or calculations were used in the Impact Forecasting Florida Flood Model that anticipates changes in future conditions.

MF-1.6 Describe if and how historical changes in topography, bathymetry, and land use land cover are treated in the flood model validation.

In the coastal flood validation, the observation data reflects the changes in topography, bathymetry, and land use land cover. The modeled storm surge also considers the changes in topography, bathymetry and land use land cover through SLOSH basins. The SLOSH basins are updated at an average rate of 3-6 basins per year, to account for changes in bathymetry and topography (NOAA, 2023b). These updates are driven by several factors including changes to bathymetry/topography due to a landfalling hurricane, changes to the coastline, addition of new flood protection devices like levees, increasing the resolution for better surge conveyance or for better representation of local features, etc.

For the inland flood hazard modelling, we assume static land use cover, bathymetry, and topography for the model simulations. These components represent a present-day model and are based on the latest data available to us at the time of modeling.

MF-1.7 If precipitation is explicitly modeled for either inland or coastal flooding, then describe the underlying data and how they are used as inputs to the flood model.

Precipitation is explicitly modeled in the Impact Forecasting Florida Flood Model, utilizing a physics-based Tropical Cyclone Rainfall (TCR) model developed by Lu et al. (2018) and Feldmann et al. (2019). Details about the model can be found in studies by Lu et al. (2018) and Feldmann et al. (2019). This model calculates rain rates and accumulated rainfall at specified Points of Interest (POI), defined here as any 0.1°×0.1° grid point in the continental United States. The key inputs for the model include:

- Two-hourly track information, encompassing details such as track position, dates, maximum sustained wind speed, and radius of maximum wind speed (RMW). These two-hourly data points are interpolated from six-hourly data derived from IF Hurricane model.
- Environmental parameters at different pressure levels including two-hourly 600 hPa (hectopascal) environmental temperature, 250, and 850 hPa environmental zonal and meridional wind speeds (m/s) interpolated to the storm center. These parameters were obtained using two sets of reanalysis data including NOAA CIRES (Cooperative Institute for Research in Environmental Sciences) Twentieth Century Global Reanalysis Version 1 (1908-1958) (Compo, G. P., et al. 2009) and NOAA NCEP-NCAR (1958 – 2023) (Kalnay, et al., 2018).
- Topography and Drag coefficient: The drag coefficient, derived from the Surface Roughness dataset of NLCD 2019 using (Lu, et al., 2018) formula. For the topography, we used a digital elevation map with a horizontal resolution of 0.1°×0.1°.
- Analytical wind profile: We employed (Emanuel & Rotunno, 2012) analytical wind profile.
- The maximum 24-hours accumulated rainfall, derived for historical and stochastic event sets, serves as input for the Fathom hydrological model.

For the pluvial flood hazard model simulations, we take extreme rainfall estimates in the form of Intensity-Duration-Frequency curves from the National Oceanic and Atmospheric Administration (NOAA) Precipitation Frequency Data Server (PFDS). These data are based on gauge data and describe rainfall intensity for different duration events for different event severities. We take these estimates for the 1-, 6- and 24-hour rainfall durations for simulation in the hydrodynamic model. Rainfall is reduced to account for soil infiltration and urban drainage and simulated within the hydrodynamic model. More detail is provided in Disclosure MF-2.6.

Within the non-TC synthetic event set, explicit precipitation fields are modeled, converted to probability (return period) space after merging with the TC event set, and are then used to sample from pre-computed hazard layers to derive inundation footprints after interpolation to National Hydrography Dataset's Hydrologic Unit Level Ten watershed boundary units. The MSWEP precipitation dataset is used as a pluvial training data input to the non-TC synthetic event set model. This dataset contains reanalysis precipitation fields across a 0.1 degree grid at 3-hourly resolution from 1979 to present. The data is also used to force the hydrological model reanalysis to provide the fluvial training data. This data is interpolated to 25 km spatial and daily temporal resolution.

MF-1.8 ***Provide citations to all data sources used to develop and support bottom friction for storm surge modeling, including publicly developed or peer reviewed information.***

The SLOSH model is based on constant eddy viscosity and bottom slip coefficients, which can reproduce reasonable steady bottom flow behavior of the wind-driven currents over an inner shelf. The SLOSH model bottom stress formulation is described in (Platzman, 1963; Jelesnianski, 1966; 1970; 1992; Kim & Chen, 1999). The values for the eddy viscosity and bottom slip coefficients were empirically determined using three historical storms with adequate meteorological and surge data for such tests – the September 1944 storm, Carol in 1956, and Donna in 1960 (Jelesnianski, et al., 1992). A tide gauge was operative just offshore at Atlantic City, New Jersey during and after each of these storms' passages. All three storms were traveling at high speed (>30mph) and waters just offshore were deep (>25ft depths). The SLOSH model was tested using several values for eddy viscosity and

slip coefficients until the peak surge matched well with the observation. It was also found that the peak surge was insensitive to a broad range of eddy viscosity and bottom slip coefficients when both were included in the bottom stress formulation (Jelesnianski, 1966). This may not always hold for shallow waters (<10ft) or for slow moving storms. Special tests with the SLOSH model for shallow depths and inland inundation with real observed data in Lakes Okeechobee and Pontchartrain imply the adopted values of eddy viscosity and bottom slip coefficients are acceptable in a universal sense, at least for the level of accuracy needed in operational storm surge forecasting.

MF-1.9 ***State whether the model includes flooding other than coastal and inland flooding. State whether the other flooding types are independent of the minimum required sub-perils of coastal and inland flooding.***

The Impact Forecasting Florida Flood Model only includes coastal and inland (fluvial and pluvial) flooding.

MF-2 Flood Parameters (Inputs)

A. *The flood model shall be developed with consideration given to flood parameters that are scientifically appropriate for modeling coastal and inland flooding. The modeling organization shall justify the use of all flood parameters based on information documented in current scientific and technical literature.*

The Impact Forecasting Florida Flood Model parameters are based on scientifically appropriate technical literatures and data sources. The justification of the flood parameters can be found in Disclosure MF-2.1.

B. *Differences in the treatment of flood parameters between historical and stochastic events shall be justified.*

The Impact Forecasting Florida Flood Model has no difference in the treatment of flood model parameters between historical and stochastic events.

C. *Grid cell size(s) used in the flood model shall be justified.*

The storm surge portion of the Impact Forecasting Florida Flood Model models surge elevation at a grid cell resolution of 0.0025-degree (equivalent to about 250 m). The 250 m resolution was determined based on the smallest SLOSH basin grid. The DEM (Digital Elevation Model) data resolution is 0.0003-degree which is equivalent to about 30m, thus the surge depth resolution is also 0.0003-degree (about 30m). The justification of grid cell size used in the storm surge portion of the Impact Forecasting Florida Flood Model can be found in Disclosure MF-2.11.

The inland flood inundation model is simulated at 1 arc second (approximately 30 m) resolution. The properties of the river channel (i.e., riverbed and bank elevation and width) are determined at a 3 arc second (approximately 90 m) resolution, with these properties interpolated to 1 arc second between the center points of these cells.

This model resolution was chosen as being fine enough to resolve primary flow pathways whilst also remaining computationally feasible to run models across the state for all three primary flood perils. This resolution is typical of regional and national scale models, and publications have demonstrated that models simulated at these resolutions are able to compare well to national scale flood maps (e.g. Bates et al. 2021; Bates et al. 2023).

The hydrological models FUSE is run on a 0.25° grid (~25km at the equator) and mizuRoute is run on the MERIT-Hydro network (median reach length of ~7km). Both models are set up to simulate all river reaches upstream and downstream of the TC/TS rainfall footprint.

For the inland event set, the final model event footprints are generated through the sampling from pre-computed hazard layer catalogs. To do this in an efficient manner, the region is discretised into pluvial and fluvial catchments, and within each, the event maximum return period is defined. This return period is used to select the most appropriate hazard layer (flood depths) to sample. Further details are provided above in Disclosure HHF-1.2.

Disclosures

MF-2.1 For coastal and inland flood model components, identify and justify the various flood parameters used in the flood model.

The following parameters are used in the storm surge portion of the Impact Forecasting Florida Flood Model:

Central Pressure

The central pressure deficit (i.e. the difference in atmospheric pressure between the storm center and the environment) will pile up the water and lead to pressure-driven surge. Lower central pressure will produce a higher surge. The central pressure is modeled in the form of relative intensity (Darling, 1991) using a multiple linear regression model. For each time step, the central pressure in a given 5x5-degree cell is modeled as a function of the relative intensities from the previous three time steps and the current and previous sea surface temperatures (Vickery, et al., 2000; Rayner, et al., 2003). A random error term which follows a normal distribution is used to model the residuals that result from the regression. Relative intensity values are taken between 0 and 1 to constrain the minimum central pressures a hurricane can physically reach under certain environmental conditions.

Radius of Maximum Winds

The radius of maximum winds is an important parameter that describes the size of a hurricane and the footprint extent of the storm surge. The winds in a larger storm will push water from a larger area of the ocean to affect a larger region on land. The strong winds in a larger storm usually tend to affect an area longer than smaller storms (NOAA, 2023b). The Rmax is modeled as a random variable which follows a lognormal distribution. The mean of the variable is described as a function of central pressure deficit and latitude (Vickery & Wadhera, 2008). The variation relative to the mean is determined from historical data through regression analysis. The historical data is obtained from the HURDAT2 Re-analysis Project (e.g., (Landsea, et al., 2004a; Landsea, et al., 2004b; Landsea, et al., 2008; Landsea, et al., 2012; Landsea, et al., 2014; Hagen & Landsea, 2012; Delgado, et al., 2018)), NOAA Technical Report NWS 38 (Ho, et al., 1987), and the Extended Best Track Dataset (Demuth, et al., 2006).

Storm Track (Translational Speed and Heading Angle)

The translational wind speed and heading angle affect the peak storm surge height. In general, a storm with a heading angle perpendicular to the coastline generates higher storm surge than a storm with heading angle close to parallel to the coastline. On the open coast, a storm with higher translational speed will produce a higher surge. However, in bays, sounds, and other enclosed bodies of water, higher surge is produced with a slower storm since slower storm will have more time to accumulate water on land (NOAA, 2023b). The hurricane translational speed and heading angle at every 6-hour time step are modeled as separate regression models, using the forward speed, heading direction, latitude, and longitude from up to two previous time steps as predictors. The regression coefficients are derived for different 5x5-degree cells across the North Atlantic Ocean (Vickery, et al., 2000; 2009c). The regression model with the corresponding set of coefficients is used when a storm moves into a given cell. The residuals from the regression are modeled as a normal distribution in each cell to address the randomness of hurricane movement.

Shape of the Coastline

Storm surge will be higher when a hurricane makes landfall on a concave coastline (curved inward, such as the Apalachee Bay in Florida) as opposed to a convex coastline (curved outward, such as the Miami Beach area on the east coast of Florida). Places with bays are especially vulnerable because the mound of water can be funneled into a small area. The shape of the coastline is defined in SLOSH basin grids (Conver, et al., 2008).

Width and Slope of the Ocean Bottom

Higher storm surge occurs on wide and gently sloping continental shelves, while lower storm surge occurs on narrow and steeply sloping shelves. Areas along the Gulf Coast, including the west coast of Florida, are vulnerable to storm surge because the ocean floor gradually deepens offshore. Conversely, areas such as the east coast of Florida have a steeper shelf, reducing the amount of storm surge (NOAA, 2023b). The slope of the coastline is defined in SLOSH basin grids through latitude, longitude, and elevation of each grid cell (Conver, et al., 2008).

Surface Drag Coefficient

The surface drag coefficient is used to quantify the drag or resistance of an object in water. A lower drag coefficient indicates the object will have less hydrodynamic drag. In the absence of suitable data to empirically formulate a variable drag coefficient for surface stress, a constant was chosen by comparing observed and computed surges for 43 historical storms (Jelesnianski, 1972). The constant drag coefficient is presently used to forecast or hindcast surges generated by all tropical storms in all basins. A constant surface drag coefficient $C_D \cdot \rho_a/\rho = 3 \times 10^{-6}\, ft^2/sec^2$ is used to calculate surface stress in SLOSH (Jelesnianski, 1972; 1992).

Vertical Eddy Viscosity Coefficient & Bottom Slip Coefficient

The SLOSH model is based on constant eddy viscosity and bottom slip coefficients, which can reproduce reasonable steady bottom flow behavior of the wind-driven currents over an inner shelf. The values for the eddy viscosity and bottom slip coefficients were empirically determined using historical storms and validation data. The vertical eddy viscosity coefficient is 0.25 ft^2/s, and the bottom slip coefficient is 0.006 ft/s for all storms and in all geographical regions. With a fast-moving storm (>20mph), empirical tests with the SLOSH model generate a storm surge that is insensitive to large changes in bottom stress coefficients (Platzman, 1963; Jelesnianski, 1966; 1970; 1992; Kim & Chen, 1999).

Wind Friction Coefficients

Strong wind friction gives weak winds with strong convergence (large inflow across pressure isobars), whereas weak friction yields strong winds with weak convergence of the wind field. These properties have compensating effects on the surge. Although large frictional changes cause large changes for the absolute surge surface stress or the computed wind speed, these frictional changes do not necessarily mean large changes for the storm surge. The computed surge is only mildly sensitive to the wind friction coefficients (Jelesnianski, et al., 1992). The wind friction coefficients in the tangential direction, k_s, and in the radial direction, k_n, are estimated using the following empirical equation:

$$k_s = 1.15k_n = \alpha\sqrt{\frac{10^{-4}R_{max}}{0.3v_{max}+60}} \tag{7}$$

Where R_{max} is the radius of maximum winds in statute miles; v_{max} is the maximum wind speed in mph for a stationary storm; α is the location parameter ($\alpha = 1$ for ocean winds, $\alpha = 4\sqrt{22/R_{max}}$ for lake winds). The above equation is based on empirical studies of many past hurricanes (Jelesnianski, et al., 1992).

The inland flood hazard model requires the following components to be parameterized:

Manning's Roughness Coefficient

The hydrodynamic model requires an estimate of the Manning's roughness coefficient as per the underlying mass conservation equations presented by (Bates, et al., 2010). This term controls the friction exerted on water flowing over the earth's surface. We apply a spatially varying Manning's friction coefficient that changes based on land cover as defined by (Chow, 1959) or (Arcement, et al., 1989), which are listed in the Table 2. This is then modified in cells that contain buildings as defined by the Microsoft building footprints dataset (Table 3). We do this so that areas within urban regions that do not contain buildings can have lower Manning's roughness coefficients than those containing buildings. In areas of no data we apply a uniform friction coefficient of 0.06, and within the sub-grid channels we apply a uniform friction coefficient of 0.04.

Table 2: Summary of spatially varying Manning's friction coefficients.

NLCD land use code	Definition	Manning's roughness coefficient
11	Open Water	0.04
12	Perennial Ice/Snow	0.04
21	Developed, Open Space	0.04
22	Developed, Low Intensity	0.04
23	Developed, Medium Intensity	0.03
24	Developed, High Intensity	0.03
31	Barren Land (Rock/Sand/Clay)	0.025
41	Deciduous Forest	0.1
42	Evergreen Forest	0.1
43	Mixed Forest	0.1
52	Shrub/Scrub	0.1
71	Grassland/Herbaceous	0.035
81	Pasture/Hay	0.03
82	Cultivated Crops	0.035
90	Woody Wetlands	0.1
95	Emergent Herbaceous Wetlands	0.07
127	Unclassified	0.06

Table 3: Spatially varying Manning's friction coefficients in the presence of buildings.

Building Coverage	Manning's roughness coefficient
>20%-50%	0.06
50%-80%	0.09
80%+	0.12

Channel Bathymetry

The model also requires the bathymetry of the river channel to be estimated. While river bathymetry information is not available over wide areas, it must at least be approximated to enable behavioral simulations of flood events (Fewtrell, et al., 2011). River widths are estimated using the Global River Widths from Landsat (GRWL) database from (Allen & Pavelsky, 2018). Channel bed elevations are then the last remaining variable to be estimated (as rectangular channels are assumed). Bankfull discharge is estimated to be equivalent to a return period of approximately 1 in 2 years (Andreadis, et al., 2013; Harman, et al., 2008). By combining bankfull discharge, channel width, and an estimate of slope calculated from the DEM, it is possible to produce an estimate of channel depth using an innovative channel solver based on the shallow water equations (Neal, et al., 2021). The Manning's equation is used to provide an initial estimate of the channel depth using the bankfull discharge, channel width, and an estimate of the Manning's friction parameter value. These Manning's-based estimates of river bed elevation (Table 2) are provided as initial conditions to a 1D gradually varying flow model that solves for nonuniform flow (Neal, et al., 2021). The solver takes the surface water profile calculated using the initial Manning's bed estimate, calculates the error between the observed bank elevation and the solved water surface elevation, and applies those differences to the Manning's bed elevation estimate to produce a new estimate of bed elevation. This process is repeated twice, allowing the solver to improve its estimate of bed elevation.

Inland Hydrological Model for Event Set Calculation

The Framework for Understanding Structural Errors (FUSE) hydrological model (Clark, et al., 2008) relies on a dozen of adjustable model parameters that control processes such as evaporation, infiltration, snow accumulation and melt, and baseflow generation. The full list of parameters and their default values (which were used here) can be found in (Clark, et al., 2008)'s Table 3. For the FUSE snow module, the parameter ranges are provided in (Clark, et al., 2008)'s Table 1. FUSE parameters are spatially uniform. MizuRoute (Mizukami N. , et al., 2016; Mizukami N. , et al., 2021), a rainfall-runoff routing model, implementation of the kinematic wave tracking, which was used here, relies on two parameters: Manning's friction coefficient, which was set to 0.01, and the river width scale factor (see equation 5 in (Mizukami, et al., 2016), which was set to 0.001. MizuRoute parameter values are the same for all river segments.

Table 4: Adjustable Model Parameters in FUSE model.

Table 3. Adjustable Model Parameters

Parameter	Description	Units	Lower Limit	Upper Limit
$S_{1,max}$	Maximum storage in the upper layer	mm	50.000	5000.000
$S_{2,max}$	Maximum storage in the lower layer	mm	100.000	10000.000
ϕ_{tens}	Fraction total storage as tension storage	-	0.050	0.950
ϕ_{rchr}	Fraction of tension storage in primary zone (upper layer)	-	0.050	0.950
ϕ_{base}	Fraction of free storage in primary reservoir (lower layer)	-	0.050	0.950
r_1	Fraction of roots in the upper layer	-	0.050	0.950
k_u	Percolation rate	mm day^{-1}	0.010	1000.000
c	Percolation exponent	-	1.000	20.000
α	Percolation multiplier for the lower layer	-	1.000	250.000
ψ	Percolation exponent for the lower layer	-	1.000	5.000
κ	Fraction of percolation to tension storage in the lower layer	-	0.050	0.950
k_i	Interflow rate	mm day^{-1}	0.010	1000.000
k_s	Base flow rate	mm day^{-1}	0.001	10000.000
n	Base flow exponent	-	1.000	10.000
v	Base flow depletion rate for single reservoir	d^{-1}	0.001	0.250
v_A	Base flow depletion rate for primary reservoir	d^{-1}	0.001	0.250
v_B	Base flow depletion rate for secondary reservoir	d^{-1}	0.001	0.250
$A_{c,max}$	Maximum saturated area (fraction)	-	0.050	0.950
b	ARNO/VIC "b" exponent	-	0.001	3.000
λ	Mean of the log-transformed topographic index distribution	m	5.000	10.000
χ	Shape parameter defining the topographic index distribution	-	2.000	5.000
μ_τ	Time delay in runoff	days	0.010	5.000

Inland non-TC Synthetic Event Set Model

The parameters within the non-TC synthetic event set model that are considered to be the most important to model outputs are the event definition threshold, the spatio-temporal windows, and the marginal tail threshold specification.

The event threshold and spatio-temporal windows used during the creation of the training data are used in the model to cluster reanalysis timeseries into unique historical events by first finding the local peaks in a timeseries at a given location, then grouping these exceedances into distinct events, using spatio-temporal clustering windows (following (Diederen, et al., 2019). In this work, we used a 1 in 0.5-year exceedance threshold to define an event of interest. The specification of this threshold is notoriously difficult in tail statistics, due to the trade-off between stability and representativeness. Due to the relatively short records (40 years), this threshold was deemed to be a suitable compromise between the two. Previous research has used thresholds of similar magnitudes (e.g. (Quinn, et al., 2019; Li, et al., 2023). Exceedances at local sites are then clustered using algorithms that contain temporal and spatial window parameters. The temporal window is given as 7 days following the research by Allen et al (2018) on the travel times of large rivers to their terminus. The spatial clustering algorithm (DBscan) is applied to the local exceedances that are found within the temporal window in order to extract unique spatial clusters. The spatial parameter within this algorithm is given as 5 decimal degrees, based on preliminary tests and qualitative assessments. The definition of the temporal and spatial parameters (and indeed the determination of what an event is) is highly uncertain, and for this reason, have been the focus of sensitivity testing (see Standard SF-2).

Once the training data has been produced, it is used to define exceedance probability curves at each site. These marginal distributions are fitted with a semi-empirical distribution (empirical below threshold, generalised pareto to the tails above) following previous literature (Heffernan & Tawn, 2004; Quinn, et al., 2019; Wing, et al., 2020). The marginal threshold above which to fit the generalised pareto model is derived following the approaches of (Varty, et al., 2021). The subsequent thresholds required for pairwise dependence characterisation and model event prediction (required by the model framework) use the same threshold as that used in the creation of the marginal distributions, for consistency.

MF-2.2 For coastal and inland flood model components, describe the dependencies among flood model parameters and specify any assumed mathematical dependencies among these parameters.

Impact Forecasting Florida Flood Model – Storm Surge

The dependencies among coastal flood model parameters are:

1. The Rmax is modeled as a random variable which follows a lognormal distribution. The mean of the variable is a function of central pressure deficit and storm eye latitude (Vickery & Wadhera, 2008). The variation relative to the mean is determined from historical data through regression analysis. The historical data is obtained from the HURDAT2 Re-analysis Project (e.g., ., (Landsea, et al., 2004a; Landsea, et al., 2004b; Landsea, et al., 2008; Landsea, et al., 2012; Landsea, et al., 2014; Hagen & Landsea, 2012; Delgado, et al., 2018)), NOAA Technical Report NWS 38 (Ho, et al., 1987), and the Extended Best Track Dataset (Demuth, et al., 2006). The Rmax model can be expressed as follows:

$$\ln(R_{max}) = r_0 + r_1 \Delta P^2 + r_2 \varphi + \varepsilon_R \quad (8)$$

   Where ΔP is the central pressure deficit, computed as the difference between the ambient air pressure and the storm central pressure; φ is the latitude of the storm eye; r_0, r_1, r_2 are the regression coefficients and ε_R is the error term. The modeled Rmax has general agreement with the observation and the effect of uncertainty is properly addressed.

2. The wind friction coefficients are functions of Rmax, Vmax (Maximum sustained wind speed), and the location parameter. The wind friction coefficients in the tangential direction, k_s, and in the radial direction, k_n, are estimated using the following empirical equation:

$$k_s = 1.15 k_n = \alpha \sqrt{\frac{10^{-4} R_{max}}{0.3 v_{max} + 60}} \quad (7)$$

   Where R_{max} is the radius of maximum winds in statute miles; v_{max} is the maximum wind speed in mph for a stationary storm; α is the location parameter ($\alpha = 1$ for ocean winds, $\alpha = 4\sqrt{22/R_{max}}$ for lake winds). The above equation is based on empirical studies of many past hurricanes (Jelesnianski, et al., 1992).

Impact Forecasting Florida Flood Model - Inland Flood

As noted in Standard MF 2.1, bankfull discharge is estimated to be equivalent to a return period of approximately 1 in 2 years (Andreadis, et al., 2013; Harman, et al., 2008)Leopold, 1994). The gauge-based discharge model is utilized to estimate the bankfull discharge for every river cell in the model. This means that the flow estimation methodology that is used for estimating the bed elevation of river channels is the same as the methodology used to estimate extreme river flows that are simulated by the model. Linking channel geometry to discharge return period in this manner ensures that the channels are appropriately sized for the flows being simulated, mitigating the problem of gross mismatches between discharge and channel conveyance.

MF-2.3 For coastal and inland flood model components, describe the dependencies that exist among the flood model components.

The tropical cyclone induced coastal flood and inland flood hazards are modeled from the same tropical cyclone track. If a location is flooded by both inland flood and coastal flood, the losses are calculated separately, and the maximum loss will be used.

MF-2.4 Identify whether physical flood parameters are modeled as random variables, functions, or fixed values for the stochastic flood event generation. Provide rationale for the choice of parameter representations.

Impact Forecasting Florida Flood Model – Storm Surge

The methods to model each flood parameter are described below:

Storm Formation Count and Genesis Parameters

The Markov Chain approach is used to model the entire track of each tropical cyclone (limited to a maximum number of time steps) on a 6-hour time step from initiation to dissipation. The number of tropical cyclones generated each year is modeled using a negative binomial distribution (Vickery, et al., 2000). The genesis location of the tropical cyclone along with its genesis date and time, initial forward speed, heading angle, and central pressure are modeled by random draws from historical genesis data (Vickery, et al., 2000; 2009c). If central pressure data is not available, a regression equation is used to estimate a central pressure value from maximum sustained wind speed and latitude. The tropical cyclone parameters at subsequent time steps are determined using regression models.

Translational/Forward Speed and Heading Angle/Direction

The tropical cyclone translational speed and heading angle at every 6-hour time step are modeled as separate regression models, using the forward speed, heading direction, latitude, and longitude from up to two previous time steps as predictors. The regression coefficients are derived for different 5x5-degree cells across the North Atlantic Ocean. The regression model with the corresponding set of coefficients is used when a storm moves into a given cell. The residuals from the regression are modeled as a normal distribution in each cell to address the randomness of storm movement.

Central Pressure

Central pressure is modeled in the form of relative intensity (Darling, 1991) using a multiple linear regression model. For each time step, the central pressure in a given 5x5-degree cell is modeled as a function of the relative intensities from the previous three time steps, the current sea surface temperature, and the previous sea surface temperature (Vickery, et al., 2000; Rayner, et al., 2003). A random error term which follows a normal distribution is used to model the residuals that result from the regression. Relative intensity values are taken between 0 and 1 to constrain the minimum central pressures a storm can physically reach under certain environmental conditions.

Radius of Maximum Winds

Radius of maximum winds is an important parameter that describes the size of a tropical cyclone. It is modeled as a random variable which follows a lognormal distribution. The mean of the variable is described as a function of central pressure deficit and latitude (Vickery, et al., 2000). The variation relative to the mean is determined from historical data through regression analysis. The historical data is obtained from the HURDAT2 Re-analysis Project (e.g., ., (Landsea, et al., 2004a; Landsea, et al., 2004b; Landsea, et al., 2008; Landsea, et al., 2012; Landsea, et al., 2014; Hagen & Landsea, 2012; Delgado, et al., 2018)), NOAA Technical Report NWS 38 (Ho, et al., 1987), and the Extended Best Track Dataset (Demuth, et al., 2006).

Surface Drag Coefficient

A constant surface drag coefficient $C_D \cdot \rho_a/\rho = 3 \times 10^{-6}\, ft^2/sec^2$ is used to calculate surface stress in SLOSH (Jelesnianski, 1972; Jelesnianski, et al., 1992). The constant drag coefficient is presently used to forecast or hindcast surges generated by all tropical storms in all basins.

Vertical Eddy Viscosity Coefficient & Bottom Slip Coefficient

The SLOSH model is based on constant eddy viscosity and bottom slip coefficients, which can reproduce reasonable steady bottom flow behavior of the wind-driven currents over an inner shelf. The values for the eddy viscosity and bottom slip coefficients were empirically determined using historical storms and validation data. The vertical eddy viscosity coefficient is 0.25 ft^2/s, and the bottom slip coefficient is 0.006 ft/s for all storms and in all geographical regions (Jelesnianski, et al., 1992).

Wind Friction Coefficients

The wind friction coefficients in the tangential direction, k_s, and in the radial direction, k_n, are estimated using the following empirical equation:

$$k_s = 1.15k_n = \alpha\sqrt{\frac{10^{-4}R_{max}}{0.3v_{max}+60}} \tag{7}$$

Where R_{max} is the radius of maximum winds in statute miles; v_{max} is the maximum wind speed in mph for a stationary storm; α is the location parameter ($\alpha = 1$ for ocean winds, $\alpha = 4\sqrt{22/R_{max}}$ for lake winds). The above equation is based on empirical studies of many past hurricanes (Jelesnianski, et al., 1992).

Impact Forecasting Florida Flood Model - Inland Flood

Manning's Roughness Coefficient

The Manning's roughness coefficient varies in space as per Disclosure MF-2.1 but is fixed both during and between events.

Channel Bathymetry

The channel bathymetry varies in space as per Disclosure MF-2.1 but is fixed both during and between events.

Inland non-TC Synthetic Event Set Model

Within the non-TC synthetic event set model, the event definition threshold, the spatio-temporal window parameters and the generalized pareto distribution fitting threshold used in the marginal distributions creation are fixed values defined by the modelers. These parameters are described in detail in Disclosure MF- 2.1.

MF-2.5 Describe if and how any physical flood parameters are treated differently in the historical and stochastic flood event sets, and provide rationale.

Physical flood parameters are not treated differently for the historical and stochastic flood event sets.

MF-2.6 If there is explicit modeling of precipitation-driven flooding, then describe how rainfall extent, duration, and rate are modeled. If the effects of precipitation are implicitly incorporated into the flood model, describe the method and implementation.

Precipitation is explicitly modeled in the Impact Forecasting US Inland Flood model, utilizing a physics-based Tropical Cyclone Rainfall (TCR) model developed by (Lu, et al., 2018) and (Feldmann, et al., 2019). You can find detailed information about the model in studies by (Lu, et al., 2018) and (Feldmann, et al., 2019). This model computes rain rates and accumulated rainfall at specified Points of Interest (POI), defined as any 0.1°×0.1° grid point in the continental United States.

The TCR model estimates rainfall by multiplying the saturation specific humidity and vertical velocity, derived from the time-evolving storm wind field and environmental winds. The TCR encompasses five physical mechanisms including topographic forcing, frictional convergence, vortex stretching, baroclinic effect, and radiative cooling to generate rainfall. The total vertical velocity is computed as the sum of the vertical velocities from these components, and the vertical vapor flux is determined by multiplying the total vertical velocity with the specific humidity.

Rain rate is then calculated by multiplying the vertical vapor flux by the assumed precipitation efficiency of 0.9. Consequently, the hourly rain rate is computed for each point of interest throughout the entire lifetime of the track.

Precipitation is explicitly modeled within the pluvial inland model simulations. Precipitation intensity for each model simulation is taken from Intensity Duration Frequency (IDF) functions defining the intensity and duration of event rainfall (and which are used to force the hydraulic model using a rain-on-grid approach), taken from the NOAA Atlas 14 precipitation frequency estimates (available at https://hdsc.nws.noaa.gov/hdsc/pfds/). To summarize, these maps are created using a regional frequency analysis approach based on L-moment statistics derived from annual maxima time series observations.

For the pluvial model, rainfall is simulated directly onto the DEM grid. Sub-grid channels are included in the model and are present for river channels with an upstream catchment area of 19.03 sq mi (50 sq km) or greater to allow rainfall to be routed through the river network. Pluvial simulations are undertaken for one-, six-, and 24-hour rainfall durations. Rainfall intensity is applied uniformly in time but is spatially variable depending on assumptions on infiltration and urban drainage, the effects of which are applied to the pluvial boundary conditions rather than modeled explicitly within the hydraulic model.

Infiltration is calculated based on a modified Horton equation (Morin & Benyamini, 1977) and varies depending on soil type as defined by the US Soil Survey Geographic Database (SSURGO) (Soil Survey Staff, 2021). An assessment of the likely standard of protection

provided by the drainage system is made by first estimating the likely standard of protection based on how urbanized a location is. We use the National Land Cover Dataset (NLCD, 2019) (Dewitz, 2021) to determine the degree to which areas are built up and classify regions into rural and urban (see Table 5). We then assign a 10-year drainage standard to urban locations. The rainfall associated with that standard of protection is then subtracted from the baseline rainfall intensity for the scenario modeled for those locations. These approaches result in a spatially variable rainfall grid, reflective of the underlying soil type and assessments of urban drainage standards.

Table 5: NLCD classification and subsequent drainage defense standard.

NLCD Classification	Fathom Classification	Drainage Defense Standard
21 - Developed, Open Space 22 - Developed, Low Intensity 23 - Developed, Medium Intensity 24 - Developed High Intensity	Urban	1-in-10 year RP
Other	Rural	Soil infiltration only

MF-2.7 For coastal flood analyses, describe how the coastline is segmented (or partitioned) in determining the parameters for flood frequency used in the flood model.

The coastline is neither segmented nor partitioned in determining any parameters for coastal flood frequency; rather, coastal segmentation is used to validate the modeled tropical cyclone landfall rate with the corresponding historical landfall rate. The modeled and measured annual landfall occurrence rates for Florida coastal segments are shown in Figure 5. The coastal segments of Florida used for calculating annual occurrence rates are shown in Figure 6.

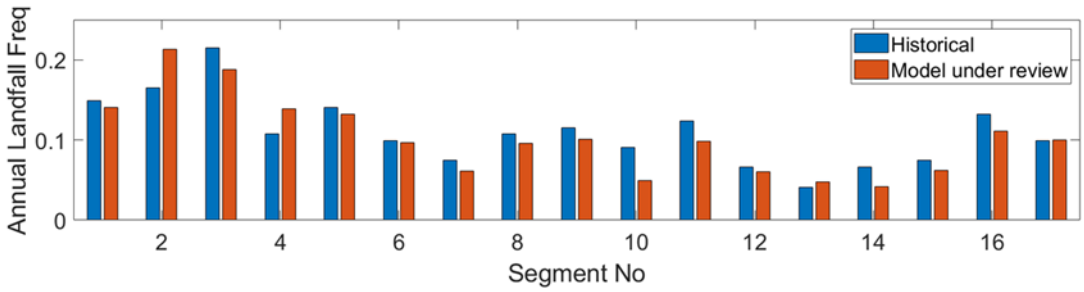

Figure 5: Comparisons between modeled and measured annual landfall occurrence rates for Florida coastal segments.

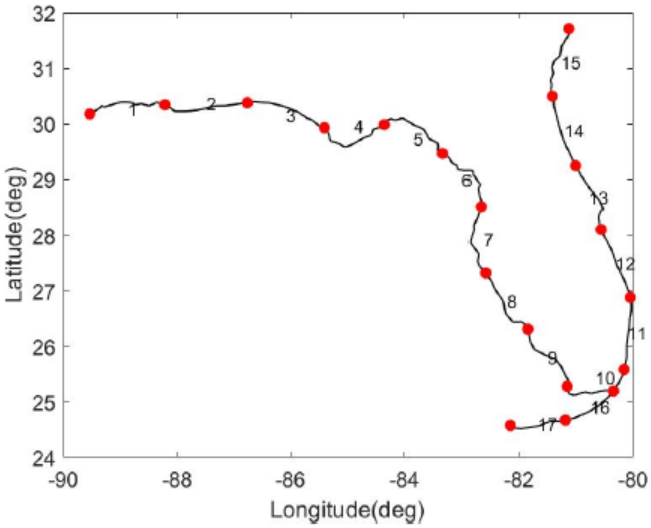

Figure 6: Coastal segments of Florida used for calculating annual occurrence rates.

MF-2.8 *For coastal flooding, describe how astronomical tides are incorporated and combined with storm surge to obtain storm tide.*

The SLOSH model incorporates the tides dynamically at every time step and at every SLOSH model grid point. The location dependent amplitudes and phases of the tidal constituents are extracted at every SLOSH grid cell from ADCIRCS's EC-2014 tidal database. This includes 37 constituents along the Atlantic and Gulf Coasts of the United States (Forbes, et al., 2014). The tide equation is then used to calculate a tide water level at each time step (Schureman, 1958).

The process of combining and advancing tides and surges can be explained below (Liu, et al., 2018):

1. Initialize with tide at time = t_0
2. SLOSH moves tide and surge to time = t_1
3. Subtract tide at time = t_{n-1} and add tide at time = t_n, for $n \geq 1$
4. Repeat steps 2 and 3.

But this process of adding and subtracting tide at every grid cell at every time step can be chaotic when dealing with cells that wet and dry. To deal with this issue, the adding and subtracting is done only for certain bathymetric depths, from the deep ocean to a specified depth. Testing and analysis of various threshold depths has determined optimum settings for each SLOSH basin. Shallower than this value, the surge model is left alone.

MF-2.9 *Describe if and how any flood parameters change or evolve during an individual flood life cycle (e.g., astronomical tide, representation of Manning's roughness varying with flood depth).*

During an individual coastal flood life cycle, several parameters driving storm surge would change. Firstly, the central pressure varies at each time step, usually increasing as the storm approaches inland. Secondly, Rmax also changes as a function of central pressure deficit and latitude (Vickery & Wadhera, 2008). Thirdly, the storm heading direction and centroid location also change as the storm moves from ocean to land. Fourthly, the wind friction coefficients also vary at each time step since they are a function of Rmax, Vmax,

and the location parameter (ocean/land). Lastly, the tidal amplitude also varies by location and time step, as described in Disclosure MF-2.8.

For inland flood, flow and precipitation increase to a peak, which is used to determine what the maximum return period of the hazard is for the individual pluvial or fluvial area of analysis.

MF-2.10 For coastal modeling, describe any wave assumptions, calculations or proxies and their impact on flood elevations.

Wave in the Impact Forecasting Florida Flood Model - Storm Surge is addressed in vulnerability functions and is assumed to be a function of the inundation depth. Detailed descriptions can be found in Disclosure VF-1.7.

MF-2.11 Provide the source, resolution, datum, and accuracy of the topography and bathymetry throughout the flood model domain.

Impact Forecasting Florida Flood Model – Storm Surge

A SLOSH basin consists of a grid definition, as well as various geographic features such as height/depth, trees, barriers, etc. used to control route, and impede the flow of water as the hurricane impacts the area (Conver, et al., 2008). These basins are currently updated at the rate of 3-6 basins per year. The updates are driven by several factors such as: changes to bathymetry or topography due to a landfalling hurricane, availability of new data, changes to coastline, and addition of flood protection structures like levees (NOAA, 2023c). The basin grid is set up to give fine resolution in the primary area of interest, and coarse resolution in the boundary region.

The vertical datum employed in the SLOSH basins is NAVD88 and the horizontal datum is NAD83. The basins are defined using topographic and bathymetric data that are averaged across each grid cell.

The USGS National Elevation Dataset (NED) is the primary source of elevation data (values above 0ft) for the SLOSH basins. NED data are available nationally in the US at resolutions of 1/9 arc-second (three-meter), 1/3 arc-second (ten-meter) and 1 arc-second (30-meter). The relative vertical accuracy of this dataset is 0.81 m (Gesch, et al., 2014). The 1 arc-second and 1/3 arcsecond data are compared for each basin, and when the differences are negligible, the 1 arc-second dataset is used to reduce the basin size. The NED is replaced when higher resolution, better quality datasets are found (Conver, et al., 2008). For elevations less than 0ft, the National Geophysical Data Center (NGDC) bathymetric data provides a comprehensive relief dataset at a resolution of 3 arc-second. The dataset extends well into the oceans, serving bathymetric data needs well. Some of the other sources of data include Tsunami datasets, LiDAR datasets (high resolution topographic data especially for shoreline areas), National Land Cover Dataset (NLCD) (for the basin trees layer that informs the model of increased friction at the momentum points), the National Geographic Digital Raster Graphics (DRGs) (shows contours, roads, rivers, etc) (Conver, et al., 2008).

The modeled water heights from SLOSH are mapped to IF grid with 0.0025-degree resolution (equivalent to about 250 m). The 250 m resolution was determined based on the smallest SLOSH basin grid for majority of the basins. The IF grid system is defined on a Cartesian coordinate system over the following region: from Longitude -162E degrees to

Longitude -64E degrees, and from Latitude 17N degrees to Latitude 50N degrees. This predefined grid methodology allows for easy data retrieval.

Impact Forecasting Florida Flood Model – Inland Flood

To use the best possible terrain information to represent the flow of water over floodplains in Florida, as there is not 100% coverage by LiDAR, Fathom have developed a new state of the art DEM for our flood maps, FABDEM+ v1.1.1. (Forest And Buildings removed Copernicus DEM). This is a merged version of FABDEM v1.1.0 (Hawker, et al., 2022; Hawker & Neal, 2021) with high quality LiDAR datasets.

Each dataset was re-gridded to a 1 arcsecond horizontal grid and converted to the EGM08 vertical datum. Blending was applied at edges of LiDAR data and FABDEM to prevent discontinuities.

FABDEM

FABDEM (Forests and Buildings removed Copernicus Digital Elevation Model) (Hawker, et al., 2022) is a digital terrain model based on the Copernicus GLO-30 digital elevation model (AIRBUS, 2020, henceforth Copernicus DEM). Copernicus DEM is a state-of-the-art satellite derived terrain dataset which dramatically improves the representation of terrain compared to datasets based on the older Shuttle Radar Topography Mission (SRTM) dataset. FABDEM uses a machine learning model to remove artifacts due to buildings and forests and obtain a bare earth model suitable for large scale flood modeling.

To correct the Copernicus DEM, a machine learning algorithm, random forest regression, was chosen to determine the height anomaly due to buildings and vegetation. As different predictor variables are applicable to estimate the heights of buildings and forests, different machine learning models were developed for each case. Forest predictor variables include forest heights and tree cover fraction, while building predictor variables include building footprints, population density, night lights, travel times to major cities, and gross domestic product per urban area. In addition to these predictor variables, image filters were applied to the Copernicus DEM and the forest heights dataset and used as predictor variables to supply information about the surrounding terrain. A full list of predictor variables is given in Hawker et al. (Hawker, et al., 2022).

Table 6: Predictor variables is given in Hawker et al. (Hawker, et al., 2022).

Table S1. Predictors for random forest models. The 'Model' column specifies which random forest model each predictor applies to: 'Forests' refers to forest corrections below 52°N, 'Boreal Forests' refers to forest corrections above 52°N, and 'Global Forests' refers to both forest models. Note, multiple predictor variables from the same dataset are separated by bullets. Unless specified otherwise, nearest neighbor resampling to COPDEM30 grid was used.

Dataset	Version	Grid Spacing (arc seconds)	Additional Information	Model	Ref.
Forest Heights	2019	1		Forests	[6]
Forest Heights Image filters	2019	1	• Sobel 3x3 • Diff of Gaussian $\sigma_1 = 0.5, \sigma_2 = 1$ • Diff of Gaussian $\sigma_1 = 1, \sigma_2 = 2$ • Diff of Gaussian $\sigma_1 = 2, \sigma_2 = 4$ • Gaussian $\sigma = 3$ • Gaussian $\sigma = 5$ • Bilateral $\sigma_{dist} = 5, \sigma_{int} = 5$ • Unsharp Masking $\sigma = 3$	Forests	[6]
Land Cover 100m – Tree Cover	3.0.1	3		Global Forests	[20]
ICESAT2 canopy heights	4	point data	• h_canopy • h_mean_canopy Inverse-distance weighted interpolation to COPDEM30 grid	Boreal forests	[21]
Travel Times	-	30	• Time to nearest city of 5–50 million people. Log transformed • Time to nearest city of 1–5 million people. Log transformed • Time to nearest city of 0.5–1 million people. Log transformed	Urban	[12]
Night Lights	2016	15		Urban	[22]
WorldPop Constrained	2020	3	Log transformed	Urban	[11]
GHS Urban Centre Database 2019A	1.2	30	• Built-up area per capita (BUCAP15) • Average greenness in the built-up area (E_GR_AV14) • Gross Domestic Product for 2015 divided by urban area and log transformed	Urban	[18]
World Settlement Footprint	2015	0.32	Fraction of COPDEM30 grid cell containing building footprint	Urban	[17]
Copernicus DEM (COPDEM30) Image filters	2020_2	1	• Sobel 3x3 • Diff of Gaussian $\sigma_1 = 0.5, \sigma_2 = 1$ • Diff of Gaussian $\sigma_1 = 1, \sigma_2 = 2$ • Diff of Gaussian $\sigma_1 = 2, \sigma_2 = 4$ • Unsharp Masking $\sigma = 1.5$ • Unsharp Masking $\sigma = 3$	• All • All • All • Global Forests • Urban • All	[1]

A key differentiator between FABDEM and other global DEMs is the 'ground truth' data used to train the machine learning models. High quality local DEMs from 12 countries around the world covering a wide range of climatic zones and urban areas were used. This enables the machine learning models to be applicable at a global scale.

To produce FABDEM, the anomalies due to forests and buildings were estimated by the machine learning models and subtracted from the Copernicus DEM separately. Then, these corrected DEMs were merged, and final post-processing steps were applied to remove artifacts from the DEM. This is shown in schematic form in Figure 7.

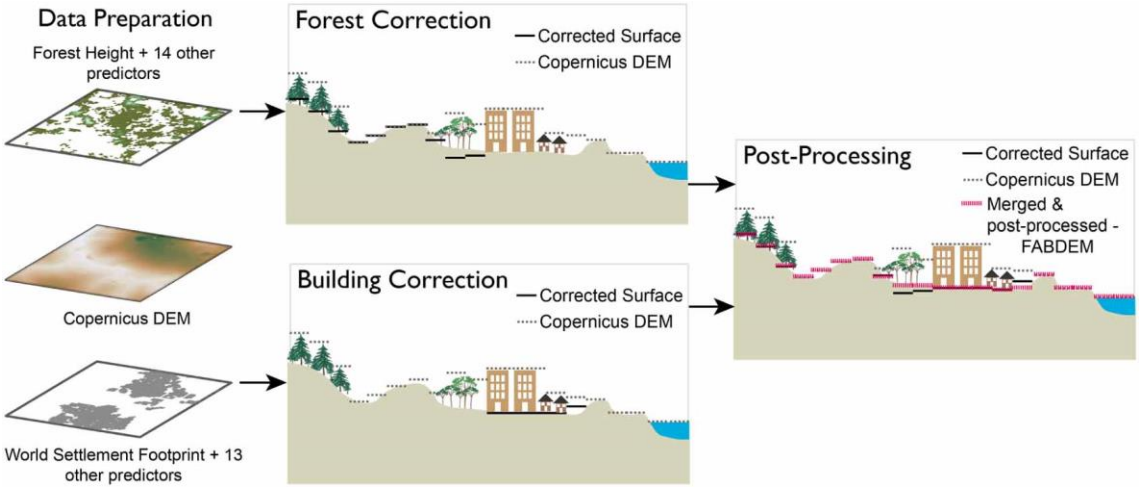

Figure 7: FABDEM methodology. 1. Processing predictor data and training data (LiDAR DEMs). 2. Applying these to a machine learning model to correct forests and building artifacts. 3. Merging and post-processing elevations from machine learning model.

FABDEM has been validated in (Hawker, et al., 2022) and performs favorably against other global DEMs. Visual inspections also show a finer and clearer depiction of floodplains when compared, for example, to the MERIT DEM (which was used in Fathom's previous global flood maps).

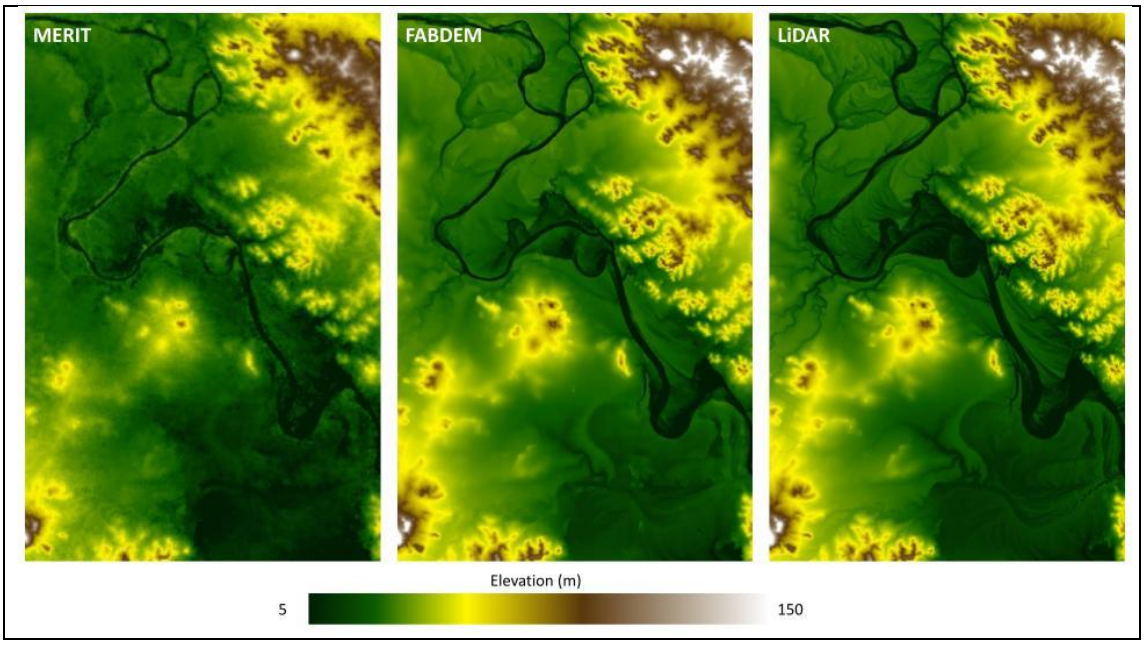

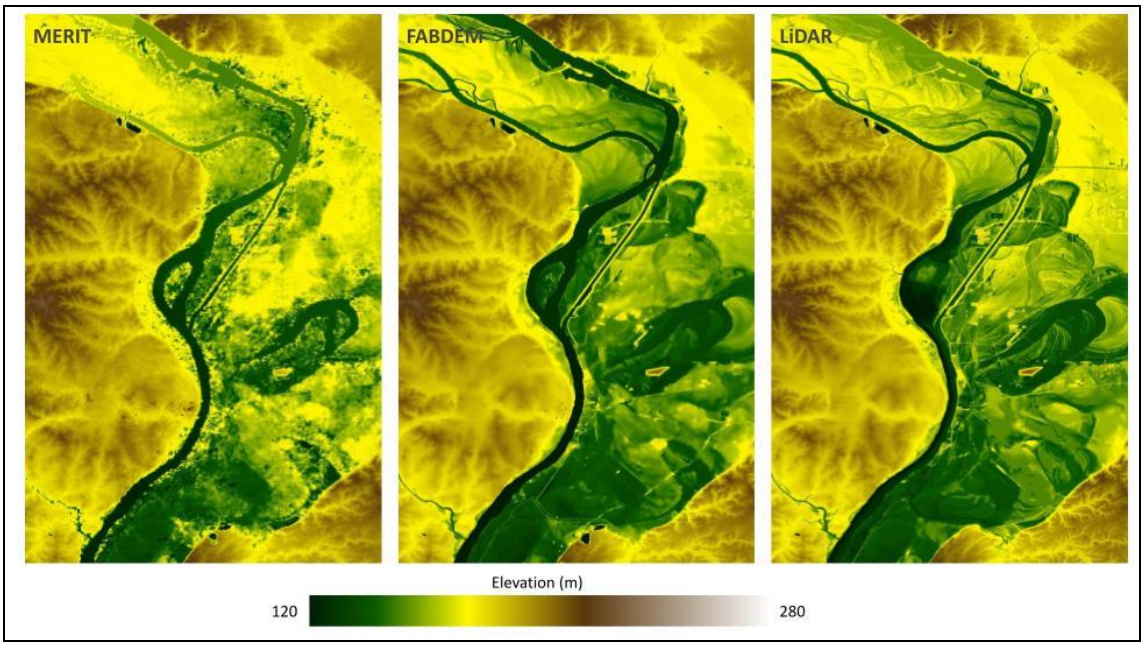

Figure 8: Comparison of FABDEM with MERIT DEM, and a high-quality local LiDAR DEM. Upper panels show Rockhampton, Australia, and Lower panels show St Louis, USA.

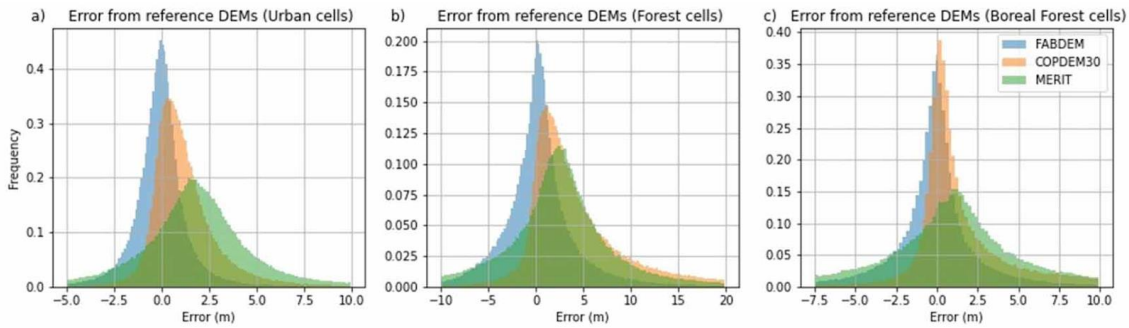

Figure 9: Histograms comparing FABDEM with COPDEM30 and MERIT DEM against reference data (reproduced from (Hawker, et al., 2022)).

LiDAR datasets

LiDAR is an acronym for Light Detection And Ranging. It describes a method which measures the time between an instrument emitting a laser and it receiving the return signal after bouncing off surface objects, from which distance can be derived accurately. This remote sensing technique, commonly using airborne sensors, produces accurate three-dimensional models of surface topography in a point cloud format. When converted to a gridded format, these provide a higher resolution and accuracy terrain dataset than the satellite-radar-based FABDEM, with LiDAR datasets' native resolution commonly resting between 0.25-5m, compared to ~30m (one arcsecond) for FABDEM, and vertical accuracy being off on the order of centimeters rather than meters. Accordingly, where LiDAR datasets exist these have been blended into FABDEM using a distance weighted blending methodology described below.

LiDAR Pre-processing

To allow integration into FABDEM, these datasets are converted to the horizontal projection EPSG:4326 and the vertical datum EGM08. As part of the vertical conversion, datasets are corrected for both differences in the underlying ellipsoid and the underlying geoid. Geoid correction follows A-B+C with A referring to the dataset in question, B EGM08, and C to the dataset's local geoid. Ellipsoid correction was applied by finding the difference between the local geoids ellipsoid and EGM08s ellipsoid and applying this to the local geoid. Datasets were resampled from their native resolution to 1 arcsecond.

Blending methodology

To combine LiDAR data with FABDEM, a blending algorithm using a distance-based weighting has been utilized. This is applied pixel-wise and blends across 10 pixels and applies distance weighting. For example, assuming LiDAR is being blended with FABDEM, a pixel that is two cells away from the edge of the LiDAR data will be assigned a LiDAR weighting of 2/10 and a FABDEM weighting of 8/10. These weighted values are combined to create the final elevation, producing a smooth blend.

In some areas there will be multiple overlapping datasets of varying quality and date of origin. To ensure that the best quality datasets are given precedence in FABDEM+, we use a hierarchical ordering system. Here data quality is given priority, with LiDAR rated above FABDEM. Where data type is the same, date of origin is the deciding factor, with more recent datasets being given precedence.

MF-2.12 Describe the grid geometry used in the coastal flood model.

The US Atlantic and Gulf of Mexico coasts are divided into 28 regions or basins. Out of these, 14 are in Florida. The basins are centered upon particularly susceptible features like inlets, large coastal centers of populations, low-lying topography, and ports. Each of the basins contains information on topography/bathymetry and terrain descriptions (heights referenced to the vertical datum, NAVD88) for each of the cells in the basin grid. A basin can be a polar, elliptical, or hyperbolic grid and is centered on the area of interest. The spatial coverage for each SLOSH basin varies from an area the size of a few counties to a few states. The grid is set up to give fine resolution in the primary area of interest, and coarse resolution in the deep-water or boundary region. The resolution of individual grid cells within each basin ranges from tens to hundreds of meters to a kilometer or more (Conver, et al., 2008). One example is the Florida Bay Basin (eke2) - Figure 10. This basin is an elliptical grid and covers the South Florida region including the Florida Keys. The resolution varies from 300 m near Marko Island on the west boundary, to 700 m on the east boundary near Miami to 2700 m on the ocean boundary on the south. The grid spacing near Key West is 1700 m. Table 7 shows the details of the Florida basins.

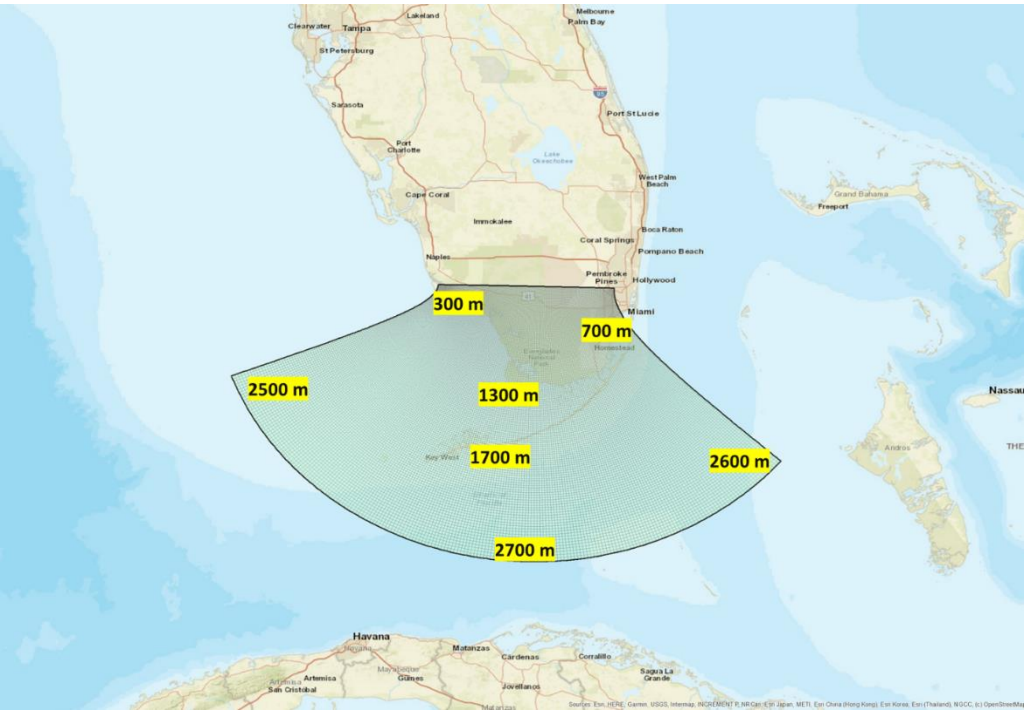

Figure 10: Geometry of the Florida Bay (eke2) SLOSH basin.

Table 7: SLOSH Basins for the Florida Region.

Basin Name	Domain Description	Dimension	Highest Resolution in FL (m)	Time step (s)
epn3	Pensacola Bay	200 x 330	300	3
hpa2	Panama City	105 x 118	300	8
ap3	Apalachicola Bay	141 x 225	300	10
esv4	Savannah / Hilton Head	152 x 200	1400	15
cd2	Cedar Key	157 x 169	500	20
ejx3	Jacksonville	333 x 381	50	8
etp3	Tampa Bay	188 x 215	200	8
co2	Cape Canaveral	69 x 89	500	8
pb3	Palm Beach	71 x 173	1200	8
efm2	Fort Myers	111 x 100	50	15
eok3	Lake Okeechobee	129 x 136	600	45
eke2	Florida Bay	170 x 200	300	6
hmi3	Biscayne Bay	125 x 190	200	4
hms8	New Orleans	655 x 852	400	6

MF-2.13 Describe if and how flood model parameters are based on or depend on National Flood Insurance Program (NFIP) Flood Insurance Rate Maps (FIRM) or other Flood Insurance Study (FIS) data.

The Impact Forecasting Florida Flood Model hazard parameters are not based on or dependent on NFIP FIRM or other FIS data. The vulnerability functions are distinguished between pre-FIRM effective year and post-FIRM effective year. The vulnerability tiers are designed based on FEMA zones.

MF-3 Wind and Pressure Fields for Storm Surge

A. *Modeling of wind and pressure fields shall be employed to drive storm surge models due to tropical cyclones.*

The storm surge portion of the Impact Forecasting Florida Flood Model employed the modeling of wind and pressure fields to drive storm surge due to tropical cyclones. Detailed descriptions of the wind and pressure field models and the choice of parameter forms can be found in Disclosure MF-3.1.

B. *The wind and pressure fields shall be based on current scientific and technical literature or developed using scientifically defensible methods.*

The SLOSH wind and pressure fields are based on scientifically defensible methods described in (Myers, et al., 1961) & (Jelesnianski, et al., 1992).

C. *Physically-based simulation of atmosphere-ocean interactions resulting in storm surge shall be conducted over a sufficiently large domain that storm surge height has converged.*

The storm surge portion of the Impact Forecasting Florida Flood Model is based on SLOSH model. The SLOSH modeling domain covers the entire U.S. Atlantic and Gulf of Mexico coastlines to ensure storm surge height convergence. In addition, coverage extends to Hawaii, Puerto Rico, Virgin Islands, and the Bahamas. SLOSH basins are being updated at an average rate of 3-6 basins per year governed by the Interagency Coordinating Committee on Hurricanes (ICCOH), a tri-agency supported by the U.S. Army Corps of Engineers (USACE), Federal Emergency Management Agency (FEMA), and the National Oceanic and Atmospheric Administration (NOAA). Updates include higher grid size resolution to improve surge representation, increasing area covered by hypothetical tracks for improved accuracy, and the latest topography or bathymetric data for better representation of barriers, gaps, passes, and other local features (NOAA, 2023c).

D. *The features of modeled wind and pressure fields shall be consistent with those of historical storms affecting Florida.*

The modeled wind and pressure fields are consistent with those of historical storms affecting Florida. Descriptions of the wind and pressure fields can be found in Disclosure MF-3.1 and MF-3.3.

Disclosures

MF-3.1 Describe the modeling of the wind and pressure fields for tropical cyclones. State and justify the choice of the parametric forms and the parameter values.

The initial location of the tropical cyclone along with its genesis date and time, initial forward speed, heading angle, and central pressure are modeled by random draws from historical genesis data using the HURDAT2 database (Vickery, et al., 2000; 2009c). If central pressure data is not available, a regression equation is used to estimate a central pressure value from maximum sustained wind speed and latitude. The Markov Chain approach is used to model the entire track of each tropical cyclone (limited to a maximum number of time steps) on a 6-hour time step from initiation to dissipation.

Rmax is modeled as a random variable which follows a lognormal distribution. The mean of the variable is described as a function of central pressure deficit and latitude (Vickery & Wadhera, 2008). The variation relative to the mean is determined from historical data through regression analysis. The historical data is obtained from the HURDAT2 Re-analysis Project (e.g., (Landsea, et al., 2004a; Landsea, et al., 2004b; Landsea, et al., 2008;

Landsea, et al., 2012; Landsea, et al., 2014; Hagen & Landsea, 2012; Delgado, et al., 2018)), NOAA Technical Report NWS 38 (Ho, et al., 1987), and the Extended Best Track Dataset (Demuth, et al., 2006).

Central pressure is modeled in the form of relative intensity (Darling, 1991) using a multiple linear regression model. For each time step, the central pressure in a given 5x5-degree cell is modeled as a function of the relative intensities from the previous three time steps and the current and previous sea surface temperatures (Vickery, et al., 2000; Rayner, et al., 2003). A random error term which follows a normal distribution is used to model the residuals that result from the regression. Relative intensity values are taken between 0 and 1 to constrain the minimum central pressures a storm can physically reach under certain environmental conditions.

SLOSH uses a parametric wind field model based on the balance of forces along and normal to the surface wind trajectory (Myers, et al., 1961; Jelesnianski, et al., 1992);

$$\frac{1}{\rho_a}\frac{dp}{dr} = \frac{k_s v^2}{\sin\phi} - v\frac{dv}{dr} \tag{1}$$

$$\frac{1}{\rho_a}\frac{dp}{dr}\cos\phi = fv + \frac{v^2}{r}\cos\phi - v^2\frac{d\phi}{dr}\sin\phi + k_n v^2 \tag{2}$$

where $p(r)$ is the pressure field; $\phi(r)$ is the inflow angle field across circular isobars towards the storm center; k_s and k_n are the wind friction coefficients in the tangential direction and radial direction, respectively; f is the Coriolis parameter; ρ_a is density of air; and $v(r)$ is the wind speed field described as follows:

$$v(r) = v_{max}\frac{2R_{max}r}{R_{max}^2+r^2} \tag{3}$$

where v_{max} is the maximum 1-minute sustained wind speed within the field. The aforementioned friction coefficients, k_s and k_n, are estimated using the following empirical equation:

$$k_s = 1.15k_n = \alpha\sqrt{\frac{10^{-4}R_{max}}{0.3v_{max}+60}} \tag{4}$$

where α is the location parameter ($\alpha = 1$ for ocean winds, $\alpha = 4\sqrt{22/R_{max}}$ for lake winds).

To solve these equations, an iteration procedure is used. v_{max} is approximated (using a table look-up procedure from pre-computations) and Eqs. (1) ~ (2) are then solved for $p(r)$ and $\phi(r)$. The discrepancy between computed and required pressure is then obviated by changing v_{max} until the pressure discrepancy is less than a preassigned value.

MF-3.2 Provide the historical data used to estimate parameters and to develop stochastic storm sets.

The tropical cyclone event set is developed using the following datasets:

- Base Hurricane Storm Set from the official HURDAT2 database (Landsea & Franklin, 2013)
- Hadley Centre Sea Ice and Sea Surface Temperature Dataset (HadISST) (Rayner, et al., 2003)

MF-3.3 ***Provide a tangential (y-axis) versus radial (x-axis) plot of the average or default wind and pressure fields for tropical cyclones used in the flood model, and justify the choice of the wind and pressure fields used. Provide such plots for non-tropical cyclones, if non-tropical cyclones are modeled explicitly. If the wind and pressure fields represent a modification from the currently accepted flood model, plot the previous and modified wind and pressure fields on the same figure using consistent axes. Describe variations between the previous and modified wind and pressure fields with references to historical tropical cyclones.***

SLOSH uses a symmetric wind field about the storm's center with maximum wind Vmax at distance Rmax from the center (Myers, et al., 1961; Schloemer & Section, 1954; Jelesnianski, 1966; Jelesnianski, et al., 1973). The SLOSH wind speed profile for a stationary storm is described in Eq. (3). Figure 11 below shows a non-dimensional wind field profile of a stationary storm.

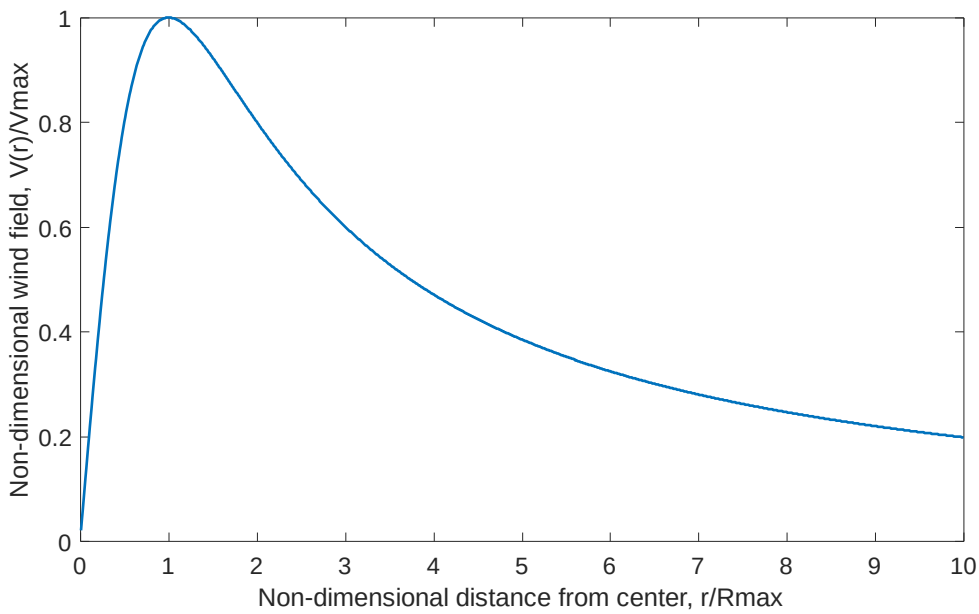

Figure 11: Non-dimensional wind field profile.

In SLOSH, the pressure field is assumed to be symmetrical with respect to the geometric center; the general relation for pressure is given in Eq. (4) (Myers, et al., 1961; Schloemer & Section, 1954):

$$\frac{p(r)-p_0}{p_\infty-p_0} = e^{-\frac{Rmax}{r}} \tag{9}$$

where r is the distance from hurricane center; Rmax is the radius of the maximum wind; p_0 is the central pressure; and p_∞ is the ambient air pressure surrounding the storm.

The radial pressure field profile is shown in Figure 12.

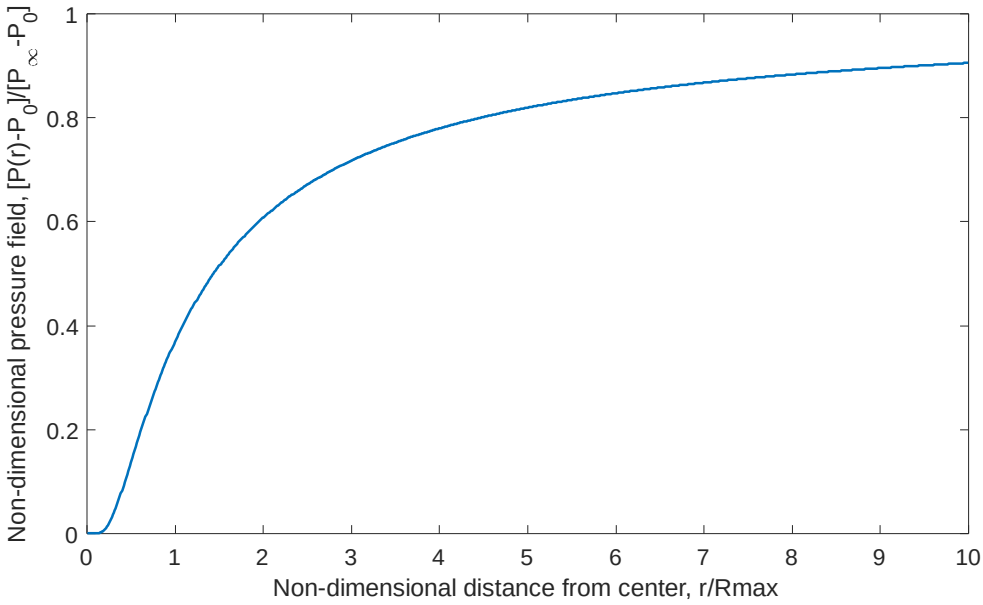

Figure 12: The non-dimensional pressure field profile.

The SLOSH wind model was not designed to accurately forecast surface winds, but to form a vector field of driving forces to generate storm surge. It was developed by the National Weather Service (NWS) of the National Oceanic and Atmospheric Administration (NOAA) in the early 1980s to delineate evacuation zones with high computational efficiency. It is still the operational storm surge model of the National Hurricane Center (NHC). Over the years, it was selected as a benchmark model for the evaluation of many other storm surge models because it is the only model in the United States that has been verified extensively against field observations for overland flooding along the East and Gulf coasts ((Mayo & Lin, 2019; Zhang, et al., 2008) investigated the potential to improve surge modeling accuracy through modification of the wind field representation. The surface background wind field, the parametric wind profile, and the maximum wind speed were modified based on empirical, physical, and observational data. The study found that the modifications to the surface background wind field and the parametric wind profile have minor impacts; however, the effect of the modification to maximum wind speed is significant—it increases the variance in the SLOSH model estimates of maximum storm surges but improves its accuracy overall. Thus, comparing to having a more accurate wind field model, the study recommended to use more accurate input parameters (e.g., observed Rmax) to increase surge modeling accuracy.

Non-tropical cyclone induced storm surges are not modeled. This is the first submission of the Impact Forecasting Florida Flood Model, so there is no comparison to be made to a prior version.

MF-3.4 ***If wind and pressure fields are modeled above the surface and translated to the surface to drive storm surge, then describe this translation; e.g., via planetary boundary layer models or empirical surface wind reduction factors and inflow angles. Discuss the associated uncertainties.***

SLOSH models surface wind and pressure fields, thus no translation is needed.

MF-3.5 If applicable, describe how the inverse barometer effect is modeled.

When low pressure systems move over a region, it creates a reduction in the vertical force acting on a column of water beneath the sea surface, causing the sea level to rise. High pressure systems, on the other hand, push down on the ocean, creating a drop in sea level. This is called the inverse barometer effect, as the higher the pressure, the lower the sea level, and vice versa. One can expect around 1 cm of water rise for each millibar of pressure drop in deep water (Anthes, 1982). The inverse barometer effect usually contributes from 10 to 15 percent of the magnitude of the storm surge (World Meteorological Organization, 2011). SLOSH accounts for this by including a hydrostatic height from pressure field (inverse barometric height from atmospheric pressure), h_0, term in the momentum equations (Jelesnianski, et al., 1992) as shown below. In deep waters, the storm's hydrostatic height is set at the height points of boundary squares.

$$\frac{\partial U}{\partial t} = -g(D+h)\left[B_r \frac{\partial(h-h_0)}{\partial x} - B_i \frac{\partial(h-h_0)}{\partial y}\right] + f(A_r V + A_i U) + C_r x_\tau - C_i y_\tau \quad (5)$$

$$\frac{\partial V}{\partial t} = -g(D+h)\left[B_r \frac{\partial(h-h_0)}{\partial y} - B_i \frac{\partial(h-h_0)}{\partial x}\right] + f(A_r U + A_i V) + C_r y_\tau - C_i x_\tau \quad (6)$$

where U, V are the components of transport, g is the gravitational constant, D is the depth of quiescent water relative to a common datum, Ar, ... Ci are the bottom stress terms, h is the height of water above datum, h_0 is the hydrostatic water height, f is the Coriolis parameter, and xτ and yτ are components of surface stress.

MF-3.6 Describe how storm translation is accounted for when computing surface wind and pressure fields.

SLOSH wind model computes surface wind and pressure fields for a stationary, circularly-symmetric storm (Jelesnianski, et al., 1992). The asymmetric wind and pressure field due to storm translation is not accounted for in the SLOSH wind model.

MF-3.7 Describe how storm surge due to non-tropical cyclones is accounted for in the flood model. If it is not accounted for, explain why.

Storm surge due to non-tropical cyclones is not accounted for in the model due to its low frequency and intensity in Florida (Shin, et al., 2022). No reliable claims data is available to calibrate or validate a model of non-tropical cyclone induced storm surge.

MF-3.8 Describe and justify the averaging time of the windspeeds used to drive the storm surge model.

SLOSH takes 6-hourly wind track points as inputs and then interpolates to hourly track points, which are then used to calculate the maximum 1-minute averaged wind speed at 10 meters of height. The 1-minute maximum sustained windspeeds are sufficient to drive the storm surge model (Jelesnianski, et al., 1992; Mayo & Lin, 2019).

MF-3.9 For methods in which storm surge is produced by physically-based simulation of atmosphere-ocean interactions and where the methodology has not been documented in the scientific and technical literature, describe the process for verifying convergence of storm surge height as a function of domain size. State the convergence criteria.

The size and resolution of the SLOSH basins are pre-determined. The SLOSH basins are being updated at an average rate of 3-6 basins per year. Priority for SLOSH basin updates are governed by the Interagency Coordinating Committee on Hurricanes (ICCOH). ICCOH is a tri-agency supported by the U.S. Army Corps of Engineers (USACE), Federal Emergency

Management Agency (FEMA), and the National Oceanic and Atmospheric Administration (NOAA). The basin updates include higher grid size resolution to improve surge representation, increasing area covered by hypothetical tracks for improved accuracy, and the latest topography or bathymetric data for better representation of barriers, gaps, passes, and other local features (NOAA, 2023c). During the basin development stages of SLOSH, results from preliminary experimental runs with past hurricanes are compared to all available observation surge data (Jelesnianski, et al., 1992). In areas of disagreement, the basin data was checked and amended if necessary. Thus, although the importance of large domains in correctly capturing regional processes and improving model solutions has been shown in literature (Blain, et al., 1994), no tests were performed by IF to verify the convergence of storm surge height as a function of domain size.

MF-4 Flood Characteristics (Outputs)

A. *Flood extent and elevation or depth generated by the flood model shall be consistent with observed historical floods affecting Florida.*

The flood extent, elevation, and depth generated by the flood model are validated with observed historical flood events affecting Florida. The comparison of flood extent and elevation/depth with observation data and FEMA return period maps can be found in Disclosure MF-4.1 and Forms HHF-1~HHF-5.

B. *Methods for deriving flood extent and elevation or depth shall be scientifically defensible and technically sound.*

The flood extent and elevation or depth are modeled using methods proposed in scientific and technical literature. The complete list of references is provided in Disclosure GF-1.6.

C. *Methods for modeling or approximating wave conditions in coastal flooding shall be scientifically defensible and technically sound.*

Wave in the storm surge portion of the Impact Forecasting Florida Flood Model is addressed in vulnerability functions and is assumed to be a function of the inundation depth. Detailed descriptions can be found in Disclosure VF-1.7.

D. *Modeled flood characteristics shall be sufficient for the calculation of flood damage.*

Modeled flood elevations or depths and flood extent are sufficient for the calculation of flood damage.

Disclosures

MF-4.1 Demonstrate that the coastal flood model component incorporates flood parameters necessary for simulating storm-tide-related flood damage in Florida. Provide justification for validation using any historical events not specified in Form HHF-1, Historical Event Flood Extent and Elevation or Depth Validation Maps.

The storm surge portion of the Impact Forecasting Florida Flood Model incorporates flood modeling parameters necessary for simulating storm surge related flood damage in Florida. The historical event footprints modeled by the storm surge portion of the Impact Forecasting Florida Flood Model were validated against ADCIRC footprints and observation data obtained from the United States Geological Survey (USGS), the National Oceanic and Atmospheric Administration (NOAA), the Federal Emergency Management Agency (FEMA), and the World's Storm Surge Data Center (SURGEDAT). Examples of the validation comparison using historical events not specified in Form HHF-1 are shown below.

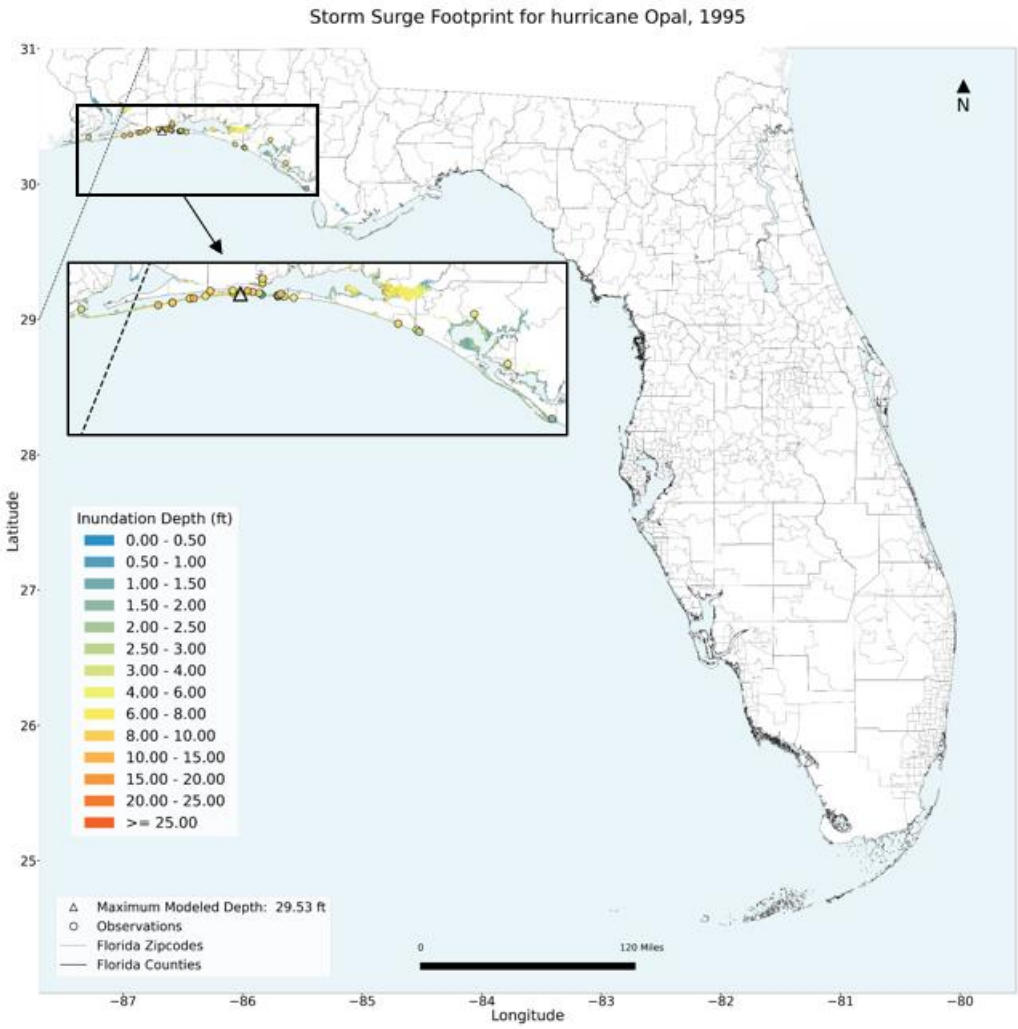

Figure 13: Storm surge Footprint compared with high water mark observation data for hurricane Opal (1995).

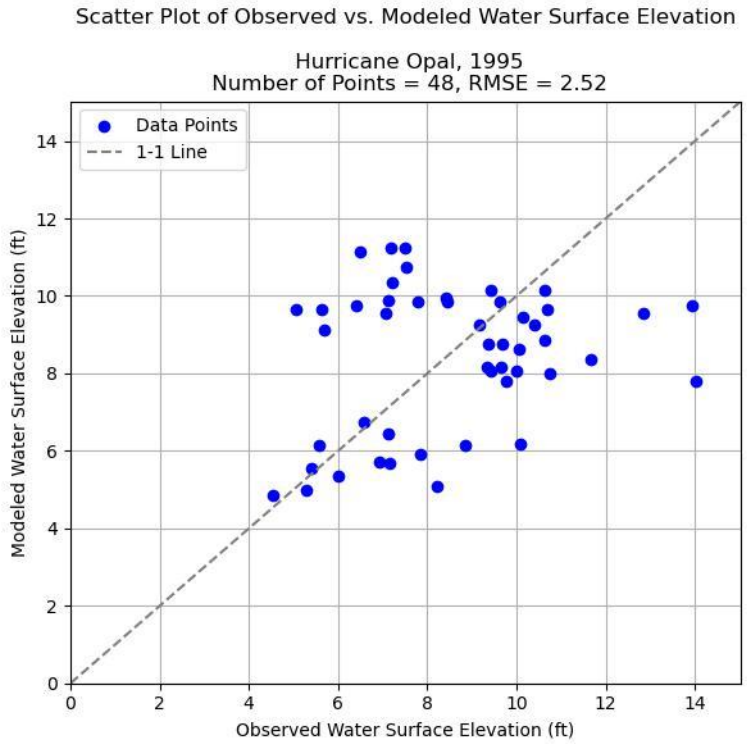

Figure 14: Scatter plot comparison of IF modeled storm surge footprint and high water mark observation data for Hurricane Opal (1995). (horizontal datum: NAD83, vertical datum: NAVD88)

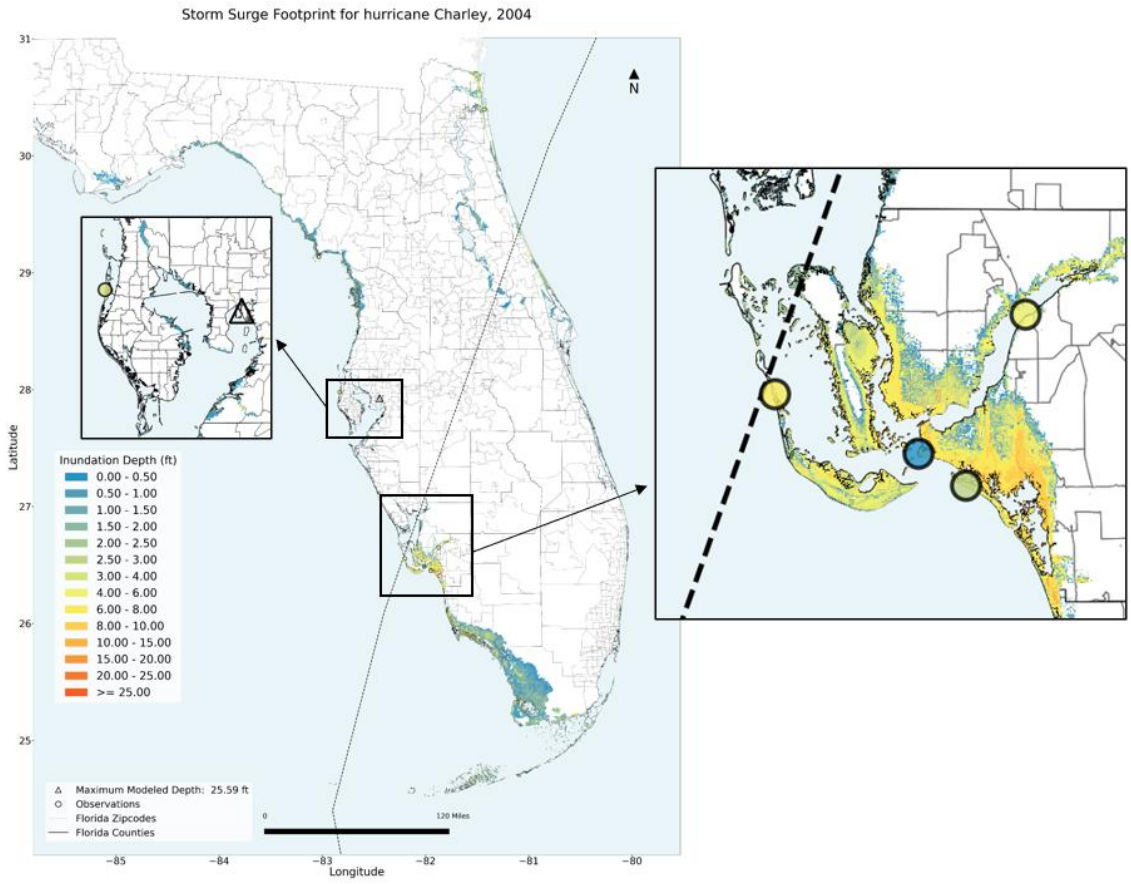

Figure 15: Storm surge Footprint compared with high water mark observation data for hurricane Charley (2004).

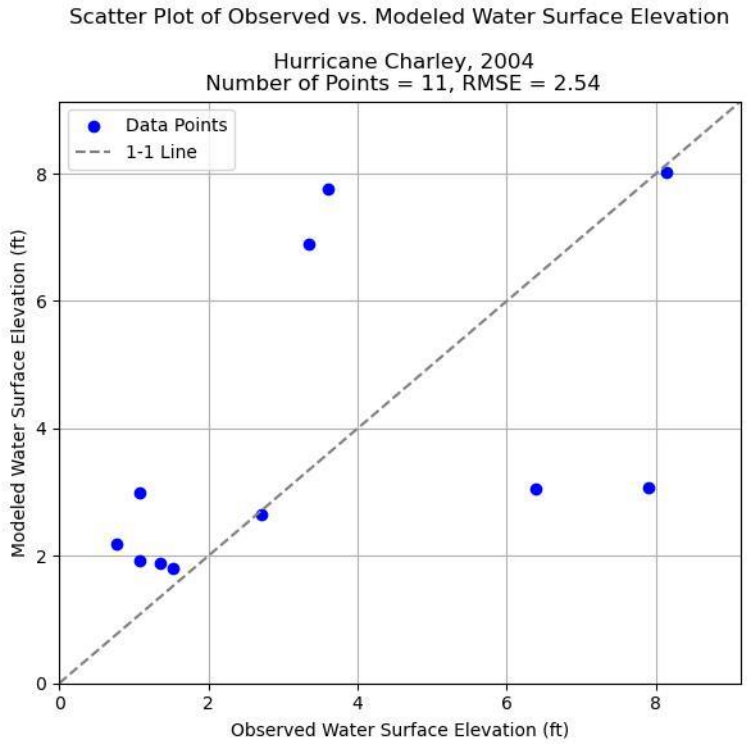

Figure 16: Scatter plot comparison of IF modeled storm surge footprint and high water mark observation data for Hurricane Charley (2004). (horizontal datum: NAD83, vertical datum: NAVD88)

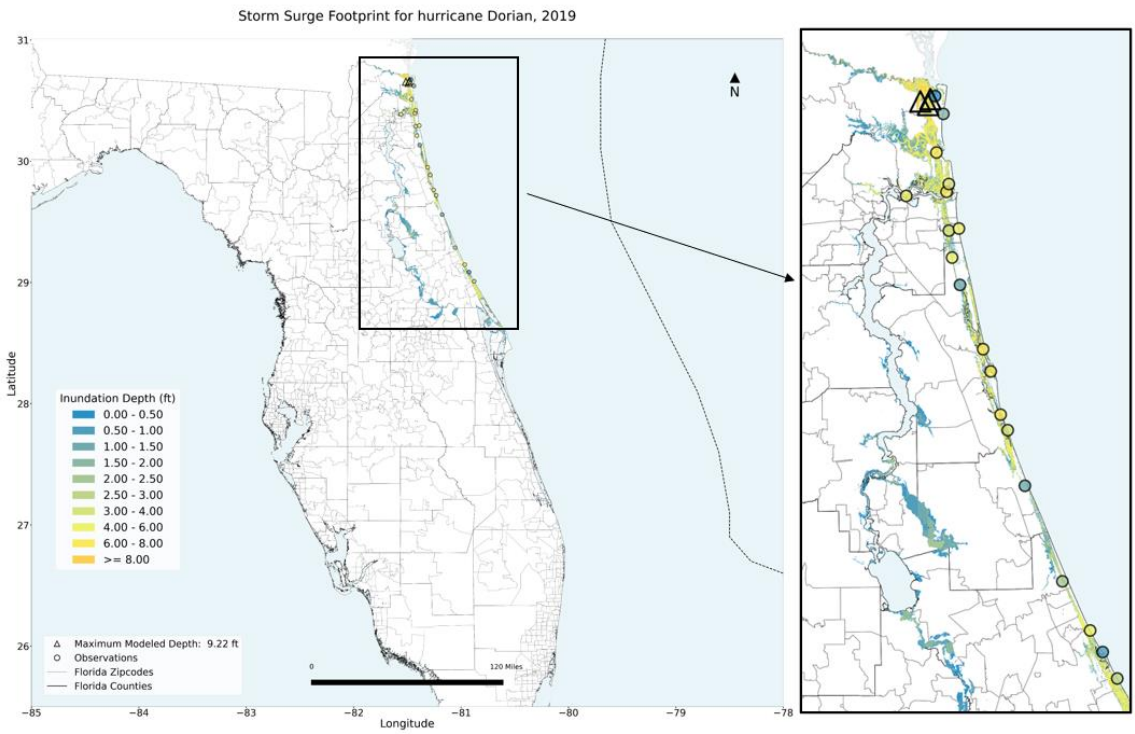

Figure 17: Storm surge Footprint compared with high water mark observation data for Hurricane Dorian (2019). There are many pixels, all with the same maximum value, located very close to each

other. These pixels have been grouped into three clusters, as shown in the figure, represented by the triangles.

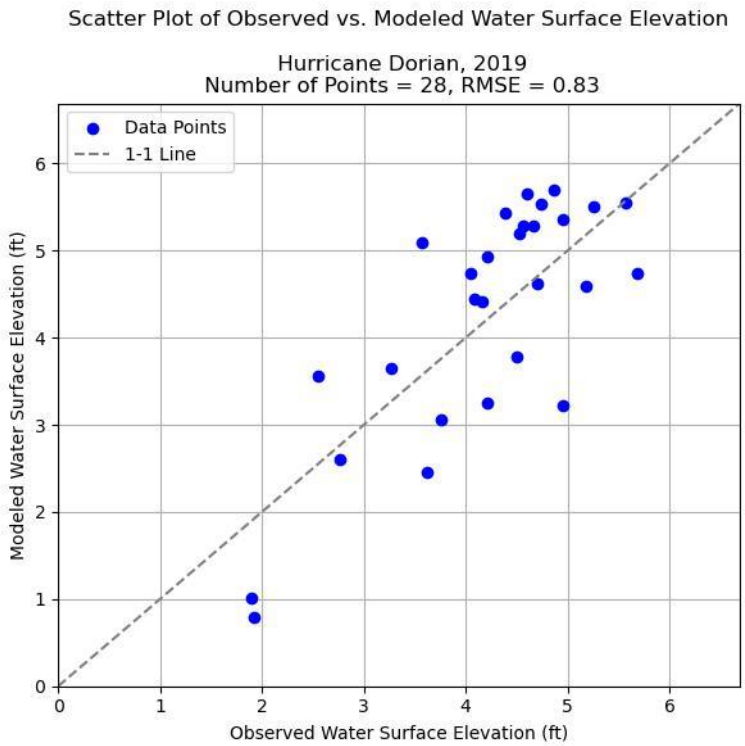

Figure 18: Scatter plot comparison of IF modeled storm surge footprint and high water mark observation data for Hurricane Dorian (2019). (horizontal datum: NAD83, vertical datum: NAVD88)

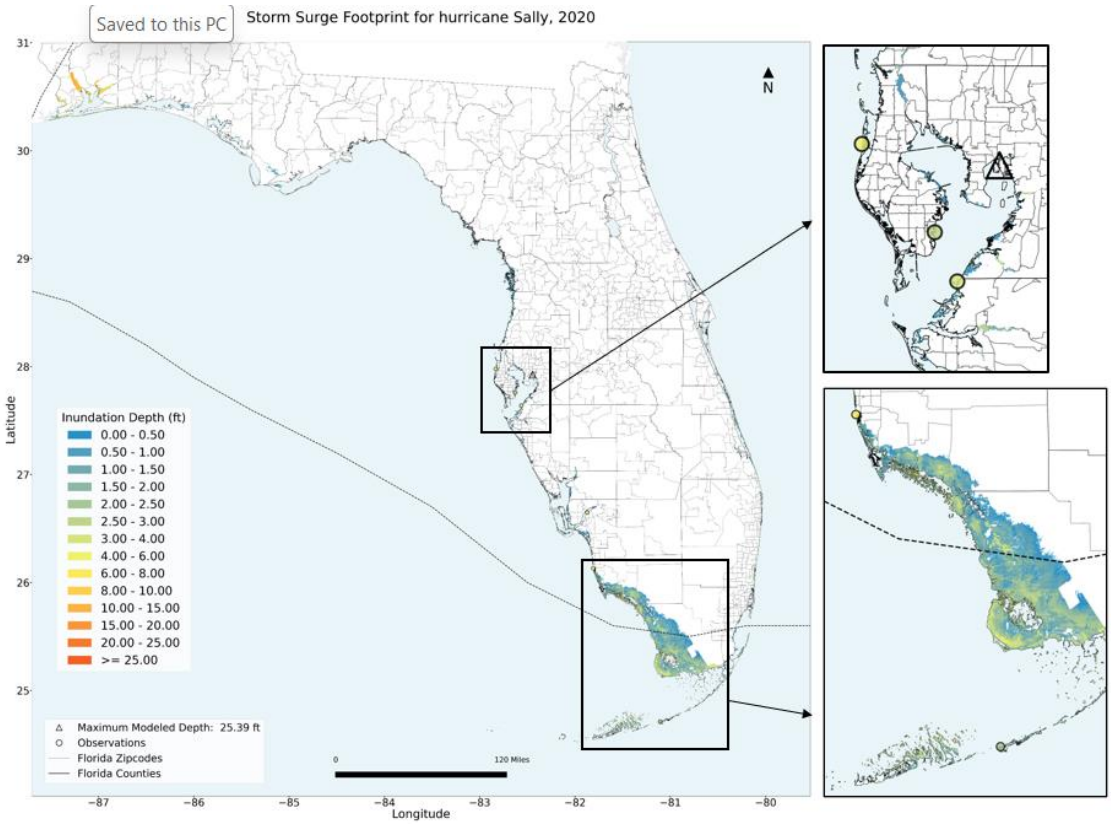

Figure 19: Storm surge Footprint compared with high water mark observation data for Hurricane Sally (2020).

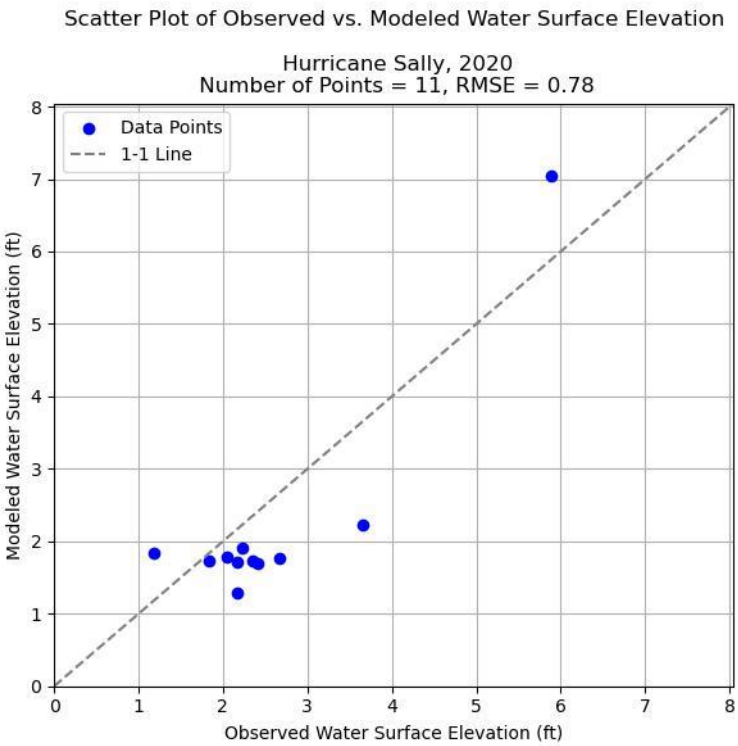

Figure 20: Scatter plot comparison of IF modeled storm surge footprint and high water mark observation data for Hurricane Sally (2020). (horizontal datum: NAD83, vertical datum: NAVD88)

MF-4.2 For coastal flooding, describe how the presence, size, and transformation of waves are modeled or approximated.

The presence, size and transformation of waves are not considered in the current version of SLOSH. The wave effects are accounted for in the vulnerability functions. Detailed descriptions can be found in Disclosure VF-1.7.

MF-4.3 For coastal modeling, describe if and how the flood model accounts for flood velocity, flood duration, flood-induced erosion, floodborne debris, salinity, and contaminated floodwaters.

The storm surge portion of the Impact Forecasting Florida Flood Model does not account for flood duration, flood-induced erosion, floodborne debris, salinity, and contaminated flood waters. The flood velocity is considered in developing the vulnerability functions. The difference between the saltwater density and freshwater density are also considered in vulnerability function development. Detailed descriptions can be found in Disclosure VF-1.8.

MF-4.4 For coastal flood waters, describe the factors that affect inland propagation and how they are modeled.

Factors affecting inland propagation of the storm surge includes the ground elevation, trees and other barriers. All these geographic features used to control, route and impede the flow of water are considered in SLOSH basins.

Each SLOSH basin is divided into multiple grid cells. The grid is set up to give fine resolution in the primary area of interest, and coarse resolution in the boundary region. The SLOSH model requires an elevation value to be assigned to each grid cell. These elevation values determine at what storm surge height the cell will flood (Conver, et al., 2008). Momentum points are located at the vertices of the grid cell. The value of the momentum point is the maximum elevation of the four surrounding grid cells. Momentum points are used by the SLOSH model to determine the flow of water across the surface and they are based solely on the value of the grid cell elevation, or the barrier points if they exist.

Flows and Cuts are needed in the SLOSH model to determine the movement of storm surge over land and water. There are two types of flow created by developers, 1-D flow and 1-D flow with banks. 1-D flow indicates that the flow of water, when the cell is wet, is across the entire cell. 1-D flow with banks indicates that the flow moves through a channel in the cell. A river which only covers fifty percent of a cell is a good example of 1-D flow with banks. Cuts are locations along a channel where the width of the flow with banks changes. These are entered into the database as the fraction (in tenths) of the cell width (Conver, et al., 2008).

Barriers are required when the average elevation of a cell does not represent a significant peak found within the cell. Examples include levees and barrier islands. Levees are manmade, narrow, linear structures that maintain an elevation significantly higher than that of the surrounding area. Because levees are usually narrow in comparison to a grid cell, they are frequently not reflected in the cell average. A barrier must be added to alert the SLOSH model that water will not go through the cell until it overtops the barrier height. Barrier islands behave similarly as they frequently have dunes with a peak higher than the cell average. Barriers are added at the vertex of the basin grid cells in the same location as the momentum point and will replace the momentum point value (Conver, et al., 2008).

Tree values inform the model of increased friction at the momentum points. Friction is important because it decreases wind speed and slows water flow.

SLOSH models the propagation of storm surge through wetting and drying of grid cells. Surge is computed at the center of each grid-square, and transport on each momentum point. The surge may travel from wet to dry cells. A two-dimensional flow will exist at a momentum point if at least one of the four surrounding grid cells is wetted and higher than the highest bed depth of the four surrounding grid cells (Jelesnianski, et al., 1992).

MF-4.5 Describe if and how inland flood affects the inland propagation of coastal flood. Describe if and how coastal flood propagation affects inland flood.

The Impact Forecasting Florida Flood Model models coastal flood and inland flood separately, so the inland flood does not affect the inland propagation of coastal flood, and vice versa.

MF-4.6 Describe if and how the coincidence and interaction of inland and coastal flooding is modeled.

The interaction of tropical cyclone induced inland and coastal flooding is accounted for in the financial component of the Impact Forecasting Florida Flood Model. The tropical cyclone induced coastal and inland flooding are modeled from the same tropical cyclone track. If a location is flooded by both inland and coastal flood, the losses are calculated separately, and the maximum loss will be used. The non-tropical cyclone induced coastal flooding is not modeled due to its low frequency and loss.

MF-4.7 ***Provide a flowchart illustrating how the characteristics of each flood model component are utilized in other components of the flood model.***

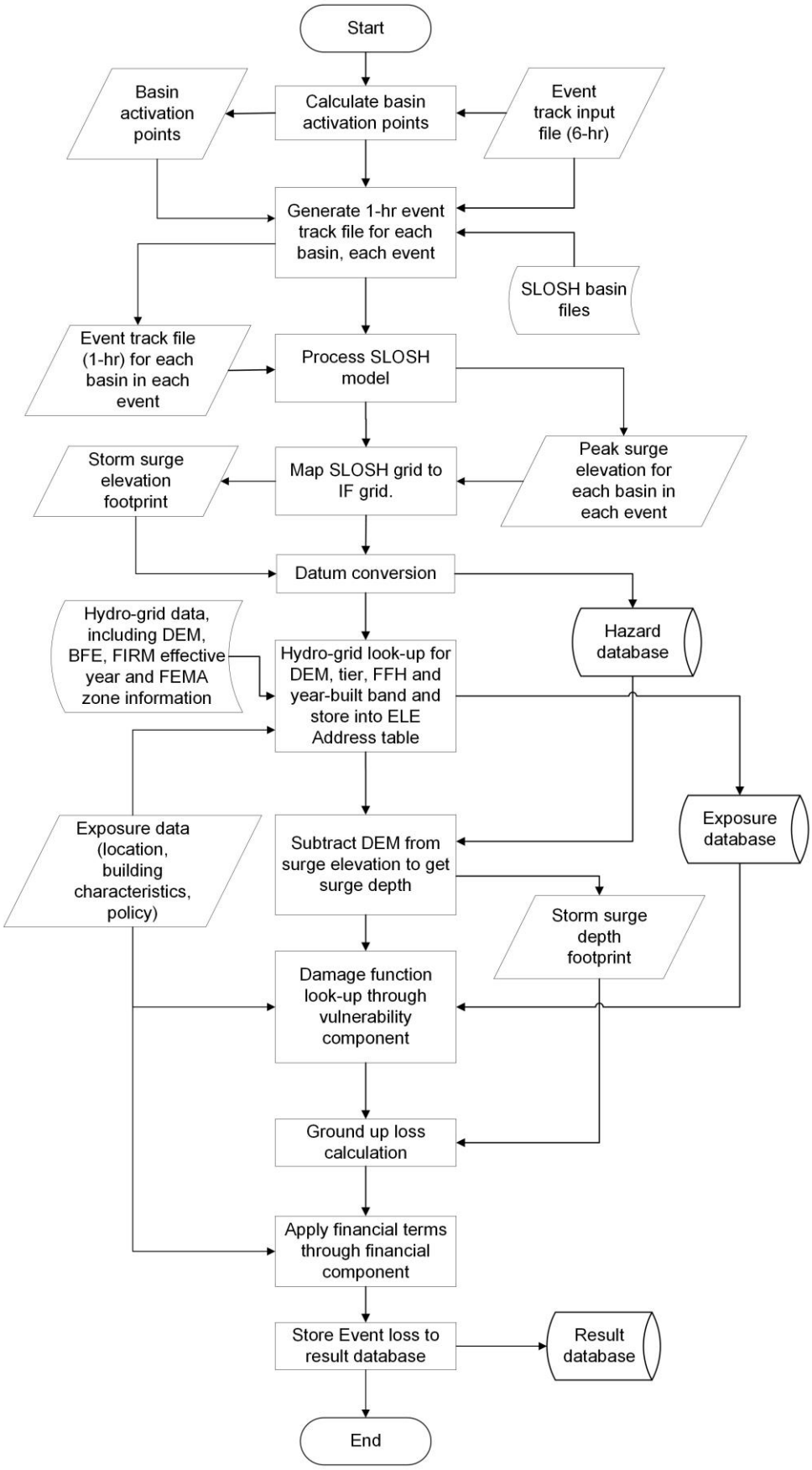
Start
Basin activation points
Calculate basin activation points
Event track input file (6-hr)
Generate 1-hr event track file for each basin, each event
SLOSH basin files
Event track file (1-hr) for each basin in each event
Process SLOSH model
Storm surge elevation footprint
Map SLOSH grid to IF grid.
Peak surge elevation for each basin in each event
Datum conversion
Hydro-grid data, including DEM, BFE, FIRM effective year and FEMA zone information
Hydro-grid look-up for DEM, tier, FFH and year-built band and store into ELE Address table
Hazard database
Exposure database
Exposure data (location, building characteristics, policy)
Subtract DEM from surge elevation to get surge depth
Storm surge depth footprint
Damage function look-up through vulnerability component
Ground up loss calculation
Apply financial terms through financial component
Store Event loss to result database
Result database
End

Figure 21: Flow chart illustrating the Impact Forecasting Florida Flood Model – Storm Surge components.

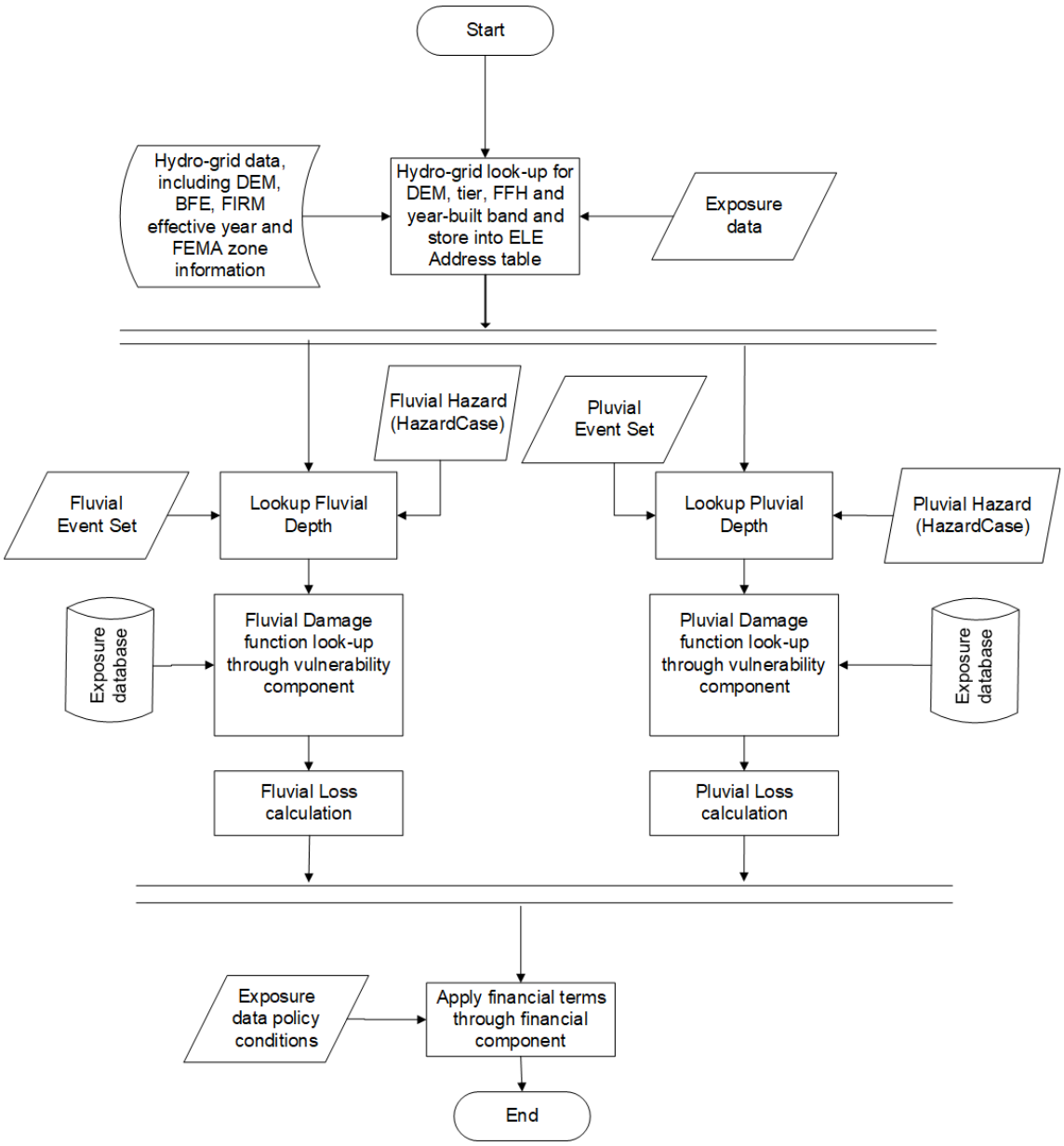

Figure 22: Flow chart illustrating the Impact Forecasting Florida Flood Model – Inland Flood components.

MF-4.8 Describe and justify the appropriateness of the databases and methods used for the calibration and validation of flood extent and elevation or depth.

Impact Forecasting Florida Flood Model – Storm Surge

The historical storm surge extent and elevation or depth modeled by the storm surge portion of the Impact Forecasting Florida Flood Model were validated against ADCIRC

footprints and observation data obtained from the United States Geological Survey (USGS), the National Oceanic and Atmospheric Administration (NOAA), the Federal Emergency Management Agency (FEMA), the World's Storm Surge Data Center (SURGEDAT) and published literatures. The comparison of flood extent and elevation/depth with observation data and FEMA return period maps can be found in Disclosure MF-4.1, Disclosure MF-5.3 and Forms HHF-1~HHF-5.

The modeled historical storm surge extent is mainly validated using the ADCIRC footprint (Coastal Emergency Risk Assessment, 2023). The ADCIRC model is a high-resolution two-dimensional, time-dependent hydrodynamic circulation model (Luettich and Westerink, 2004; Westerink et al., 2008). It functions as a highly developed computer program for solving equations for a moving fluid on a rotating earth. The ADCIRC modelling system has been used for long-term planning and design, evaluation of surge mitigation systems, and operational forecasting (Vijayan et al., 2021; Massey et al., 2022).

The modeled historical storm surge elevation or depth is validated against observed peak storm surge height records or high water marks (HWM) data obtained from various sources like United States Geological Survey (USGS), National Oceanic and Atmospheric Administration (NOAA), World's Storm Surge Data Center (SURGEDAT), Federal Emergency Management Agency (FEMA) studies and other published literatures and reports. During and following large storm events, the USGS specialist collects streamflow and additional data (including storm tide, wave height, HWM, etc.) to aid in documenting and validating the major storm events. The NOAA Storm Event Database contain records of the occurrence of storms and their associated significant meteorological features, such as inundation locations and depths. SURGEDAT is a global storm surge data center which maintains surge maps and peak surge height data for major historical storm surges. For older storms, limited records or observation data is available, so the modeled footprint is validated against reports from FEMA, NOAA, US Army Corps of Engineers and other literatures.

For stochastic events, the modeled return period surge maps are validated against NFIP extents. Detailed comparison maps are shown in Form HHF-3. The modeled stochastic storm surge elevation exceedance probabilities at several NOAA tidal station locations were compared with the observed frequencies (NOAA, 2023a). The validation of the return period storm surge elevation at several NOAA tidal stations are shown in Disclosure MF-5.3.

Impact Forecasting Florida Flood Model – Inland Flood

The inland model framework has been developed over the many years, with both the modelling methodologies and model outputs being extensively validated against observed data in the US (e.g. (Wing, et al., 2017; Wing, et al., 2018; Bates, et al., 2021)).

Most recently, the flood hazard data simulated using the modelling framework presented here have been validated across the US, with the models shown to perform well in comparison to FEMA flood maps and also flood maps from the IOWA flood centre (Bates et al. 2021).

The comparisons in this paper were of flood extents with the main performance metric being the Critical Success Index (CSI). The CSI represents the proportion of cells correctly modeled as flooded and is calculated as:

CSI = True Positive / (True Positive + False Positive + False Negative)

Scores range from 0, meaning no match between modeled and benchmark data, to 1, perfect match between modeled and benchmark data.

In comparisons to the FEMA 1% annual probability flood maps and the high quality, engineering-grade model based IOWA flood centre 5 year and 100 year flood maps, the model produced Critical Success Index scores of between 0.69 and 0.87 which represents good agreement given the underlying uncertainties in both modeled and benchmark data.

Comparing against both high and low frequency events demonstrates that the model performs well for both small and large flood events, whilst the US-wide analysis shows that the model is able to perform well across a range of climatological and hydrological conditions.

MF-4.9 Describe any variations in the treatment of the flood model flood extent and elevation or depth for stochastic versus historical floods, and justify this variation.

For historical events, when gauge data is available, it is used to determine the return period of flow for the fluvial catchment that the gauge falls within. There is no additional variation in the treatment of flood hazard between events in the stochastic and historical catalog.

MF-4.10 Describe the effects of storm size, bathymetry, and windspeed on storm surge height and its variation along the coast for the coastal flood model.

The impact of bathymetry on the storm surge is captured in the SLOSH model by having basins that represent the local bathymetry at a sufficient resolution to capture all the necessary natural and manmade features. Storm surge will be higher when a hurricane makes landfall on a concave coastline (curved inward, such as the Apalachee Bay in Florida) as opposed to a convex coastline (curved outward, such as the Miami Beach area on the east coast of Florida). Places with bays are especially vulnerable because the mound of water can be funneled into a small area. In terms of the slope of the continental shelves, higher storm surge occurs on wide and gently sloping continental shelves, while lower storm surge occurs on narrow and steeply sloping shelves. Areas along the Gulf Coast, including the west coast of Florida, are vulnerable to storm surge because the ocean floor gradually deepens offshore. Conversely, areas such as the east coast of Florida have a steeper shelf, reducing the amount of storm surge (NOAA, 2023b).

Stronger winds will produce a higher surge since more water will be pushed toward the shore by the force of winds moving cyclonically around the storm.

The radius of maximum winds, Rmax, is an important parameter that describes the size of a hurricane and the footprint extent of the storm surge. The winds in a larger storm will push water from a larger area of the ocean to affect a larger region on land. The strong winds in a larger storm usually tend to affect an area longer than smaller storms (NOAA, 2023b).

Lower central pressure will produce a higher surge. The central pressure deficit (i.e. the difference in atmospheric pressure between the storm center and the environment) will pile up the water and lead to pressure-driven surge (NOAA, 2023b).

To test the influence of Cp (central pressure) and Rmax on modeled storm surge height, the effect of some hypothetical storm tracks on the Florida Bay (eke2) basin were modeled using SLOSH. The track of Hurricane Irma (2017) was used as the default track. The Rmax and central pressure difference (ΔP) in the default track were increased and decreased by 25% and 50%, while keeping other factors constant. These simulations are named Rmax $\pm$X and $\Delta P \pm$X (Table 8) where the X in the subscript indicates the percentage change, and the sign ($\pm$) indicates an increase or decrease. For example, "Rmax+25" and "ΔP-50" indicate simulations where the Rmax was increased by 25%, and ΔP was decreased by

50% respectively. "Def" indicates the default track simulation without any parameter change.

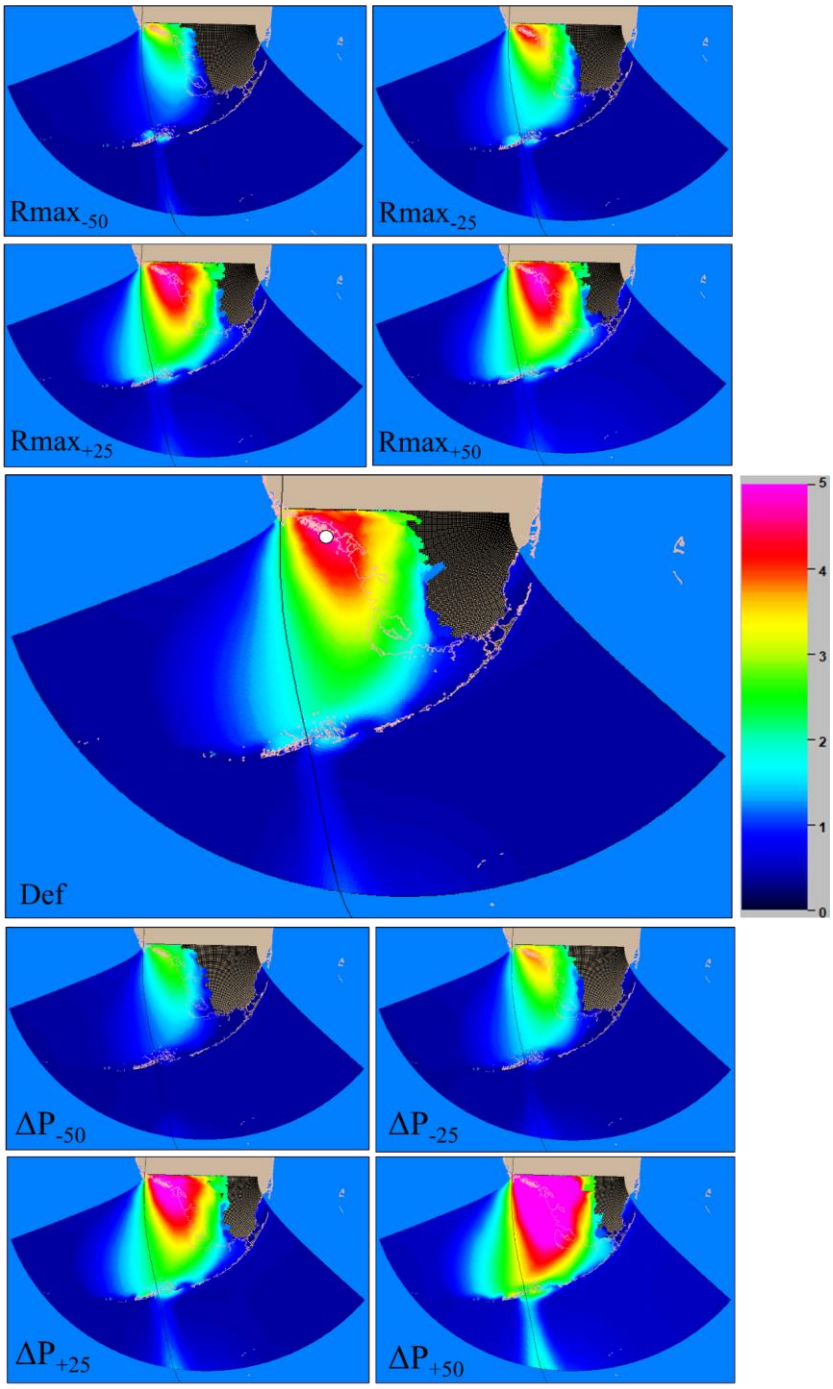

Figure 23: Surface map of maximum modeled water levels (m, relative to NAVD88).

In Figure 23, the gray area indicates Florida and the ellipsoidal area represents the SLOSH basin. The rows correspond to: (top two) simulations where Rmax was varied by 25 and 50%; (center) The default run with no change in storm parameters; and (bottom two) simulations where ΔP was changed by 25% and 50%. The white circle in the "Def"

figure (center row) indicates the location where the maximum water level values are shown in Table 8 and the black line shows the storm track.

Table 8: Peak water levels (m, relative to NAVD88) at the location shown in Figure 22.

Changing Rmax		Changing ΔP	
Simulation	Peak Storm Tide (m, NAVD88)	Simulation	Peak Storm Tide (m, NAVD88)
Rmax-50	3.23	ΔP -50	2.86
Rmax-25	4.27	ΔP -25	3.84
Def	4.72	Def	4.72
Rmax+25	4.79	ΔP +25	5.52
Rmax+50	4.92	ΔP +50	6.16

Comparisons of modeled storm surge (Figure 20) show that the peak surge increases as the storm size (Rmax) increases, indicating that the storm size effectively increases the distance over which the wind acts. At a location along the coast close to the storm peak (the white dot in Figure 23), the peak water level decreases from 4.72 m to 3.23 m with a 50% decrease in Rmax, and increases from 4.72 m to 4.92 m with a 50% increase in Rmax. A similar trend is observed with a change in ΔP as well. The surge increases with an increase in the central pressure difference (ΔP), but the percentage change is much higher. At the same location, the maximum water level increased to 6.16 m with a 50% increase in ΔP (about 30% change) and decreased from 4.72 m to 2.86 m with a 50% decrease in ΔP (about 40% change). These findings are in line with the case study results in Irish et al. 2008.

MF-4.11 Describe the effects of windspeed, depth, fetch, and wind duration on locally generated wave heights or wave proxies for the coastal flood model.

The storm surge portion of the Impact Forecasting Florida Flood Model addresses wave heights in developing the vulnerability functions. The breaking wave height is assumed to be a function of the inundation depth and the additional forces due to waves are accounted for when developing building vulnerability functions. The modeled storm surge inundation depth depends on windspeed, fetch and wind duration, thus the wave heights can be considered as implicitly affected by these variables. Detailed descriptions can be found in Disclosure VF-1.7.

MF-4.12 Describe if and how model flood characteristics are based on or depend on NFIP FIRM or other FIS data.

The vulnerability functions of the Impact Forecasting Florida Flood Model are distinguished between pre-FIRM effective year and post-FIRM effective year. The vulnerability tiers are designed based on FEMA zones. The default first floor height for different types of buildings at each 30m resolution grid is determined based on FEMA zone, FIRM effective year and Community Rating System (CRS) score. No other FIS data is used.

MF-4.13 ***Provide a completed Form HHF-2, Coastal Flood Characteristics by Annual Exceedance Probability. Provide a link to the location of the form [Form HHF-2: Coastal Flood Characteristics by Annual Exceedance Probability].***

MF-4.14 ***Provide a completed Form HHF-3, Coastal Flood Characteristics by Annual Exceedance Probabilities (Trade Secret Item), if not considered as Trade Secret. Provide a link to the location of the form [Form HHF-3: Coastal Flood Characteristics by Annual Exceedance Probabilities (Trade Secret Item)].***

MF-5 Flood Probability Distributions

A. *Flood probability, its geographic variation, and the associated flood extent and elevation or depth shall be scientifically defensible and shall be consistent with flooding observed for Florida.*

The flood probability, geographic variation and modeled flood extent and elevation or depth are validated using observations from historical events. The rationale of the probability distributions for flood modeling parameters is described in Disclosure MF-5.2. The validation of flood extent and elevation or depth can be found in Disclosure MF-4.1 and Forms HHF-1~HHF-5.

B. *Flood probability distributions for storm tide affected areas shall include tropical, and if modeled, non-tropical events.*

Flood probability distributions for coastal areas include tropical cyclone induced events. The non-tropical cyclone induced storm surge events are not considered in the storm surge portion of the Impact Forecasting Florida Flood Model due to its low frequency and low impact. Detailed response can be found in Disclosure MF-3.7.

C. *Probability distributions for coastal wave conditions, if modeled, shall arise from the same events as the storm tide modeling.*

The coastal wave conditions are implicitly modeled in vulnerability functions. Detailed descriptions can be found in Disclosure VF-1.7.

D. *Any additional probability distributions of flood parameters and modeled characteristics shall be consistent with historical floods for Florida resulting from coastal and inland flooding.*

The probability distributions of all flood parameters and characteristics are consistent with historical flood events affecting Florida. The rationale of the probability distributions for flood modeling parameters can be found in Disclosure MF-5.2.

Disclosures

MF-5.1 Describe how non-tropical and tropical event coastal storm tide flood probability distributions are combined, if applicable. Provide an example demonstrating the process.

Non-tropical cyclone induced storm surge is not modeled in the storm surge portion of the Impact Forecasting Florida Flood Model.

MF-5.2 Provide the rationale for each of the probability distributions used for relevant flood parameters and characteristics.

Impact Forecasting Florida Flood Model – Storm Surge

The rationale for each of the probability distributions used for relevant coastal flood parameters and characteristics are:

Storm Formation Count and Genesis Parameters

The Markov Chain approach is used to model the entire track of each tropical cyclone (limited to a maximum number of time steps) on a 6-hour time step from initiation to

dissipation. The number of tropical cyclones generated each year is modeled using a negative binomial distribution (Vickery, et al., 2000). The genesis location of the tropical cyclone along with its genesis date and time, initial forward speed, heading angle, and central pressure are modeled by random draws from historical genesis data (Vickery, et al., 2000; 2009c). If central pressure data is not available, a regression equation is used to estimate a central pressure value from maximum sustained wind speed and latitude. The tropical cyclone parameters at subsequent time steps are determined using regression models.

Translational/Forward Speed and Heading Angle/Direction

The tropical cyclone translational speed and heading angle at every 6-hour time step are modeled as separate regression models, using the forward speed, heading direction, latitude, and longitude from up to two previous time steps as predictors. The regression coefficients are derived for different 5x5-degree cells across the North Atlantic Ocean (Vickery et al., 2000, 2009c). The regression model with the corresponding set of coefficients is used when a storm moves into a given cell. The residuals from the regression are modeled as a normal distribution in each cell to address the randomness of storm movement.

Central Pressure

Central pressure is modeled in the form of relative intensity (Darling, 1991) using a multiple linear regression model. For each time step, the central pressure in a given 5x5-degree cell is modeled as a function of the relative intensities from the previous three time steps, the current sea surface temperature, and the previous sea surface temperature (Vickery, et al., 2000; 2009a; Rayner, et al., 2003). A random error term which follows a normal distribution is used to model the residuals that result from the regression. Relative intensity values are taken between 0 and 1 to constrain the minimum central pressures a storm can physically reach under certain environmental conditions.

Radius of Maximum Winds

Radius of maximum winds is an important parameter that describes the size of a tropical cyclone. It is modeled as a random variable which follows a lognormal distribution. The mean of the variable is described as a function of central pressure deficit and latitude (Vickery & Wadhera, 2008). The variation relative to the mean is determined from historical data through regression analysis. The historical data is obtained from the HURDAT2 Re-analysis Project (e.g., ., (Landsea, et al., 2004a; Landsea, et al., 2004b; Landsea, et al., 2008; Landsea, et al., 2012; Landsea, et al., 2014; Hagen & Landsea, 2012; Delgado, et al., 2018)), NOAA Technical Report NWS 38 (Ho, et al., 1987), and the Extended Best Track Dataset (Demuth, et al., 2006)

Impact Forecasting Florida Flood Model – Inland flood

For TC-induced inland flood, no distribution is used on the top of what is mentioned above, as only rainfall rates are calculated on the top of hurricane tracks.

Within the non-TC synthetic event set model the number of events per year across the region and the probability of a given site being the conditional site are conditioned upon the historical training data following previous literature (see (Quinn, et al., 2019; Wing, et al., 2020)) and are non-parametric. Furthermore, the reanalysis training data is converted into

semi-empirical marginal distributions, which provide the exceedance probability of a given magnitude event at each site. They are semi-empirical in that they are constructed by fitting a Generalised Pareto distribution to data above a specified threshold (calculated at each site), while an empirical distribution is fitted below. For calculation of the tail dependence between sites, the model utilizes a further conversion, transforming all the data from their semi-empirical distributions to a common Laplace distribution. This is a continuous distribution that is commonly used in similar applications as it enables a simplification of pairwise tail dependence model fitting and inferences, particularly in weakly associated variables (Keef et al 2013a). These transformations, and the utilised distributions are commonplace within the literature. See work by (Heffernan & Tawn, 2004; Keef, et al., 2013) for early model introduction and approach justification, as well as more recent literature including (Quinn, et al., 2019; Wing, et al., 2020; Southworth, 2022; Diederen & Liu, 2020), and (Li, et al., 2023) for similar applications to that utilized in this submission. The marginal threshold above which to fit the generalized pareto model is derived following the approaches of (Varty, et al., 2021).

For the hydraulic hazard modeling, the Generalized Extreme Value (GEV) and Generalized Pareto distributions are used as part of the Regionalized Flood Frequency Analysis (RFFA) that is used to calculate extreme streamflow. Discharge estimates using these distributions have been validated against independently derived flood frequency curves contained in the USGS StreamStats data and compared against an earlier version of the RFFA published by (Wing, et al., 2017) (v1) that used a smaller pool of gauges than the 6,902 USGS river gauges used here (v2). StreamStats data were obtained for 1095 USGS gauging stations and contain discharge frequencies computed in accordance with Bulletin 17C guidelines (England et al., 2019). Figure 24 displays the results of this validation, presenting the errors from the v1 and v2 RFFA approaches against USGS defined discharge estimates. Overall, we see substantial improvement in model skill, particularly for higher frequency events, for the newer RFFA. For example, the 5 years flow magnitude is computed with 25% error on average compared with 54% in v1. 80% of sites match the 5 years USGS flow within 50%, compared to only 46% of sites in v1. Improvements in model skill, particularly at low return periods, are unsurprising given the updated index flood approach that utilizes local gauge data where possible. Model skill at high return periods is also improved, with absolute errors in 100 years flow quantification reducing from 75% to 47% and biases brought down from 72% to 29%. Given that errors in return period flows estimated from river gauges can themselves be considerable, particularly where the gauge time series is significantly shorter than the target return period (Benson, 1958), the RFFA performance against the StreamStats benchmark can be considered reasonable.

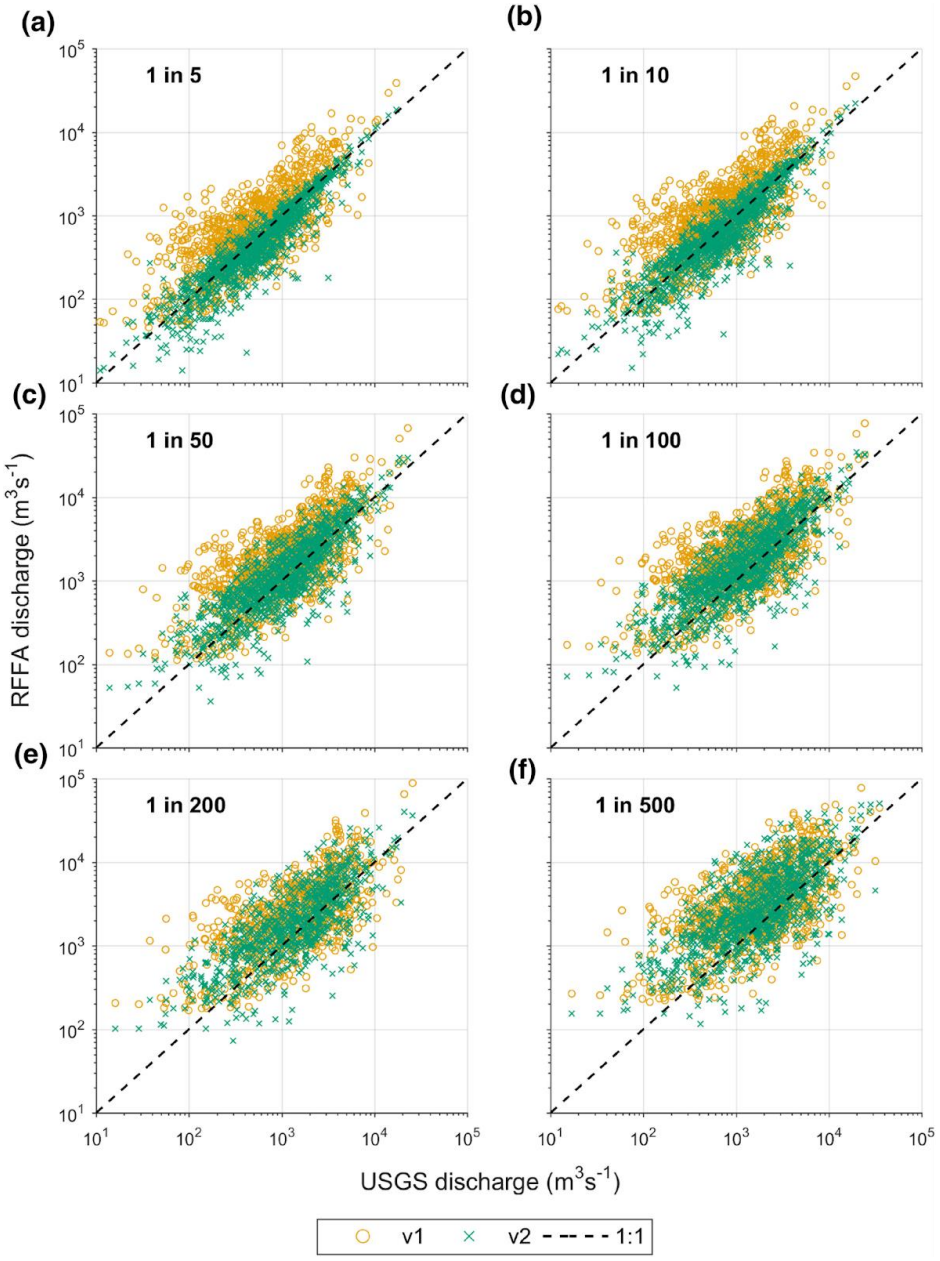

Figure 24: Validation of RFFA methods applied by Wing et al. (2017), v1, and the updated version, v2, used in this study. The figure displays the errors in estimated discharge, computed using benchmark data from USGS StreamStats data, for the 1 in 5 (a), 10 (b), 50 (c), 100 (d), 200 (e), and 500 years (f) events. RFFA, Regionalized Flood Frequency Analyses; USGS, United States Geological Survey.

MF-5.3 Demonstrate that simulated flood elevation or depth frequencies are consistent with historical frequencies.

Impact Forecasting Florida Flood Model – Storm Surge

The simulated coastal flood elevation frequencies are consistent with historical observed frequencies. The modeled storm surge elevation exceedance probabilities at a location on land closest to several NOAA tidal station locations were compared with the observed

frequencies, as is shown in Figure 25 below. NOAA provided the annual exceedance probability curve with 95% confidence intervals for varies stations along Florida coastline (NOAA, 2023a). All stations have at least 30 years of data. The comparison in Figure 25 shows that in general, the modeled flood elevation frequencies are in line with the historical frequencies. The simulated water elevation tends to be a bit lower (less than 0.5m lower) than the measurements for low return period but such small water elevation is unlikely to cause damage on land.

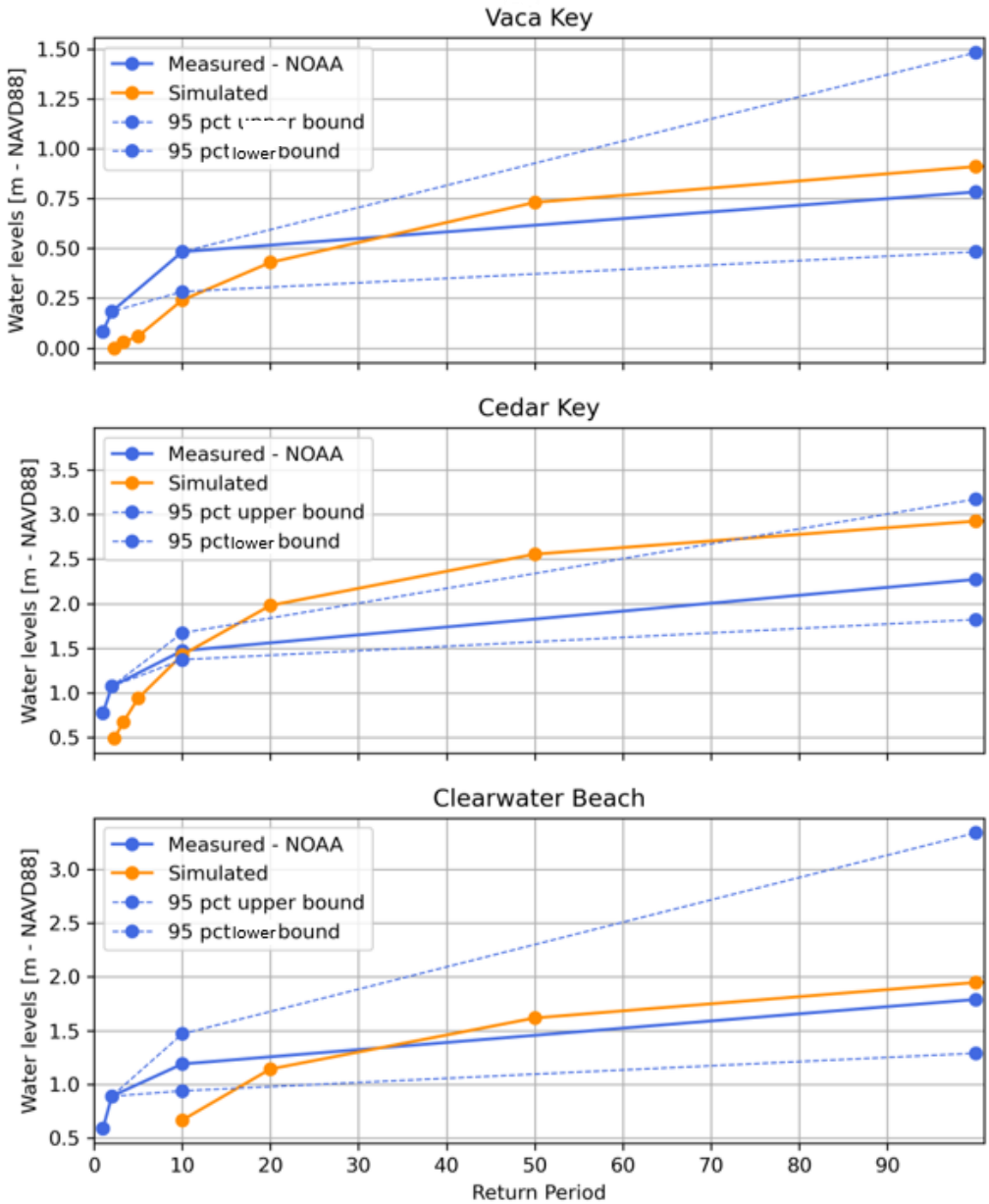

Figure 25: Comparison of simulated flood elevation at different frequencies (orange line and markers) with historic frequencies from NOAA (blue line and markers). The upper and low bounds of the 95 percent confidence interval of the measured flood elevation frequencies are also included with dashed blue lines and markers. The comparison was conducted for Vaca Key (top), Cedar Key (middle) and Clearwater Beach (bottom).

Impact Forecasting Florida Flood Model – Inland Flood

The simulated inland flood elevation frequencies are consistent with historical observed frequencies as shown in Table 9.

Table 9: Annual rates of unique event impacts across Florida. Bracket values represent Wald confidence bounds obtained from a bootstrapping analysis of the historical dataTC– Tropical Cyclone, NTC – non-Tropical cyclone.

Metric (at 10 year threshold)	Synthetic	Historic
Number of impacts annually (process agnostic)	2.7	3 [2.4, 3.6]
Number of impacts annually (TC)	0.9	1 [0.6, 1.3]
Number of impacts annually (NTC)	1.8	2 [1.6, 2.5]

The hazard layers have been validated at different frequencies. For example (Bates, et al., 2021) compared the model framework underpinning the Florida flood hazard model across the US and (as shown in Table 10 of (Bates, et al., 2021) and summarized in the table below) found that the model performed well in comparison to national (FEMA) flood maps, as well as regional flood maps (IOWA) at both higher (5 year) and lower (100 year) frequency events.

Table 10: Summary of validation Test Performance Metrics reported in (Bates, et al., 2021).

Metric	Hit rate (HR)	False alarm ratio (FAR)	Critical success index (CSI)	Error bias (EB)
Iowa Flood Center 5 years	0.77	0.15	0.69	0.38
Iowa Flood Center 100 years	0.93	0.07	0.87	0.49
FEMA 100 years	0.85	0.09	0.78	0.38
FEMA 100 years, coastal only	0.92	0.12	0.82	0.62

In terms of the synthetic event set modelling, the simulated frequencies are forced to be correct. The model is forced to sample from hazard layers at the correct frequencies. Further details regarding the non-TC synthetic event set model and the merged event set are given in Standard SF-1.

HYDROLOGICAL AND HYDRAULIC FLOOD STANDARDS

HHF-1 Flood Parameters (Inputs)

A. *Treatment of land use and land cover (LULC) effects shall be consistent with current scientific and technical literature. Any LULC database used shall be consistent with the National Land Cover Database (NLCD) 2016 or later. Use of alternate datasets shall be justified.*

The land use and land cover dataset is based on the National Land Cover Database (vintage 2019) and is used to serve as a base dataset for hydraulic roughness used in the flood hazard simulation. The details of the sources as well as the processing steps and values of Manning's roughness are described in depth in Disclosure HHF-1.9, Disclosure HHF-1.10, and when it comes to infiltration in the hydrological model, a Soil Survey Geographic Database (SSURGO) dataset is described in Disclosure HF-1.11 and Disclosure MF-2.6. Additional information can be found in Disclosure MF-1.6 and Disclosure MF-2.1. No alternative datasets besides the aforementioned are used.

B. *Treatment of soil effects on inland flooding shall be consistent with current scientific and technical literature.*

The Disclosures HHF-1.9 and HF-1.11 describe the use of the SSURGO dataset, and the principles of soil water mechanisms in hydrological models are discussed in the section dedicated to the FUSE model in Disclosure HHF-1.14.

C. *Treatment of watersheds and hydrologic basins shall be consistent with current scientific and technical literature.*

For inland flood simulation, there are multiple uses of watersheds and hydrological units. Datasets (mainly from NHD+) used in the process of hazard maps generation are described in Disclosures HHF-1.3, HHF-1.12, and HHF-1.13. On the topic of event set discretization, HUC10 units (NHD) are used for the pluvial event set (with further description available in Disclosure HHF-1.2). The discretization of fluvial hazard is unrelated to pre-defined hydrological units primarily because it is necessary to have overlaps in flood hazard maps (with further description available in Disclosure HHF-1.2).

D. *Treatment of hydraulic systems, including conveyance, storage, and hydraulic structures, shall be consistent with current scientific and technical literature.*

These systems are considered on only a limited basis in the direct application of flood hazard simulations. Largely, the use and application of flood protection structures is described in Standard HHF-3. To avoid limitations caused by the lack of state-wide data, a 1D sub grid channel network that is coupled to the 2D floodplain ensures a continuous channel network is modeled throughout the domain, including in areas that have been highly modified. This is described in depth in Disclosures HHF-1.13 and HHF-1.14. The impact of urban drainage systems are also considered, as described in Disclosure HHF-1.10.

.

Disclosures

HHF-1.1 For inland flood analyses associated with riverine and lacustrine flooding,

A. Describe how the rivers, lakes, and associated floodplains are segmented (or partitioned) in determining the parameters for flood frequency used in the flood model,

Rivers are discretized into reaches such that tributaries are simulated in a separate simulation to the main river channels they join. Larger river channels are also split into smaller sections when they reach the maximum river length (approximately 100km) or where there is a significant change in upstream catchment area (i.e. at the confluence of a large tributary). Boundary conditions (i.e. inflow hydrographs) are calculated at the start of each river section with smaller additional inflows added on a cell-by-cell basis further downstream as upstream catchment area increases.

Lakes for which the lacustrine modeling was done were isolated based on available gauge data and/or presence and absence of neighboring lakes with any observations. Subsequently, a frequency analysis was conducted on observed annual maxima for the lakes with a minimum of 10 years of recorded data. The recurrence interval was computed using a Weibull formula (U.S. Interagency Advisory Committee on Water Data, 1982). Each lake's annual recurrence interval versus water elevation curve was plotted and fitted with the optimal distribution. Using the chosen distribution, water elevation was calculated for the model's return periods.

B. Describe how the interaction between riverine and lacustrine components are represented in the flood model, and

Lacustrine modeling was merged (replacing the original flood hazard) into Fathom's inland hazard and simply assumes the same return period on the lake as well as in the hazard map. However, the return-period on the lake segment comes from the event set and depends on the hazard map segmentation and which return period is assigned to each segment. Here, for larger lakes, the segment could be comprised entirely of the lake or, for smaller lakes, also part of the river network system (and thus excluded from lacustrine simulation).

C. If groundwater is accounted for in the flood model, describe how the interaction between groundwater and inland flooding is represented.

Groundwater determines the state of the system (initial conditions in particular). For non-TC model (based on the hydrological hindcast), the groundwater stores are constantly updated as part of the continuous simulation, so groundwater variations are accounted for. For the TC model, we use same set of initial conditions for all events, so all events experience the same groundwater contribution (i.e. groundwater variations are not represented).

HHF-1.2 For inland flood analyses associated with surface water flooding, describe how the affected area is segmented (or partitioned) in determining the parameters for flood frequency used in the flood model.

The modeling framework samples from existing hazard layers which correspond to specified return period forcing levels. For this reason, the absolute magnitudes in the merged event

set at the site locations are not relevant; rather, only the quantile they represent is relevant. Therefore, the merged event sets were then converted to empirical quantiles at each site. To remove bias between the event set magnitudes and the return period levels of the boundary conditions in the hazard layers, the empirical quantiles were calculated with respect to the event set data (rather than linking the event set magnitudes to the marginal distributions of the hazard layers). A simple rank-select method was used to assign the expected return period to each event magnitude at each event set site.

Next, the point-based return periods needed to be interpolated over the entire Florida as well as the whole US region. Within the pluvial peril, this is done by discretizing the US into unique catchment units within which an assumption is made that every cell is experiencing the same return period magnitude. The units used were those provided in the NHD HUC 10 dataset (USGS, 2021), an example of which is provided in Figure 26.

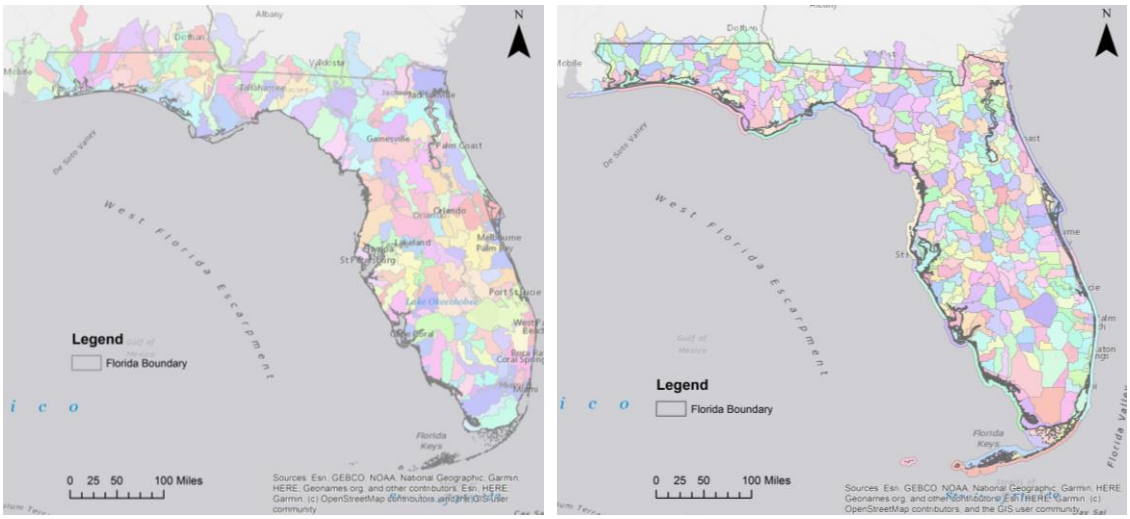

Figure 26: Fluvial (left) and pluvial (right) discretization of the region.

To extract the relevant hazard layers within each catchment, these return period estimates were intersected with the Fathom hazard layers on a catchment-by-catchment basis, iteratively stitching together a full flood depth map. Figure 27 provides a schematic example of this 'cookie-cutter' approach in a single catchment.

Unlike in the pluvial catchment discretization, the fluvial catchments can overlap. This is important, particularly at confluences where a given pixel may be part of a flood due to an extreme event occurring on more than one river. If we were to use static catchment units, whichever gauge was linked to the catchment the pixel was found within would be the only source of flooding at that site, which, in reality, is not the case. Instead, the river network is discretized into catchment units that correspond to a flood extent linked to two selected flood return period simulations (100yr and 1000yr) by a given input boundary condition. Each of these units are assigned a link gauge (where synthetic event magnitudes are produced), and then when constructing the event footprint, the relevant hazard layers' depths within the polygon unit are taken. In this way the full extent of a flood on each river reach can be examined during an event, unrestricted by (often arbitrary) catchment boundaries. The maximum depth of any overlapping catchment units is retained as the fluvial flood depth for a given event. An example is provided in Figure 28.

Once the fluvial and pluvial flood depths have been extracted across all catchments, for a given event, the final event depth at a location is given as the maximum of the two sub-

perils. The evaluation of these hazard depths against asset exposures in the region is conducted within the Impact Forecasting ELEMENTS platform.

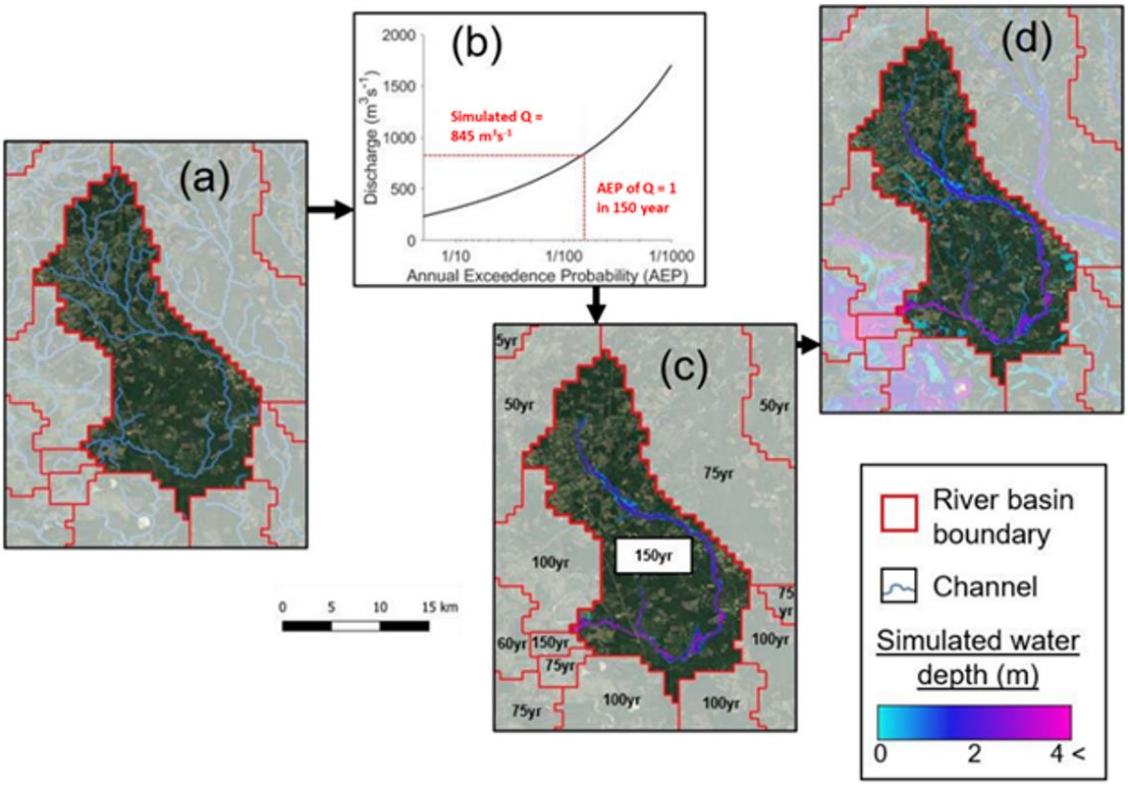

Figure 27: An example demonstrating the process of extracting flood maps for a catchment unit.

Figure 27 shows an example demonstrating the process of extracting flood maps for a catchment unit where no overlapping is allowed for a given flood event. The graph in (b) shows that the annual exceedance probability of the simulated Q occurring at the outlet of the catchment in (a) is 1 in 150 years. The 150-year Fathom depth grid, already simulated, is then extracted for the catchment in (c), while AEPs (Aggregate Exceedance Proabability) of all other catchments are computed too. The final flood inundation map is shown in (d), where this extraction process has been repeated for all river basins in the domain for both fluvial and pluvial sub-perils. In this project, static units are used for pluvial events, while overlapping units (see below) are used for fluvial events.

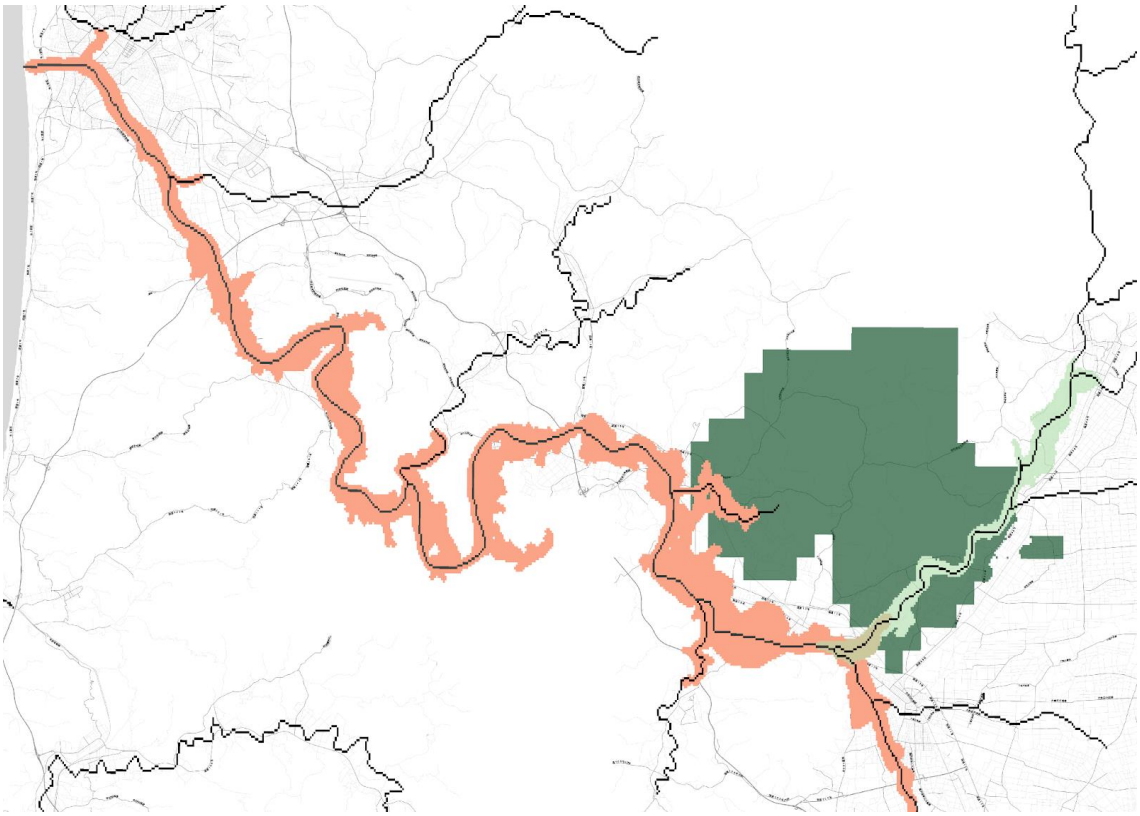

Figure 28: An example of the overlapping fluvial catchments in three river reaches, with RP100 masks shown in orange and green.

Figure 28 shows an example of the overlapping fluvial catchments in three river reaches, with the RP100 masks shown in orange and green, respectively. These masks will be used to sample from the underlying hazard layers when these reaches are impacted during an event. Note the overlapping of the catchments at the confluence, enabling a more realistic representation of flooding of pixels in the region, which can be inundated by an extreme event on either reach.

HHF-1.3 Describe any assumptions or calculations used in the inland flood model relating to initial and boundary conditions (e.g., groundwater levels, lake levels, river flows and discharge locations, tides, river confluences, soil moisture).

At single locations with sufficiently lengthy time series of observed annual flow maxima, return period flood flows can be estimated using extreme value distributions. However, gauged flow data is available only for a small number of rivers globally. Furthermore, the number of years of data at a given gauge is generally too small for robust estimates of extreme floods (100-year return period or more). In order to estimate flood flows in ungauged regions, Fathom uses a Regional Flood Frequency Analysis (RFFA) approach (Smith, et al., 2015). The implementation adopted was first described in (Sampson, et al., 2015). This approach pools gauged annual maxima from hydrologically similar regions together, deriving an index flood, used to scale data in the same pool. Flood frequency analysis is subsequently applied to the scaled pooled data to obtain growth curves. Application of the growth curve to the index flood of a given location yields estimated flood quantiles. The index flood is globally derived by calculating the index flood at all gauges

with sufficient data, then using a log – log multiple linear regression to relate the index flood to catchment descriptors which are available globally. The index flood can thus be estimated anywhere, and the pooled regional growth curves can be applied, allowing derivation of flood return periods anywhere. Pooling of gauges increases the number of data points that can be used to estimate extreme return periods.

While this approach worked surprisingly well over the US (refer to the validation study of (Wing, et al., 2017), it ignores obvious sources of high-quality local data that could lead to valuable improvement. To further improve this method, we upgraded the algorithm to use a much larger set of annual maxima data from 6,902 USGS river gauges. To best utilize the far denser USGS gauge network, gauges were carefully partitioned in space to estimate the index flood. This partitioning was undertaken using a hierarchical approach whereby the model moves from smaller scale catchments to larger catchment zones until a set of pooled gauge requirements are satisfied. These requirements were based on upstream catchment area, defining whether gauges with both small and large upstream areas were present in the pooling group. Once the catchment zone has enough gauges, representative of the required range of catchment areas, the gauges were pooled together into a single group. Therefore, only gauges from the same river or hydrological zone were used in the estimation of the index flood for a particular site. However, for the estimation of the growth curves, gauges were pooled together across all catchment zones to increase the sample size.

For the TC fluvial simulations, initial conditions for FUSE (e.g. soil moisture) and mizuRoute (river levels) were retrieved from the FUSE-mizuRoute hindcast driven by MSWEP (Beck, et al., 2019) and MSWX (Beck, et al., 2022) over 1980 to 2020. Model states from a few days before hurricane Katrina made landfall were considered to be indicative of pre-TC conditions and were used for all events. The main advantages of extracting initial conditions from a continuous distributed FUSE-mizuRoute historical simulation (instead of e.g. randomly generating them) are that the fields are spatially coherent, physically constrained, and that the FUSE and mizuRoute states are in sync. For Non-TC events, model states for FUSE and mizuRoute are updated every day as part of the 1980-2020 hydrological hindcast (continuous simulation driven by reanalysis), i.e., we do not use pre-Katrina conditions for these events. Instead, initial model states depend on the atmospheric conditions over the period preceding each event. The footprint for each event is then determined by a dynamical simulation based on these initial conditions (the hindcast).

As discussed in Disclosure HHF 1.1.C, soil moisture was not considered in the hydraulic modeling, except for the infiltration calculations for which soils were assumed to be dry, as discussed in further detail in Disclosure HHF 1.11.

HHF-1.4 Document the sensitivity of the flood model results to assumptions for values of initial and boundary conditions, including soil moisture, lake level, and tide height if relevant.

(Newman, et al., 2021) developed a stochastic framework relying on FUSE to explore the relative importance of key hydrological modeling decisions (initial conditions, model parameters, model structure and precipitation event forcing) when simulating extreme flooding events in two US catchments (a semi-arid catchment in Oklahoma and a snow dominated one in Idaho, which is less relevant for modeling in Florida). They generated millions of flood events and decomposed the variance of flood magnitudes for different return periods. They found that for the most extreme events, rainfall intensity is the dominant driver, and that initial conditions (including soil moisture) only play a secondary

role. For the more frequent events, the initial conditions play the dominant role. Their study is relevant here because, like our framework, it uses FUSE, but the hydroclimatic conditions of the two study catchments are quite different from that of Florida. Studies like Newman et al. (2021) that are based on a large number of stochastic simulations are typically limited to a few sites because of their computational cost. This applies to the study by Zhu et al. (2018), which focuses on the Turkey River in the Midwestern US. Importantly, while they demonstrate the importance of antecedent soil moisture, they also show that the importance diminishes as event magnitude increases.

Similar conclusions were drawn by Wasko and Nathan (2019) who showed that antecedent soil moisture plays a more important role in modest flooding events whereas precipitation is the most important driver affecting flooding associated with extreme precipitation episodes. They used long flow records in Australia and identified a recurrence interval dependent tipping point beyond which the trends in catchment rainfall outweigh those of soil moisture trends and dominate the flood response. They report that for regions where soil moisture has decreased, this tipping point occurs at an average recurrence interval of ten years or more. Additional evidence is provided by Brunner et al. (2020) using a large ensemble of extreme rainfall events over Bavaria, Germany. For the majority of the catchments, they identified a 'return interval threshold' in the relationship between precipitation and flood increases: at return intervals above this threshold, further increases in extreme precipitation frequency and magnitude clearly yield increased flood magnitudes; below the threshold, flood magnitude is modulated by land surface processes, including those involving soil moisture.

In the context of TC modeling, an implication is that flow simulations at the edges of the TC footprint would benefit most from using a range of initial conditions, while simulations at locations close to the TC/TS track are likely to be less sensitive.

In the hydraulic flood model, the impact of tide height is not modelled. Instead the downstream boundary of the fluvial hydraulic models at the coast are set to a fixed water height equal to the bank height of the channel to assume a full channel at the coast. This is to ensure that fluvial flood hazard is separated from the impacts of any coastal flooding which are modelled separately.

Likewise, the impact of lake levels were also not explicitly modelled by the hydraulic models and were instead modelled separately (as discussed in Disclosure HHF-1.1).

No assumptions on fluctuation of water levels in lakes and sea are considered, FUSE-mizuRoute does not account for lake level and tide height.

The analyses of several important storm surge model input parameters are explained in detail in Disclosures HHF-4.1 and SF-2.2.

HHF-1.5 Describe the source and representation of topography in the flood model. Describe the horizontal resolution and the vertical accuracy of the topographic representation. Identify the horizontal and vertical datum of the topographic information. Describe any modelling organization modifications to the topographic representation. Describe the sensitivity of simulated floods to uncertainties in the topographic representation.

This item is mainly covered in Disclosure MF-2.11; the topography is primarily composed of LiDAR with FABDEM (Hawker, et al., 2022) filling in any gaps. The horizontal resolution of the topography is 1 arc second (approximately 30 m). The vertical accuracy of LiDAR is typically in the order of 0.25 m, though there is greater uncertainty in the small number of

locations underpinned by FABDEM. The horizontal datum is WGS84, and the vertical datum is EGM08.

Following the compiling of the DTM as described in Disclosure MF-2.11, no further modifications to the topography were made. The flood model will be sensitive to significant uncertainties in the DTM. Research by (Savage, et al., 2016) shows that localized water depths can be sensitive to DTM uncertainties, however the model tends to be most sensitive to DTM uncertainty during the drying phase of the flood, with the sensitivity of the model to DTM uncertainty being negligible in comparison to uncertainties in boundary conditions and model friction parameters. Furthermore, given that the vast majority of Florida is covered with LiDAR, particularly areas with significant exposure, uncertainty in the topography here will be small and therefore the sensitivity of the model to realistic uncertainties here will also be small.

The topography representation used for surge modeling (embedded in the SLOSH model) is described in detail in Disclosure MF-2.11.

HHF-1.6 Provide the grid resolution or other area partitioning used to model the inland flood extent and depth and how the hydrological and hydraulic characteristics are determined on these scales.

The flood inundation model is simulated at 1 arc second (approximately 30 m) resolution. The properties of the river channel (i.e. riverbed and bank elevation and width) are determined at a 3 arc second (approximately 90 m) resolution, with these properties interpolated to 1 arc second between the center points of these cells.

The hydrological model FUSE is run on a 0.25° grid (~25km at the equator) and mizuRoute is run on the MERIT-Hydro network (median reach length of ~7km). Both models are set up to simulate all river reaches upstream and downstream of the TC rainfall footprint.

For the inland event set, the final model event footprints are generated through the sampling from pre-computed hazard layer catalogs. To do this in an efficient manner, the region is discretized into pluvial and fluvial catchments, and within each, the event maximum return period is defined. This return period is used to select the most appropriate hazard layer (flood depths) to sample. Further details are provided in Disclosure HHF-1.2.

HHF-1.7 Describe any assumptions or calculations used in the inland flood model relating to flood-induced erosion or topographic changes.

No assumptions or calculations were made in relation to flood induced erosion or topographic changes.

HHF-1.8 Provide citations to all data sources used to develop and support the land-use evaluation methodology, including publicly developed or peer-reviewed information.

This is answered in Disclosure MF-2.1 and partially replicated here.

The National Land Cover Dataset (2019) (Dewitz, 2021) is applied to the model to define the spatially varying Manning's roughness coefficient and the urbanization that is applied to estimate urban drainage, as described in Disclosure MF-2.1. These coefficients are based on values developed by (Arcement, et al., 1989) or (Chow, 1959). This is then modified in cells that contain buildings as defined by the Microsoft building footprints dataset (Microsoft, 2018).

For the storm surge model, the National Land Cover Dataset (Dewitz, 2021) is necessary for the Trees layer in SLOSH basins. The input for this layer is downloaded from the National Land Cover Dataset website which is hosted by the Multi-Resolution Land Characteristics Consortium (MRLC). Based on field observations, basin developers have found the NLCD to be accurate and use it to determine land cover classifications for SLOSH basins (Conver, et al., 2008).

HHF-1.9 Provide the collection and publication dates of the LULC and soil data used in the flood model and justify the applicability and timeliness of the data for Florida.

The LULC dataset used by the model is the 2019 version of the National Land Cover Dataset (Dewitz, 2021). This was the latest version of the dataset available at the time of modeling. The soil data applied in the model is the Soil Survey Geographic Database (SSURGO) (Soil Survey Staff, 2021). A digitized version of the data was downloaded when we started building the flood model in 2018.

We have compared our SSURGO dataset to the latest version that has most recently been released (2023) and any differences are relatively small and primarily confined to the wildlife management areas in Southern Florida rather than the areas where there is the most financial risk. Furthermore, the way in which this data is used by the model means that the introduction of a newer dataset would not significantly change the model outputs. This is because although the soil dataset is used to determine infiltration rates which are modeled as a reduction in rainfall intensity within the pluvial model, the dominant driver to changes in the precipitation data is the urban drainage allowances that are defined instead by the newer NLCD dataset, as land cover has a greater control on this than soil type.

HHF-1.10 Describe the methodology used to convert LULC information into a spatial distribution of hydrological parameters, including roughness coefficients, throughout the flood model domain.

This is described in Disclosures MF-2.1 and MF-2.6 but is repeated here for completeness.

Manning's roughness coefficient - The hydrodynamic model requires an estimate of the Manning's roughness coefficient as per the underlying mass conservation equations presented by (Bates, et al., 2010). This term controls the friction exerted on water flowing over the earth's surface. We apply a spatially varying Manning's friction coefficient that changes based on land cover as defined by the NLCD (2019) (see Table 11). These coefficients are based on values published at (Arcement, et al., 1989) or (Chow, 1959) and references therein. This is then modified in cells that contain buildings as defined by the Microsoft building footprints dataset, as shown in Table 12). We do this so that areas within urban regions that do not contain buildings can have lower Manning's roughness coefficients than those containing buildings. In areas of no data, we apply a uniform friction coefficient of 0.06, and within the sub-grid channels we apply a uniform friction coefficient of 0.04. For the mizuRoute routing model providing the fluvial boundary conditions, a Manning's friction coefficient of 0.01 was used across the whole river network. A sensitivity test was run with a value of 0.03 across the whole river network, the differences in model performance were found to be minor (see Disclosure SF-2.3).

Table 11: Summary of spatially varying Manning's friction coefficients.

NLCD land use code	Definition	Manning's roughness coefficient
11	Open Water	0.04

NLCD land use code	Definition	Manning's roughness coefficient
12	Perennial Ice/Snow	0.04
21	Developed, Open Space	0.04
22	Developed, Low Intensity	0.04
23	Developed, Medium Intensity	0.03
24	Developed, High Intensity	0.03
31	Barren Land (Rock/Sand/Clay)	0.025
41	Deciduous Forest	0.1
42	Evergreen Forest	0.1
43	Mixed Forest	0.1
52	Shrub/Scrub	0.1
71	Grassland/Herbaceous	0.035
81	Pasture/Hay	0.03
82	Cultivated Crops	0.035
90	Woody Wetlands	0.1
95	Emergent Herbaceous Wetlands	0.07
127	Unclassified	0.06

Table 12: Spatially varying Manning's friction coefficients in the presence of buildings.

Building Coverage	Manning's roughness coefficient
>20%-50%	0.06
50%-80%	0.09
80%+	0.12

Urban drainage standards - We use the National Land Cover Dataset (NLCD, 2019) (Dewitz, 2021) to determine the degree to which areas are built up and classify regions into rural and urban (see Table 13). We then assign a 10-year drainage standard to urban locations. The rainfall associated with that standard of protection is then subtracted from the baseline rainfall intensity for the scenario modeled for those locations. These approaches result in a spatially variable rainfall grid, reflective of the underlying soil type and assessments of urban drainage standards.

Table 13: NLCD classification and subsequent drainage defense standard

NLCD Classification	Fathom Classification	Drainage Defense Standard
21 - Developed, Open Space 22 - Developed, Low Intensity 23 - Developed, Medium Intensity	Urban	1-in-10 year RP

24 - Developed High Intensity		
Other	Rural	Soil infiltration only

For the storm surge model, the National Land Cover Dataset (Dewitz, 2021) is necessary for the Trees layer in SLOSH basins. The tree height values are added at the corner points of the SLOSH basin grids to inform the model of increased friction. Friction is important because it decreases wind speed and slows water flow (Conver, et al., 2008).

HHF-1.11 Describe the methods used to account for soil infiltration and percolation rates and soil moisture conditions in the inland flood model, if applicable. Provide citations to all data sources used to develop and support the soil infiltration and percolation rates and soil moisture conditions methodology, including publicly developed or peer-reviewed information. Justify the selection of antecedent soil conditions.

Infiltration is calculated based on a modified Horton equation (Morin & Benyamini, 1977) and varies depending on soil type as defined by the Soil Survey Geographic Database (SSURGO) (Soil Survey Staff, 2021) .

Initial infiltration rates were defined based on values published within (Hillel, 2013) and vary based on soil type. These initial rates represent dry initial soil conditions; however, these rates decrease to a final steady-state evaporation/infiltration date, again with values taken from (Hillel, 1982) and infiltration calculated using the modified Horton equation in (Morin & Benyamini, 1977).

In the FUSE implementation of VIC (Liang, et al., 1994) used here, soil moisture in the upper soil layer is determined by computing the balance between precipitation minus evaporation, surface runoff, and percolation of water from upper to lower soil layer; see (Clark, et al., 2008). The balance is computed for each time step of the hindcast, which is used to generate the initial conditions, and is then computed for each time step of the TC runs.

HHF-1.12 Describe the methods used to develop watershed and hydrologic basin boundaries, and the hydrologic connectivity in the flood model, or any assumptions used in lieu of representing watersheds and hydrologic basins in the flood model.

The hydrological connectivity of the river channels is defined by the NHD+ accumulation network (Buto, 2020) from which catchment masks are defined. River channels are modeled within the hydraulic model as sub-grid channels. Rivers with an upstream catchment area greater than 193.051 sq mi (500 sq km) (as defined by the NHD+ accumulation network) are modeled within the fluvial model, whilst rivers smaller than this are represented by the pluvial model.

The catchment masks are defined based on NHD+, but mizuRoute uses the MERIT-Hydro river (Yamazaki, et al., 2019) network. Hence, locations on the NHD+ network where boundary conditions are needed are mapped onto the MERIT-Hydro river network, and this determines where mizuRoute flow time series are extracted.

HHF-1.13 Describe the methods used to develop the hydraulic network (e.g., riverine, lacustrine) in the flood model, the treatment of hydraulic structures (e.g., bridges, culverts) within the hydraulic network, and any assumptions used in lieu of the physical representation of hydraulic structures in the flood model.

As described in Disclosure HHF-1.12, the river network modeled within the hydraulic model is defined from NHD+ and as described in Disclosure HHF-3.1; areas protected by the levees contained with the National Levee Database (NLD) are post processed onto the flood hazard maps. This is achieved by removing flooding from defended areas for return periods up to the respective levee's standard of protection. For example, if an area is defended up to and including a flood with a 100 year return internal, then flood hazard layers for more frequent floods (i.e. return intervals of 100 years or less) will show no flooding within the defended area. No hydraulic structures other than the levees are considered. The use of sub-grid channels within the hydraulic models (see Disclosure HHF-1.14 for full details) ensures that the hydraulic network remains connected in the presence of bridges, culverts, and other structures as the channels are modeled within a 1D sub-grid channel network that is coupled to the 2D floodplain.

The lacustrine modeling is a static simulation done on top of the inland modeling. Here, after the extent generation, every modeled lake outlet was investigated, and generated flood hazard was adjusted (clipped out) according to its outlet type (natural outflow) or outlet structure as well as the link to fluvial flood hazard downstream of the modeled water body.

For the storm surge portion of the model, various geographic features such as continental shelf, inland terrain, inland water bodies (e.g. rivers, lakes, bays, estuaries), trees, and barriers are considered in the SLOSH basins (Jelesnianski, et al., 1992; Conver, et al., 2008). Two hurricane levees in Florida were added to the SLOSH basin files as barriers using location and height data from the National Levee Database. Levees will be overtopped if modeled surge height exceeds the levee height.

HHF-1.14 Characterize the hydrologic and hydraulic mathematical models used, and the corresponding sources and citations.

IF Flood model – Inland Flood

LISFLOOD-FP model description

Fathom's hydraulic modeling framework is an implementation of the LISFLOOD-FP numerical scheme (Bates, et al., 2010), a novel simplification of the shallow water equations which yields an algorithm for which the minimum stable time step scales linearly with decreasing grid size, making it computationally more efficient than previous diffusive wave formulations, e.g. (Hunter, et al., 2005) which scale quadratically. Combined with improvements in implementation and optimization through parallelization on central and graphical processing units, this has provided dramatic reductions in model runtimes, vital for applications across continental scales (Neal, et al., 2018).

(Bates, et al., 2010) provide a validation of the model accuracy through a series of idealized test cases in which flows are contrasted with analytical solutions and an existing diffuse wave model. They report that depth errors were typically within that of higher resolution terrain data in simple beach test cases, increasing in complex test cases involving wetting and drying, noting however that results were near identical to model benchmark solutions

yet achieved at a fraction of the computational cost. Similar results were found by (de Almeida & Bates, 2013) during a validation study of the inertial model implementation over a wider range of idealized test cases, contrasting model flows with those from analytical solutions and full shallow water models. Here they also reported that the inertial model performed very well within subcritical flow conditions, which are typically found in floodplain and lowland river flows of practical interest, while requiring a fraction of the computational runtime.

An important limitation of many 2D approaches over large domains is the inability to represent rivers whose widths are considerably smaller than the grid size. (Neal, et al., 2012)This issue is addressed within the LISFLOOD-FP model through the implementation of a 'sub-grid' solver, in which channel characteristics and flows are represented using a 1D model while floodplain flows occurring when conveyance capacities are exceeded are propagated using the 2D inertial model solver of (Bates, et al., 2010). In summary, the 2D base model LISFLOOD-FP uses an explicit forward difference scheme on a staggered grid (Figure 29). The model comprises two equations that handle the continuity of mass in each cell and continuity of momentum between cells. Although arranged in two dimensions, the momentum equation implemented across each face of each grid cell is in fact a one-dimensional calculation such that the fluxes through each cell face are decoupled from each other. For each cell, the continuity equation over a time step Δt is:

$$h_{i,j}^{t+\Delta t} = h_{i,j}^{t} + \Delta t \frac{Q_{x\,i-1/2j}^{t+\Delta t} - Q_{x\,i+\frac{1}{2}j}^{t+\Delta t} + Q_{y\,i,j-1/2j}^{t+\Delta t} - Q_{y\,i,j+1/2j}^{t+\Delta t}}{A_{i,j}} \tag{10}$$

Where Q is the flow between cells (m^3s^{-1}), h is the water depth at the center of each cell (m), A is the water surface/cell area (m^2), and subscripts i and j are cell spatial indices in x and y directions, respectively. Because flows in the x and y directions are calculated using the same approach, the method of description below presents only the calculation of flow in the x direction, dropping references to x and y directions from the notation. The momentum equation to calculate flow Q between two cells is described by the following equation:

$$Q_{i+1/2}^{t+\Delta t} = \frac{q_{i+1/2}^{t} - g h_{flow}^{t} \Delta t . S_{i+1/2}^{t}}{\left[1 + g \Delta t n^2 \left| q_{i+\frac{1}{2}}^{t} \right| \left(h_{flow}^{t}\right)^{7/3}\right]} \Delta x \tag{11}$$

Where Δx is the cell width (m), g is the acceleration due to gravity (ms^{-2}), q^t (m^2s^{-1}) is the flow from the previous time step Q^t (m^3s^{-1}) divided by cell width Δx (m), S is the water surface slope between cells (unitless), n is Manning's roughness coefficient ($sm^{1/3}$), and h_{flow} is the depth between cells through which water can flow (m).

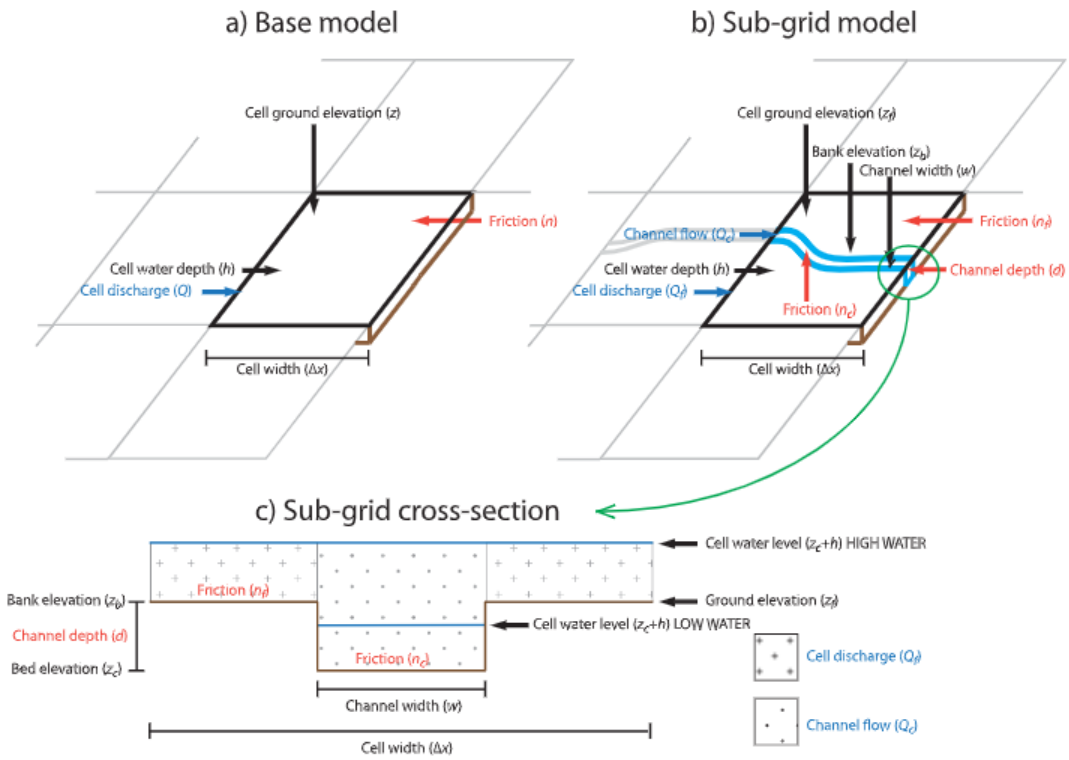

Figure 29: Conceptual diagram of (a) LISFLOOD-FP base model, (b) sub-grid channels model and (c) sub-grid section.

Introducing a sub-grid channel to the base model is relatively simple because each cell face can be treated as a one-dimensional model and therefore be implemented as a series of separate flow calculations with a shared water surface height but with different widths and bed elevations representing the floodplain and channel, respectively. Two variables are added to the base model to represent the channel, namely bed elevation *zc* and channel width *w*. The channel and flow calculations can then be solved independently before being combined to obtain the cell face discharge that is needed by the continuity equation. For a complete solver schematic and full calculation chain see (Neal, et al., 2012; Bates, et al., 2010) in which this model implementation was validated over an 800 km reach of the River Niger in Mali by comparing four different model structures: 1D only (no floodplain), 2D only (no channels), coupled 1D/2D (main channels with floodplain), and a 2D sub-grid model (main channels, smaller sub-grid floodplain channels, and floodplain). The study determined that inclusion of both the channel network and floodplain was essential, and that inclusion

of the smaller sub-grid channels on the floodplain yielded significantly increased simulation accuracy in terms of water level, wave propagation speed, and inundation extent.

The application of a hydraulic solver at high resolution across the complete land surface of our planet does require the solver to be stable across all conceivable slope profiles including, for example, large topographic discontinuities such as cliff faces. While the inertial formulation of the shallow water equations is appropriate for simulating the types of gradually varying water surface that typify low gradient areas such as flood plains, it may be invalid in areas of very steep terrain where supercritical flow may be expected. Under such conditions, the solver limits flow depth to the critical depth (i.e. the Froude number is not allowed to exceed 1) to ensure that simulated flow does not exceed critical flow and become supercritical. This means that in areas of very steep terrain, modeled water velocities may be reduced and depths increased, but the model will remain stable and mass conservative.

This hybrid model enables all river channels to be explicitly modeled except for rivers with upstream accumulations < 193.051 sq mi (500 sq km), since these types of reaches are often too small to be accurately predicted and are commonly well represented by the pluvial flood drivers. The pluvial model involves gridded rainfall intensities of given duration and probability inputting water directly onto the 2D grid with, importantly, 1D sub-grid channels retained so that rivers can still convey flood waters for smaller channels with catchment areas >19.03 sq mi (50 sq km) (there are large uncertainties with estimating the bathymetry of river channels with a smaller upstream area than this).

FUSE and mizuRoute model description

To produce flow simulations, the hydrological model FUSE (Clark, et al., 2008) was combined with the routing model mizuRoute (Mizukami, et al., 2016; 2021). FUSE was used to simulate runoff over a 0.25° grid, and its simulations were run through mizuRoute to convert runoff into flow and to account for all (upstream) grid cells contributing to flow along the MERIT-Hydro river network (median length around 7km). A key strength of FUSE and mizuRoute is their high computation efficiency, which is essential to dynamically simulate the large number of synthetic events this project is based on over a domain covering a large fraction of the CONUS (Contiguous United States).

FUSE is a modular framework for hydrological modelling. It is based on four conceptual models (VIC, PRMS, SACRAMENTO and TOPMODEL). The components (e.g., evaporation or baseflow generation) of these four models were taken apart and, through the FUSE framework, can be recombined to create new models and understand differences between models. Here the FUSE implementation of the VIC model, see e.g., (Newman, et al., 2021) was used. The original FUSE version documented in (Clark, et al., 2008) operates as a lumped model but the version used here is distributed, i.e., it operates on a regular grid and each grid cell contains an instance of the model. Furthermore, the FUSE version used here leverages the snow module developed by (Henn, et al., 2015). Elevation heterogeneity within each grid cell and its influence on precipitation and temperature are captured using elevation bands computed using MERIT DEM.

mizuRoute is used as routing model, i.e. to post-processes runoff outputs from FUSE to produce spatially distributed streamflow at various spatial scales from headwater basins to continental-wide river systems. mizuRoute is a vector-based model and here it uses the MERIT-Hydro river network (Yamazaki, et al., 2019). It offers two main options for river channel routing: a kinematic wave tracking routing procedure and an impulse response function – unit-hydrograph (IRF-UH) routing procedure. The former was used here.

Streamflow estimates at the boundary locations used by LISFLOOD were extracted from the output of mizuRoute.

To produce what is referred to here as “hydrological hindcast” the MSWEP2.8 (Beck, et al., 2019) precipitation and MSWX1.0 (Beck, et al., 2022) temperature products were obtained. Both MSWEP and MSWX are based on the ERA5 (Hersbach, 2023) reanalysis, which they refine by merging it with rain gauge observations and satellite rainfall data and by applying bias-correction based on records from meteorological and flow stations. Daily rainfall accumulation and temperature data for approximately 40 years (1980-2020) was extracted and aggregated over each grid cell of a 0.25° grid covering the CONUS and used to force FUSE-mizuRoute.

Non-TC Synthetic Event Set:

The non-TC synthetic event set is fundamentally centered on a derivative of the multivariate extreme value model first introduced by (Heffernan & Tawn, 2004) which aims to characterize tail dependence between a series of datasets, then use those characteristics to inform the creation of synthetic event footprints. The model, first, derives marginal distributions at a series of selected data sites through the fitting of semi-empirical distributions (Generalized Pareto fitted above a specified threshold) and then converting these to a common Laplace margin. Once on Laplace margins, tail dependence models are fitted between each data site in a pairwise fashion, resulting in a matrix of regression parameters and a corresponding matrix of residuals. Sampling from these pairwise regression models, and associated residuals, can then be used to provide event predictions across all sites under the condition that the conditional site is experiencing a threshold exceeding event. The fundamental equation behind the model is given as:

$$Y_{-i}: Y_i = \alpha Y_i + Y_i^b Z_{-i} \; for \; Y_i > u \tag{12}$$

Where $Y_{-i}$is a vector of marginal distributions excluding Y_i, u is the threshold above which dependence is modeled, α and b are vectors describing the strength of the dependence and how the dependence changes, respectively, and Z_{-i} is a vector of d-1 residuals.

This modelling framework has been used in numerous similar studies across many different environmental perils, see for instance: (Keef, et al., 2013; Quinn, et al., 2019; Wing, et al., 2020; Southworth, 2022), and (Li, et al., 2023) for similar applications to that utilized in this submission. This model draws inputs from the hydrological model (described above) and the precipitation reanalysis provided by MWSEP.

Storm Surge

To compute surge heights, SLOSH uses the following equations of motion to balance the surface forces, including surface friction:

$$\frac{\partial U}{\partial t} = -g(D+h)\left[B_r \frac{\partial(h-h_0)}{\partial x} - B_i \frac{\partial(h-h_0)}{\partial y}\right] + f(A_r V + A_i U) + C_r x_\tau - C_i y_\tau \tag{5}$$

$$\frac{\partial V}{\partial t} = -g(D+h)\left[B_r \frac{\partial(h-h_0)}{\partial y} - B_i \frac{\partial(h-h_0)}{\partial x}\right] + f(A_r U + A_i V) + C_r y_\tau - C_i x_\tau \tag{6}$$

where *U* and *V* are the components of transport, *g* is the gravitational constant, *D* is the depth of quiescent water relative to a common datum, A_r, C_i are the bottom stress terms, h is the height of water above datum, h_0 is the hydrostatic water height, *f* is the Coriolis parameter, and x_τ and y_τ are components of surface stress.

SLOSH models the propagation of storm surge through wetting and drying of grid cells. Surge is computed at the center of each grid-square, and transport is computed on each momentum point. A two-dimensional flow will exist at a momentum point if at least one of the four surrounding grid cells is wetted and higher than the highest bed depth of the four surrounding grid cells (Jelesnianski, et al., 1992).

Factors affecting inland propagation of the storm surge include the ground elevation, trees, levees, and other barriers. All these geographic features used to control, route, and impede the flow of water are considered in SLOSH basins.

Each SLOSH basin is divided into multiple grid cells. The grid is set up to give fine resolution in the primary area of interest, and coarse resolution in the boundary region. The SLOSH model requires an elevation value to be assigned to each grid cell. These elevation values determine at what storm surge height the cell will flood (Conver, et al., 2008). Momentum points are located at the vertices of the grid cell. The value of the momentum point is the maximum elevation of the four surrounding grid cells. Momentum points are used by the SLOSH model to determine the flow of water across the surface, and they are based solely on the value of the grid cell elevation, or the barrier points if they exist.

Flows and Cuts are needed in the SLOSH model to determine the movement of storm surge over land and water. There are two types of flow created by developers, 1-D flow and 1-D flow with banks. 1-D flow indicates that the flow of water, when the cell is wet, is across the entire cell. 1-D flow with banks indicates that the flow moves through a channel in the cell. A river which only covers fifty percent of a cell is a good example of 1-D flow with banks. Cuts are locations along a channel where the width of the flow with banks changes. These are entered into the database as the fraction (in tenths) of the cell width (Conver, et al., 2008).

Barriers are required when the average elevation of a cell does not represent a significant peak found within the cell. Examples include levees and barrier islands. Levees are manmade, narrow, linear structures that maintain an elevation significantly higher than that of the surrounding area. Because levees are usually narrow in comparison to a grid cell, they are frequently not reflected in the cell average. A barrier must be added to alert the SLOSH model that water will not go through the cell until it overtops the barrier height. Barrier islands behave similarly as they frequently have dunes with a peak higher than the cell average. Barriers are added at the vertex of the basin grid cells in the same location as the momentum point and will replace the momentum point value (Conver, et al., 2008)

Tree values inform the model of increased friction at the momentum points. Friction is important because it decreases wind speed and slows water flow.

HHF-1.15 Describe if and how flood model parameters are based on or depend on NFIP FIRM or other FIS data.

For parametrization of hydrological and hydraulic models, no FIRM or local FIS studies were used, but several benchmark studies were done and published comparing results with FEMA zones; see (Wing, et al., 2017; 2018), and (Bates, et al., 2021).

HHF-2 Flood Characteristics (Outputs)

A. *Flood extent and elevation or depth generated by the flood model shall be consistent with observed historical floods affecting Florida.*

As there is limited observation data for depth-based flood extents, the evaluation of modeled flood elevations, depths, and extents against historical depths was based mainly on specific control points where such data was available, including the events listed in Form HHF-1. The modeled and observed extent, water level, and discharge were compared for several historical examples, listed in Form HHF-1 A and C and in Disclosure HHF-2.3. The required map outputs are available in Form HHF-1, HHF-3, and HHF-5.

B. *Methods for deriving flood extent and depth shall be scientifically defensible and technically sound.*

For inland flood as well as for storm-surge, except for lacustrine simulation, the use of 2-dimensional hydrodynamic modeling is done with both approaches using the widely spread and highly peer-reviewed models SLOSH and LISFLOOD-FP as well as the corresponding workflow. 2-dimensional hydrodynamic modeling is the most advanced technique used even on a single-site scale in engineering practice and shifts the overall modeling uncertainties to input characteristics / boundary conditions superseding the uncertainties in the hydrodynamic simulation. Models are extensively described in the Disclosure HHF-1.14.

C. *Modeled flood characteristics shall be sufficient for the calculation of flood damage.*

A flood depth (expressed in centimeters above the earth surface) is the only hazard intensity that is subsequently linked with a damage function to calculate damage. This corresponds with the common practice used in country-wide probabilistic damage modeling as is described in (Mitchell-Wallace, et al., 2017; Meyer, et al., 2009).

Disclosures

HHF-2.1 Provide comparisons of the modeled and historical flood extents and elevations or depths for the storm events listed in Form HHF-1, Historical Event Flood Extent and Elevation or Depth Validation Maps. For any storms where sufficient data are not available, the modelling organization may substitute an alternate historical storm of their choosing. Describe how each substituted storm provides similar coastal and inland flooding characteristics to the storm being replaced.

Please refer to Form HHF-1 for the modeled vs observed comparison hazard maps and other related matrices.

The Unnamed Panhandle Storm (2013) was replaced by Hurricane Hermine (2016) because of the similarities in impacted and recorded rainfall intensities and due to the lack of available observations of extent and intensity for the 2013 event.

Tropical Storm Fay (2008) was replaced by Hurricane Ian (2022) due to the similarity in track and rainfall footprint between the storms and the lack of observed flood hazard data for Fay.

Hurricane Eta (2020) replaces the East Florida Storm (2009) due to similarities in areas impacted and recorded rainfall intensities and due to the lack of available observations of extent and intensity for the 2009 event.

HHF-2.2 Demonstrate that the inland flood model component incorporates flood parameters necessary for simulating inland flood damage and accommodates the varied geographic, geologic, hydrologic, hydraulic, and LULC conditions in Florida. Provide justification for validation using any historical events not specified in Form HHF-1, Historical Event Flood Extent and Elevation or Depth Validation Maps.

The mathematical models used are described in detail in Disclosure HHF-1.14; the used input data, input parameters, and input boundary conditions are described in multiple sections of Standard MF-1, in Standard MF-2, and in the following HHF Disclosures: HHF-1.3, HHF-1.5, HHF-1.9 and HHF-1.10. All models used are widely used tools based on a solid scientific background, are largely peer-reviewed, and the input data used do meet the source and vintage requirements. Prior to the submission, Hurricane Ian's hydrologic validation was ongoing, but due to computational limitations it was unable to be included at the time of both the initial submission and the resubmission for deficiency corrections. As such, the hydrologic validation for Ian is limited to water surface elevation and extent validation that was included in Form HHF-1 in Figure 109, Figure 110, Figure 125, and Figure 126.

IF modeled all the events named in Form HHF-1, though after an extensive search of local, state, and federal databases we were unable to find high quality validation data for the following events:

1. Hurricane Jeanne (2004)
2. Tropical Storm Fay (2008)
3. Unnamed Storm in East Florida (May 2009)
4. Unnamed Storm in Panhandle (July 2013)

The following replacement storms were selected based on similarity in track and precipitation footprint/amount to the removed storms.

1. Hurricane Frances (2004) replaces Hurricane Jeanne (2004)
2. Hurricane Ian (2022) replaces Tropical Storm Fay (2008)
3. Hurricane Eta (2020) replaces the East Florida Storm (2009)
4. Hurricane Hermine (2016) replaces the Panhandle storm (2013)

The full list then is:

1. Hurricane Andrew (Aug 1992)
2. Hurricane Frances (Sep 2004)
3. Hurricane Ivan (Sep 2004)
4. Hurricane Wilma (Oct 2005)
5. Hurricane Hermine (Sep 2016)
6. Hurricane Matthew (Oct 2016)
7. Hurricane Irma (Sep 2017)
8. Hurricane Michael (Oct 2018)
9. Hurricane Eta (Nov 2020)
10. Hurricane Ian (Sep 2022)

HHF-2.3 For each of the storm events in Form HHF-1, Historical Event Flood Extent and Elevation or Depth Validation Maps, resulting in inland flooding, provide a comparison of the modeled flood flow to recorded flow data from selected USGS or FWMD gauging stations. Provide the rationale for gauging station selections.

We worked with flow data from USGS gauges that were originally selected to perform extreme value analyses and train Fathom's Regional Flood Frequency Analysis (Smith, et al., 2015) model. These stations meet the following requirements:

1. At least 20 years of flow record
2. At least 19.03 sq mi (50 sq km) upstream area
3. Annual maximum flow (MAF) data free of outliers – determined by calculating z-score and log z-score of gauge MAFs and filtering out outliers (z-score >3)
4. Realistic MAF data in arid regions – determined by calculating mean MAF over catchment area and filtering out overly dry gauges.
5. Gauge coordinates and upstream area consistent with river network used for fluvial modeling – gauges too far from the network or with upstream area too different from that of the network were excluded.

In addition to these five requirements, all the gauges used here must be in the state of Florida. This resulted in 291 gauges being selected for the evaluation of the hydrological simulations. For all these gauges, we extracted flow simulations from the FUSE-mizuRoute hindcast driven by MSWEP (Beck, et al., 2019) and MSWX (Beck, et al., 2022) for each historical TC listed in Disclosure HHF-2.2, except for Ian. We did not evaluate the runs for Ian because the hindcast finished in 2020 and hence Ian is not covered by the hindcast. This leads to a total of 9 TCs for which hydrological simulations were evaluated using a combination of maps showing the event spatial pattern and hydrographs illustrating the temporal dynamic of the event (Figure 30 to Figure 38).

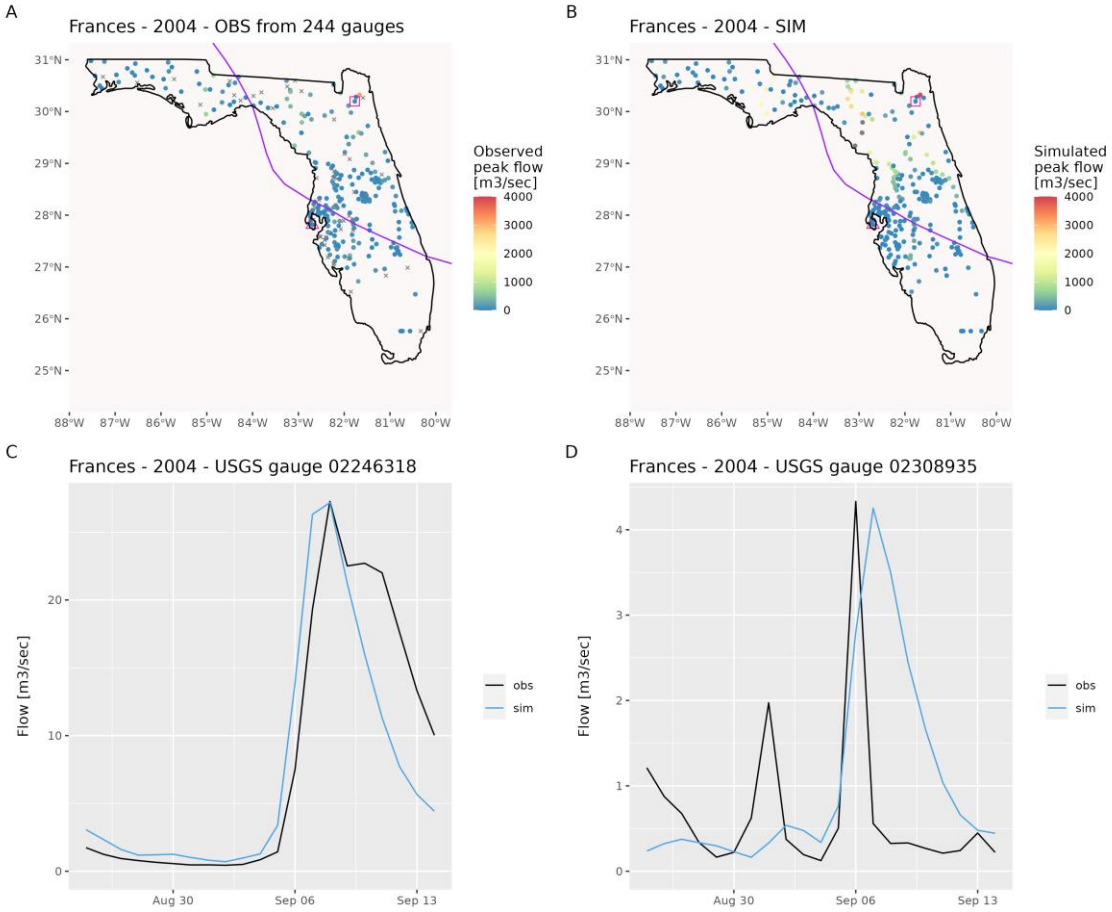

Figure 30: Evaluation of the flow simulation for tropical cyclone Frances (2004): A) Observed peak flow, the total number of gauges with available data is indicated in the title, gauges with no data are indicated by a cross, the TC track is shown in purple; B) Simulated peak flow at all 291 gauges, the TC track is shown in purple; C) and D) example hydrographs, observed and simulated flow. Gauge locations are marked with a square (for the location in example C), and a triangle (for the location in example D).

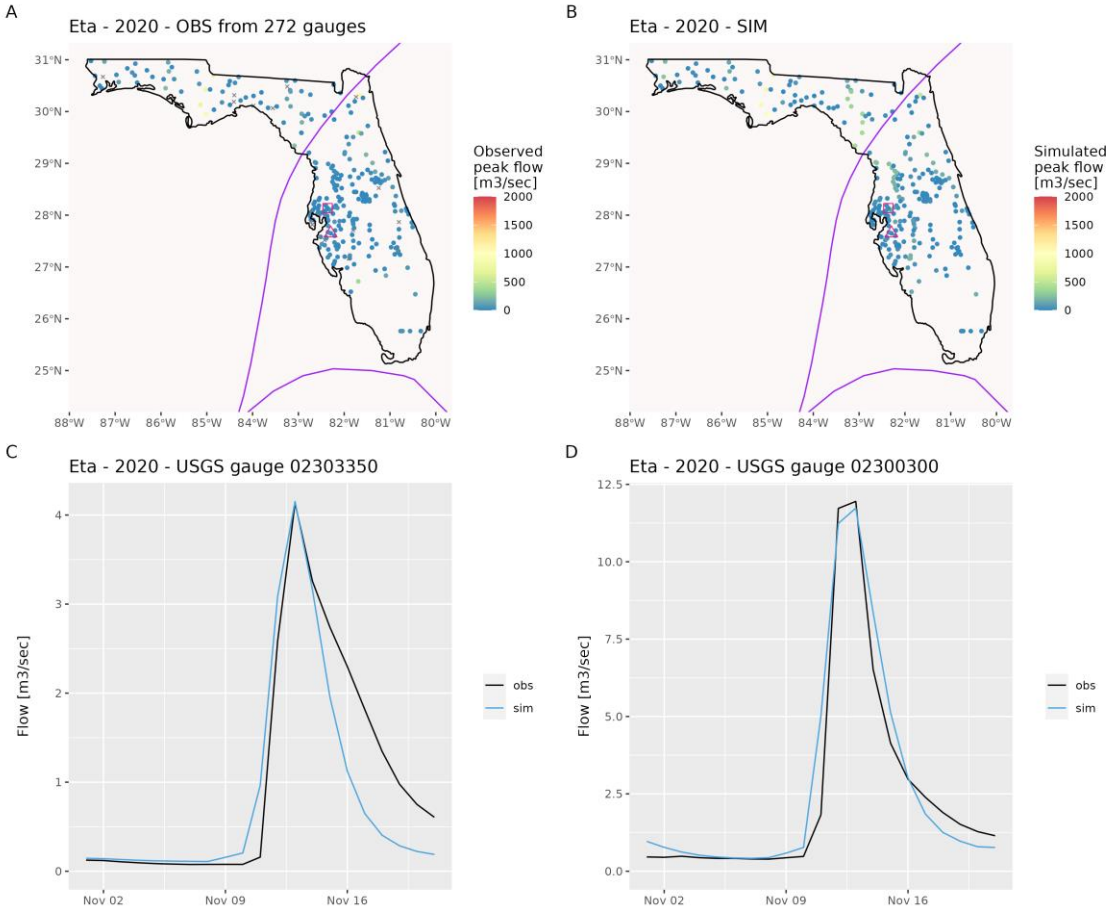

Figure 31: Evaluation of the flow simulation for cyclone Eta (2020): A) Observed peak flow, the total number of gauges with available data is indicated in the title, gauges with no data are indicated by a cross, the TC track is shown in purple; B) Simulated peak flow at all 291 gauges, the TC track is shown in purple; C) and D) example hydrographs, observed and simulated flow. Gauge locations are marked with a square (for the location in example C), and a triangle (for the location in example D).

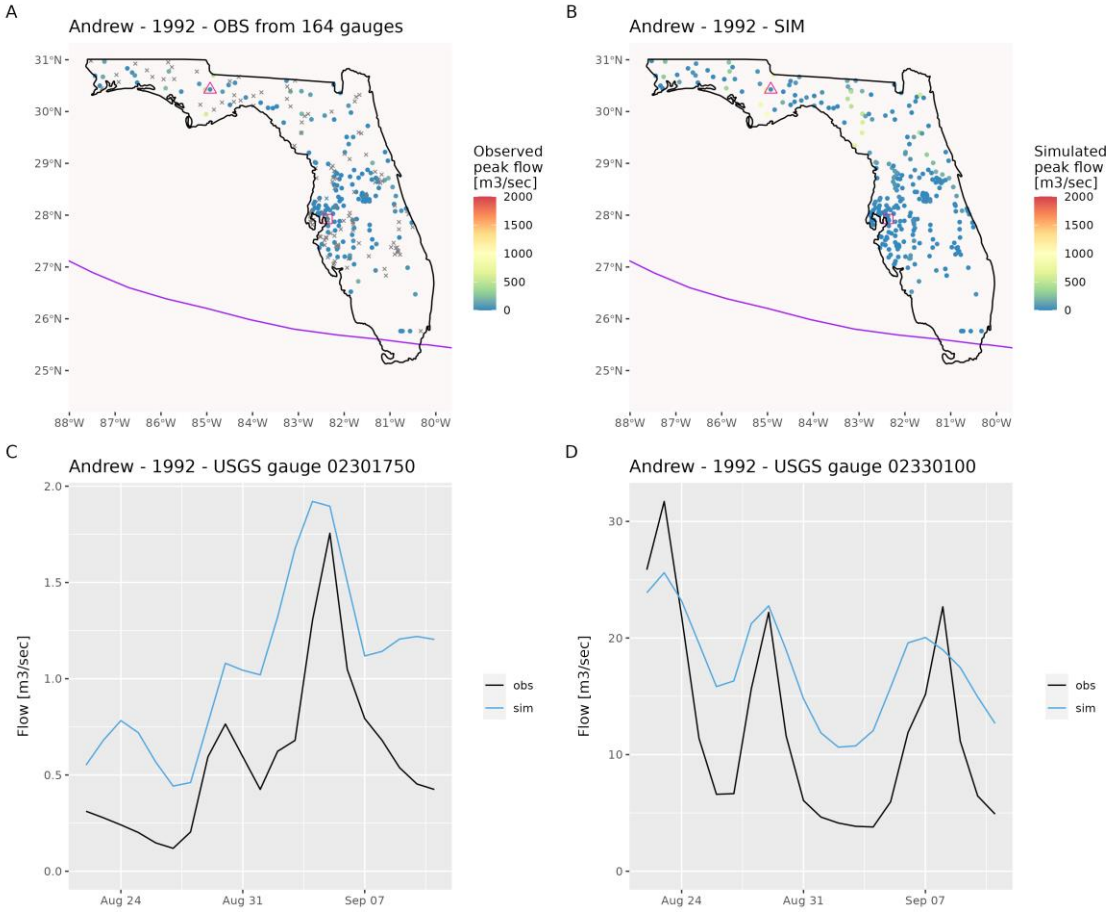

Figure 32: Evaluation of the flow simulation for cyclone Andrew (1992): A) Observed peak flow, the total number of gauges with available data is indicated in the title, gauges with no data are indicated by a cross, the TC track is shown in purple; B) Simulated peak flow at all 291 gauges, the TC track is shown in purple; C) and D) example hydrographs, observed and simulated flow. Gauge locations are marked with a square (for the location in example C), and a triangle (for the location in example D).

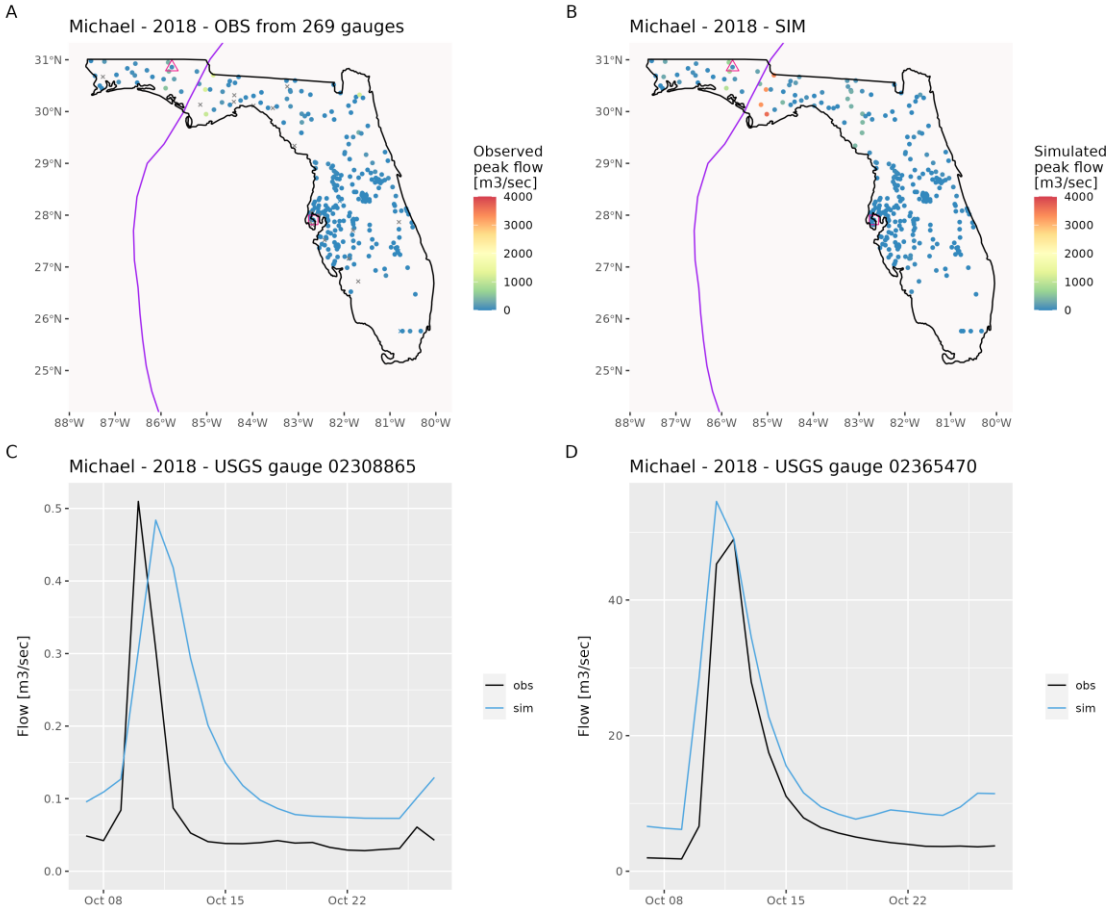

Figure 33: Evaluation of the flow simulation for cyclone Michael (2018): A) Observed peak flow, the total number of gauges with available data is indicated in the title, gauges with no data are indicated by a cross, the TC track is shown in purple; B) Simulated peak flow at all 291 gauges, the TC track is shown in purple; C) and D) example hydrographs, observed and simulated flow. Gauge locations are marked with a square (for the location in example C), and a triangle (for the location in example D).

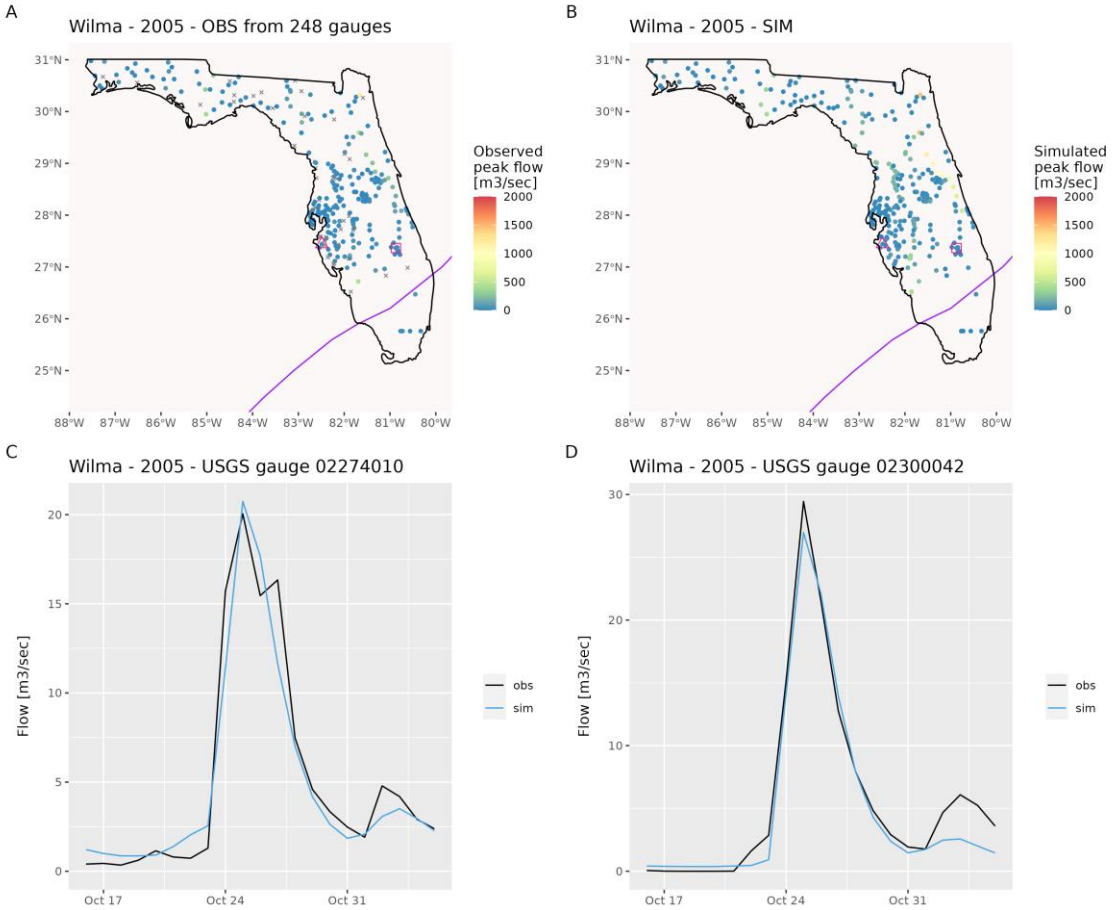

Figure 34: Evaluation of the flow simulation for cyclone Wilma (2005): A) Observed peak flow, the total number of gauges with available data is indicated in the title, gauges with no data are indicated by a cross, the TC track is shown in purple; B) Simulated peak flow at all 291 gauges, the TC track is shown in purple; C) and D) example hydrographs, observed and simulated flow. Gauge locations are marked with a square (for the location in example C), and a triangle (for the location in example D).

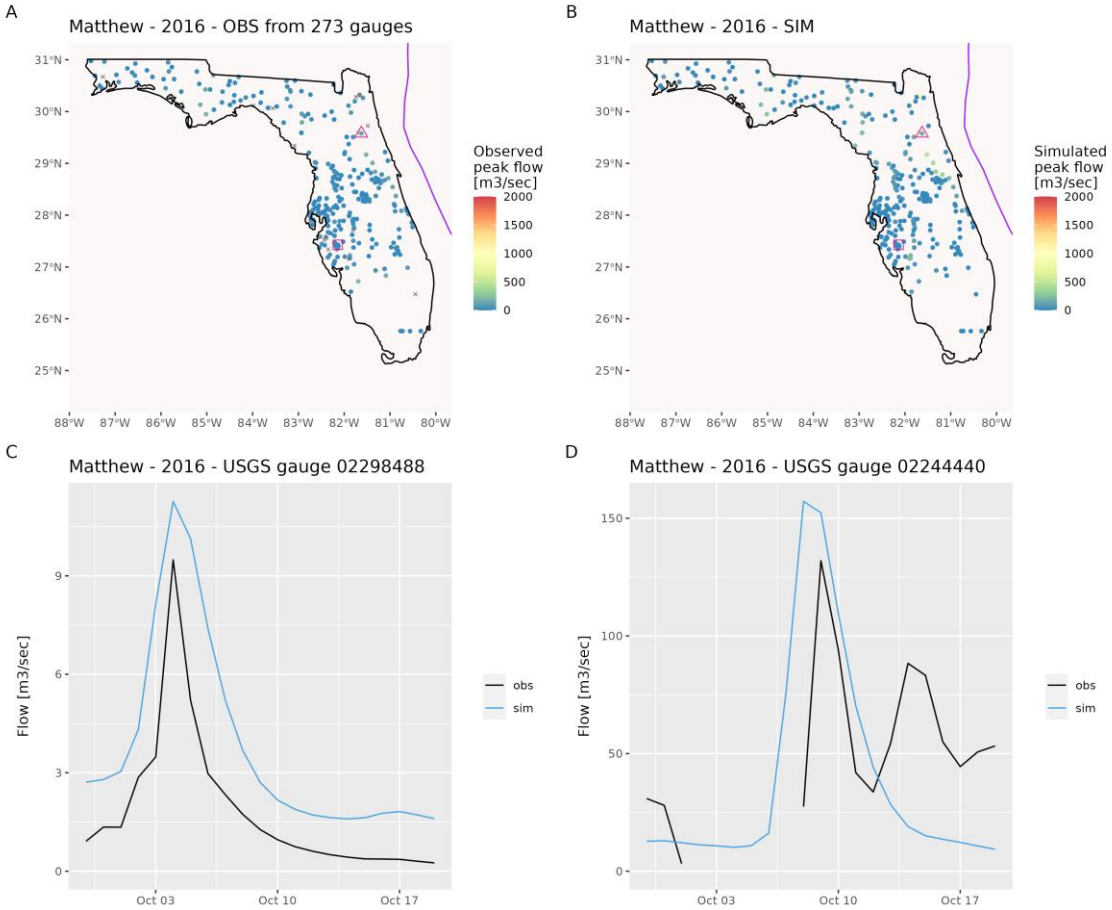

Figure 35: Evaluation of the flow simulation for cyclone Matthew (2016): A) Observed peak flow, the total number of gauges with available data is indicated in the title, gauges with no data are indicated by a cross, the TC track is shown in purple; B) Simulated peak flow at all 291 gauges, the TC track is shown in purple; C) and D) example hydrographs, observed and simulated flow. Gauge locations are marked with a square (for the location in example C), and a triangle (for the location in example D).

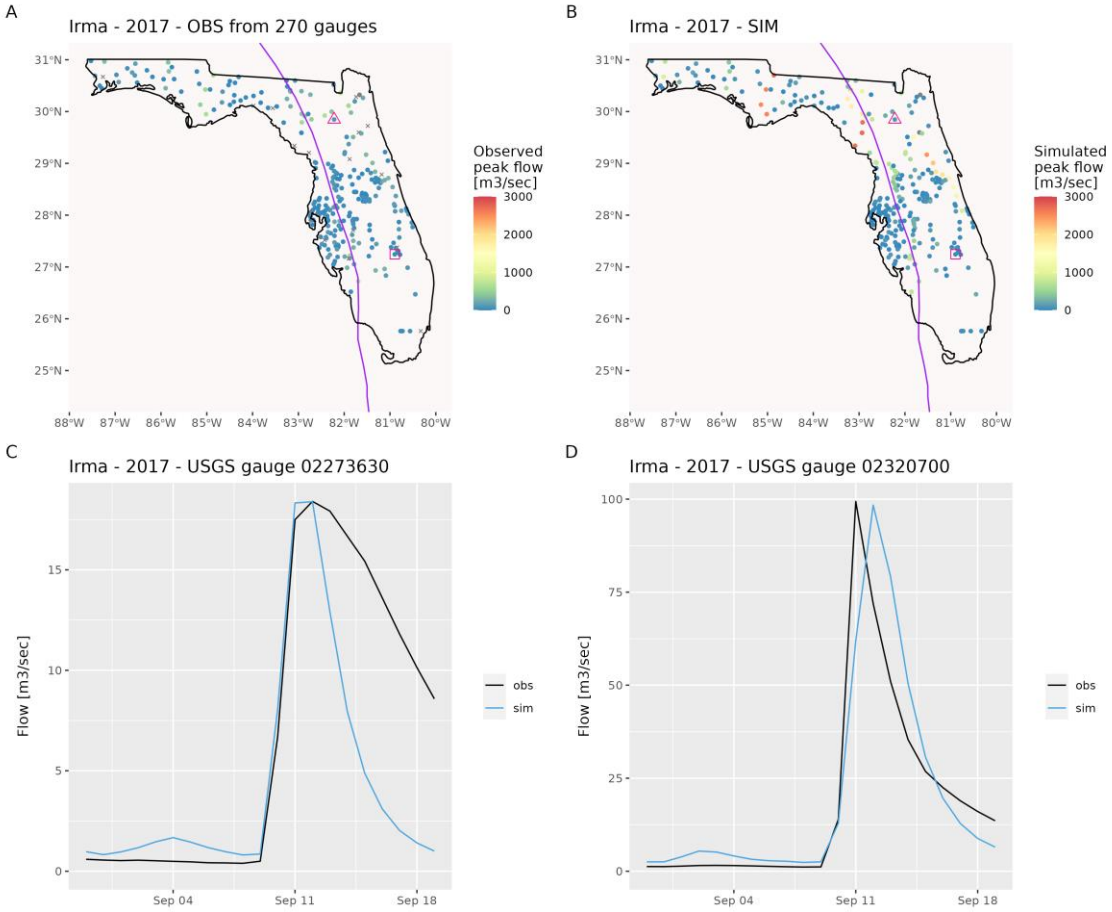

Figure 36: Evaluation of the flow simulation for cyclone Irma (2017): A) Observed peak flow, the total number of gauges with available data is indicated in the title, gauges with no data are indicated by a cross, the TC track is shown in purple; B) Simulated peak flow at all 291 gauges, the TC track is shown in purple; C) and D) example hydrographs, observed and simulated flow. Gauge locations are marked with a square (for the location in example C), and a triangle (for the location in example D).

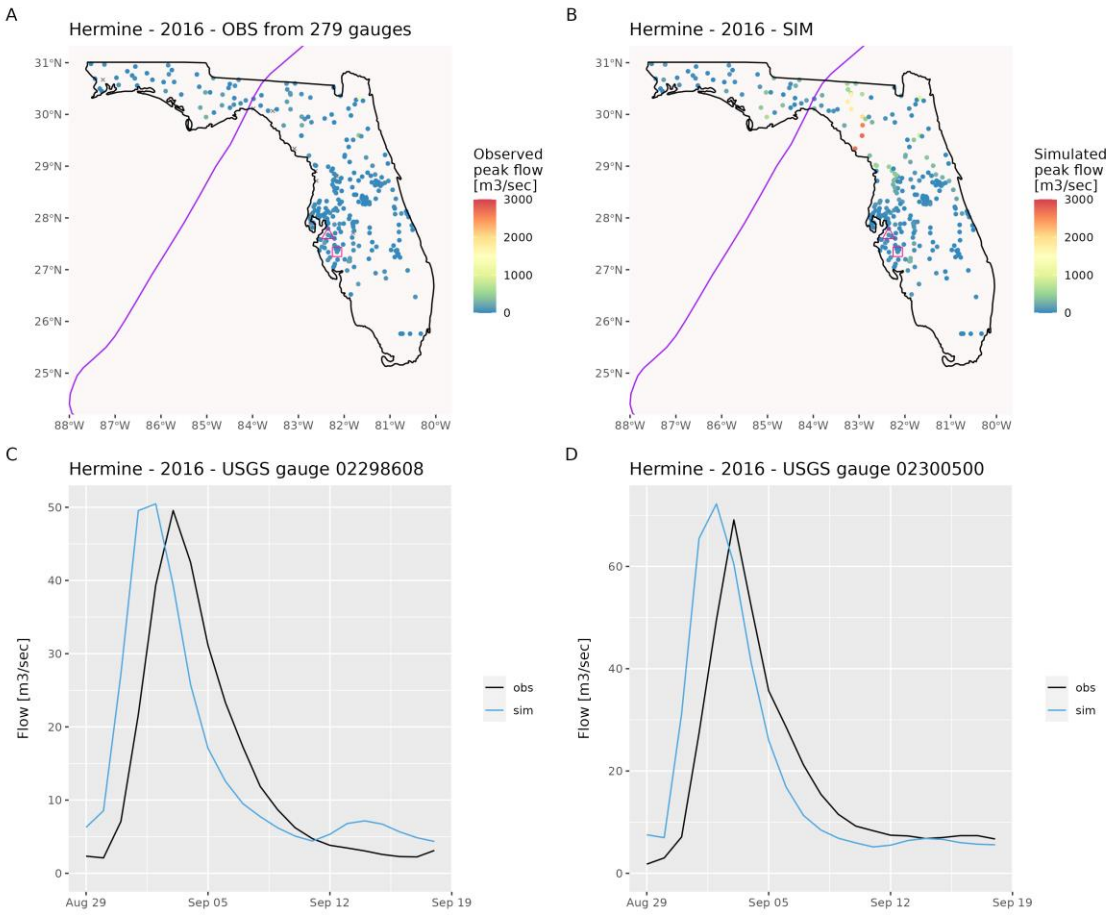

Figure 37: Evaluation of the flow simulation for cyclone Hermine (2016): A) Observed peak flow, the total number of gauges with available data is indicated in the title, gauges with no data are indicated by a cross, the TC track is shown in purple; B) Simulated peak flow at all 291 gauges, the TC track is shown in purple; C) and D) example hydrographs, observed and simulated flow. Gauge locations are marked with a square (for the location in example C), and a triangle (for the location in example D).

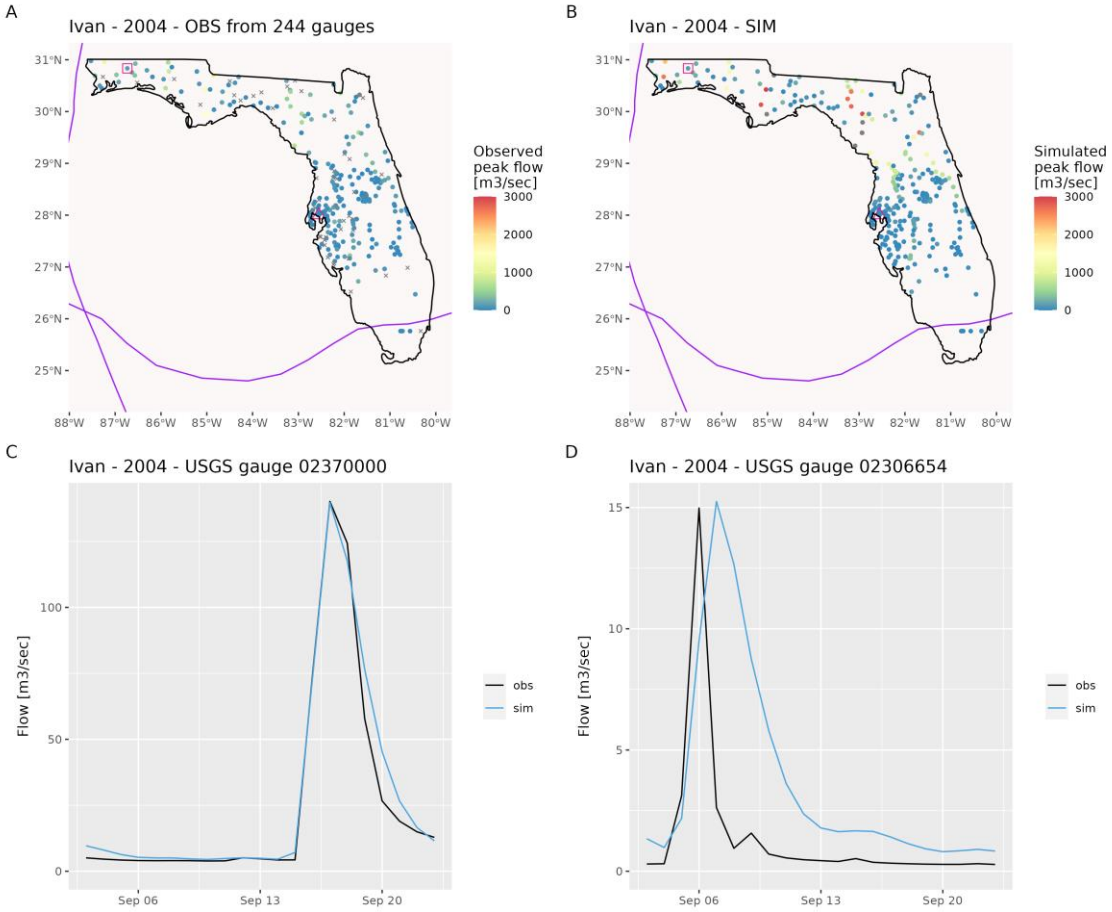

Figure 38: Evaluation of the flow simulation for cyclone Ivan (2004): A) Observed peak flow, the total number of gauges with available data is indicated in the title, gauges with no data are indicated by a cross, the TC track is shown in purple; B) Simulated peak flow at all 291 gauges, the TC track is shown in purple; C) and D) example hydrographs, observed and simulated flow. Gauge locations are marked with a square (for the location in example C), and a triangle (for the location in example D).

In addition to evaluating the hydrological simulations for individual TC events, we evaluated them across the events. We asked if the model can correctly rank the 9 events and used the Spearman rank correlation coefficient to quantify this. For each gauge, we extracted the observed and simulated peak flow for all events for which observations are available. Then we computed the rank correlation coefficient for each gauge. A perfect match between the observed and simulated ranks leads to a correlation of 1. Figure 39 shows that high correlations are achieved across Florida, with a median correlation across all gauges of 0.79. This illustrates the ability of the hydrological model to differentiate between events and correctly capture a wide range of peak flows across a wide range of river sizes.

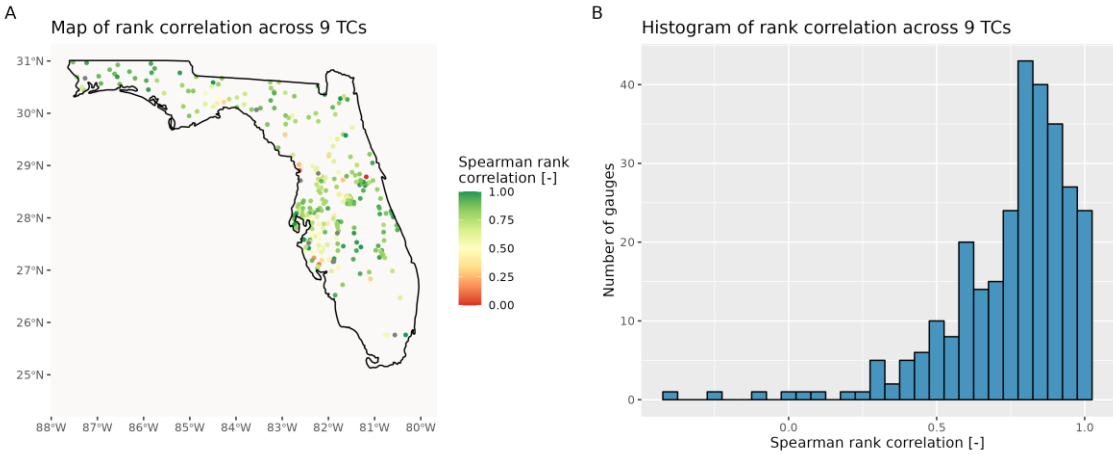

Figure 39: Spearman rank correlation computed for each gauge across all 9 tropical cyclones and shown as A) a map and B) a histogram.

HHF-2.4 ***Identify all hydrological and hydraulic variables that affect the flood extent, elevation, depth, and other flood characteristics. Provide the units of these variables.***

All sub-perils (storm surge, fluvial and pluvial components of inland floods, excluding the lacustrine) are solved using 2-dimensional hydrodynamic modeling using St. Venant's equation. The following variables are included in the calculation of inland flood:

- Discharge [$m^3.s^{-1}$] for inland flood (fluvial simulation),
- Rainfall [$mmhr^{-1}$] for pluvial inland flood simulation
- Topography [m] and slope [%], however in the numerical solvers of partial differential equations it is taken from the computational mesh placed on the DTM cells.
- Hydraulic roughness – a Manning's "n" [$s.m^{-1/3}$] is taken and adjusted from the original combination of Chezi/Manning's equation to 1- and 2-dimensional application.

The variables for the storm surge portion of the model are listed below with detailed description available in Disclosure MF-2.1.

- Topography [m]
- Central Pressure [mb]
- Radius of Maximum Winds [km]
- Storm Track (Latitude and Longitude at 6hr interval) [degree]
- Surface drag coefficient [$ft^2.s^{-2}$]
- Vertical Eddy Viscosity Coefficient [$ft2.s^{-1}$]
- Bottom Slip Coefficient [$ft.s^{-1}$]
- Wind Friction Coefficients ks, kn [$mph^{-1/2}$]

HHF-2.5 ***For inland flood modeling, describe if and how the flood model accounts for flood velocity, flood duration, flood-induced erosion, foodborne debris, and contaminated floodwaters.***

The hydraulic model (LISFLOOD-FP) simulates depth, flow velocity (in x- and y- directions), and flood duration dynamically, but only flood depth is used as hazard intensity when evaluating flood loss. No flood-induced erosion or flood-borne debris are included in the actual hydrodynamic calculation, nor are they included later in the loss calculation process.

HHF-2.6 ***Describe the effect of any assumptions or calculations relating to initial and boundary conditions on the flood characteristics.***

The final flood hazard maps were developed with parameters and initial boundary conditions based on the best current practice, expert judgement, and several peer-reviewed publications (Sampson, et al., 2015; Smith, et al., 2015; Wing, et al., 2017; 2018). The sensitivity is partially tested, with results shown in Disclosure HHF-4.1.

The initial conditions of the hydraulic model are limited to applying a within-channel baseflow to the sub-grid channels that is less than any of the modeled peak flows simulated, meaning it does not impact on the modeled flood extents. Further information on the methodologies applied to calculate the boundary conditions are provided in Disclosures MF-2.6 and MF-5.2

HHF-2.7 Describe and justify the appropriateness of the databases and methods used for the calibration and validation of flood extent and elevation or depth.

In the inland flood model; the calibration and validation of inland flood hazard was initially performed by Fathom with methodology and results available in (Wing, et al., 2017; 2018). Further validation of flood extents was performed by the Aon Impact Forecasting team using the following datasets and methods:

- NFIP FIRM – for RPs of 1 in 100 (zones V, VE, A, AE, A1-30, AH, AO, AR, IN) and 1 in 500 (Zones: B, X500)
  - Flood extent agreement between the most recently available NFIP maps and the corresponding Fathom return period maps were compared using the methods set forth by (Millones, 2011). This comparison provides no indication of flood hazard depth. Larger deviations were identified on areas with older date of NFIP version, often with limited contribution of pluvial hazard.
- Local FIS study, mainly to determine and check the flood protection measures but also flood hazard in close proximity to the particular measure.
  - The same limitations as above apply for FIS reports.
- The ICEYE dataset (and other satellite derived flood hazard map) was used to validate the historical flood footprint of Hurricane Ian, as it was a storm with important inundation observed during the model development process.
  - The ICEYE product provides flood depth information after the captured inundation extent is subtracted from a DTM, but several limitations of this product were observed. In some areas the flood extent was insufficiently captured (likely caused by the satellite imagery being taken long before or after the flood's peak). While this limitation dealt with insufficient flood capture, there were also observations of different areas where inundation appeared even though it was obvious that no flooding had occurred (USGS data appearance), likely caused by incorrect satellite extent interpretation due to high soil moisture.
- In the Inland flood model, validation of historical flood extent and elevation/depth involves utilizing high-water mark data and gauge water levels from reliable sources like the United States Geological Survey (USGS), the National Oceanic and Atmospheric Administration (NOAA), and the Federal Emergency Management Agency (FEMA). It is essential to recognize certain limitations, such as the limited availability of inland flood observations for all historical events and potential inaccuracies associated with older observation data. Despite these challenges, the comparisons of flood extent and elevation/depth with observation data and FEMA return period maps are detailed in Forms HHF-1 to HHF-5. These constraints emphasize the necessity of interpreting the model's accuracy considering both data availability and potential discrepancies related to the age of the observation data.

In the storm surge model, the historical storm surge extent and modeled elevation or depth were validated against ADCIRC footprints and observation data obtained from the United States Geological Survey (USGS), the National Oceanic and Atmospheric Administration (NOAA), the Federal Emergency Management Agency (FEMA), the World's Storm Surge Data Center (SURGEDAT), and published literatures. The comparison of flood extent and

elevation/depth with observation data and FEMA return period maps can be found in Disclosure MF-4.1, Disclosure MF-5.3, and Forms HHF-1~HHF-5.

The modeled historical storm surge extent is mainly validated using the ADCIRC footprint (Coastal Emergency Risks Assessment , 2023). The ADCIRC model is a high-resolution two-dimensional, time-dependent hydrodynamic circulation model (Luettich & Westerink, 2004; Westerink, et al., 2008). It functions as a highly developed computer program for solving equations for a moving fluid on a rotating earth. The ADCIRC modeling system has been used for long-term planning and design, evaluation of surge mitigation systems, and operational forecasting (Vijayan, et al., 2021; Massey, et al., 2022).

The modeled historical storm surge elevation or depth is validated against observed peak storm surge height records or high-water marks (HWM) data obtained from various sources like the United States Geological Survey (USGS), the National Oceanic and Atmospheric Administration (NOAA), World's Storm Surge Data Center (SURGEDAT), Federal Emergency Management Agency (FEMA) studies, and other published literatures and reports. During and following large storm events, the USGS specialist collects streamflow and additional data (including storm tide, wave height, HWM, etc.) to aid in documenting and validating the major storm events. The NOAA Storm Event Database contains records of the occurrence of storms and their associated significant meteorological features, such as inundation locations and depths. SURGEDAT is a global storm surge data center that maintains surge maps and peak surge height data for major historical storm surges. For older storms, limited records or observation data is available, so the modeled footprint is validated against reports from FEMA, NOAA, the US Army Corps of Engineers, and other literatures.

For stochastic events, the modeled return period surge maps are validated against NFIP extents. Detailed comparison maps are shown in Form HHF-3. The modeled stochastic storm surge elevation exceedance probabilities at several NOAA tidal station locations were compared with the observed frequencies (NOAA; Tides & Currents, 2023a). The validation of the return period storm surge elevation at several NOAA tidal stations are shown in Disclosure MF-5.3.

HHF-2.8 Describe any variations in the treatment of the flood model flood extent and elevation or depth for stochastic versus historical floods and justify this variation.

There is no difference in the treatment of flood extent or elevation between historical and stochastic events for the IF US Flood Model. This concerns both stochastic (TC and non-TC) models and sub-perils: fluvial, pluvial, and surge. The only practical difference might be in using observed data in historical event processing as they are expected to be of higher quality than the hydrological model outputs; however, the hydrological and hydraulic connectivity and workflow discussed in Disclosures HHF-1.2, HHF-1.12, and HHF-1.13 remains exactly the same as in stochastic events generation.

HHF-2.9 Identify whether flood characteristics are based on or depend on NFIP FIRM or other FIS data.

Similarly, as in the Disclosure HHF-1.15, no flood characteristics based on or dependent on NFIP FIRM or FIS data were natively used. Several benchmark studies were done and published comparing results with FEMA zones, see (Wing, et al., 2017; 2018).

HHF-2.10 Provide a completed Form HHF-1, Historical Event Flood Extent and Elevation or Depth Validation Maps. Provide a link to the location of the form [Form HHF-1: Historical Coastal and Inland Event Flood Extent and Elevation or Depth Validation Maps].

The Form HHF-1, Historical Coastal and Inland Event Flood Extent and Elevation or Depth Validation Map (items A – H) is completed and presented in its respective section under a hyperlink above.

HHF-2.11 Provide a completed Form HHF-4, Inland Flood Characteristics by Annual Exceedance Probability. Provide a link to the location of the form [Form HHF-4: Inland Flood Characteristics by Annual Exceedance Probability].

The Form HHF-4, Inland Flood Characteristics by Annual Exceedance Probability (items A – C) are completed and presented in its respective section under a hyperlink above.

HHF-2.12 Provide a completed Form HHF-5, Inland Flood Characteristics by Annual Exceedance Probabilities (Trade Secret Item), if not considered as Trade Secret. Provide a link to the location of the form [Form HHF-5: Inland Flood Characteristics by Annual Exceedance Probabilities (Trade Secret Item)].

The data for the Trade-Secret Items of HHF-5, Inland Flood Characteristics by Annual Exceedance Probabilities (items A and B) is completed and presented in its respective section under a hyperlink above.

HHF-3 Modeling of Major Flood Control Measures

A. *The flood model's treatment of major flood control measures and their performance shall be consistent with available information and current state-of-the-science.*

Besides the dataset available in the USACE's National Levee Database, which is applied to the hydraulic model output, the availability of any other consolidated datasets across Florida is not known. Some information can be obtained from county or commune level, but its use is limited due to the fact that many measures have a much wider purposes than flood protection, and extraction of such information for the flood loss model used is not simple. Rigorous efforts were taken to process this information in the key exposed areas as described in Disclosure HHF-3.5. Additionally, in the fluvial component of the model, the effect of many of such measures is bypassed by the sub-grid model implemented in the LISFLOOD-FP model.

B. *The modeling organization shall have a documented procedure for reviewing and updating information about major flood control measures and if justified, shall update the flood model flood control databases.*

As the new implementation of new or existing flood protection measures is a common task, the model can be updated in several simple steps described below; however, the exact process depends on the flood protection type, which can be:

- Technical flood protection measures (flood walls and levees)
- Flood volume mitigation measures (retention measures: reservoirs, polders)

The HazardCase table (table(s) in model database holding the hazard information) update requires knowledge of a protected polygon and its standard of protection (the hydrological return period the measure is expected to withstand). This is converted to model cell IDs (FineCellIDs), whose records are subsequently updated.

For the Flood Volume mitigation measures, the reduction of discharge return period needs to be identified along with segments that are affected by such change. The return periods on those segments are subsequently adjusted in the EventDefinition (table(s) in model database holding the event set information).

C. *Treatment of the potential failure of major flood control measures shall be based upon current scientific and technical literature, empirical studies, or engineering analyses.*

As described in more detail in Disclosure HHF-3.4, the model does not simulate flood protection failure; rather, it only simulates its overtopping in case the event set return period is exceeded for inland flood model or water level exceed levee height for storm surge model, and, in such a case, the originally modeled flood hazard is assumed.

Disclosures

HHF-3.1 List the major flood control measures incorporated in the flood model and the sources of all data employed.

Storm Surge

The National Levee Database (NLD) is used to incorporate hurricane levees in the SLOSH basins. There are two hurricane levees in Florida, and the levee heights are added to the SLOSH basin files to serve as one type of barrier. The barrier is used to alert the SLOSH model that water will not go through the cell until it overtops the barrier height. The two levee systems in Florida are:

The Fort Pickens Seawall in Escambia County is located at the western end of Santa Rosa Island in Pensacola Beach, with a maximum height of 9 feet (NAVD88), a total length of 1.28 miles, and a leveed area of 0.12 square miles.

The L-31 East levee system in Miami-Dade County along the Biscayne Bay coastline, with a maximum height of 9.50 feet (NAVD88), a total length of 18.85 miles, and a leveed area of 54.56 square miles.

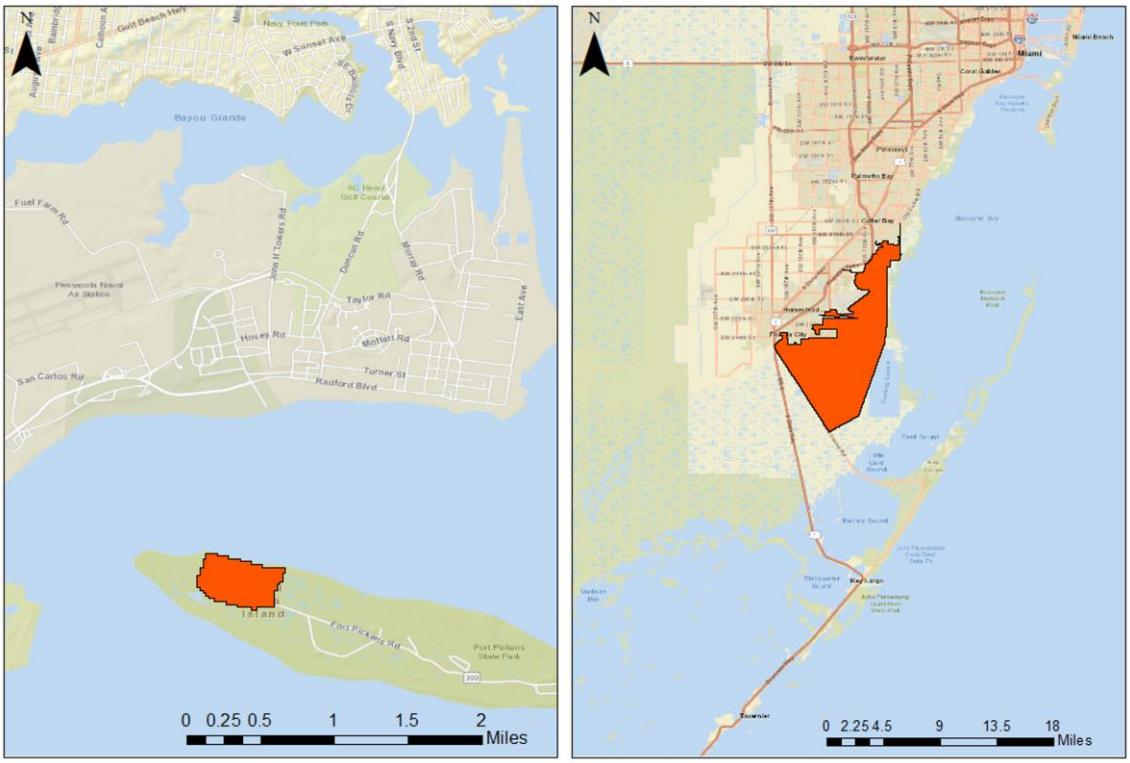

Figure 40: Location of the two levee systems in Florida: (left) Fort Pickens Seawall; and (right) L-31 East levee system.

Inland Flood

For the inland flood portion of the model, the core of the flood protection information comes from the National Levee Database (NLD) managed by the US Army Corps of Engineers https://levees.sec.usace.army.mil/ (US Army Corps of Engineers, 2007) with a 2020 vintage. From here the location of protected land is taken, along with the SoP (Standard of Proection) of designed structures.

Apart from the NLD, an intensive internal survey on the county level, and on a more detailed level for major cities in Florida, was conducted to isolate various flood protections that the NLD may exclude. To incorporate these additional flood protections, relatively high exposure regions surrounding major waterbodies, as derived from the NHD database (Buto, 2020), were scrutinized across the state of Florida. The assessment involved the utilization of LiDAR-based high-resolution Digital Elevation Models (DEM) along with satellite imagery to look for elevated defensive structures.

In instances where defensive structures exhibited visibility within the elevation dataset and optical imagery yet remained absent from the National Levee Database, a manual intervention was undertaken to introduce the requisite defenses in alignment with the prevailing elevation patterns. The Standard of Protection for flood defense structures was estimated by referencing nearby or similar local-scale defenses and based on engineering standard practices, providing an informed estimation aligned with the perceived flood risks in their respective areas.

HHF-3.2 Describe the methodology to account for major flood control measures in the flood model and indicate if these measures can be set (either to on or off) in the flood model.

For the storm surge portion of the model, the flood control measures are modeled as barriers in the SLOSH basin. Barrier heights are added at the vertex of the SLOSH basin grid cells to alert the SLOSH model that water will not go through the cell until it overtops the barrier height. Since barrier heights are pre-determined and included in the SLOSH basin files, it is not possible to toggle them on or off.

For inland flood, the defended areas within a fluvial or pluvial hydrographic zone are assigned a standard of protection associated with a given return period based on available data from federal, state, and local studies. When the return period of flow within a hydrographic zone for a given event is below the return period of the standard of protection, no loss will be calculated. When the return period of flow within a hydrographic zone for a given event exceeds the return period of the standard of protection, it is assumed that the defenses will fail, and the loss will be calculated for exposures within the flooded cells. Because these calculations are done before loss model run time, it is not possible to toggle flood defenses on or off.

For pluvial simulation, the effect of man-made drainage system can be assumed as flood protection; these parameters are reflected in the rainfall infiltration rates and are shown in Disclosure HHF-1.10 in Table 13.

HHF-3.3 *Describe if and how major flood control measures that require human intervention are incorporated into the flood model.*

The storm surge portion of the model simulates levee overtopping through adding barrier heights in the SLOSH basin files. However, the flood control measures that require human interventions (e.g., placing sandbags, controlling flow, or shutting down dams) are not considered.

The inland flood portion of the model assumes failure of structural flood barriers and storm water drainage systems when they are overtopped, but it does not consider human intervention into the strengthening (i.e. sandbagging) unless it propagates into regional frequency analysis used to derive discharge or rainfall used in the hydraulic simulation, nor the strategic failure (i.e. intentional levee breaching) of flood defense infrastructure.

HHF-3.4 *Describe and justify the methodology used to account for the potential failure or alteration of major flood control measures in the flood model and if the level of failure can be adjusted in the flood model.*

In the flood protection data set, each polygon is assigned a standard of protection (SoP) which equals the hydrological return period (in years) to which it is designed to withstand flooding.

For any stochastic or historical event, the hydrological return period is assigned to that particular hazard unit, the SoP is compared the RP if the

$$RP_{event}(U) \leq SoP \overset{event}{\Longrightarrow} D^{afterSoP}(U) = 0 \tag{13}$$

$$RP_{event}(U) > SoP \overset{event}{\Longrightarrow} D^{afterSoP}(U) = D^{beforeSoP}(U) \tag{14}$$

Where $RP_{event}(U)$ is a hydrological return period [years] provided for each Unit (U) [-]; SoP standard of protection [years], $D^{x}(U)$ is the inundation depth [centimeters] before or after the SoP was applied. The examples results are shown in Disclosure HHF 3.5.

HHF-3.5 *Provide an example of the flood extent and elevation or depth showing the potential impact of a major flood control measure failure.*

Figure 41 comprises of multiple map panels portraying examples of some levee systems in Florida. Each panel consists of three maps, with the first map providing a satellite imagery overview of the respective levee. The second map displays the same levee with a defended flood map having a return period one below the corresponding overtop threshold. In contrast, the third map reveals the impact of flooding without the levee, illustrated by an undefended flood map. This sequence offers a perspective on the impact of various levee failures on the fluvial flood rasters. Same cases but shown in different parts of Florida are shown in Figure 41, Figure 42 and Figure 43.

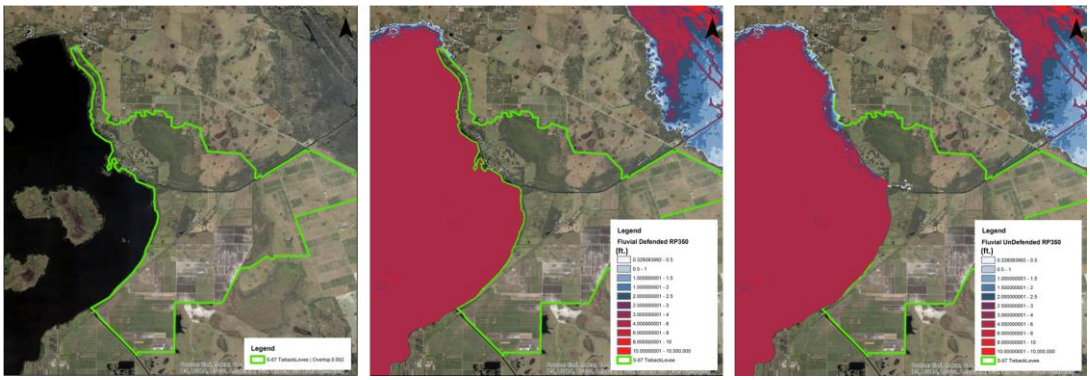

Figure 41: S-67 Tieback Levee: Levee over satellite imagery(left), levee with defended 350-year flood map (center) & levee with undefended 350-year flood map(right)

Figure 42: Abruckle Creek Levee: Levee over satellite imagery(left), levee with defended 40-year flood map (center) & levee with undefended 40-year flood map(right)

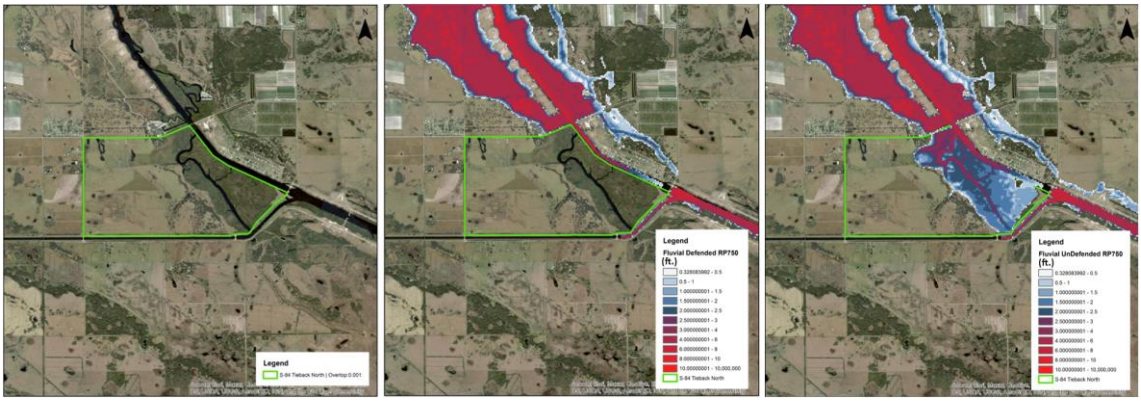

Figure 43: S-84 Tieback North Levee: Levee over satellite imagery(left), levee with defended 750-year flood map (center) & levee with undefended 750-year flood map(right)

Figure 44 also comprises of three figures showing the L-31 East levee system in the storm surge model (left), the surge inundation footprint without levee failure (middle) and the surge footprint with levee overtopping (right).

Figure 44: S-84 L-31 East Levee: Levee over satellite imagery(left), surge footprint without levee failure (center) & surge footprint with levee failure (right).

HHF-4 Logical Relationships Among Flood Parameters and Characteristics

A. At a specific location, water surface elevation shall increase with increasing terrain roughness at that location, all other factors held constant.

As shown in Figure 47, all locations demonstrate an increased peak water surface elevation with increased terrain roughness. This is expected due to the model solver resolving a form of the shallow water equations, which takes roughness as a parameter, so with everything else remaining constant roughness will increase water surface elevation. At the start of some simulations, water surface elevation is reduced since flow at the assessment location is reduced at the start of simulations due to the increased roughness upstream increasing the time to peak of the flow reaching the assessment point.

B. Rate of discharge shall increase with increase in steepness in the topography, all other factors held constant.

As shown in Figure 48, all locations demonstrate an increased peak discharge (in some cases on the falling limb a lower discharge is seen; this is due to the full hydrograph passing through the location). This is expected due to the model solver resolving a form of the shallow water equations, which evaluates water surface slope between cells, so with everything else remaining constant an increased topographic slope, and hence water surface slope, will increase the rate of discharge.

C. Rate of discharge shall increase with increase in imperviousness of LULC, all other factors held constant.

As shown in Figure 49, increased imperviousness is shown to increase the peak discharge rate. This is expected since increasing imperviousness reduces infiltration. This is represented by a comparative increase in rainfall rate modeled (as by default the rainfall input accounts for infiltration). This causes additional run-off, which in channel is seen as a clear increase in discharge.

D. Inland flood extent and depth associated with riverine and lacustrine flooding shall increase with increasing discharge, all other factors held constant.

As shown in Figure 50, Figure 51, Figure 52, Figure 53 and Figure 54 without changing other parameters, increasing discharge will increase water surface elevation and inundation extents, as to resolve the equations used within the solver without changing other input parameters, to balance additional flow, either flooding must be deeper or a larger extent (which provides a shallower water surface slope).

E. The coincidence of storm tide and inland flooding shall not decrease the flood extent and depth, all other factors held constant.

The inland and coastal flooding is calculated within separate models and therefore are not impacted by each other.

Disclosures

HHF-4.1 Provide a sample graph of water surface elevation and discharge versus time associated with inland flooding for modelling-organization-defined locations within each region in Florida identified in Figure 1. Discuss how the flood characteristics exhibit logical relationships.

Table 14 below shows the parameters of locations selected for sensitivity simulations selected in such a way as to provide reference behavior for required checks of using the hydraulic model (LISFLOOD-FP).

The range of parameters listed, and some additional discussion is provided at the end of Disclosure HHF-4.2.

Table 14: Information for selected assessment locations

Location	Region	County	Watercourse	Location (lat, lon)
#1	Panhandle	Santa Rosa	Blackwater River	30.624, -87.035
#2	North Florida	Clay	Black Creek	30.080, -81.761
#3	Southwest Florida	Hillsborough	Alafia River	27.857, -82.269
#4	East Florida	St. Lucie	Tributary of North Fork Saint Lucie River	27.402, -80.352
#5	Southeast Florida	Miami-Dade	Little River Canal	25.853, -80.197

Locations listed in Table 14 were selected to be suitable to perform the analysis requested and to represent large variety of conditions in Florida. In some cases, they also represent the areas that are challenging for hydraulic simulation, but they should serve well as basis for additional discussion. Figure 45 shows their location in Florida, individually, they are shown in detail in Figure 46.

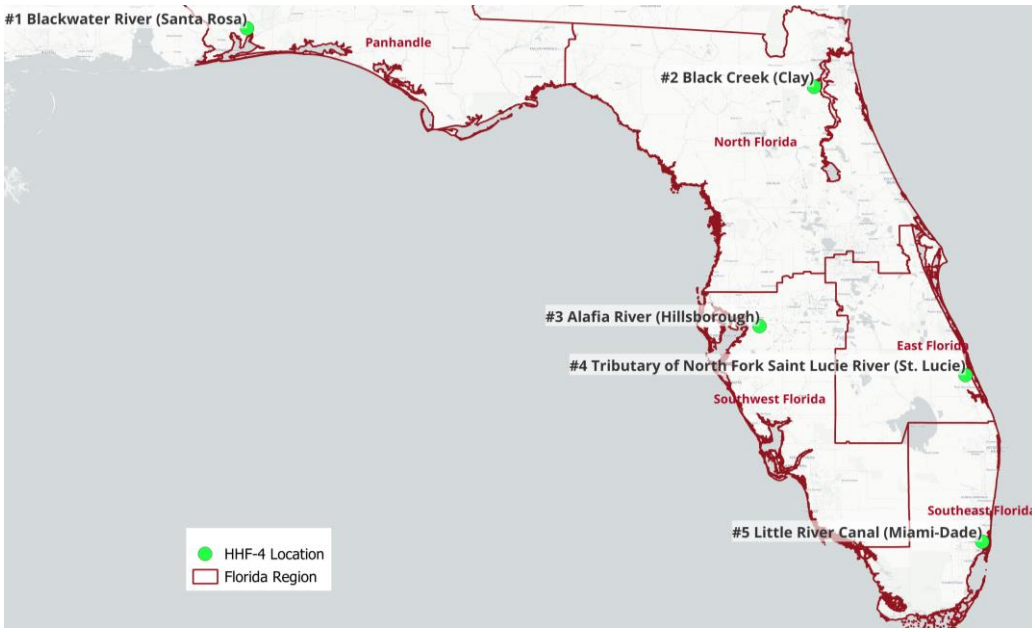

Figure 45: Location of points selected for HHF-4

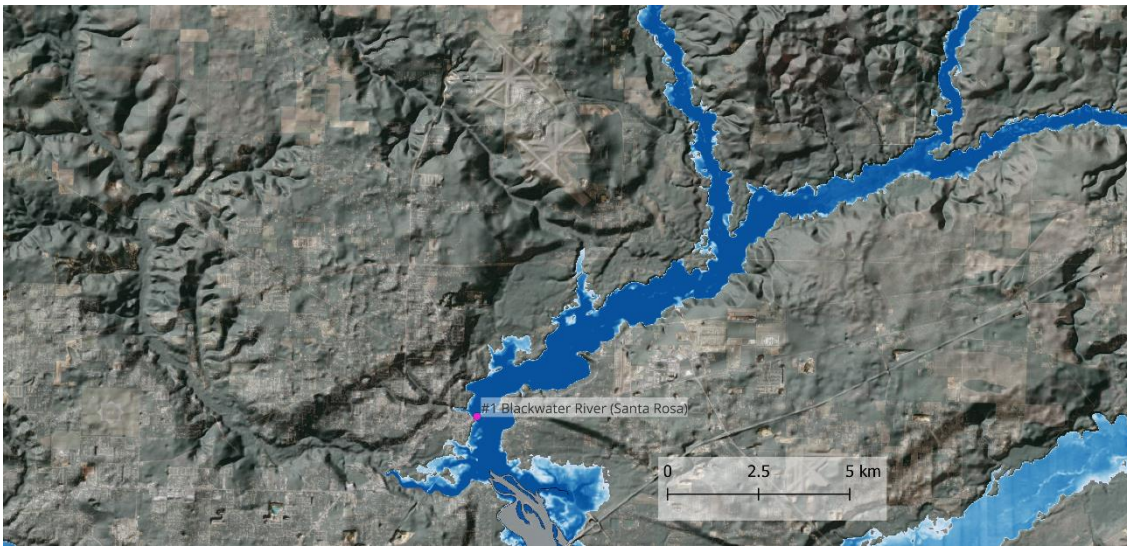
#1 Blackwater River (Santa Rosa)
0
2.5
5 km

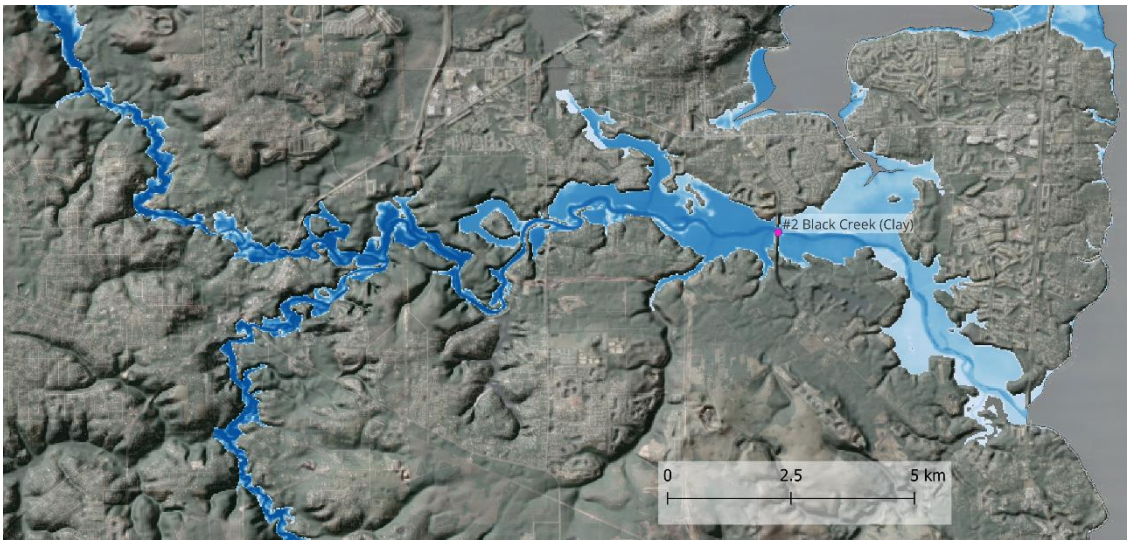
#2 Black Creek (Clay)
0
2.5
5 km

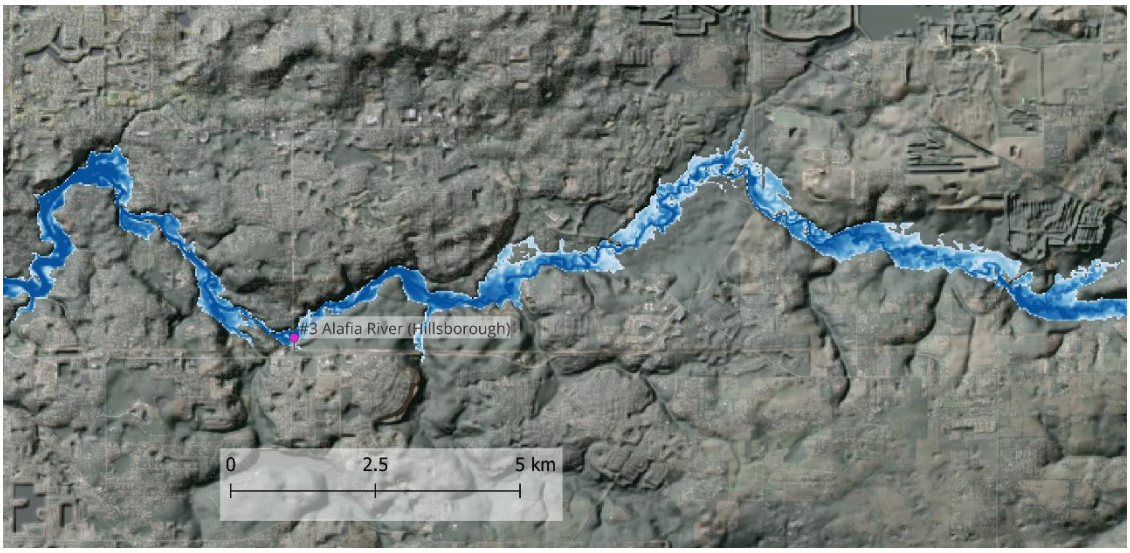
#3 Alafia River (Hillsborough)
0
2.5
5 km

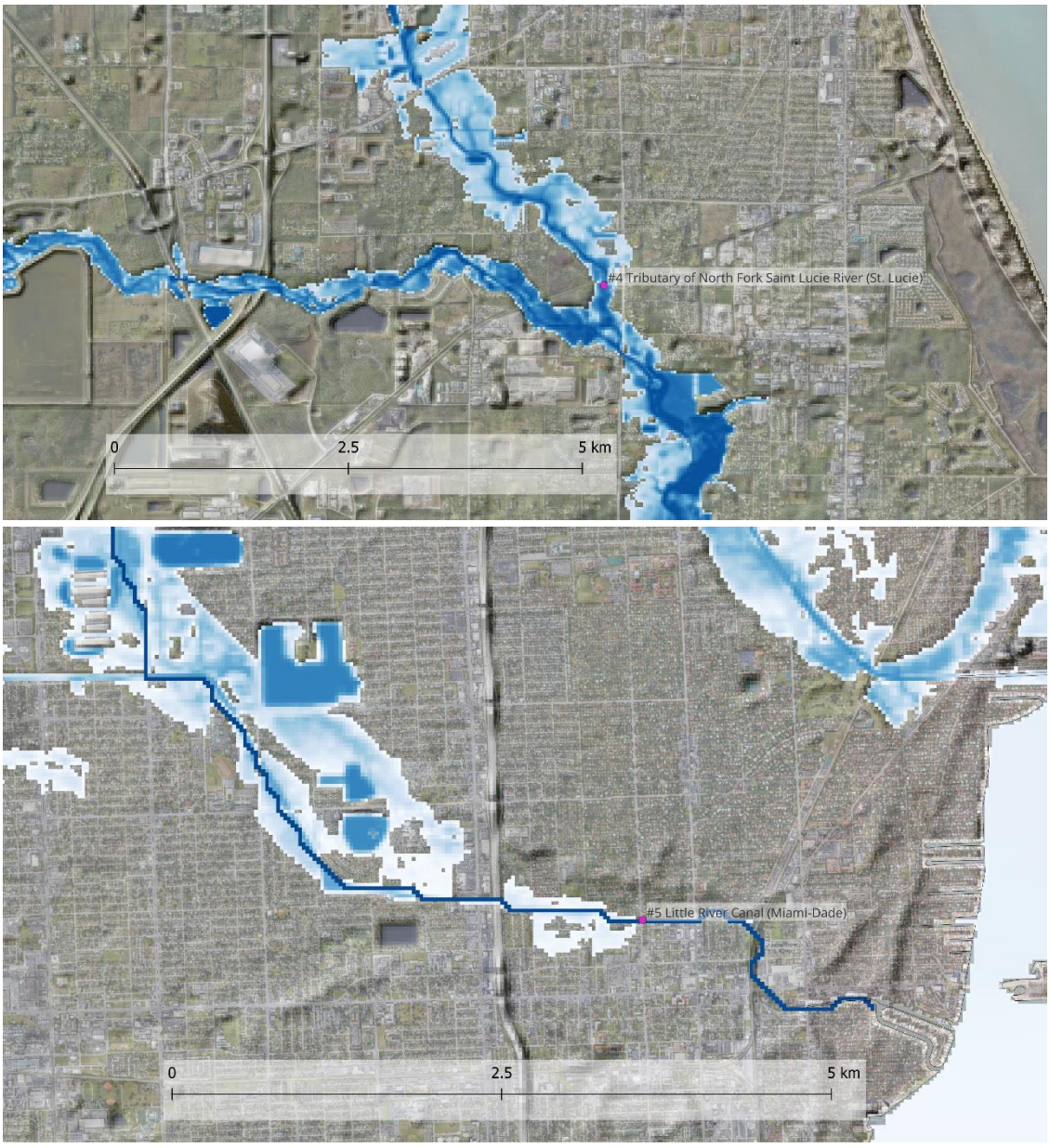

Figure 46: Situation of locations selected for HHF-4 analysis, with modeled 1 in 100 years (base-model) hazard illustrating the on-site flood flow conditions.

Reflecting HHF-4-A: Change in the hydraulic roughness (Manning's "n")

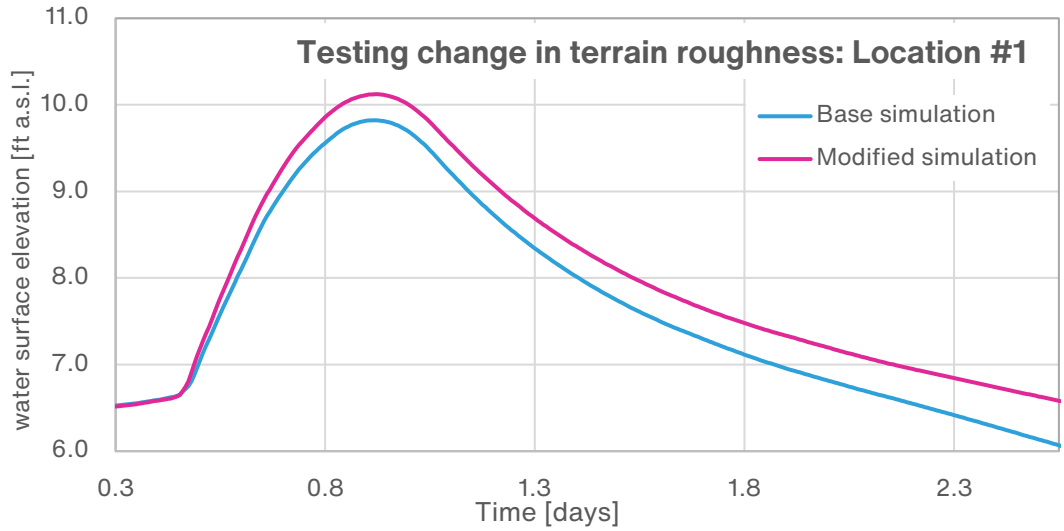

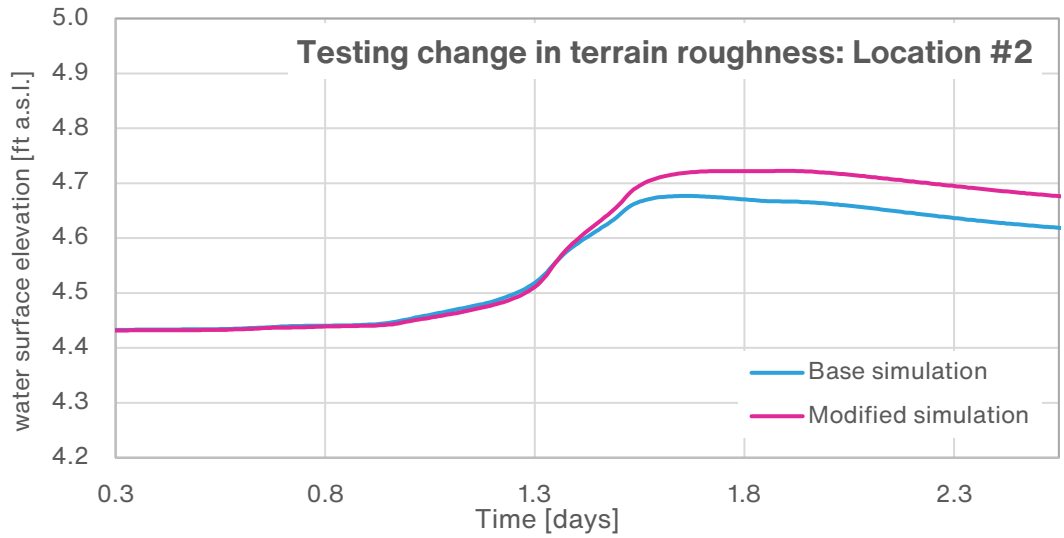

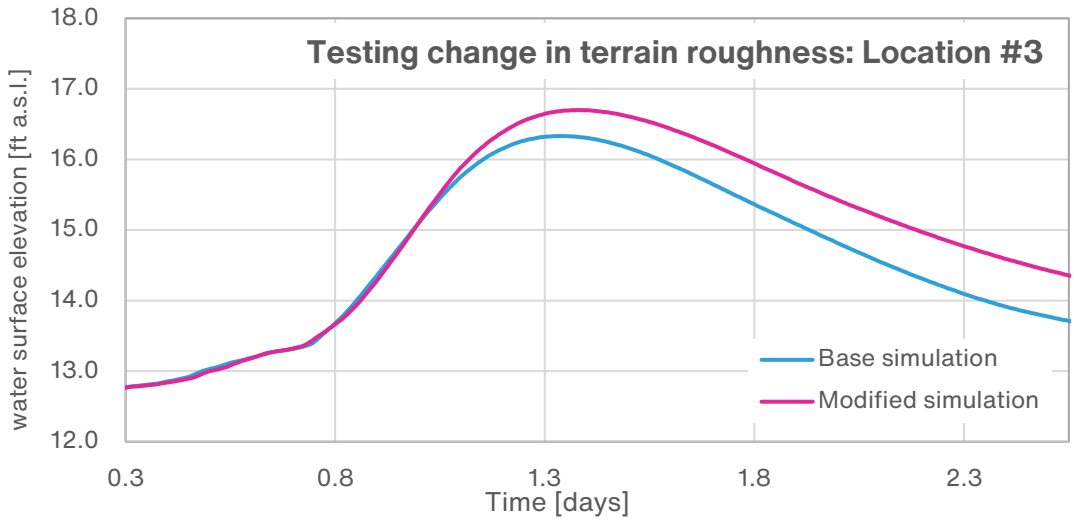

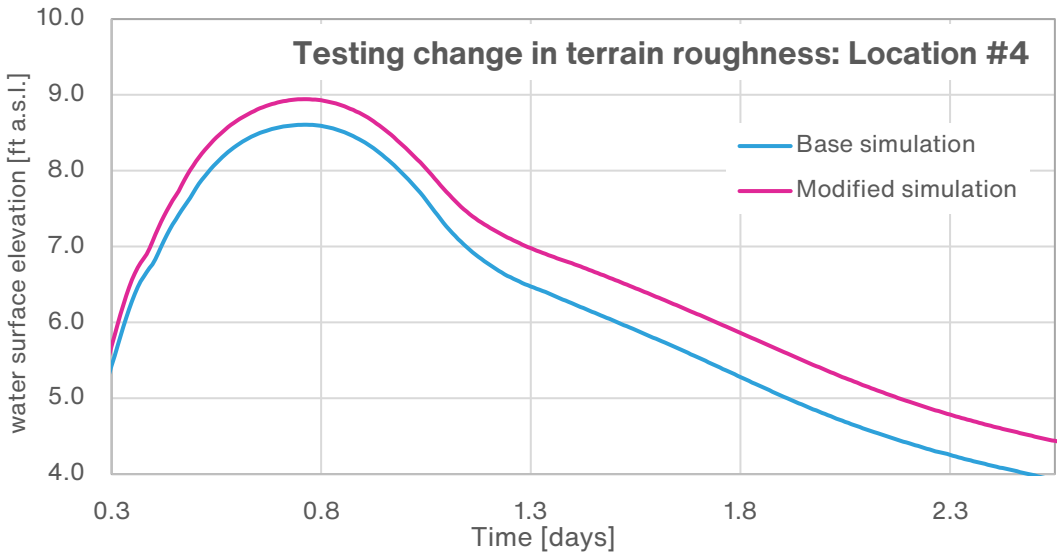

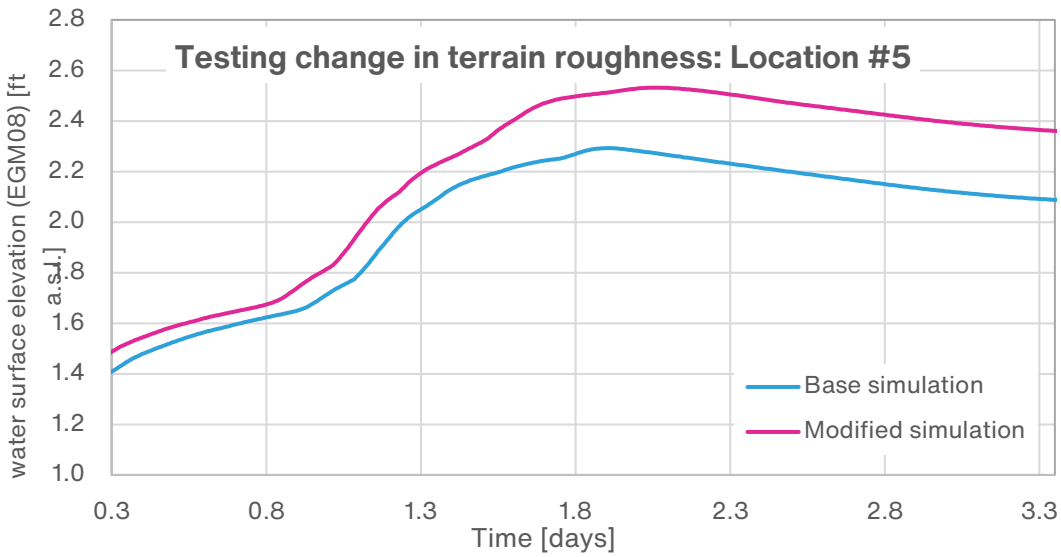

Figure 47: Demonstration of increased water surface elevation (in feet above the mean sea level) with increased roughness in each of the 5 assessment locations during 100yr fluvial event

Reflecting HHF-4 B: Steepness in model topography

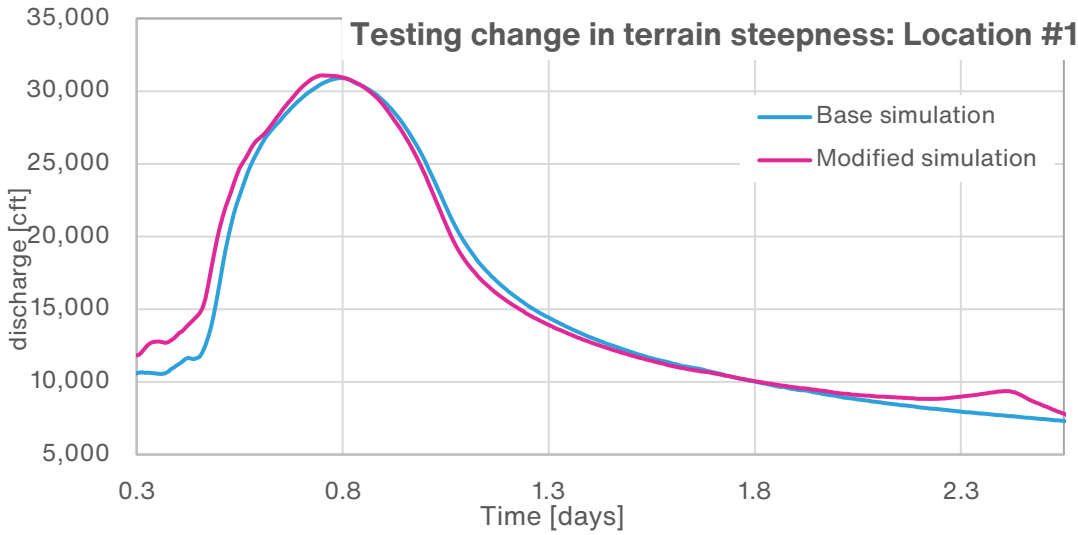

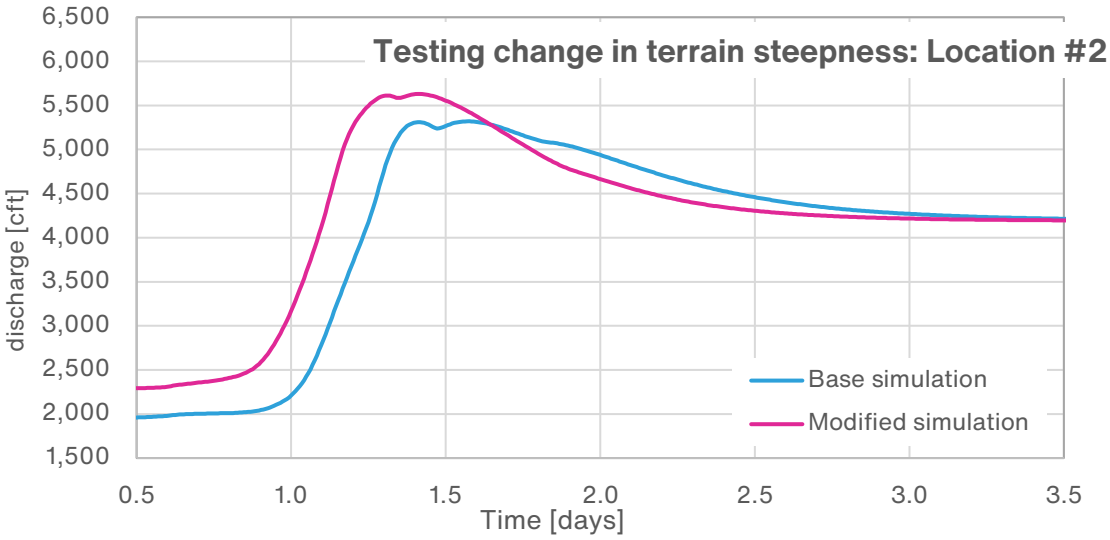

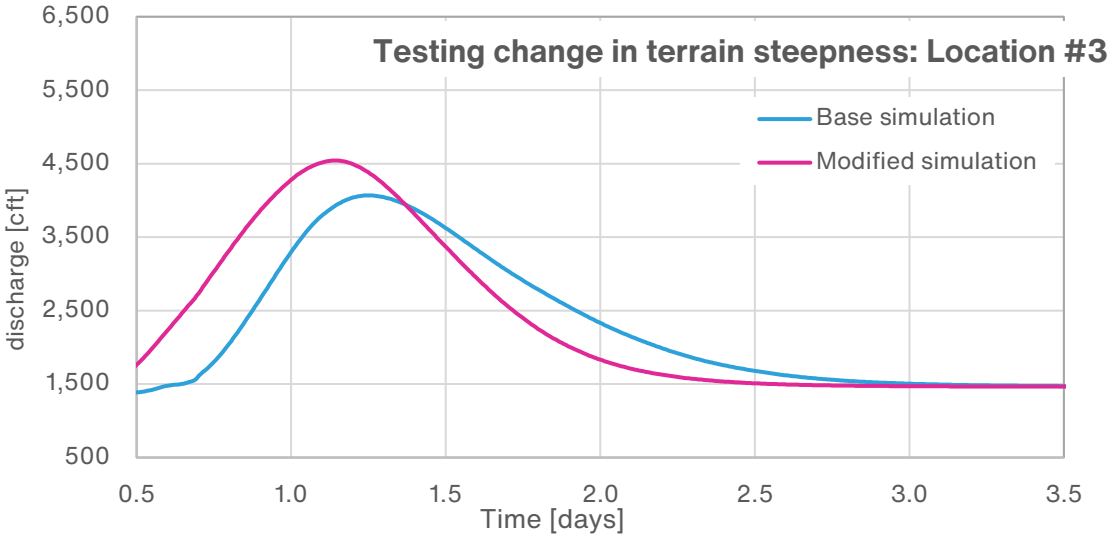

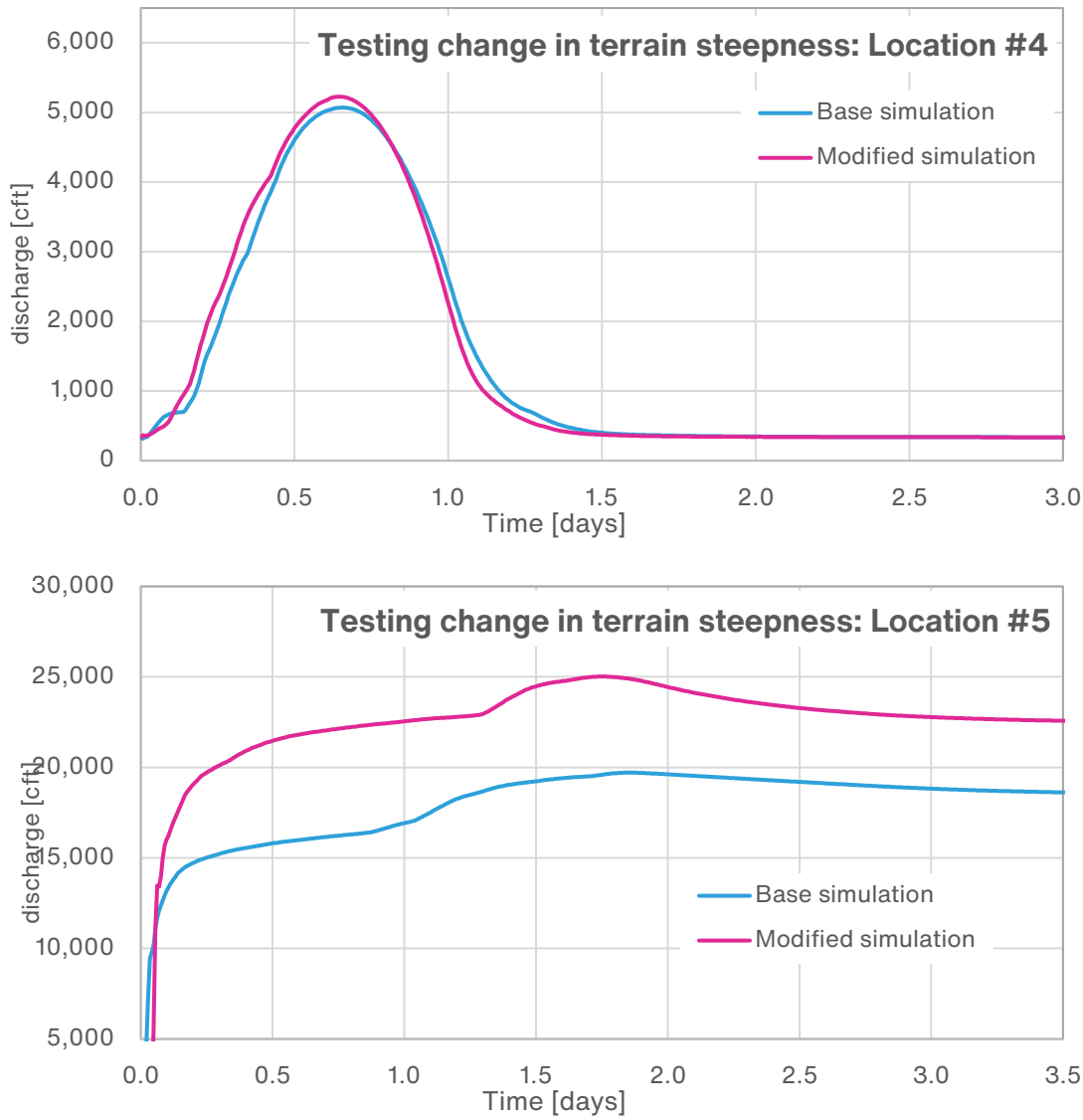

Figure 48: Demonstration of increased discharge with increased steepness in each of the 5 assessment locations during 100yr fluvial event

Reflecting HHF-4 C: Change in the surface permeability.

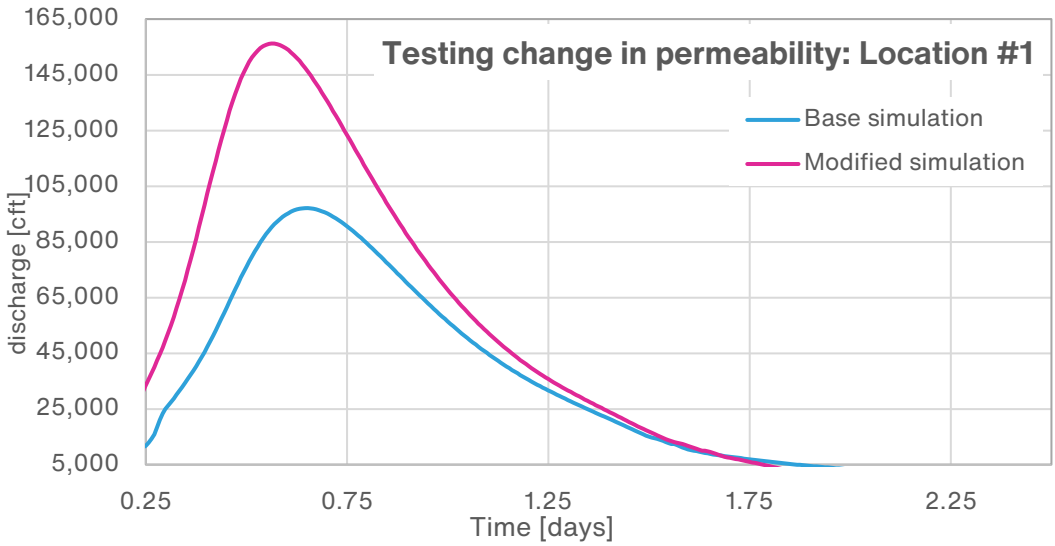

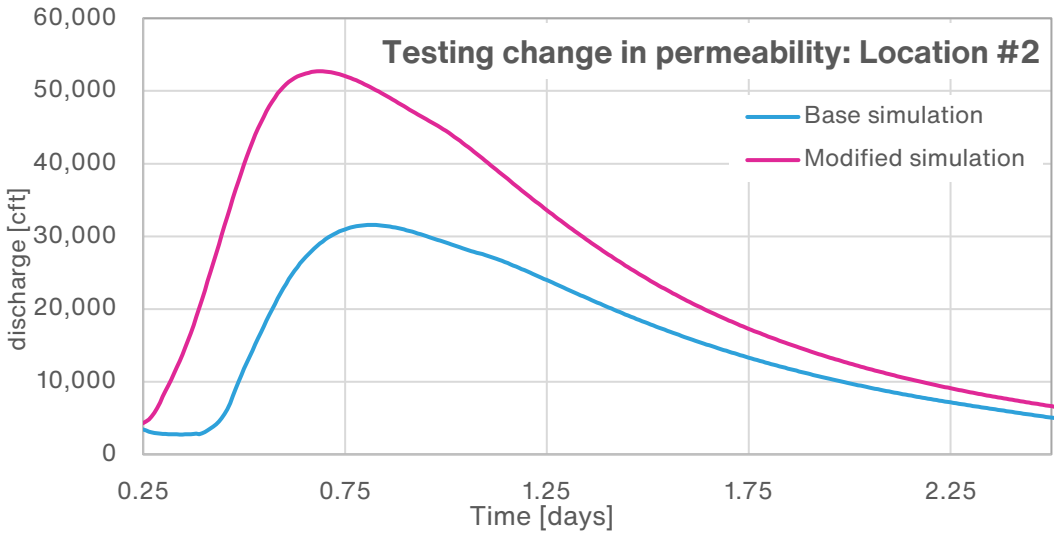

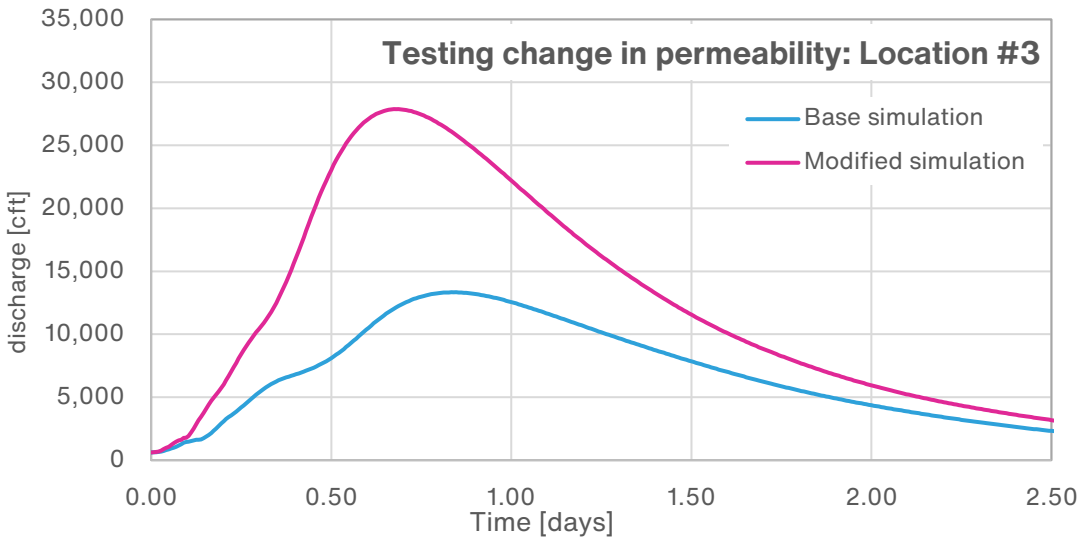

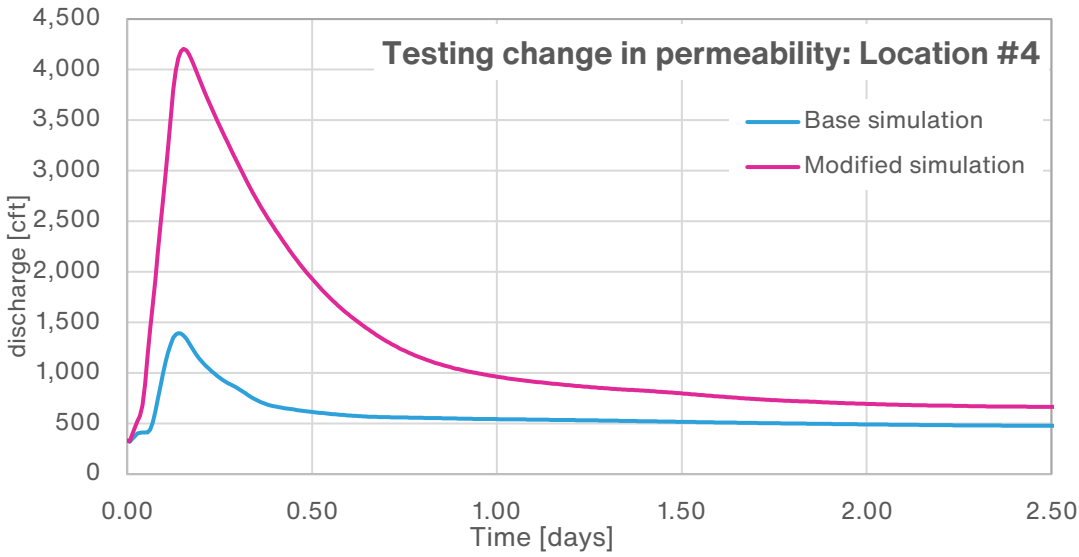

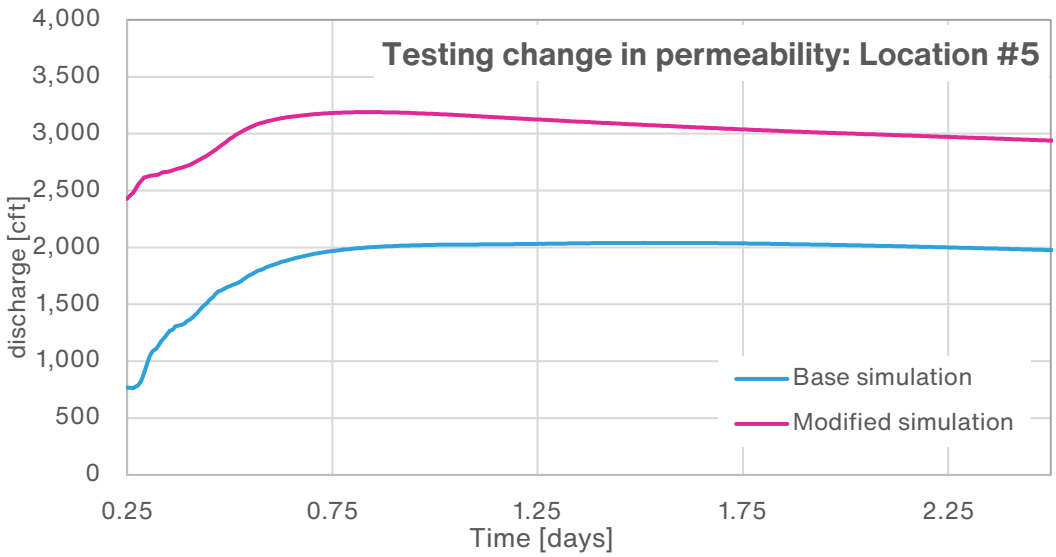

Figure 49: Demonstration of increased discharge with increased imperviousness in each of the 5 assessment locations during 100yr pluvial event

Reflecting HHF-4 D: Change in input discharge

Location #1

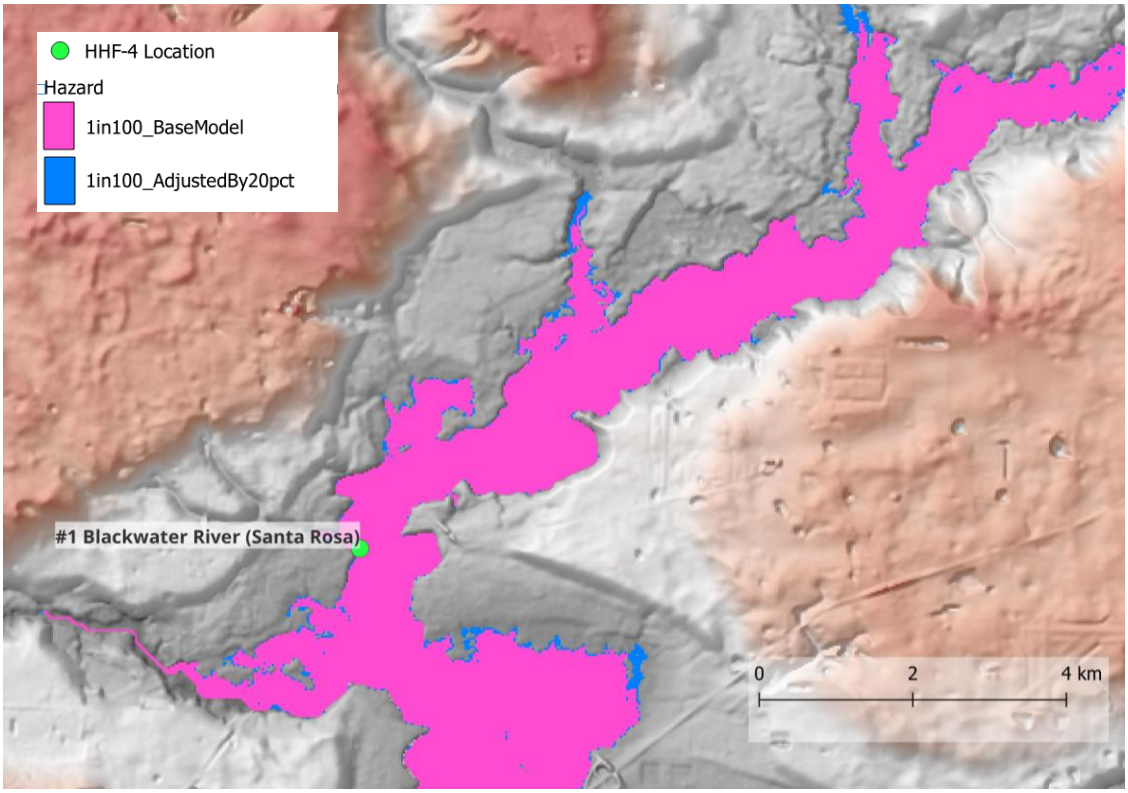

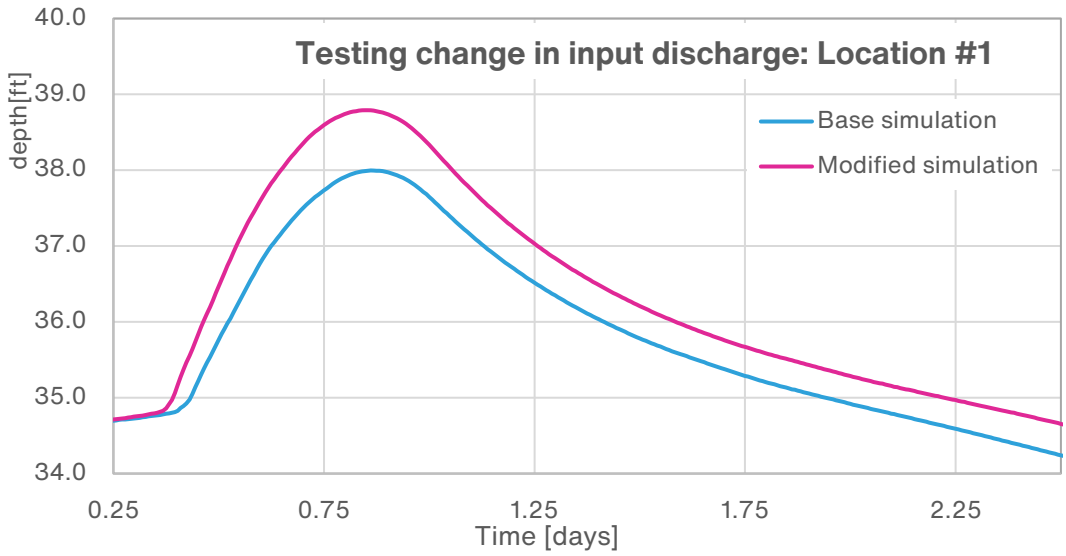

Figure 50: Flood hazard comparison (1 in 100 years) and inundation depth for HHF-4 location #1

Location #2

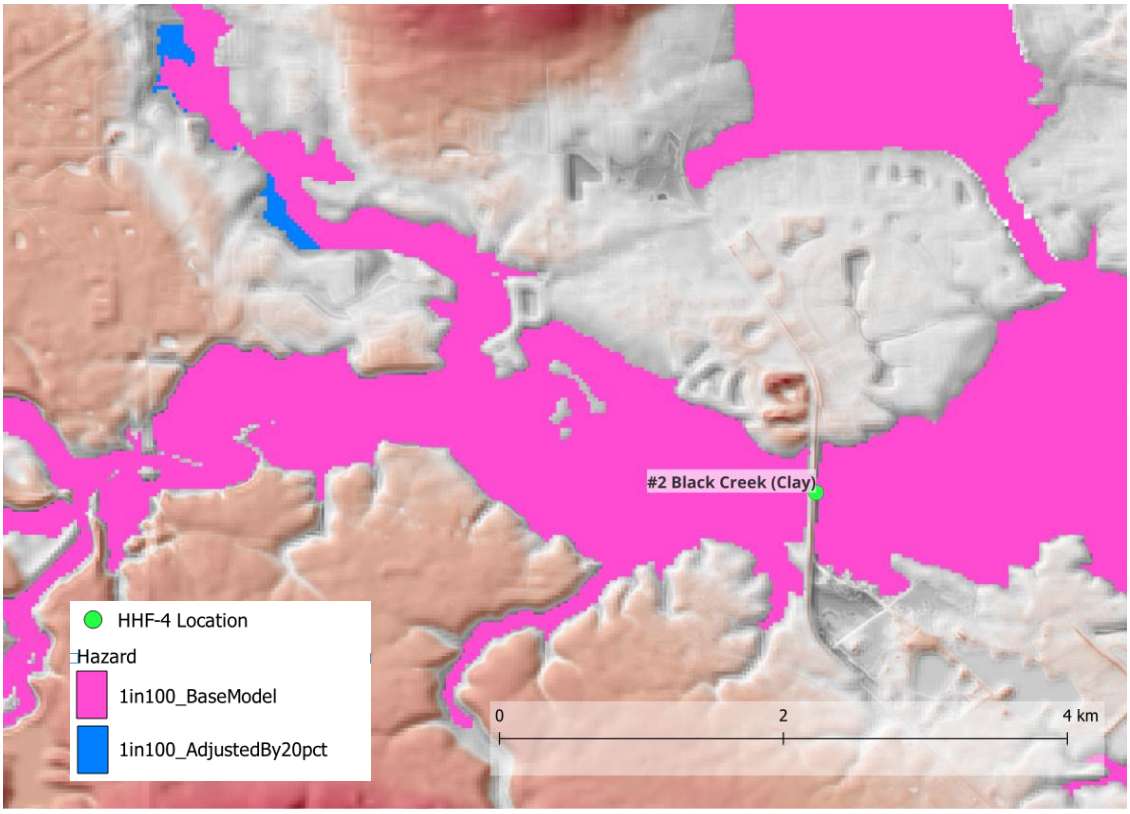

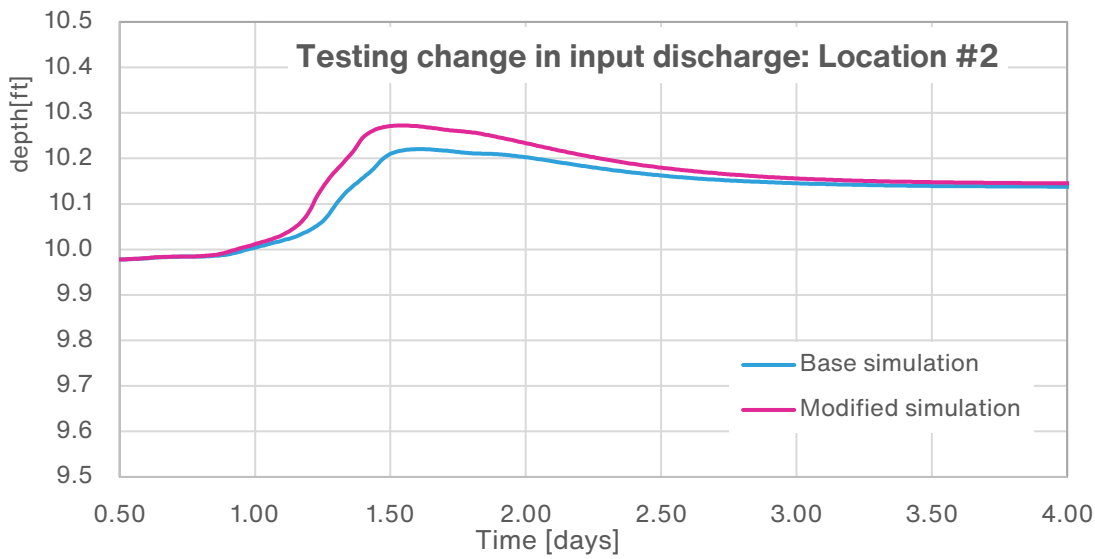

Figure 51: Flood hazard comparison (1 in 100 years) and inundation depth for HHF-4 location #2

Location #3

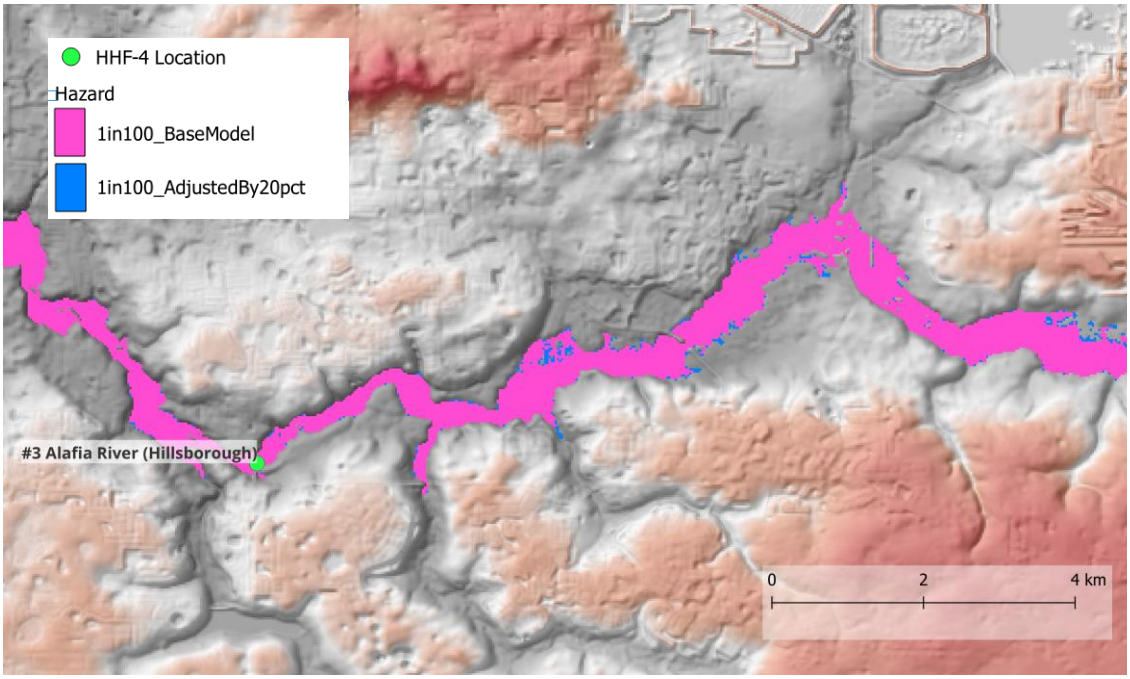

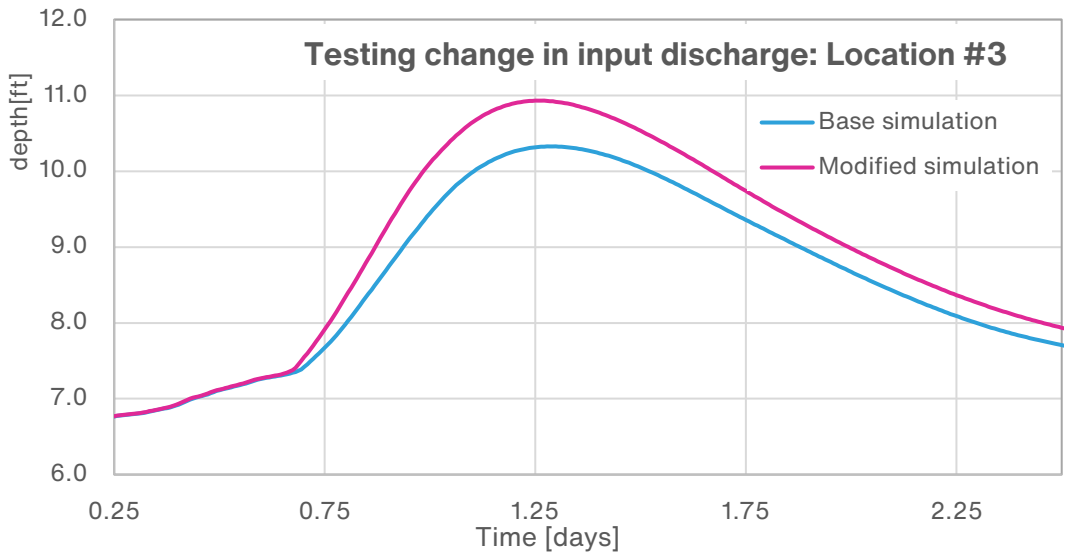

Figure 52: Flood hazard comparison (1 in 100 years) and inundation depth for HHF-4 location #3

Location # 4

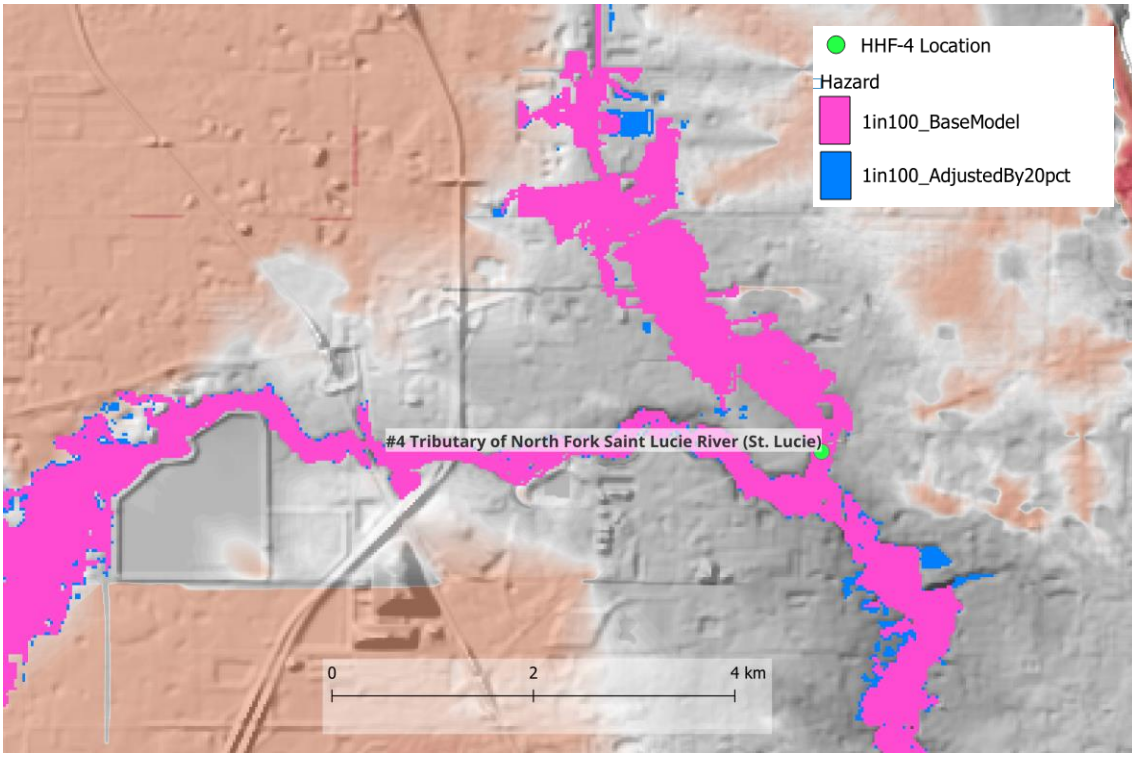

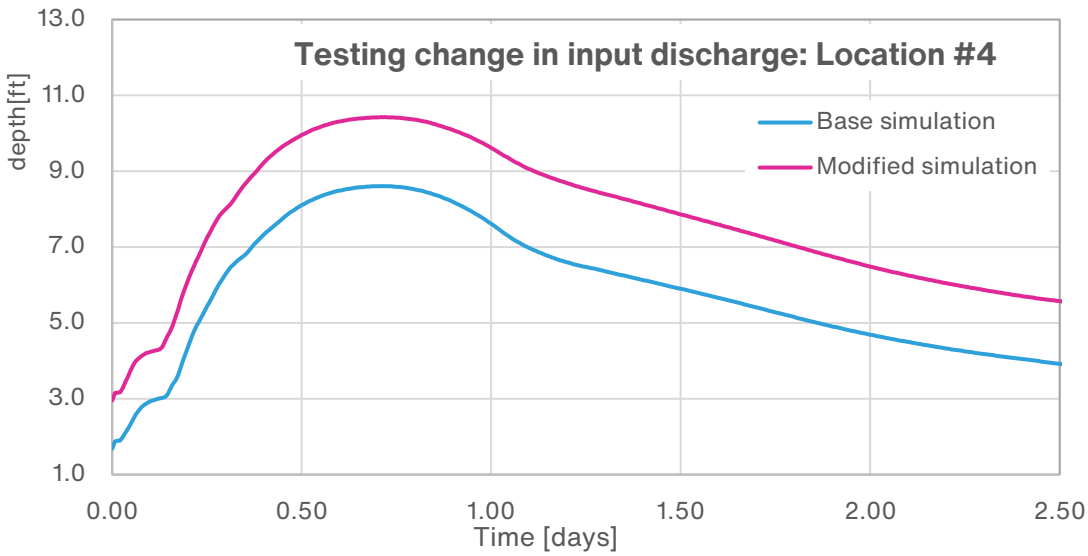

Figure 53: Flood hazard comparison (1 in 100 years) and inundation depth for HHF-4 location #4

Location # 5

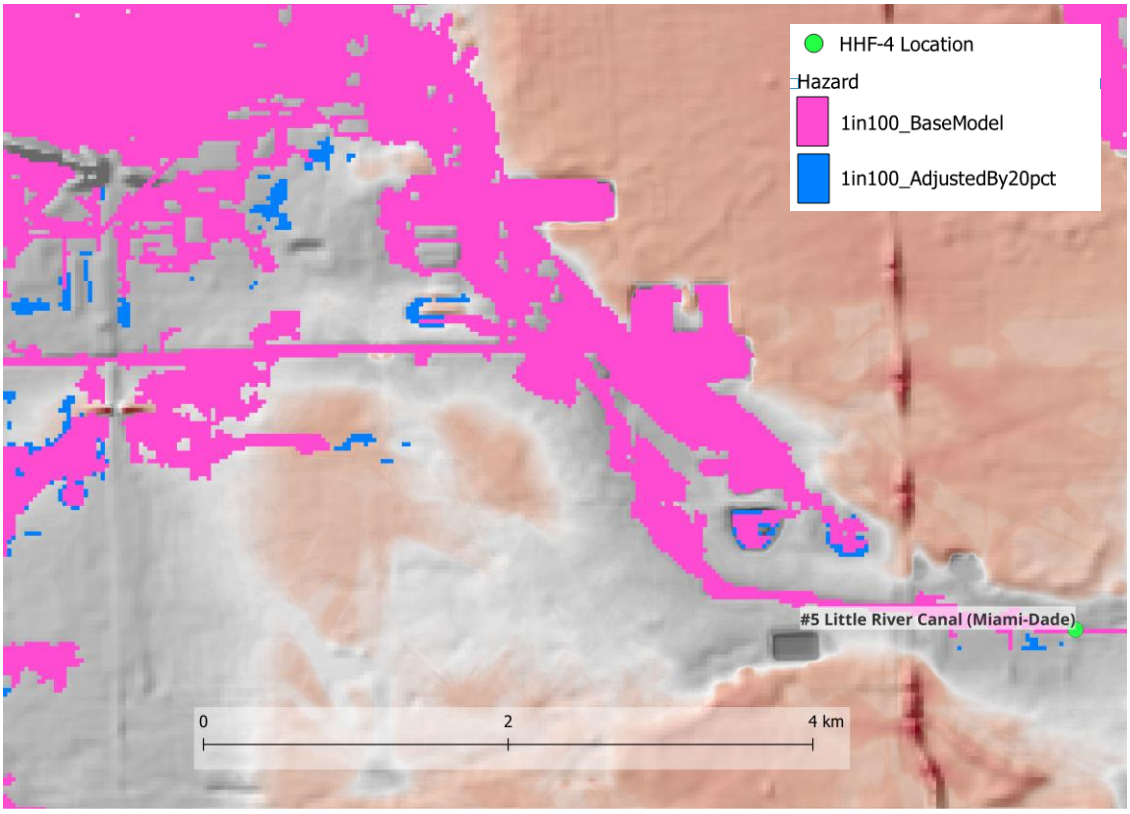

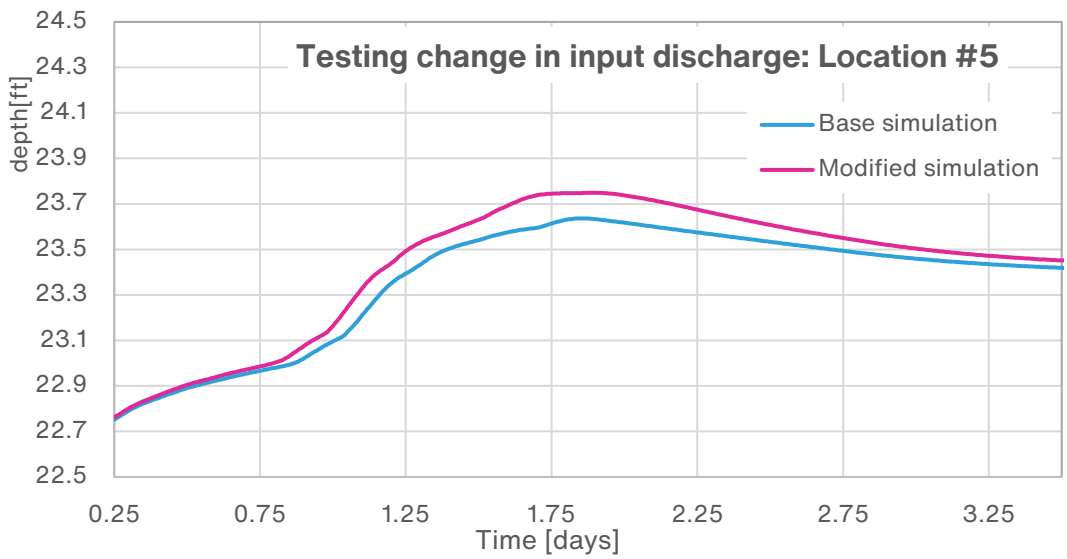

Figure 54: Flood hazard comparison (1 in 100 years) and inundation depth for HHF-4 location #5

HHF-4.2 *Describe the analysis performed in order to demonstrate the logical relationships in this standard.*

To demonstrate these relationships, Fathom developers adjusted the model parameters or other adjustments as outlined below to achieve the assessment required.

Fathom's hydraulic solver is an implementation of the LISFLOOD-FP numerical scheme (Bates, et al., 2010). An important limitation of many 2D approaches over large domains is the inability to represent rivers whose width is considerably smaller than the grid size. (Neal, et al., 2012) addressed this issue within the LISFLOOD-FP model through the implementation of a 'sub-grid' solver in which channel characteristics and flows are represented using a 1D model, while floodplain flows occurring when conveyance capacities are exceeded are propagated using the 2D inertial model solver of (Bates, et al., 2010). This inertial sub-grid formulation of LISFLOOD-FP is the model schema used for Fathom's highly optimized implementation.

The model comprises two equations that handle the continuity of mass in each cell and continuity of momentum between cells. For each cell, the continuity equation over a time step Δt is:

$$h_{i,j}^{t+\Delta t} = h_{i,j}^{t} + \Delta t \frac{Q_{x\,i-1/2j}^{t+\Delta t} - Q_{x\,i+\frac{1}{2}j}^{t+\Delta t} + Q_{y\,i,j-1/2j}^{t+\Delta t} - Q_{y\,i,j+1/2j}^{t+\Delta t}}{A_{i,j}} \tag{9}$$

Where *Q* is the flow between cells, *h* is the water depth at the center of each cell, *A* is the water surface / cell area, and subscripts *i* and *j* are cell spatial indices in x and y directions, respectively. The momentum equation to calculate flow *Q* between two cells is described by the following equation:

$$Q_{i+1/2}^{t+\Delta t} = \frac{q_{i+1/2}^{t} - g h_{flow}^{t} \Delta t . S_{i+1/2}^{t}}{\left[1 + g \Delta t n^2 \left| q_{i+\frac{1}{2}}^{t} \right| \left(h_{flow}^{t}\right)^{7/3}\right]} \Delta x \tag{10}$$

Where *⊿x* is the cell width, *g* is the acceleration due to gravity, *qt* is the is flow from the previous time step Q^t divided by cell width *⊿x*, *S* is the water surface slope between cells, *n* is Manning's roughness coefficient, and *h flow* is the depth between cells through which water can flow.

Further detail on the model solver is available in (Bates, et al., 2010) and (Neal, et al., 2012).

The underlying model remains the same for fluvial and pluvial model runs; however, the method of representing the boundary conditions is changed. Fluvial model setup involves a time-varying volumetric boundary condition point at the top of each river reach being used to input a design hydrograph. Any smaller lateral inflows along the reach will be input using a time-invariant volumetric boundary condition at appropriate locations. For the pluvial model, rainfall is simulated directly onto the DTM grid. Sub-grid channels are included in the model and are present for river channels with an upstream catchment area of 19.03 sq mi (50 sq km) or greater to allow rainfall to be routed through the river network.

Unless otherwise detailed, the fluvial model has been used for these assessments, as it has larger, more concentrated flows, so relationships are more clearly demonstrated.

The methodologies deployed to demonstrate the logical relationships among flood parameters and characteristics are as follows:

A. Manning's 'n' roughness coefficient is a key component of the calculations undertaken by the model solver (Equation 6) and is parameterized as part of the

inputs to the model. Therefore, to undertake this assessment this value was increased by 20%.

B. Whilst slope between cells is accounted for by the model solver (Equation 5), this is calculated based on the model DTM topography and channel parameters provided, as opposed to being parameterized. Therefore, to demonstrate this relationship the underlying topography used in the model has had to be altered. All elevation values have been increased by 20%; this makes all slopes in the model steeper.

C. The Fathom modeling methodology calculates hydrological inputs to the model that account for losses due to infiltration into the ground. To account for reduced porosity, these inputs have been adjusted so that infiltration is not accounted for. For this test the pluvial model has been used; the reduction in infiltration can be more clearly seen due to the direct rainfall on grid methodology used, due to the increased rainfall rate.

D. The model hydrological inputs are pre-calculated as part of the build process. The effect of increased discharge is shown by increasing these values by 20% over the full time series.

E. The inland and coastal flooding is calculated within separate models and therefore are not impacted by each other. Therefore, no testing is required for this characteristic.

Table 15, Table 16, Table 17 and Table 18 shows additional statistic relevant for the tests and the overall effect on inundation depth at precise location placed in Table 14. These tests are discussed in Disclosure SF-2.2.

Table 15: Testing the effect of water-level and depth increments on fluvial simulation when hydraulic roughness is increased by 20%

Pt.	Modifi-cation	WL – base (ft)	WL-modif. (ft)	Base Depth (ft)	Modified Depth (ft)	Depths ratio	Depths difference
						%	ft
#1	+20%	9.82	10.12	38.00	38.30	0.78%	0.301
#2	+20%	4.68	4.72	10.22	10.27	0.44%	0.046
#3	+20%	16.33	16.70	10.33	10.69	3.44%	0.367
#4	+20%	8.61	8.94	9.88	10.22	3.30%	0.337
#5	+20%	2.29	2.53	23.64	23.88	1.00%	0.239

Table 16: Testing the effect of depth change on fluvial simulation when topography is increased by 20%

Pt.	Modifica-tion	WL – base (ft)	WL-moif. (ft)	Base Depth (ft)	Modified Depth (ft)	Depths ratio %	Depths difference ft
#1	+20%			38.00	44.05	13.75%	6.055
#2	+20%			10.22	11.34	9.87%	1.119
#3	+20%			10.33	10.93	5.51%	0.603
#4	+20%			9.88	10.58	6.65%	0.704

Pt.	Modifica-tion	WL – base (ft)	WL-moif. (ft)	Base Depth (ft)	Modified Depth (ft)	Depths ratio %	Depths difference ft
#5	+20%			23.64	27.79	14.95%	4.156

Table 17: Testing the effect of water-level and depth increment on pluvial simulation when soil permeability is switched off.

Pt.	Modifica-tion	WL – base (ft)	WL-modif. (ft)	Base Depth (ft)	Modified Depth (ft)	Depths ratio %	Depths difference ft
#1	turned off	13.75	16.72	41.921	44.895	6.63%	2.974
#2	turned off	8.44	10.81	13.987	16.351	14.46%	2.364
#3	turned off	21.56	26.03	15.560	20.021	22.28%	4.461
#4	turned off	5.61	9.47	6.886	10.745	35.91%	3.859
#5	turned off	4.80	5.44	26.141	26.782	2.39%	0.641

Table 18: Testing the effect of water-level and depth increments on fluvial simulation when input discharge is increased by 20%

Pt.	Modifica-tion	WL – base (ft)	WL-modif. (ft)	Original Depth (ft)	Base Depth (ft)	Depths ratio %	Depths difference ft
#1	+20%	9.82	10.62	38.00	38.79	2.05%	0.795
#2	+20%	4.68	4.73	10.22	10.27	0.50%	0.052
#3	+20%	16.33	16.94	10.33	10.93	5.53%	0.604
#4	+20%	8.61	9.15	9.88	10.42	5.24%	0.546
#5	+20%	2.29	2.41	23.64	23.75	0.48%	0.113

In the inland modeling, no other variables impact the magnitude of the output. The model does show some sensitivity to input variables including hydraulic roughness and discharge changes. However, the resulting impact from these is smaller than impacts from changes in pluvial input modification (impermeability) and slope testing and the inaccuracy in these parameters will be small (eg. steepness is based on the elevation model used, which is determined by LiDAR, with relatively small inaccuracies), and therefore the sensitivity value tested is much larger than any expected inaccuracy in the model input for these variables.

STATISTICAL FLOOD STANDARDS

SF-1 Modeled Results and Goodness-of-Fit

A. The use of historical data in developing the flood model shall be supported by rigorous methods published in current scientific and technical literature.

Parameters and characteristics used are modeled using regression equations and probability distributions fitted to historical data. These equations and distributions are developed and validated based on methods documented in current scientific and technical literature. Moreover, the inland flooding related event set was modeled using derivations of statistical approaches first introduced by (Heffernan & Tawn, 2004), together with reanalysis precipitation and discharge model datasets, following methods consistent with current scientific and technical literature. References are provided, where appropriate, throughout the disclosure documents and a complete list of references is provided in Disclosure GF-1.6.

B. Modeled results and historical observations shall reflect statistical agreement using current scientific and statistical methods for the academic disciplines appropriate for the various flood model components or characteristics.

Modeled results and historical observations are made sure to be consistent across all aspects of the model. This is achieved by performing statistical tests in all stages of model development. Good agreement is observed between modeled and measured statistics of various parameters and characteristics of flood events. Synthetic event set results were contrasted with historical reanalysis data using quantitative and qualitative tests throughout the model development process. Details of the various tests conducted can be found in Disclosure SF-1.5. Good agreement is demonstrated between modeled and reanalysis characteristics.

Disclosures

SF-1.1 Provide a completed Form SF-1, Distributions of Stochastic Flood Parameters (Coastal, Inland). Identify the form of the probability distributions used for each function or variable, if applicable. Identify statistical techniques used for estimation and the specific goodness-of-fit evaluations applied along with appropriate metrics. Describe whether the fitted distributions provide a reasonable agreement with available historical data. Provide a link to the location of the form [Form SF-1: Distributions of Stochastic Flood Parameters (Coastal, Inland)].

The probability distributions used to model different flood model parameters are discussed below in Disclosure SF-1.5 and in the Form SF-1.

SF-1.2 Describe the insurance flood claims data used for validation and verification of the flood model.

Impact Forecasting validated and verified the flood model using NFIP claims from “OpenFEMA Dataset: FIMA NFIP Redacted Claims – v2”. The NFIP writes over 90% of the residential insurance policies in Florida (Kousky, et al., 2018), though property owners are

only required to purchase it if their property is encumbered by a federally backed mortgage and located within a special flood hazard area (SFHA). This dataset contains claims from 1978 to 2023. The claims data used consists of personal residential building exposure totalling $535,614.90 million from 2,302,459 policies, and personal residential content exposure totalling $24,249.79 million from 397,169 policies. Prior to utilizing the claims and policy data, extensive processing was used to identify and correct/remove erroneous records from both datasets. This included removing records where flood depths were listed as zero but the pay-out for the event was non-zero, removal of commercial policies and claims, and removing claims where the location attributes were contradictory with respect to the policy or claim being in Florida. The NFIP observed data presented in SF-5.1 is derived from this claims database.

The Aon residential industry exposure database (IED) represents all residential risks, regardless of insured status, and the losses produced using this IED are not comparable to the observed NFIP losses. To correctly validate the modeled loss projections for each storm, the team created an estimated NFIP Take Up Rate (TUR) for each county in Florida. Utilizing the IED, the number of policies within each of the SFHAs, within a county, was compared against the number of total exposures within the same area. This factor was then multiplied against the total modeled gross losses to create a "modeled NFIP" loss value. In consideration of the increase in value of exposures that has occurred between the event's occurrence date and the IED's representative building stock date, a trending factor based on (Collins, 2001) was applied to the NFIP loss data.

For additional validation of the model's historical loss projections, please see section SF5.

To consider the increase in value of exposures that has occurred between the event's occurrence date and the IED's representative building stock date, a trending factor based on (Collins, 2001) was applied to the NFIP loss data.

SF-1.3 Provide an assessment of uncertainty in flood probable maximum loss levels and in flood loss costs for flood output ranges using confidence intervals or other scientific characterizations of uncertainty.

The uncertainty in flood loss costs is studied and presented in Standard SF-3. For the storm surge portion of the model, the parameters studied include central pressure (Cp), radius of maximum winds (Rmax), translational velocity (VT), and far field pressure (FFP). The far field pressure (FFP) is the major contributor to the uncertainty in storm surge loss costs for Category 1 storms. For Category 3 and Category 5 hurricanes, Rmax has the greatest impact. For inland modelling exploratory analyses of effects of changing slope, roughness, permeability and discharge are demonstrated in Standard SF-2 and Standard HHF-4.

To assess the uncertainty in flood probable maximum loss levels, the expected flood loss and 10% and 90% flood loss levels were computed using Impact Forecasting's personal residential exposure, and the AEP and OEP (occurrence exceedance probability) results are provided in Form AF-8. Each event in the stochastic event set was simulated 10 times to capture the variation of loss due to uncertainty in the flood vulnerability functions. Those were then converted to year losses by taking either the max or sum of the individual event losses for a given year. The return period for each year was calculated based on the averaged sample loss for each year. The expected flood loss and 10% and 90% flood loss levels for the desired return periods were computed from the 10 samples of certain years.

SF-1.4 ***Justify any differences between the historical and modeled results using current scientific and statistical methods in the appropriate disciplines.***

The agreement between historical and modeled results is justified using appropriate statistical methods including goodness-of-fit tests from scientific and technical literature.

SF-1.5 ***Provide graphical comparisons of modeled and historical data and goodness-of-fit evaluations. Examples to include are flood frequencies, flow, elevations or depths, and available damage.***

The text below provides a comprehensive summary of statistics taking from all significant observed hydro-meteorological data and their reflectance in the model.

In one set of comparisons, the historical training data for the non-TC synthetic event set model was contrasted with the non-TC synthetic event set footprints in a variety of tests. These tests fundamentally aim to assess if the synthetic event set can recreate the general patterns seen in the training data, following common approaches used in previous research including (Diederen, et al., 2019; Quinn, et al., 2019; Wing, et al., 2020; Li, et al., 2023), and many others. In particular we examine the re-creation of the marginal distributions, the event sizes, the pairwise dependence, and the seasonality. The event frequency and seasonality plots, in particular, show strong agreement between the two datasets. While it is true that dissimilarities can be seen between the datasets across each metric tested, this is expected given the use of a 10yr event threshold and a historical record comprising only 40 years in length.

Another set of comparisons form part of the assessment of the final merged event set, including the outputs from the non-TC and TC synthetic event sets. Event-peril-catchment return periods in this event set are calculated after merging the two event sets and then ranking (by magnitude) and assigning return periods simply as event catalog duration (years) / rank. The event set assessment characterizes the frequency of impacts across the state of Florida (TC and non-TC), the spatial pattern of the proportion of TC and non-TC events across catchments, and the seasonality of their occurrence. Each metric is contrasted with the same metrics obtained from the historical training data (based on MSWEP and our in-house hydrological model reanalysis). The various qualitative and quantitative analyses indicate that the model is providing events that are similar with expectations provided in the historical training data, in terms of recreation exceedance probabilities, event footprint sizes, pairwise co-occurrence rates, and seasonality.

Within these tests the historical training data refers to Multi-Source Weighted-Ensemble Precipitation (MSWEP) reanalysis precipitation fields provided by (Beck, et al., 2019) and corresponding discharge simulations from Fathoms FUSE-mizuRroute hydrological model framework. For non-TC analyses, historical TC events are then removed from the records using the IBTrACS historical database (Knapp, et al., 2010; 2018), before then applying spatio-temporal clustering to the data to derive unique historical events.

Landfall Frequency for TC Events

The comparison between modeled and measured annual landfall frequencies of Florida landfalling tropical cyclones per category is provided in Figure 55. The p-value from a two-sample Pearson's chi-squared test performed on the count data is 0.94. It indicates reasonable agreement between modeled and measured counts of landfalling tropical cyclones in Florida at the 5% level of significance.

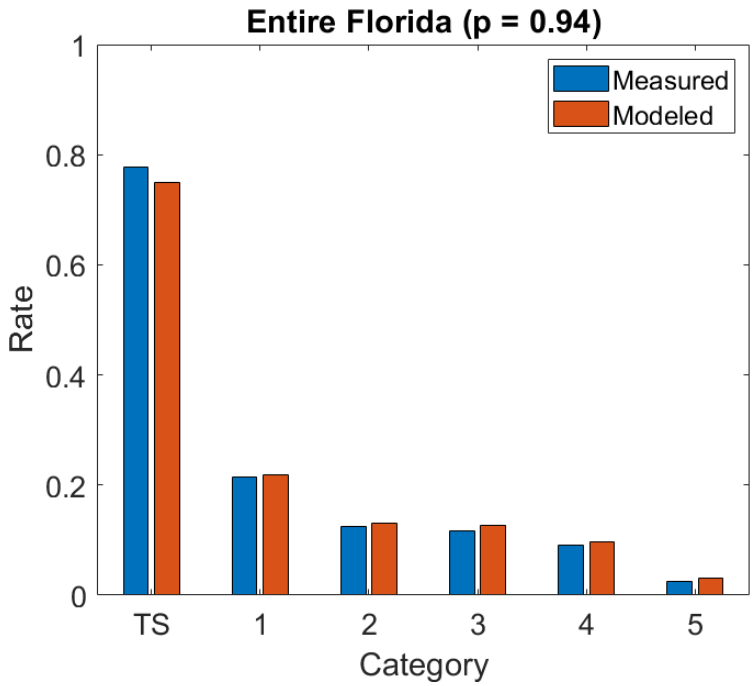

Figure 55: Comparison of modeled and observed frequencies of Florida landfalling tropical cyclones per category.

Marginal distributions of rainfall and discharge

The exhibit is a comparison of the non-TC synthetic event set and training data return period distributions at the unique sites used within the non-TC synthetic event set model training data. This metric fits marginal distributions to the historical training data and the synthetic event set, and then contrasts the results. Here in Figure 56 we present the 20yr and 100yr examples, merging both pluvial and fluvial perils, together with 10th, 50th and 90th quantiles of the proportional errors. Pluvial units are given in terms of mm daily accumulation while fluvial units used are cumecs, plotted on log axis. Median error (%) for the example RP (return period) plots are 10% and 9% in the 20yr and 100yr plots, respectively. Both datasets however are strongly correlated, namely 99.8% for 20yr and 99.7% for 100yr case and the shift in intercept is deemed not important as the mapping of events to actual flood extents auto-corrects this bias almost completely. No work has been undertaken to correct it at this stage as, primarily, the use of the non-TC synthetic event set is to characterize event tail dependence (correlations between sites), and therefore the absolute magnitudes of the flow / accumulations are secondary. Further, no absolute flows or precipitation values are used in deriving the resulting hazard maps; instead, all values are converted to frequency space, and those values (e.g. 1 in 50yr) are used to sample from pre-existing hazard layers based on frequency matching. That being said, the merging of the TC model precipitation with this non-TC synthetic event set could be susceptible to biases, the result of which would be errors in the proportion of extreme events that are attributed to TC or non-TC processes. However, given the dominance of TCs in the region, the apparent biases shown were not expected to lead to significant uncertainties in the final model output. For context, considering all pluvial sites in the region, if we were to apply a 9% uplift to all non-TC event accumulations in the synthetic event set model (in line with median bias shown), the resulting proportion of ≥100yr events attributed to TC events

would decrease by only 2% from approximately 96% to 94%. Even in the higher frequency events (e.g. 10yr) we see a change of less than 3.5% (78% to 74.5%).

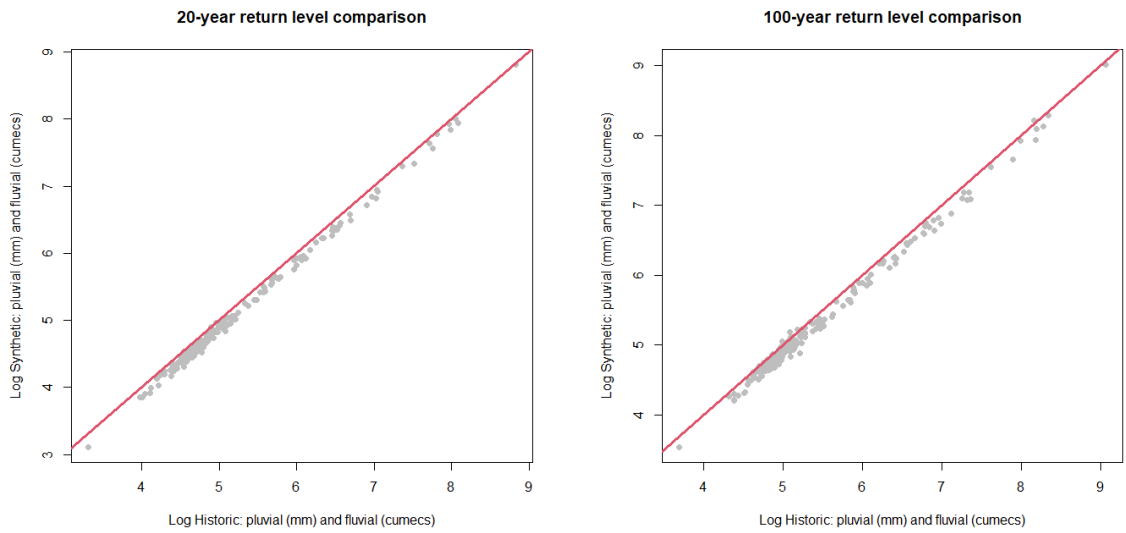

Figure 56: 20yr and 100yr return period comparisons between the non-TC synthetic event set and the historical training data

Inland flooding event size

This test contrasted the event sizes (in terms of spatial footprint) in the non-TC synthetic event set against the historical training data. Event size in this instance relates to the number of sites that are threshold exceeding within a given event. For each unique site, each event in which it was threshold exceeding was found, and for each the number of other sites also exceeding their event threshold were counted. Example empirical CDFs (cumulative distribution functions) of event sizes conditioned at 2 unique sites representing the smallest absolute mean error score (left) and largest absolute mean error score (right) across all sites are also provided in Figure 57. The associated Kolmogorov-Smirnov test statistic (KS) and P-values are also reported.

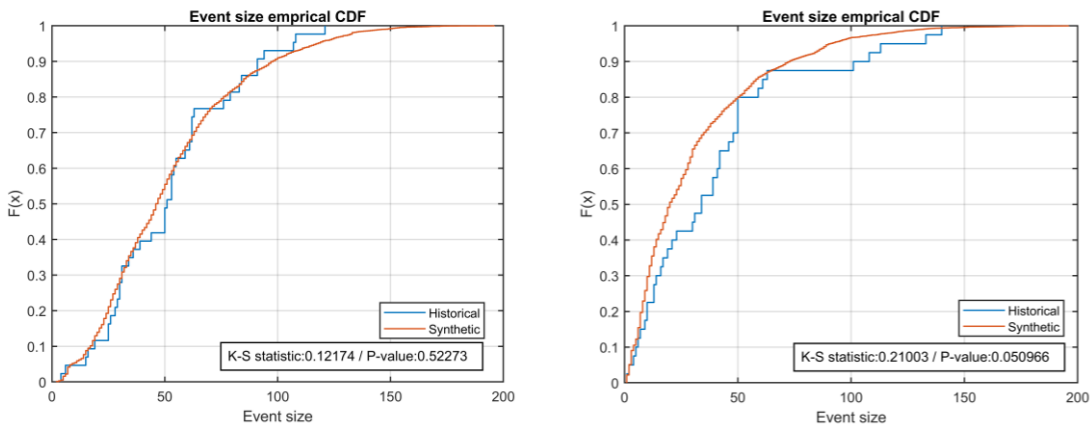

Figure 57: Historical training data and non-TC synthetic event set event size distributions from 2 example data locations representing the best (left) and worst (right) performance.

Then, we considered all event sizes across the entire region. Figure 58 plots the empirical distribution of all event sizes within the historical training data against the distribution obtained from all events in the non-TC synthetic event set.

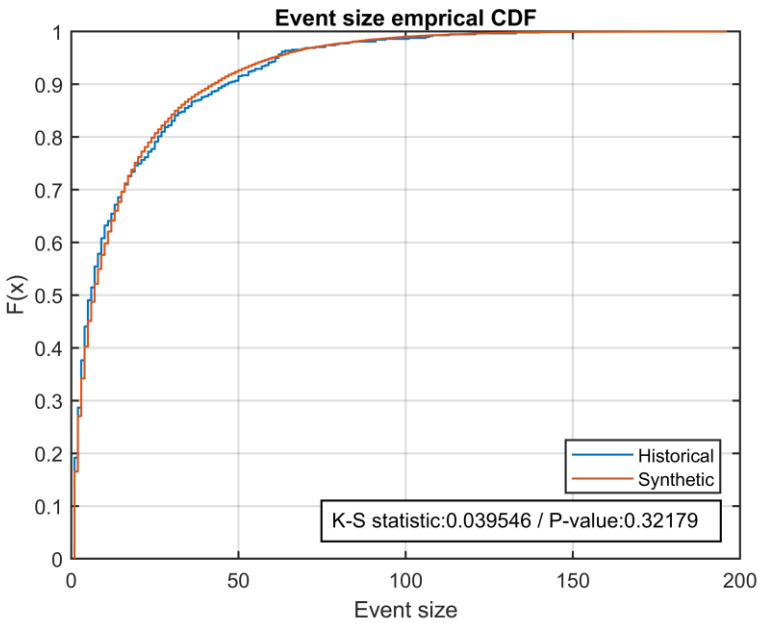

Figure 58: Historical training data and synthetic event set event size distributions.

Inland flooding event location co-occurrence

This exhibition aims to contrast the co-occurrence rates between sites within the historical training data and non-TC synthetic event set, i.e. addressing whether particular pairs of gauges show the same dependence in the training data as in the non-TC synthetic event set. We do this by iteratively selecting each gauge site, finding all events in which it was threshold exceeding, and then for every other site we record the proportion of these events that both sites were threshold exceeding (i.e. if the conditioning site was large 10 times, a neighbor was large during all 10 of those events, then the score would be 1). We generate a scatter plot of each conditioning site, plotting this score against all other sites. Each point on the scatter gives the synthetic pairwise co-occurrence score against the corresponding historic co-occurrence score. We then calculate the r2 score of this scatter. We then plot the distribution of all the r2 scores in Figure 60.

Below in Figure 59 we also provide 6 example conditional site scatter plots provided for the best and worst fluvial and pluvial sites (in terms of r2 scores), as well as a fluvial and pluvial site example near Miami.

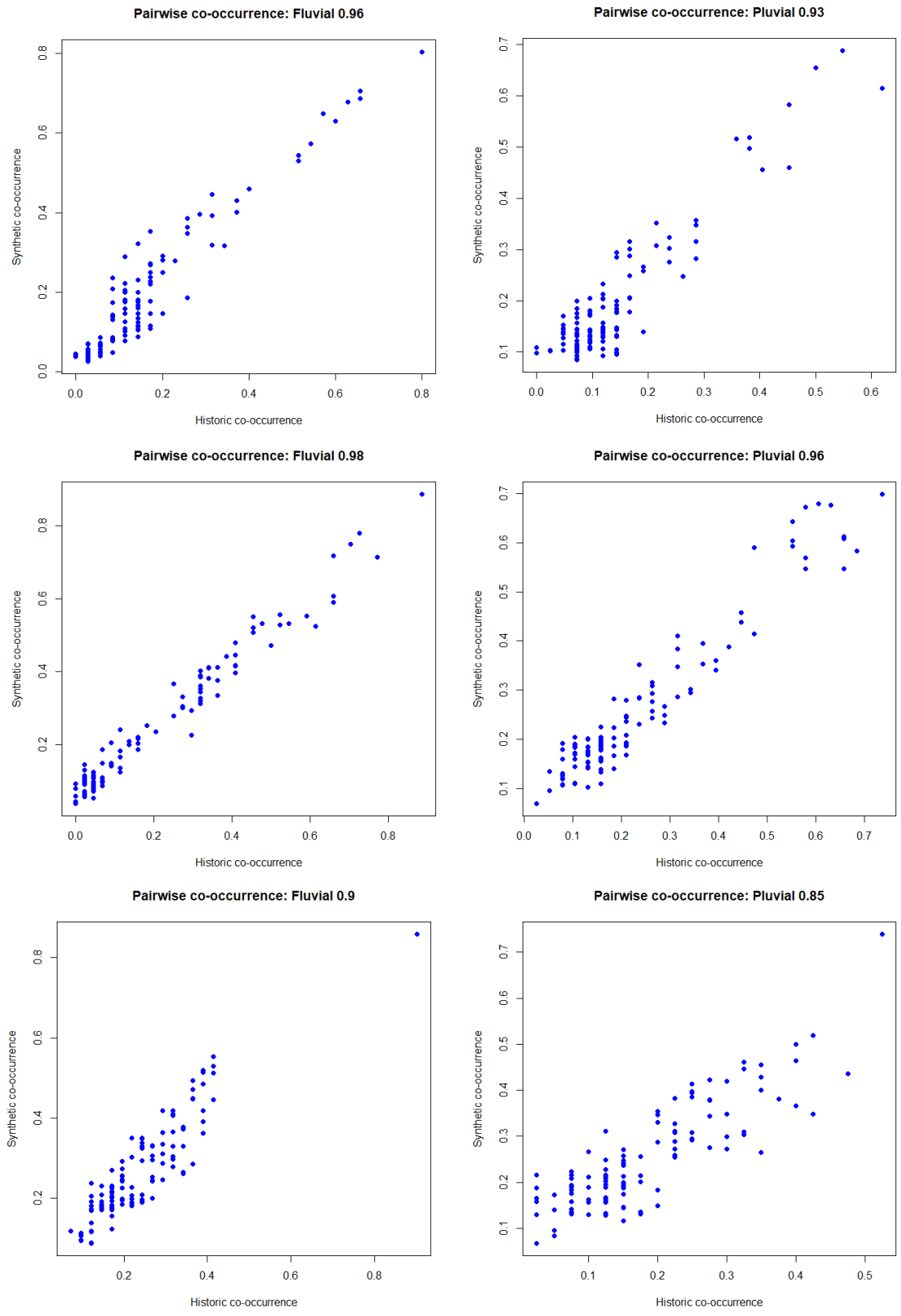

Figure 59: Site example co-occurrence plots; top (Miami), middle (best scoring), bottom (worst scoring) examples

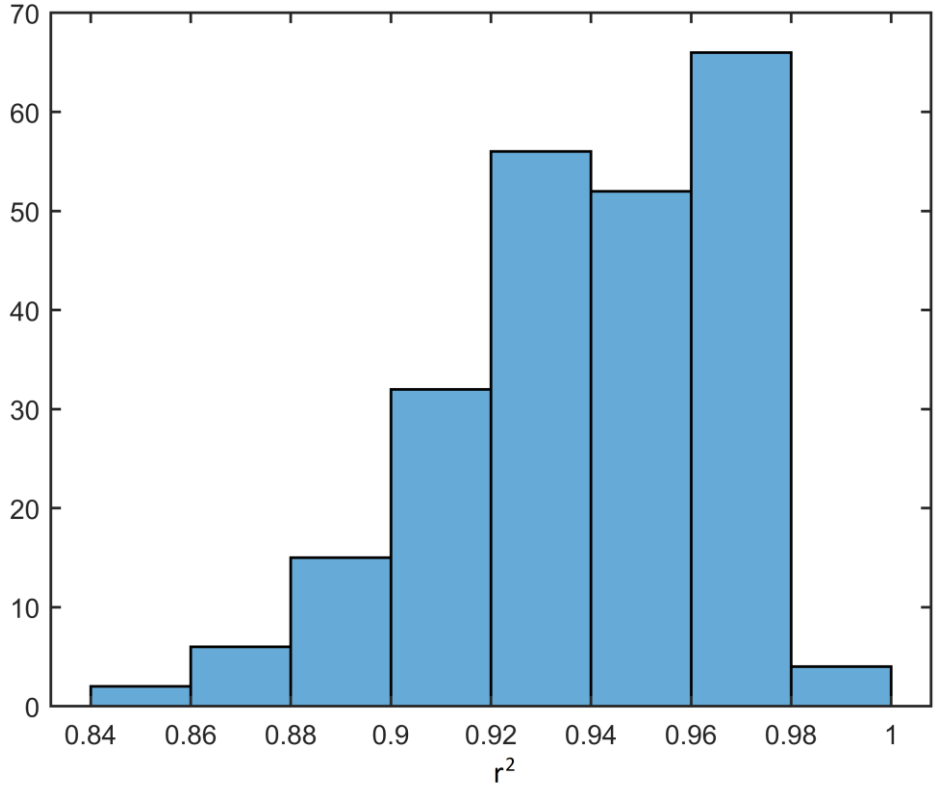

Figure 60: The histogram of co-occurrence r2 scores across all Florida data locations

Another similar metric, Chi, is provided Figure 61. Chi (Coles, et al., 2001) is commonly used to characterize the tail dependence between 2 sets of data, quantifying the extremal dependence between them (effectively the likelihood one is extreme given that the other is). Here we plot the non-TC synthetic event set and historic training data Chi values between 5,000 pairs of data locations. While the paired difference Wilcoxon test rejected the symmetry of differences (likely due to sample size as well as due to visible shift for lower Chi values), the difference is not substantial and the overall performance is satisfactory.

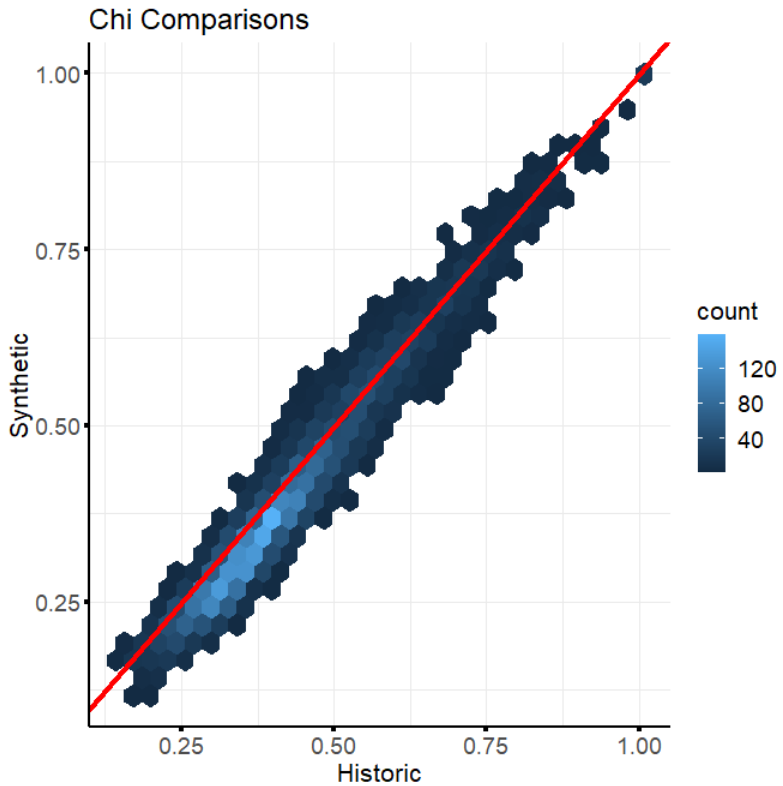

Figure 61: Chi statistics (Coles, et al., 2001) over 5,000 data site pairs in the historical training data and the synthetic data.

Spatial co-occurrence patterns

Here we provide qualitative examples of the event co-occurrence between sites. In each plot below (Figure 62 and Figure 63), for a given conditioning site, we plot the probability that each neighbor is threshold exceeding, given the site of interest is threshold exceeding. We do this for the historical training data and the non-TC synthetic event set for 2 example conditional sites, providing a pluvial and fluvial example. For clarity, we restrict neighbor plots to those with values ≥ 30%.

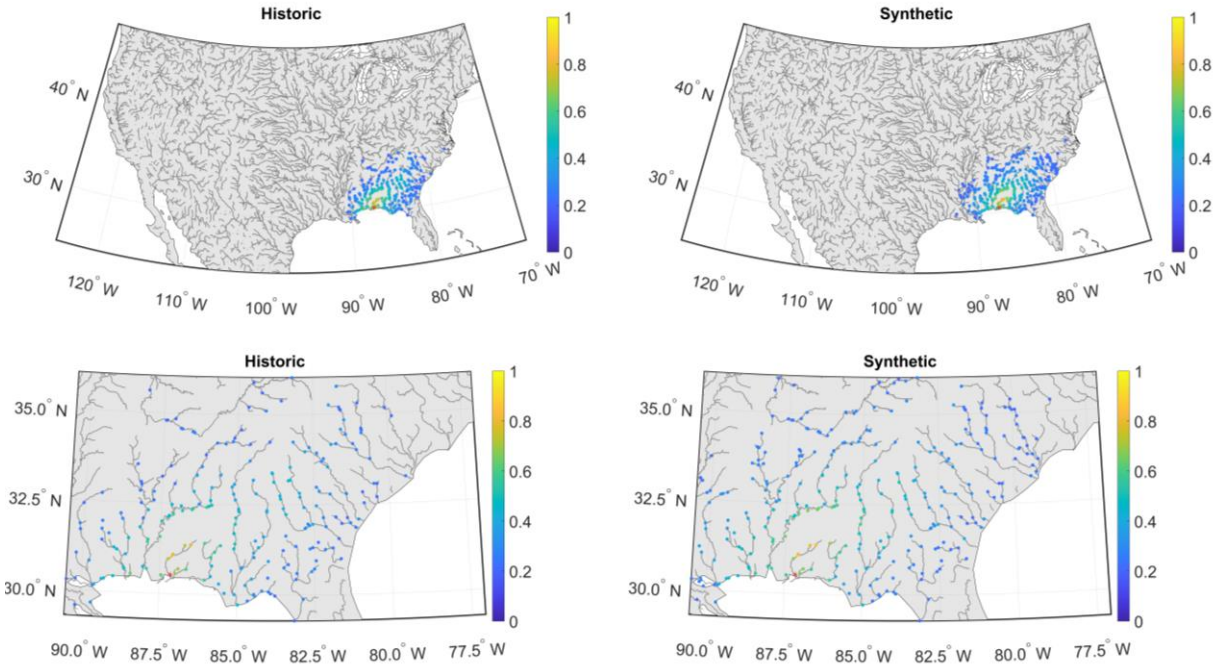

Figure 62: Example fluvial likelihood maps (SiteID = 1398).

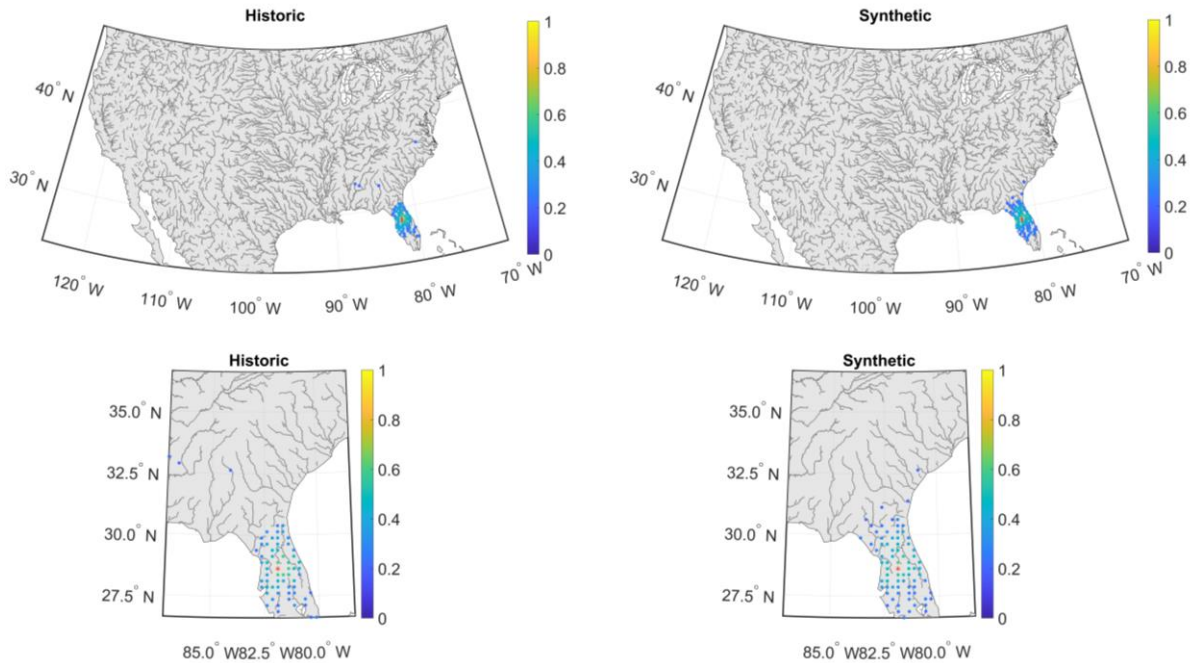

Figure 63: Example fluvial likelihood maps (SiteID = 5679).

Number of events

In this test we contrast the number of unique events seen across Florida each year, either TC or non-TC, on average, in the synthetic and historic event sets. Each event in the event sets is extracted and a 'hit' recorded if at least one catchment, in either peril (exceeds our potential loss causing threshold (10yr). Table 19 provides the event rates above this threshold. Upper and lower Wald confidence bounds are provided in the brackets for the

historical period. Figure 64 (left) plots the empirical distributions of the agnostic event rates, while Figure 64 (right) plots empirical CDFs from 5,000 samples of 40yrs of data from the synthetic event set with the historical CDF overlain in red.

Table 19: Annual rates of unique event impacts across Florida. Bracket values represent Wald confidence bounds obtained from a bootstrapping analysis of the historical data.

Metric (at 10yr threshold)	Synthetic	Historic
Number of impacts p/y (process agnostic)	2.7	3 [2.4, 3.6]
Number of impacts p/y (TC)	0.9	1 [0.6, 1.3]
Number of impacts p/y (NTC)	1.8	2 [1.6, 2.5]

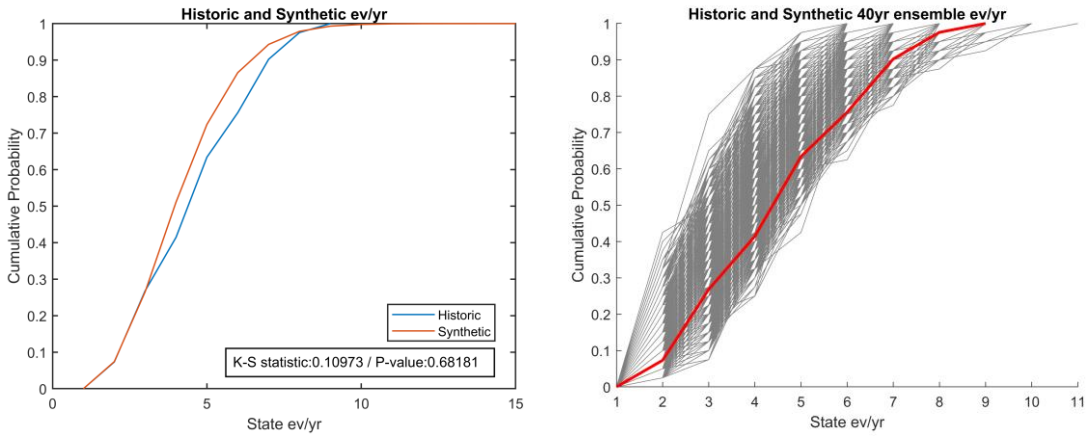

Figure 64: The synthetic event set and historic agnostic empirical distributions of events per year (left), an ensemble of CDFs from 5000 iterations of 40yrs of data from the synthetic event set with historical (red) overlain (right). For clarity, the CDFs are linearly interpolated within these figures.

Seasonality of TC events

The TC event occurrence date information was obtained from HURDAT2 database. The comparison between modeled and measured TC event occurrence rate per month is provided in Figure 65. The p-value from a two-sample Pearson's chi-squared test performed on the data is 0.15. The test was performed on the counts of the TC events occurred each month. The number of TC event occurrence was aggregated in months that have very few occurrence (e.g. January ~ May, November ~ December). The p-value indicates reasonable agreement between modeled and measured occurrence rate of tropical cyclones affecting Florida at the 5% level of significance.

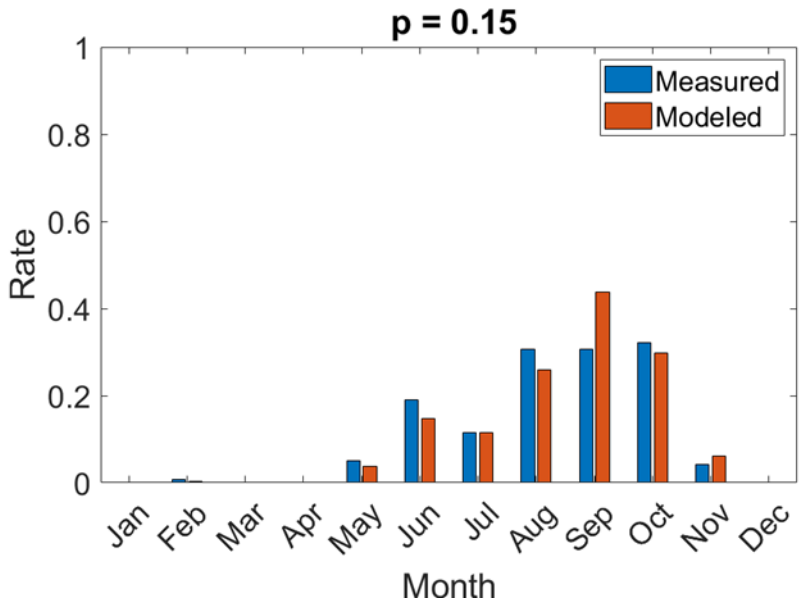

Figure 65: The monthly event occurrence rate for TC events affecting Florida.

Seasonality of non-TC events

In Figure 66 we plot the proportion of events occurring in each month in both the historical training data and the non-TC synthetic event set. Note that these are not loss causing events, nor are they related to any final RP magnitudes associated with the merged TC and non-TC products; rather they are non-TC synthetic events only, where the event threshold is the 1 in 0.5 yr non-TC magnitude. We don't provide specific statistics as the model framework effectively enforces correspondence. For context, the largest difference in monthly ratios does not exceed 0.5%. In subsequent analysis below, we will demonstrate how these patterns change in the final merged event set over thresholds of relevance to flooding.

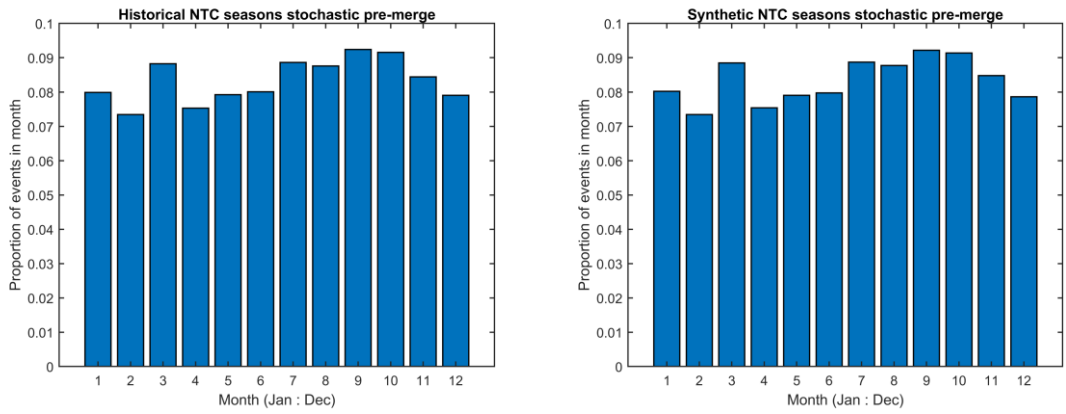

Figure 66: The seasonality of threshold exceedances in the historical training data and synthetic data event sets.

Seasonality of events combined

This test evaluates the synthetic event set and historical data in terms of the seasonal frequency of events. The event threshold used is the 1 in 10yr RP. A Chi Square test was performed on the seasons counts within both datasets producing a value of 7.51 for Chi and

a corresponding P value of 0.757. Figure 67 provides the historic and synthetic event set event rates given as a proportion of all events for ease of comparison.

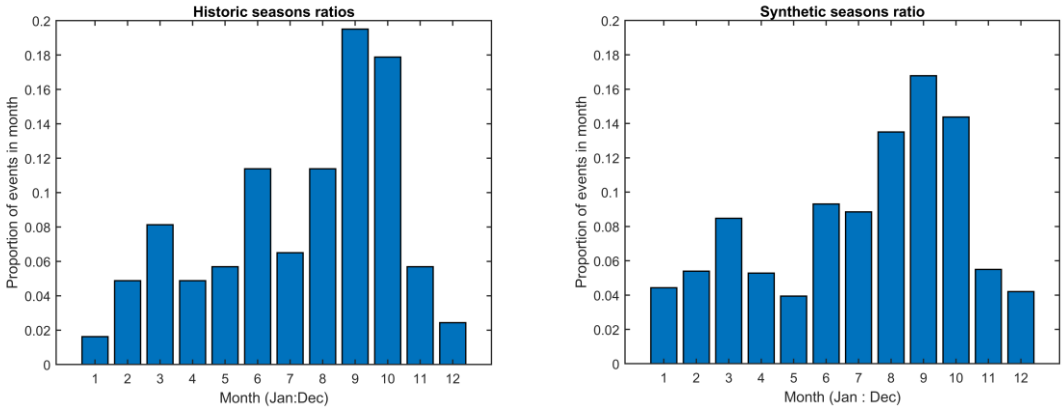

Figure 67: The historic (left) and synthetic event set (right) proportional month event rates.

Presence of non-TC 'historical' events

This procedure was performed to qualitatively assess whether the non-TC synthetic event set was able to reproduce sample footprints found within the historical (non-TC) training data. In this instance we present a 'significant' event in the training record, defined in this case as the event that contained both the largest RP sum across all catchments and the largest number of unique catchments exceeding our event threshold. The target event footprint (defined at site point locations) is provided in Figure 69. Plot scales report return periods at sample points.

Each event in the non-TC synthetic event set was assessed and retained for comparison if it met all the following criteria:

- RP match at our largest site in the historical of +/- 50%
- Match the regional sum RP value within +/- 50%
- Match the regional sum of unique site exceedances within +/-50%

12 events remained that matched the specified criteria. Plots of their 3 metric values against the target event are given below (Figure 68), with 2 example footprints provided in Figure 70.

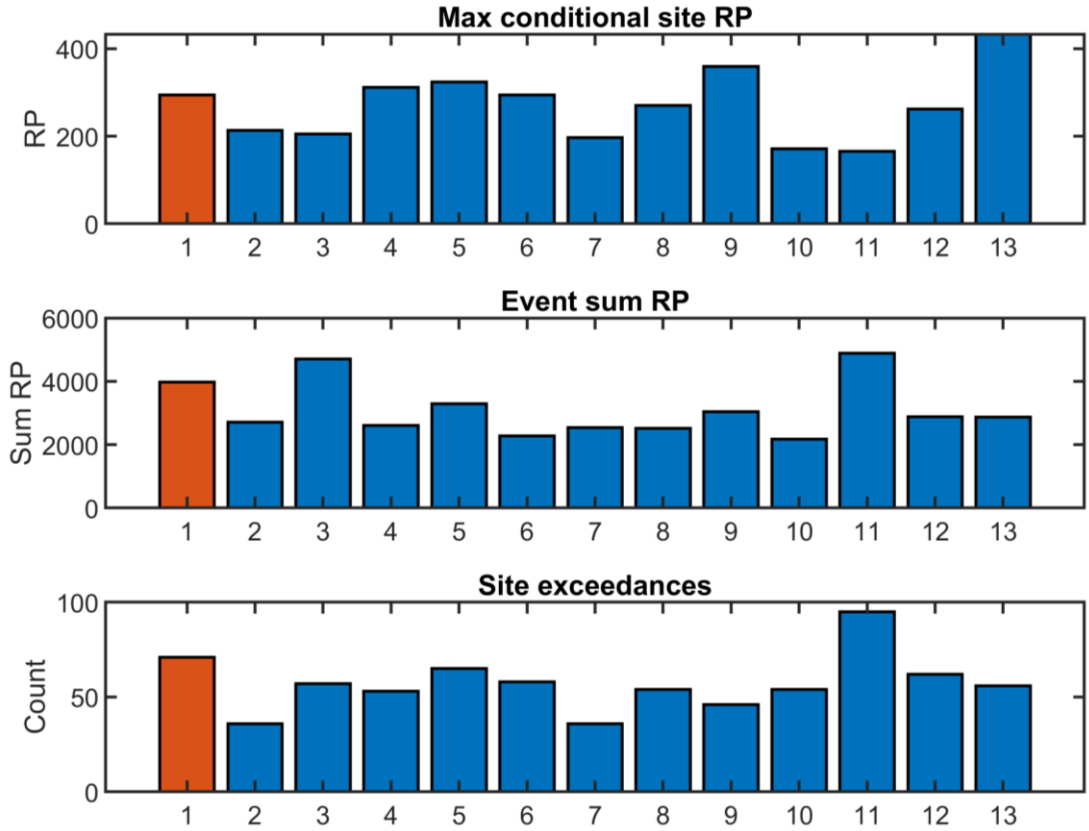

Figure 68: The target event metric scores (orange) and the 12 'similar' events from the statistical model non-TC synthetic event set (blue).

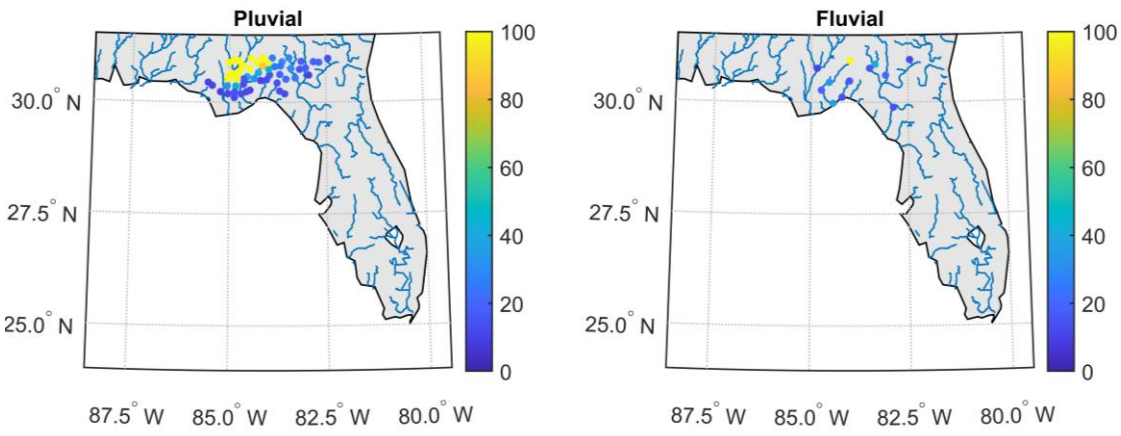

Figure 69: The fluvial and pluvial footprints associated with the target event chosen from the historical training data.

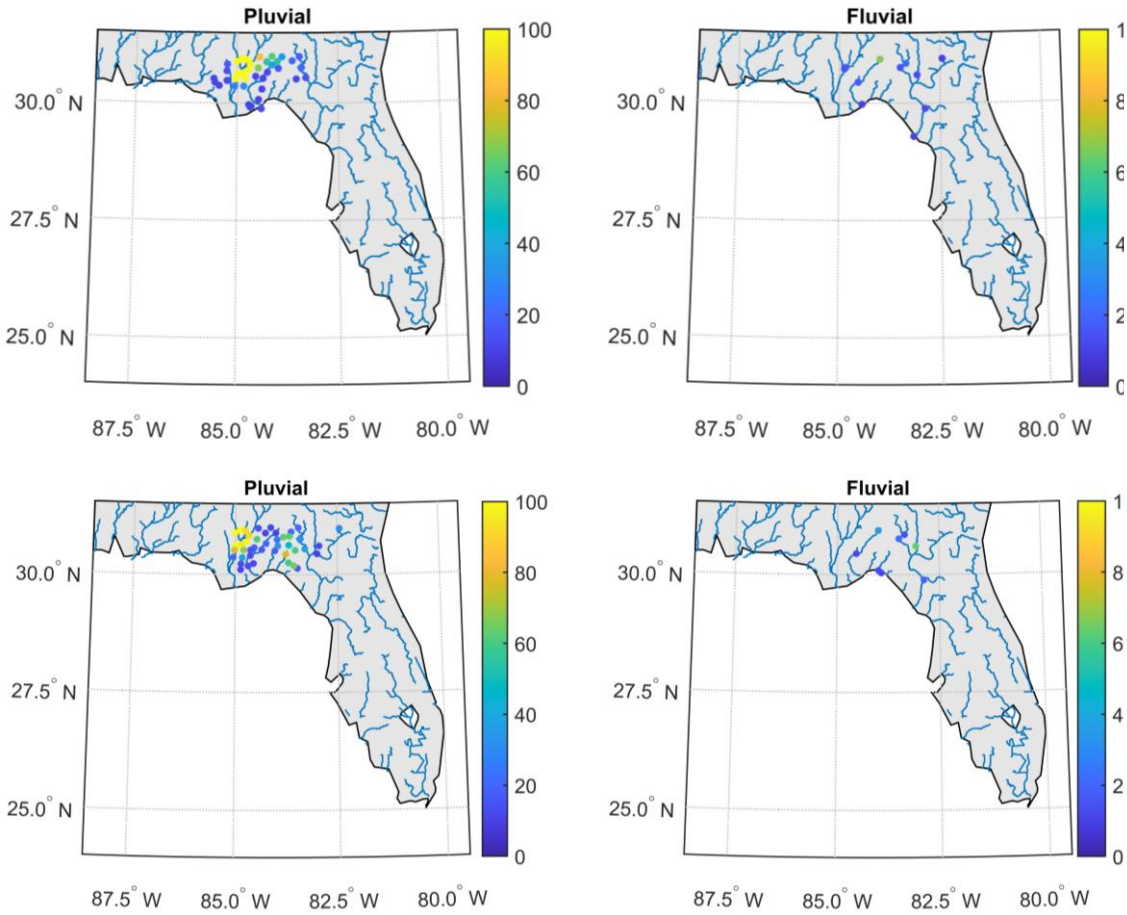

Figure 70: Example events (EventID = 296732 -top and Event ID = 935658 -bottom) from the non-TC synthetic event set that met the specified criteria to be 'similar' to the target event. Magnitudes given in terms of return period.

Vulnerability

To show our building damage ratios are statistically significant, we compared a set of our modeled losses to a subset of the NFIP claims data from August 2023. We included Welch's t-tests for both inland flooding and storm surge Residential Single-Family losses to ensure our modeled losses are similar to that of claimed losses. Through this we see that our damage ratios pass t-tests among 1 ft bins from 1-4ft for storm surge and 2-4ft for inland as provided in the below tables. The claims data is provided at the censustract level and has more uncertainty for the inland data at smaller flood depths. This added uncertainty, along with a larger number of outlier claims, result in the inland curves not passing on the 1-2ft bin like storm surge. Figure 71 shows our losses compared to storm surge claims, while Figure 73 shows our losses compared to inland claims.

Flood Depth (ft)	P.value	Average Claims	Average Modeled	Claims Count	Test of Significance
0 – 1	0.00	0.06	0.04	11,823	
1 – 2	0.68	0.10	0.11	8,311	*
2 – 3	0.94	0.19	0.19	5,946	*
3 – 4	0.23	0.18	0.22	3,778	*
4 – 5	0.05	0.21	0.31	1,285	
5 – 6	0.00	0.13	0.37	1,120	
6 – 10	0.00	0.17	0.55	3,507	

Figure 71: Storm Surge Building Damage Functions Statistical Significance Test

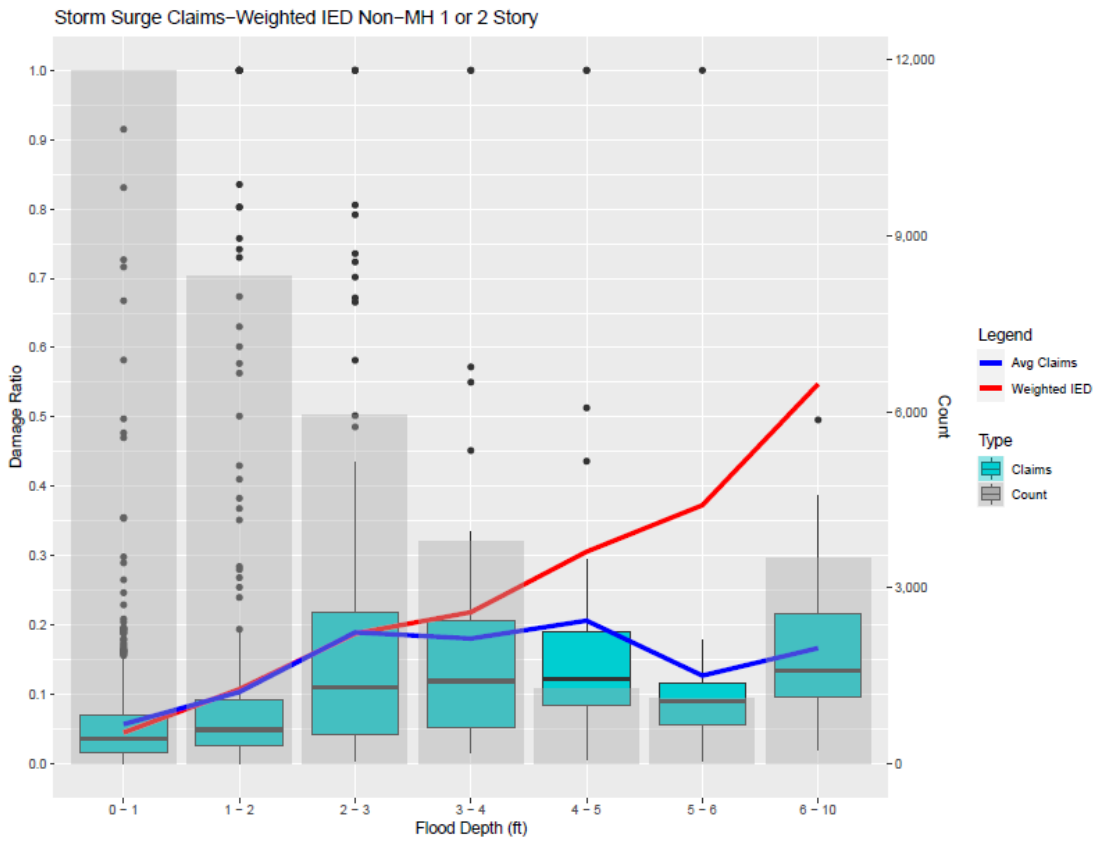

Figure 72: Box Plot Of Storm Surge Depth/Damage Ratios with NFIP Claims

Flood Depth (ft)	P.value	Average Claims	Average Modeled	Claims Count	Test of Significance
0 – 1	0.00	0.10	0.06	22,083	
1 – 2	0.00	0.13	0.08	5,305	
2 – 3	0.82	0.14	0.13	1,154	*
3 – 4	0.23	0.16	0.21	132	*
4 – 5	0.00	0.09	0.32	15	
5 – 10	0.00	0.19	0.36	723	

Figure 73: Inland Flood Building Damage Function Statistical Significance Test

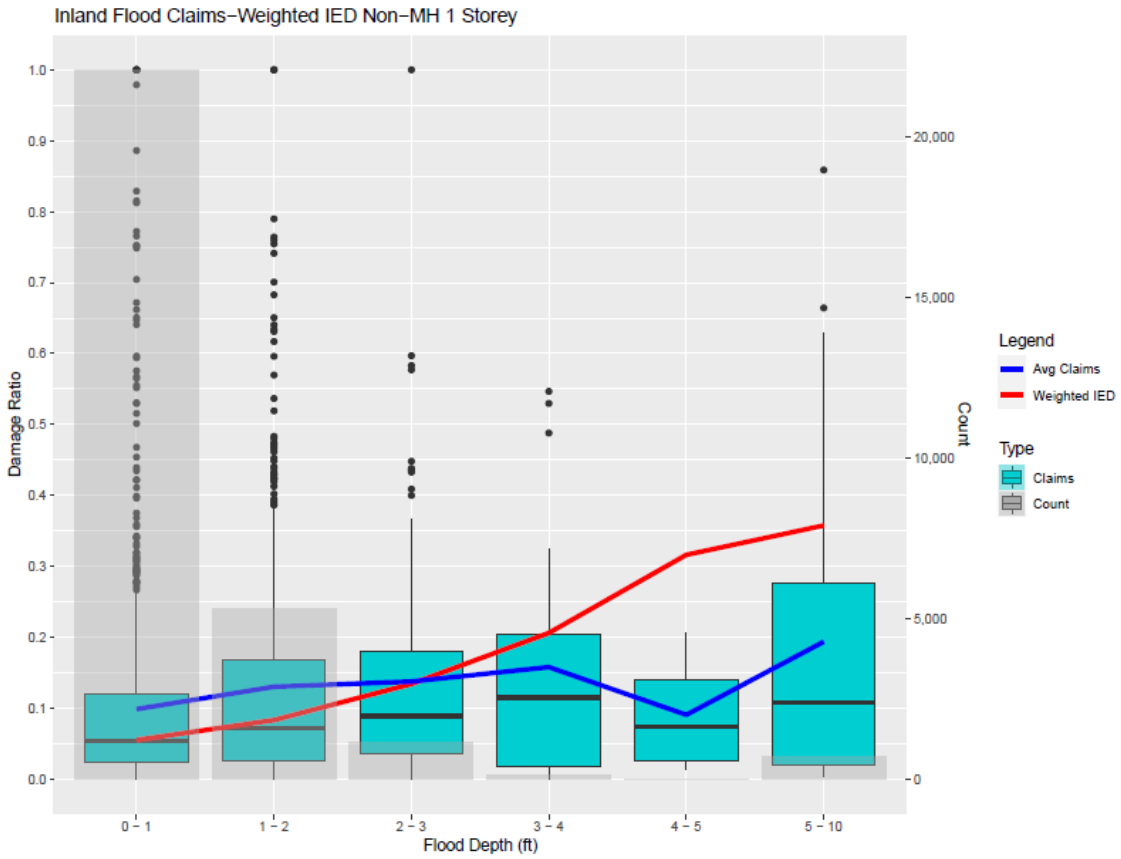

Figure 74: Box Plot Of Inland Flood Depth/Damage Ratios with NFIP Claims

SF-1.6 ***Provide a completed Form SF-2, Examples of Flood Loss Exceedance Estimates (Coastal and Inland Combined). Provide a link to the location of the form [Form SF-2: Examples of Flood Loss Exceedance Estimates (Coastal and Inland Combined)].***

The completed Form SF-2 is provided in the hyperlink above.

SF-2 Sensitivity Analysis for Flood Model Output

The modeling organization shall have assessed the sensitivity of temporal and spatial outputs with respect to the simultaneous variation of input variables using current scientific and statistical methods in the appropriate disciplines and shall have taken appropriate action.

Impact Forecasting has assessed the sensitivity of outputs with respect to the simultaneous variation of input variables using current scientific and statistical methods. The sensitivity analysis results can be found in Disclosure SF-2.1.

Disclosures

SF-2.1 Identify the most sensitive aspects of the flood model and the basis for making this determination.

The most sensitive aspects of the Storm Surge component in the Impact Forecasting Flood Model are far field pressure (FFP), radius of maximum winds (Rmax), and central pressure (Cp). This conclusion is based on the results of the sensitivity analysis following the guidelines from Form S-6 of the FCHLPM Hurricane Standards Report of Activities as of November 1, 2021.

The hurricane input variables, track direction, landfall points, and exposure information are from Form S-6 of the FCHLPM Hurricane Standards Report of Activities as of November 1, 2021. The sensitivity analysis is based on the standardized regression coefficients (SRC) of each input variable. The calculation of SRC follows the methodology from (Iman, et al., 2001). Four model input variables are included in the sensitivity analysis: central pressure (Cp), radius of maximum winds (Rmax), translational velocity (VT) and far field pressure (FFP).

The results of the SRCs from the sensitivity analysis are summarized in Table 20 and Figure 75 below. Figure 75 shows that FFP and Cp have the most influence on the magnitude of the storm surge loss cost for a Category 1 hurricane. The relationship is positive for FFP and negative for CP. VT and Rmax have little influence. The Category 3 results in Figure 75 show that Rmax and FFP have large influence while the influence of Cp is reduced. The influence of VT to Category 3 storms increases compared to Category 1 storms, and the relationship is negative. For Category 5 hurricanes, Figure 75 shows that Rmax has the largest influence (positive) on the magnitude of the loss cost. The VT (negative), FFP (positive) and Cp (negative) have SRCs that are similar to each other, and they have small influence on storm surge loss cost.

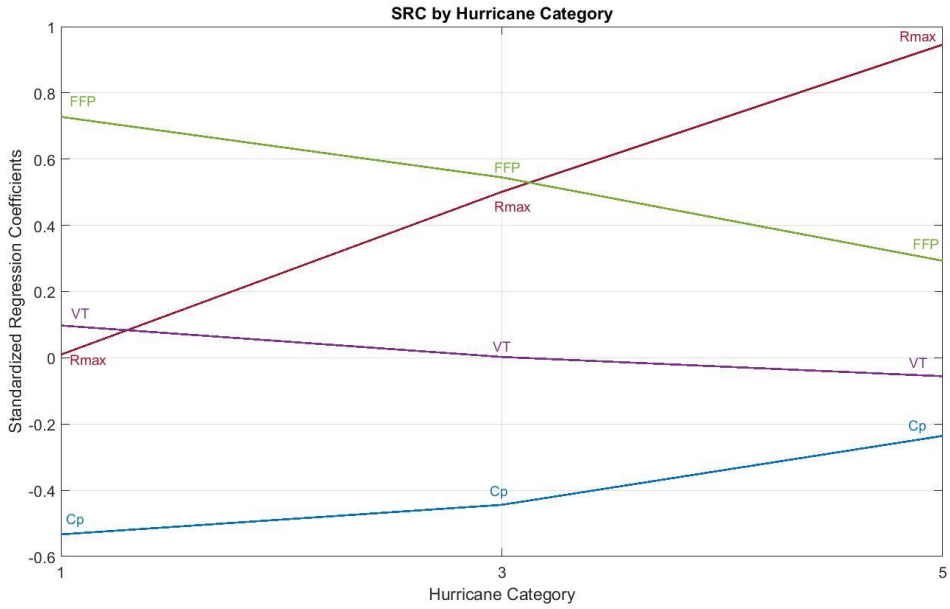

Figure 75 SRCs for expected storm surge loss costs for all input variables for all hurricane categories.

Table 20 Calculated SRCs for expected storm surge loss costs for all input variables for all hurricane categories.

Category	Cp	Rmax	FFP	VT
1	-0.5332	0.0095	0.7276	0.0976
3	-0.4439	0.5012	0.5448	0.0026
5	-0.2357	0.9457	0.2929	-0.0556

For the inland modeling the individual inundation hazard maps are fixed, and events are compiled from cut-outs of individual areas as defined by the local return periods in the fixed event set. While each flooding event is ultimately corresponding to certain discharges and rainfalls, those are not considered input variables as such. Impact Forecasting performed a set of exploratory analyses to illustrate the effect of changing key model parts and model parameters, presented in Disclosure SF-2.2 and Disclosure SF-2.3 as well as Disclosure HHF-4.1.

The analysis of the temporal sensitivities of loss costs was not performed since loss costs depend on the peak surge or flood inundation and not the temporal variation of the surge or flood inundation.

SF-2.2 Identify other input variables that impact the magnitude of the output when the input variables are varied simultaneously. Describe the degree to which these sensitivities affect output results and illustrate with an example.

In modeling surge Impact Forecasting has identified no other input variables that impact the magnitude of the output when input variables varied simultaneously.

Inland Modeling

In this section, we provide values that come from analyses carried out in the frame of Standard HHF-4. The complexity and cost do not allow proper sensitivity analysis.

Tasks below follows the structure of HHF 4 standard and provide a short insight how the flood depth differs after the input parameters were modified. The depth ratios in the exhibitions are calculated as $1 - \frac{Modified\ simulaton}{Base\ simulation}$.

From the simulations demonstrated, the highest effect is visible in the model setup when permeability is switched off.

A: Hydraulic roughness

Hydraulic roughness was increased by 20% causing changes shown in the following table. Figure 76 shows changes in the water-level progress (as requested in HHF-4 A), while Table 21 demonstrate the peak flood depth of base and modified simulation.

Table 21: Testing the effect of water-level and depth increments on fluvial simulation when hydraulic roughness is increased by 20%

Point	Modification	Base Depth (ft)	Modified Depth (ft)	Depths ratio	Depths difference
				%	ft
#1	+20%	38.00	38.30	0.78%	0.301
#2	+20%	10.22	10.27	0.44%	0.046
#3	+20%	10.33	10.69	3.44%	0.367
#4	+20%	9.88	10.22	3.30%	0.337
#5	+20%	23.64	23.88	1.00%	0.239

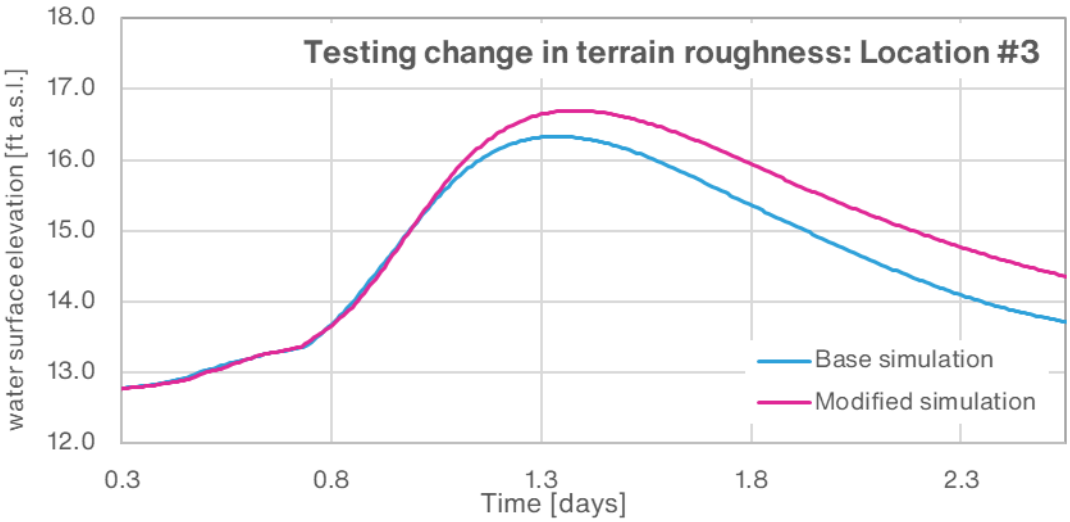

Figure 76 Example of water-level increment after hydraulic roughness was increased by 20% (Alafia River in Hillsborough County)

B: Steepness

In this analysis, the altitude was increased by 20% that caused increase in the terrain slopes. Figure 77 shows progress of base and modified simulation, while Table 22 shows peak flood discharge.

Table 22: Testing the effect of depth change on fluvial simulation when topography is increased by 20%

Point	Modification	Base Depth (ft)	Modified Depth (ft)	Depths ratio	Depths difference
				%	ft
#1	+20%	38.00	44.05	13.75%	6.055
#2	+20%	10.22	11.34	9.87%	1.119
#3	+20%	10.33	10.93	5.51%	0.603
#4	+20%	9.88	10.58	6.65%	0.704
#5	+20%	23.64	27.79	14.95%	4.156

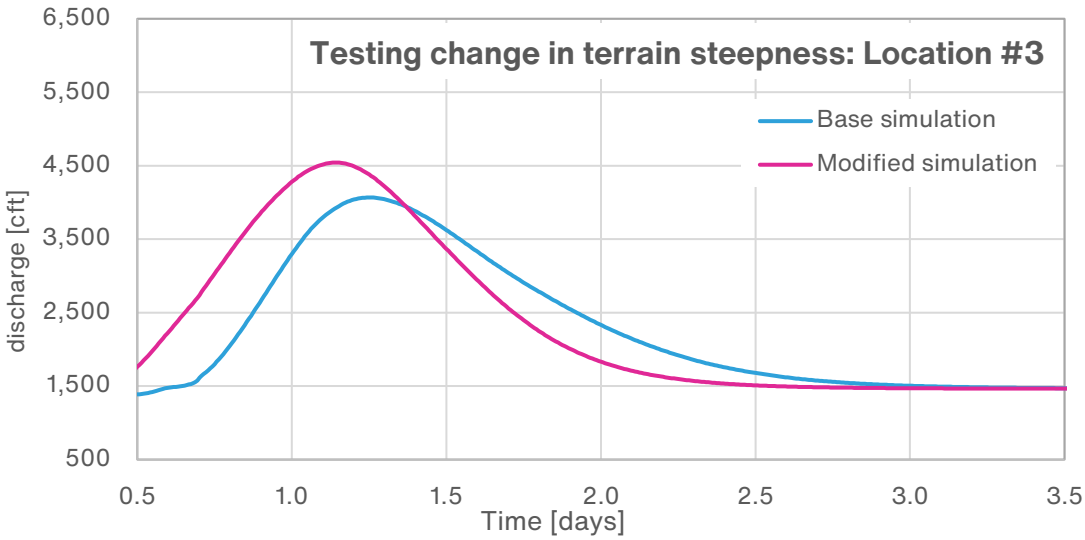

Figure 77 Example of discharge increment after DTM elevation was increased by 20% (Alafia River in Hillsborough County)

C: Impermeability

In this analysis, the surface permeability was switched off. As this parameter is not used (and not differentiated) in fluvial simulation, this test evaluates the results of pluvial simulation and absolute depth can't be therefore directly compared.

Figure 78 shows effect on outflow discharge (as requested in HHF-C) and Table 23 shows peak depth reached during the simulations.

Table 23: Testing the effect of water-level and depth increment on pluvial simulation when soil permeability is switched off.

Point	Modification	Base Depth (ft)	Modified Depth (ft)	Depths ratio	Depths difference
				%	ft
#1	turned off	41.921	44.895	6.63%	2.974
#2	turned off	13.987	16.351	14.46%	2.364
#3	turned off	15.560	20.021	22.28%	4.461
#4	turned off	6.886	10.745	35.91%	3.859
#5	turned off	26.141	26.782	2.39%	0.641

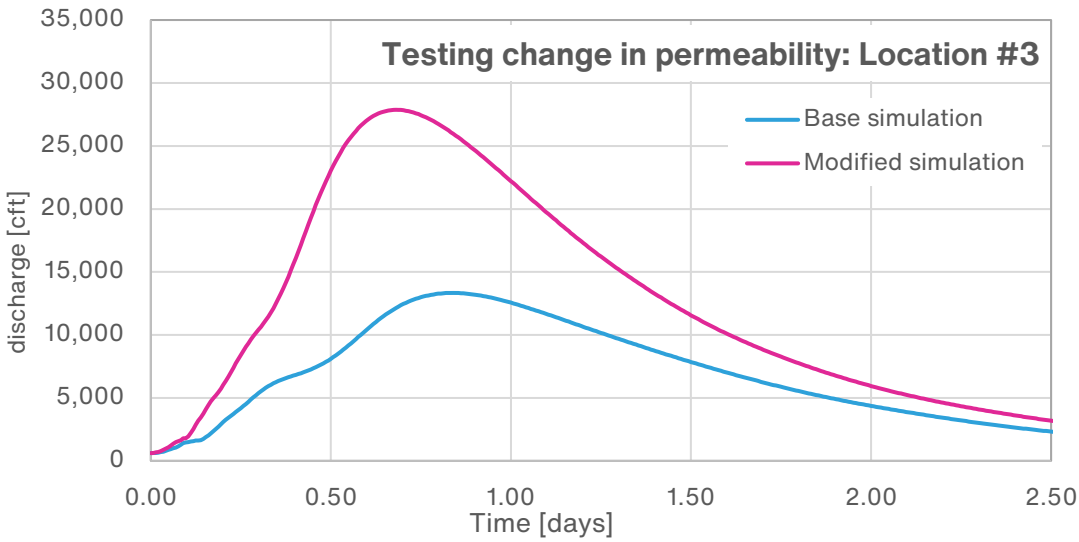

Figure 78 Example of water-level increment after surface permeability is switched off (Alafia River in Hillsborough County)

D: Discharge

In this section the input discharge was increased by 20%. Figure 79 shows the effect on inundation depth (as requested by Standard HHF-4 D), while Table 24 shows peak flood depth in base and modified simulation.

Table 24: Testing the effect of water-level and depth increments on fluvial simulation when input discharge is increased by 20%

Point	Modification	Base Depth (ft)	Modified Depth (ft)	Depths ratio	Depths difference
				%	ft
#1	+20%	38.00	38.79	2.05%	0.795
#2	+20%	10.22	10.27	0.50%	0.052
#3	+20%	10.33	10.93	5.53%	0.604
#4	+20%	9.88	10.42	5.24%	0.546
#5	+20%	23.64	23.75	0.48%	0.113

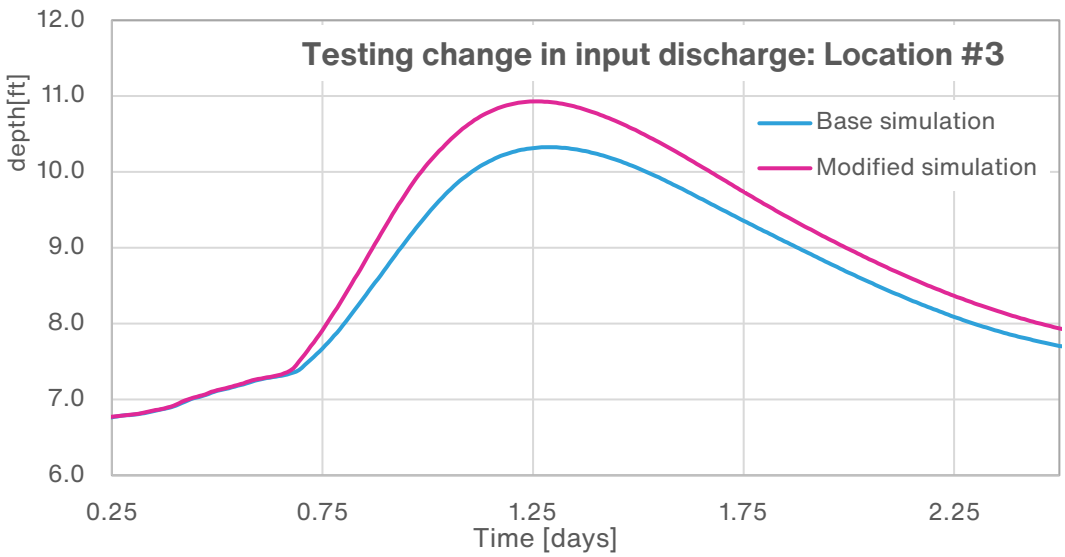

Figure 79 Example of water-level increment after input discharge was increased by 20% (Alafia River in Hillsborough County)

SF-2.3 Describe how other aspects of the flood model may have a significant impact on the sensitivities in output results and the basis for making this determination.

The storm surge loss costs may also be sensitive to the storm landfall location, angle of approach to the coast, the shape and characteristics of coastal features such as bays and estuaries and the slope of the continental shelf. This determination is made based on studies performed by IF scientists through changing the heading direction and landfall locations of the hypothetical storms.

The rainfall parameters used in pluvial situation are schematized as the RP set of design-rainfalls used is derived for one rainfall duration and the temporal progress of rainfall intensity of any real rainfall will be different.

One of the important parameters in routing models, and in mizuRoute in particular, is Manning's roughness coefficient. The model setup uses a value of 0.01 across the US, which can be low for river channels. To assess the potential effect a hindcast using a value of 0.03 (closer to the value of 0.04 used by LISFLOOD-FP for river channels) was run. Figure 80 shows that, in Florida, there is a marginal gain in KGE, that barely improves the performance of FUSE-mizuRoute.

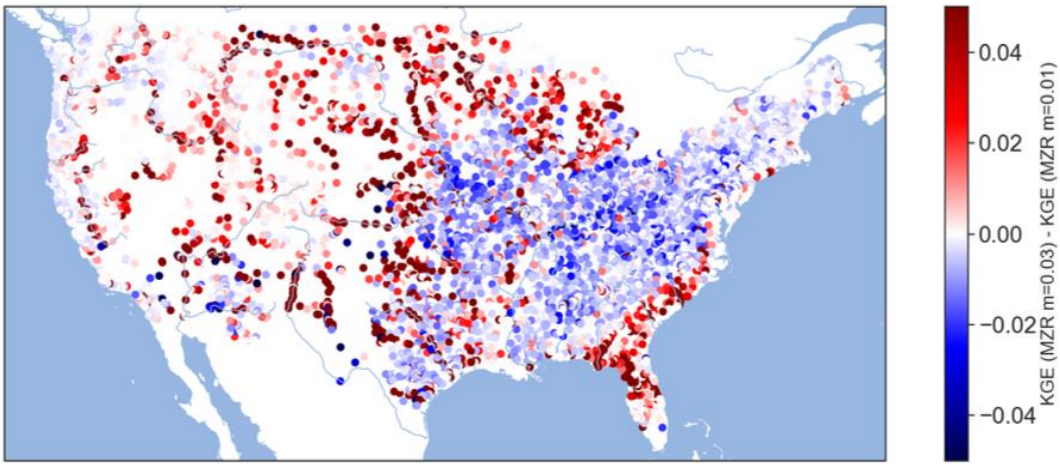

Figure 80 Difference in KGE between the hindcasts using Manning's coefficient of 0.03 versus 0.01. Values greater than 0 indicate a higher KGE with n=0.03, while values smaller than 0 indicate a better performance with n=0.01.

There are a number of parameter decisions required within the non-TC synthetic event set modeling framework. Here we present an effect of change of two parameters that we believe are both influential and uncertain: the clustering temporal and spatial windows. These parameters are used in the pre-processing stage of the framework and influence what the model defines as a unique 'event' in the historical records. These events form our training dataset upon which the synthetic event set model is built, so they are potentially influential to the output, yet it is difficult to define what an 'event' is (or should be). This combination of influence and uncertainty makes these parameters interesting to assess.

It is important to note, however, that these sensitivity tests relate only to the non-TC synthetic event set model outputs, specifically the impact on the size distributions (extent and duration) from uncertainty in the spatio-temporal clustering algorithms implemented. Further, this data (and its sensitivities) have no impact upon the hydraulic simulation of the flood hazard; they can only impact the footprint used to sample from the underlying hazard layers, after return periods are calculated from the non-TC and TC merged event sets. For this reason, it would be extremely difficult to fully capture the impact of these sensitivities on the final flood event set hazard, let alone the ultimate losses, without re-generating the full CAT model for each iteration. Therefore, here we examine the influence of parameter choice only on the resulting non-TC footprint characteristics, and do not consider downstream impacts.

In this test we re-run the non-TC synthetic event set model twice, once with 'relaxed' clustering constraints (i.e. events are clustered with longer time windows and larger spatial search windows) and once with more severe clustering constraints.

Table 25 provides the parameter values tested and the corresponding defaults.

Table 25: Sensitivity testing parameter choices

Run set	EV temporal window (days)	Dbscan spatial radius (deg)
Default	7	5
R1 relaxed constraints	10	7.5
R2 tightened constraints	4	2.5

The resulting synthetic event sets were then contrasted using 3 metrics: the total number of events, the empirical CDF of event durations, and the empirical CDF of event sizes. Table 26 provides a summary of these metrics while Figure 81 plots the empirical CDFs of event size and duration.

Table 26: Sensitivity assessment result metrics

Metric (FL impacts only)	Default	R1 (relaxed)	R2 (tightened)
Total events	739	596	935
CDF of duration 5,50,95,99	1, 3, 12, 17	1,4,15,20	1,2,8,11
CDF of event sizes (count) 5,50,95,99	1,10,96,142	1, 12, 104, 171	1,7,84,126

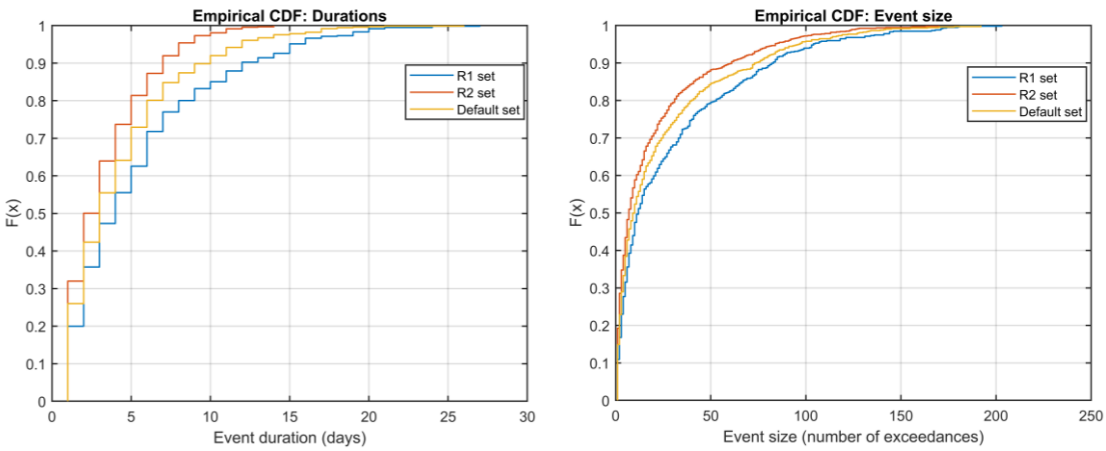

Figure 81: Sensitivity analysis empirical CDFs of event duration (left) and event size (right)

SF-2.4 *Describe and justify action or inaction as a result of the sensitivity analyses performed.*

The results of the sensitivity analysis have been carefully reviewed and were found to be reasonable. No action was taken.

SF-3 Uncertainty Analysis for Flood Model Output

The modeling organization shall have performed an uncertainty analysis on the temporal and spatial outputs of the flood model using current scientific and statistical methods in the appropriate disciplines and shall have taken appropriate action. The analysis shall identify and quantify the extent that input variables impact the uncertainty in flood model output as the input variables are simultaneously varied.

Impact Forecasting has assessed the uncertainty of the flood outputs with respect to the simultaneous variation of input variables using current scientific and statistical methods. The uncertainty analysis results can be found in Disclosure SF-3.1.

Disclosures

SF-3.1 Identify the major contributors to the uncertainty in flood model outputs and the basis for making this determination. Provide a full discussion of the degree to which these uncertainties affect output results and illustrate with an example.

The far field pressure (FFP) is the major contributor to the uncertainty in storm surge loss costs for Category 1 storms. For Category 3 and Category 5 hurricanes, Rmax has the greatest impact. This conclusion is based on the results of the uncertainty analysis following the guidelines from Form S-6 of the FCHLPM Hurricane Standards Report of Activities as of November 1, 2021.

The hurricane input variables, track direction, landfall points and exposure information are from Form S-6 of the FCHLPM Hurricane Standards Report of Activities as of November 1, 2021. The uncertainty analysis is based on the expected percentage reduction (EPR) in the variance of storm surge loss cost. The calculation of EPR follows the methodology from Iman, Johnson, and Schroeder (2001). Four model input variables are included in the uncertainty analysis: central pressure (Cp), radius of maximum winds (Rmax), translational velocity (VT) and far field pressure (FFP).

The results of the EPRs from the uncertainty analysis are summarized in Table 27 and Figure 82 below. Figure 82 shows that FFP contributes most to the uncertainty in storm surge loss cost for a Category 1 storms. Cp makes the second largest contribution to uncertainty while Rmax and VT have little influence. For Category 3 storms, Rmax makes the largest contribution to the uncertainty in storm surge loss cost, followed by FFP and CP. VT continues to have little influence. The contribution of Rmax increases as the storm intensity increases. It becomes the dominant contributor to the uncertainty of storm surge loss cost for Category 5 storms. The contributions of the other 3 parameters are comparably negligible for Category 5 storms.

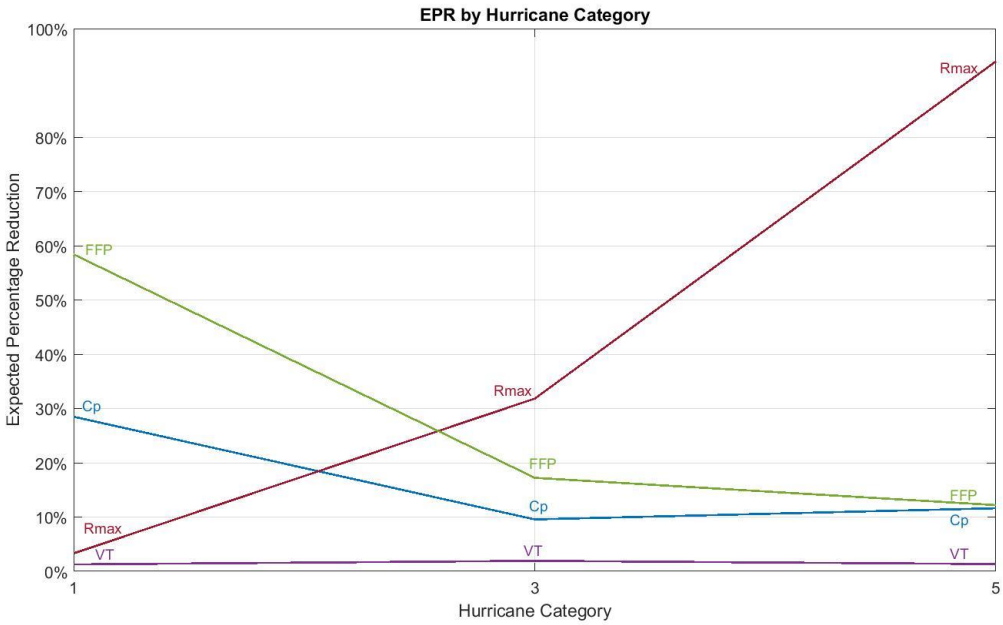

Figure 82: EPRs for expected storm surge loss costs for all input variables for all hurricane categories.

Table 27: Calculated EPRs for expected storm surge loss costs for all input variables for all hurricane categories.

Category	Cp	Rmax	FFP	VT
1	0.2849	0.0330	0.5840	0.0127
3	0.0956	0.3182	0.1723	0.0193
5	0.1162	0.9396	0.1220	0.0134

The largest contributors to uncertainty in inland flood model are expected to be the spatio-temporal parameters governing the event clustering, outlined and assessed within Disclosure SF-2.3. No further uncertainty analysis has been conducted on the non-TC synthetic event set model, as discussed above. The direct impact of any uncertainties in the synthetic event footprints upon the final model results would be very costly to explicitly calculate.

The analysis of the temporal uncertainties of loss costs was not performed since loss costs depend on the peak surge or flood inundation and not the temporal variation of the surge or flood inundation.

SF-3.2 *Describe how other aspects of the flood model may have a significant impact on the uncertainties in output results and the basis for making this determination.*

The uncertainties in the storm surge loss costs may also be related to the storm landfall location, angle of approach to the coast, the shape and characteristics of coastal features such as bays and estuaries, and the slope of the continental shelf. This determination is made based on studies performed by IF scientists through changing the heading direction and landfall points of the hypothetical storms.

The uncertainties in the inland flood loss costs can be driven by the presence, capacity, operation and failure of flood defenses, inaccuracies in the representation of floodplain and channel morphology by the Digital Terrain Model, variations in rainfall rates that occur at a temporal scale below the modeled temporal scale for rainfall, and flood wave celerity. This determination was made by IF scientists based on experience with these factors in other flood models developed by them. Yet another type of uncertainty can arise from the selection of training data or from clustering algorithm selection, which define the final properties of the events.

SF-3.3 Describe and justify action or inaction as a result of the uncertainty analyses performed.

The results of the uncertainty analyses have been thoroughly reviewed and were found to be reasonable. No action was taken as a result of the analyses performed.

SF-4 Flood Model Loss Cost Convergence by Geographic Zone

At a modeling-organization-determined level of aggregation utilizing a minimum of 30 geographic zones encompassing the entire state, the contribution to the error in flood loss cost estimates attributable to the sampling process shall be negligible for the modeled coastal and inland flooding combined.

The Impact Forecasting Florida Flood Model (FCHLPM) stochastic event set is constructed using 200,000 years of simulation. As described in Disclosure SF-4.1, the standard error in flood loss cost is lower than 5% of the estimated loss cost value for every county in Florida.

Disclosures

SF-4.1 Describe the sampling plan used to obtain the average annual flood loss costs and flood output ranges. For a direct Monte Carlo simulation, indicate steps taken to determine sample size. For an importance sampling design or other sampling scheme, describe the underpinnings of the design and how it achieves the required performance.

The general model structure, as described in Disclosure GF-1.2, consists of two probabilistic models (TC and non-TC) implemented in the ELEMENTS platform and a post-processing script that combines these to create a complete flood view of 200,000 years.

For the tropical cyclone induced flooding, IF uses a direct Monte Carlo simulation approach to estimate flood loss costs and flood output ranges. A sample size of 200,000 years was deemed adequate as the error in flood loss cost estimation associated with sampling becomes negligible at this sample size. In a sensitivity analysis during tropical cyclone event set development, the sample size was increased gradually, and the corresponding standard errors in flood loss costs at county level were calculated. With 200,000 years of simulation, the maximum standard error at county level becomes smaller than 5% of the loss cost estimate for every county in Florida. The event clustering was then performed to reduce the size of the event set. Tropical cyclone events were grouped based on region of landfall with similar wind speeds, radius of maximum winds, and decay rates. A single event is selected from each group, and the frequency is adjusted accordingly. A new event set was constructed using the representative events from all groups. The annual landfall frequency of the sampled TC events is in good agreement with the original event set.

A non-TC induced flooding event set is generated by Fathom in the 10,000 years of simulations with the appropriate length taken as industry standard discussed in (Diederen, et al., 2019; Li, et al., 2023; Quinn, et al., 2019; Wing, et al., 2020),or (Bates, et al., 2023). To provide an event catalog that matches the TC model, the non-TC event set is replicated 20 times to achieve the same 200,000 years of simulation.

The maximum standard error at county level for the combined TC and non-TC model is smaller than 5% of the loss cost estimate for every county in Florida.

SF-4.2 ***Describe the nature and results of the convergence tests performed to validate the expected flood loss projections generated. If a set of simulated flood events or simulation trials was used to determine these flood loss projections, specify the convergence tests that were used and the results. Specify the number of flood events or trials that were used.***

For each of the 67 counties in Florida, the mean (μ) and standard deviation (σ) of the flood loss cost for modeled coastal and inland flood combined were computed. The standard error was then calculated as $\frac{\sigma}{\sqrt{200000}}$ for each county and verified to be within 5% of the mean loss cost for all counties.

SF-5 Replication of Known Flood Losses

The flood model shall estimate incurred flood losses in an unbiased manner on a sufficient body of past flood events, including the most current data available to the modeling organization. This standard applies to personal residential exposures. The replications shall be produced on an objective body of flood loss data by county or an appropriate level of geographic detail.

The Impact Forecasting Florida Flood Model (FCHLPM) reasonably replicates incurred hurricane losses for 10 historical events from 1992 through 2022 for observed NFIP losses, as shown in Figure 83.

Disclosure

SF-5.1 Describe the nature and results of the analyses performed to validate the flood loss projections generated for personal residential losses. Include analyses for the events listed in Form HHF-1, Historical Event Flood Extent and Elevation or Depth Validation Maps.

The Aon US flood model team has performed extensive analysis of the input industry exposure database and the National Flood Insurance Program's (NFIP) policy and claims data sets. The NFIP loss databases were used by the team's analysts, scientists, and engineers as the basis of validation of event level losses.

Accurately performing validation of modeled event level industry losses compared to the NFIP's observed losses required significant analysis and processing of the NFIP's claims and policy database. The claims were partitioned in time and space using storm track and hydrologic data to assign claims to each of the individual events included in Form HHF-1. To take into account the increase in value of exposures that has occurred between the event's occurrence date and the IED's representative building stock date, a trending factor based on Collins and Low (2001) was applied to the NFIP loss data.

The NFIP writes over 90% of the residential insurance policies in Florida (Kousky, et al., 2018), though property owners are only required to purchase it if their property is encumbered by a federally backed mortgage and located within a special flood hazard area (SFHA). The Aon residential industry exposure database (IED) represents all residential risks, regardless of insured status, and the losses produced using this IED are not comparable to the observed NFIP losses. Therefore, to correctly validate the loss projections for each storm, the team created an estimated NFIP Take Up Rate (TUR) for each county in Florida. Utilizing the IED, the number of policies within each of the SFHAs, within a county, was compared against the number of total exposures within the same area. This factor was then multiplied against the total modeled gross losses to create a "modeled NFIP" loss value.

The differences between the modeled losses and the observed losses can be attributed to numerous factors that lie in a model's inability to fully resolve the physical processes that underlie the meteorological, hydrological, hydraulic, and mechanical processes that occurred during the modeled events. These limitations, as well as the uncertainties of the models themselves, are discussed at length in the other sections of this submission.

Additionally, the changes in the building stock, NFIP take up rates, and the built environment were all analyzed to determine how each assumption contributes to the difference between the observed and modeled NFIP losses. The most striking and yet obvious conclusion of this analysis was that after each event, the number of structures in all counties in Florida that were impacted by the modeled historical events in Form HHF-1 experienced an increase in the number of post-FIRM and decrease in pre-FIRM structures insured by the NFIP. Post-FIRM structures are far more resilient to damage from flooding due to a combination of elevation of the first habitable floor, relocation of building services and contents above the BFE, and the use of water-resistant building materials. In addition to changes to the risk profile of the NFIP's insured book, infrastructure improvements to mitigate flood hazards have been undertaken by state and federal authorities. These infrastructure improvements have resulted in a reduction of economic flood losses due to flooding of over $1.8bn since 2004.

Table 28: Modeled historical losses (Industry and NFIP) and trended observed NFIP losses

Storm Name	Modeled Industry Gross Loss	Modeled NFIP Gross Loss	Trended Observed NFIP Loss
Hurricane Andrew	7,123,030,163	1,042,239,634	1,294,513,377
Hurricane Frances	2,832,370,654	547,661,290	324,905,822
Hurricane Ivan	3,292,682,493	542,702,700	2,102,627,561
Hurricane Wilma	1,208,699,461	530,616,387	975,490,244
Hurricane Hermine	273,322,157	32,757,509	118,005,301
Hurricane Matthew	1,594,962,169	292,476,387	292,320,949
Hurricane Irma	2,914,512,298	784,048,467	979,526,059
Hurricane Michael	448,996,398	35,080,878	298,770,955
Hurricane Eta	1,853,300,717	429,794,469	167,548,951
Hurricane Ian	28,122,945,609	7,856,307,941	4,292,311,545

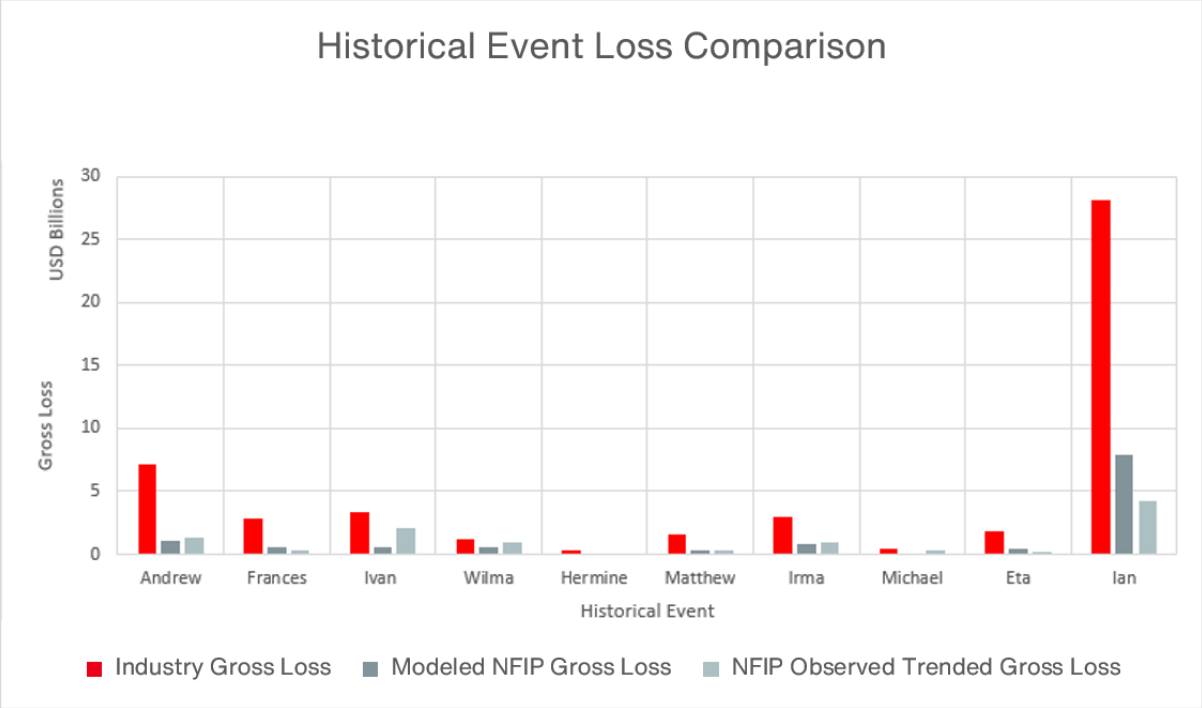

Figure 83 Historical Event Loss Comparison

VULNERABILITY FLOOD STANDARDS

VF-1 Derivation of Building Flood Vulnerability Functions

A. *Development of the building flood vulnerability functions shall be based on two or more of the following: (1) rational structural analysis, (2) post-event site investigations, (3) scientific and technical literature, (4) expert opinion, (5) laboratory or field testing, and (6) insurance claims data. Building flood vulnerability functions shall be supported by historical and other relevant data.*

The development of the building flood vulnerability functions incorporates rational structural analysis together with supporting information from scientific (Baradaranshoraka, et al., 2017), (Becker, et al., 2011), (Cantelmo & Cuomo, 2021), (Chidambarathanu & Retnan, 2013), (Custer & Nishijima, 2015), (Friedland & Levitan, 2009), (Herbert, et al., 2012), (Li & Ellingwood, 2006), (Li, et al., 2012), (Nasiri, et al., 2016), (Tomiczek, et al., 2014), (Masoomi, et al., 2019), (Kelman & Spence, 2003) and technical literature ((ACI Committee, 2008), (ASCE, 2014), (ASCE, 1998), (ASCE, 2016), (ASCE, 1988), (ASCE, 2022), (FBC, 2001), (FBC, 2004), (FBC, 2007), (FBC, 2010), (FBC, 2014), (FBC, 2017), (FBC, 2020), (FEMA, 2021b), (FEMA, 2011), (FEMA, 2010), (FEMA, 2009), (HUD, 2007), (HUD-MHCSS, 1994), (NDS, 2018)), post-event reconnaissance (Fritz, et al., 2007), (Genovese, et al., 2011), (Gurley, et al., 2017), (Prevatt, et al., 2018), (Prevatt, et al., 2019), (Smith & Scyphers, 2019), (Suppasri, et al., 2019), and expert opinion. The model methodology is detailed in Disclosure VF-1.3. The development of the vulnerability functions was calibrated/validated using NFIP claims. These data are described in Disclosure VF-1.4.

B. *The derivation of building flood vulnerability functions and the treatment of associated uncertainties shall be theoretically sound and consistent with fundamental engineering principles.*

The building flood vulnerability functions are developed based on sound engineering principles using a component-based approach (Porter, et al., 2001), (Park, et al., 2014), (Nadal, et al., 2010), (Nadal, et al., 2006) combined with Monte Carlo simulations. The uncertainties in loading, flood-resistant capacity, and repair cost for each component (Gordian, 2024) are counted using appropriate probabilistic distributions. The suite of vulnerability functions is calibrated/validated using NFIP claims (National Flood Insurance Program, 2023), (Frimpong, et al., 2020), (Kousky & Michel-Kerjan, 2017), (Shin, et al., 2022), (Vishnu, et al., 2021), (Wing, et al., 2020)) from multiple historical events and by publicly available research, such as USACE ((Gulf Engineers & Consultants (GEC), 1997), (Gulf Engineers & Consultants (GEC), 2006), (Davis & Skaggs, 1992)) and HAZUS ((FEMA, 2013), (FEMA, 2022a) models.

C. *Residential building stock classification shall be representative of Florida construction for personal residential buildings.*

Impact Forecasting's residential building stock is classified based on a review of construction inventories from the Aon industrial exposure dataset, the U.S. Census data, the Florida Hurricane Catastrophe Fund (FHCF), and post-event reconnaissance surveys (Fritz, et al., 2007), (Genovese,

et al., 2011), (Smith & Scyphers, 2019), (Suppasri, et al., 2019). In addition, the residential building stock classification was compared with exposure data from NFIP claims (National Flood Insurance Program, 2023). These resources were used to compile standard structure types for personal residential buildings.

D. The following flood characteristics shall be used or accounted for in the derivation of building flood vulnerability functions: depth above ground, and in coastal areas, damaging wave action.

Impact Forecasting's building flood vulnerability functions relate flood damage to the depth of inundation experienced by the building, accounting for the action of the hydrostatic and hydrodynamic loads applied to the building (ASCE, 1988), (ASCE, 2016), (Cantelmo & Cuomo, 2021), (Hatzikyriakou & Lin, 2017), (FEMA, 2011). In coastal areas, the damaging wave action, specifically for the breaking wave (ASCE, 1988), (ASCE, 2016), (FEMA, 2011), is considered as part of the acting loads on the building envelope.

E. The following primary building characteristics shall be used or accounted for in the derivation of building flood vulnerability functions: lowest floor elevation relative to ground, foundation type, construction materials, number of stories, and year of construction.

The derivation of Impact Forecasting's flood vulnerability functions accounted for the primary building characteristics, including occupancy type, construction material, year of construction, number of stories, foundation type, first-floor height (derived from the lowest floor elevations), (FEMA, 2010), (FEMA, 2020a), (Florida Division of Emergency Management, 2017) and geographical tier. The usage of the following building characteristics: first-floor height relative to the ground, foundation type, construction materials, number of stories, and year of construction, is further explained in Disclosure VF-1.9.

F. Flood vulnerability functions shall be separately derived for personal residential buildings and manufactured homes.

The vulnerability functions of personal residential buildings and manufactured homes are developed based on rational structural analysis. Impact Forecasting accounted for the difference in structural characteristics among personal residential buildings and manufactured homes and derived their vulnerability functions separately. These vulnerability functions are calibrated/validated using NFIP claims data (National Flood Insurance Program, 2023) with supporting information from scientific (Baradaranshoraka, et al., 2019), (Carol J. Friedland, 2009), (Gerl, et al., 2016), (Jones & Krecic, 2011), (Marshall & Haag, 2014), (Weekes, 2014) and technical literature (ACI Committee, 2008), (ASCE, 2016), (FBC, 2020), (HUD, 2007), (Yokel, et al., 1981), (NDS, 2018) and expert opinion.

Disclosures

VF-1.1 Describe any modifications to the building vulnerability component of the flood model since the currently accepted flood model.

This is the first submission of the Impact Forecasting Florida Flood Model.

VF-1.2 Provide a flowchart documenting the process by which the building flood vulnerability functions are derived and implemented.

A flowchart which provides the derivation and implementation of building vulnerability functions is shown in Figure 84.

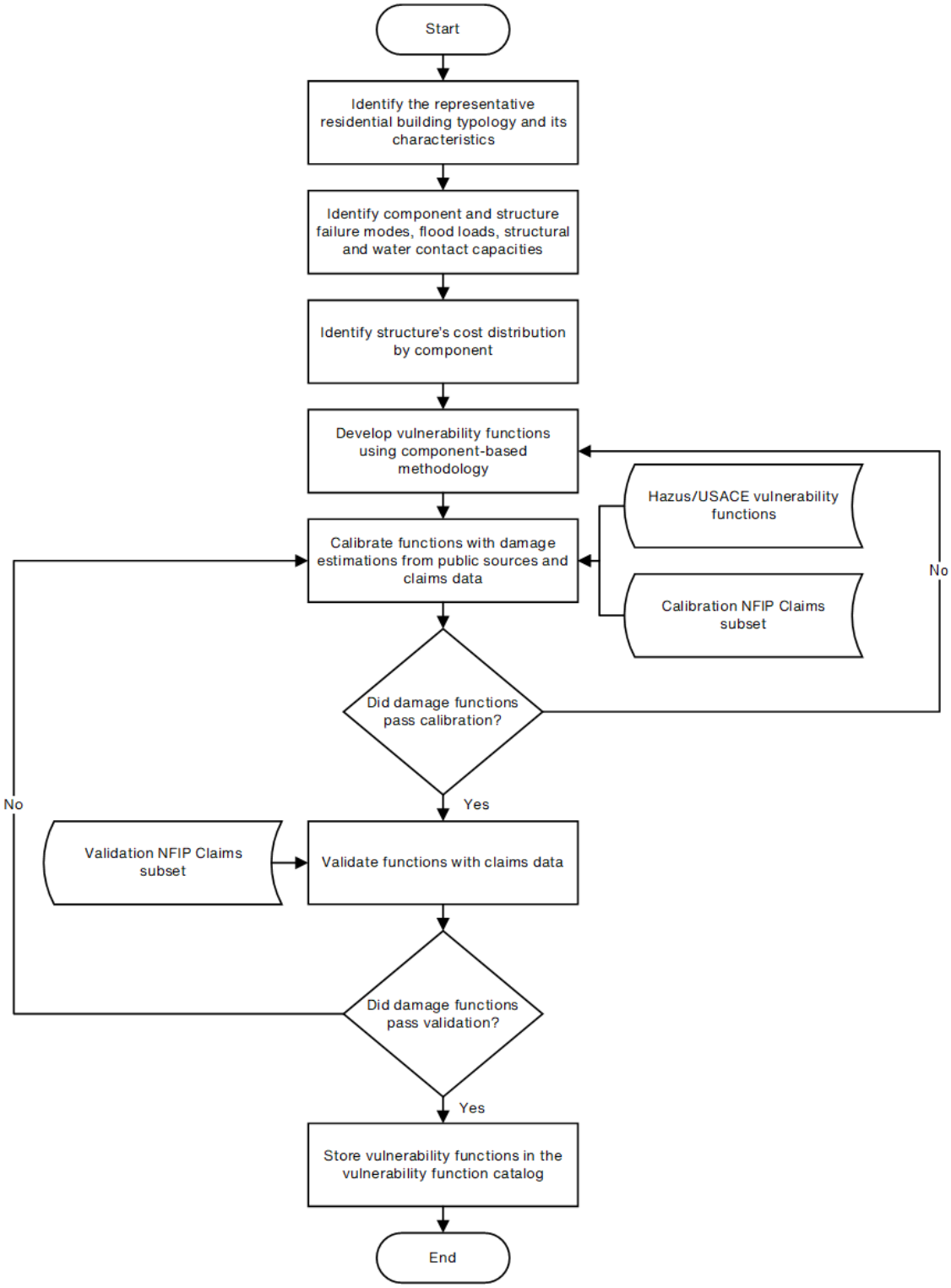

Figure 84. Development and implementation of building flood vulnerability functions.

VF-1.3 Describe the assumptions, data, methods, and processes used for the development of the building flood vulnerability functions.

In the present model, the development of vulnerability functions can be divided into the following steps:

Numerical Simulation – Vulnerability Engine

This step generates simulator-based vulnerability functions that includes the assessment of the following parameters for different hazard intensities (still water level): flow velocity, level of infiltrated water, assessment of flood load (ASCE, 2016), (FEMA, 2011) and corresponding mechanical damage of components based on a structural engineering approach (ACI Committee, 2008), (HUD, 2007), (NDS, 2018), assessment of water-contact damage of the building components, structural integrity check, and assessment of the building damage. The damage condition is then transferred into loss terms via the component costs breakout. It is important to note that the damage functions for inland and coastal conditions were obtained separately due to different sets of the acting loads and thus different structural responses of the simulated buildings.

Application of Relativity Factors

This step applies precalculated piecewise linear factors to the simulator-based curves to generate relativity-derived vulnerability functions. The application of relativity factors allows a reduction of the number of simulation-based curves and, thus, reduce the computational cost of simulation while maintaining the flexibility of the model. The relativity factors were defined in order to keep correspondence between the simulator-based curves and the relativity-derived curves. The initial relativity factors were calculated for different number of story values based on the distribution of sum insured in a building's height, for different construction types based on the bending capacity of the wall material, and for different occupancy types based on the building area estimation. The relativity factors were applied as piecewise linear factors. The factors remain constant up to First Floor Height (FFH); after the FFH, factors change linearly and reach 1 at the highest point of the building. Thus, all the damage functions can reach total damage, regardless of whether a relativity factor is increasing or decreasing. This implementation ensures that the model's handling of different vulnerability characteristics is sufficiently robust.

Calculation of Unknown Characteristics

The unknown characteristics are calculated by weighting the completely defined vulnerability functions (with known characteristics). The weight of each individual function is derived from the available statistics by region, tier, and occupancy classes of the relevant building stock, the data source for which in this case is the Aon Industry Exposure Data (furthermore, IED). Due to limited information on foundation type in the IED, the model was further refined by the statistics available in (FEMA, 2022a) and by evaluating requirements in the relevant construction codes (FBC, 2001), (FBC, 2004), (FBC, 2007), (FBC, 2010), (FBC, 2014), (FBC, 2017), (FBC, 2020), (HUD-MHCSS, 1994), (HUD, 2007), (FEMA, 2009), (FEMA, 2013), (FEMA, 2020a), (FEMA, 2022a) (accompanied by expert judgment) in cases of insufficient data.

Mapping

This step includes the assignment of the previously obtained damage functions to the non-modeled construction classes, tiers, and coverages with similar flood-related behavior. The mapping scheme is based on engineering judgment and the experience of team members.

.

VF-1.4 ***As applicable, describe the nature and extent of actual insurance company flood claims data used to develop the building flood vulnerability functions. Describe in detail the breakdown of data into number of policies, number of insurers, dates of flood loss, amount of flood loss, and amount of dollar exposure, separated into personal residential and manufactured homes.***

Impact Forecasting validated the vulnerability functions using NFIP claims from "OpenFEMA Dataset: FIMA NFIP Redacted Claims – v2" (National Flood Insurance Program, 2023). The claims data are derived from the NFIP system of record, staged in the NFIP reporting platform.

The claims data used in the development and validation of the building vulnerability functions include the personal residential exposure in an amount totaling $ 535,614.90 million, spanning 2,302,459 policies. The amount of flood building losses involved is about $ 61,655.62 million. The exposure amount and number of policies used are given in Table 29.

Table 29: Number of building policies and exposure value by construction type.

	Number of policies	Total building value in million $
Non-MH	2,270,979	533,237.38
MH	31,480	2,377.52

VF-1.5 ***Describe any new insurance company flood claims datasets reviewed since the currently accepted flood model.***

This is the first submission of the Impact Forecasting Florida Flood Model.

VF-1.6 ***Summarize post-event site investigations, including the sources, and provide a brief description of the resulting use of these data in the development or validation of building flood vulnerability functions.***

Impact Forecasting structural engineers, wind engineers, and research team members have traveled to various locations with high or moderate hurricane-induced damage to perform post-event reconnaissance. The post-event reconnaissance consists of site inspections that are used to compare actual observed damage with expected model results across various locations in the flooded field.

Impact Forecasting experience includes post-event reconnaissance for Hurricane Katrina (2005), Hurricane Wilma (2005), and Hurricane Sandy (2012). Recent post-event reconnaissance includes Hurricane Matthew (2016) (Gurley, et al., 2017), Hurricane Harvey (2017), Hurricane Irma (2017) (Prevatt, et al., 2018), Hurricane Michael (2018) (Prevatt, et al., 2019), and Hurricane Ian (2022).

The obtained knowledge was used to calibrate and validate the model's damage functions.

VF-1.7 Describe how the building flood vulnerability functions incorporate depth of flooding (above ground and above lowest floor) and damaging wave action (in coastal areas). For coastal areas, define the thresholds indicating the presence of damaging wave action for buildings and manufactured homes. Describe the area over which building flood vulnerability functions for damaging wave action or wave proxies are applied.

The vulnerability functions rely on flood inundation depth above ground as the intensity measure, with the mean damage ratio (MDR) increasing as inundation depth rises. These functions incorporate the first floor height from the ground (first floor height, or FFH) as a primary building characteristic, and distinct vulnerability functions have been developed for buildings with varying FFHs.

Notably, direct damage to the building interior occurs only when the above-ground inundation surpasses the FFH. However, it's important to highlight that exterior components of the building can sustain damage even before flood depth reaches the FFH, mainly due to wave slamming in coastal areas.

When developing the flood vulnerability functions, the expected hydrostatic (due to differences in depth of flooding between the inside and the outside of the structure), hydrodynamic (due to the water speed), and wave action (hydrostatic, hydrodynamic and wave slam in coastal flooding) loading at each inundation depth were considered. The hydrostatic, hydrodynamic, and wave forces are calculated using published engineering studies including (ASCE, 2016), and (FEMA, 2011).

The vulnerability functions assume that inland flooding inundation will produce hydrostatic and hydrodynamic loads, as shown in Figure 85. It should be noted that the intruded water and corresponding hydrostatic forces are not shown in Figure 85 to ensure figure simplicity. As can be seen, the hydrostatic load is not acting in the building when the envelope is breached and the water levels inside and outside the building are equalized.

The vulnerability functions assume that coastal flooding inundation will be accompanied by waves, and hence wave forces, proportional to the still-water inundation depth. During a coastal flooding event, a building can experience wave forces due to breaking, non-breaking, and broken waves. The model considers that every building should experience breaking wave action at least once; thus, the effects of non-breaking and broken waves are considered insignificant as their influence on a structure is lesser than that of a breaking wave.

The coastal flood vulnerability functions estimate breaking wave impacts at every inundation depth. As per (FEMA, 2011) and (ASCE, 2016) guidelines, the breaking wave height is calculated as 0.78 of the still-water inundation depth, with 70% above the inundation depth (wave crest) and 30% below (wave trough). Consequently, the crest of the incident wave is at 1.55x the still-water inundation depth with respect to the ground level. This approach is used for calculation of loads on piles, piers, and posts (see Figure 85(a)). It is important to note that only the first row of piles, piers, and posts are subjected to breaking wave loads while the hydrodynamic loads are applied to all piles, piers, and posts in the manner shown in Figure 85(c) and (d).

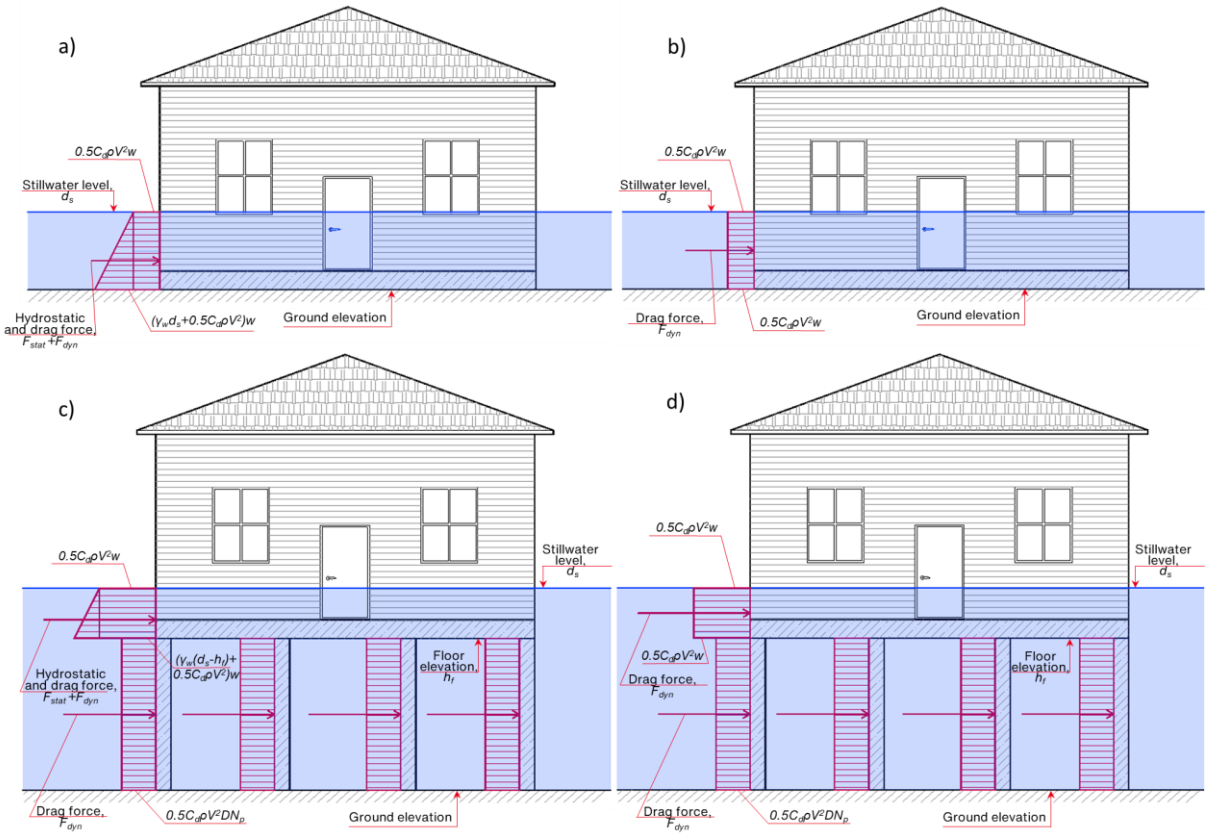

Figure 85. Hydrostatic and hydrodynamic forces action: a) on an unelevated building for enclosed dry space behind wall; b) on an unelevated building after envelope breach; c) on an elevated building for enclosed dry space behind wall; d) on an elevated building after envelope breach. Legend: Fstat – hydrostatic force; Fdyn – drag (hydrodynamic) force; Cd – drag coefficient (this coefficient differs for piles and walls); ds – still water level; D – pile diameter; Np – number of piles in one row; hf – floor elevation; w – width of wall; ρ – mass density of water; γw – specific weight of water. Intruded water and corresponding hydrostatic forces are not shown to ensure figure simplicity.

Similarly, for elevated structures the wave slam effect is considered with the crest of the incident wave being at 1.55x the still-water inundation depth (calculating from the ground level). The slam of breaking wave generates a hydrodynamic force acting on the part of the wall which is lower than 1.55x of still-water level measured from the ground level; see Figure 86 (b).

When the water level reaches vertical walls (for both elevated and unelevated structures), breaking wave loads resulting from a normally incident breaking wave acting on a rigid vertical wall cause reflected or standing waves against the waterward side of the wall, with the crest of the reflected wave being at 2.2x the still-water inundation with respect to the ground level ((FEMA, 2011), (ASCE, 2016)), see Figure 86 (c). The forces acting on a wall if the crest of a reflected wave overtops the building are shown in Figure 86 (d).

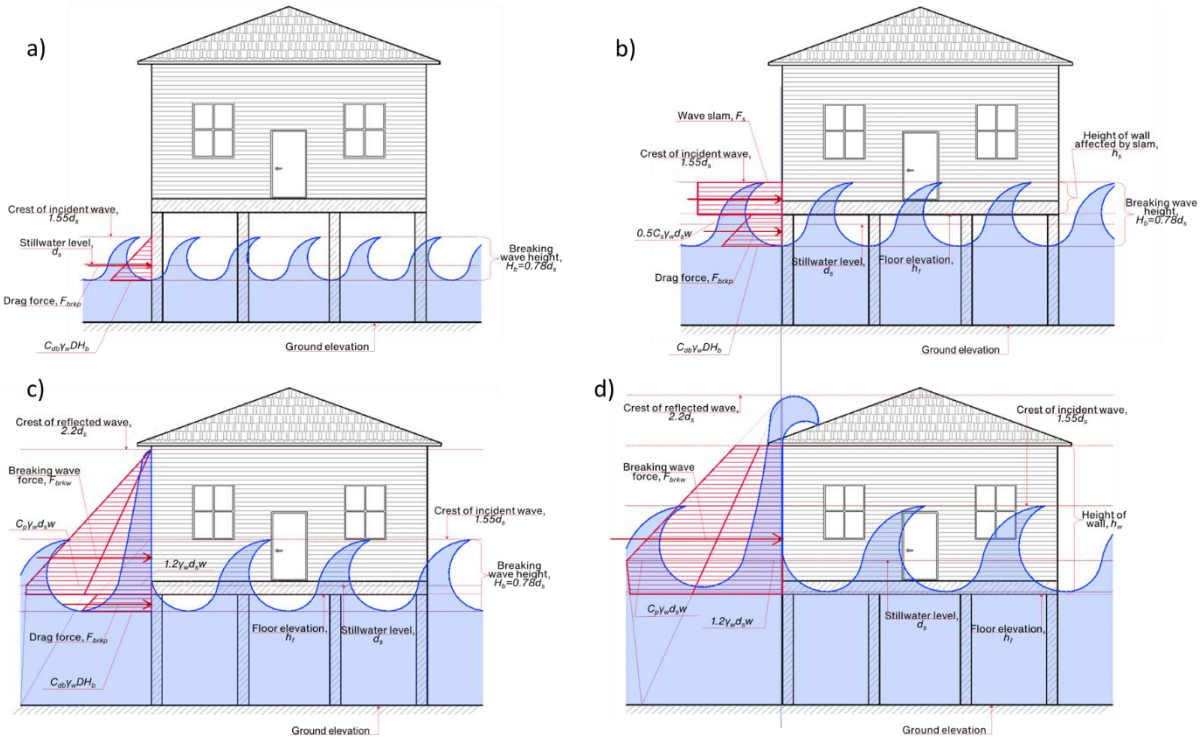

Figure 86. Breaking wave force action (for enclosed dry space behind wall): a) on piles; b) on piles and wave slam; c) on piles and reflecting wave; d) reflecting wave crest overtops the building wall. Legend: Fbrkp – drag force on pile; Fbrkw – breaking wave force on wall; Fs – wave slam force; Cdb – breaking wave drag coefficient; Cp – dynamic pressure coefficient; Cs – slam coefficient; ds – still water level; Hb – breaking wave height; D – pile diameter; hf – floor elevation; w – width of wall; hs = (1.55ds-hf) – height of wall affected by slam ; γw – specific weight of water.

For all exposures inundated by coastal flooding, wave action is considered, and there are no specific distance-from-coast thresholds at which wave action begins or ends. The still water level specified herein controls wave heights.

Coastal flooding introduces hydrostatic, hydrodynamic, and wave forces, with the assumed wave action imparting distinct loads on buildings during storm surge. Additionally, the hydrostatic pressure arising from coastal flooding exceeds that of inland flooding due to the wave depth contributing to increased pressure on the structures.

VF-1.8 *State if the following flood characteristics are considered in the development of the building flood vulnerability functions, and if so, how; if not, explain why:*

A. Flood velocity,

Flood velocity plays a significant role in the formulation of both coastal and inland vulnerability functions. Within the framework of component-based engineering analysis, the hydrodynamic forces acting on building components depend on the flood velocity, which affects potential damage to building elements. The link between inundation depth and flood velocity, as outlined in (FEMA, 2011), is applied. (FEMA, 2011) offers both upper and lower bound estimates of flood velocity, established as functions of the respective inundation depths. The model uses a beta distribution between upper and lower flood velocity bounds, such that the average flood velocity is closer to the lower bound than to the higher bound

because the thresholds shown in FEMA (2011) are design values, which are conservative. The beta distribution is applied indistinctly for inland and coastal flooding.

B. Flood duration,

The vulnerability functions implicitly account for the duration of flooding through their calibration and validation process using claims data (National Flood Insurance Program, 2023). Claims data capture the damage caused by flood events without distinction based on flood duration. This approach ensures that the vulnerability assessment encompasses the full spectrum of flood impacts, from brief inundations to protracted events.

C. Flood-induced erosion,

The flood-induced erosion was not modeled explicitly. The omission of explicit modeling for flood-induced erosion was primarily driven by its high variability, which is closely tied to soil type. Nevertheless, it is important to note that flood-induced erosion is factored into the vulnerability functions indirectly through their calibration and validation process using claims data (National Flood Insurance Program, 2023). This approach accounts for the erosion effects within the vulnerability assessment, acknowledging the nuanced interplay between soil characteristics and flooding impacts.

D. Flood-borne debris,

The explicit modelling of flood-borne debris was not considered for most types of buildings. However, it's noteworthy that the vulnerability functions have undergone calibration and validation using claims data (National Flood Insurance Program, 2023). Consequently, the effects of flood-borne debris have been implicitly accounted for within the vulnerability functions, ensuring a comprehensive assessment of the impacts associated with debris in real-world flood events.

The assessment of flood-borne debris effects was specifically taken into account for buildings equipped with breakaway walls, primarily after the breakage of these walls (FEMA, 2021a). This is due to the fact that breakaway walls can serve as a potential source of significant flood-borne debris. Incorporating the debris factor, an additional damage source was considered in the vulnerability assessment for such buildings, acknowledging the increased risk and potential harm resulting from debris generated by the breakage of these walls.

E. Salinity (saltwater versus freshwater flooding), and

In the present model, the vulnerability functions have been distinctly developed for freshwater (inland flood) and saltwater (coastal flood) flooding scenarios. This approach explicitly captures the distinctions between these two types of flooding.

Furthermore, it's important to note that saltwater has a higher density compared to freshwater. This disparity in density is taken into consideration when estimating the flood-induced forces, which are then integrated into the vulnerability functions. This comprehensive approach ensures that the unique characteristics of saltwater and freshwater flooding are appropriately accounted for within the vulnerability assessment.

F. Contaminated floodwaters.

The incorporation of contaminated floodwaters was not a direct focus during the development of the building flood vulnerability functions. However, it is worth noting that

vulnerability functions have undergone calibration and validation using claims data. As a result, the influence of contaminated floodwaters has been implicitly factored into the vulnerability assessment.

VF-1.9 Describe how the building flood vulnerability functions incorporate the following primary building characteristics:

A. Lowest floor elevation relative to ground,

The vulnerability model accounts for the first-floor height (FFH) in the development of the flood building vulnerability functions. The first-floor heights are derived from the lowest floor elevations. Different vulnerability functions have been developed for a range of FFH values, for more details, refer to Standard VF-1, Disclosure 12.

FFH has a significant impact on flood vulnerability. The vulnerability model takes FFH from exposure input as precedence. For exposure data where information on FFH is not available or unknown, the model assigns a default FFH value derived from information on the base flood elevation (BFE) and freeboard together with the building occupancy, construction, foundation type, year built, and flood zone.

In cases where BFE is not available, the FFH is inferred based on expert judgement or it is taken directly from public sources (FEMA, 2013).

B. Foundation type,

Impact Forecasting recognizes seven types of foundations: slab-on-grade; crawlspace; basement; dry-stack concrete; pier or post; solid wall; and piles. Among them, the dry-stack concrete foundation is supported to be used for mobile homes (MH) only. For more details, refer to Standard VF-1, Disclosure 12.

In the case of unidentified foundations, Impact Forecasting offers an unknown type of foundation, which is a weighting of various foundations based on statistics available in (FEMA, 2022a) and requirements in the construction codes (FBC, 2001), (FBC, 2004), (FBC, 2007), (FBC, 2010), (FBC, 2014), (FBC, 2017), (FBC, 2020), (HUD-MHCSS, 1994), (HUD, 2007) accompanied by expert judgment where there is a lack of data.

C. Primary construction materials,

Primary construction materials used in the present model are shown in Table 30. For more details, refer to Standard VF-1, Disclosure 12.

Table 30: Primary construction materials.

Construction materials
Unknown
Wood
Masonry veneer
Masonry
Unreinforced masonry
Reinforced masonry
Reinforced concrete
Reinforced concrete – tilt up
Wind resistive
Very wind resistive
Steel frame
Light metal building
Mobile home unknown tie down state
Mobile home not tied down
Mobile home tied down
Mobile home double wide

D. Number of stories, and

The number of stories bands that are used in the model are shown in Table 31. For more details refer to Standards VF-1, Disclosure 12.

Table 31: Modeled number of stories.

Number of stories
Unknown
1
2
3
4 ~ 6
7 ~ 10
>= 11

E. Year of construction.

Impact Forecasting assigned construction year-built bands, based on Florida's construction practices and code (ASCE, 2014), (ASCE, 1998), (ASCE, 2016), (ASCE, 1988), (ASCE, 2022), (FBC, 2001), (FBC, 2004), (FBC, 2007), (FBC, 2010), (FBC, 2014), (FBC, 2017), (FBC, 2020), (FEMA, 2017), (FEMA, 2011), (FEMA, 2010), (FEMA, 2009), (HUD, 2007), (HUD-MHCSS, 1994) enforcement of FIRM and building codes, to reflect changes in a

building's flood resistant capacities over the years. Table 32 and Table 33 summarize the code enforcement and construction practice associated with each band for non-MH and MH buildings.

Table 32: The code enforcement and construction practice for non-MH buildings.

Year built band		Description
Pre-FIRM		A building for which construction or substantial improvement occurred on or before December 31,1974, or before the effective date of an initial Flood Insurance Rate Map (FIRM).
Post-FIRM	<= 1981	For coastal communities, the BFEs shown on FIRMs published before 1981 are water elevations, including only the effects of tide and storm surges.
	> 1981 and <= 2001	Incorporate wave heights into base flood elevations in coastal areas.
2002 ~ 2011		Coastal A Zone is used to facilitate the application of load combinations. Minimum elevation requirements for the lowest floor, including freeboard requirements for certain structures. Flood load is counted in the design.
2012 ~ 2017		The Florida Building Code (FBC) includes flood provisions that meet or exceed the NFIP requirements for building and structures. All countries, cities and towns are required to enforce the FBC. Many Florida communities enforce some "higher standards" than those required by the FBC.
2018 and Newer		Starting with the 6th Edition, the Florida Building Code requires all buildings to be elevated to at least BFE plus 1 foot. Some Florida communities enforce some "higher standards" than those required by the FBC.

Table 33: The code enforcement and construction practice for MH.

Year-built bands	Code enforcement and construction practice
Pre-1976	Before 1976, manufactured homes were essentially unregulated, and had wide variations in construction quality and strength.
1976 – 1993	The first HUD (U.S. Department of Housing and Urban Development) code specified minimum wind pressures for MH design and contained general criteria for anchoring homes to resist wind forces. The minimum wind pressures

Year-built bands	Code enforcement and construction practice
	corresponded to a sustained (fastest mile) wind speed of 70 mph in an exposure C category. Since 1976, the NFIP has also regulated the installation of manufactured homes in floodplains.
1994 – 1998	MHs were designed and manufactured with increased wind-resistant capacities based on HUD Zones: 100 mph in the fastest mile for Zone II, and 110 mph in the fastest mile for Zone III. In 1996, HUD published the Permanent Foundations Guide for Manufactured Housing, and established a new minimum anchor load resistance capacity, along with new horizontal and vertical tie down requirements.
1999 – 2007	In 1999, the Florida Department of Highway Safety and Motor Vehicles promulgated an amended version of installation Standards for Mobile/Manufactured Homes. Combined with the design of chassis/floor systems for perimeter support, the performance of HUD-Code homes was closer to what was standard in the site-built homes.
2008 – 2017	In 2007, the Federal government established standards requiring all new MH to meet minimum requirements for installation and anchoring. Florida established stricter installation standards than the HUD code.
Post-2017	The NFIP encourages participating communities to adopt and enforce freeboard requirements as part of their local floodplain management ordinance. The community with CRS class 8 or above must adopt and enforce at least a 1-foot freeboard requirement for all residential buildings constructed, substantially improved, and/or reconstructed due to substantial damage, throughout its Special Flood Hazard Area.

VF-1.10 State if the following building characteristics are considered in the development of the building flood vulnerability functions, and if so, how; if not, explain why:

A. Use of each story (e.g., habitable space, parking, storage, other),

The use of each story within buildings was not integrated into the vulnerability functions due to its limited availability in insurer exposure and claims data.

B. Presence of basement,

The presence of a basement is an important factor that has been included during the development of the vulnerability functions. Buildings with basements are more vulnerable when inundation reaches these lower levels, resulting in damage to both the building interior and its contents. An unfinished and not floodproofed basement is considered as one of the possible foundation types. Basement floodproofing is taken into account via available secondary modifiers.

C. Replacement value of building,

In the present model, for simulator-based vulnerability functions, the cost of individual components is taken into account (Gordian, 2024). The sum of these individual component costs equals the replacement value of building. Thus, the damage to individual components directly corresponds to a fraction of the building's replacement value. Consequently, the total damage of the building (damage is equal to 1) reflects the replacement value of the entire building.

D. Structure value by story,

The inclusion of structure value by story was omitted from the vulnerability functions due to its limited availability in insurer exposure and claims data.

E. Square footage of living area,

In the present model, for all the simulator-based vulnerability functions, a constant square footage of each floor of the building was considered. Thus, the vulnerability functions do not take into account the varying square footage of living areas.

F. Other construction characteristics, as applicable, and

In the present model, various construction materials are considered, and this is reflected in the strengths of load-bearing components. It is important to highlight that the strength of these components depends not only on the type of construction materials, but also on the year-built band. The buildings that fall into the oldest year-built bands tend to exhibit greater vulnerability due to differences in construction codes ((ASCE, 2014), (ASCE, 1998), (ASCE, 2016), (ASCE, 1988), (ASCE, 2022), (FBC, 2001), (FBC, 2004), (FBC, 2007), (FBC, 2010), (FBC, 2014), (FBC, 2017), (FBC, 2020), (FEMA, 2017), (FEMA, 2011), (FEMA, 2010), (FEMA, 2009), (HUD, 2007), (HUD-MHCSS, 1994)), mechanical properties of historical materials, and the impact of time-dependent degradation or damage of construction materials.

G. Distance from building to flood source(s) (e.g., river, lake, coast).

The distance between a building and the flood source was indirectly accounted for with the tier definitions; however, it was not factored directly into the vulnerability module due to its limited availability in insurer exposure and claims data.

VF-1.11 Describe the process by which local construction practices, statewide and local building code, and floodplain management regulation adoption and enforcement are considered in the development of building flood vulnerability functions.

The building flood vulnerability functions for Florida vary both spatially and temporally to represent the regional variation in construction practices, including considerations for compliance with NFIP (FEMA, 2021b), building code adoption and enforcement over time (ASCE, 2014), (ASCE, 1998), (ASCE, 2016), (ASCE, 1988), (ASCE, 2022), (FBC, 2001),

(FBC, 2004), (FBC, 2007), (FBC, 2010), (FBC, 2014), (FBC, 2017), (FBC, 2020), (FEMA, 2017), (FEMA, 2011), (FEMA, 2010), (FEMA, 2009), (HUD, 2007), (HUD-MHCSS, 1994). These variations are captured by vulnerability tiers and year built bands.

The vulnerability tiers are derived following the design guidelines of FEMA flood zones from NFIP and the Florida Building Codes, which represent distinct spatial regions in Florida with varied requirements in the design load and provisions to protect the building from damage. Tier 1 refers to the coastal areas with a 1% or greater chance of flooding and an additional hazard associated with storm waves. Tier 2 refers to the designated areas that are subject to a 100-year flood. Tier 3 covers the remaining areas of Florida.

The year built is used to temporally vary the vulnerability of risks that are in the same spatial region but were built in different periods with different building code requirements. Year built values are grouped into year-built bands that represent distinct points in time when meaningful building code changes occurred that would impact the structural performance of a risk in a flood event.

VF-1.12 Provide the total number of building flood vulnerability functions available for use in the flood model. Describe which building flood vulnerability functions are used for personal residential buildings, manufactured homes, condo unit owners, and apartment renters.

The model incorporates 483,384 structure vulnerability functions, which are applicable to both building coverage and appurtenant structure coverage. The robust nature of the available vulnerability functions is primarily due to the numerous Foundation Type options, which are further broken into bins of FFH, as detailed in Table 34.

All the primary characteristics and their combinations for personal residential buildings, manufactured homes, condo unit owners, and apartment renters are shown in Table 34 and Table 35.

Table 34: Primary modifiers used in personal residential buildings, condo unit owners and apartment renters vulnerability functions.

Primary modifier	Values
Coverage	Structure, Appurtenant structure
Sub Peril	Fluvial, Pluvial, Storm surge
Tier	Zone V and coastal A zone, Zone A, Non-Special Flood Hazard Area (non SFHA)
Construction classes	Unknown, Wood, Masonry veneer, Masonry, Unreinforced masonry, Reinforced masonry, Reinforced concrete, Reinforced concrete – tilt up, Wind resistive, Very wind resistive, Steel frame, Light metal building
Number of stories	Unknown, 1 story, 2 stories, 3 stories, 4-6 stories, 7-10 stories, 11 stories or more
Year-built band	Unknown, Pre-FIRM, 1981 or older, 1981-2002, 2002-2012, 2012-2018, 2018 or newer

Primary modifier	Values
Foundation type and FFH	Unknown foundation (unknown FFH, FFH lower than 3.5 ft, 3.5-5.5 ft FFH, FFH higher than 5.5 ft), Slab on grade foundation (unknown FFH, FFH lower than 0.5 ft, 0.5-1.5 ft FFH, 1.5-2.5 ft FFH, 2.5-3.5 ft FFH, FFH higher than 3.5 ft), Crawlspace foundation (unknown FFH, FFH lower than 3.5 ft, 3.5-4.5 ft FFH, FFH higher than 4.5 ft), Above grade crawlspace foundation (unknown FFH, FFH lower than 3.5 ft, 3.5-4.5 ft FFH, FFH higher than 4.5 ft), Below grade crawlspace foundation (unknown FFH, FFH lower than 1.5 ft, 1.5-2.5 ft FFH, FFH higher than 2.5 ft), Building with basement Solid wall foundation (unknown FFH, FFH lower than 5.5 ft, 5.5-6.5 ft FFH, 6.5-7.5 ft FFH, 7.5-8.5 ft FFH, 8.5-9.5 ft FFH, FFH higher than 9.5 feet), Pier or post foundation (unknown FFH, FFH lower than 4.5 ft, 4.5-5.5 ft FFH, 5.5-6.5 ft FFH, 6.5-7.5 ft FFH, FFH higher than 7.5 ft), Pile foundation (unknown FFH, FFH lower than 6.5 ft, 6.5-7.5 ft FFH, 7.5-8.5 ft FFH, 8.5-9.5 ft FFH, 9.5-10.5 ft FFH, 10.5-11.5 ft FFH, 11.5-12.5 ft FFH, 12.5-13.5 ft FFH, 13.5-14.5 ft FFH, 14.5-15.5 ft FFH, 15.5-16.5 ft FFH, 16.5-17.5 ft FFH, 17.5-18.5 ft FFH, 18.5-19.5 ft FFH, FFH higher than 19.5 ft)

Table 35: Primary modifiers used in MH vulnerability functions.

Primary modifier	Values
Coverage	Structure, Appurtenant structure
Sub Peril	Fluvial, Pluvial, Storm surge
Tier	Zone V and coastal A zone, Zone A, Non-Special Flood Hazard Area (non SFHA)
Construction classes	Mobile home double wide, Mobile home not tied down, Mobile home tied down, Mobile home unknown tie down state
Number of stories	Unknown, 1 story
Year-built band	Unknown, 1976 or older, 1976-1994, 1994-1999, 1999-2008, 2008-2017, 2018 or newer

Primary modifier	Values
Foundation type and FFH	Dry stack concrete foundation (unknown FFH, FFH lower than 3.5 ft, FFH higher than 3.5 ft)

VF-1.13 Describe the assumptions, data, methods, and processes used to develop building flood vulnerability functions when:

A. personal residential construction types are unknown, or

The unknown construction type is calculated by the weighting of the completely defined vulnerability functions with known construction types. The weight of each individual function is derived from the available statistics on construction type depending on tier (Zone V and coastal A zone, Zone A, or non SFHA) and occupancy classes of the building stock data, which is the Aon IED and (FEMA, 2022a)

B. one or more primary building characteristics are unknown, or

One or more unknown primary building characteristics are calculated in the same way as the unknown construction type. The unknown characteristics are calculated by the weighting of the completely defined vulnerability functions (known modifiers). The weight of each individual function is derived from the available statistics which depends on tier (Zone V and coastal A zone, Zone A, or non SFHA) and occupancy classes of the building stock data, which is the Aon IED and (FEMA, 2022a) .

C. building input characteristics are conflicting.

In the case of conflicting building characteristic combinations, the vulnerability functions are mapped to functions that align with the model's coverage, which represents realistic building characteristic combinations. This mapping helps ensure that the assessment remains consistent and applicable within the framework of the model's existing parameters and capabilities.

During the import of exposure information, the Impact Forecasting exposure module assigns vulnerability function identification codes based on each risk's primary and secondary characteristics. No adjustments are made when secondary risk characteristics are not provided. The Impact Forecasting exposure module relies on the user to provide realistic building characteristics.

VF-1.14 Describe similarities and differences in how the building flood vulnerability functions are developed and applied for coastal and inland flooding.

In the model, the coastal flood and inland flood vulnerability functions share identical primary building characteristics and component strengths (Nadal, et al., 2010). However, they are developed separately because the forces acting on a building during coastal and inland floods differ significantly (ASCE, 2016), (ASCE, 1988). Coastal floods involve wave action, which introduces specific load combinations that are not present in inland floods. Additionally, the salinity of coastal floodwaters, characterized by higher water density, impacts buildings differently, and this is reflected in the distinct vulnerability functions. Both sets of vulnerability functions are created using the component method as described in Standard VF-1, Disclosure 3.

VF-1.15 Describe if and how building flood vulnerability functions are based on or depend on NFIP FIRM or other FIS data.

Some inputs of building vulnerability functions are based on the information provided by NFIP FIRM data. The vulnerability functions are distinguished between pre-FIRM effective year and post-FIRM effective year; for more details, refer to Standard VF-1, Disclosure 9, part E. The vulnerability tiers are designed based on FEMA zones (see Standard VF-1, Disclosure 11), where for the development of vulnerability function with unknown primary building characteristics, the weight of each individual function is derived from the available statistics which depends on tier (see Standard VF-1, Disclosure 13, parts A and B).

VF-1.16 For a building in an area subject to coastal and inland flooding, describe how the flood model calculates and reports flood damage.

Impact Forecasting's catastrophe modeling software employs a multi-peril approach, combining coastal and inland flood hazards. Each peril (coastal and inland (fluvial and pluvial) flood) has its own intensity footprint for each event. In locations where these footprints overlap, the software calculates damage and loss separately for each peril. It then reports the maximum loss among them, ensuring a comprehensive assessment that considers the most significant impact from either the coastal or inland flood, resulting in a more robust risk analysis. For more details, refer to Standard AF-2, Disclosure 3.

VF-1.17 Describe the treatment of uncertainties associated with the building flood vulnerability functions.

The uncertainty in the damage ratio for each flood depth range is addressed by adopting the OASIS format (Oasis LMF, 2023), which probabilistically represents damage to assets susceptible to flooding. This distribution is derived from simulations conducted within a Monte Carlo framework (Wagenaar, et al., 2015), involving statistical sampling across various flood loading scenarios, diverse structural components, and different mechanical properties of construction materials. These simulations are designed to capture and reflect the inherent uncertainty in damage outcomes. This comprehensive approach ensures a robust probabilistic representation of potential losses in the face of flooding events.

VF-1.18 Provide a completed Form VF-1, Coastal Flood with Damaging Wave Action. Provide a link to the location of the form [Form VF-1: Coastal Flood with Damaging Wave Action].

Form VF-1 is provided in the link above.

VF-1.19 Provide a completed Form VF-2, Inland Flood by Flood Depth. Provide a link to the location of the form [Form VF-2: Inland Flood by Flood Depth].

Form VF-2 is provided in the link above.

VF-2 Derivation of Contents Flood Vulnerability Functions

A. Development of the contents flood vulnerability functions shall be based on some combination of the following: (1) post-event site investigations, (2) scientific and technical literature, (3) expert opinion, (4) laboratory or field testing, and (5) insurance claims data. Contents flood vulnerability functions shall be supported by historical and other relevant data.

Following the same procedure in the development of the building vulnerability functions, the content vulnerability functions are derived using a component-based approach together with supporting information from the scientific literature (Gulf Engineers & Consultants (GEC), 1997, 2006; Endendijk, et al., 2023; Baradaranshoraka, 2017; Mosimann, et al., 2018) and expert opinions. The suite of vulnerability functions is calibrated/validated using NFIP claims from multiple historical events (National Flood Insurance Program, 2023) and by publicly available research (FEMA, 2013, 2022a). The model methodology is detailed in Disclosure VF-2.4.

B. The relationship between building and contents flood vulnerability functions shall be reasonable.

The contents vulnerability functions are developed based on sound engineering principles using a component-based approach (Porter, et al., 2001), (Park, et al., 2014), (Nadal, et al., 2010), (Nadal, et al., 2006). The relationship between building and contents flood vulnerability functions is reasonable and the functions are calibrated/validated using historical NFIP claims data (National Flood Insurance Program, 2023) and by publicly available reports (Gulf Engineers & Consultants (GEC), 1997), (Gulf Engineers & Consultants (GEC), 2006), (Davis & Skaggs, 1992), (FEMA, 2013), (FEMA, 2022a).

Disclosures

VF-2.1 Describe any modifications to the contents vulnerability component of the flood model since the currently accepted flood model.

This is the first submission of the Impact Forecasting Florida Flood Model.

VF-2.2 Provide a flowchart documenting the process by which the contents flood vulnerability functions are derived and implemented.

A flowchart which provides the derivation and implementation of content vulnerability functions is shown in Figure 87.

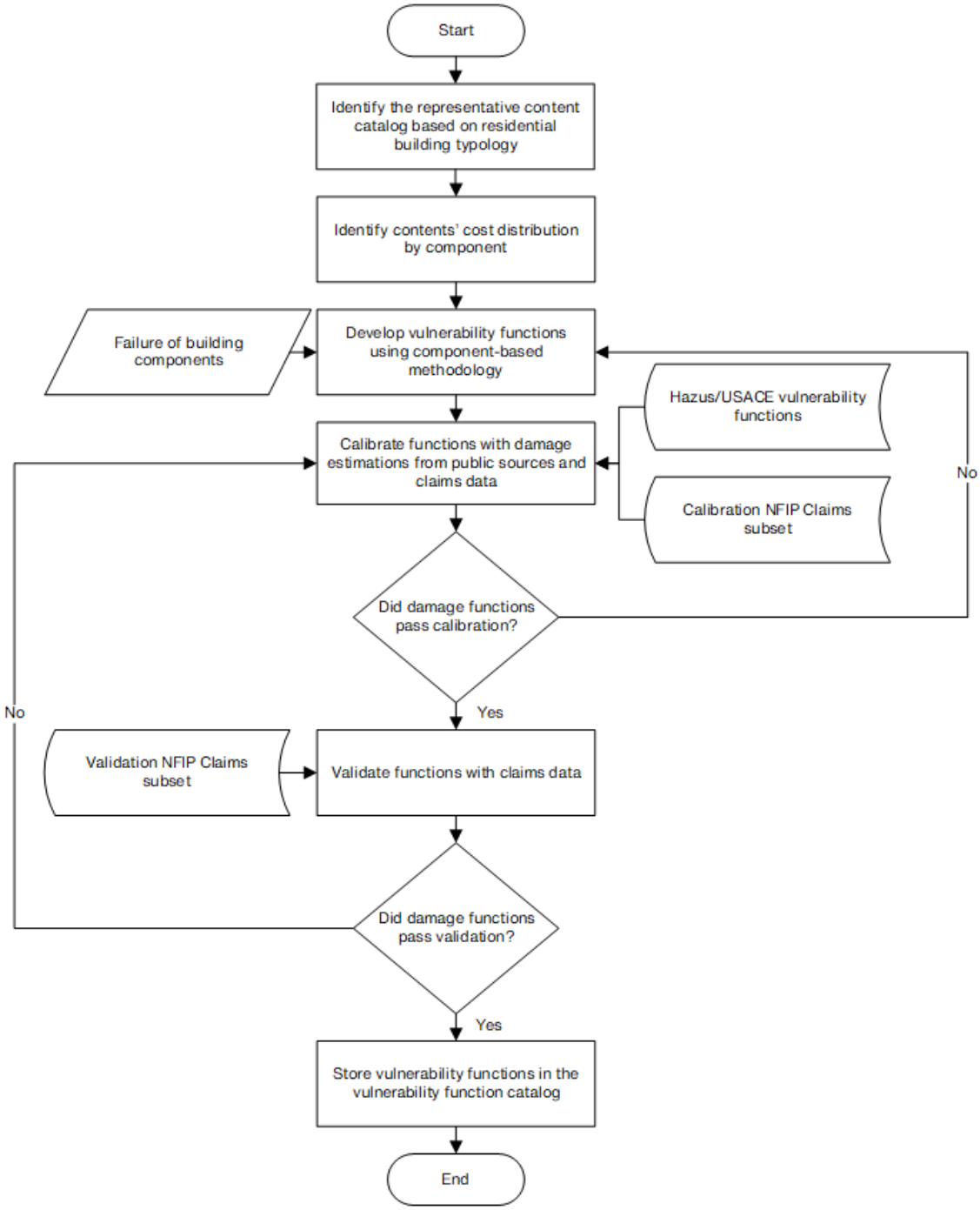

Figure 87. Development and implementation of content vulnerability functions.

VF-2.3 Describe the relationship between contents and building flood vulnerability functions.

Contents vulnerability functions are intricately tied to the building damage due to the dependency between the envelope breakage (i.e., windows, doors, envelope walls) and the flood depth inside the building, which generates the loss to contents due to water contact. The contents damage ratio changes monotonically with the building damage ratio (Baradaranshoraka, 2017), (Mosimann, et al., 2018). However, the relationship between contents damage and building damage is not linear due to the distribution on the height of

the building and content components. Most contents are allocated directly on the floor, experiencing loss at shallow water levels due to water infiltration (before envelope breakage). At the instance of envelope breakage, a sudden increase to the water level inside the building generates a sharp increase in both contents and building vulnerability curves. Additionally, there is a building-to-contents relationship regarding the complete loss in the sense that under a building structural failure condition, which could occur due to different failure mechanisms, the complete loss of contents is expected.

VF-2.4 Describe any assumptions, data, methods, and processes used to develop and validate the contents flood vulnerability functions.

The process considered in the development of the contents flood vulnerability functions is shown in Standard VF-2, Disclosure 2. The contents damage functions were developed using the Impact Forecasting damage simulator based on engineering analysis and judgement. Similar to the building vulnerability function development, the development of the contents vulnerability functions includes the application of relativity factors, derivation of functions with unknown characteristics, and mapping, as described in the Standard VF-1, Disclosure 3. These contents vulnerability functions provide loss behavior as the sum of the individual loss for each component of the contents catalog due to water contact (Gulf Engineers & Consultants (GEC), 1997), (Gulf Engineers & Consultants (GEC), 2006), (Natural Resources Canada (NRCan), 2021). The contents damage functions were later calibrated and validated using detailed coverage-level insurance claims data and vulnerability functions available on USACE reports.

VF-2.5 As applicable, describe the nature and extent of actual insurance company flood claims data used to develop the contents flood vulnerability functions. Describe in detail the breakdown of contents flood claims data into number of policies, number of insurers, dates of flood loss, amount of flood loss, and amount of dollar exposure, separated into personal residential buildings and manufactured homes.

Impact Forecasting developed and validated the contents vulnerability functions using NFIP claims from “OpenFEMA Dataset: FIMA NFIP Redacted Claims – v2” (National Flood Insurance Program, 2023). The personal residential content exposure used is in an amount totalling $ 24,249.79 million, spanning 397,169 policies. The amount of flood contents losses involved is about $ 5,472.57 million. Table 36 summarizes the number of policies and exposure value by construction type.

Table 36: Number of content policies and exposure value by construction type.

	Number of policies	Total content value in million $
Non-MH	389,744	23,769.08
MH	7,425	480.71

VF-2.6 Describe any new contents flood claims datasets used in the flood model since the currently accepted flood model.

This is the first submission of the Impact Forecasting Florida Flood Model.

VF-2.7 Provide the total number of contents flood vulnerability functions available for use in the flood model. Describe whether different contents flood vulnerability functions are used for buildings, manufactured homes, unit location for condo owners and apartment renters, and various building classes.

The model incorporates 483,384 contents flood vulnerability functions available to use. Due to the linkage between the building damage state (i.e. envelope breakage and structural integrity) and the contents damage, the model accounts for unique contents flood vulnerability functions used for different building occupancy types, including personal residential building structures, manufactured homes, condo owners and apartment renters, and various building classes. Contents vulnerability functions incorporate all the primary characteristic combinations that are shown in Standard VF-1 Disclosure 12, but for contents coverage.

VF-2.8 Describe any relationships between flood characteristics and contents flood vulnerability functions.

Separate contents flood vulnerability functions are developed for coastal and inland flood. Contents flood vulnerability functions are intricately tied to the water level inside the building and the building's failure, making them highly dependent on various flood characteristics such as water velocity, wave action, water salinity, etc. Since these flood characteristics influence the water level within the building and the likelihood of building failure differently, the content flood vulnerability functions naturally vary across different flood scenarios, ensuring a nuanced assessment of contents vulnerability under varying conditions.

VF-2.9 State the minimum threshold, if any, at which contents flood damage is calculated (e.g., contents flood damage is estimated for building damage greater than x percent or flood depth greater than y inches). Provide documentation of assumptions and available validation data to verify the approach used.

Contents flood vulnerability functions are influenced by the water level within the building and the potential for building failure. This dynamic interaction can lead to scenarios where contents damage occurs without any structural damage to the building itself, such as damage to low-lying contents due to water infiltration. In these cases, there is no minimum threshold of structural damage required for contents damage to be calculated, highlighting the importance of assessing contents vulnerability independently from the initiation of structural damage.

Moreover, it's noteworthy that the contents flood vulnerability functions have been validated through comparisons with publicly available models from USACE reports (Gulf Engineers & Consultants (GEC), 1997), (Gulf Engineers & Consultants (GEC), 2006) and HAZUS ((FEMA, 2013), (FEMA, 2022a), further reinforcing their accuracy and reliability in predicting contents-related flood damage.

VF-2.10 Describe similarities and differences in how contents flood vulnerability functions are developed and applied for coastal and inland flooding.

Contents flood vulnerability functions for coastal and inland flooding were developed in exactly the same way, using the same assumptions; however, it is important to note that they were developed separately. The development of separate contents vulnerability functions for coastal and inland flooding is essential because contents flood vulnerability functions are inherently tied to the water level inside the building and building failure, both

of which differ between inland and coastal flood scenarios. Consequently, contents flood vulnerability functions naturally exhibit variations to accurately reflect these differences and ensure precise assessments under varying flood conditions.

VF-2.11 Describe if and how contents flood vulnerability functions are based on or depend on NFIP FIRM or other FIS data.

Since certain inputs for building vulnerability functions rely on data from NFIP FIRM, and contents vulnerability functions depend on building vulnerability functions, it follows that contents vulnerability functions are likewise grounded in the data from NFIP FIRM; for more details, refer to Standard VF-1, Disclosure 15. The contents flood vulnerability functions distinguish between pre-FIRM effective year and post-FIRM effective year. Likewise, the vulnerability tiers are based on FEMA zones.

VF-3 Derivation of Time Element Flood Vulnerability Functions

A. Development of the time element flood vulnerability functions shall be based on one or more of the following: (1) post-event site investigations, (2) scientific and technical literature, (3) expert opinion, (4) laboratory or field testing, and (5) insurance claims data.

The time element vulnerability functions were developed using a component-based approach to estimate the building damage and subsequently establish the amount of time required for the restoration of each building component. The vulnerability model also considers the emergency response time after a flood event (e.g. the time required for evacuation or drying and cleaning after a flood event) (FEMA, 2013), (MLIT, 2005). Additionally, expert opinion together with published peer-reviewed research ((Lamond, et al., 2013), (Baradaranshoraka, 2017), and post-event reconnaissance reports were utilized for the calibration / validation of the vulnerability functions. The model methodology is detailed in Standard VF-3, Disclosure 3.

B. The relationship among building, contents, and time element flood vulnerability functions shall be reasonable.

The time element vulnerability functions were derived considering two main concepts: the emergency response time and the required restoration time. The latter corresponds to the linkage between the building component incurred damage and the expected time in days necessary to physically restore the damaged components (Baradaranshoraka, 2017). Furthermore, there is a consistent pattern among the building, contents, and time element flood vulnerability functions. An example of this relationship is the condition of complete loss, such as in the building-to-content relationship described in Standard VF-2, Disclosure 3; this condition applies also to the time element vulnerability functions.

C. Time element flood vulnerability functions derivations shall consider the estimated time required to repair or replace the property.

The time element vulnerability functions were developed using a component-based methodology that considers the time required for the repair/replacement of each building component. The sum of the time assigned for each component corresponds to the total time for the repair/replacement of the property. Due to this, the time element vulnerability functions describe loss behavior as a function of the building damage ratios and an additional time linked to the emergency response.

Disclosures

VF-3.1 Describe any modifications to the time element vulnerability component of the flood model since the currently accepted flood model.

This is the first submission of the Impact Forecasting Florida Flood Model.

VF-3.2 Provide a flowchart documenting the process by which the time element flood vulnerability functions are derived and implemented.

A flowchart that provides the derivation and implementation of time element vulnerability functions is shown in Figure 88.

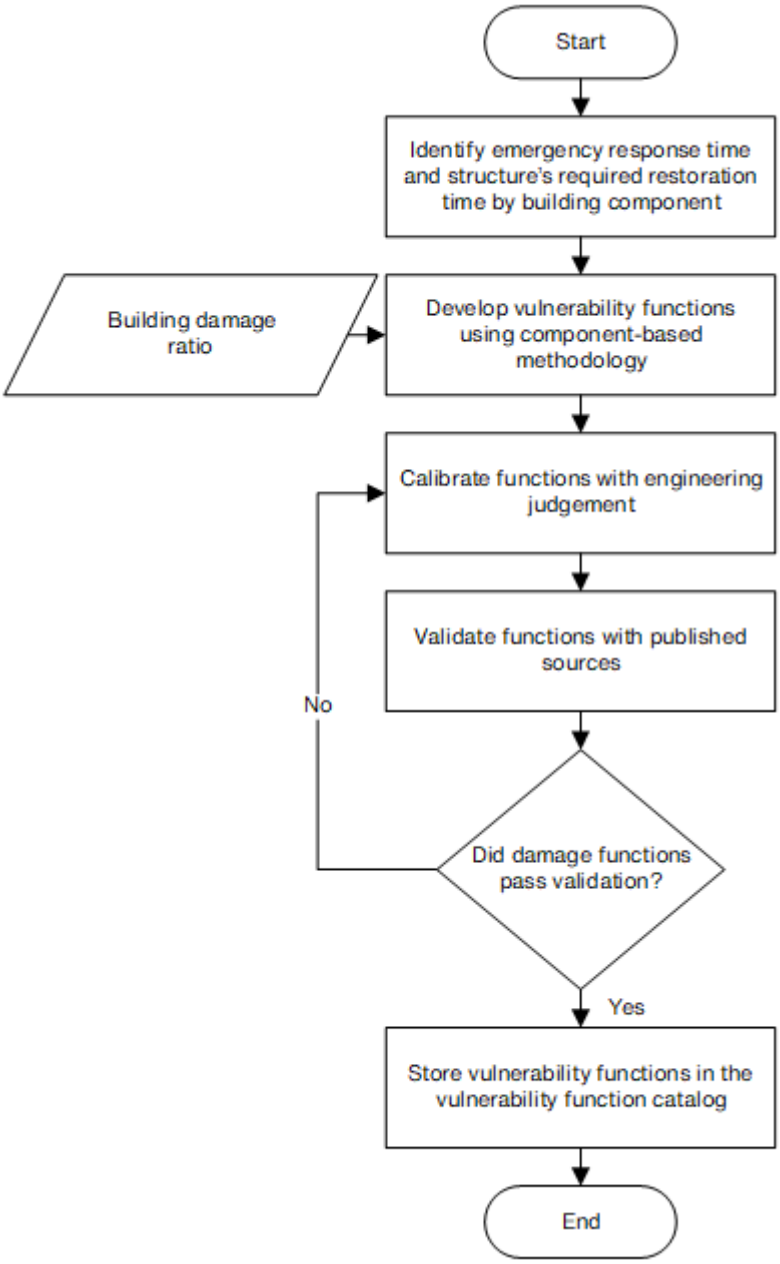

Figure 88. Development and implementation of time element vulnerability functions.

VF-3.3 *Describe the assumptions, data, methods, and processes used to develop and validate time element flood vulnerability functions.*

The overall procedure for the development of the time element flood vulnerability functions is shown in Standard VF-3, Disclosure 2. The time element vulnerability functions were derived considering the required restoration time (RRT) and the emergency response time (ERT). Following a component-based approach, a residential building consists of several components which may be damaged during a flood event. For each of these components, certain restoration time is required and will be based on the component characteristics and the procedures for repair/replacement. Then, the sum of the restoration time of all the components is an indicator of the required restoration time (RRT) of the building. The data on the amount of labor hours required to repair and replace each unit of a given component

were obtained from the RSMeans database (Gordian, 2024). The emergency response time (ERT) is the time required for evacuation, drying, and cleaning after a flood event. The ERT is a function of inundation depth and was obtained from the Manual for Economic Evaluation of Flood Control Investment (MLIT, 2005).

VF-3.4 Describe the relationships among building, contents, and time element flood vulnerability functions.

The time element vulnerability functions were derived considering two main concepts: the emergency response time (ERT); and the required restoration time (RRT). The RRT reflects the time required to repair or reconstruct the damaged building to full function. At low building damage levels, the repair of the damaged building components is relatively fast and not significant enough to force the occupants to leave the dwelling for an extended period of time. However, as the building damage level increases, the repair time also increases significantly. A similar trend is observed in the emergency response time (ERT), accounting for a longer period as the inundation depth experienced in the location is higher (MLIT, 2005).

VF-3.5 As applicable, describe the nature and extent of actual insurance company flood claims data used to develop the time element flood vulnerability functions. Describe in detail the breakdown of time element flood claims data into number of policies, number of insurers, dates of flood loss, amount of flood loss, and amount of dollar exposure, separated into personal residential buildings and manufactured homes.

Claims data was not used for development of time element flood vulnerability functions due to the limited availability of claims information on time element coverage.

VF-3.6 Describe any new time element flood claims datasets used in the flood model since the currently accepted flood model.

This is the first submission of the Impact Forecasting Florida Flood Model.

VF-3.7 Provide the total number of time element flood vulnerability functions available for use in the flood model. Describe whether different time element flood vulnerability functions are used for personal residential, manufactured homes, unit location for condo owners and apartment renters, and various building classes.

The model incorporates 483,384 time element flood vulnerability functions available to use. Due to the linkage between the building component incurred damage and the expected time necessary to physically restore the damaged components, the model accounts for unique time element flood vulnerability functions used for different building occupancy types, including personal residential building structures, manufactured homes, condo owners and apartment renters, and various building classes. Time element vulnerability functions incorporate all the primary characteristics shown in Standard VF-1, Disclosure 12.

VF-3.8 Describe similarities and differences in how time element flood vulnerability functions are developed and applied for coastal and inland flooding.

The coastal flood and inland flood vulnerability models share identical primary building characteristics, component cost, and repair time. Because the time element flood vulnerability functions are derived based on the experienced damage of the building components, the differences in the coastal and inland flooding vulnerability functions for

buildings are reflected into the time element functions. In general terms, as discussed in Standard VF-1, Disclosure 14, the vulnerability functions are developed separately due to the difference in the forces exerted on the building during coastal and inland floods.

VF-3.9 ***Describe whether and how building classification and characteristics, and flood characteristics, are incorporated into the time element flood vulnerability functions.***

The time element vulnerability functions were derived considering the required restoration time (RRT) and the emergency response time (ERT), as described in Standard VF-3, Disclosure 3. Due to the relationship between the building damage and the required restoration time, the building classification and characteristics affect the time element vulnerability functions. Additionally, as described in Standard VF-1, Disclosures 7 and 8, the flood characteristics are different for inland and coastal flood, leading to differentiated building vulnerability functions for those two different kinds of flooding. In the same way, the time element flood vulnerability functions are different depending on building and flood characteristics. Additionally, regarding the emergency response time, the model considers a longer period of relocation as the inundation depth experienced at a given location increases.

VF-3.10 ***Describe whether and how time element flood vulnerability functions take into consideration the damage to local and regional infrastructure, or time element vulnerability resulting from a governmental mandate associated with flood events (e.g., evacuation and re-entry mandates).***

The time element vulnerability functions were derived considering the required restoration time (RRT) and the emergency response time (ERT). The RRT deals with the direct loss (i.e. losses related to building repair time), while the ERT considerers the indirect loss. In this sense, the damage to local and regional infrastructure, or time element vulnerability resulting from a governmental mandate associated with flood events, is implicitly considered in the emergency response time after a flood event (i.e. the time required for evacuation, drying, and cleaning after a flood event). Additionally, the effects of local and regional infrastructure disruptions are implicitly accounted for during calibration and validation by comparing expert opinion with published peer-reviewed research (Baradaranshoraka, 2017), (Lamond, et al., 2013) and post-event reconnaissance reports.

VF-4 Flood Mitigation Measures

A. *Modeling of flood mitigation measures to improve flood resistance of buildings, and the corresponding effects on flood vulnerability and associated uncertainties shall be theoretically sound and consistent with fundamental engineering principles. These measures shall include design, construction, and retrofit techniques that affect the flood resistance or flood protection of personal residential buildings.*

The impact of the flood mitigation measures on flood resistance of buildings and associated uncertainties are modeled based on sound engineering principles (FEMA, 2022b), (FEMA, 2021a), (FEMA, 2020b), (Paleo-Torres, 2020) using a component-based approach. The flood mitigation measures cover flood-resistant design, construction, and retrofit techniques, including utility elevation, floodproofing, and flood openings. Standard VF-4, Disclosure 2 describes the procedures used to calculate the impact of flood mitigation measures.

B. *The modeling organization shall justify all flood mitigation measures considered by the flood model.*

The flood mitigation measures, summarized in Standard VF-4, Disclosure 4, are identified based on structural engineering expertise principles (FEMA, 2022b), (FEMA, 2021a), (FEMA, 2020b), (Paleo-Torres, 2020) and post-event reconnaissance (Endendijk, et al., 2023) of historical flood damage. Their impacts on the flood resistance of buildings were assessed consistent with fundamental engineering principles. The mitigation measures and their impacts on the building performance for given flood hazards are well documented.

C. *Application of flood mitigation measures that affect the performance of personal residential buildings and the damage to contents shall be justified as to the impact on reducing flood damage whether done individually or in combination.*

The mitigation measures reduce the vulnerabilities of personal residential buildings and the damage to contents. In the flood model, every individual mitigation measure is applied to the primary vulnerability function directly; if several mitigation measures are present, the effects of multiple mitigation measures are combined systematically as described in Standard VF-4, Disclosure 7. The application of the mitigation measures and the resulting building and contents vulnerability functions, both individually and in combination, is reasonable and in agreement with engineering principles (FEMA, 2022b), (FEMA, 2021a), (FEMA, 2020b), (Paleo-Torres, 2020).

Disclosures

VF-4.1 Describe any modifications to flood mitigation measures used by the flood model since the currently accepted flood model.

This is the first submission of the Impact Forecasting Florida Flood Model.

VF-4.2 Describe the procedures used to calculate the impact of flood mitigation measures, including software, its identification, and current version. Describe whether or not such procedures have been modified since the currently accepted flood model.

Mitigation measures and secondary characteristics are assessed based on their influence on the flood performance of a structure ((Paleo-Torres, 2020), (Endendijk, et al., 2023). The simulator, utilized for calculating primary vulnerability functions, is also employed to define secondary modifiers. Typically, mitigation measures and secondary modifiers are

factored into the analysis by adjusting properties associated with each secondary modifier. These property adjustments may include aspects like equipment location, water infiltration, and more. For instance, to account for dry floodproofing, the simulator restricts water infiltration up to the dry floodproofing height, effectively incorporating this mitigation measure into the flood performance assessment of the structure. This approach allows for a comprehensive consideration of how various factors impact a building's resilience against flooding.

The secondary modifier adjustments are initially applied to the damage ratio distributions for the primary damage function. Subsequently, the damage ratios required for loss analysis are determined by sampling from the combined damage ratio distributions for the given hazard. This process ensures that the influence of secondary modifiers is appropriately integrated into the overall damage assessment, providing a more accurate representation of the potential losses associated with the hazard.

This is the first submission of the Impact Forecasting Florida Flood Model.

VF-4.3 ***Provide a completed Form VF-3, Flood Mitigation Measures, Range of Changes in Flood Damage. Provide a link to the location of the form [Form VF-3: Flood Mitigation Measures, Range of Changes in Flood Damage].***

Form VF-3 is provided in the link above.

VF-4.4 ***Provide a description of all flood mitigation measures used by the flood model, whether or not they are listed in Form VF-3, Flood Mitigation Measures, Range of Changes in Flood Damage.***

Table 37 and Table 38 provide an overview of the secondary characteristics and flood risk mitigation measures integrated into the present model.

Table 37: Secondary characteristics included in the present model.

Secondary Characteristics	Options	In Form VF-3	Description
Building Enclosure	Unknown enclosure		Evaluating the building enclosure, including features like closed or open foundations, breakaway walls, and flood openings, is important in flood vulnerability modeling as it directly influences a structure's vulnerability to flood damage. The type and condition of building enclosures significantly impact the degree of protection against floodwaters, making it imperative to accurately assess their vulnerability for
	Enclosed walls, with flood openings	✓	
	Enclosed walls, without flood openings		
	Breakaway walls, with flood openings		
	Breakaway walls, without flood openings		
	Open Foundation		

Secondary Characteristics	Options	In Form VF-3	Description
			more precise risk analysis and mitigation planning.

Table 38: Mitigation measures included in the present model.

Mitigation Measures	Options	In Form VF-3	Description
Elevate or Protect Utility Equipment	Unknown		The assessment of elevated or protected utility equipment is important in building vulnerability analysis because it directly affects a building's vulnerability to flood-related disruptions. Properly elevated or protected utility systems reduce the risk of damage, ensuring the building remains functional and resilient during and after flood events.
	Not elevated or protected		
	Up to 1 foot	✓	
	Up to 2 feet	✓	
	Up to 3 feet	✓	
Wet Floodproofing	Unknown		Incorporating wet floodproofing measures is essential in building vulnerability assessments because it directly impacts a structure's vulnerability to flood damage. Properly implemented wet floodproofing strategies can mitigate damage by allowing controlled entry and exit of floodwaters, reducing the risk of extensive structural harm and supporting overall flood resilience.
	Not floodproofed		
	Up to 1 foot	✓	
	Up to 2 feet	✓	
	Up to 3 feet	✓	
Dry Floodproofing	Unknown		The consideration of dry floodproofing is important in vulnerability assessments as it directly influences a building's vulnerability to flood damage. Effective dry floodproofing measures can prevent floodwaters from entering the structure, significantly reducing the risk of damage to building contents and preserving the building's overall resilience.
	Not floodproofed		
	Up to 1 foot	✓	
	Up to 2 feet	✓	
	Up to 3 feet	✓	

VF-4.5 Describe how time element flood losses are affected by performance of flood mitigation measures. Identify any assumptions.

The time element vulnerability functions are linked to the building vulnerability functions. When mitigation measures or secondary characteristics are applied, they impact the building vulnerability functions, leading to a decrease in vulnerability with mitigation measures or potentially altering vulnerability (either decreasing or increasing) for secondary characteristics.

As a result, the time element vulnerability functions are adjusted accordingly to reflect these changes. Importantly, the required restoration time, which is a fraction of the time element flood losses, changes in direct proportion to the building damage. No additional assumptions are introduced, ensuring that the time element losses align with the modified building vulnerabilities, providing a consistent and realistic representation of the evolving risk over time.

VF-4.6 Describe how building and contents damage and the treatment of associated uncertainties are affected by flood mitigation measures. Identify any assumptions.

Building damage is reduced when flood mitigation measures are implemented, as they decrease vulnerability. Secondary characteristics, however, can either increase or decrease building vulnerability depending on the value selected and its overall impact on a building's vulnerability to flood.

Contents vulnerability functions are intricately tied to water levels inside the building and building failure. Consequently, mitigation measures can affect contents damage if they influence the water level inside the building, such as in the case of dry floodproofing. Additionally, if mitigation measures or secondary characteristics affect the pace of building failure, they can also impact contents damage.

Secondary modifiers were calculated using a simulator. Thus, the uncertainties were treated in the same way as for damage functions without secondary modifiers; see Standard VF-1, Disclosure 17. When the secondary modifiers are obtained, the OASIS distribution (Oasis LMF, 2023) for a non-modified damage function (without secondary modifiers) is scaled proportionally to the secondary modifiers.

Importantly, these adjustments are made without introducing any additional assumptions, ensuring that the model accurately accounts for the complex interplay between mitigation measures, secondary characteristics, and the resulting damage patterns for buildings and contents.

VF-4.7 Describe how the effects of multiple flood mitigation measures are combined in the flood model and the process used to ensure that multiple flood mitigation measures are correctly combined.

The combined effects of multiple flood mitigation measures and secondary characteristics are managed using a multiplicative methodology. To maintain control and ensure realistic results, limits, including lower and upper bounds, are established to govern the maximum change that can occur when numerous secondary characteristics are applied concurrently.

These limitations and the impacts of multiple flood mitigation measures and secondary characteristics have been rigorously calibrated and validated through structural engineering analysis and reference to publicly available research (Endendijk, et al., 2023), (Paleo-Torres, 2020). This robust approach ensures that the model accurately reflects the complex

interactions and realistic outcomes associated with the implementation of various flood risk reduction measures.

VF-4.8 ***Provide a completed Form VF-4, Differences in Flood Mitigation Measures. Provide a link to the location of the form [Form VF-4: Differences in Flood Mitigation Measures].***

This is the first submission of the Impact Forecasting Florida Flood Model. No Form VF-4 is valid.

ACTUARIAL FLOOD STANDARDS

AF-1 Flood Model Input Data and Output Reports

A. Adjustments, edits, inclusions, or deletions to insurance company or other input data used by the modeling organization shall be based upon generally accepted actuarial, underwriting, and statistical procedures.

Any adjustments, edits, inclusions, or deletions made to insurance company or other input data are based upon accepted actuarial, underwriting, and statistical procedures.

B. All modifications, adjustments, assumptions, inputs and input file identification, and defaults necessary to use the flood model shall be actuarially sound and shall be included with the flood model output report. Treatment of missing values for user inputs required to run the flood model shall be actuarially sound and described with the flood model output report.

Model input data is provided by the user for each flood model analysis. The Impact Forecasting Florida Flood Model (FCHLPM) version 3.0 performs validation tasks during exposure data import and includes any anomalies in the import log file to help users ensure data integrity. All modifications, adjustments, assumptions, inputs and input file identification, and defaults necessary to use the flood model are actuarially sound and are included with the flood model output report and in the Impact Forecasting documentation. Treatment of missing values required to run the flood model is actuarially sound.

Disclosures

AF-1.1 Identify insurance-to-value assumptions and describe the methods and assumptions used to determine the property value and associated flood losses. Provide a sample calculation for determining the property value.

The Impact Forecasting Florida Flood Model (FCHLPM) version 3.0 does not make assumptions regarding insurance-to-value. The insured value and insurance limits are provided as separate inputs by the user. Users may enter different values for insurance limit and replacement value to reflect certain policy terms such as underinsurance or guaranteed replacement cost. No adjustments are made to these values within the model. As such, no sample calculation has been provided.

AF-1.2 Identify depreciation assumptions and describe the methods and assumptions used to reduce insured flood losses on account of depreciation. Provide a sample calculation for determining the amount of depreciation and the actual cash value (ACV) flood losses.

The Impact Forecasting Florida Flood Model (FCHLPM) version 3.0 does not make assumptions of depreciation and does not reduce insured flood losses on account of depreciation. Users have the option to code the actual cash values instead of the

replacement cost values into the flood model input file. As such, no sample calculation has been provided.

AF-1.3 Describe the different flood policies, contracts, and endorsements as specified in s. 627.715, F.S., that are modeled.

The Impact Forecasting Florida Flood Model (FCHLPM) version 3.0 does not account for losses from non-flood water intrusion. All policy terms, conditions, and endorsements as outlined in s.627.715, F.S., including the incorporation of building, time element, and contents coverages, as well as other flexible terms, can be accommodated by the Impact Forecasting Florida Flood Model (FCHLPM) version 3.0.

AF-1.4 Provide a copy of the input form(s) used by the flood model with the flood model options available for selection by the user for the Florida flood model under review. Describe the process followed by the user to generate the flood model output produced from the input form. Include the flood model name, version identification, and platform identification on the input form. All items included in the input form should be clearly labeled and defined.

Multiple import formats are supported for importing exposure information into the Impact Forecasting exposure database. The ELEMENTS Input Data Format document (see Disclosure CIF-2.1) describes input field names and data types that are supported during import, including the fields which are required in order to generate loss estimates.

The Impact Forecasting model supports 3 different types of input file formats to import exposure:

1. Two File Format (optional: secondary modifier)
2. Four File Format (optional: treaty and secondary modifier)
3. ENF (ELEMENTS Normalized Format)

These three input file formats will generate identical loss results if the same assumptions, data mappings, and analysis settings are applied.

- The input form(s) used by the flood model are provided Appendix E: Flood Model Input Form
- Location data fields are provided in Table 61
- Policy data fields are provided in Table 62
- Treaty data fields (optional) are provided in Table 63
- Secondary modifiers fields (optional)
- Screenshots of a sample data file and import options are provided in: Figure 161, Figure 162, Figure 163, and Figure 164.

The process for the user to generate the model output produced by such input is shown below:

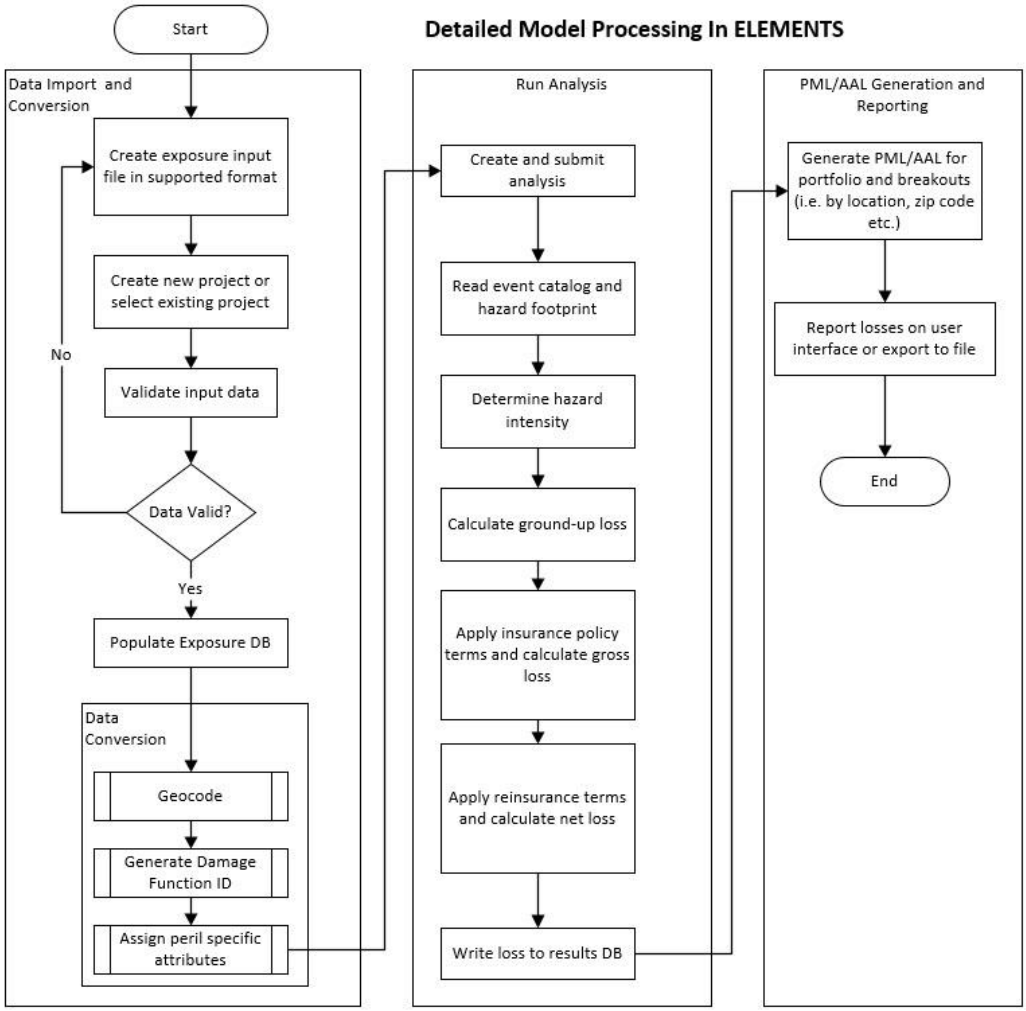

Figure 89: User workflow to create flood model output

To produce rate filing compliant results, the user should additionally take the following steps:

- Analyses must be performed for the peril types: Tropical Cyclone Induced Flooding (FCHLPM) and Non Tropical System Induced Flooding (FCHLPM) with the 'Florida rate filing compliance' check box selected (as detailed in Figure 164 through Figure 168).
- After analysis completion, the user uses the FCHLPM Florida Flood TC/Non-TC Loss Compiler tool to combine the two analyses, as seen in Figure 90. This will produce a compilation of losses for Tropical and Non Tropical analyses.
- This compiled report contains compliant results, and the produced report will additionally contain both the analysis settings and results for the Tropical Cyclone, Non Tropical Cyclone, and compiled analyses, as seen in Figure 171.

Figure 90: Screenshot of the Florida Flood TC/Non-TC Loss Compiler tool that can be used to combine Tropical Cyclone and Non Tropical Cyclone results to create a compiled analysis appropriate for rate filing.

AF-1.5 ***Disclose, in a flood model output report, the specific inputs required to use the flood model and the options of the flood model selected for use in a personal residential property flood insurance rate filing in Florida. Include the flood model name, version identification, and platform identification on the flood model output report. All items included in the flood model output report should be clearly labeled, highlighted, and defined.***

Analysis options for Florida rate making are specified by Florida Statute FS 627.0628. The following Impact Forecasting Florida Flood Model (FCHLPM) version 3.0 options are required for Florida personal lines ratemaking model runs (Table 39, Table 40, and Table 41).

AF-1.6 ***Provide a list of all options available (e.g., flood event data source, vulnerability functions) to the user. Identify the specific options acceptable for a Florida rate filing.***

All options available and options acceptable for a Florida rate filing have been included in Table 39, Table 40, and Table 41.

Table 39: Required Impact Forecasting Florida Flood Model (FCHLPM) Model v3.0 analysis settings for Florida ratemaking (common settings)

Option	For All Available Settings	For Florida Rate Filing	Note
ELEMENTS Version	18.0.0.0	18.0.0.0	Version of ELEMENTS platform
Region	United States	United States	Region selection
Peril	Flood	Flood	Peril selection
Model Suite	Impact Forecasting FCHLPM	Impact Forecasting FCHLPM	Model suite selection
Loss Cases	With/Without Demand Surge	With Demand Surge	Demand surge option provides losses that include increased cost of labor and material following major catastrophe.

Option	For All Available Settings	For Florida Rate Filing	Note
Include Damage Uncertainty	Yes/No	Yes	This option allows the user to run damage calculation with a defined number of samples to account for damage uncertainty.
Custom Damage Samples	Yes/No	No	This option allows the user to change the default number of samples suggested for given model.
Custom Event selection	Yes/No	No	This option enables the user to generate losses for selected events out of the full event catalog.
Custom Damage Function	Yes/No	No	This option allows the user to overwrite the default damage function with custom vulnerability curve.
Parameter Adjustment	Yes/No	No	This option allows the user to adjust ground up losses based on given criteria.
Use location-based seed	Yes/No	Yes	Use of location-based seed ensures result repeatability (the same location will always generate the same losses irrespective of order of record in given portfolio).

Table 40: Required Impact Forecasting Florida Flood Model (FCHLPM) Model v3.0 analysis settings for Florida ratemaking (Tropical Cyclone Induced Flooding (FCHLPM) peril settings)

Option	For All Available Settings	For Florida Rate Filing	Note
Peril Type	Tropical Cyclone Induced Flood v.3.0	Tropical Cyclone Induced Flood (FCHLPM) v.3.0	Peril Selection
Damage Options	Fluvial Pluvial Storm Surge Fluvial and Pluvial Fluvial and Storm Surge Pluvial and Storm Surge Fluvial Pluvial and Storm Surge	Fluvial Pluvial Storm Surge Fluvial and Pluvial Fluvial and Storm Surge Pluvial and Storm Surge Fluvial Pluvial and Storm Surge	Sub peril option selection

Table 41: Required Impact Forecasting Florida Flood Model (FCHLPM) Model v3.0 analysis settings for Florida ratemaking (Non-Tropical Induced Flooding (FCHLPM) peril settings)

Option	For All Available Settings	For Florida Rate Filing	Note
Peril Type	Non Tropical System Induced Flood v.3.0	Non Tropical System Induced Flood (FCHLPM) v.3.0	Peril Selection
Damage Options	Fluvial Pluvial Fluvial and Pluvial	Fluvial Pluvial Fluvial and Pluvial	Sub peril option selection

The flood model output report is provided in Appendix F: Flood Model Output Form.

Screenshots of analysis settings and report viewing options referred to in Table 39, Table 40, and Table 41 are in:

- Figure 165
- Figure 166
- Figure 167
- Figure 168

Example screenshots of the hurricane model output (results) are provided in:

- Figure 169
- Figure 170

AF-1.7 Explain the differences in data input and flood model output required for coastal and inland flood modeling.

The data input and flood model output are same for inland and coastal flood modelling in the Impact Forecasting Florida Flood Model (FCHLPM) version 3.0.

AF-1.8 Describe actions performed to ensure the validity of insurer or other input data used for flood model inputs or for validation/verification.

The Impact Forecasting model performs validation tasks during exposure data import. Below is a list of assumptions for treatment of data during import.

Insurance to Value

The model does not make assumptions regarding insurance to value. The insured value and insurance limits are provided as separate inputs. No adjustments are made to these values within the model. Users may enter different values for insurance limit and replacement value to reflect certain policy terms such as underinsurance or guaranteed replacement cost.

Missing Values

If building characteristics are missing, the model defaults to an unknown value. Unknown values are based on the weighted average of known characteristic(s) (see Disclosure VF-1.13). If policy conditions are missing, the model does not make additional assumptions.

Appurtenant Structures

Limits and values of appurtenant structures for each location are user inputs. The model does not make assumptions regarding the value of appurtenant structures.

Contents

Contents limits and values are part of the user input. No assumptions are made within the model.

Time Element Coverage

Time element coverage limits and values are part of the user input. No assumptions are made within the model.

Geocoding

As discussed in Disclosure GF-3.4, there are four ways to geocode portfolio data within the Impact Forecasting model. If both address and longitude/latitude information are available, users are given an option to select how geocoding should be performed. If the policy's address is incorrect, ZIP Code centroid geocoding is performed for the policy. If a location does not geocode (for example, if a ZIP Code is invalid), the location is excluded from the analysis. All locations that are not included in the analysis are recorded in a log file.

The Portfolio Import Summary (Figure 91) and Portfolio Import Log (Figure 92) are available upon completion of data import. It is recommended that the logs and exposure summary be reviewed prior to running the model in order to ensure data integrity prior to analysis. Upon

review, the user may correct any errors and re-import the data. Invalid locations are omitted from the import.

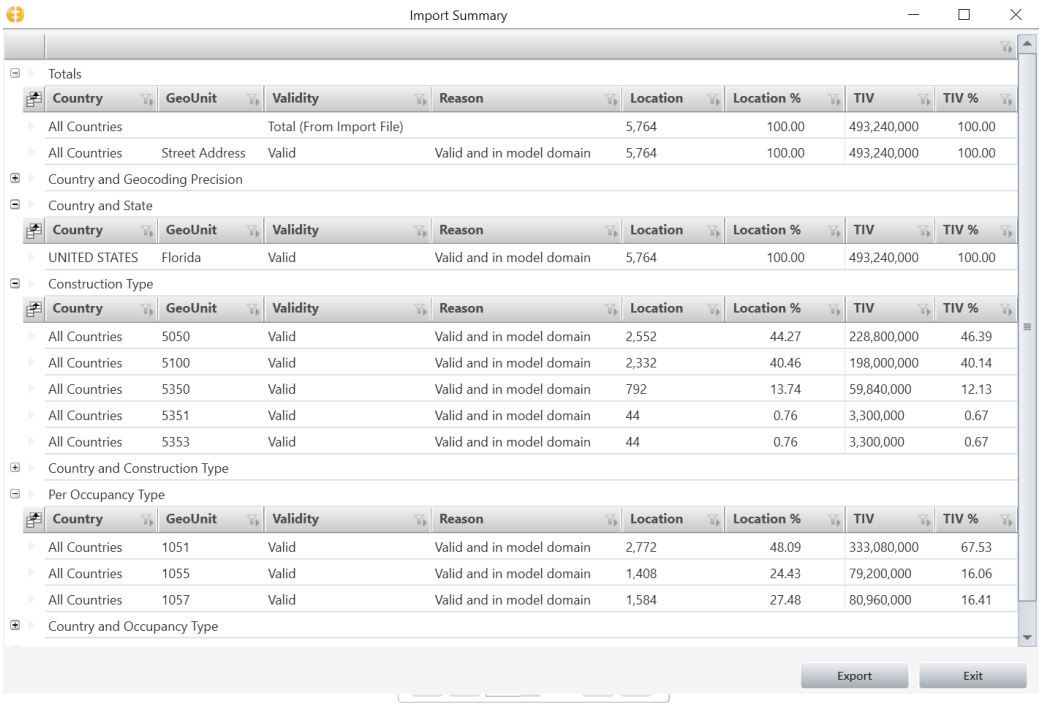

Country	GeoUnit	Validity	Reason	Location	Location %	TIV	TIV %
Totals							
All Countries		Total (From Import File)		5,764	100.00	493,240,000	100.00
All Countries	Street Address	Valid	Valid and in model domain	5,764	100.00	493,240,000	100.00
Country and Geocoding Precision							
Country and State							
Country	GeoUnit	Validity	Reason	Location	Location %	TIV	TIV %
UNITED STATES	Florida	Valid	Valid and in model domain	5,764	100.00	493,240,000	100.00
Construction Type							
Country	GeoUnit	Validity	Reason	Location	Location %	TIV	TIV %
All Countries	5050	Valid	Valid and in model domain	2,552	44.27	228,800,000	46.39
All Countries	5100	Valid	Valid and in model domain	2,332	40.46	198,000,000	40.14
All Countries	5350	Valid	Valid and in model domain	792	13.74	59,840,000	12.13
All Countries	5351	Valid	Valid and in model domain	44	0.76	3,300,000	0.67
All Countries	5353	Valid	Valid and in model domain	44	0.76	3,300,000	0.67
Country and Construction Type							
Per Occupancy Type							
Country	GeoUnit	Validity	Reason	Location	Location %	TIV	TIV %
All Countries	1051	Valid	Valid and in model domain	2,772	48.09	333,080,000	67.53
All Countries	1055	Valid	Valid and in model domain	1,408	24.43	79,200,000	16.06
All Countries	1057	Valid	Valid and in model domain	1,584	27.48	80,960,000	16.41
Country and Occupancy Type							

Figure 91: Sample Portfolio Import Summary

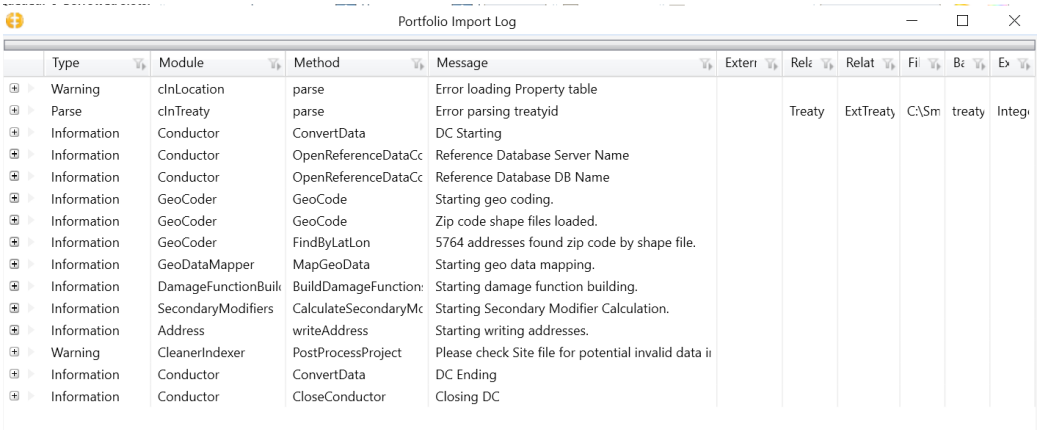

Type	Module	Method	Message	Extern	Rela	Relat	Fi	Ba	Ex
Warning	clnLocation	parse	Error loading Property table						
Parse	clnTreaty	parse	Error parsing treatyid		Treaty	ExtTreaty	C:\Sm	treaty	Integ
Information	Conductor	ConvertData	DC Starting						
Information	Conductor	OpenReferenceDataCc	Reference Database Server Name						
Information	Conductor	OpenReferenceDataCc	Reference Database DB Name						
Information	GeoCoder	GeoCode	Starting geo coding.						
Information	GeoCoder	GeoCode	Zip code shape files loaded.						
Information	GeoCoder	FindByLatLon	5764 addresses found zip code by shape file.						
Information	GeoDataMapper	MapGeoData	Starting geo data mapping.						
Information	DamageFunctionBuil	BuildDamageFunction:	Starting damage function building.						
Information	SecondaryModifiers	CalculateSecondaryMc	Starting Secondary Modifier Calculation.						
Information	Address	writeAddress	Starting writing addresses.						
Warning	CleanerIndexer	PostProcessProject	Please check Site file for potential invalid data i						
Information	Conductor	ConvertData	DC Ending						
Information	Conductor	CloseConductor	Closing DC						

Figure 92:Sample Portfolio Import Log

AF-1.9 ***Disclose if changing the order of the flood model input exposure data produces different flood model output or results.***

The order of flood model input exposure data does not affect the flood model output or results.

AF-1.10 ***Disclose if removing or adding policies from the flood model input file affects the flood model output for the remaining policies.***

Adding or removing policies from the flood model input file does not affect the output or results for the remaining policies.

AF-2 Flood Events Resulting in Modeled Flood Losses

A. *Modeled flood loss costs and flood probable maximum loss levels shall reflect insured flood related damages from both coastal and inland flood events impacting Florida.*

Modeled flood losses and flood probable maximum loss levels reflect all insured flood-related damages from coastal and inland flood events impacting Florida.

B. *The modeling organization shall have a documented procedure for distinguishing flood-related losses from other peril losses.*

Impact Forecasting has a documented procedure for distinguishing flood losses from other peril losses. As shown in Figure 165, the Impact Forecasting Florida Flood Model (FCHLPM) version 3.0 only provides users the option to model flood-related losses.

Disclosures

AF-2.1 Describe how damage from flood model generated floods (originating either inside or outside of Florida) is excluded or included in the calculation of flood loss costs and flood probable maximum loss levels for Florida.

The Impact Forecasting Florida Flood Model (FCHLPM) version 3.0 is a subset of the Impact Forecasting US flood model, which simulates flood events and the losses arising from them as a direct result of tropical and non tropical precipitation. The Impact Forecasting Florida Flood Model (FCHLPM) version 3.0 was isolated by removing all hydrologic areas that do not cross the boundary of the state of Florida. Only exposures falling within the boundary of Florida will be used to calculate losses for a given event, and the PMLs for the stochastic catalog. In the case where a hydrologic area does cross the boundary of Florida, the hazard from a given event that occurs within the area inside the boundary of Florida is used for loss calculation. Additionally, in the case where a river flows into Florida from a neighboring state, riverine discharge that occurs as a result of precipitation that falls entirely outside of Florida will be propagated down the river network to the river segment(s) within Florida and will be transformed into depths within the state of Florida boundary. These depths will then be used to estimate losses arising from the causative event.

AF-2.2 Describe how wind losses associated with coastal and inland flooding are treated in the calculation of flood loss costs and flood probable maximum loss levels for Florida.

Flood loss costs and flood probable maximum loss levels do not account for wind losses related to coastal and inland flooding.

AF-2.3 Describe how the flood model considers the correlation and potential overlap of flood losses associated with coastal and inland flooding.

The Impact Forecasting Florida Flood Model (FCHLPM) version 3.0 calculates the losses from coastal and inland flooding separately. For locations where the two footprints overlap, the maximum loss for each location will be reported.

AF-2.4 ***Other than coastal and inland flooding, state whether any other types of flooding events are modeled. If so, describe how damage resulting from these flood type events is treated in the calculation of flood loss costs and flood probable maximum loss levels for Florida.***

No other types of flooding events are modeled other than coastal and inland flooding.

AF-2.5 ***Describe which non-flood water losses are considered flood losses from water intrusion. Describe how water intrusion losses are considered in the calculation of flood loss costs and flood probable maximum loss levels for Florida.***

The Impact Forecasting Florida Flood Model (FCHLPM) version 3.0 does not consider non-flood water losses to be flood losses caused by water intrusion. The flood loss costs and flood probable maximum loss levels for Florida do not account for these losses.

AF-3 Flood Coverages

A. *The methods used in the calculation of personal residential structure flood loss costs, including the effect of law and ordinance coverage, shall be actuarially sound.*

The methods used in the development of personal residential structure flood loss costs are actuarially sound. The vulnerability functions are developed based on well-established structural and flood engineering science in literature and calibrated and validated by analyzing historical claims data. IF model doesn't explicitly model the Law and Ordinance as FL Statute doesn't require Law and Ordinance for Flood policies.

B. *The methods used in the calculation of personal residential appurtenant structure flood loss costs shall be actuarially sound.*

The methods used in the calculation of appurtenant structure flood loss costs are actuarially sound. The Impact Forecasting Florida Flood Model (FCHLPM) version 3.0 calculates personal residential appurtenant structure flood loss costs separately from building, contents, and time element flood loss costs. The methods used in the calculation of appurtenant structure flood loss costs are same as the methods used for the calculation of building flood loss costs.

C. *The methods used in the calculation of personal residential contents flood loss costs shall be actuarially sound.*

The methods used in the development of contents flood loss costs are actuarially sound. The Impact Forecasting Florida Flood Model (FCHLPM) version 3.0 calculates contents loss cost separately from building, appurtenant structure, and time element flood loss costs. The model has been validated against actual loss data.

D. *The methods used in the calculation of personal residential time element flood loss costs shall be actuarially sound.*

The methods used in the development of time element flood loss costs are actuarially sound. The Impact Forecasting Florida Flood Model (FCHLPM) version 3.0 calculates time element losses based on the emergency response time and the required restoration time. The required restoration time is determined based on the estimated damage to the structure. Time element damage functions have been calibrated and validated against publicly available model since NFIP does not offer coverages regarding time element losses induced by flooding damage.

Disclosures

AF-3.1 Describe the methods used in the flood model to calculate flood loss costs for residential structure coverage associated with personal residential properties.

1. Based on the latitude/longitude, year built, number of stories, foundation type, first floor height (FFH), construction and occupancy types, all secondary modifiers, a vulnerability function is assigned to the exposure.
2. Flood depth is determined for each simulated event and location. A damage ratio distribution (from which samples are drawn) is generated for that exposure. A Monte Carlo simulation approach is used to produce the damage samples at the coverage level.

3. Ground up loss is calculated based on the damage ratio distribution for building coverage
4. Gross loss is calculated after applying limits, deductibles, coinsurance, etc., at the coverage, location, and policy levels.
5. Average Annual Loss (AAL) is the sum product of event rate and event loss across all simulated events.
6. Loss cost is the average annual loss per $1,000 of insured value (loss is divided by the insured value, then multiplied by 1,000).

AF-3.2 Describe the methods used in the flood model to calculate flood loss costs for appurtenant structure coverage associated with personal residential properties.

The Impact Forecasting Florida Flood Model (FCHLPM) version 3.0 estimates flood losses for appurtenant structure coverage associated with personal residential properties using the same method as for building coverage, as described in Disclosure AF-3.1, but using the input appurtenant structure coverage values. The IF model can assign a different vulnerability function for appurtenant structures if the appurtenant structure is separately coded with different characteristics in the input file.

AF-3.3 Describe the methods used in the flood model to calculate flood loss costs for contents coverage associated with personal residential properties.

The Impact Forecasting Florida Flood Model (FCHLPM) version 3.0 estimates flood losses for contents coverage associated with personal residential properties using the method described in Disclosure AF-3.1 but using the input contents coverage values.

AF-3.4 Describe the methods used in the flood model to calculate flood loss costs for time element coverage associated with personal residential properties.

The Impact Forecasting Florida Flood Model (FCHLPM) version 3.0 estimates flood losses for time element coverage associated with personal residential properties using the method described in Disclosure AF-3.1 but using the input time element coverage values.

AF-3.5 Describe the methods used in the flood model to account for law and ordinance coverage associated with personal residential properties.

L&O is not considered in the Impact Forecasting Florida Flood Model (FCHLPM) version 3.0, since it's not required by law.

AF-4 Modeled Flood Loss Cost and Flood Probable Maximum Loss Level Considerations

A. Flood loss cost projections and flood probable maximum loss levels shall not include expenses, risk load, investment income, premium reserves, taxes, assessments, or profit margin.

Flood losses and probable maximum loss levels generated by the Impact Forecasting Florida Flood Model (FCHLPM) version 3.0 do not include expenses, risk load, investment income, premium reserves, taxes, assessments, or profit margins.

B. Flood loss cost projections and flood probable maximum loss levels shall not make a prospective provision for economic inflation.

The Impact Forecasting Florida Flood Model (FCHLPM) version 3.0 does not make a prospective provision for economic inflation.

C. Flood loss cost projections and flood probable maximum loss levels shall not include any explicit provision for wind losses.

The Impact Forecasting Florida Flood Model (FCHLPM) version 3.0 provides users the option to model only storm surge and inland flood losses. Wind loss is excluded from the results.

D. Damage caused from inland and coastal flooding shall be included in the calculation of flood loss costs and flood probable maximum loss levels.

Damage caused from inland and coastal flooding are included in the calculation of flood loss costs and flood probable maximum loss levels.

E. Flood loss cost projections and flood probable maximum loss levels shall be capable of being calculated from exposures at a geocode (latitude-longitude) level of resolution including the consideration of flood extent and depth.

The Impact Forecasting Florida Flood Model (FCHLPM) version 3.0 is capable of calculating flood loss cost projections and flood probable maximum loss levels based on exposures at a geocode (latitude-longitude) level of resolution.

F. Demand surge shall be included in the flood model's calculation of flood loss costs and flood probable maximum loss levels using relevant data and actuarially sound methods and assumptions.

Demand surge is included in the IF model's calculation of flood loss costs and probable maximum loss levels. The demand surge function exists individually for both TC and non-TC components of the model, capturing the difference in the type of damage and subsequent recovery caused by individual perils. The TC portion of the model function is developed based on analysis of the pricing information for the construction sector from Xactimate and XactContents. For the Non-TC portions of the model, demand surge is represented by a separate function developed using historical loss data and fluctuations in the labor and material costs specific to the construction sector following a major event.

Disclosures

AF-4.1 Describe the method(s) used to estimate annual flood loss costs and flood probable maximum loss levels and the treatment of associated uncertainties. Identify any source documents used and any relevant research results.

The Impact Forecasting Flood Model contains two event sets: the tropical cyclone (TC) induced flooding and non-tropical cyclone (non-TC) induced flooding. The TC induced flooding is simulated for 200,000 years and the non-TC induced flooding is simulated for 10,000 years. In order to provide a combined view of flood risk, Impact Forecasting developed a linking table that connects the two event sets into a unified table of 200,000 years, which is the same time span as the TC event set. To achieve this, 20 copies of the non-TC event set are used to produce a matching catalog size.

OEP and AEP PMLs can be calculated using the following steps:

1. Each event in the TC and non-TC event sets were simulated several times to capture the variation of the loss due to uncertainty in the flood vulnerability functions. The final event level loss is the averaged sample loss per each event.
2. The event losses from the TC and non-TC event sets are mapped to 200,000 years of event losses using the aforementioned linking table.
3. Taking either the maximum (for OEP) or the sum (for AEP) of the individual event losses for a given year to create a year loss table (YLT).
4. Calculate the return period for each year to get PML for certain return periods.

$$\frac{1}{RP(L_i)} = \frac{1}{200{,}000}\sum_{j=1}^{200{,}000} \mathbf{1}_{L_j \geq L_i} \tag{15}$$

   where L_i or L_j is either the year's maximum (for OEP) or aggregate loss (for AEP). **1** indicates a conditional statement where count + 1 (the year) if $L_j \geq L_i$ is true.

5. The annual averaged loss (AAL) is calculated as the averaged of annual losses.

$$AAL = \sum_{i=1}^{N} f_i L_i = \sum_{i=1}^{200{,}000} \frac{1}{200{,}000} L_i \tag{16}$$

$$AAL = annual\ averaged\ loss$$
$$N = number\ of\ simulated\ years$$
$$f_i = the\ frequency\ for\ year\ i$$
$$L_i = the\ loss\ for\ year\ i$$

.

AF-4.2 ***Identify all possible resolutions available for the reported flood output ranges. Identify the finest level of resolution (i.e., the most granular level) for which flood loss costs and flood probable maximum loss levels can be provided.***

In the Impact Forecasting Florida Flood Model (FCHLPM) version 3.0, flood loss costs and flood probable maximum loss can be produced at the location. Flood loss costs and flood probable maximum loss levels can then be calculated at any geographic level, such as ZIP Code, county, state, etc.

AF-4.3 ***Describe how the flood model incorporates demand surge in the calculation of flood loss costs and flood probable maximum loss levels. Indicate if there are any differences in the manner that demand surge is incorporated for coastal and inland flooding.***

The Impact Forecasting Florida Flood Model (FCHLPM) version 3.0 considers demand surge as a factor at event level, driven by the loss produced by each event without considering DS. Different event have different scale of impact and intensity and are assigned a factor associated with demand surge which is multiplied with the loss produced. There are no differences in the manner that demand surge is incorporated for inland and coastal flooding, but differentiate DS (Demand Surge) factor for TC and non-TC events.

AF-4.4 ***Provide citations to published papers, if any, or modeling-organization studies that were used to develop how the flood model estimates demand surge.***

The following references were used to guide the development of the demand surge model:

Ahmadi, N., & Shahandashti, S. M. (2018). Role of predisaster construction market conditions in influencing postdisaster demand surge. Natural Hazards Review, 19(3), 04018010.

Döhrmann, D., Gürtler, M., & Hibbeln, M. (2017). Insured loss inflation: How natural catastrophes affect reconstruction costs. Journal of Risk and Insurance, 84(3), 851-879.

EM-DAT Database (2020). Retrieved from https://www.emdat.be/. Accessed 30 July 2020.

Hallegatte, S. (2008). An adaptive regional input-output model and its application to the assessment of the economic cost of Katrina. Risk Analysis: An International Journal, 28(3), 779-799.

Hallegatte, S., Boissonnade, A., Schlumberger, M. E., & Muir-Wood, R. (2008). Demand surge and worker migrations in disaster aftermaths: application to Florida in 2004 and 2005. Journal of Regional Science. Retrieved from http://www2.centre-cired.fr/IMG/pdf/Migration_Final.pdf

Olsen, A. H., & Porter, K. A. (2011a). What we know about demand surge: Brief summary. Natural Hazards Review, 12(2), 62-71.

Olsen, A. H., & Porter, K. A. (2011b). On the contribution of reconstruction labor wages and material prices to demand surge. Report No. SESM-11-1, Dept. of Civil, Environmental, and Architectural Engineering, Univ. of Colorado at Boulder, Boulder, CO.

Property Claim Services (2020). Catastrophe Bulletins. Retrieved from https://pcs.iso.com/pcs/app/start.do. Accessed 30 July 2020.

Rachel Personius (2020). Construction Cost: The Impacts of Hurricanes Harvey and Irma. Retrieved from https://www.fgould.com/americas/articles/construction-cost-the-impacts-of-hurricanes/. Accessed 30 July 2020.

Rick Lloyd (2020). The Cost Impact of Hurricane Harvey on The Texas Construction Market. Retrieved from https://www.mgac.com/blog/the-cost-impact-of-hurricane-harvey-on-the-texas-construction-market/. Accessed 30 July 2020.

Significant Flood Events (2020). Retrieved from https://www.fema.gov/significant-flood-events. Accessed 30 July 2020.

Smith, A. B., & Katz, R. W. (2013). US billion-dollar weather and climate disasters: data sources, trends, accuracy and biases. Natural Hazards, 67(2), 387-410.

Trish Hopkinson (November, 2017). Hurricanes drive demand surge in reconstruction costs. Retrieved from https://www.verisk.com/insurance/visualize/hurricanes-drive-demand-surge-in-reconstruction-costs/. Accessed 30 July 2020.

Xactware (2020). Xactware's pricing data. Retrieved from https://www.xactware.com/en-us/resources/pricing-data-services/overview/#. Accessed 30 July 2020.

AF-4.5 Describe how economic inflation has been applied to past insurance experience to develop and validate flood loss costs and flood probable maximum loss levels.

When past insurance experience was used to develop and validate flood loss costs and flood probable maximum losses, Impact Forecasting apply economic inflation to the data. To take into account the increase in value of exposures that has occurred between the event's occurrence date and the IED's representative building stock date, a trending factor based on Collins and Lowe (2001) was applied to the NFIP loss data. The in-force exposure at the time of the event was used to generate the modeled losses. Modeled losses were then compared to NFIP trended claims.

AF-5 Flood Policy Conditions

A. *The methods used in the development of mathematical distributions to reflect the effects of deductibles, policy limits, and flood policy exclusions shall be actuarially sound.*

The methods used in the development of mathematical distributions to reflect the effects of deductibles, policy limits and flood policy exclusions are actuarially sound. Deductible methodology is discussed in Disclosure AF-5.1.

B. *The relationship among the modeled deductible flood loss costs shall be reasonable.*

The relationship among the modeled deductible flood loss costs is reasonable. When other variables are held constant, loss costs decrease as deductibles increase.

C. *Deductible flood loss costs shall be calculated in accordance with s. 627.715, F.S.*

The Impact Forecasting Florida Flood Model (FCHLPM) version 3.0 is capable of handling deductibles. It complies with s. 627.715, F.S.

Disclosures

AF-5.1 Describe the methods used in the flood model to treat deductibles, policy limits, policy exclusions, loss settlement provisions, and insurance-to-value criteria when projecting flood loss costs and flood probable maximum loss levels. In particular, specify the loss settlement options available for manufactured homes.

Expected loss at each location is estimated using the probability density function of the damage ratio. Damage ratio is defined as ground up loss divided by replacement value.

$$\boldsymbol{E(L)= \int_{ded}^{ded+lim}(x-ded)*f(x)dx+lim*(1-F(lim+ded))} \quad (17)$$

Where:

ded = deductible

lim = limit

x = ground up loss, x ≥ 0

f(x) = probability density function of ground up loss

E(L)= expected gross loss net of deductible and limit

F(x) = cumulative distribution function of ground up loss

Percentage deductibles are converted to dollar deductibles during import.

The calculation of gross loss given above is based on well-established actuarial methodology. The method is discussed in various publications listed below.

- Homer, D., & Li, M. (2017, June). Notes on using property catastrophe model results. In Casualty Actuarial Society E-Forum (Vol. 2). Retrieved from https://www.casact.org/community/affiliates/camar/0517/CatNotes.pdf

- Heckman, P. E., & Meyers, G. G. (1983). The calculation of aggregate loss distributions from claim severity and claim count distributions. In Proceedings of the Casualty Actuarial Society (Vol. 70, No. 133-134, pp. 49-66). Casualty Actuarial Society.

- Waszink, H. E. (2006, March). The report of the research working party on correlations and dependencies among all risk sources. Part 4: Serial correlations of interest and inflation rates. The Casualty Actuarial Society Forum, Winter 2006 Edition (p. 255-276).

Model users have the options to reflect Mobile Home loss settlement options or actual cash value in coverage limits. Impact Forecasting model does not model loss settlement options explicitly.

AF-5.2 Describe if and how the flood model treats policy exclusions and loss settlement provisions.

Regarding policy exclusions, if the user removes a coverage amount from the input file, the model would not generate losses for the excluded coverage. Loss settlement and other exclusions that are not explicitly reflected in the exposure data cannot be quantified by the model. However, loss settlement and other exclusions may be implicitly included in the model results to the extent that the claims data used to calibrate the model reflected these conditions. Loss settlement for mobile home is not currently modeled by Impact Forecasting due to lack of claims data.

AF-5.3 Describe if and how the flood model treats annual deductibles.

The Impact Forecasting Florida Flood Model (FCHLPM) version 3.0 does not have annual deductible functionality applied.

AF-6 Flood Loss Outputs and Logical Relationships to Risk

A. *The methods, data, and assumptions used in the estimation of flood loss costs and flood probable maximum loss levels shall be actuarially sound.*

The methods, data, and assumptions used in the estimation of flood loss costs and probable maximum loss levels are actuarially sound.

B. *Flood loss costs shall not exhibit an illogical relation to risk, nor shall flood loss costs exhibit a significant change when the underlying risk does not change significantly.*

Loss costs generated by the Impact Forecasting model do not show an illogical relation to risk, and do not exhibit a significant change when the underlying risk does not change significantly.

C. *Flood loss costs cannot increase as the structure flood damage resistance increases, all other factors held constant.*

Flood loss costs do not increase as structure flood damage resistance increases, all other factors held constant, flood loss cost maps for various construction types are provided in Form AF-6: Logical Relationships to Flood Risk (Trade Secret Item) which will be available for review by the Professional Team.

D. *Flood loss costs cannot increase as flood hazard mitigation measures incorporated in the structure increase, all other factors held constant.*

Flood loss costs do not increase as flood hazard mitigation measures increase, all other factors held constant.

E. *Flood loss costs shall be consistent with the effects of major flood control measures, all other factors held constant.*

Flood loss costs are consistent with the effects of major flood control measures, all other factors held constant.

F. *Flood loss costs cannot increase as the flood resistant design provisions increase, all other factors held constant.*

Flood loss costs do not increase as the flood resistant design provisions increase, all other factors held constant. Flood loss cost sensitivity tests performed in Form AF-6: Logical Relationships to Flood Risk (Trade Secret Item) will be available for review by the Professional Team.

G. *Flood loss costs cannot increase as building code enforcement increases, all other factors held constant.*

Flood loss costs do not increase as building code enforcement increases, all other factors held constant. Flood loss cost sensitivity tests performed in Form AF-6: Logical Relationships to Flood Risk (Trade Secret Item) will be available for review by the Professional Team.

H. Flood loss costs shall decrease as deductibles increase, all other factors held constant.

Flood loss costs decrease as deductibles increase, all other factors held constant. Flood loss cost sensitivity tests performed in Form AF-6: Logical Relationships to Flood Risk (Trade Secret Item) will be available for review by the Professional Team.

I. The relationship of flood loss costs for individual coverages (e.g., personal residential structure, appurtenant structure, contents, and time element) shall be consistent with the coverages provided.

The relationship of flood loss costs for individual coverages is consistent with the coverages provided. Flood loss cost sensitivity tests performed in Form AF-6: Logical Relationships to Flood Risk (Trade Secret Item) will be available for review by the Professional Team.

J. Flood output ranges shall be logical for the type of risk being modeled and apparent deviations shall be justified.

Flood output ranges are logical for the type of risk being modeled. There are no deviations other than those counterintuitive relationships as a result of the characteristics of the underlying data, as discussed in Disclosure AF-6.8.

L. All other factors held constant, flood output ranges produced by the flood model shall in general reflect lower flood loss costs for personal residential structures that have a higher elevation versus those that have a lower elevation.

All other factors held constant, flood output ranges produced by the Impact Forecasting Florida Flood Model (FCHLPM) version 3.0 reflects lower flood loss costs for personal residential structures that have a higher elevation versus those that have a lower elevation.

M. For flood loss costs and flood probable maximum loss level estimates derived from and validated with historical insured flood losses or other input data and information, the assumptions in the derivations concerning (1) construction characteristics, (2) policy provisions, and (3) contractual provisions shall be appropriate based on the type of risk being modeled.

Disclosures VF-1.2 and VF-1.4 discuss how historical loss information has been used in the development of the Impact Forecasting vulnerability functions. Disclosures VF-1.2 and VF-1.4 also discuss that construction characteristics, lines of business, policy terms, insured value/limits, deductibles and sublimits, etc., were supplied by insurance companies to Impact Forecasting along with the claim information. Data mapping schemes were provided by insurance companies as well. Impact Forecasting scientists thoroughly reviewed the exposure, claims data, and data assumptions. Additional communications and clarifications were carried out with the data providers in case there were ambiguities and anomalies.

Disclosures

AF-6.1 Provide a completed Form AF-1, Zero Deductible Personal Residential Standard Flood Loss Costs. Provide a link to the location of the form [

Form AF-1: Zero Deductible Personal Residential Standard Flood Loss Costs].

AF-6.2 Provide a completed Form AF-2, Total Flood Statewide Loss Costs. Provide a link to the location of the form [Form AF-2: Total Flood Statewide Loss Costs].

AF-6.3 Provide a completed Form AF-3, Personal Residential Standard Flood Losses by ZIP Code. Provide a link to the location of the form [Form AF-3: Personal Residential Standard Flood Losses by ZIP Code].

AF-6.4 Provide a completed Form AF-4, Flood Output Ranges, using the modeling-organization-specified, predetermined, and comprehensive exposure dataset. Provide a link to the location of the form [Form AF-4: Flood Output Ranges].

AF-6.5 Provide a completed Form AF-5, Percentage Change in Flood Output Ranges. Provide a link to the location of the form [Form AF-5: Percentage Change in Flood Output Ranges].

This is the first Impact Forecasting Florida Flood Model submission.

AF-6.6 Provide a completed Form AF-6, Logical Relationships to Flood Risk (Trade Secret Item), if not considered as Trade Secret. Provide a link to the location of the form [Form AF-6: Logical Relationships to Flood Risk (Trade Secret Item)].

AF-6.7 Provide a completed Form AF-7, Percentage Change in Logical Relationships to Flood Risk. Provide a link to the location of the form [Form AF-7: Percentage Change in Logical Relationships to Flood Risk].

This is the first Impact Forecasting Florida Flood Model submission.

AF-6.8 Explain any assumptions, deviations, and differences from the prescribed exposure information in Form AF-6, Logical Relationships to Flood Risk (Trade Secret Item), and Form AF-7, Percentage Change in Logical Relationships to Flood Risk. In particular, explain how the treatment of unknown is handled in each sensitivity exhibit.

When preparing the exposure file as specified in the file “NotionalInput21.xlsx”, Impact Forecasting coded any “unknown” value with an equivalent “unknown” code for the risk characteristics in the Impact Forecasting model. Deductibles prescribed in “NotionalInput21.xlsx” were mapped to the policy deductible data field. The all other perils deductible field used by the Impact Forecasting model was defaulted to zero. There were no additional assumptions and deviations.

AF-6.9 ***Provide a completed Form AF-8, Flood Probable Maximum Loss for Florida. Provide a link to the location of the form [Form AF-8: Flood Probable Maximum Loss for Florida].***

AF-6.10 ***Describe the calculation of uncertainty intervals.***

The expected flood loss and 10% and 90% flood loss levels were computed using Impact Forecasting's personal residential exposure and the AEP and OEP results were provided in Form AF-8: Flood Probable Maximum Loss for Florida. Each event in the stochastic event set were simulated 10 times to capture the variation of loss due to uncertainty in the flood vulnerability functions. Those were then converted to year losses by taking either max or sum of the individual event losses for a given year. The return period for each year was calculated based on the averaged sample loss for each year. The expected flood loss and 10% and 90% flood loss levels for the desired return periods were computed from the 10 samples of certain years.

AF-6.11 ***Describe how the flood model produces flood probable maximum loss levels.***

The methodology used by the Impact Forecasting Florida Flood Model (FCHLPM) version 3.0 to estimate flood probable maximum loss levels has been discussed in Disclosure AF-4.1.

AF-6.12 ***Provide citations to published papers, if any, or modeling-organization studies that were used to estimate flood probable maximum loss levels.***

Homer, D., & Li, M. (2017, June). Notes on using property catastrophe model results. In Casualty Actuarial Society E-Forum (Vol. 2). Retrieved from https://www.casact.org/community/affiliates/camar/0517/CatNotes.pdf

Impact Forecasting (2020). ELEMENTS Computational & Financial Model. (Internal documentation).

Heckman, P. E., & Meyers, G. G. (1983). The calculation of aggregate loss distributions from claim severity and claim count distributions. In Proceedings of the Casualty Actuarial Society (Vol. 70, No. 133-134, pp. 49-66). Casualty Actuarial Society.

Meyers, G. (2006, March). The report of the research working party on correlations and dependencies among all risk sources. Part 3: The common shock model for correlated insurance. The Casualty Actuarial Society Forum, Winter 2006 Edition (p. 231-254).

Kuzak, D., & Larsen, T. (2005). Use of catastrophe models in insurance rate making. Catastrophe modeling: A new approach to managing risk, Chap. 5 (Springer, New York), 97–118.

AF-6.13 Explain any differences between the values provided on Form AF-8, Flood Probable Maximum Loss for Florida, and those provided on Form SF-2, Examples of Flood Loss Exceedance Estimates (Coastal and Inland Combined).

The results of Form AF-8: Flood Probable Maximum Loss for Florida match with Form SF-2: Examples of Flood Loss Exceedance Estimates (Coastal and Inland Combined).

AF-6.14 Provide an explanation for all flood loss costs that are not consistent with the requirements of this standard.

Flood loss costs are consistent with the requirements of Standard AF-6.

AF-6.15 Provide an explanation of the differences in flood output ranges between the currently accepted flood model and the flood model under review.

This is the first Impact Forecasting Florida Flood Model submission.

COMPUTER/INFORMATION FLOOD STANDARDS

CIF-1 Flood Model Documentation

A. *Flood model functionality and technical descriptions shall be documented formally in an archival format separate from the use of correspondence including emails, presentation materials, and unformatted text files.*

Impact Forecasting maintains the following three sets of documentation related to flood model development and implementation:

1. Model development documentation created by the Research and Development (R&D) team detailing all components, formulas, and test data for the flood model;
2. Technical notes produced by the Software Team based on model methodology described in the R&D document. The technical notes describe architectural and design strategies to implement the flood model in the ELEMENTS platform; and
3. High-level documentation created for end users that describes the components of the flood model and their usage in the ELEMENTS platform.

All documents are maintained in Microsoft Team Foundation Server (TFS) and are version controlled.

B. *A primary document repository shall be maintained, containing or referencing a complete set of documentation specifying the flood model structure, detailed software description, and functionality. Documentation shall be indicative of current model development and software engineering practices.*

Impact Forecasting maintains a document repository in TFS and SharePoint where all documents are stored and versioned. These documents describe major components of the flood model as well as interactions between components of the model using sequence diagrams, flowcharts, and other graphical descriptions where applicable. A list of such documents is provided in Disclosure CIF-2.1.

C. *All computer software (i.e., user interface, scientific, engineering, actuarial, data preparation, and validation) relevant to the flood model shall be consistently documented and dated.*

Documents describing model requirements, system architecture, design strategy, implementation details, and the user interface are produced by the Software Team. In addition, a document related to testing plans and test results is produced by the QA (Quality Assurance) Team.

D. *The following shall be maintained: (1) a table of all changes in the flood model from the currently accepted flood model to the initial submission this year, and (2) a table of all substantive changes in the flood model since this year's initial submission.*

This is the first Impact Forecasting submission to the FCHLPM.

E. Documentation shall be created separately from the source code.

The Impact Forecasting Software Team produces requirements, architecture, and design documents separate from the source code. These documents are used by the QA Team to prepare test cases and perform tests.

F. A list of all externally acquired currently used flood model-specific software and data assets shall be maintained. The list shall include (1) asset name, (2) asset version number, (3) asset acquisition date, (4) asset acquisition source, (5) asset acquisition mode (e.g., lease, purchase, open source), and (6) length of time asset has been in use by the modeling organization.

A list of externally acquired software and data assets is created and maintained by the Impact Forecasting team and will be available for review by the Professional Team.

CIF-2 Flood Model Requirements

A complete set of requirements for each software component, as well as for each database or data file accessed by a component, shall be maintained. Requirements shall be updated whenever changes are made to the flood model.

Impact Forecasting maintains a set of documentation containing the requirements for each component and its features. These documents are modified and tracked when the model changes. Documents listed in Disclosure CIF-2.1 will be available for review by the Professional Team.

Disclosure

CIF-2.1 Provide a description of the flood model and platform(s) documentation for interface, human factors, functionality, system documentation, data, human and material resources, security, and quality assurance.

Impact Forecasting maintains documentation for major software components along with a database schema, technical notes, a user guide, an installation guide, and a deployment guide for successful deployment and usage of the models on the ELEMENTS platform.

Impact Forecasting produces various types of internal (i.e., used only by Impact Forecasting) and external (i.e., client-facing) documents at different phases of the model development process. Documentation produced and maintained by the Impact Forecasting Software Team includes:

- Software Development Process: Describes the ELEMENTS software development process including various phases of development and delivery (e.g., requirements gathering, architecting, designing, implementation, testing, deployment, and support)
- Feature Requirement Specification: Captures requirements for new features or enhancements to existing ones
- Architecture/Design Document: Describes overall architecture and design of the system
- Technical Notes: Describes each major feature in detail along with dataflow diagrams and flowcharts when applicable
- Test Plans and Test Cases: Captures test cases for each feature and test plans for each iteration of internal and external releases
- Database Schema: Describes database schema for Exposure, Results, and Model databases
- Product Release Notes (Internal and External): Documents the addition of new features and the enhancement of existing features for every internal and external release
- ELEMENTS User Guide: Contains operational instructions for end users of the ELEMENTS platform
- Input Data Format: Describes each exposure field and indicates the supported format to successfully import exposure data to ELEMENTS
- ELEMENTS Installation and Deployment Guide: Provides guidance on server configuration and product setup for IT administrators
- Additional Tools User Guide: Consists of a user guide for administration tools for managing product setup and configuration by IT administrator
- Coding Standard: Details coding standards to be followed when developing applications

CIF-3 Flood Model Organization and Component Design

A. The following shall be maintained and documented: (1) detailed control and data flowcharts and interface specifications for each software component, (2) schema definitions for each database and data file, (3) flowcharts illustrating flood model-related flow of information and its processing by modeling organization personnel or consultants, (4) network organization, and (5) system model representations associated with (1)-(4) above. Documentation shall be to the level of components that make significant contributions to the flood model output.

Impact Forecasting develops and maintains documents which describe the database schema and relationships between data, including flowcharts to show the flow of information and links between data from various components of the software system. This includes schema of the Exposure, Results, and Model databases. Interaction between software components and sub-components is captured in architecture and design documentation, including the interactions between hazard and vulnerability modules. A separate document describing interactions between multiple Impact Forecasting groups and team members is maintained using a diagram.

B. All flowcharts (e.g., software, data, and system models) in the submission or in other relevant documentation shall be based on (1) a referenced industry standard (e.g., UML, BPMN, SysML), or (2) a comparable internally-developed standard which is separately documented.

All flowcharts developed and maintained by Impact Forecasting follow industry standards based on ISO (International Organization for Standardization) 5807, Unified Modeling Language (UML) and Business Process Model and Notation (BPMN). Figure 93 is an example of the detailed modeling process in ELEMENTS using Impact Forecasting's Flowchart Standards.

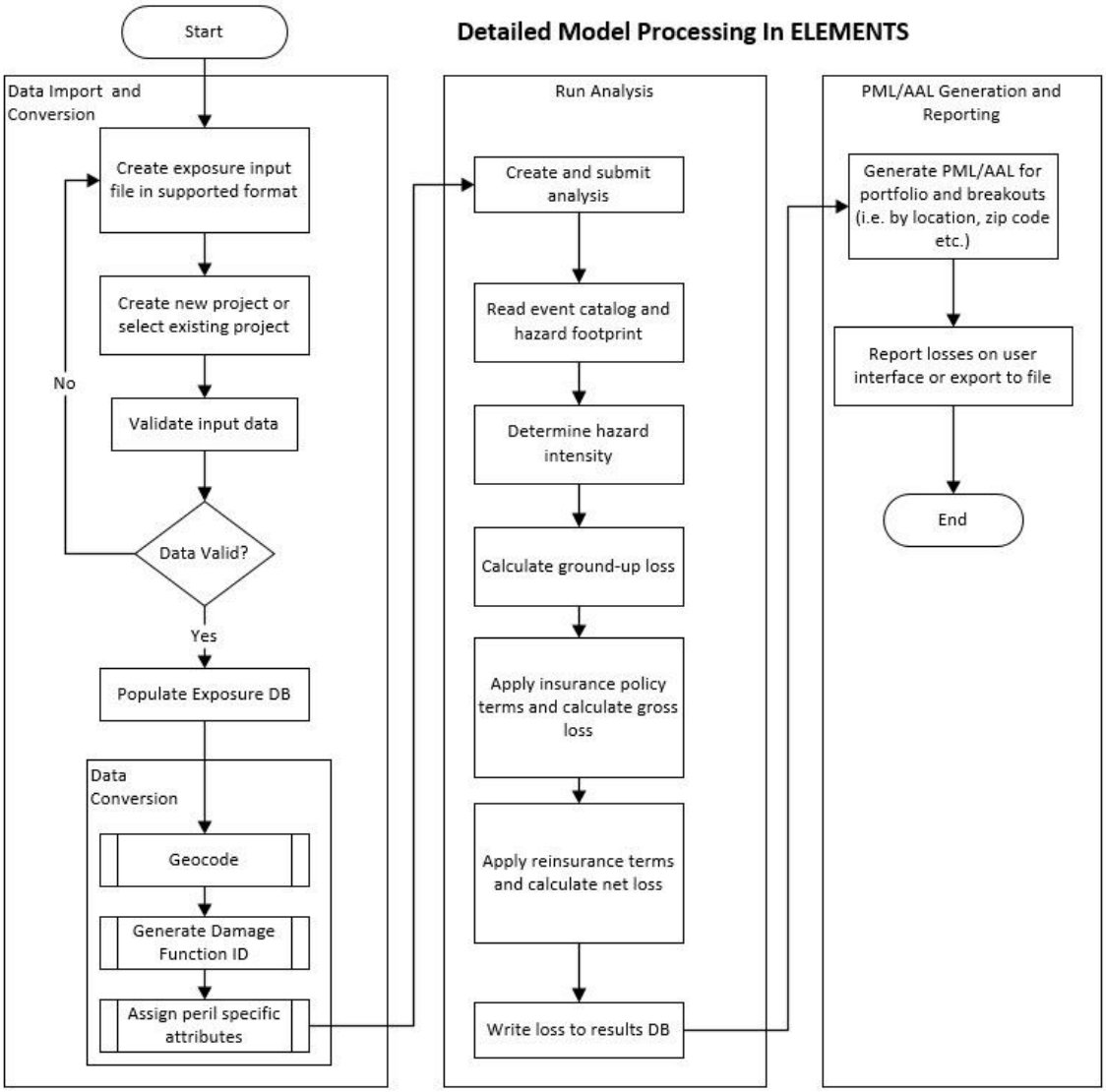

Figure 93: Example of a modeling process flowchart

CIF-4 Flood Model Implementation

A. A complete procedure of coding guidelines consistent with current software engineering practices shall be maintained.

Impact Forecasting maintains coding guidelines and a handbook of good coding practice. Developers are encouraged to follow documented best practices to ensure a robust product.

B. Network organization documentation shall be maintained.

Impact Forecasting maintains a network organization diagram involving all the servers and hardware components involved in running the flood model on the ELEMENTS platform.

C. A complete procedure used in creating, deriving, or procuring and verifying databases or data files accessed by components shall be maintained.

All model files and databases provided by the R&D group are stored and backed up regularly. The Software Team compares production-ready files and databases with original copies using MD5 Hash comparison.

D. All components shall be traceable, through explicit component identification in the flood model representations (e.g., flowcharts) down to the code level.

Descriptions of all static components and interactions between components are documented at various levels of detail using flowcharts and other depictions. This documentation can be used to track implementation details in actual code.

E. A table of all software components affecting flood loss costs and flood probable maximum loss levels shall be maintained with the following table columns: (1) component name, (2) number of lines of code, minus blank and comment lines, and (3) number of explanatory comment lines.

Impact Forecasting maintains a list of all components affecting flood loss cost and probable maximum loss calculations along with implementation details, such as number of lines of code and number of lines of comments for each component and sub-component.

F. Each component shall be sufficiently and consistently commented so that a software engineer unfamiliar with the code shall be able to comprehend the component logic at a reasonable level of abstraction.

All components including Classes and Methods are sufficiently commented in the code as per industry guidelines. All Classes are commented with each class's purpose and linkage to other Classes. All methods are commented with Input and Output parameters along with inner workings of the method, exceptions, and logic. An important line of code is commented in detail with linkage to work items in the source control system (TFS) when applicable.

G. The following documentation shall be maintained for all components or data modified by items identified in Flood Standard GF-1, Scope of the Flood Model and Its Implementation, Disclosure 8 and Audit 9:

1. **A list of all equations and formulas used in documentation of the flood model with definitions of all terms and variables.**
2. **A cross-referenced list of implementation source code terms and variable names corresponding to items within G.1 above.**

A list of all components referred to in Standard GF-1 and used in software implementation is maintained and tracked. A cross-referenced list of equations and variables used in implementation is documented and maintained.

H. Flood model code and data shall be accompanied by documented maintenance, testing, and update plans with their schedules. The vintage of the code and data shall be justified.

Flood model code has been stored and maintained in a TFS source control system. Changes to the flood model methodology have been documented as a part of new requirements. A plan was prepared to implement and test new requirements, and a schedule was prepared to introduce changes. Flood model code has been updated based on the change in requirements, and changes to the code have been tracked using a source control system. Both during and upon completion of coding, new and updated functionalities have been tested to match the outcome with expected results. Code is stored with a time stamp in the source control system, and the difference between new and old code can be compared upon request. The vintage of data used in modeling can be accessed upon request.

Disclosure

CIF-4.1 Specify the hardware, operating system, and essential software required to use the flood model on a given platform.

Table 42 shows various hardware and software components along with configuration and supported versions of the Impact Forecasting Florida Flood Model on the ELEMENTS platform.

Table 42: Hardware and software requirements for the Impact Forecasting Florida Flood Model on the ELEMENTS Version 18.0 platform

Component	Configuration or Supported Versions	Remarks
Operating system (Server)	Microsoft Windows 2016 or higher	
Operating system (Client)	Microsoft Windows 10 or higher - 64 bit	
CPU Speed (Minimum)	2.0 GHz of higher	
RAM (Minimum)	4 GB per core	JobManager - min. 4 cores
AnalysisServer - min. 12 cores	10 GB (RAM) or higher per core	
Exposure/Results/Model database server - min. 12 cores	64 GB (RAM) or higher	
Hard disk space	Minimum 300 GB (base - no models), max. 3.5TB (base + all models)	
SQL Server Database	Minimum 32 GB (base - no models), recommended 64 GB per instance	Recommend hosting exposure/result and model databases on separate servers.

Component	Configuration or Supported Versions	Remarks
SQL Native Client	SQL Server Native Client version 11	Impact Forecasting also has installation files which use MSOLEDBSQL
SQL Server Management Object (SMO)	SQL Server 2017 SMO	
.Net Framework	Ver. 4.8	
Visual Studio	Visual Studio 2019 or higher	
Precisely Spectrum Geocoding engine	Spectrum 2019 with May 2022 dataset	
Infragistics Windows Presentation Foundation (WPF) controls	Ver. 14.2, 20.1	

CIF-5 Flood Model Verification

A. General

For each component, procedures shall be maintained for verification, such as code inspections, reviews, calculation crosschecks, and walkthroughs, sufficient to demonstrate code correctness. Verification procedures shall include tests performed by modeling organization personnel other than the original component developers.

Any change in a model component is usually performed by engineers from the Research & Development group. These changes are documented and developed by engineers in their choice of language or other product (e.g., FORTRAN, Python, R, Excel, MATLAB) depending on the complexity of the change. These components are then peer reviewed and approved. Test portfolios, including approved client books, are then run with approved changes. Results and documentation of changes are shared with the Software Team. The Software Team independently implements these changes in the production-ready software following industry standard processes. At the end, the QA Team performs various tests in which results (hazard and losses) are compared with original runs performed by model development engineers and, upon successful comparison, changes are approved and released in the final product.

B. Component Testing

1. **Testing software shall be used to assist in documenting and analyzing all components.**

The Impact Forecasting Software Team uses the Team Foundation Server (TFS) Unit testing framework to perform unit tests on all components when applicable. All unit test cases are documented and stored in the TFS repository.

2. **Unit tests shall be performed and documented for each updated component.**

Unit tests for all components are performed where applicable. For all eligible components and sub-components, an input, along with the expected output, is defined and tests are run to match expected results. Only upon passing the unit tests is the code allowed to be checked in as a part of the final build.

In addition to the unit tests, automated tests, which go through sets of sub-components and check the correctness of the results, are also performed.

3. **Regression tests shall be performed and documented on incremental builds.**

Sets of regression tests are documented and performed with each iteration of internal and production releases. New regression tests are added with newly added features to complete the coverage of all cases.

4. **Integration tests shall be performed and documented to ensure the correctness of all flood model components. Sufficient testing shall be performed to ensure that all components have been executed at least once.**

End-to-end tests involving all flood model components are performed regularly by the QA team with each internal and production release. Multiple test cases are created to make sure all possible interactions among sub-components and components are covered.

C. Data Testing

1. **Testing software shall be used to assist in documenting and analyzing all databases and data files accessed by components.**

Specific test cases are developed for components which access model data from a database or files and are compared against expected results. These tests are run periodically with every internal and production release cycle. The Unified Function Test (UFT) suite by MicroFocus is used to automate test cases in addition to manual testing to verify communications between various components. The combination of log files, intermediate files, and SQL databases are also used to verify data flow and inter-component communication. Microsoft Excel and Word are used to document the testing process and its outcome.

2. **Integrity, consistency, and correctness checks shall be performed and documented on all databases and data files accessed by the components.**

A data hash mechanism is used when copying data from one server to another to ensure that no data are corrupted which can corrupt results. All data used by the flood model is regularly backed up.

Disclosures

CIF-5.1 State whether any two executions of the flood model with no changes in input data, parameters, code, and seeds of random number generators produce the same flood loss costs and flood probable maximum loss levels.

The Impact Forecasting Florida Flood Model will produce the same loss cost and probable maximum loss levels when fed with the same set of input data multiple times. The model will use the same seed for a given location based on its latitude and longitude. This will also ensure that the same result is produced even when the ordering of locations changes in the input file. Loss repeatability is tested as part of the regular testing suite.

CIF-5.2 Provide an overview of the component testing procedures.

Flood model component testing consists of the following types of tests:

Hazard Component Testing

Once implemented in the ELEMENTS software, the hazard intensity values (flood depth) for strategically selected locations and for selected events are extracted from the ELEMENTS analysis and compared with the hazard intensity from model development.

Vulnerability Component Testing

A unit test for selected damage functions to check for boundary conditions and interpolation is performed and compared with manual calculations. A portfolio is prepared to cover all possible combinations of damage functions and is analyzed against a selected hazard value and compared with manual calculations.

Aggregation Testing

A full analysis (hazard and loss) is performed on the test portfolio and the results are compared with baseline numbers to ensure hazard and vulnerability components are working together as expected and are providing expected results.

Regression Testing

Test portfolios and approved client portfolios are run with every internal and release build to ensure consistency in results. Automation tests are run with every release build to ensure end-to-end product integrity.

Performance Testing

With every release build, a performance test is run to ensure runtime is consistent with expectations based on the new or modified features.

CIF-5.3 Provide a description of verification approaches used for externally acquired data, software, and models.

Data and software received from external sources go through quality checks before they are deemed usable by the group. These checks are described in Table 43.

In addition, Impact Forecasting also performs the following data checks on externally acquired data sources when possible:

- Creation of a Hash of the received data which is verified against data copied to the destination
- Check data accuracy against other available sources
- Compare current version with previous version in the case of an upgrade

Table 43: Impact Forecasting verification approaches for externally-acquired data and software

Externally-Acquired Data	Verification Approach
Atlantic Hurricane Database (HURDAT2)	Verified by spot checks against the online version at the time of verification. Also validated by visually comparing the HURDAT2 data with historical storm tracks/intensities provided by NOAA (National Oceanic and Atmospheric Administration).
Tropical Cyclone Extended Best Track Dataset	Verified by spot checks against the latest version as well as comparing with HURDAT2 for parameters that are in both datasets.
HURDAT Reanalysis Data	Verified by spot checks against the online version at the time of verification. The data were also compared with that available in the NOAA Report NWS (National Weather Service) 38 - Hurricane Climatology for the Atlantic and Gulf Coasts of the United States.
Hadley Centre Sea Ice and Sea Surface Temperature Dataset (HadISST)	Verified by comparing the SST plots with the latest version available as well as other data sources, such as the Extended Reconstructed Sea Surface Temperature (ERSST), for consistency.
USGS National Elevation Dataset (NED)	Data verified through data visualisation software packages
US river flow data from USGS National Water Information System (NWIS)	River flows underwent QC checks before being incorporated into the Regionalised Flood Frequency Analysis

Externally-Acquired Data	Verification Approach
US extreme precipitation data from the National Oceanic and Atmospheric Administration (NOAA) Precipitation Frequency Data Server (PFDS)	Data verified through data visualisation software packages
USGS National Hydrography Data, High resolution (NHDPlus).	Data verified through data visualisation software packages
US Army Corps of Engineers National Levee Database	Data verified through data visualisation software packages
US Soil Survey Geographic Database (SSURGO)	Data verified through data visualisation software packages
Koppen Geiger Climate Classification	Data verified through data visualisation software packages
HydroBASINS database	Data verified through data visualisation software packages
Multi-Source Weighted-Ensemble Precipitation (MSWEP)	A comparison of 11 gauge-corrected rainfall datasets over the US (https://hess.copernicus.org/articles/23/207/2019/) showed that MSWEP has the best overall performance. The MSWEP v2 paper has been cited more than 600 times in peer-reviewed studies, which reflects its quality and its status as top rainfall dataset.
Multi-Source Weather (MSWX)	As the MSWX data is primarily based on the widely used and reliable ECMWF Reanalysis v5 (ERA5), and was generated by the same group as MSWEP, so is considered to be particularly reliable.
MERIT-Hydro	The MERIT-Hydro river network is one of the best dataset available, its paper has been cited more than 450 times. MERIT-Hydro is one of the key building blocks of the Fathom's global flood maps, so it was repeatedly verified.
The International Best Track Archive for Climate Stewardship (IBTrACS)	Data verified though data visualisation and spot checks against historical storm reports (i.e. location and timing)
Postal Code Information from Zip-Codes.com	ZIP Code boundaries are examined for consistency and quality, and are compared with previous vintages for accuracy and appropriateness.
U.S. Census (2020) Data	Verified by spot checks against the online version at the time of verification.
Precisely Spectrum - Enterprise Geocoding Module	Sets of addresses are passed to the geocoder engine, and the retrieved coordinates are compared with other sources, such as Google Maps. Various combinations of address components (street, city,

Externally-Acquired Data	Verification Approach
	state, county) are tested for validity of the address and the returned coordinate values.
NFIP Claims Data	Data cleansing procedure, data entries were revised by filtering over selected fields to avoid entries with incomplete or presumably incorrect data.
NFIP Policy Data	Data cleansing procedure, data entries were revised by filtering over selected fields to avoid entries with incomplete or presumably incorrect data.
Hazus Flood Assessment Structure Tool Damage Functions	Verified by revising original sources of expert-judgement derived damage functions.

CIF-6 Human-Computer Interaction

A. *Interfaces shall be implemented as consistent with accepted principles and practices of Human-Computer Interaction (HCI), Interaction Design, and User Experience (UX) engineering.*

The user interface is designed using accepted principles and practices of HCI by Impact Forecasting UX design engineer and considers various human factors to implement requirements, making the interface intuitive and easy to use for end users. The user interface is designed to minimize common user errors and to streamline workflows. Catastrophe modeling domain specific vocabulary is used on the user interface to communicate tasks and workflows effectively. The UX design is finalized using industry standard software packages and UX engineering principles prior to coding.

B. *Interface options used in the flood model shall be unique, explicit, and distinctly emphasized.*

The option to run a FCHLPM approved model is uniquely emphasized on the user interface by having “FCHLPM” as a part of the model’s name along with the model version.

C. *For a Florida rate filing, interface options shall be limited to those options found acceptable by the Commission.*

An option to run the FCHLPM approved model rate filing is available in the interface. When this option is selected, all other options are set to approved default values, limiting users only to options found acceptable by the Commission.

Disclosure

CIF-6.1 Identify procedures used to design, implement, and evaluate interface options.

- Clearly defined description of available analysis options.
- Define default values for all applicable options when submitting analysis for filing using the FCHLPM approved model.
- Provide option (Default) to run the FCHLPM approved model for rate filing purposes.
- Set all options to approved default value and lock options (not allowing users to change values) when the FCHLPM approved model is used for rate filing.

CIF-7 Flood Model Maintenance and Revision

A. *A clearly written policy shall be implemented for review, maintenance, and revision of the flood model and network organization, including verification and validation of revised components, databases, and data files.*

Impact Forecasting created policies and processes to be followed when changing model components in any form. This includes the production of a business case which includes the driving factor(s) that necessitate the change and the objective and impact of the change.

Detailed documentation also includes the proposed solution by R&D, the methodology, and the impact of changes on model results. New proposed changes are peer reviewed and, upon approval, this information is passed on to the Software Team for implementation along with relevant modified components.

The Software Team follows the process to perform quality checks of components received from R&D. New methodology is documented by software engineers, and architecture and design documents are revised accordingly. Once new changes are implemented in the software, software engineers and the QA Team follow the process to test new changes. The type of tests performed to check the quality of the model change depends on the nature of the change that was made.

B. *A revision to any portion of the flood model that results in a change in any Florida personal residential flood loss cost or flood probable maximum loss level shall result in a new flood model version identification.*

Impact Forecasting maintains one version identifier for the flood model and a separate version identifier for the ELEMENTS platform. As the Impact Forecasting Florida Flood Model periodically changes to reflect new learning and advancement in understanding of the model components, new versions are assigned for internal and external releases.

C. *Tracking software shall be used to identify and describe all errors, as well as modifications to code, data, and documentation.*

Impact Forecasting uses Team Foundation Server (TFS) as the code, documentation (including feature and change requests and requirements), and requirements repository. Any changes to the model components are tracked using TFS source control system, which records the change, author, and date/time of the change.

D. *A list of all flood model versions since the initial submission for this year shall be maintained. Each flood model description shall have an unique version identification and a list of additions, deletions, and changes that define that version.*

This is the first Impact Forecasting flood model submission to the FCHLPM. Impact Forecasting will maintain a list of flood model changes after the initial submission. A unique version identifier will be assigned according to the versioning scheme established by Impact Forecasting (see Disclosure CIF-7.2).

Disclosures

CIF-7.1 Identify procedures used to review and maintain code, data, and documentation.

New development in the ELEMENTS platform and flood model components starts with creating a requirement specification for approved changes. Once a requirement

specification and scope of the project is finalized, the project is assigned to R&D and/or the Software Team depending on the nature of the changes.

Based on the requirements and scope, functional specifications with technical details are prepared. Once the functional specifications are finalized, the QA Team starts creating test cases, and the software team prepares architecture, design, and/or technical documentation depending on the complexity of the change. Upon finalization of architecture and design changes, the Software Team creates a new branch in TFS, implements the changes, and performs unit testing when appropriate. After completion of implementation, new changes are merged into the main branch, and an internal product release gets built, which is then submitted for testing by the QA Team. The QA Team performs tests based on the created test cases for the given changes to make sure the new changes are performing as expected. New changes are then tested along with rest of the existing components as a part of the regression test. Once approved by QA, new features are considered ready for release. A description of new features is added into Release Notes for the next release, and the User Guide and Deployment Guide (see Disclosure CIF-2.1) are updated appropriately.

Figure 94 shows the high-level model implementation and release process.

Model implementation in ELEMENTS and deployment process

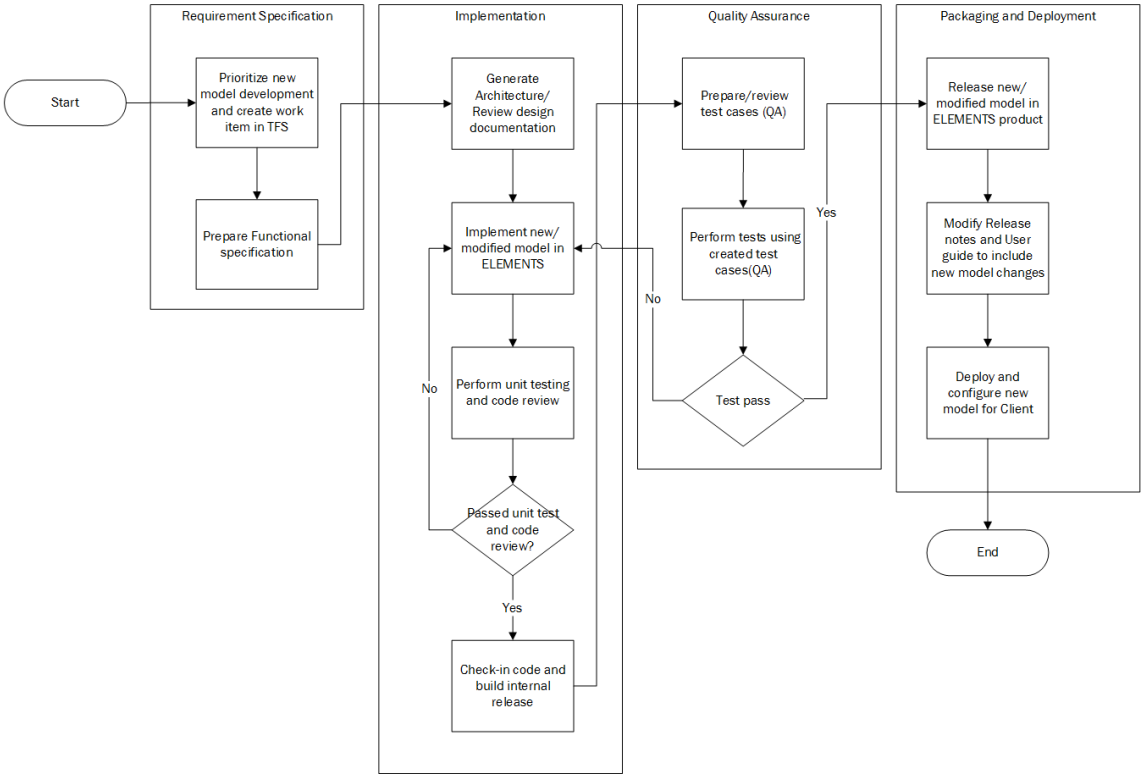

Figure 94: Model implementation in ELEMENTS software and deployment process

CIF-7.2 Describe the rules underlying the flood model and code revision identification systems.

The Impact Forecasting Florida Flood Model is deployed on the Impact Forecasting ELEMENTS platform. Any changes in model components or the ELEMENTS platform that result in a change in loss results are carefully managed by providing version identification to the flood model and platform independently. Figure 95 shows an example of the version progression of the ELEMENTS platform and an example model independently.

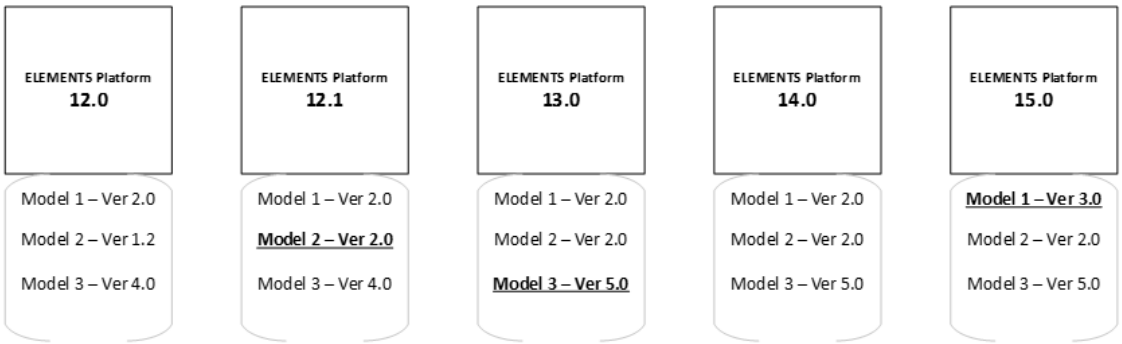

Figure 95: Example of models hosted on the ELEMENTS platform

Impact Forecasting uses the following versioning scheme for the ELEMENTS platform and models.

[Major Release].[Minor Release].[Beta]

All major releases of the model or platform follow a whole number format (e.g., Ver. 1.0, Ver. 2.0, etc.). Minor releases which may include patches receive a minor release number (e.g., Ver. 10.1, Ver. 12.2, etc.). If Impact Forecasting is releasing a beta model or platform to clients, “b” will be added at the end of the beta version (e.g., Ver. 2.0.1b).

CIF-8 Flood Model Security

Security procedures shall be implemented and fully documented for (1) secure access to individual computers where the software components or data can be created or modified, (2) secure operation of the flood model by clients, if relevant, to ensure that the correct software operation cannot be compromised, (3) anti-virus software installation for all machines where all components and data are being accessed, and (4) secure access to documentation, software, and data in the event of a catastrophe.

Impact Forecasting documents and follows security processes to secure access to the code, data, and documentation as prescribed by the company's policy and industry standard.

Disclosure

CIF-8.1 Describe methods used to ensure the security and integrity of the code, data, and documentation. These methods include the security aspects of each platform and its associated hardware, software, and firmware.

Secured Computer Access

Office Security:

- Aon facilities employ 24-hour security staff and building access monitoring.
- Only employees with authorized electronic badges may enter Aon facilities.
- Only authorized employees of Aon may enter areas of the building designated for Aon employees.
- All Aon floors feature doors that close and lock automatically.

Data Center Access:

- Data center access is restricted to only administrators.
- Access to servers is monitored 24 hours per day, 7 days per week.
- Data center access requires specific security badges and biometric scans.

Secured Model

Firewall and Network Security:

- Cisco Next-Gen Firewalls are used for controlling traffic in and out of the network.
- Intrusion detection systems (IDS) and intrusion protection systems (IPS) software are used to detect and prevent network intrusions.
- Proxy servers are used to filter user traffic to only approved external web sites.

User Account Access:

- Authorized Aon user accounts are required for network access. Former employees' user accounts are immediately closed following their last day of employment.
- Access to files and folders on all servers is regulated by Windows permissions. Permissions are set on a server-by-server, folder-by-folder, or file-by-file basis as appropriate. Access to SQL instances is set on a user-by-user basis.

- Access to the Aon network from outside the firewall is granted using a VPN gateway. VPN access is tied to a user's Windows account and is controlled by Aon IT and Security.
- All company personnel are required to pass a background check upon employment.
- All employees require an authorized user account to log in to any workstation or server. Passwords must adhere to strict, industry-standard requirements.
- User accounts are managed by the Aon's UAM (User Access Management) teams.
- Server and workstation accounts are locked out after 5 unsuccessful logins.
- All servers are located in a secured data center, which requires electronic badge access and biometric hand scans. Datacenter access is restricted to administrators only.
- Windows updates and patches are administered by the IT department and run monthly. The distribution of updates is controlled by Group Policy at the domain level.
- Anti-virus:
- All servers and workstations are installed with Symantec Hosted Endpoint antivirus software.
- Virus definitions are updated daily.
- Updates to the antivirus software are managed by Aon IT department via a web-based management console.

Secured Documentation, Software, and Data

Code:

- Only developers have access to Impact Forecasting code.
- Microsoft Team Foundation Server is used for version control, and only specified developers have access to the necessary Collections, Projects, and Solutions.
- Only administrators have physical access to the TFS server.
- TFS server(s) are backed-up to tape on a weekly basis. Backup tapes are stored offsite.
- Data Security:
- All confidential data can be sent via SFTP (Secure File Transfer Protocol) with PGP encryption.
- All confidential data must be stored in our physically secured datacenter.
- File shares and SQL servers are not accessible outside the Aon network.
- Both remote access (RDP) and file access are restricted to only authorized users.
- File servers containing client and/or sensitive data must have Symantec Endpoint Protection antivirus software installed, be encrypted with BitLocker, and be backed up nightly via ShadowProtect.
- Data access is regulated to authorized users only. This includes access to the Team Foundation Server for version control, file shares and SQL Server databases.
- All servers are backed up using StorageCraft ShadowProtect, with full backups monthly and incremental backups nightly. Tape backups are made monthly and shipped off-site to Iron Mountain, a third-party storage company.
- All old hard drives are wiped clean by an administrator when they are no longer needed. Non-solid state drives (SSD) are wiped using Darik's Boot and Nuke (DBAN), and SSD drives are wiped using SecureErase.

Documentation:

- SharePoint is used to manage and version control documentation.
- Users are granted permissions to SharePoint sites on an as needed basis.
- Access to SharePoint is managed by the SharePoint administrators.
- Windows authentication is used for managing, granting, and denying access.

Security of code, data, and documentation for each client organization is governed by strict licensing, mutually acceptable requirements under which they cannot reverse engineer or modify any of the binaries provided to them under the terms and conditions of the license, and secure installations involving both parties' IT departments.

Appendix A: FCHLPM Forms

Form GF-1: General Flood Standards Expert Certification

I hereby certify that I have reviewed the current submission of Impact Forecasting Florida Flood (FCHLPM) Model Version 3.0 for compliance with the 2021 Flood Standards adopted by the Florida Commission on Hurricane Loss Projection Methodology and hereby certify that:

1. The flood model meets the General Flood Standards (GF-1–GF-5);
1. The disclosures and forms related to the General Flood Standards section are editorially and technically accurate, reliable, unbiased, and complete;
2. My review was completed in accordance with the professional standards and code of ethical conduct for my profession;
3. My review involved ensuring the consistency of the content in all sections of the submission; and
4. In expressing my opinion I have not been influenced by any other party in order to bias or prejudice my opinion.

Daniel Rees	M.A., Geographic Information Science
Name	Professional Credentials (Area of Expertise)
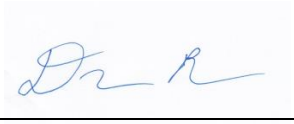	January 27, 2024
Signature (original submission)	Date
Xian He	Ph.D. Civil Engineering
Name	Professional Credentials (Area of Expertise)
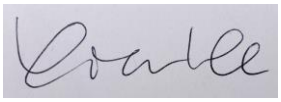	January 28, 2024
Signature (original submission)	Date
	April 24, 2024
Signature (response to deficiencies, if any)	Date
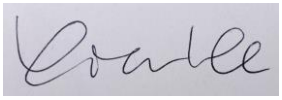	April 24, 2024
Signature (response to deficiencies, if any)	Date
	May 10, 2024
Signature (revisions to submission, if any)	Date

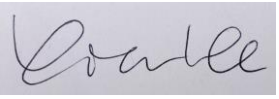

May 10, 2024

Signature (revisions to submission, if any) Date

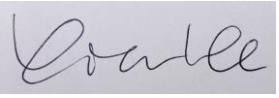

Aug 30, 2024

Signature (revisions to submission, if any) Date

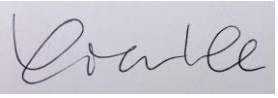

October 22, 2024

Signature (final submission) Date

October 23, 2024

Signature (final submission) Date

An updated signature and form are required following any modification of the flood model and any revision of the original submission. If a signatory differs from the original signatory, provide the printed name and professional credentials for any new signatories. Additional signature lines should be added as necessary with the following format:

Signature (revisions to submission) Date

Note: A facsimile or any properly reproduced signature will be acceptable to meet this requirement.

Include Form GF-1, General Flood Standards Expert Certification, in a submission appendix.

Form GF-2: Meteorological Flood Standards Expert Certification

I hereby certify that I have reviewed the current submission of Impact Forecasting Florida Flood (FCHLPM) Model Version 3.0 for compliance with the 2021 Flood Standards adopted by the Florida Commission on Hurricane Loss Projection Methodology and hereby certify that:

1. The flood model meets the Meteorological Flood Standards (MF-1–MF-5);
2. The disclosures and forms related to the Meteorological Flood Standards section are editorially and technically accurate, reliable, unbiased, and complete;
3. My review was completed in accordance with the professional standards and code of ethical conduct for my profession; and
4. In expressing my opinion I have not been influenced by any other party in order to bias or prejudice my opinion.

Niall Quinn	Ph.D., Geographical Sciences
Name	Professional Credentials (Area of Expertise)
	January 27, 2024
Signature (original submission)	Date
Radovan Drinka	M.S., Physics
Name	Professional Credentials (Area of Expertise)
	January 27, 2024
Signature (original submission)	Date
	April 24, 2024
Signature (response to deficiencies, if any)	Date
	April 24, 2024
Signature (response to deficiencies, if any)	Date
	May 10, 2024
Signature (revisions to submission, if any)	Date
	May 10, 2024
Signature (revisions to submission, if any)	Date

	Aug 30, 2024
Signature (revisions to submission, if any)	Date
	October 22, 2024
Signature (final submission)	Date
	October 21, 2024
Signature (final submission)	Date

An updated signature and form are required following any modification of the flood model and any revision of the original submission. If a signatory differs from the original signatory, provide the printed name and professional credentials for any new signatories. Additional signature lines should be added as necessary with the following format:

Signature (revisions to submission)	Date

Note: A facsimile or any properly reproduced signature will be acceptable to meet this requirement.

Include Form GF-2, Meteorological Flood Standards Expert Certification, in a submission appendix.

Form GF-3: Hydrological and Hydraulic Flood Standards Expert Certification

I hereby certify that I have reviewed the current submission of Impact Forecasting Florida Flood (FCHLPM) Model Version 3.0 for compliance with the 2021 Flood Standards adopted by the Florida Commission on Hurricane Loss Projection Methodology and hereby certify that:

1. The flood model meets the Hydrological and Hydraulic Flood Standards (HHF-1–HHF-4);
2. The disclosures and forms related to the Hydrological and Hydraulic Flood Standards section are editorially and technically accurate, reliable, unbiased, and complete;
3. My review was completed in accordance with the professional standards and code of ethical conduct for my profession; and
4. In expressing my opinion I have not been influenced by any other party in order to bias or prejudice my opinion.

James Savage
Name

Ph.D., Geographical Sciences
Professional Credentials (Area of Expertise)

State: N/A Expiration Date: N/A
Professional License Type: N/A

Signature (original submission)

January 27, 2024
Date

Petr Puncochar
Name

Ph.D., Hydrology and Open-Channel Hydraulics
Professional Credentials (Area of Expertise)

State: N/A Expiration Date: N/A
Professional License Type: N/A

Signature (original submission)

January 27, 2024
Date

Signature (response to deficiencies, if any)

April 24, 2024
Date

Signature (response to deficiencies, if any)

April 24, 2024
Date

Signature (revisions to submission, if any)

May 10, 2024
Date

Signature (revisions to submission, if any)

May 10, 2024
Date

	July 16, 2024
Signature (revisions to submission, if any)	Date
	October 23, 2024
Signature (final submission)	Date
	October 23, 2024
Signature (final submission)	Date

An updated signature and form are required following any modification of the flood model and any revision of the original submission. If a signatory differs from the original signatory, provide the printed name and professional credentials for any new signatories. Additional signature lines should be added as necessary with the following format:

Signature (revisions to submission)	Date

Note: A facsimile or any properly reproduced signature will be acceptable to meet this requirement.

Include Form GF-3, Hydrological and Hydraulic Flood Standards Expert Certification, in a submission appendix.

Form GF-4: Statistical Flood Standards Expert Certification

I hereby certify that I have reviewed the current submission of Impact Forecasting Florida Flood (FCHLPM) Model Version 3.0 for compliance with the 2021 Flood Standards adopted by the Florida Commission on Hurricane Loss Projection Methodology and hereby certify that:

1. The flood model meets the Statistical Flood Standards (SF-1–SF-5);
2. The disclosures and forms related to the Statistical Flood Standards section are editorially and technically accurate, reliable, unbiased, and complete;
3. My review was completed in accordance with the professional standards and code of ethical conduct for my profession; and
4. In expressing my opinion I have not been influenced by any other party in order to bias or prejudice my opinion.

Name Professional Credentials (Area of Expertise)

Radek Solnicky	M.S., Mathematical Statistics
Name	Professional Credentials (Area of Expertise)
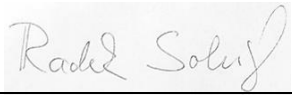	January 27, 2024
Signature (original submission)	Date
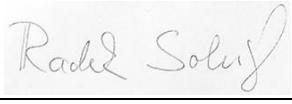	April 24, 2024
Signature (response to deficiencies, if any)	Date
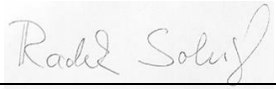	May 10, 2024
Signature (revisions to submission, if any)	Date
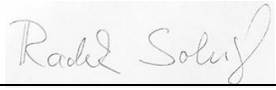	June 06, 2024
Signature (revisions to submission, if any)	Date
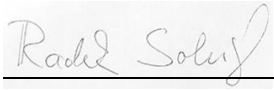	October 22, 2024
Signature (final submission)	Date

An updated signature and form are required following any modification of the flood model and any revision of the original submission. If a signatory differs from the original signatory, provide the printed name and professional credentials for any new signatories. Additional signature lines should be added as necessary with the following format:

Signature (revisions to submission)	Date

Note: A facsimile or any properly reproduced signature will be acceptable to meet this requirement.

Include Form GF-4, Statistical Flood Standards Expert Certification, in a submission appendix.

Form GF-5: Vulnerability Flood Standards Expert Certification

I hereby certify that I have reviewed the current submission of Impact Forecasting Florida Flood (FCHLPM) Model Version 3.0 for compliance with the 2021 Flood Standards adopted by the Florida Commission on Hurricane Loss Projection Methodology and hereby certify that:

1. The flood model meets the Vulnerability Flood Standards (VF-1–VF-4);
2. The disclosures and forms related to the Vulnerability Flood Standards section are editorially and technically accurate, reliable, unbiased, and complete;
3. My review was completed in accordance with the professional standards and code of ethical conduct for my profession; and
4. In expressing my opinion I have not been influenced by any other party in order to bias or prejudice my opinion.

Yujin Liang	Ph.D., Structural Engineering; P.E.
Name	Professional Credentials (Area of Expertise)
	State: Minnesota Expiration Date:06/30/2026
	Professional License Type: Structural
	January 27, 2024
Signature (original submission)	Date
	April 24, 2024
Signature (response to deficiencies, if any)	Date
	May 10, 2024
Signature (revisions to submission, if any)	Date
	Aug 30, 2024
Signature (revisions to submission, if any)	Date
	October 22, 2024
Signature (final submission)	Date

An updated signature and form are required following any modification of the flood model and any revision of the original submission. If a signatory differs from the original signatory, provide the printed name and professional credentials for any new signatories. Additional signature lines should be added as necessary with the following format:

Signature (revisions to submission) Date

Note: A facsimile or any properly reproduced signature will be acceptable to meet this requirement.

Include Form GF-5, Vulnerability Flood Standards Expert Certification, in a submission appendix.

Form GF-6: Actuarial Flood Standards Expert Certification

I hereby certify that I have reviewed the current submission of Impact Forecasting Florida Flood (FCHLPM) Model Version 3.0 for compliance with the 2021 Flood Standards adopted by the Florida Commission on Hurricane Loss Projection Methodology and hereby certify that:

1. The flood model meets the Actuarial Flood Standards (AF-1–AF-6);
2. The disclosures and forms related to the Actuarial Flood Standards section are editorially and technically accurate, reliable, unbiased, and complete;
3. My review was completed in accordance with the Actuarial Standards of Practice and Code of Conduct; and
4. In expressing my opinion I have not been influenced by any other party in order to bias or prejudice my opinion.

Minchong Mao	FCAS, MAAA
Name	Professional Credentials (Area of Expertise)
	January 28, 2024
Signature (original submission)	Date
	April 24, 2024
Signature (response to deficiencies, if any)	Date
	May 10, 2024
Signature (revisions to submission, if any)	Date
	Aug 09, 2024
Signature (revisions to submission, if any)	Date
	October 24, 2024
Signature (final submission)	Date

An updated signature and form are required following any modification of the flood model and any revision of the original submission. If a signatory differs from the original signatory, provide the printed name and professional credentials for any new signatories. Additional signature lines should be added as necessary with the following format:

Signature (revisions to submission) Date

Note: A facsimile or any properly reproduced signature will be acceptable to meet this requirement.

Include Form GF-6, Actuarial Flood Standards Expert Certification, in a submission appendix.

Form GF-7: Computer/Information Flood Standards Expert Certification

I hereby certify that I have reviewed the current submission of Impact Forecasting Florida Flood (FCHLPM) Model Version 3.0 for compliance with the 2021 Flood Standards adopted by the Florida Commission on Hurricane Loss Projection Methodology and hereby certify that:

1. The flood model meets the Computer/Information Flood Standards (CIF-1–CIF-8);
2. The disclosures and forms related to the Computer/Information Flood Standards section are editorially and technically accurate, reliable, unbiased, and complete;
3. My review was completed in accordance with the professional standards and code of ethical conduct for my profession; and
4. In expressing my opinion I have not been influenced by any other party in order to bias or prejudice my opinion.

Sushma Bhat — Name

B.S., Computer Science — Professional Credentials (Area of Expertise)

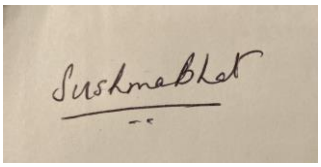

Signature (original submission)

January 27, 2024 — Date

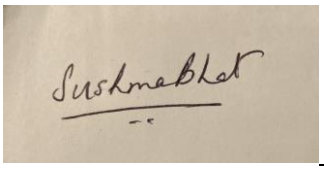

Signature (response to deficiencies, if any)

April 24, 2024 — Date

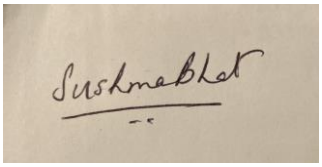

Signature (revisions to submission, if any)

May 10, 2024 — Date

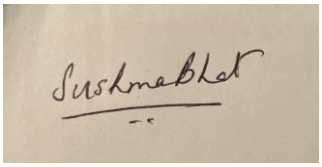

_____	October 24
Signature (final submission)	Date

An updated signature and form are required following any modification of the flood model and any revision of the original submission. If a signatory differs from the original signatory, provide the printed name and professional credentials for any new signatories. Additional signature lines should be added as necessary with the following format:

_____	_____
Signature (revisions to submission)	Date

Note: A facsimile or any properly reproduced signature will be acceptable to meet this requirement.

Include Form GF-7, Computer/Information Flood Standards Expert Certification, in a submission appendix.

Form GF-8: Editorial Review Expert Certification

I hereby certify that I have reviewed the current submission of Impact Forecasting Florida Flood (FCHLPM) Model Version 3.0 for compliance with the "Process for Determining the Acceptability of a Computer Simulation Flood Loss Model" adopted by the Florida Commission on Hurricane Loss Projection Methodology in its Flood Standards Report of Activities as of November 1, 2021, and hereby certify that:

1. The flood model submission is in compliance with the Notification Requirements and General Flood Standard GF-5, Editorial Compliance;
2. The disclosures and forms related to each flood standards section are editorially accurate and contain complete information and any changes that have been made to the submission during the review process have been reviewed for completeness, grammatical correctness, and typographical errors;
3. There are no incomplete responses, charts or graphs, inaccurate citations, or extraneous text or references;
4. The current version of the flood model submission has been reviewed for grammatical correctness, typographical errors, completeness, the exclusion of extraneous data/ information and is otherwise acceptable for publication; and
5. In expressing my opinion I have not been influenced by any other party in order to bias or prejudice my opinion.

David Colbus	M.A., Climate and Society
Name	Professional Credentials (Area of Expertise)
	January 27, 2024
Signature (original submission)	Date
Alec Killoran	B.A., English
Name	Professional Credentials (Area of Expertise)
	April 24, 2024
Signature (response to deficiencies, if any)	Date
	May 10, 2024
Signature (revisions to submission, if any)	Date
	Aug 30, 2024
Signature (revisions to submission, if any)	Date
	October 24, 2024
Signature (final submission)	Date

An updated signature and form are required following any modification of the flood model and any revision of the original submission. If a signatory differs from the original signatory, provide the printed name and professional credentials for any new signatories. Additional signature lines should be added as necessary with the following format:

Signature (revisions to submission) Date

Note: A facsimile or any properly reproduced signature will be acceptable to meet this requirement.

Include Form GF-8, Editorial Review Expert Certification, in a submission appendix.

Form HHF-1: Historical Coastal and Inland Event Flood Extent and Elevation or Depth Validation Maps

A. Provide color-coded contour or high-resolution maps with appropriate base map data illustrating modeled coastal and inland flood extents and elevations or depths for the following historical Florida flood events:

- **Hurricane Andrew (1992)**
- **Hurricane Ivan (2004)**
- **Hurricane Jeanne (2004)**
- **Hurricane Wilma (2005)**
- **Tropical Storm Fay (2008)**
- **Unnamed Storm in East Florida (May 2009)**
- **Unnamed Storm in Panhandle (July 2013)**
- **Hurricane Matthew (2016)**
- **Hurricane Irma (2017)**
- **Hurricane Michael (2018)**

For any storms where sufficient data are not available, the modeling organization may substitute an alternate historical storm of their choosing.

High-resolution maps illustrating modeled storm surge and inland flood extents and water depths are provided in Figure 96 to Figure 111 for the following historical Florida flood events:

- Hurricane Andrew (1992)
- Hurricane Ivan (2004)
- Hurricane Frances (2004)
- Hurricane Wilma (2005)
- Hurricane Matthew (2016)
- Hurricane Hermine (2016)
- Hurricane Irma (2017)
- Hurricane Michael (2018)
- Hurricane Eta (2020)
- Hurricane Ian (2022)

B. Plot the locations and values associated with validation points (e.g., maximum flood elevations or depths from observations such as gauge data, high-water marks) on each contour or high-resolution map for the historical events.

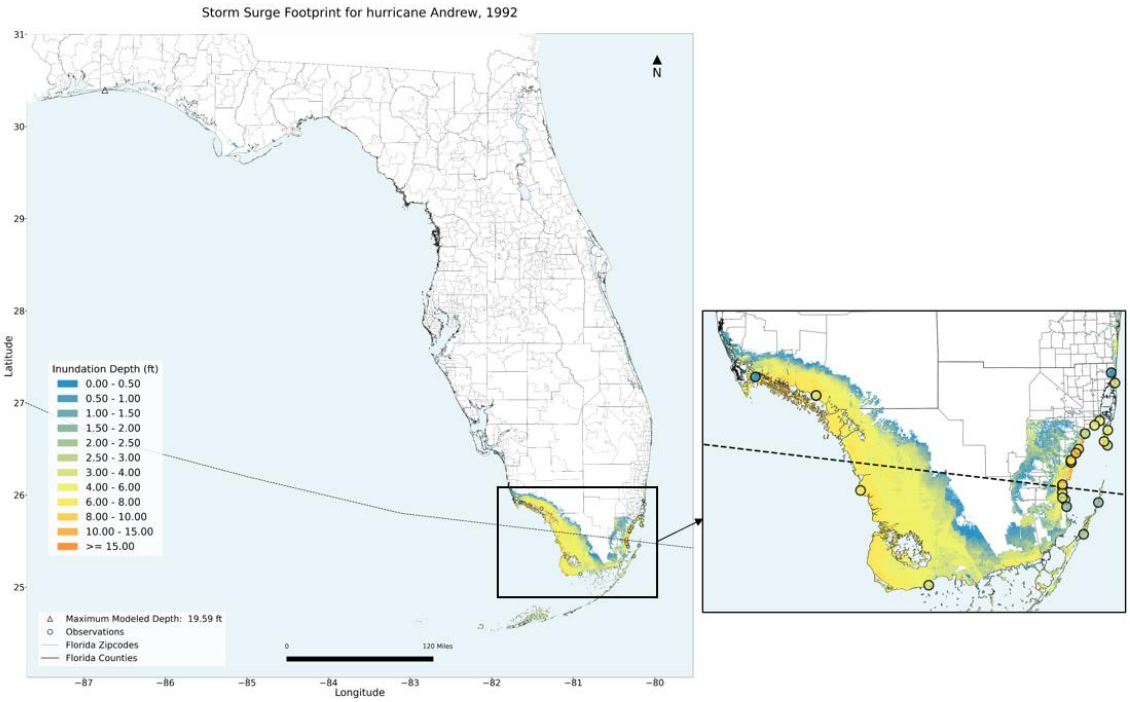

Figure 96: Storm surge validation footprint for Hurricane Andrew (1992).

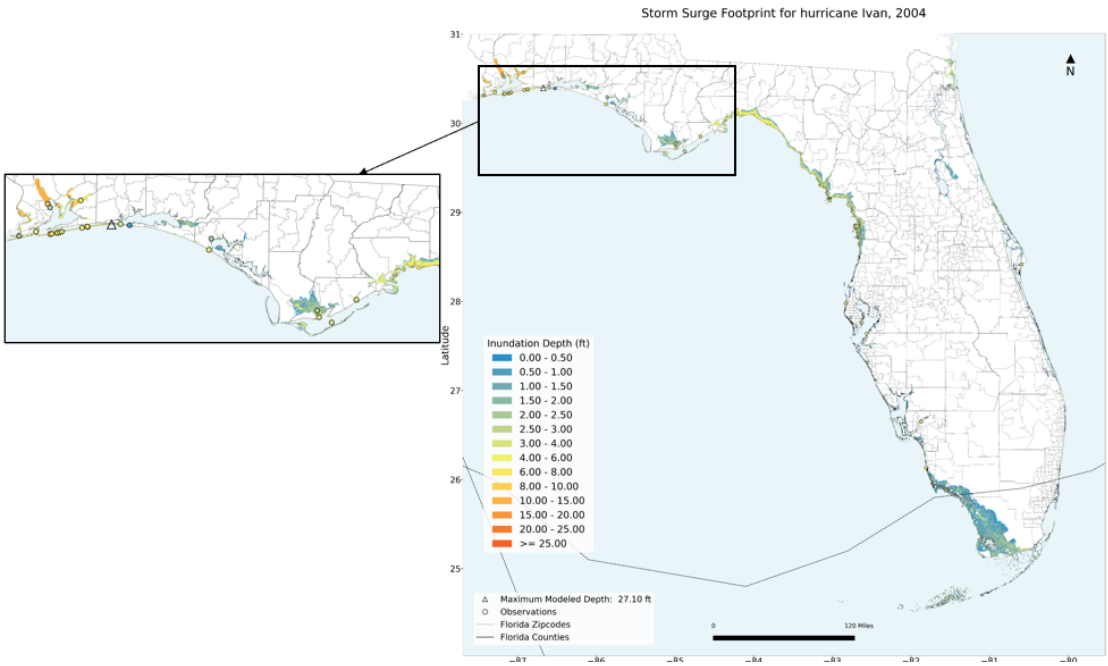

Figure 97: Storm surge validation footprint for Hurricane Ivan (2004).

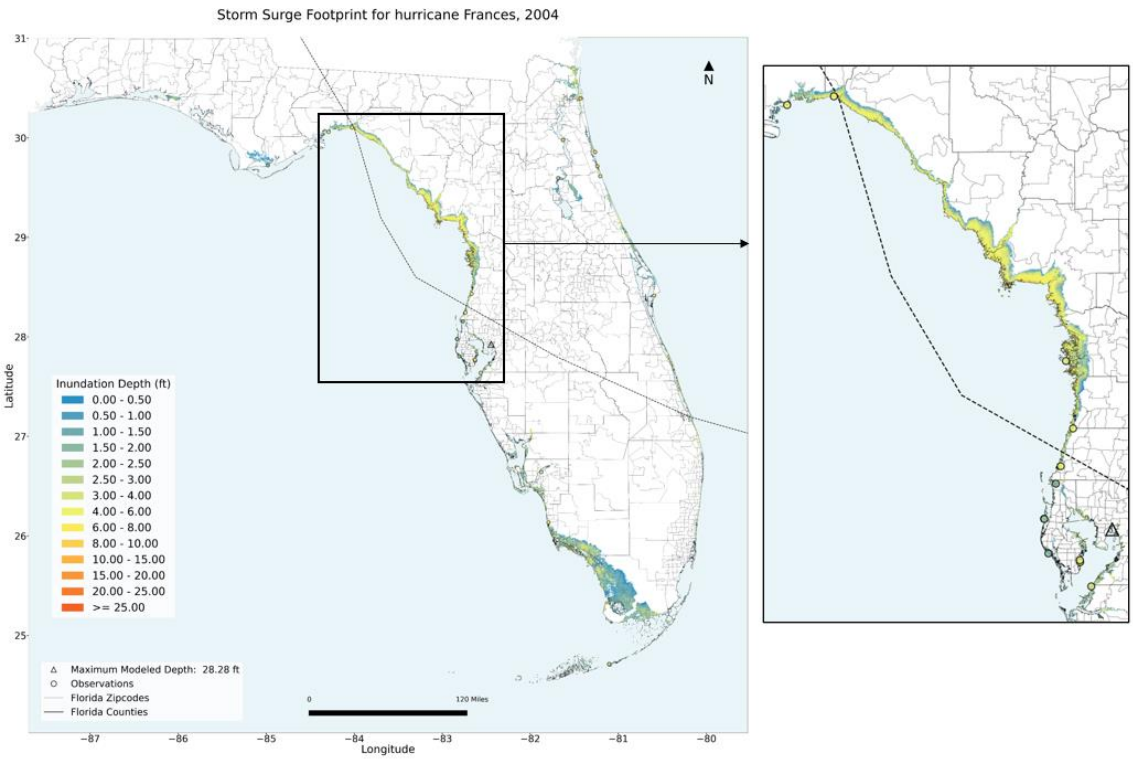

Figure 98: Storm surge validation footprint for Hurricane Frances (2004).

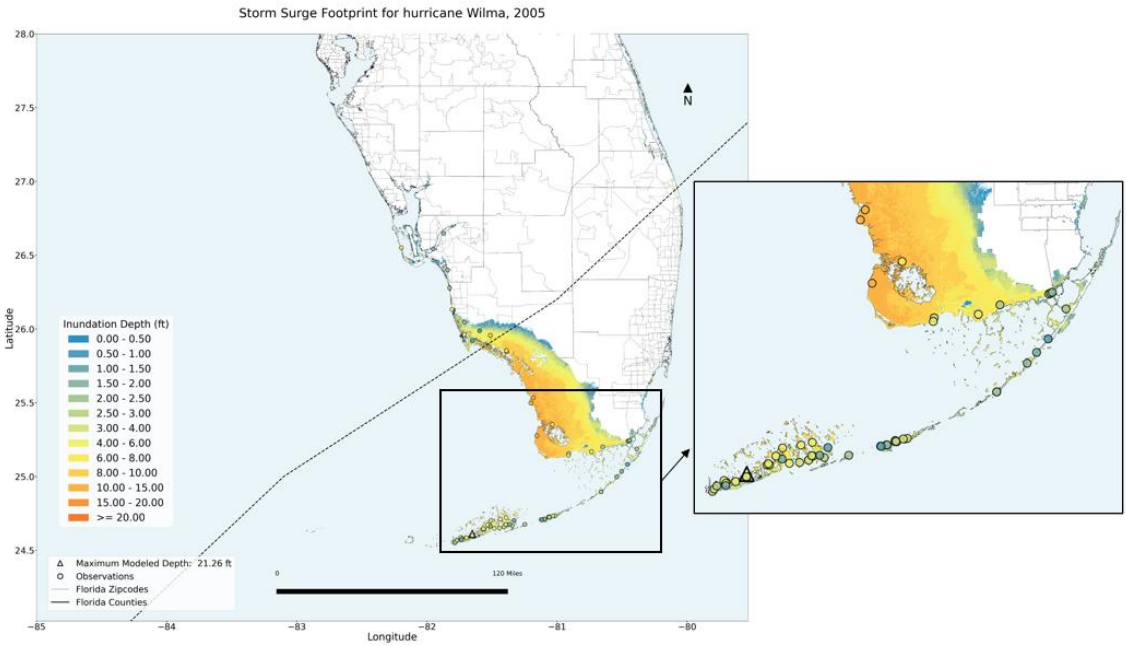

Figure 99: Storm surge validation footprint for Hurricane Wilma (2005).

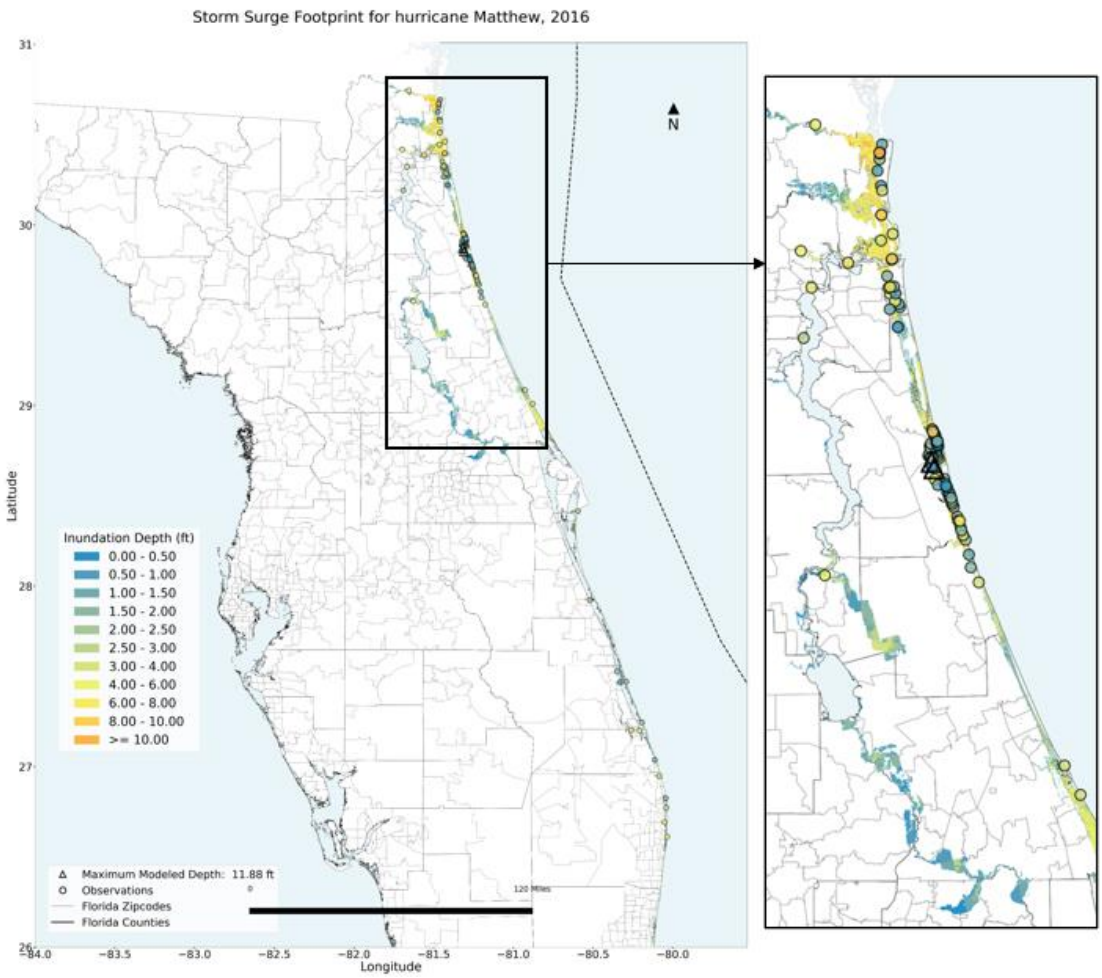

Figure 100: Storm surge validation footprint for Hurricane Matthew (2016). There are 25 pixels, all with the same maximum value, located very close to each other. These pixels have been grouped into two clusters, as shown in the figure, represented by the triangles.

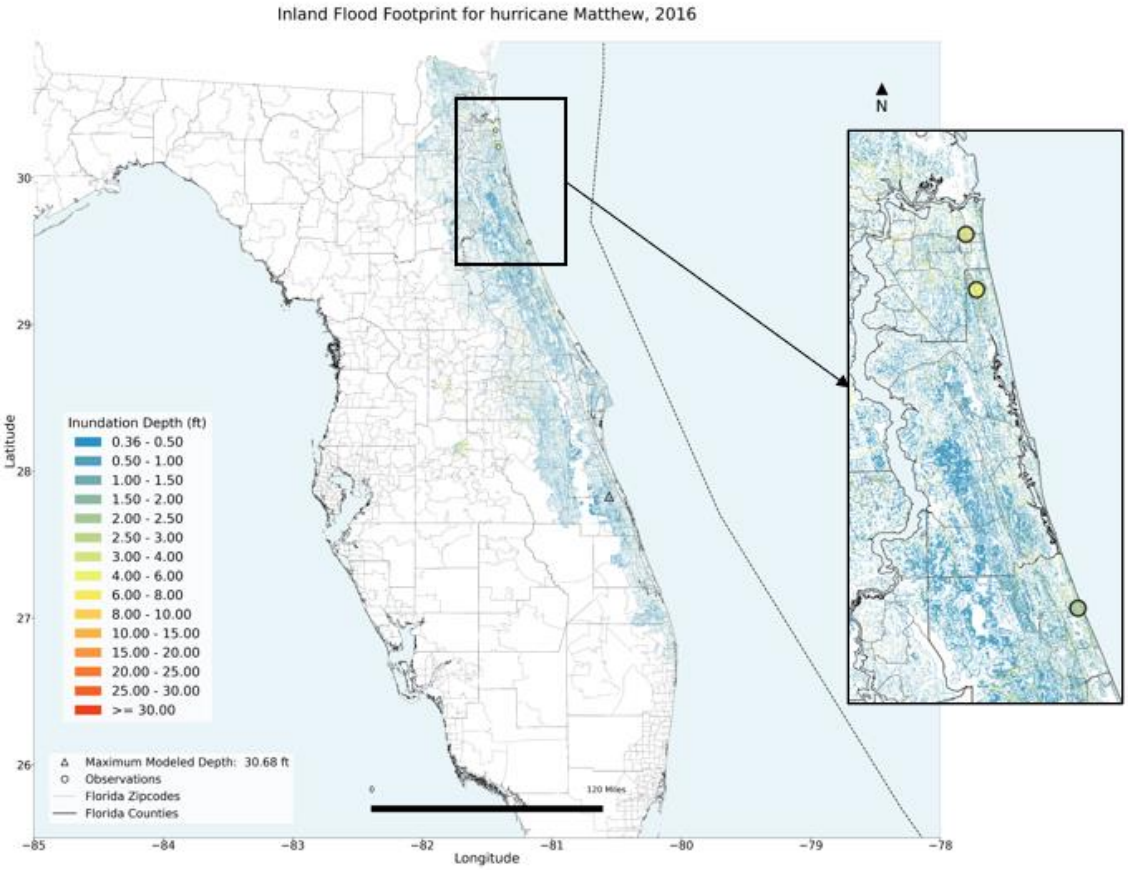

Figure 101: Inland flood validation footprint for Hurricane Matthew (2016).

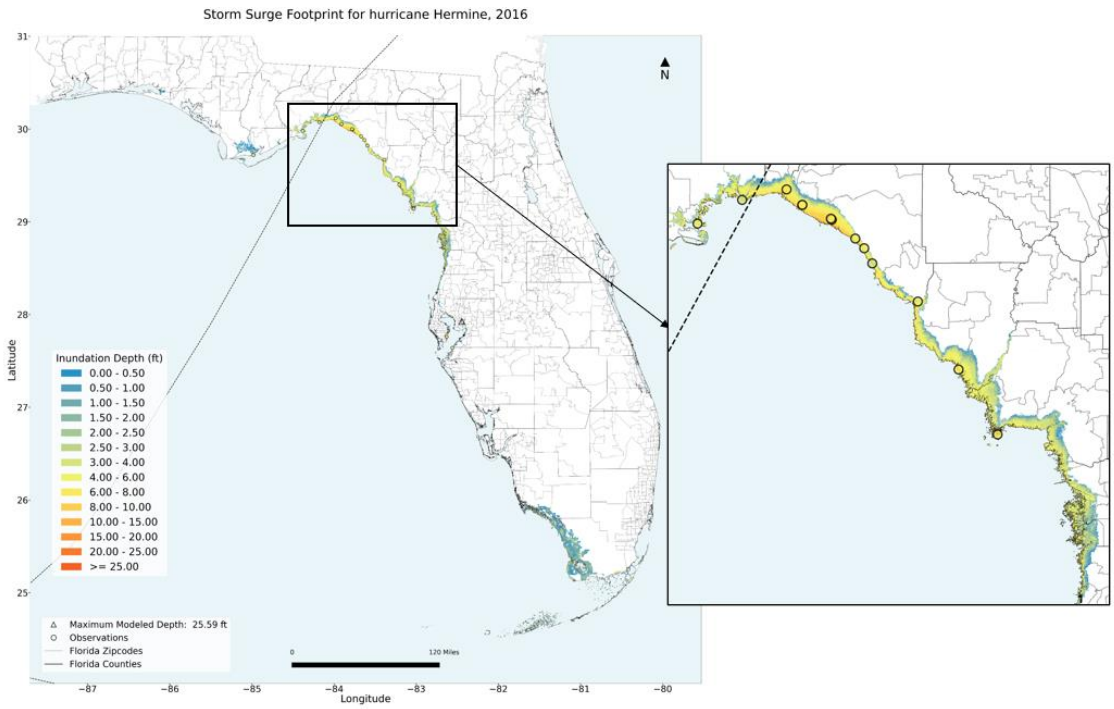

Figure 102: Storm Surge validation footprint for Hurricane Hermine (2016).

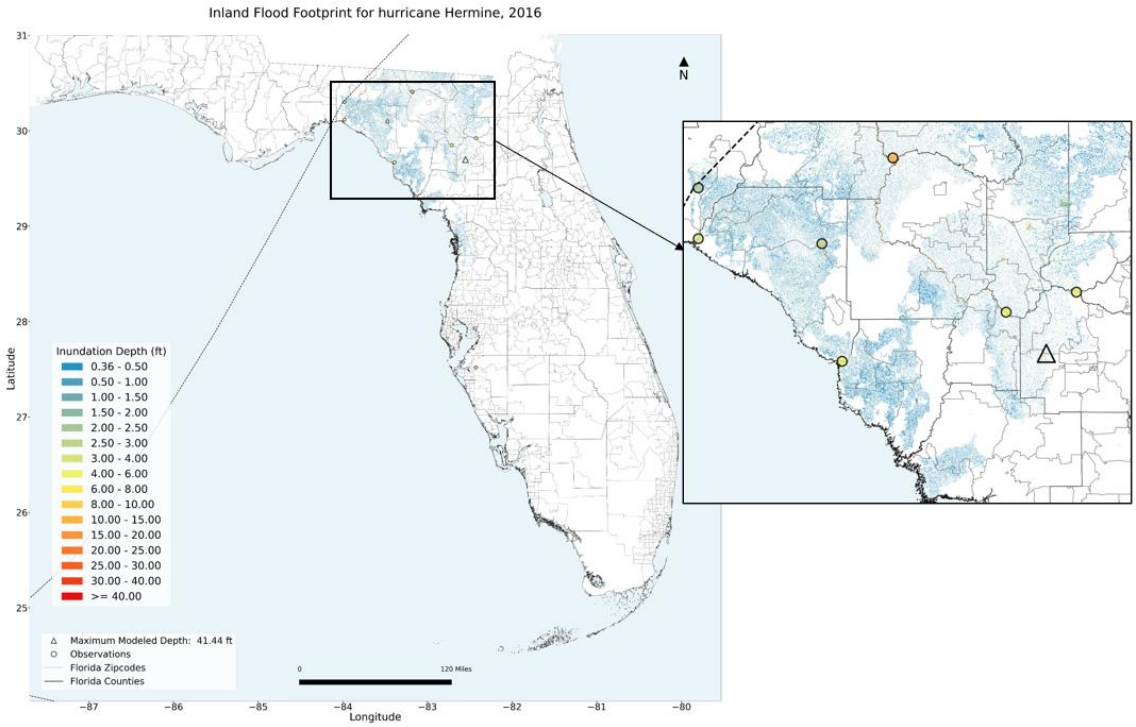

Figure 103: Inland flood validation footprint for Hurricane Hermine (2016).

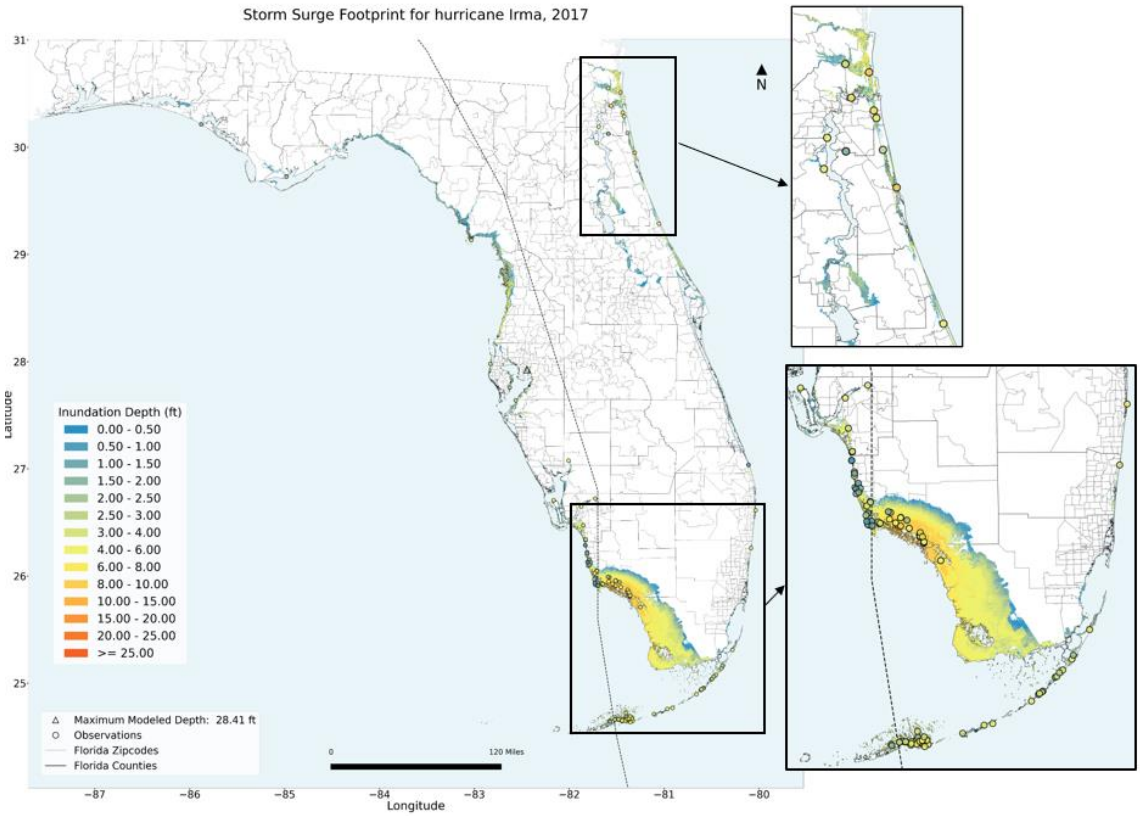

Figure 104: Storm surge validation footprint for Hurricane Irma (2017).

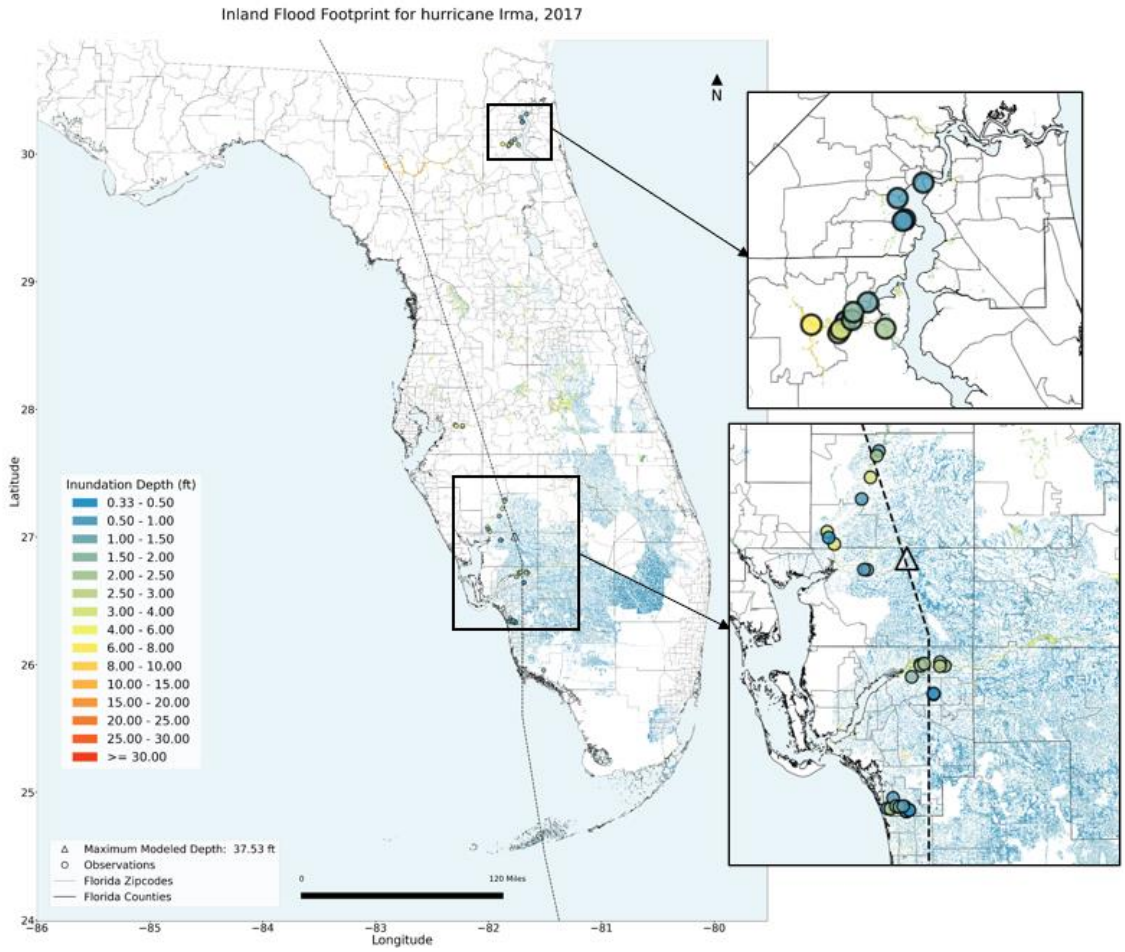

Figure 105: Inland flood validation footprint for Hurricane Irma (2017).

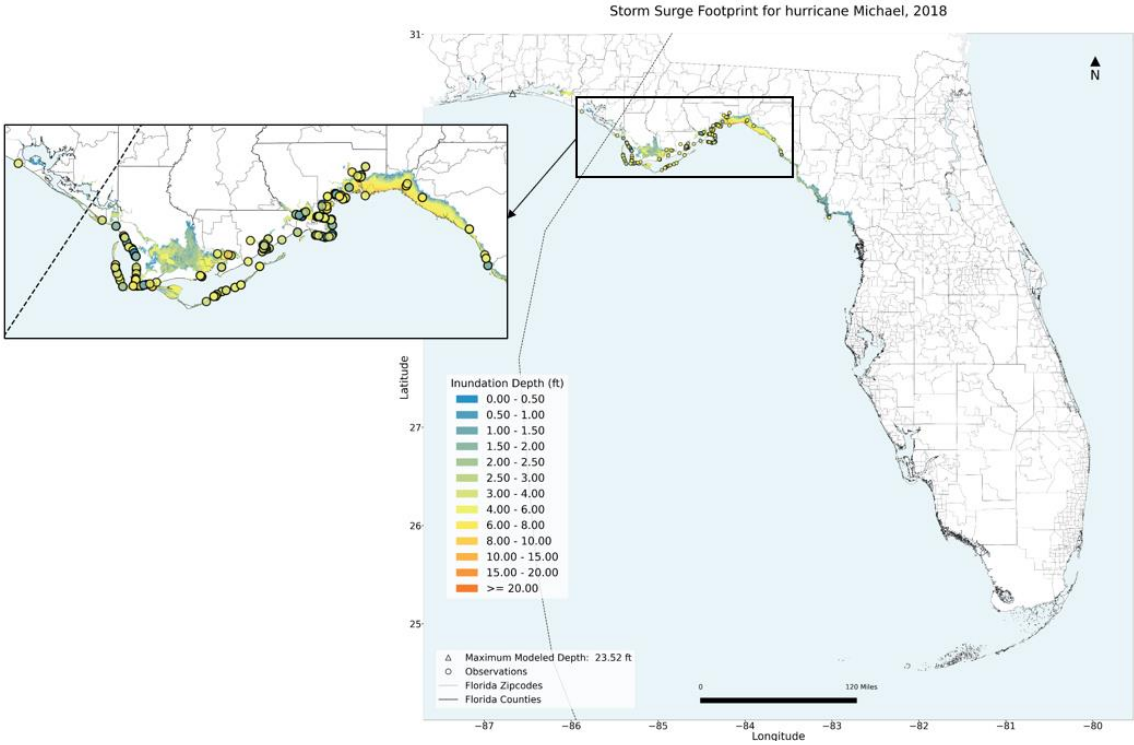

Figure 106: Storm surge validation footprint for Hurricane Michael (2018).

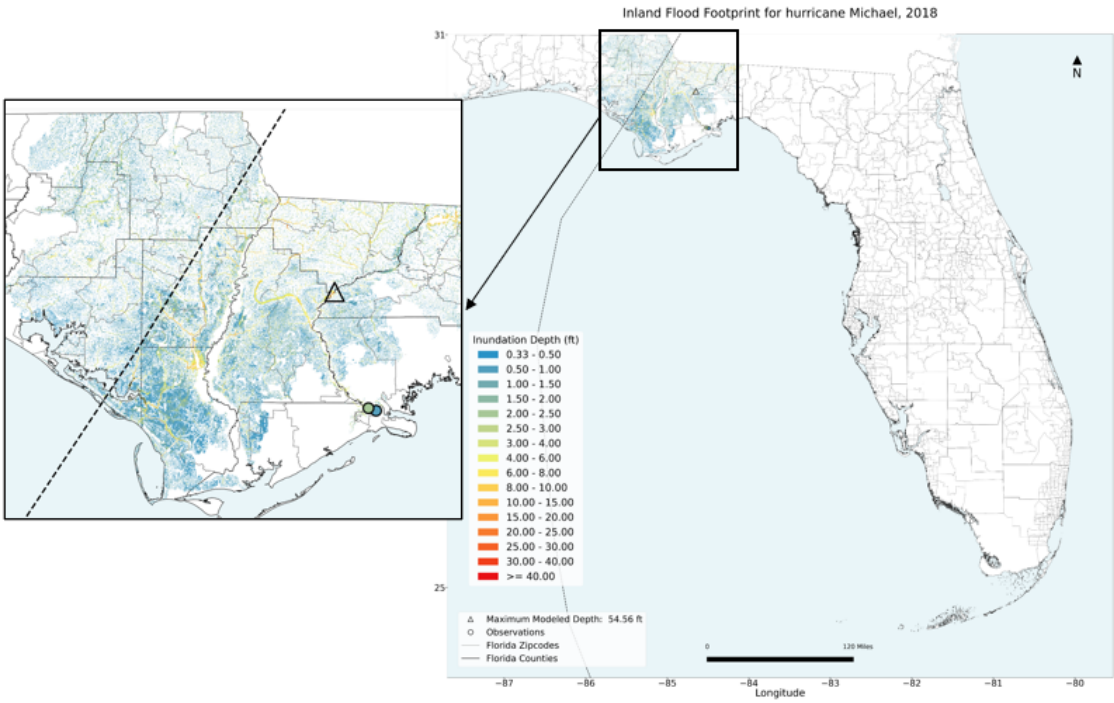

Figure 107: Inland flood validation footprint for Hurricane Michael (2018).

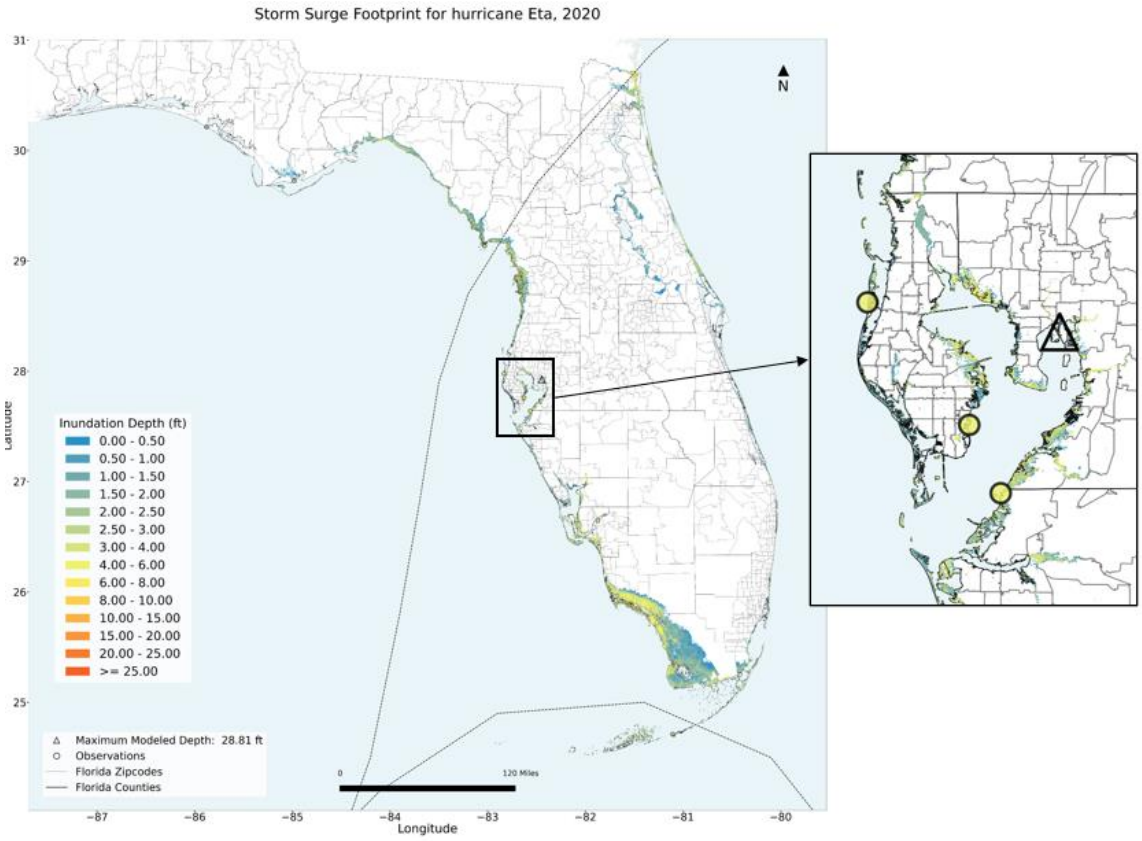

Figure 108: Storm surge validation footprint for Hurricane Eta (2020).

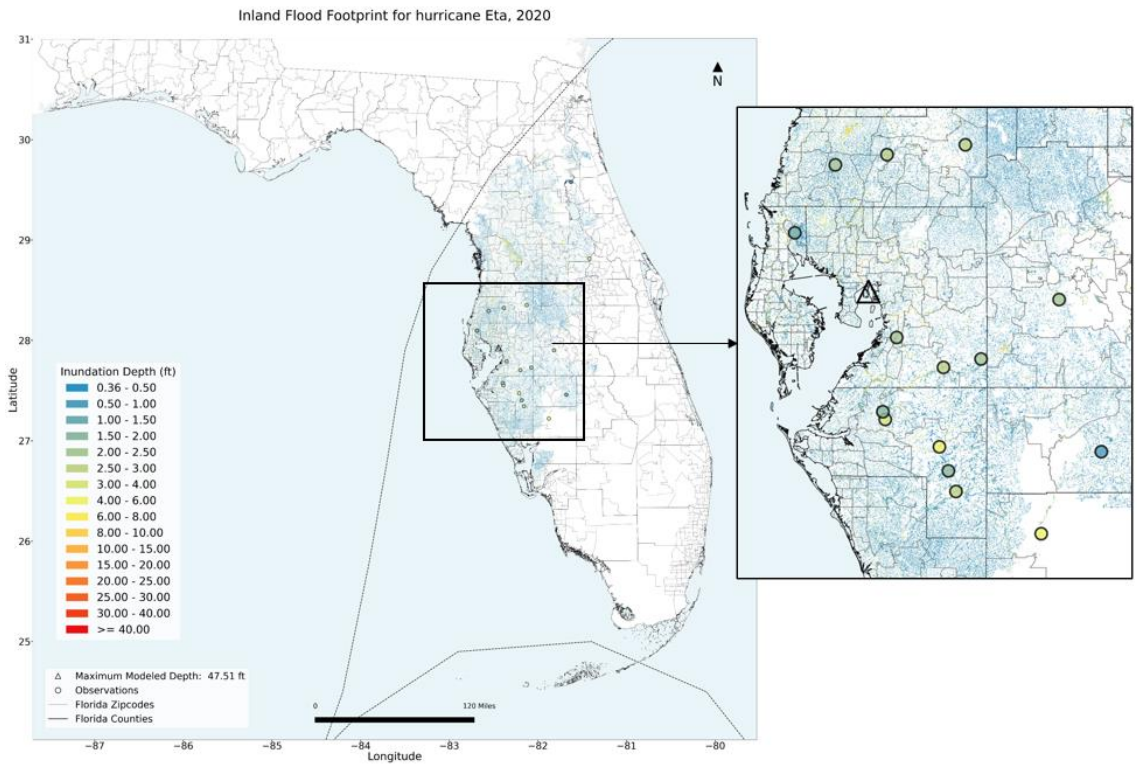

Figure 109: Inland Flood validation footprint for Hurricane Eta (2020).

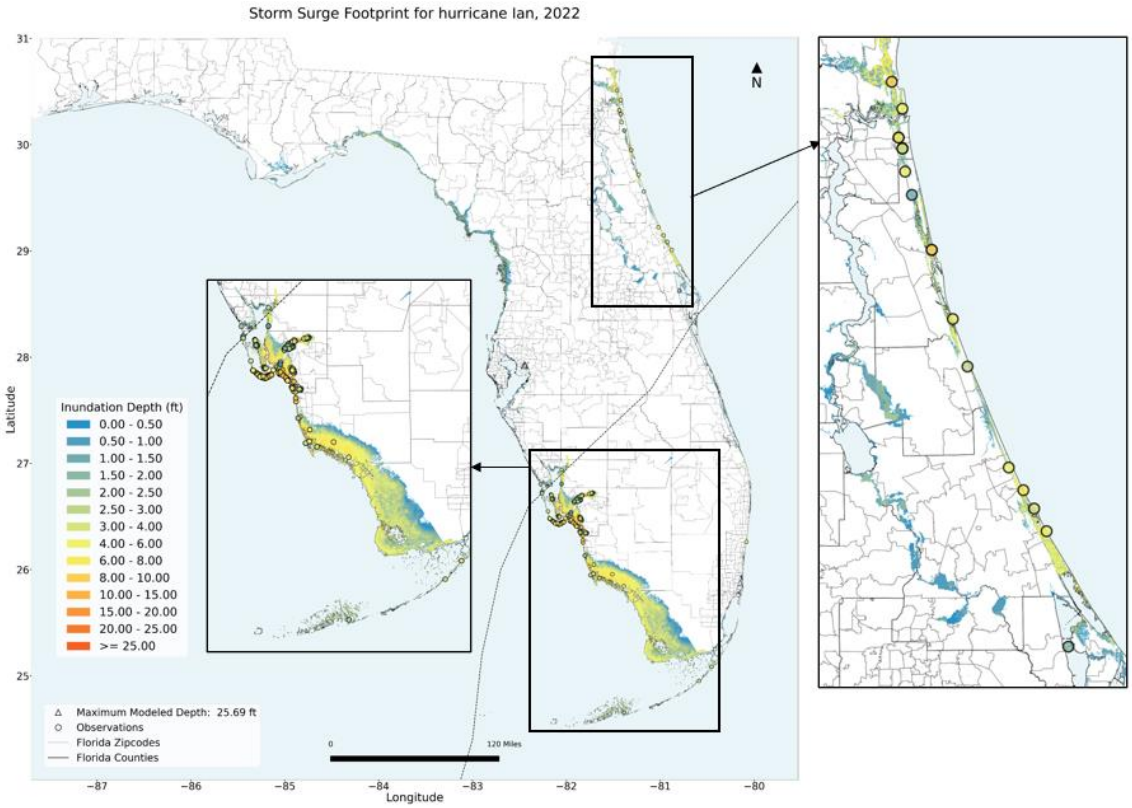

Figure 110: Storm surge validation footprint for Hurricane Ian (2022).

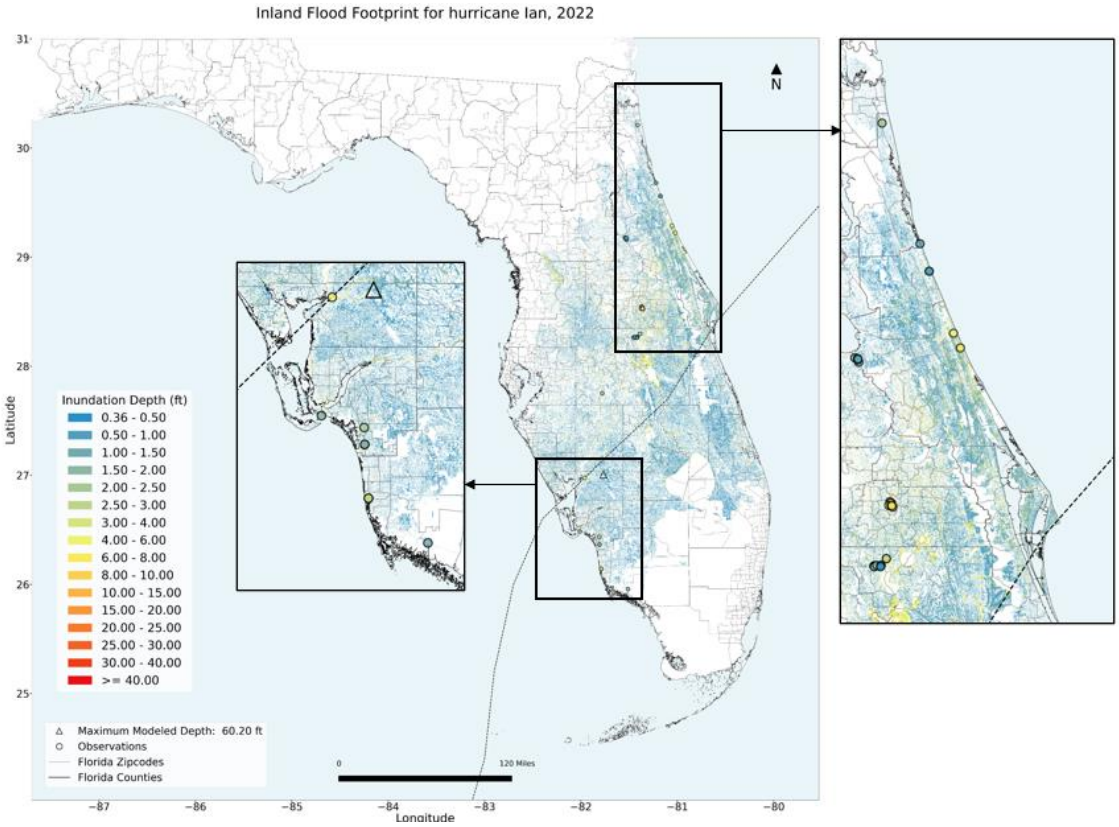

Figure 111: Inland flood validation footprint for Hurricane Ian (2022).

C. Provide scatter plots of simulated versus observed elevation or depth at the validation points.

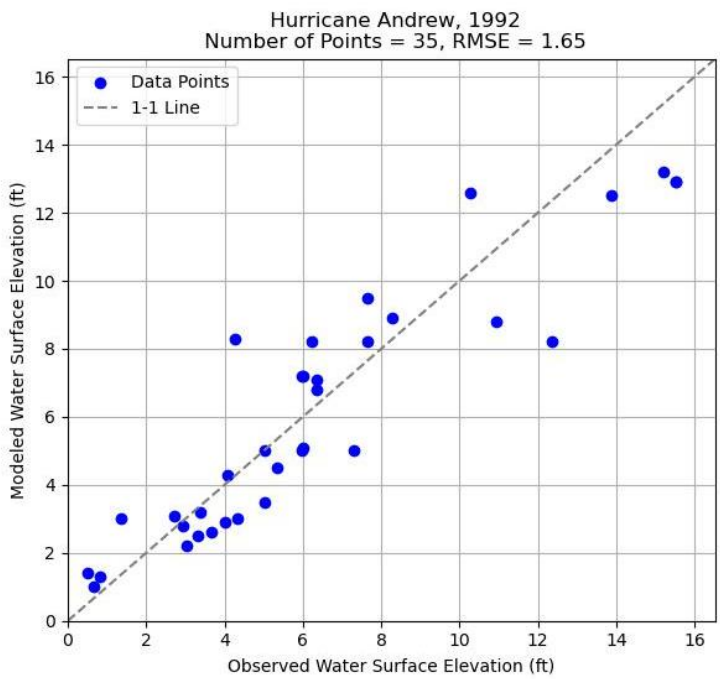

Figure 112: Storm surge validation scatter plots for Hurricane Andrew (1992). (horizontal datum: NAD83, vertical datum: NAVD88)

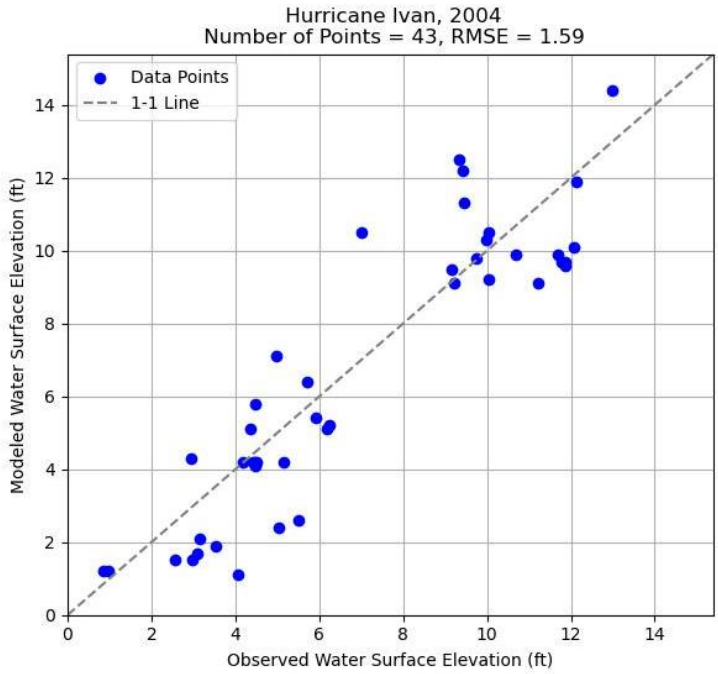

Figure 113: Storm surge validation scatter plots for Hurricane Ivan (2004). (horizontal datum: NAD83, vertical datum: NAVD88)

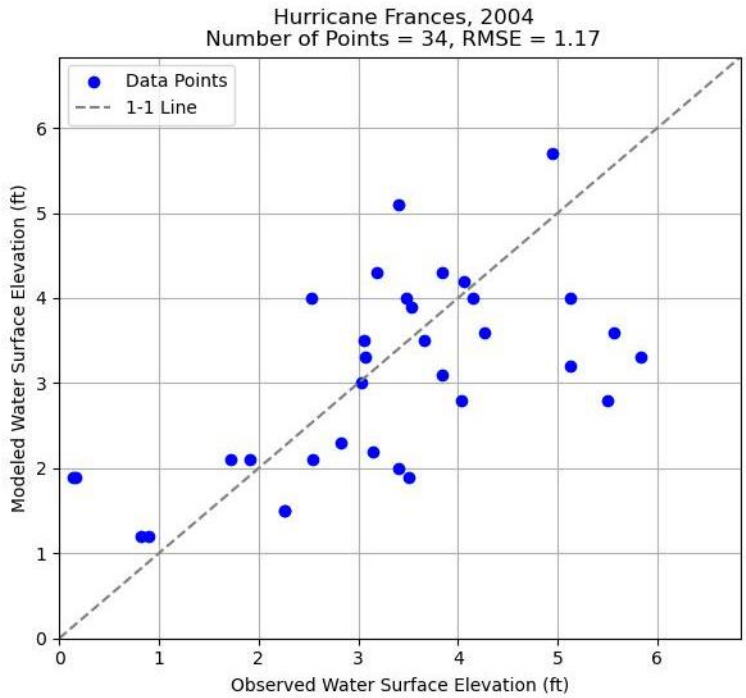

Figure 114: Storm surge validation scatter plots for Hurricane Frances (2004). (horizontal datum: NAD83, vertical datum: NAVD88)

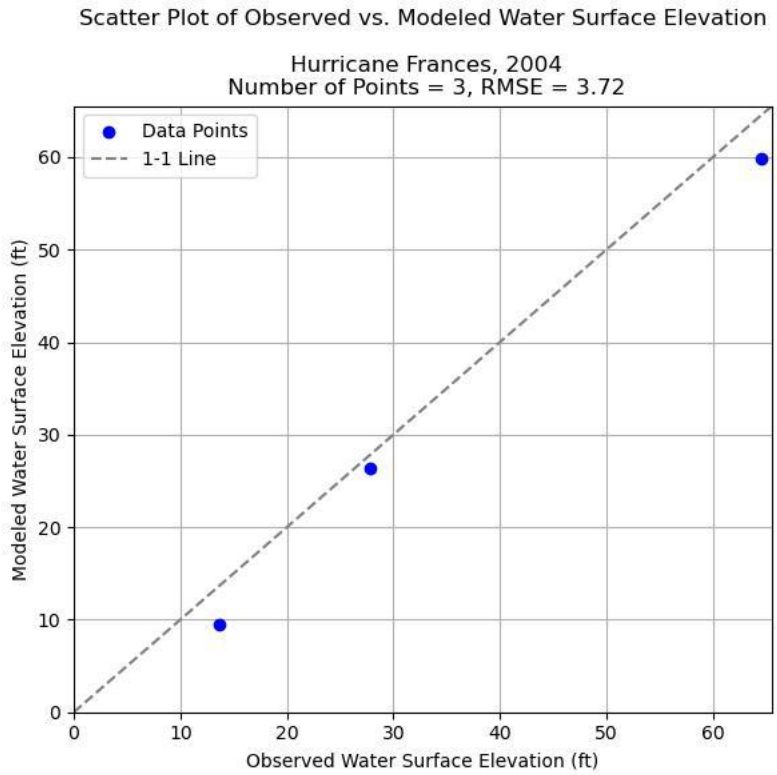

Figure 115: Inland validation scatter plots for Hurricane Frances (2004). (Vertical datum: EGM 08)

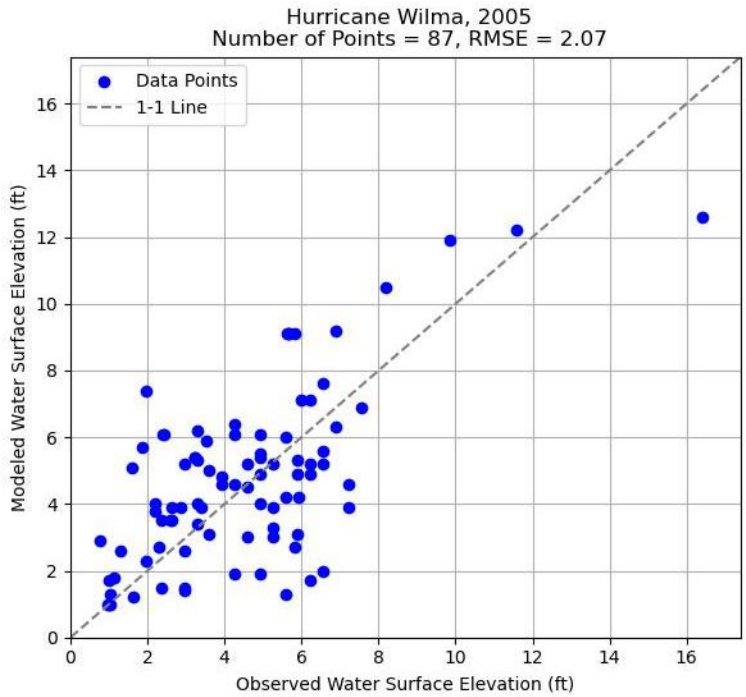

Figure 116: Storm surge validation scatter plots for Hurricane Wilma (2005). (horizontal datum: NAD83, vertical datum: NAVD88)

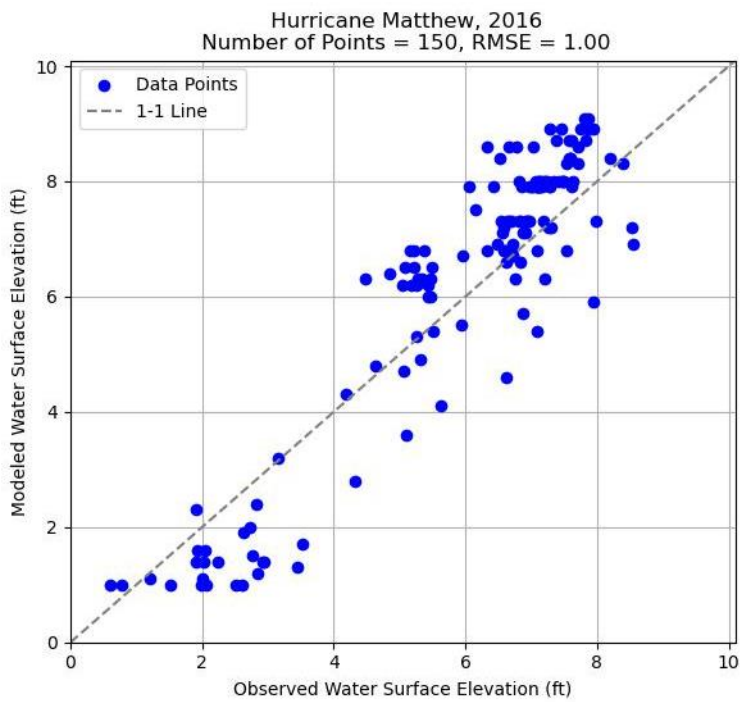

Figure 117: Storm surge validation scatter plots for Hurricane Matthew (2016). (horizontal datum: NAD83, vertical datum: NAVD88)

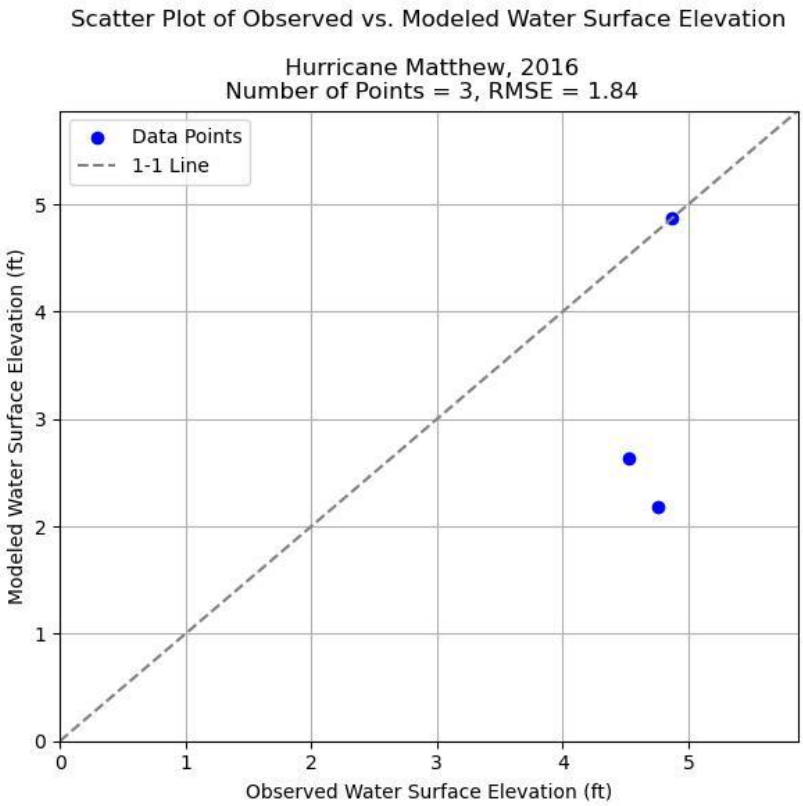

Figure 118: Inland Flood validation scatter plots for Hurricane Matthew (2016). (Vertical datum: EGM 08)

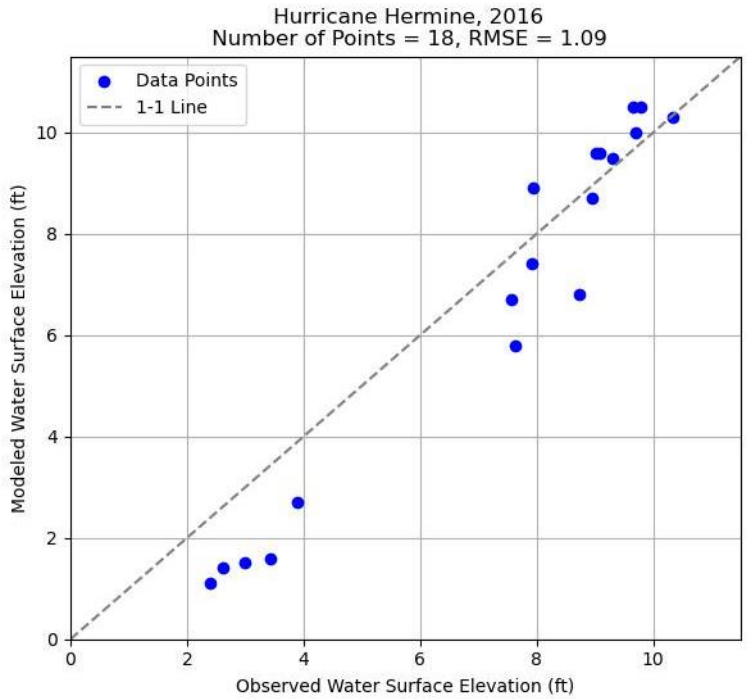

Figure 119: Storm surge validation scatter plots for Hurricane Hermine (2016). (horizontal datum: NAD83, vertical datum: NAVD88)

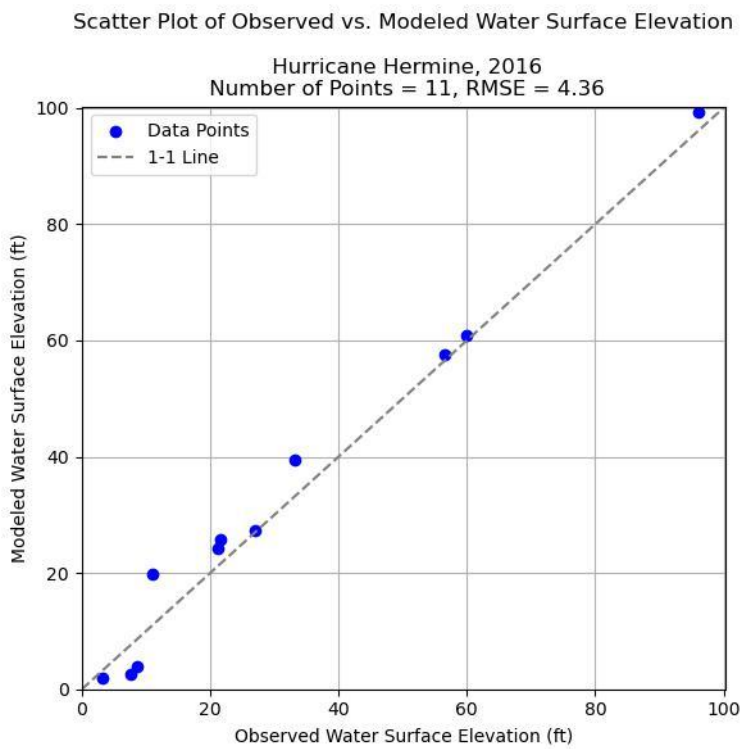

Figure 120: Inland Flood validation scatter plots for Hurricane Hermine (2016). (Vertical datum: EGM 08)

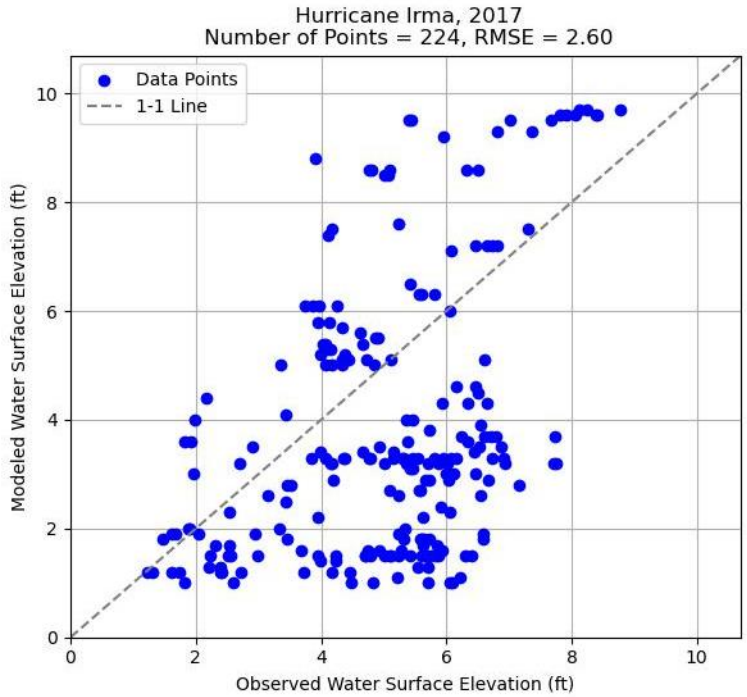

Figure 121: Storm surge validation scatter plots for Hurricane Irma (2017). (horizontal datum: NAD83, vertical datum: NAVD88)

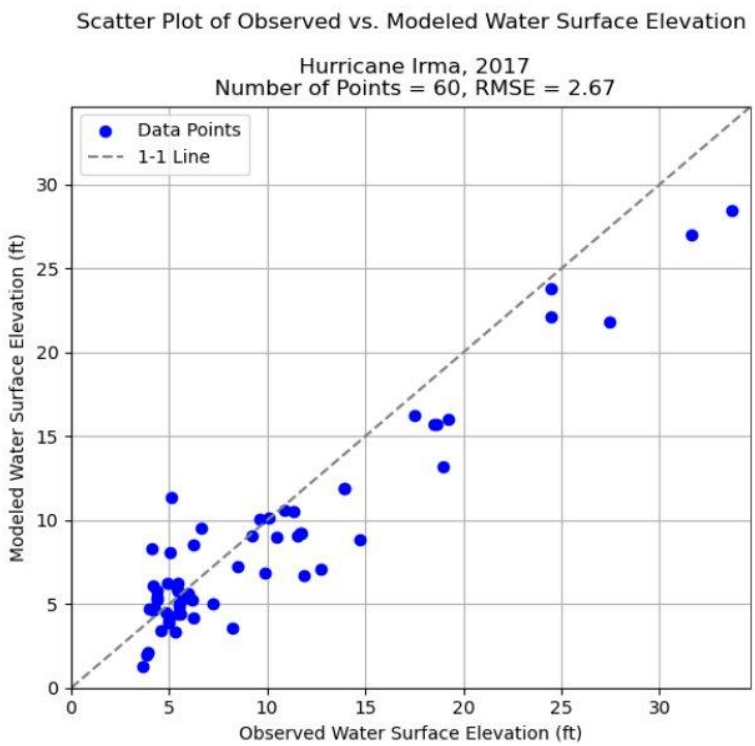

Figure 122: Inland Flood validation scatter plots for Hurricane Irma (2017). (Vertical datum: EGM 08)

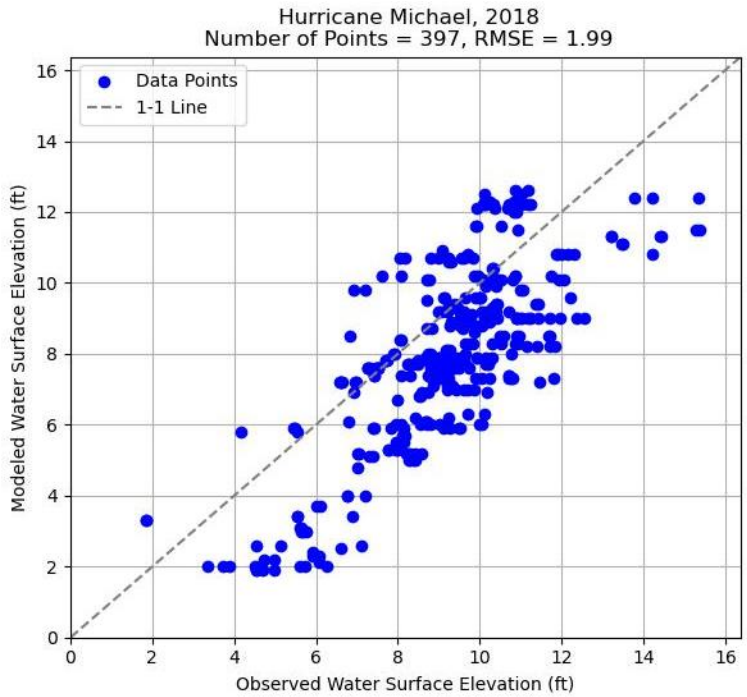

Figure 123: Storm surge validation scatter plots for Hurricane Michael (2018). (horizontal datum: NAD83, vertical datum: NAVD88)

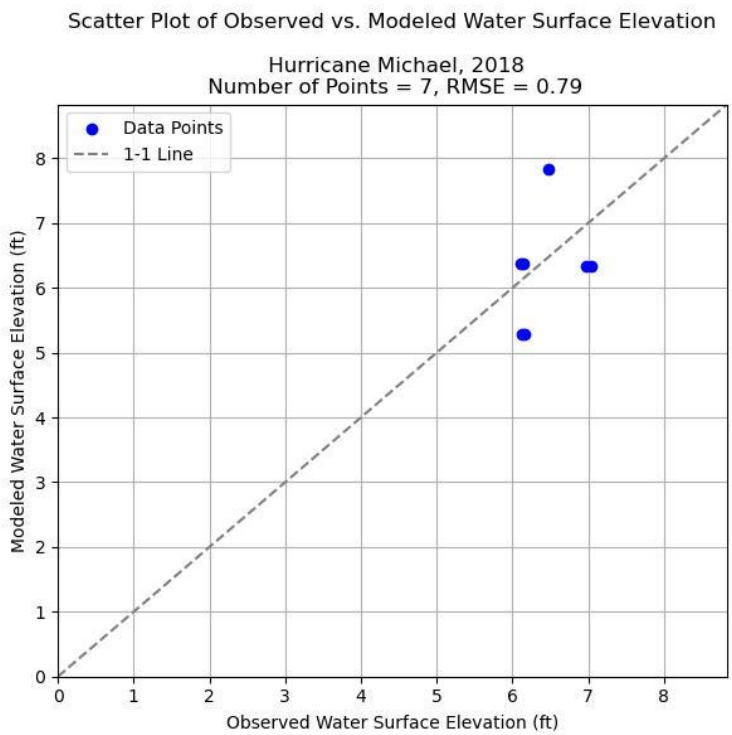

Figure 124: Inland Flood validation scatter plots for Hurricane Michael (2018). (Vertical datum: EGM 08)

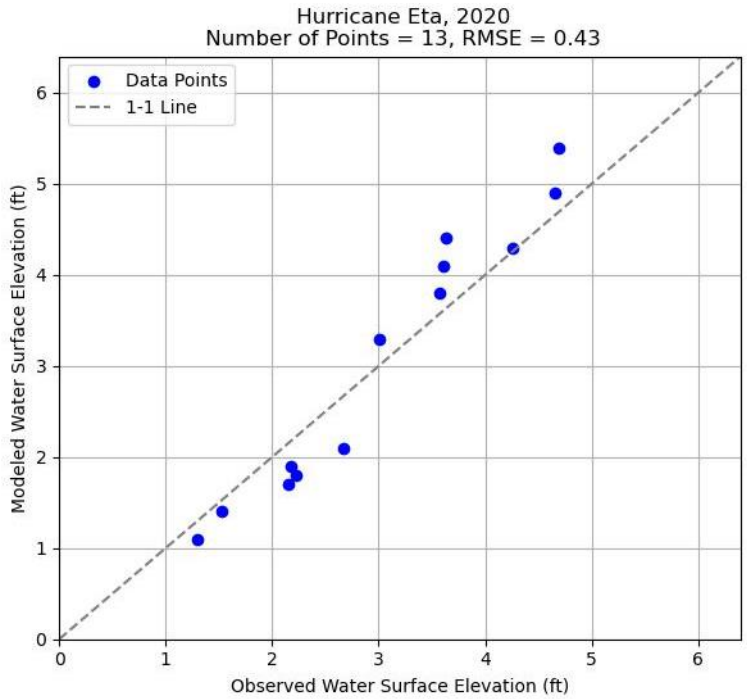

Figure 125: Storm surge validation scatter plots for Hurricane Eta (2020). (horizontal datum: NAD83, vertical datum: NAVD88)

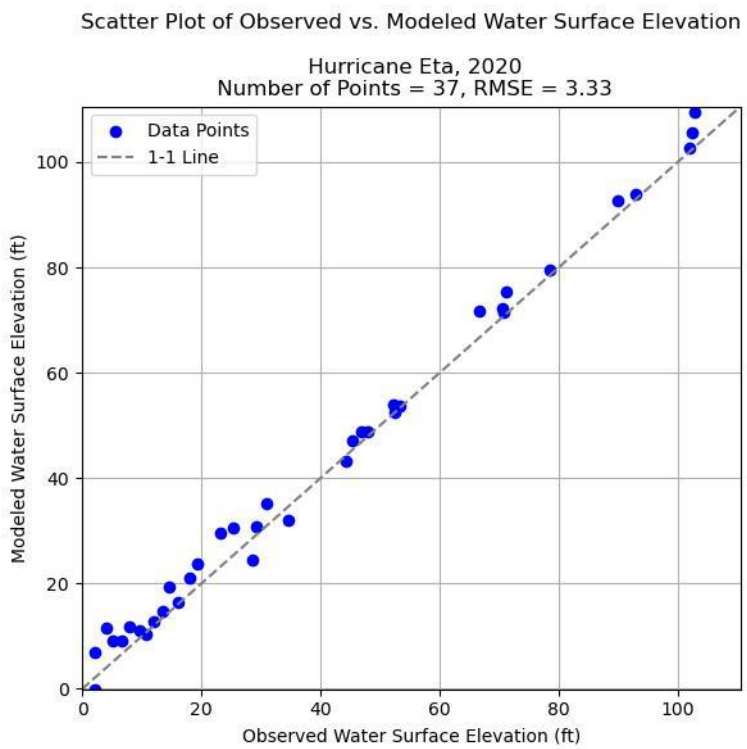

Figure 126: Inland flood validation scatter plots for Hurricane Eta (2020). (Vertical datum: EGM 08)

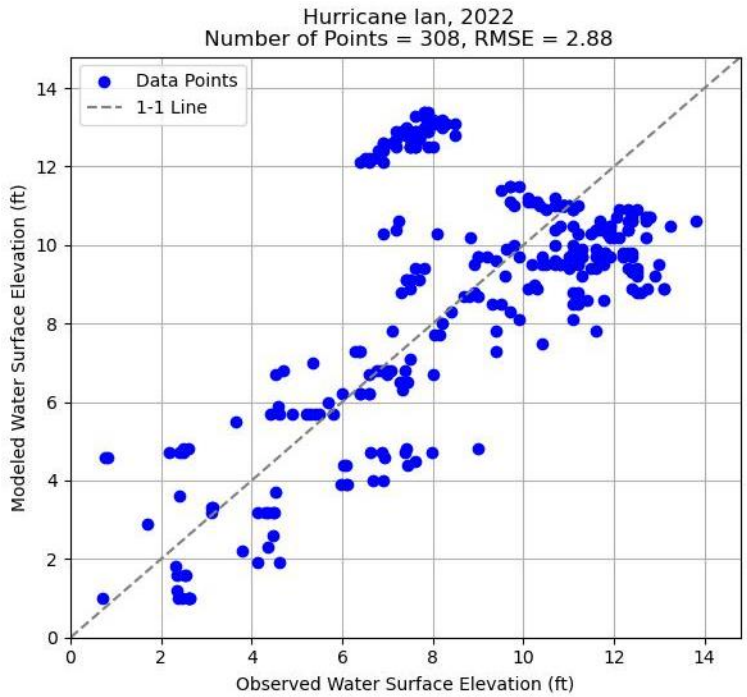

Figure 127: Storm surge validation scatter plots for Hurricane Ian (2022). (horizontal datum: NAD83, vertical datum: NAVD88)

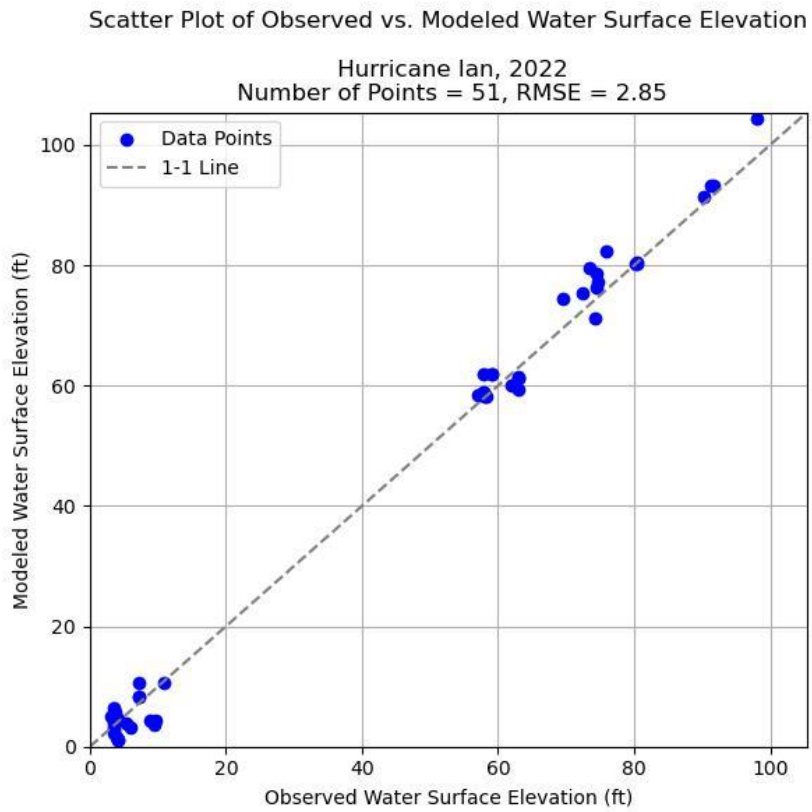

Figure 128: Inland Flood validation scatter plots for Hurricane Ian (2022). (Vertical datum: EGM 08)

D. Indicate the resolution of the flood model elevation or depth grid used on each contour or high-resolution map.

The resolution of the storm surge and inland flood depth grid used on each high-resolution map above is approximately 30m by 30m, which is consistent with the DEM resolution.

E. Demonstrate the consistency of the modeled flood extent and elevation or depth with observed flood extent and elevation or depth for each historical event.

As shown in Disclosure MF-4.1 and Form HHF-1 part B and C, the Impact Forecasting Flood Model – Storm Surge and inland flood can produce comparable flood extent and elevation or depth with observed data for various historical events in different geographic regions. As demonstrated in the scatter plots, the root-mean-square-error is less than 1 meter for all events except Inland flood scatter plots for Frances and Hermine for which we could not find enough inland flood observation data.

F. Explain any differences between the modeled flood extent and elevation or depth and the historical floods observations. Include an explanation if the differences are impacted by major flood control measures.

As demonstrated in Disclosure MF-4.1 and Form HHF-1 part B and C, the Impact Forecasting Flood Model – Storm Surge can produce comparable surge footprints with historical observation data overall. Some differences are expected due to modelling resolution, not including the wave runup in the modeled surge height, the non-functioning of tide station measuring instruments and subjective or inaccurate high water marks data.

- Inland flood can produce comparable flood footprints with historical observation data overall. Some differences are expected due to modelling resolution, and subjective or inaccurate high water marks data.

G. If additional assumptions are necessary to complete this form, provide the rationale for the assumptions as well as a detailed description of how they are included.

No additional assumptions were made to complete this form.

H. Include Form HHF-1, Historical Event Flood Extent and Elevation or Depth Validation Maps, in a submission appendix.

Form HHF-2: Coastal Flood Characteristics by Annual Exceedance Probability

A. *Define one study area subject to coastal flooding within each of the five Florida geographic regions identified in Figure 1. The extent of each study area is to be determined by the modeling organization and should be large enough to encompass at least one county. The modeling organization is to create the underlying grid for this form.*

The study areas selected for each of the five Florida geographic regions identified in Form HHF-2 are:

- Wakulla county in Panhandle region
- Levy county in North Florida region
- Pinellas county in Southwest Florida region
- Broward county in Southeast Florida region
- Brevard county in East Florida region

The grid resolution is 30m by 30m, which is consistent with the DEM resolution.

B. *Provide, for each study area, color-coded contour or high-resolution maps showing the modeled flood extent and elevation or depth corresponding to 0.01 annual exceedance probability. Flood extent and elevation or depth should incorporate waves or wave proxies, if modeled. For locations subject to both coastal and inland flooding, this information should reflect only coastal flooding.*

The high-resolution maps showing modeled storm surge extent and depth corresponding to the 0.01 annual exceedance probabilities are shown in Figure 129 to Figure 133 below.

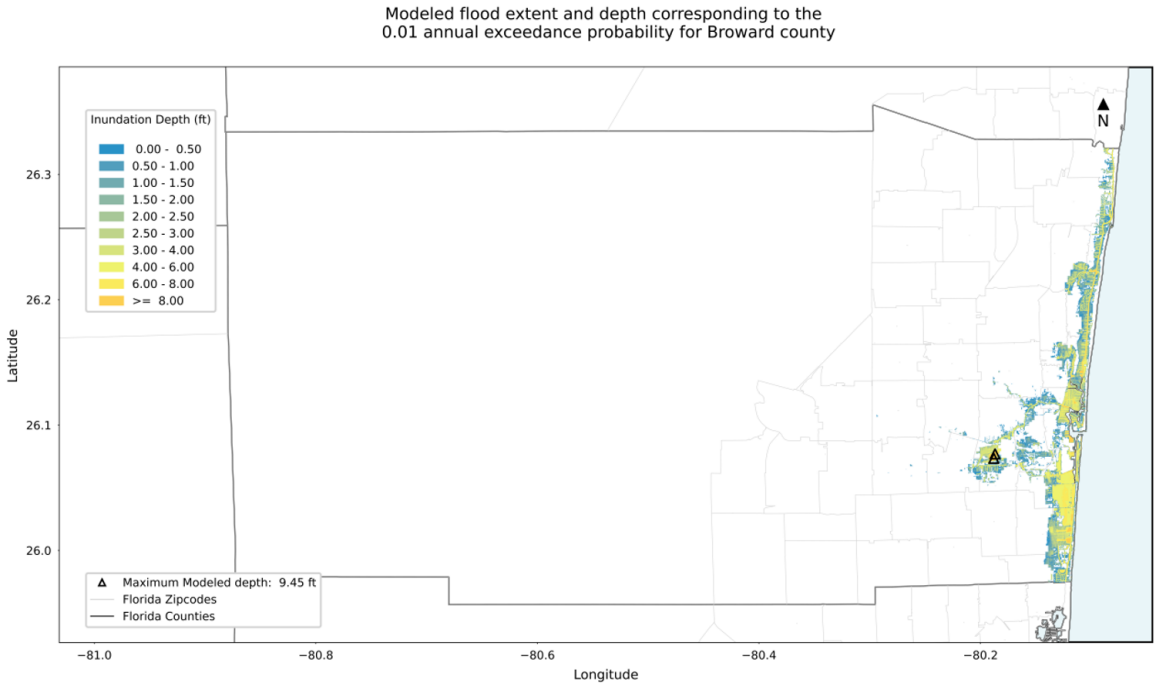

Figure 129: Modeled storm surge extent and depth corresponding to the 0.01 annual exceedance probability for Broward County. There are 306 pixels, all with the same maximum value, located very close to each other. These pixels have been grouped into two clusters, as shown in the figure, represented by the triangles. (horizontal datum: WGS84, vertical datum: EGM08)

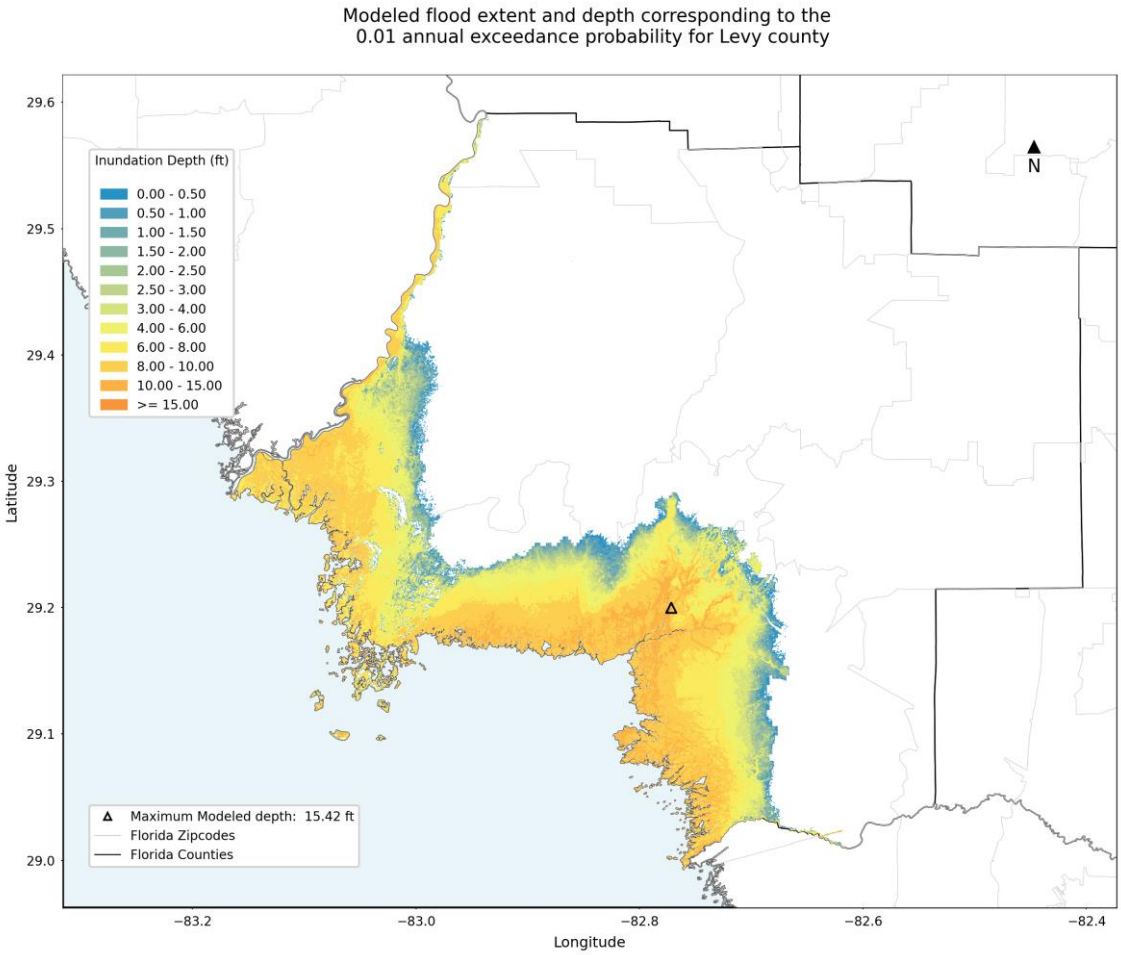

Figure 130: Modeled storm surge extent and depth corresponding to the 0.01 annual exceedance probability for Levy County. (horizontal datum: WGS84, vertical datum: EGM08)

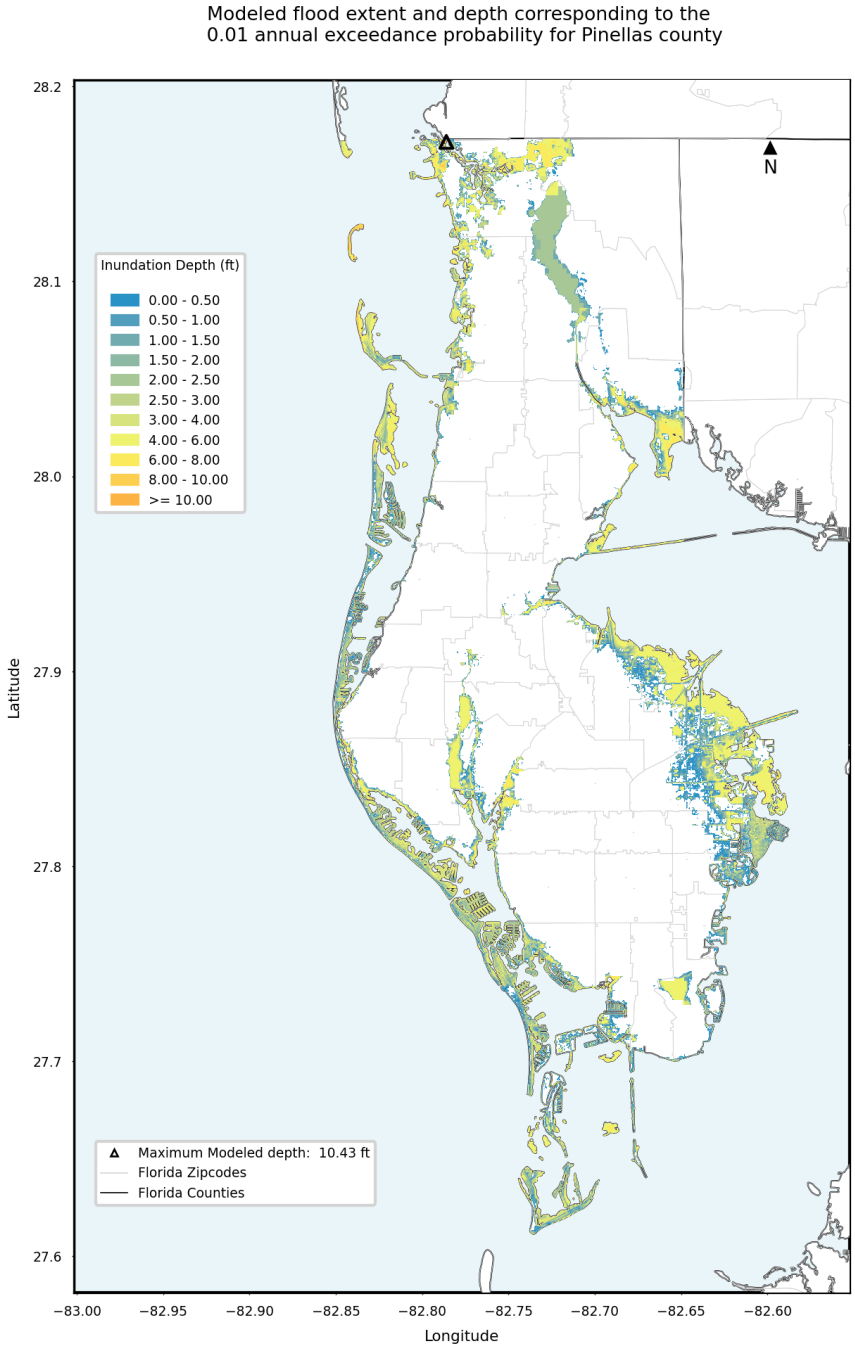

Figure 131: Modeled storm surge extent and depth corresponding to the 0.01 annual exceedance probability for Pinellas County. (horizontal datum: WGS84, vertical datum: EGM08)

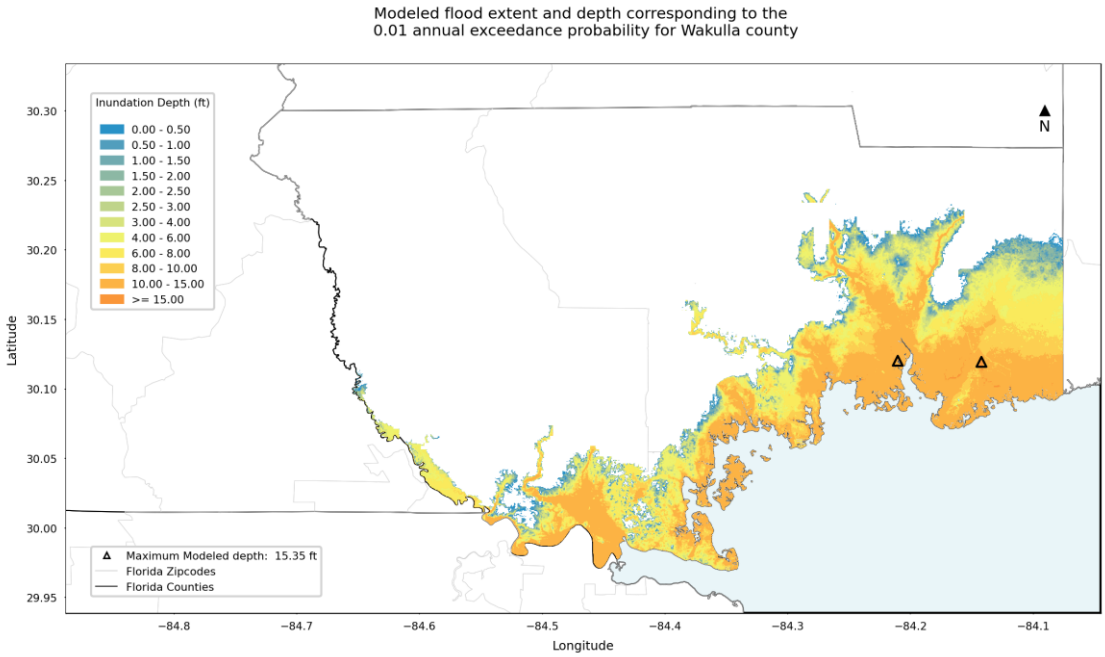

Figure 132: Modeled storm surge extent and depth corresponding to the 0.01 annual exceedance probability for Wakulla County. There are 56 pixels, all with the same maximum value. These pixels

have been grouped into two clusters, represented by the triangles. (horizontal datum: WGS84, vertical datum: EGM08)

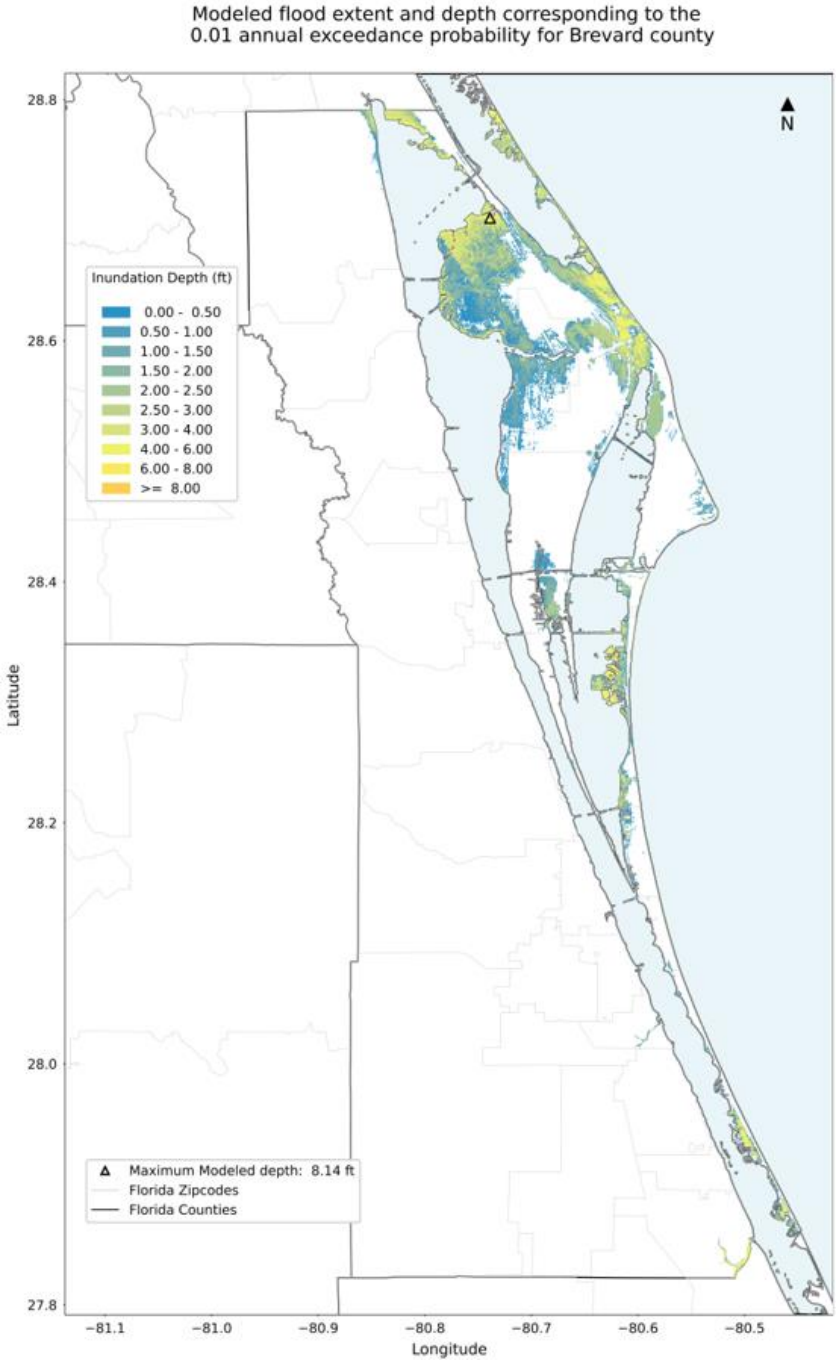

Figure 133: Modeled storm surge extent and depth corresponding to the 0.01 annual exceedance probability for Brevard County. (horizontal datum: WGS84, vertical datum: EGM08)

C. Include Form HHF-2, Coastal Flood Characteristics by Annual Exceedance Probability, in a submission appendix.

Figure 1

Form HHF-3: Coastal Flood Characteristics by Annual Exceedance Probabilities (Trade Secret Item)

Form HHF-3 is considered to be trade secret material and will be provided to the Professional Team for review during the on-site visit and to the Commission during the closed portion of the Acceptability Meeting.

Form HHF-4: Inland Flood Characteristics by Annual Exceedance Probability

A. Define one study area subject to inland flooding within each of the five Florida geographic regions identified in Figure 1. The extent of each study area is to be determined by the modeling organization and should be large enough to encompass at least one county. The modeling organization is to create the underlying grid for this form.

The study areas selected for each of the five Florida geographic regions identified in Form HHF-4 are:

- Washington County in Panhandle region
- Clay County in North Florida region
- Hardee County in Southwest Florida region
- Broward County in Southeast Florida region
- Indian River County in East Florida region

The grid resolution is 30m by 30m, which is consistent with the DEM resolution.

B. Provide, for each study area, color-coded contour or high-resolution maps showing the modeled flood extent and elevation or depth corresponding to the 0.01 annual exceedance probability. Flood extent and elevation or depth should incorporate the effects of flood-induced erosion, if modeled. For locations subject to both inland and coastal flooding, this information should reflect only inland flooding.

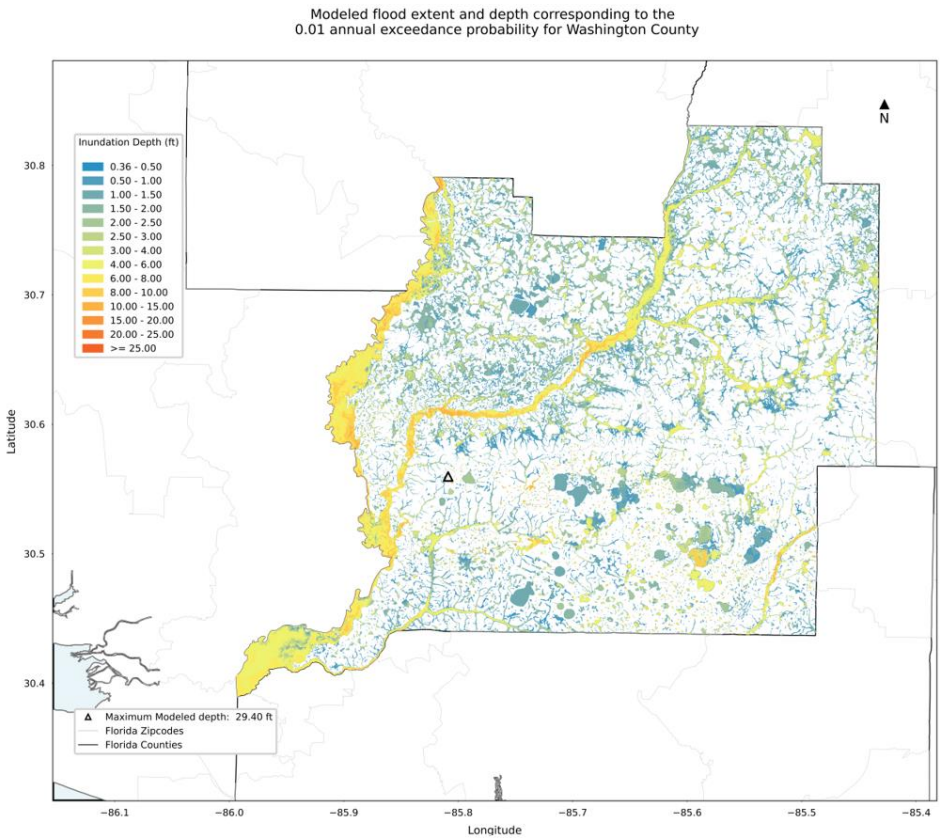

Figure 134: Modeled inland flood extent and depth corresponding to the 0.01 annual exceedance probability for Washington County in Panhandle region.

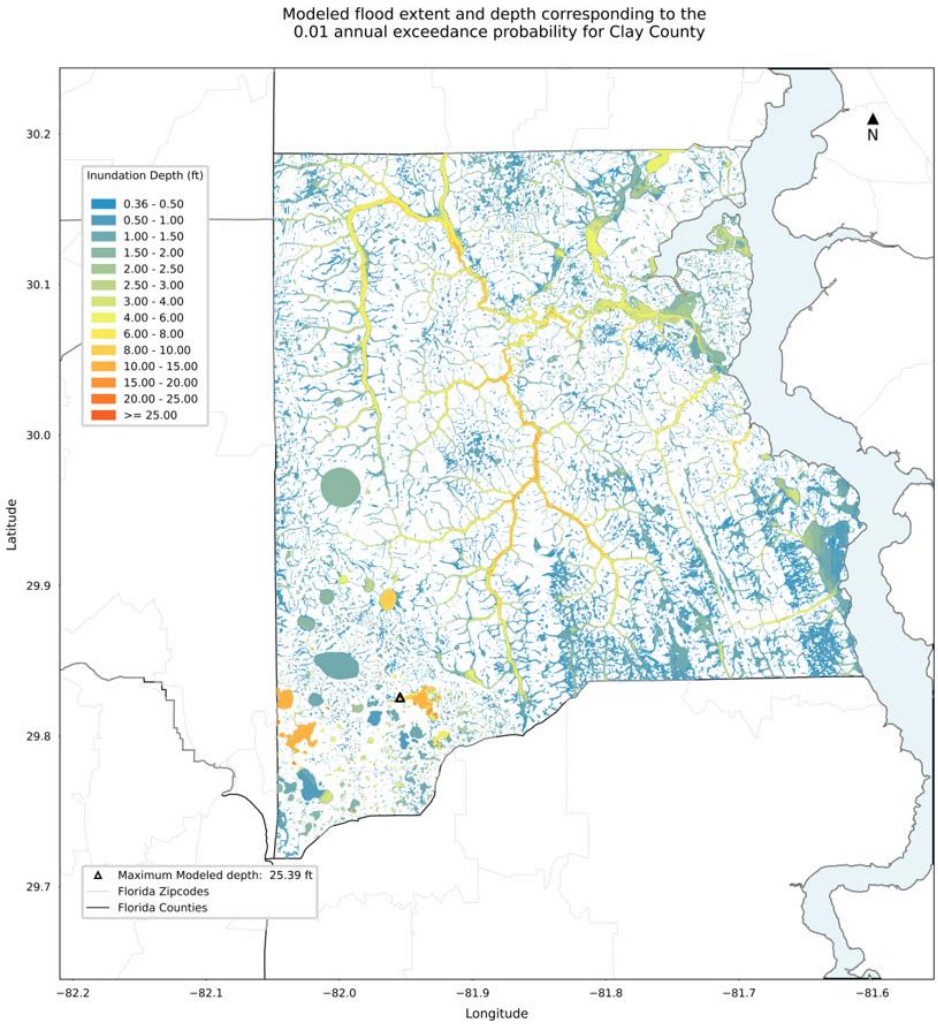

Figure 135: Modeled inland flood extent and depth corresponding to the 0.01 annual exceedance probability for Clay County in North Florida region.

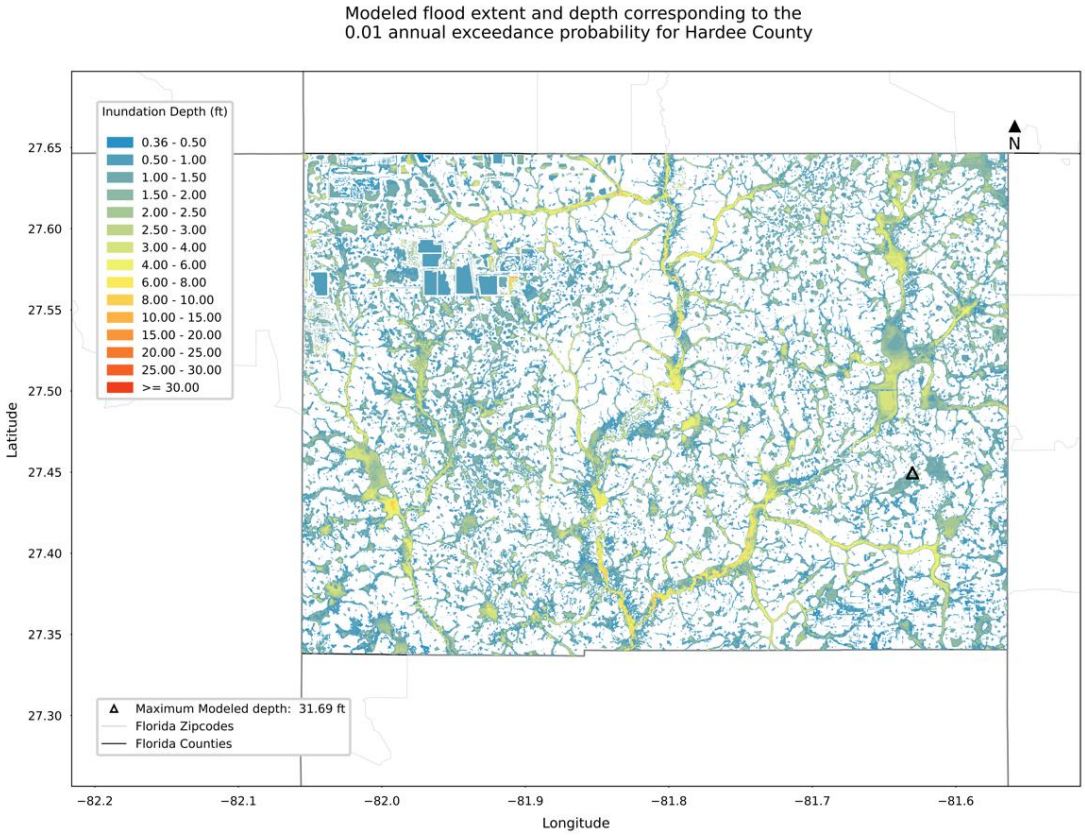

Figure 136: Modeled inland flood extent and depth corresponding to the 0.01 annual exceedance probability for Hardee County in Southwest Florida region.

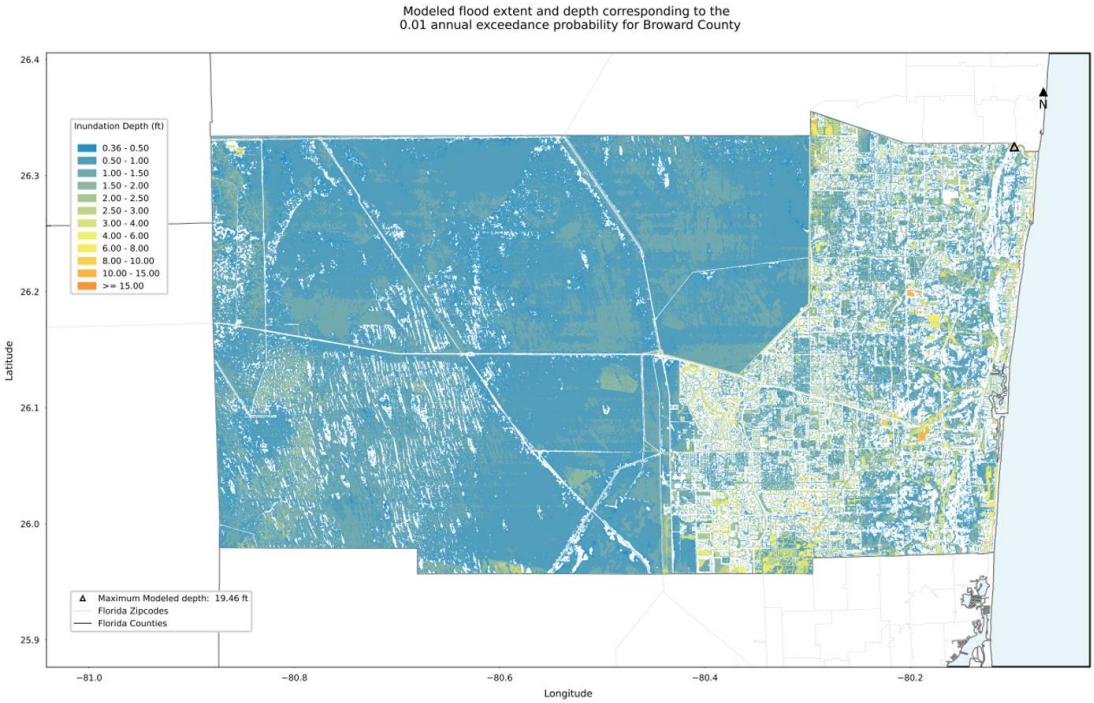

Figure 137: Modeled inland flood extent and depth corresponding to the 0.01 annual exceedance probability for Broward County in Southeast Florida region.

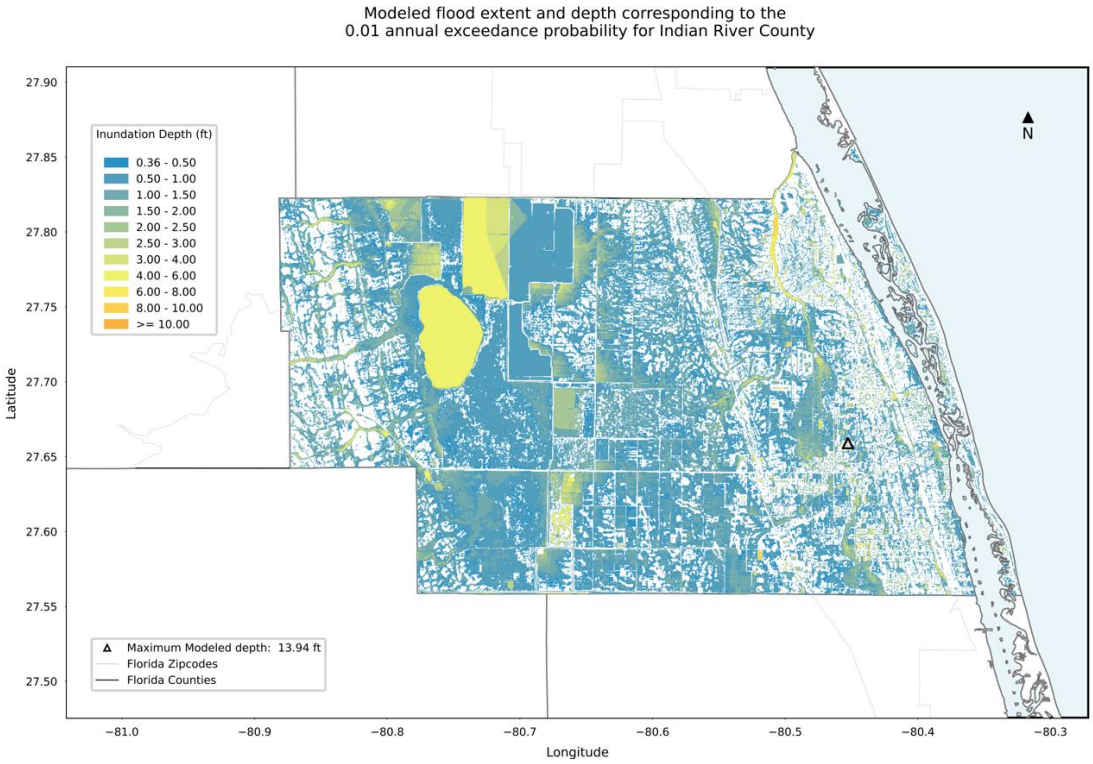

Figure 138: Modeled inland flood extent and depth corresponding to the 0.01 annual exceedance probability for Indian River County in East Florida region.

C. Include Form HHF-4, Inland Flood Characteristics by Annual Exceedance Probability, in a submission appendix.

Figure 1

Form HHF-5: Inland Flood Characteristics by Annual Exceedance Probabilities (Trade Secret Item)

Form HHF-5 is considered to be trade secret material and will be provided to the Professional Team for review during the on-site visit and to the Commission during the closed portion of the Acceptability Meeting.

Form SF-1: Distributions of Stochastic Flood Parameters (Coastal, Inland)

A. Provide the probability distribution functional form used for each stochastic flood parameter in the flood model (one each for coastal and inland flooding). Provide a summary of the justification for each functional form selected for each general classification. Specify the relevant classification (coastal or inland) for each distribution.

Year Range Used for Fitting refers to the year range of data upon which the flood model distribution parameters are estimated.

Year Range Used for Validation refers to the year range of data upon which the goodness-of-fit statistics are based.

B. Include Form SF-1, Distributions of Stochastic Flood Parameters (Coastal, Inland), in a submission appendix.

Form SF-1 is provided in Table 44

Table 44: Distributions of stochastic flood parameters (Coastal, Inland)

Stochastic Flood Parameter (Function or Variable)	Classification: Coastal or Inland	Functional Form of Distribution	Data Sources	Year Range Used		Justification for Functional Form and Parameter Estimates
				For Filing	For Validation	
Annual number of events (non-TC synthetic event set)	Inland	Empirical	MSWEP / FUSE-Mizoroute model reanalysis outputs	1980-2020	1980-2020	Commonly used in environmental applications of the multivariate extreme value model (example references in Disclosure SF-1.5)
Marginal distributions (non-TC synthetic event set)	Inland	Semi-empirical (GPD tails)	Fitted to MSWEP / FUSE-Mizoroute model reanalysis outputs	1980-2020	1980-2020	Commonly used in environmental applications of the multivariate extreme value model (example references in Disclosure SF-1.5)
Normalized margins for tail fitting (non-TC synthetic event set)	Inland	Laplace distribution	Fitted to MSWEP / FUSE-Mizoroute model reanalysis outputs	1980-2020	1980-2020	Commonly used in environmental applications of the multivariate extreme value model (example references in Disclosure SF-1.5)
Conditioning site selection (non-TC	Inland	Multinomial sampling	Applied to MSWEP / FUSE-Mizoroute model	1980-2020	1980-2020	Commonly used in environmental applications of the

Stochastic Flood Parameter (Function or Variable)	Classification: Coastal or Inland	Functional Form of Distribution	Data Sources	Year Range Used		Justification for Functional Form and Parameter Estimates
				For Filing	For Validation	
synthetic event set)			reanalysis outputs			multivariate extreme value model (example references in Disclosure SF-1.5)
Residual Sampling (non-TC synthetic event set)	Inland	Empirical (with rejection sampling)	Derived from reanalysis events within MSWEP / FUSE-Mizoroute model outputs	1980-2020	1980-2020	Commonly used in environmental applications of the multivariate extreme value model (example references in Disclosure SF-1.5)
Water Level Frequency Curve for lacustrine modelling	Inland	Log-Pearson distribution Type III	United States Geological Survey (USGS)	1857-2023	1857-2023	Following Advisory Committee on Water Information (ACWI) guidelines, the graphical frequency analysis was employed for lake frequency assessment. The procedure included referencing Bulleting-17-B guideline (page 2) for flood frequency analysis and specifying a

Stochastic Flood Parameter (Function or Variable)	Classification: Coastal or Inland	Functional Form of Distribution	Data Sources	Year Range Used		Justification for Functional Form and Parameter Estimates
				For Filing	For Validation	
						record length of at least 10 years for statistical analysis. Probability positions were computed using the Bulleting 17-B formula (Weibull formula, equation 11, page 27), and then plotted against untransformed lake levels on an arithmetic-normal probability grid. The shape of the plotted curve was utilized to determine the appropriate distribution.
Annual number of storms	Tropical cyclone induced coastal and inland flooding	Negative binomial	HURDAT2	1900-2020	1900-2020	Negative binomial distribution fits historical data well which is supported by standard statistical tests. It works better than Poisson distribution.

Stochastic Flood Parameter (Function or Variable)	Classification: Coastal or Inland	Functional Form of Distribution	Data Sources	Year Range Used		Justification for Functional Form and Parameter Estimates
				For Filing	For Validation	
Storm genesis parameters	Tropical cyclone induced coastal and inland flooding	Uniform	HURDAT2	1900-2020	1900-2020	Storm genesis parameters (e.g., initial location, forward speed, etc.) are sampled randomly from historical data to preserve spatial and temporal patterns of historical genesis.
Translational speed and heading angle	Tropical cyclone induced coastal and inland flooding	Empirical (regression models with residuals fitted to normal distributions)	HURDAT2	1900-2020	1900-2020	Both translational speed and heading angle are modeled using a Markov Chain approach. The approach is based on the published work of (Vickery, et al., 2000). The resultant empirical distributions match historical data well.
Central pressure	Tropical cyclone induced coastal and inland flooding	Empirical (regression model with residuals fitted to	HURDAT2, HadISST	1900-2020	1900-2020	Central pressure is modeled as a function of sea surface temperature. Sea surface

Stochastic Flood Parameter (Function or Variable)	Classification: Coastal or Inland	Functional Form of Distribution	Data Sources	Year Range Used		Justification for Functional Form and Parameter Estimates
				For Filing	For Validation	
		normal distribution)				temperature has been found to have a positive correlation with hurricane intensity. The modeling method is adopted from (Vickery, et al., 2000). The resultant empirical distribution agrees with historical data.
Radius of maximum winds	Tropical cyclone induced coastal and inland flooding	Lognormal (regression model with residuals fitted to normal distribution)	HURDAT2, HURDAT2 Reanalysis, NWS 38, Extended Best Track	1900-2020	1900-2020	Radius of maximum winds is modeled using an empirical equation documented in (Vickery & Wadhera, 2008). The coefficients in the equation are estimated using a multi-linear regression. The model fits historical data well.

Form SF-2: Examples of Flood Loss Exceedance Estimates (Coastal and Inland Combined)

A. One or more automated programs or scripts should be used to generate and arrange the data in Form SF-2, Examples of Flood Loss Exceedance Estimates (Coastal and Inland Combined).

An automated script is used to generate and arrange data in Form SF-2.

B. Provide estimates of the annual aggregate personal residential insured flood losses for various probability levels using a modeling-organization-specified, predetermined, and comprehensive exposure dataset justified by the modeling organization. Provide the total average annual flood loss for the loss exceedance distribution. If the modeling methodology does not allow the flood model to produce a viable answer for certain return periods, state so and why.

The annual aggregate personal residential insured flood losses for various return periods based on the Impact Forecasting Industry Exposure Dataset are provided in Table 45 below. The results are for TC and non-TC model combined with demand surge factor included.

C. Include Form SF-2, Examples of Flood Loss Exceedance Estimates (Coastal and Inland Combined), in a submission appendix.

Form SF-2 is provided in Table 45 and Table 46.

Part A

Table 45: Examples of flood loss exceedance estimates

Return Period (Years)	Annual Probability of Exceedance	Estimated Flood Loss Modeling Organization Exposure Dataset
Top Event	NA	185,743,902,149
10,000	0.0001	122,914,381,384
5,000	0.0002	114,131,227,458
2,000	0.0005	101,382,675,078
1,000	0.0010	89,502,542,800
500	0.0020	78,906,907,251
250	0.0040	66,523,139,201
100	0.0100	48,436,340,018
50	0.0200	31,725,207,355
20	0.0500	12,409,850,818
10	0.1000	4,523,920,264
5	0.2000	1,463,207,788

Part B

Table 46: Average annual loss for the flood loss exceedance distribution

	Estimated Flood Loss Notional Risk Dataset
Mean (Total Average Annual Flood Loss)	2,460,609,450
Median	137,191,687
Standard Deviation	8,655,585,288
Interquartile Range	1,008,100,491
Sample Size	200,000

Form VF-1: Coastal Flood with Damaging Wave Action

A. Sample personal residential exposure data for 8 reference buildings as defined below and 26 stillwater flood depths (0-25 feet at 1-foot increments) are provided in the file named "VFEventFormsInput21.xlsx."

Model the sample personal residential exposure data provided in the file versus the stillwater flood depths, and provide the damage/exposure ratios summarized by flood depth and construction type. Estimated Damage for each individual flood depth is the sum of ground up loss to all reference buildings in the flood depth range, excluding demand surge.

Personal residential contents, appurtenant structures, or time element coverages are not included.

Reference Buildings

Wood Frame	Masonry	Manufactured Home
#1 One story Crawlspace foundation Top of foundation wall 3 feet above grade	#4 One story Slab foundation Top of slab 1 foot above grade Unreinforced masonry exterior walls	#7 Manufactured post 1994 Dry stack concrete foundation Pier height 3 feet above grade Tie downs Single unit
#2 Two story Slab foundation Top of slab 1 foot above grade 5/8" diameter anchors at 48" centers for wall/slab connections	#5 Two story Slab foundation Top of slab 1 foot above grade Reinforced masonry exterior walls	#8 Manufactured post 1994 Reinforced masonry pier foundation Pier height 6 feet above grade Tie downs Single unit
#3 Two story Timber pile foundation Top of pile 8 feet above grade Wood floor system bolted to piles	#6 Two story Concrete pile foundation Concrete slab Top of pile 8 feet above grade Reinforced masonry exterior walls	

The 8 reference buildings versus 26 Stillwater flood depths with damaging wave action are modeled.

B. Confirm that the buildings used in completing the form are identical to those in the above table for the reference buildings.

The buildings used in completing this form are identical to those in the above table for the reference building, with the exception of the manufactured homes in cases 7 and 8. Impact Forecasting's vulnerability function set does not include a single year band for all the years post-1994 for mobile homes. There are multiple more granular year bands available, as detailed in Standard VF-1, Disclosure 12. For cases 7 and 8 in the table above, Impact Forecasting assigned a year built value of 2000, corresponding to the year band covering 1999-2010, which is the predominant year band (amongst available options post-1994) in which most mobile homes were built.

C. If additional assumptions are necessary to complete this form, provide the rationale for the assumptions as well as a description of how they are included.

A separate damage function for manufactured homes on 6 ft pier foundations were made in order to fill-in this form. The damage function is simulator based. Thus, all the assumptions which are valid for simulation-based functions are also valid for this function.

There were no further assumptions made to complete this form.

D. Provide a plot of the stillwater flood depth versus estimated damage/subject exposure data.

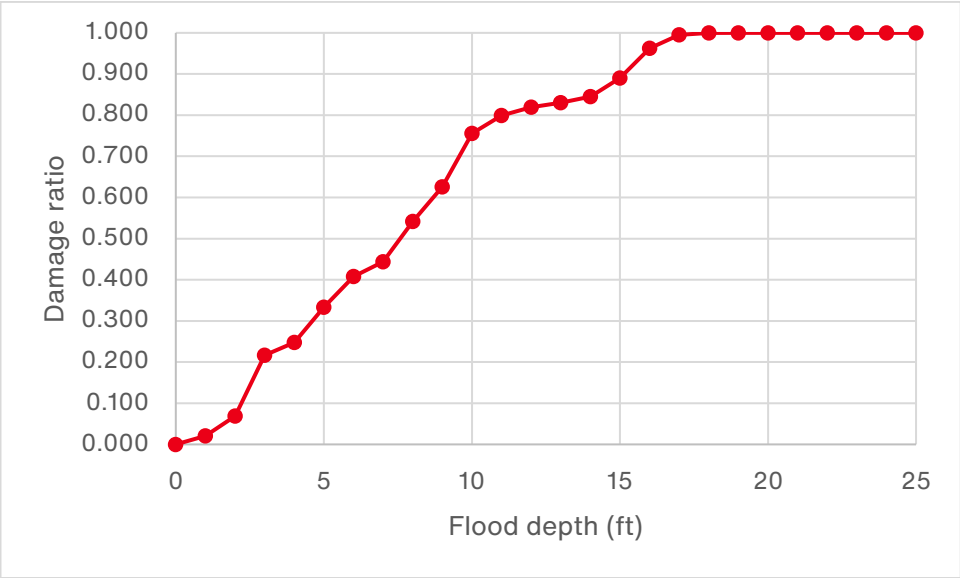

Figure 139: Estimated structure damage ratios by ranges of flood depths for Coastal Flood.

E. Include Form VF-1, Coastal Flood with Damaging Wave Action, in a submission appendix.

Form VF-1 is provided in Table 47.

Table 47: Coastal Flood with Damaging Wave Action

Stillwater Flood Depth (Feet)	Estimated Damage/ Subject Exposure
Above Ground Level	0.000
0	0.000

Stillwater Flood Depth (Feet)	Estimated Damage/ Subject Exposure
1	0.021
2	0.069
3	0.216
4	0.248
5	0.333
6	0.408
7	0.444
8	0.542
9	0.626
10	0.756
11	0.799
12	0.819
13	0.830
14	0.845
15	0.890
16	0.962
17	0.995
18	1.000
19	1.000
20	1.000
21	1.000
22	1.000
23	1.000

Form VF-2: Inland Flood by Flood Depth

A. Sample personal residential exposure data for 8 reference buildings as defined below and 26 flood depths (0-25 feet at 1-foot increments) are provided in the file named "VFEventFormsInput21.xlsx."

Model the sample personal residential exposure data provided in the file versus the flood depths, and provide the damage/exposure ratios summarized by flood depth and construction type. Estimated Damage for each individual flood depth is the sum of ground up loss to all reference buildings in the flood depth range, excluding demand surge.

Personal residential contents, appurtenant structures, or time element coverages are not included.

Reference Buildings

Wood Frame	Masonry	Manufactured Home
#1 One story Crawlspace foundation Top of foundation wall 3 feet above grade	#4 One story Slab foundation Top of slab 1 foot above grade Unreinforced masonry exterior walls	#7 Manufactured post 1994 Dry stack concrete foundation Pier height 3 feet above grade Tie downs Single unit
#2 Two story Slab foundation Top of slab 1 foot above grade 5/8" diameter anchors at 48" centers for wall/slab connections	#5 Two story Slab foundation Top of slab 1 foot above grade Reinforced masonry exterior walls	#8 Manufactured post 1994 Reinforced masonry pier foundation Pier height 6 feet above grade Tie downs Single unit
#3 Two story Timber pile foundation Top of pile 8 feet above grade Wood floor system bolted to piles	#6 Two story Concrete pile foundation Concrete slab Top of pile 8 feet above grade Reinforced masonry exterior walls	

B. Confirm that the buildings used in completing the form are identical to those in the above table for the reference buildings.

The 8 reference buildings versus 26 Stillwater flood depths are modeled.

C. If additional assumptions are necessary to complete this form, provide the rationale for the assumptions as well as a description of how they are included.

The buildings used in completing this form are identical to those in the above table for the reference building, with the exception of the manufactured homes in cases 7 and 8. Impact Forecasting's vulnerability function set does not include a single year band for all the years post-1994 for mobile homes. There are multiple more granular year bands available, as detailed in Standard VF-1, Disclosure 12. For cases 7 and 8 in the table above, Impact Forecasting assigned a year built value of 2000, corresponding to the year band covering 1999-2010, which is the predominant year band (amongst available options post-1994) in which most mobile homes were built.

D. Provide a plot of the flood depth versus estimated damage/subject exposure data.

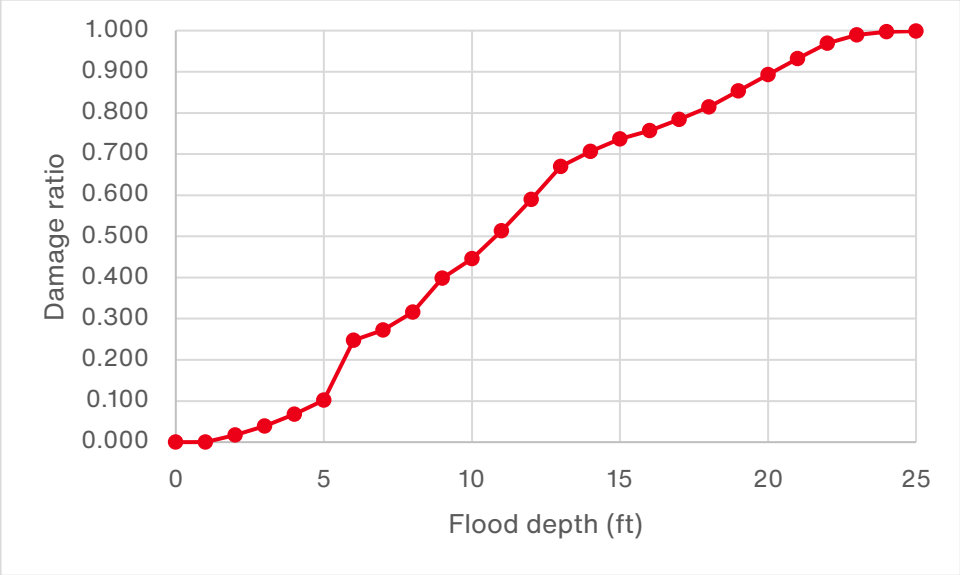

Figure 140: Estimated structure damage ratios by ranges of flood depths for Inland Flood.

E. Include Form VF-2, Inland Flood by Flood Depth, in a submission appendix.

Form VF-2 is provided in Table 48.

Table 48: Inland Flood by Flood Depth

Flood Depth (Feet) Above Ground Level	Estimated Damage/ Subject Exposure
Above Ground Level	0.000
0	0.000
1	0.000
2	0.018
3	0.039
4	0.068
5	0.102
6	0.247

Flood Depth (Feet) Above Ground Level	Estimated Damage/ Subject Exposure
7	0.273
8	0.316
9	0.398
10	0.446
11	0.514
12	0.590
13	0.670
14	0.707
15	0.737
16	0.757
17	0.784
18	0.814
19	0.853
20	0.893
21	0.932
22	0.969
23	0.990
24	0.997
25	0.999

Form VF-3: Flood Mitigation Measures, Range of Changes in Flood Damage

A. Provide the change in the personal residential reference building damage ratio (not loss cost) for each individual flood mitigation measure listed in Form VF-3, Flood Mitigation Measures, Range of Changes in Flood Damage, as well as for the combination of the flood mitigation measures. Personal residential contents, appurtenant structures, or time-element coverages are not included.

The change in the personal residential reference building damage ratio for each flood mitigation measure is provided in the file "IF2021FormVF3.xlsx".

B. If additional assumptions are necessary to complete this form, provide the rationale for the assumptions as well as a detailed description of how they are included.

In the model, the structure elevation is considered a primary modifier, and not a secondary modifier.

There were no further assumptions made to complete this form.

C. Provide this form in Excel format without truncation. The file name should include the abbreviated name of the modeling organization, the flood standards year, and the form name. Also include Form VF-3, Flood Mitigation Measures, Range of Changes in Flood Damage, in a submission appendix.

Form VF-3 in Excel format is provided in the file "IF2021FormVF3.xlsx" at the link provided to the FCHLPM, and in Table 49.

Reference Buildings

Wood Frame	Masonry
One story Crawlspace foundation Top of foundation wall 3 feet above grade	One story Slab foundation Top of slab 1 foot above grade Unreinforced masonry exterior walls
Two story Timber pile foundation Top of pile 8 feet above grade Wood floor system bolted to piles	

D. Place the reference buildings at the following locations, with latitude and longitude referenced to the World Geodetic System of 1984 (WGS84) datum, and provide the aggregated results.

Gulf of Mexico	***St. Johns River***
Latitude: 27.9957517	***Latitude: 29.3768881***
Longitude: -82.8277373	***Longitude: -81.6190223***

The reference buildings are placed at the locations listed above. The aggregated results are provided in Table 49.

E. Provide the ground elevation used from the flood model elevation database for both reference points.

The ground elevations used from the flood model elevation database are 1.81 m for the Gulf of Mexico location and 1.59 m for the St. Johns River location.

Table 49: Flood Mitigation Measures, Range of Changes in Flood Damage

INDIVIDUAL FLOOD MITIGATION MEASURES		PERCENTAGE CHANGES IN DAMAGE ((REFERENCE DAMAGE RATIO - MITIGATED DAMAGE RATIO) / REFERENCE DAMAGE RATIO) * 100									
		TWO-STORY WOOD FRAME STRUCTURE					MASONRY STRUCTURE				
		FLOOD DEPTH (FT) ABOVE GROUND					FLOOD DEPTH (FT) ABOVE GROUND				
		7	9	11	13	15	1	3	5	7	9
	REFERENCE STRUCTURE	—	—	—	—	—	—	—	—	—	—
ELEVATE STRUCTURE	Elevate Floor 1 Foot	1.29	48.63	16.96	14.45	16.77	—	—	—	—	—
	Elevate Floor 2 Feet	32.35	75.96	35.94	29.77	27.27	—	—	—	—	—
	Elevate Floor 3 Feet	49.64	76.31	81.45	37.78	39.44	—	—	—	—	—
UTILITY EQUIPMENT	Elevate or Protect 1 Foot	0.00	1.00	2.00	2.00	0.50	–	2.00	2.50	0.50	0.00
	Elevate or Protect 2 Feet	0.00	1.00	4.50	1.00	0.50	–	2.00	3.00	1.00	0.00
	Elevate or Protect 3 Feet	0.00	1.00	5.00	1.50	0.50	–	2.00	5.00	1.00	0.00
FLOODPROOFING	Wet 1 Foot	0.00	51.00	13.00	8.50	5.00	–	56.00	17.50	9.50	5.00
	Wet 2 Feet	0.00	62.50	13.00	8.50	4.00	–	56.00	25.50	9.50	5.00
	Wet 3 Feet	0.00	62.50	20.00	8.50	5.50	–	65.00	29.00	9.50	5.00
	Dry 1 Foot	—	—	—	—	—	–	0.00	0.00	0.00	0.00
	Dry 2 Feet	—	—	—	—	—	–	0.00	0.50	0.00	0.00
	Dry 3 Feet	—	—	—	—	—	–	50.00	0.00	0.00	0.00
FLOOD OPENINGS		ONE-STORY WOOD FRAME STRUCTURE									
		FLOOD DEPTH (FT) ABOVE GROUND									
		1	3	5	7	9					
	Flood Openings in Foundation Walls	–	1.00	1.00	1.00	1.00	—	—	—	—	—
FLOOD MITIGATION MEASURES IN COMBINATION		PERCENTAGE CHANGES IN DAMAGE ((REFERENCE DAMAGE RATIO - MITIGATED DAMAGE RATIO) / REFERENCE DAMAGE RATIO) * 100									
		TWO-STORY WOOD FRAME STRUCTURE					MASONRY STRUCTURE				
		FLOOD DEPTH (FT) ABOVE GROUND					FLOOD DEPTH (FT) ABOVE GROUND				
		7	9	11	13	15	1	3	5	7	9
Elevate Utility Equipment 2 Feet Above Floor and Wet Floodproof Structure to 2 Feet		0.00	63.00	17.00	9.50	4.50	–	58.00	27.50	10.50	5.00

Form VF-4: Differences in Flood Mitigation Measures

A. Provide the differences between the values reported in Form VF-3, Flood Mitigation Measures, Range of Changes in Damage, relative to the equivalent data compiled from the currently accepted flood model.

This is the first submission of the Impact Forecasting flood model. No Form VF-4 valid.

B. Provide a list and describe any assumptions made to complete this form.

C. Provide a summary description of the differences.

D. Provide this form in Excel format without truncation. The file name should include the abbreviated name of the modeling organization, the flood standards year, and the form name. Also include Form VF-4, Differences in Flood Mitigation Measures, in a submission appendix.

Form AF-1: Zero Deductible Personal Residential Standard Flood Loss Costs

A. ***Provide three maps, color-coded by rating areas or geographic zones (with a minimum of seven value ranges), displaying zero deductible personal residential standard flood loss costs per $1,000 of exposure for wood frame, masonry, and manufactured homes.***

Three maps color-coded by ZIP Code, displaying zero deductible personal residential flood loss costs per $1,000 of exposure appear in Figure 141 (frame owners), Figure 142(masonry owners), and Figure 143 (manufactured homes) below.

Note: Standard Flood in Florida is equivalent to the NFIP. Rating areas or geographic zones are to be defined by the modeling organization.

B. ***Create exposure sets for these exhibits by modeling the frame and masonry building and manufactured homes from Notional Set 3 described in the file "NotionalInput21_Flood.xlsx" geocoded to each rating area or geographic zone in the state, as provided in the flood model. Define the flood rating areas or geographic zones. Provide the predominant County name and the Federal Information Processing Standards (FIPS) Code (Figure 2) associated with each rating area or geographic zone. Refer to the Notional Standard Flood Policy Specifications below for additional modeling information. Explain any assumptions, deviations, and differences from the prescribed exposure information.***

No additional assumptions were made for this form. The created exposure is consistent with Notional Set 3 assumptions in "NotionalInput21_Flood.xlsx", geocoding the zip-code level exposure according to the provided FIPS code.

C. ***Describe if and how Law and Ordinance is included in this form.***

IF model doesn't explicitly model the Law and Ordinance as FL Statute doesn't require Law and Ordinance for Flood policies.

D. ***If additional assumptions are necessary to complete this form, provide the rationale for the assumptions as well as a detailed description of how they are included.***

No additional assumptions were made for this form.

E. ***Provide, in the format given in the file named "2021FormAF1.xlsx" in both Excel and PDF format, the underlying standard flood loss cost data, rounded to three decimal places, used for A. above. The file name should include the abbreviated name of the modeling organization, the flood standards year, and the form name.***

Form AF-1 is provided in Excel format in the file "IF2021FormAF1.xlsx" and in PDF format in the file "IF2021FormAF1.pdf" at the link provided to the FCHLPM.

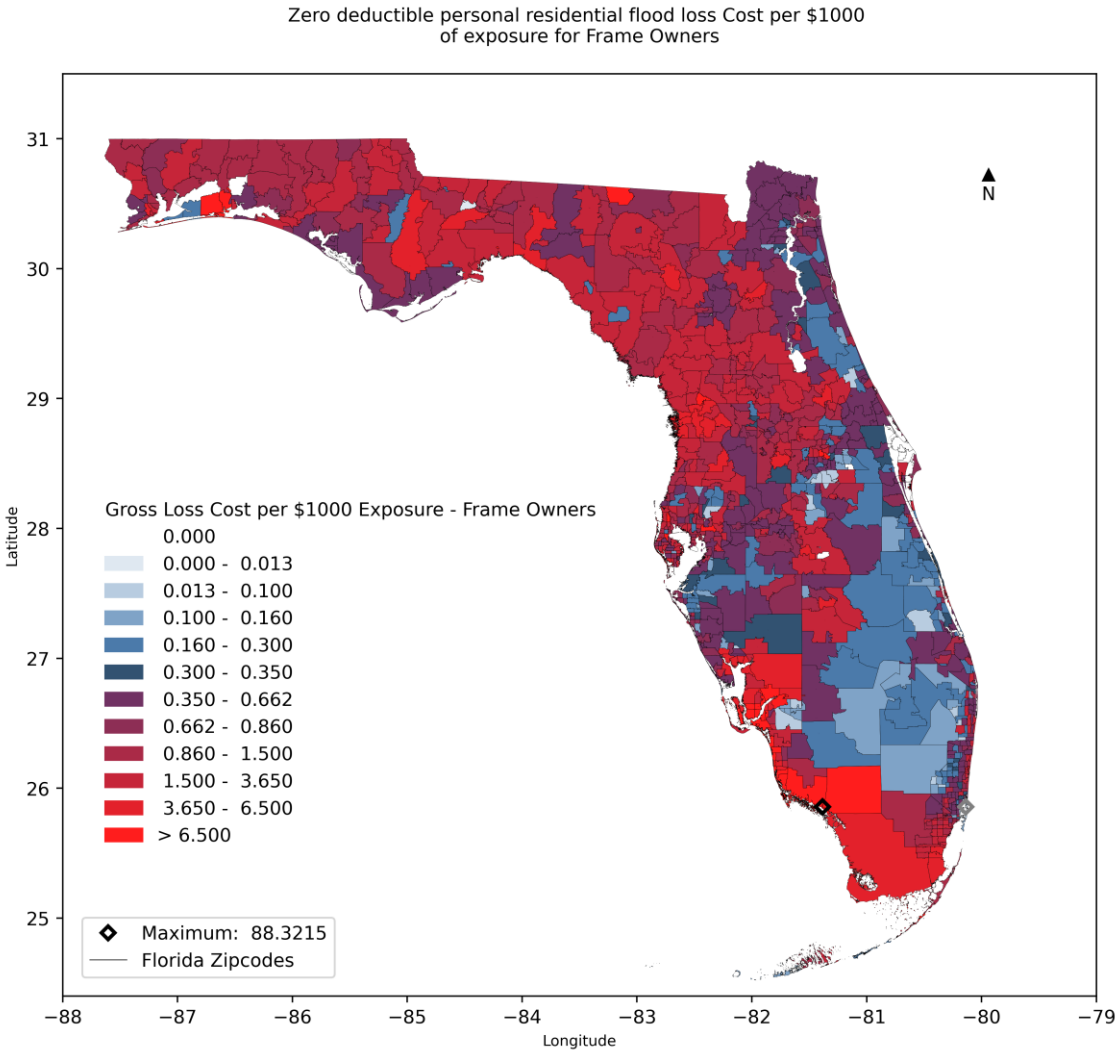

Figure 141: Zero deductible standard flood loss costs by county for frame owners.

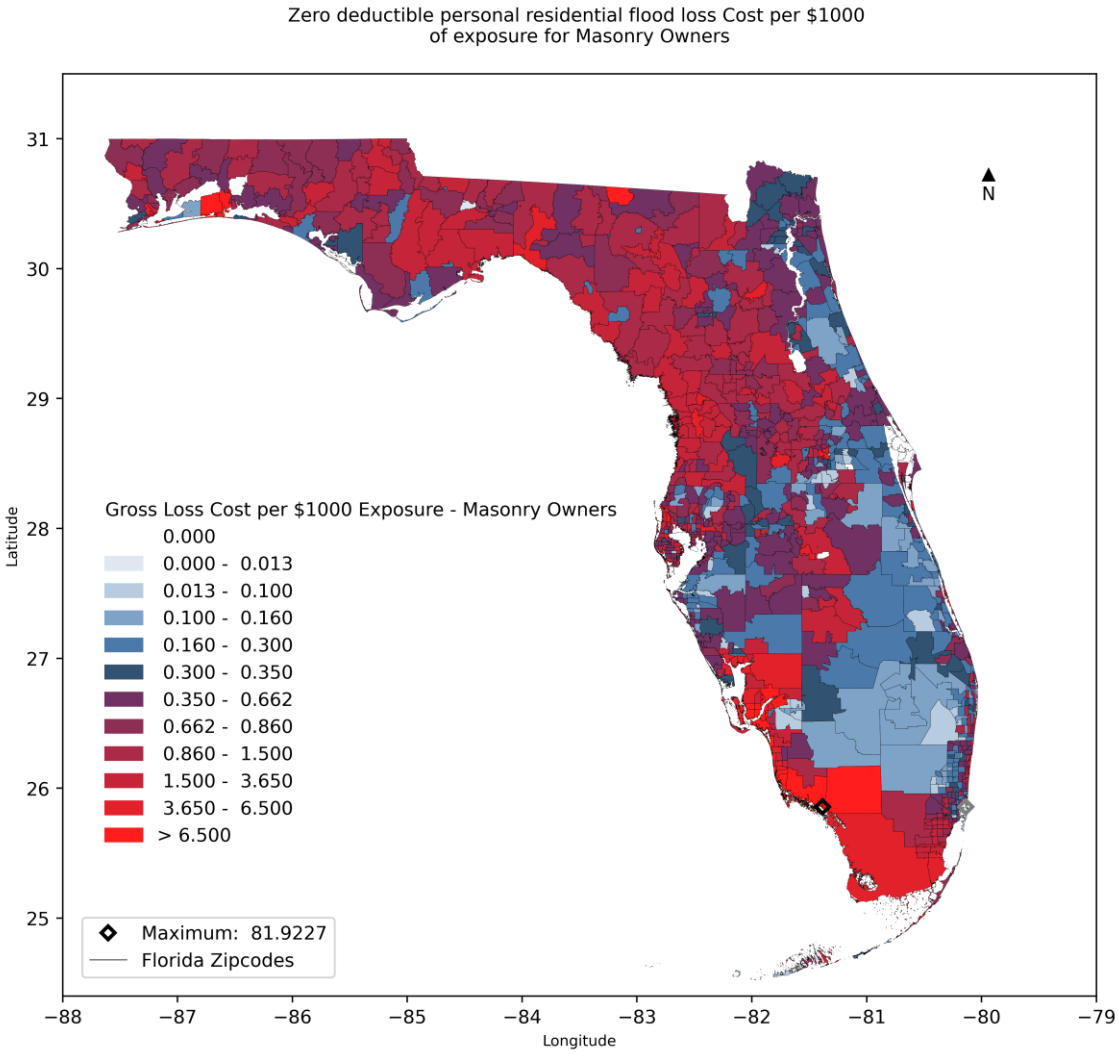

Figure 142: Zero deductible standard flood loss costs by county for masonry owners.

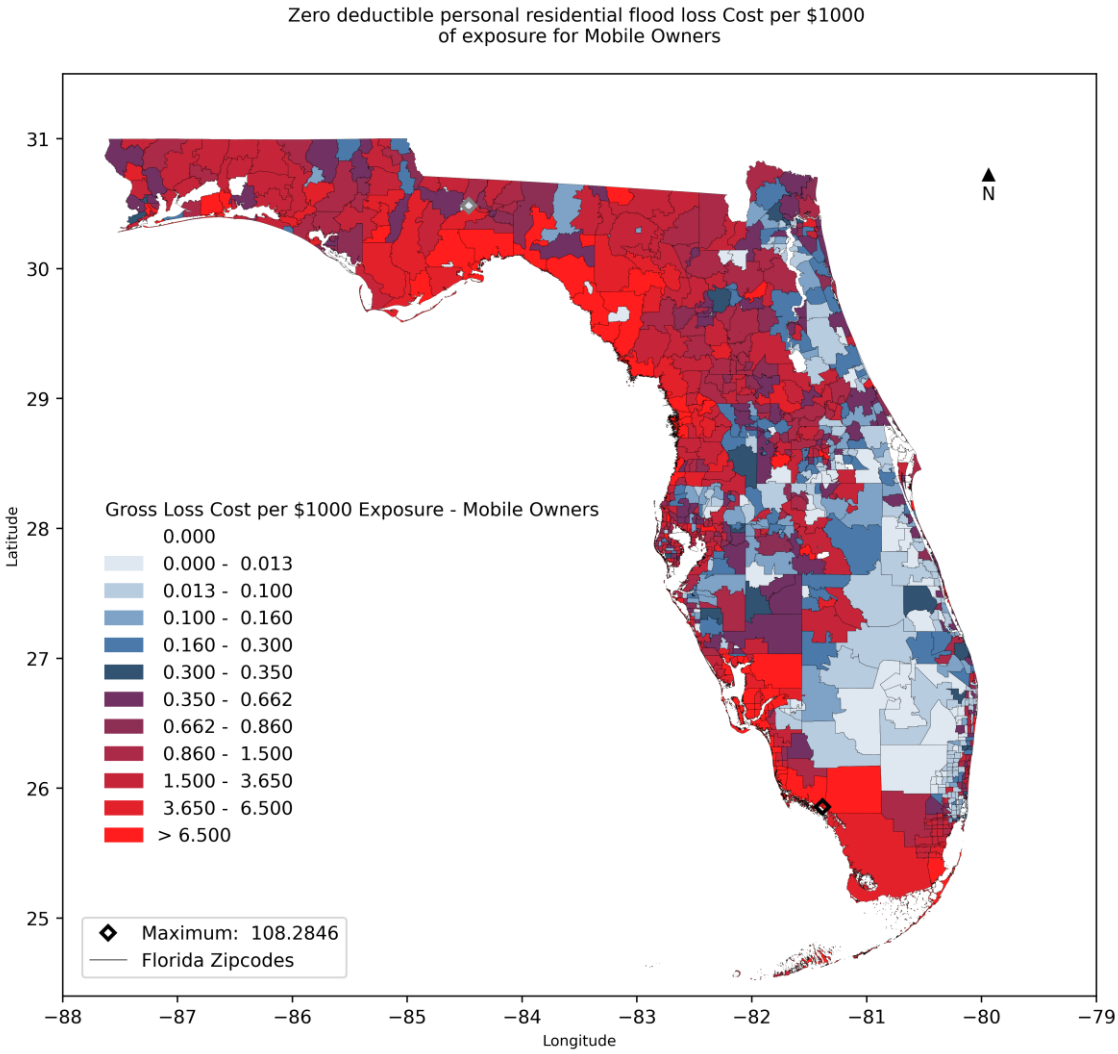

Figure 143: Zero deductible standard flood loss costs by county for manufactured owners.

Figure 2

Florida County Codes

County Code	County Name	County Code	County Name	County Code	County Name
001	Alachua	049	Hardee	093	Okeechobee
003	Baker	051	Hendry	095	Orange
005	Bay	053	Hernando	097	Osceola
007	Bradford	055	Highlands	099	Palm Beach
009	Brevard	057	Hillsborough	101	Pasco
011	Broward	059	Holmes	103	Pinellas
013	Calhoun	061	Indian River	105	Polk
015	Charlotte	063	Jackson	107	Putnam
017	Citrus	065	Jefferson	109	St. Johns
019	Clay	067	Lafayette	111	St. Lucie
021	Collier	069	Lake	113	Santa Rosa
023	Columbia	071	Lee	115	Sarasota
027	De Soto	073	Leon	117	Seminole
029	Dixie	075	Levy	119	Sumter
031	Duval	077	Liberty	121	Suwannee
033	Escambia	079	Madison	123	Taylor
035	Flagler	081	Manatee	125	Union
037	Franklin	083	Marion	127	Volusia
039	Gadsden	085	Martin	129	Wakulla
041	Gilchrist	086	Miami-Dade	131	Walton
043	Glades	087	Monroe	133	Washington
045	Gulf	089	Nassau		
047	Hamilton	091	Okaloosa		

Note: These codes are derived from the Federal Information Processing Standards (FIPS) Codes.

Notional Standard Flood Policy Specifications

Policy Type	Assumptions
Owners	**Coverage A = Building Property** • Replacement cost equal to Coverage A limit • Excludes all appurtenant structures **Coverage B = Personal Property** • Actual cash value equal to Coverage B limit **Time Element Coverage** • To be defined by the modeling organization

✧ Flood loss costs per $1,000 should be related to the Coverage A limit for Coverage A, to the Coverage B limit for Coverage B, and to the Time Element limit for Time Element Coverage

Manufactured Homes	**Coverage A = Building Property** • Replacement cost equal to Coverage A limit **Coverage B = Personal Property** • Actual cash value equal to Coverage B limit **Time Element Coverage** • To be defined by the modeling organization

✧ Flood loss costs per $1,000 should be related to the Coverage A limit for Coverage A, to the Coverage B limit for Coverage B, and to the Time Element limit for Time Element Coverage

Form AF-2: Total Flood Statewide Loss Costs

A. ***Provide the total personal residential insured flood loss assuming zero deductible policies for individual historical flooding events using a modeling-organization-specified, predetermined and comprehensive exposure dataset. The list of flooding events in this form should include meteorological and hydrological events and circumstances occurring inside or outside of Florida that resulted in or contributed to flooding in Florida included in the modeling organization flood-event dataset (e.g., Florida and by-passing hurricanes, tropical cyclones below hurricane strength that caused flood losses in Florida, rainfall events that caused flood losses in Florida).***

The table below contains the tropical cyclones from HURDAT2 and rainfall events to be included in the modeling organization flood-event dataset. The modeling organization should populate the table with its own flood-event dataset. Each tropical cyclone and rainfall event has been assigned an ID number. For tropical cyclones resulting in zero loss, the table entry should be left blank. Additional tropical cyclones and rainfall events included in the modeling organization flood-event dataset should be added to the table in order of year and assigned an intermediate ID number within the bounding ID numbers.

As defined, a by-passing hurricane (ByP) is a hurricane which does not make landfall on Florida, but produces minimum damaging windspeeds or greater on Florida. For the by-passing hurricanes included in the table only, the hurricane intensity entered is the maximum windspeed at closest approach to Florida as a hurricane, not the windspeed over Florida.

B. ***If additional assumptions are necessary to complete this form, provide the rationale for the assumptions as well as a detailed description of how they are included.***

No additional assumptions were made for this form.

C. ***Provide this form in Excel format. The file name should include the abbreviated name of the modeling organization, the flood standards year, and the form name. Also include Form AF-2, Total Flood Statewide Loss Costs, in a submission appendix.***

Form AF-2 is provided in Excel format in the file “IF2021FormAF2.xlsx” at the link provided to the FCHLPM and appears in Table 50 below.

Table 50: Total Flood Statewide Loss Costs

ID	Tropical Cyclone/ Hurricane Landfall/Closest Approach Date	Year	Name	Hurricane Landfall Region as defined in Figure 3 - Category	Personal Residential Insured Flood Losses ($)
005	10/25/1921	1921	TampaBay06-1921	B-3	22,833,488,016.18
010	09/18/1926	1926	GreatMiami07-1926	C-4/A-3	41,669,395,505.51
015	09/17/1928	1928	LakeOkeechobee04-1928	C-4	4,961,735,414.04
020	09/03/1935	1935	LaborDay03-1935	C-5/A-2	7,143,531,937.29
025	08/31/1950	1950	Baker-1950	F-1/ByP-1	340,668.83
030	09/05/1950	1950	Easy-1950	A-3	10,998,041,679.77
035	10/18/1950	1950	King-1950	C-4	225,006,893.29
040	09/26/1953	1953	Florence-1953	A-1	128,076,520.90
045	10/09/1953	1953	Hazel-1953	B-1	12,594,800,912.57
050	09/25/1956	1956	Flossy-1956	A-1	5,458,677.85
055	09/10/1960	1960	Donna-1960	B-4	28,361,430,085.38
060	09/15/1960	1960	Ethel-1960	F-1	57,298.76
065	08/27/1964	1964	Cleo-1964	C-2	384,899,362.64
070	09/10/1964	1964	Dora-1964	D-2	991,012,243.60
075	10/14/1964	1964	Isbell-1964	B-2	268,335,553.70
080	09/08/1965	1965	Betsy-1965	C-3	2,646,869,323.33
085	06/09/1966	1966	Alma-1966	A-1	468,990,001.02
090	10/04/1966	1966	Inez-1966	C-1	74,863,192.05
095	10/19/1968	1968	Gladys-1968	A-1	2,946,739,616.38
100	08/18/1969	1969	Camille-1969	F-5	79,597.38
105	06/19/1972	1972	Agnes-1972	A-1	24,407,689.64
110	09/23/1975	1975	Eloise-1975	A-3	51,656,593.99
115	09/04/1979	1979	David-1979	C-2/E-2	329,088,966.18
120	09/13/1979	1979	Frederic-1979	F-3	357,362,980.14
125	09/02/1985	1985	Elena-1985	F-3/ByP-3	64,200,024.16
130	11/21/1985	1985	Kate-1985	A-2	193,275,238.33
135	10/12/1987	1987	Floyd-1987	B-1	27,862,715.88
140	08/24/1992	1992	Andrew-1992	C-5	7,300,245,763.39
145	08/03/1995	1995	Erin-1995	C-1/A-1	273,212,081.10
150	10/04/1995	1995	Opal-1995	A-3	965,511,869.79

ID	Tropical Cyclone/ Hurricane Landfall/Closest Approach Date	Year	Name	Hurricane Landfall Region as defined in Figure 3 - Category	Personal Residential Insured Flood Losses ($)
155	07/19/1997	1997	Danny-1997	F-1	354,858,883.12
160	09/03/1998	1998	Earl-1998	A-1	760,519,323.17
165	09/25/1998	1998	Georges-1998	B-2/F-2	924,771,724.22
170	10/15/1999	1999	Irene-1999	B-1	2,475,451,676.32
175	06/04/2001	2001	Tropical Storm Allison-2001	---	18,932.83
180	08/13/2004	2004	Charley-2004	B-4	1,203,303,924.76
185	09/05/2004	2004	Frances-2004	C-2	2,940,790,402.14
190	09/16/2004	2004	Ivan-2004	F-3/ByP-3	3,345,817,829.59
195	09/26/2004	2004	Jeanne-2004	C-3	1,038,257,627.11
200	0710/2005	2005	Dennis-2005	A-3	1,115,954,836.91
205	08/25/2005	2005	Katrina-2005	C-1	434,646,228.31
210	09/20/2005	2005	Rita-2005	ByP-2	64,525,654.41
215	10/24/2005	2005	Wilma-2005	B-3	1,251,910,787.50
220	08/18/2008	2008	Tropical Storm Fay-2008	---	1,814,200,913.71
225	---	2009	Unnamed Storm in East Florida-May 2009		37,748,374.39
230	---	2013	Unnamed Storm in Panhandle-July 2013	---	10,480,884.44
235	09/02/2016	2016	Hermine-2016	A-1	284,783,780.19
240	10/07/2016	2016	Matthew-2016	ByP-3	1,662,216,351.85
245	0910/2017	2017	Irma-2017	B-4	2,988,870,215.46
250	10/08/2017	2017	Nate-2017	F-1	142,251.98
255	10/10/2018	2018	Michael-2018	A-5	460,311,858.54
260	09/04/2019	2019	Dorian-2019	ByP-2	112,730,672.35
265	09/16/2020	2020	Sally-2020	F-2	1,270,246,480.45
270	10/28/2020	2020	Zeta-2020	ByP-3	59,616.80
275	11/11/2020	2020	Eta-2020	ByP-1	1,949,658,393.14
			Total:		172,792,254,046.78

Figure 3

State of Florida and Neighboring States by Region

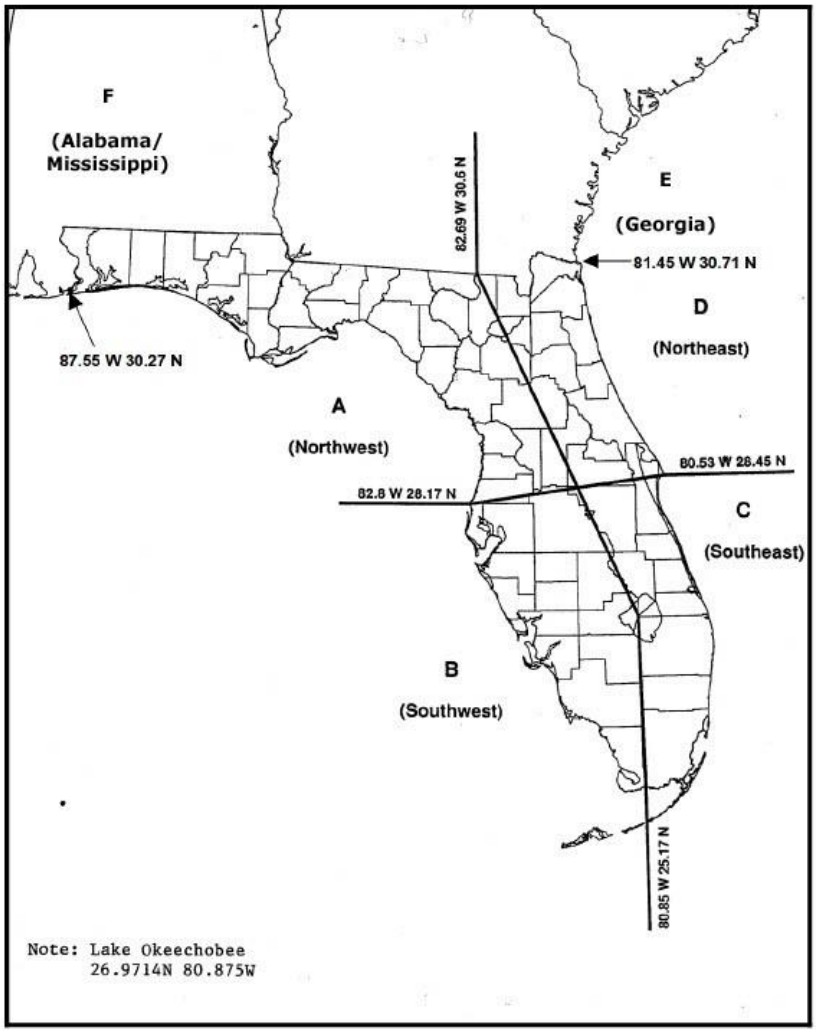

Form AF-3: Personal Residential Standard Flood Losses by ZIP Code

A. One or more automated programs or scripts should be used to generate and arrange the data in Form AF-3, Personal Residential Standard Flood Losses by ZIP Code.

An automated script is used to generate and arrange the data in Form AF-3.

B. Provide the percentage of total personal residential zero deductible standard flood loss, rounded to four decimal places, and the modeled loss from the events listed below using the modeling-organization-specified, predetermined, and comprehensive exposure dataset.

- **Hurricane Andrew (1992)**
- **Hurricane Ivan (2004)**
- **Hurricane Jeanne (2004)**
- **Hurricane Wilma (2005)**
- **Tropical Storm Fay (2008)**
- **Unnamed Storm in East Florida (May 2009)**
- **Unnamed Storm in Panhandle (July 2013)**
- **Hurricane Matthew (2016)**
- **Hurricane Irma (2017)**
- **Hurricane Michael (2018)**

C. Provide maps color-coded by ZIP Code depicting the percentage total personal residential standard flood loss from each flood event using the following interval coding:

- **Red > 5%**
- **Light Red > 2% to 5%**
- **Pink > 1% to 2%**
- **Light Pink > 0.5% to 1%**
- **Light Blue > 0.2% to 0.5%**
- **Medium Blue > 0.1% to 0.2%**
- **Blue > 0% to 0.1%**
- **White 0%**

Maps color-coded by ZIP Code depicting the percentage of total residential flood losses from each event are provided in Figure 144 (Hurricane Andrew), Figure 145 (Hurricane Ivan), Figure 146

(Hurricane Jeanne),

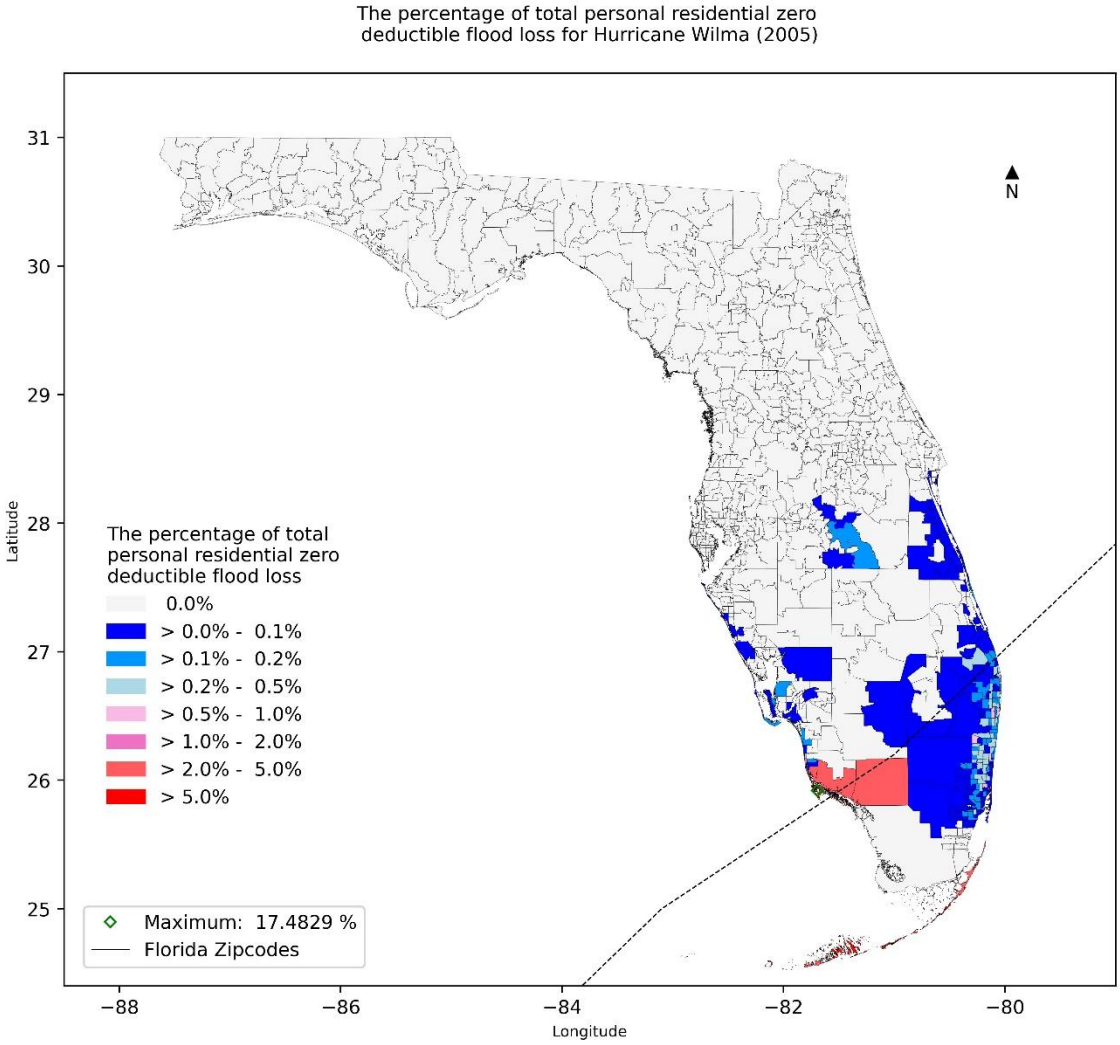

Figure 147 (Hurricane Wilma), Figure 148 (Tropical Storm Fay), Figure 149 (Unnamed Storm in East Florida), Figure 150 (Unnamed Storm in Panhandle), Figure 151 (Hurricane Matthew), Figure 152 (Hurricane Irma) and Figure 153 (Hurricane Michael).

D. *If additional assumptions are necessary to complete this form, provide the rationale for the assumptions as well as a detailed description of how they are included.*

No additional assumptions were made for this form.

E. *Provide, in the format given in the file named "2021FormAF3.xlsx" in both Excel and PDF format, the total flood losses by ZIP Code. The file name should include the abbreviated name of the modeling organization, the flood standards year, and the form name.*

Form AF-3 is provided in Excel format in the file "IF2021FormAF3.xlsx" at the link provided.

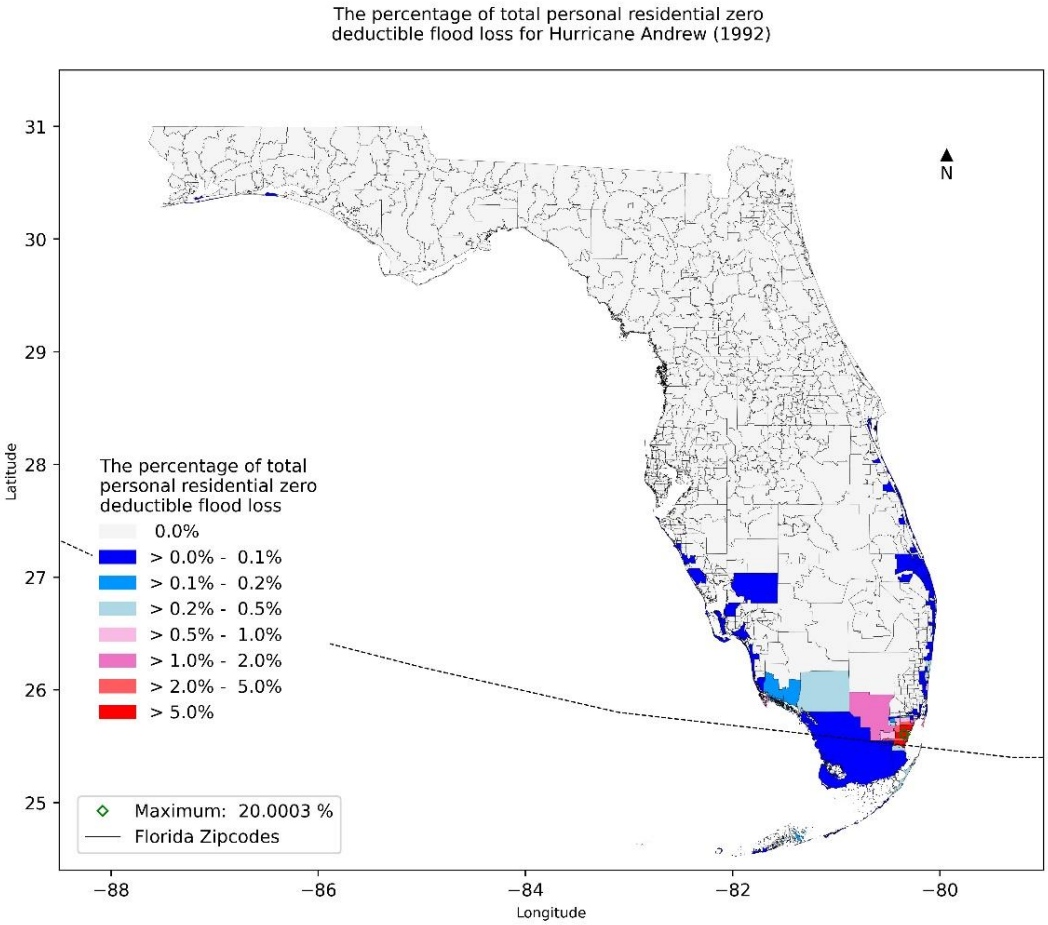

Figure 144: Percentage of total residential flood losses for Hurricane Andrew (1992) by Zip Code

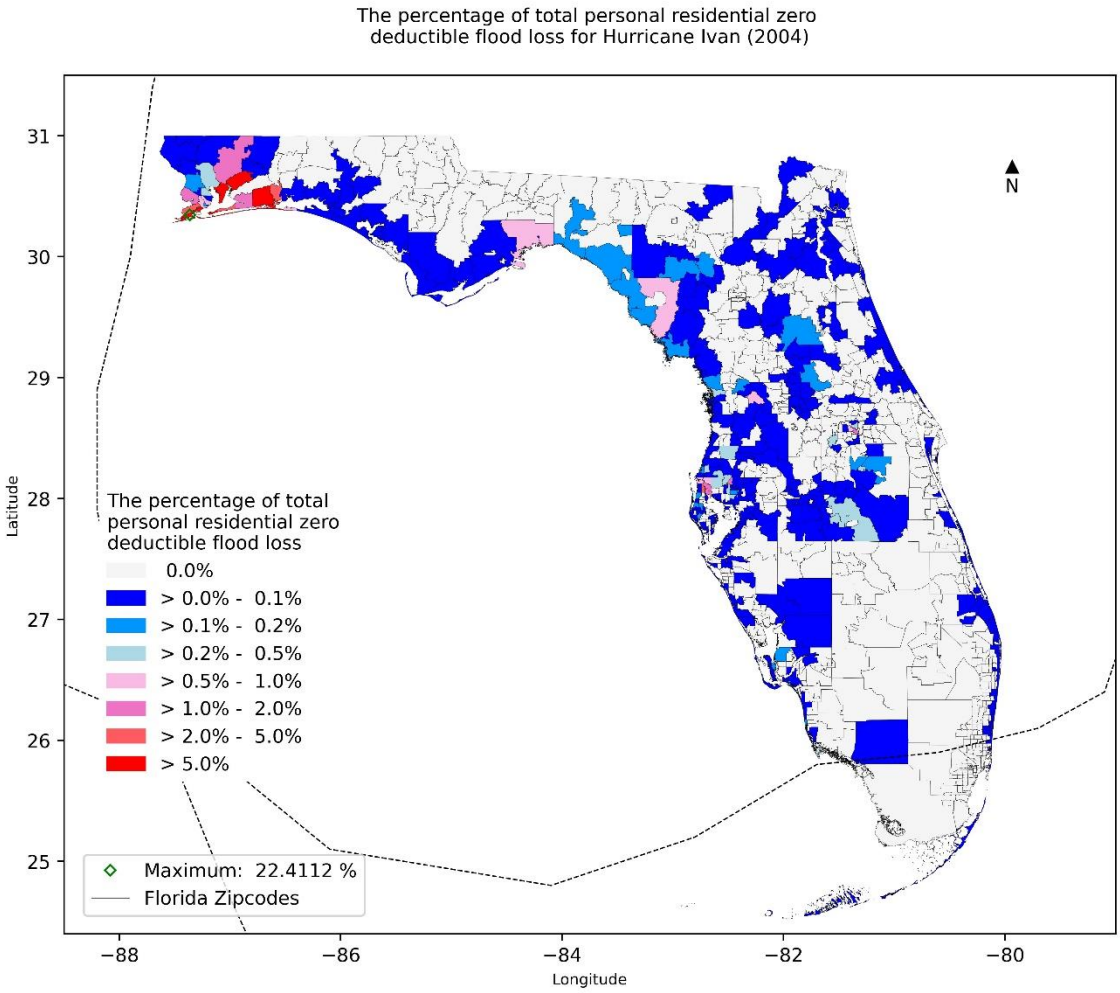

Figure 145: Percentage of total residential flood losses for Hurricane Ivan (2004) by Zip Code

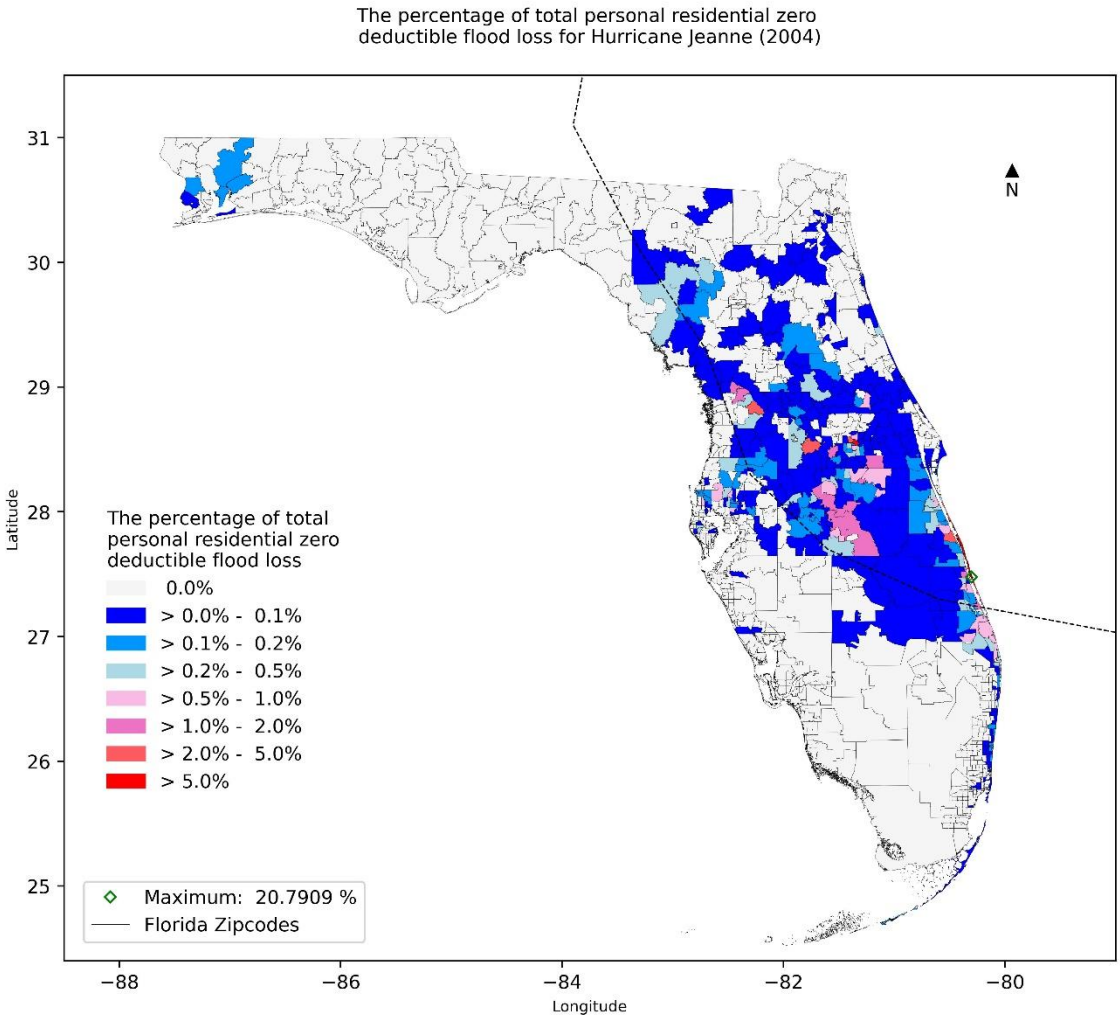

Figure 146: Percentage of total residential flood losses for Hurricane Jeanne (2004) by Zip Code

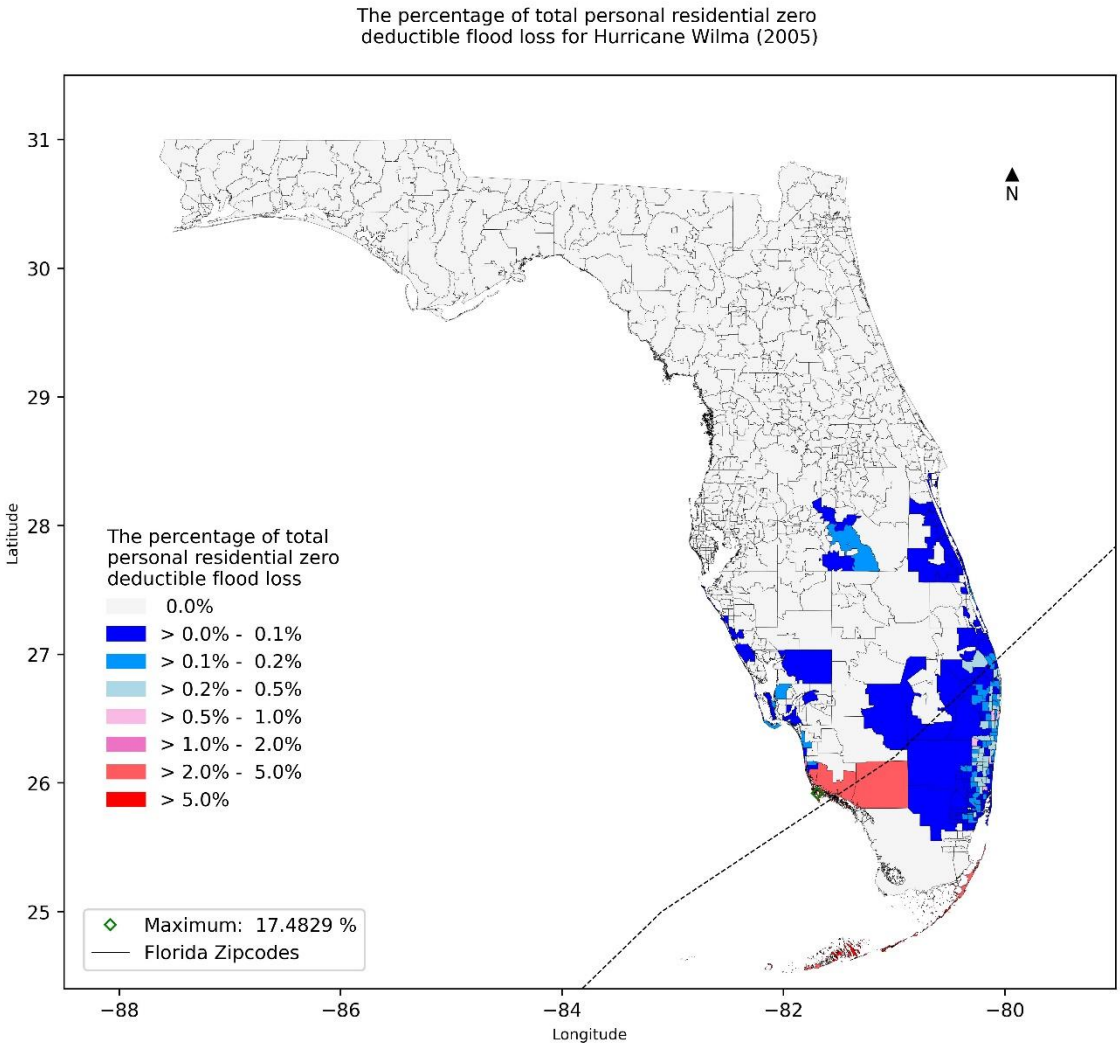

Figure 147: Percentage of total residential flood losses for Hurricane Wilma (2005) by Zip Code

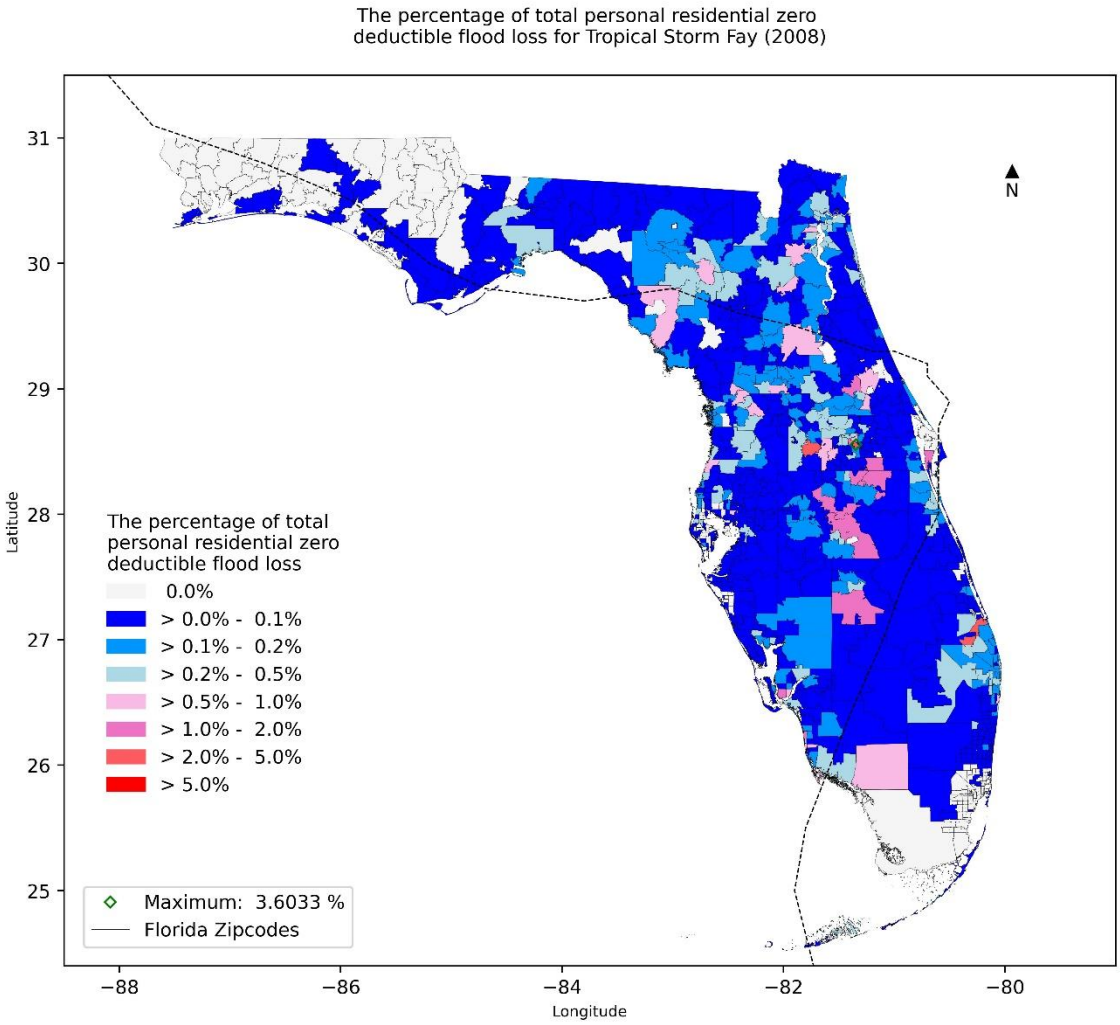

Figure 148: Percentage of total residential flood losses for Tropical Storm Fay (2008) by Zip Code

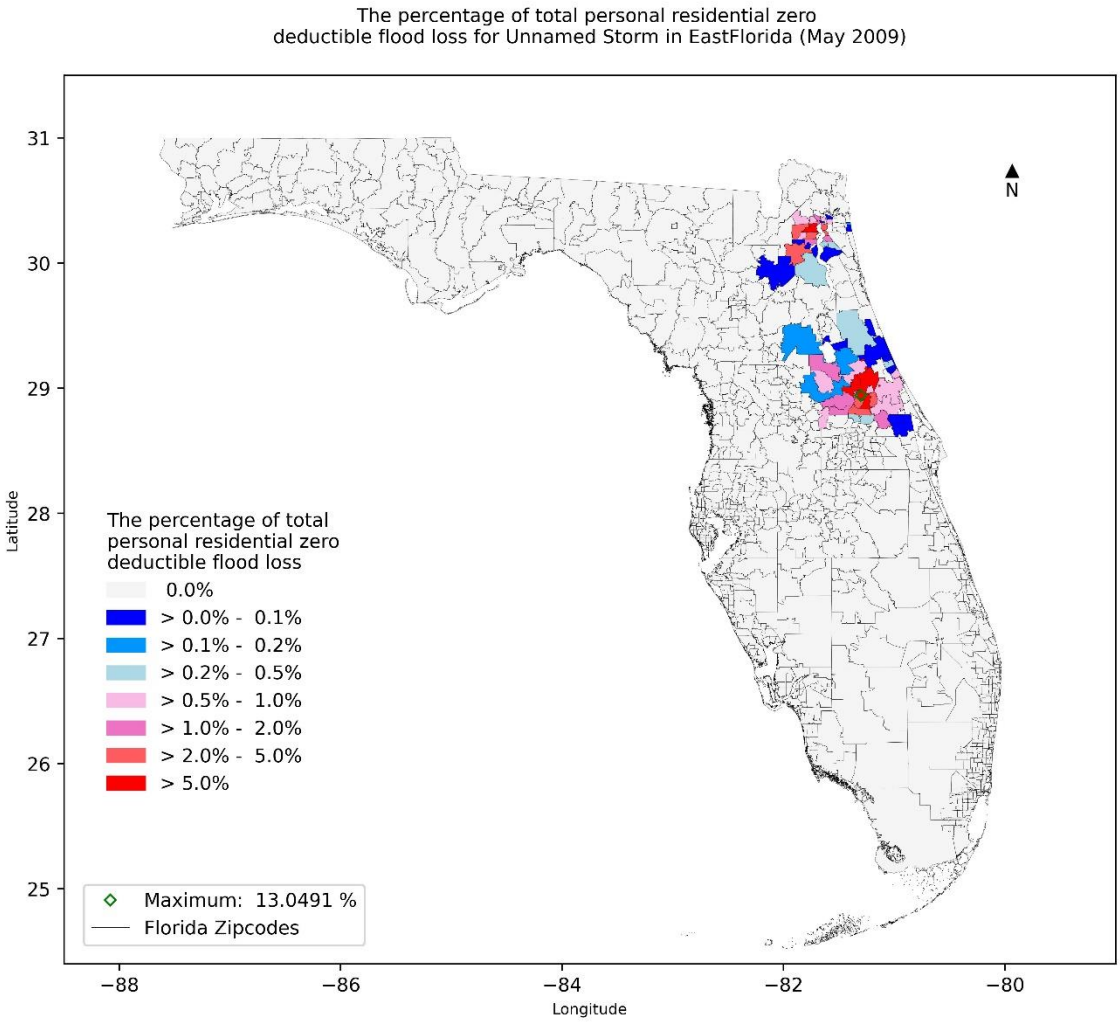

Figure 149: Percentage of total residential flood losses for Unnamed Storm in East Florida (May 2009) by Zip Code

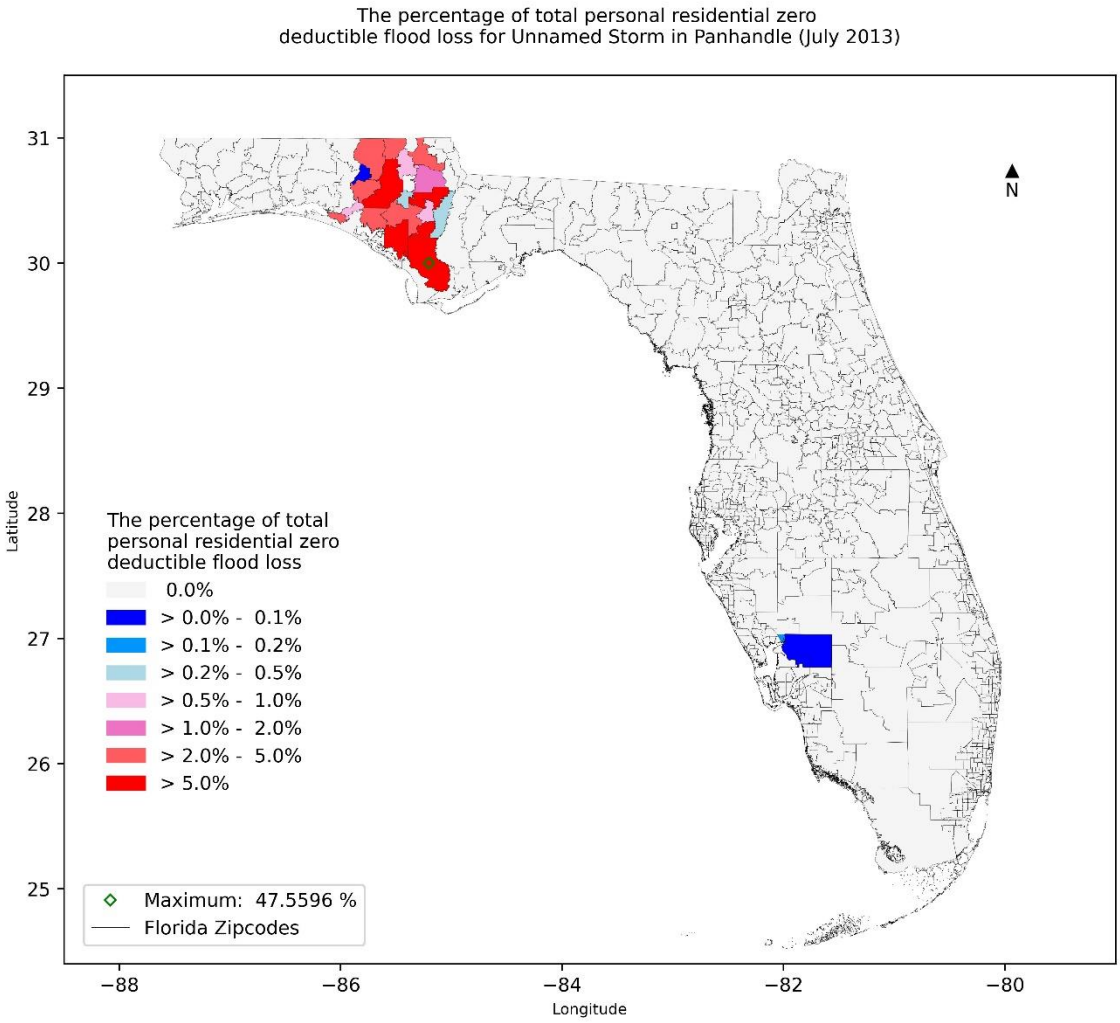

Figure 150: Percentage of total residential flood losses for Unnamed Storm in Panhandle (July 2013) by Zip Code

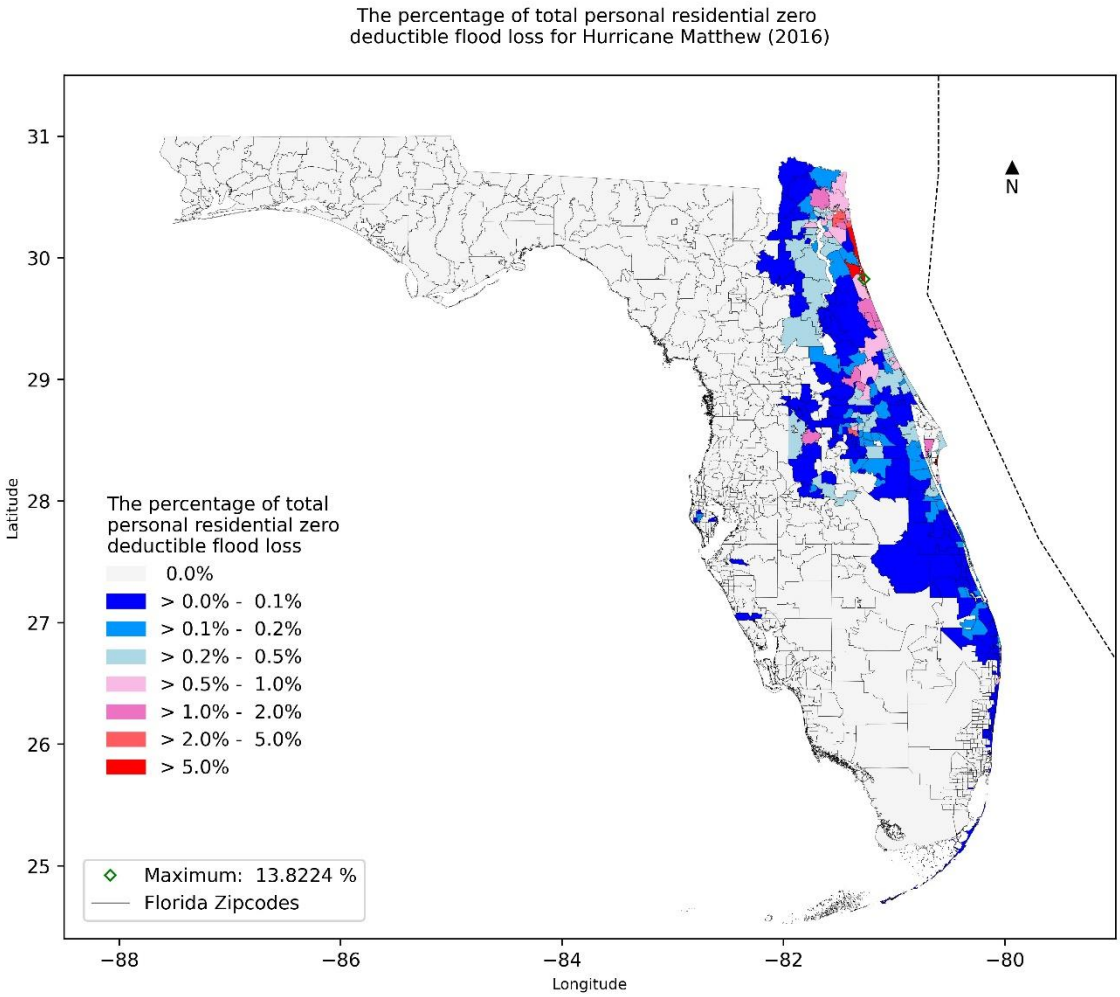

Figure 151: Percentage of total residential flood losses for Hurricane Matthew (2016) by Zip Code

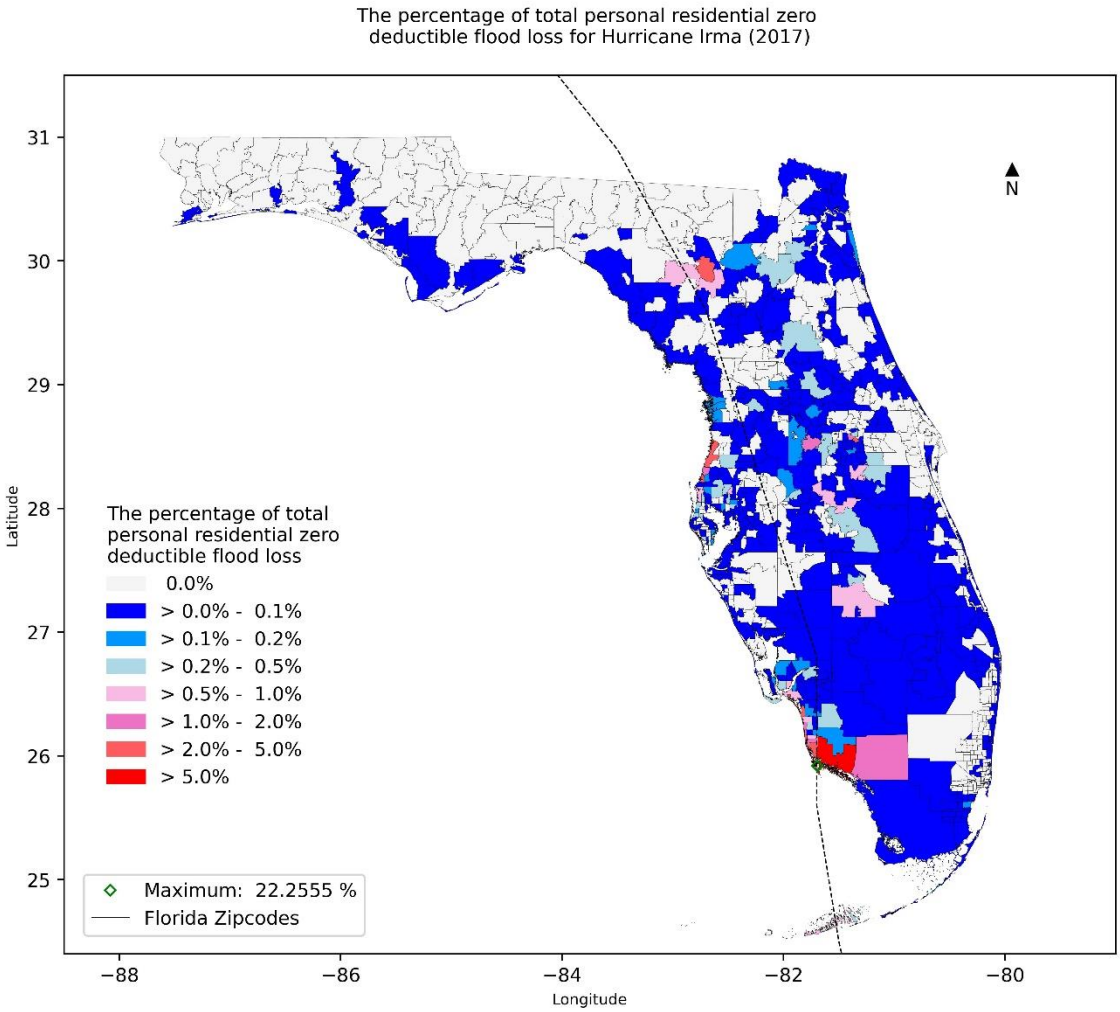

Figure 152: Percentage of total residential flood losses for Hurricane Irma (2017) by Zip Code

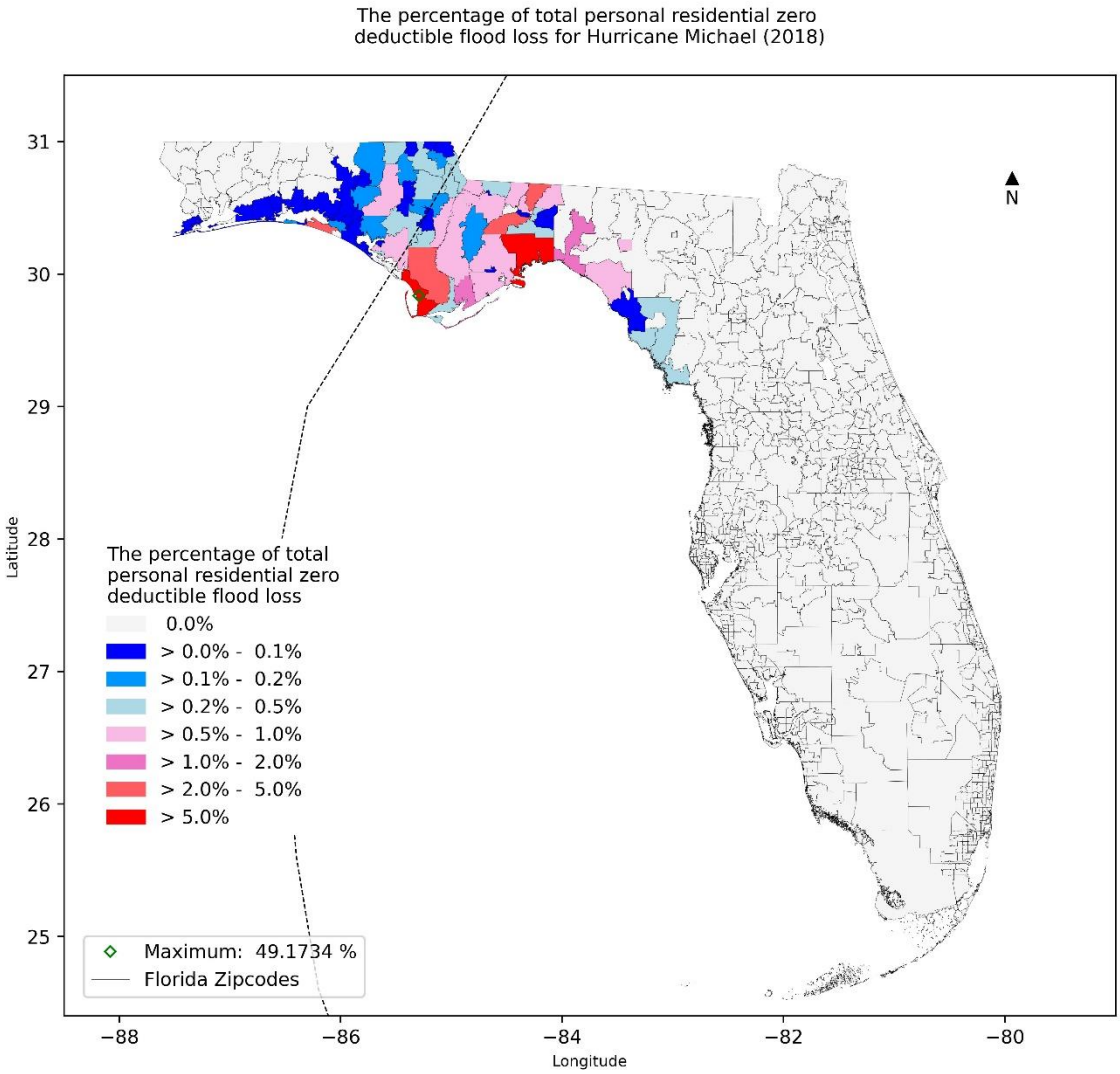

Figure 153: Percentage of total residential flood losses for Hurricane Michael (2018) by Zip Code

Form AF-4: Flood Output Ranges

A. One or more automated programs or scripts should be used to generate the personal residential flood output ranges in the format shown in the file named "2021FormAF4.xlsx."

An automated script is used to generate and arrange the data in Form AF-4.

B. Provide this form in Excel format. The file name should include the abbreviated name of the modeling organization, the flood standards year, and the form name. Also include Form AF-4, Flood Output Ranges, in a submission appendix.

C. Provide flood loss costs, rounded to three decimal places, by county (Figure 4). Within each county, flood loss costs should be shown separately per $1,000 of exposure for frame owners, masonry owners, frame renters, masonry renters, frame condo unit owners, masonry condo unit owners, and manufactured homes. For each of these categories using rating areas or geographic zones, the flood output range should show the highest flood loss cost, the lowest flood loss cost, and the weighted average flood loss cost. The aggregate personal residential exposure data for this form is to be developed from the modeling-organization-specified, predetermined, and comprehensive exposure dataset except for insured values and deductibles information. Insured values are to be based on the flood output range specifications given below. When calculating the weighted average flood loss costs, weight the flood loss costs by the total insured value calculated above. Include the statewide range of flood loss costs (i.e., low, high, and weighted average).

Form AF-4, Flood Output Ranges, is provided in Excel format in the file "IF2021FormAF4.xlsx" at the link provided to the FCHLPM and appears below in Table 51 (zero deductible), Table 52 (specified deductible), Table 53 (Time Element zero deductible), and Table 54 (Time Element specified deductible).

D. If a modeling organization has flood loss costs for a rating area or geographic zone for which there is no exposure, give the flood loss costs zero weight (i.e., assume the exposure in that rating area or geographic zone is zero). Provide a list in the flood model submission document of those rating areas or geographic zones where this occurs.

There are no instances of flood loss costs for a county for which there is no exposure.

E. If a modeling organization does not have flood loss costs for a rating area or geographic zone for which there is some exposure, do not assume such flood loss costs are zero, but use only the exposures for which there are flood loss costs in calculating the weighted average flood loss costs. Provide a list in the flood model submission document of the rating areas or geographic zones where this occurs.

There are no counties in which there is exposure and no loss cost.

F. NA should be used in cells to signify no exposure.

NA is used in the cells of Form AF-4 for which there is no exposure in Exposure Data.

G. Describe how Law and Ordinance is included in the flood output ranges.

The Impact Forecasting Flood model doesn't explicitly model the Law and Ordinance as FL Statute doesn't require Law and Ordinance for Flood policies.

H. If additional assumptions are necessary to complete this form, provide the rationale for the assumptions as well as a detailed description of how they are included.

No additional assumptions were made for this form.

Table 51: Standard Flood loss costs per $1,000 of exposure for 0% deductibles

County	Loss Costs	Frame Owners	Masonry Owners	Manufactured Homes	Frame Renters	Masonry Renters	Frame Condo Unit	Masonry Condo Unit
Alachua	LOW	0.000	0.000	0.000	0.002	0.001	0.001	0.001
	AVERAGE	1.153	0.798	1.194	0.232	1.029	0.226	0.988
	HIGH	87.286	61.192	106.603	6.935	28.575	6.798	27.465
Baker	LOW	0.001	0.001	0.000	0.077	NA	0.074	NA
	AVERAGE	1.366	0.441	2.645	0.282	NA	0.271	NA
	HIGH	67.558	15.119	127.985	0.486	NA	0.469	NA
Bay	LOW	0.000	0.000	0.000	0.000	0.000	0.000	0.000
	AVERAGE	0.423	0.404	0.686	0.185	1.058	0.184	1.050
	HIGH	73.626	51.543	92.100	19.575	7.637	19.254	7.590
Bradford	LOW	0.002	0.002	0.000	0.001	0.004	0.001	0.004
	AVERAGE	2.479	0.691	0.500	0.038	0.591	0.037	0.565
	HIGH	94.385	20.034	136.368	0.192	1.703	0.185	1.627
Brevard	LOW	0.000	0.000	0.000	0.000	0.000	0.000	0.000
	AVERAGE	0.416	0.434	0.121	0.759	0.641	0.741	0.623
	HIGH	84.262	67.651	76.384	44.983	29.760	44.178	28.640
Broward	LOW	0.000	0.000	0.000	0.000	0.000	0.000	0.000
	AVERAGE	0.532	0.362	0.190	0.298	0.328	0.298	0.318
	HIGH	29.049	129.045	3.444	5.819	35.521	5.836	34.584
Calhoun	LOW	0.000	0.001	0.000	NA	NA	NA	NA
	AVERAGE	1.848	2.162	4.799	NA	NA	NA	NA
	HIGH	101.463	129.972	195.789	NA	NA	NA	NA
Charlotte	LOW	0.000	0.000	0.000	0.000	0.000	0.000	0.000
	AVERAGE	3.594	3.518	8.468	1.965	1.478	1.961	1.470
	HIGH	57.700	140.493	120.078	9.980	11.064	9.990	11.051

County	Loss Costs	Frame Owners	Masonry Owners	Manufactured Homes	Frame Renters	Masonry Renters	Frame Condo Unit	Masonry Condo Unit
Citrus	LOW	0.001	0.000	0.000	0.027	0.000	0.027	0.000
	AVERAGE	5.120	5.519	7.787	3.202	4.113	3.194	4.077
	HIGH	89.124	105.724	154.179	15.776	45.105	15.721	44.763
Clay	LOW	0.000	0.000	0.000	0.000	0.000	0.000	0.000
	AVERAGE	1.011	0.355	1.081	0.090	0.107	0.087	0.103
	HIGH	151.307	77.267	152.556	4.584	1.610	4.441	1.539
Collier	LOW	0.000	0.000	0.000	0.000	0.044	0.000	0.043
	AVERAGE	7.290	0.262	30.958	5.851	1.349	5.839	1.338
	HIGH	344.040	5.630	155.344	109.475	53.471	109.587	53.118
Columbia	LOW	0.000	0.001	0.000	NA	NA	NA	NA
	AVERAGE	2.559	1.704	2.823	NA	NA	NA	NA
	HIGH	117.750	106.960	114.919	NA	NA	NA	NA
De Soto	LOW	0.000	0.000	0.000	0.002	0.000	0.002	0.000
	AVERAGE	1.299	1.471	0.581	0.151	0.086	0.145	0.085
	HIGH	42.542	53.582	24.482	0.604	9.903	0.579	9.916
Dixie	LOW	0.000	0.000	0.000	0.003	0.030	0.002	0.029
	AVERAGE	9.251	2.175	9.960	0.791	0.030	0.792	0.029
	HIGH	374.082	72.119	143.173	6.118	0.030	6.146	0.029
Duval	LOW	0.000	0.000	0.000	0.000	0.000	0.000	0.000
	AVERAGE	0.413	0.343	0.368	0.297	0.319	0.291	0.306
	HIGH	69.838	56.832	28.640	16.756	15.331	16.546	14.957
Escambia	LOW	0.035	0.000	0.000	0.000	0.000	0.000	0.000
	AVERAGE	1.336	1.046	0.871	0.634	0.852	0.630	0.821
	HIGH	106.297	96.192	66.559	36.590	43.318	36.356	41.670
Flagler	LOW	0.000	0.000	0.000	0.000	0.000	0.000	0.000
	AVERAGE	0.285	0.184	0.107	0.343	0.121	0.343	0.119
	HIGH	15.262	10.866	3.810	9.316	4.800	9.338	4.735

County	Loss Costs	Frame Owners	Masonry Owners	Manufactured Homes	Frame Renters	Masonry Renters	Frame Condo Unit	Masonry Condo Unit
Franklin	LOW	0.000	0.000	0.000	0.000	0.001	0.000	0.001
	AVERAGE	1.293	1.148	0.862	0.291	0.487	0.291	0.483
	HIGH	210.535	49.045	29.578	2.830	0.610	2.822	0.606
Gadsden	LOW	0.001	0.002	0.000	NA	NA	NA	NA
	AVERAGE	1.802	0.860	1.473	NA	NA	NA	NA
	HIGH	103.535	15.963	104.294	NA	NA	NA	NA
Gilchrist	LOW	0.000	0.000	0.000	0.011	0.003	0.011	0.003
	AVERAGE	2.569	0.781	2.112	0.460	0.003	0.444	0.003
	HIGH	89.779	21.668	145.153	1.323	0.003	1.278	0.003
Glades	LOW	0.001	0.001	0.000	0.002	0.115	0.002	0.110
	AVERAGE	0.272	0.086	0.054	0.092	0.140	0.089	0.133
	HIGH	8.117	1.882	10.646	0.550	0.164	0.530	0.156
Gulf	LOW	0.000	0.000	0.000	0.000	0.002	0.000	0.002
	AVERAGE	1.323	0.785	2.695	0.661	0.397	0.656	0.390
	HIGH	194.643	97.695	209.748	21.961	2.600	21.813	2.570
Hamilton	LOW	0.000	0.002	0.000	NA	0.002	NA	0.002
	AVERAGE	3.419	0.281	1.941	NA	0.118	NA	0.113
	HIGH	55.954	0.742	97.625	NA	0.951	NA	0.907
Hardee	LOW	0.000	0.000	0.000	NA	NA	NA	NA
	AVERAGE	1.377	0.564	0.182	NA	NA	NA	NA
	HIGH	81.654	31.465	21.081	NA	NA	NA	NA
Hendry	LOW	0.001	0.001	0.000	0.001	0.002	0.001	0.002
	AVERAGE	0.265	0.226	0.012	0.090	0.216	0.086	0.206
	HIGH	12.756	108.868	6.052	1.075	5.588	1.039	5.348
Hernando	LOW	0.000	0.000	0.000	0.000	0.000	0.000	0.000
	AVERAGE	3.874	1.345	4.690	0.407	0.382	0.401	0.370
	HIGH	92.922	81.998	111.763	13.776	7.771	13.796	7.725
Highlands	LOW	0.001	0.001	0.000	0.001	0.001	0.001	0.001
	AVERAGE	2.877	1.193	0.298	3.102	3.276	3.032	3.142

County	Loss Costs	Frame Owners	Masonry Owners	Manufactured Homes	Frame Renters	Masonry Renters	Frame Condo Unit	Masonry Condo Unit
	HIGH	105.126	93.581	24.299	30.881	25.857	30.366	24.825
Hillsborough	LOW	0.000	0.000	0.000	0.000	0.000	0.000	0.000
	AVERAGE	1.111	0.813	1.587	0.477	0.676	0.471	0.659
	HIGH	130.057	190.581	109.259	9.987	21.608	9.798	20.753
Holmes	LOW	0.000	0.000	0.000	NA	NA	NA	NA
	AVERAGE	1.450	1.800	1.090	NA	NA	NA	NA
	HIGH	85.135	48.327	96.101	NA	NA	NA	NA
Indian River	LOW	0.000	0.000	0.000	0.000	0.000	0.000	0.000
	AVERAGE	0.233	0.176	0.232	0.091	0.101	0.088	0.098
	HIGH	165.247	39.231	63.734	4.813	5.271	4.749	5.044
Jackson	LOW	0.000	0.001	0.000	0.033	0.006	0.032	0.005
	AVERAGE	1.634	0.936	1.065	0.232	0.240	0.223	0.229
	HIGH	51.573	37.282	106.764	0.484	0.569	0.467	0.543
Jefferson	LOW	0.000	0.002	0.000	0.013	0.083	0.013	0.079
	AVERAGE	6.957	4.693	4.555	0.356	0.214	0.344	0.204
	HIGH	89.024	50.822	109.157	0.912	0.341	0.879	0.325
Lafayette	LOW	0.001	0.002	0.000	NA	NA	NA	NA
	AVERAGE	3.006	0.908	2.333	NA	NA	NA	NA
	HIGH	130.620	41.486	94.616	NA	NA	NA	NA
Lake	LOW	0.000	0.000	0.000	0.001	0.002	0.001	0.002
	AVERAGE	2.251	0.919	1.395	0.736	1.176	0.718	1.147
	HIGH	151.542	41.179	154.305	42.882	2.731	42.164	2.657
Lee	LOW	0.000	0.000	0.000	0.000	0.000	0.000	0.000
	AVERAGE	5.549	8.841	17.180	4.084	4.177	4.089	4.158
	HIGH	353.672	156.715	333.806	108.207	61.631	108.655	61.517
Leon	LOW	0.000	0.001	0.000	0.000	0.003	0.000	0.003
	AVERAGE	1.440	0.067	1.990	0.670	0.928	0.658	0.891
	HIGH	119.025	0.616	154.522	48.535	10.625	47.859	10.231

County	Loss Costs	Frame Owners	Masonry Owners	Manufactured Homes	Frame Renters	Masonry Renters	Frame Condo Unit	Masonry Condo Unit
Levy	LOW	0.001	0.000	0.000	0.002	0.000	0.002	0.000
	AVERAGE	1.355	3.520	2.818	4.097	2.823	4.029	2.803
	HIGH	17.437	219.244	373.535	14.055	44.020	13.910	43.633
Liberty	LOW	0.001	0.002	0.000	NA	NA	NA	NA
	AVERAGE	2.373	0.986	2.779	NA	NA	NA	NA
	HIGH	70.126	13.740	120.276	NA	NA	NA	NA
Madison	LOW	0.002	0.002	0.000	0.002	0.622	0.002	0.594
	AVERAGE	1.373	0.928	1.372	0.397	0.622	0.385	0.594
	HIGH	34.440	15.596	103.189	2.402	0.622	2.352	0.594
Manatee	LOW	0.000	0.000	0.000	0.000	0.000	0.000	0.000
	AVERAGE	1.085	0.587	2.126	0.416	0.429	0.415	0.422
	HIGH	42.509	30.506	48.021	15.031	10.637	15.018	10.566
Marion	LOW	0.000	0.000	0.000	0.001	0.001	0.001	0.001
	AVERAGE	1.751	1.262	1.674	0.980	0.677	0.960	0.649
	HIGH	149.815	107.123	120.538	46.551	14.364	46.051	13.760
Martin	LOW	0.000	0.000	0.000	0.000	0.000	0.000	0.000
	AVERAGE	0.761	0.325	1.155	0.438	0.149	0.426	0.145
	HIGH	82.774	63.499	55.872	15.543	11.505	15.344	11.428
Miami-Dade	LOW	0.000	0.000	0.000	0.000	0.000	0.000	0.000
	AVERAGE	0.695	0.942	1.001	0.038	0.443	0.037	0.433
	HIGH	9.058	62.771	85.815	6.195	62.316	6.141	61.856
Monroe	LOW	0.000	0.000	0.000	0.000	0.000	0.000	0.000
	AVERAGE	1.762	2.396	15.788	0.720	0.427	0.724	0.425
	HIGH	116.079	114.333	140.338	15.153	13.629	15.117	13.561
Nassau	LOW	0.000	0.000	0.000	0.000	0.000	0.000	0.000
	AVERAGE	0.317	0.284	0.341	0.261	0.066	0.258	0.065
	HIGH	39.507	9.811	22.061	2.843	1.757	2.796	1.719
Okaloosa	LOW	0.000	0.000	0.000	0.000	0.000	0.000	0.000

County	Loss Costs	Frame Owners	Masonry Owners	Manufactured Homes	Frame Renters	Masonry Renters	Frame Condo Unit	Masonry Condo Unit
	AVERAGE	7.331	7.825	1.222	5.213	7.769	5.256	7.809
	HIGH	131.810	119.950	95.415	75.279	81.285	76.058	82.106
Okeechobee	LOW	0.000	0.001	0.000	0.001	0.001	0.001	0.001
	AVERAGE	0.241	0.131	0.109	0.185	0.100	0.179	0.096
	HIGH	9.029	3.740	129.832	2.120	3.436	2.051	3.278
Orange	LOW	0.000	0.000	0.000	0.001	0.001	0.001	0.001
	AVERAGE	2.034	0.945	0.617	0.450	0.817	0.437	0.784
	HIGH	168.007	167.276	48.250	58.003	86.055	57.131	83.916
Osceola	LOW	0.000	0.000	0.000	0.001	0.001	0.001	0.001
	AVERAGE	0.752	0.510	0.145	0.272	0.341	0.264	0.326
	HIGH	99.961	82.530	20.726	7.633	5.551	7.414	5.316
Palm Beach	LOW	0.000	0.000	0.000	0.000	0.000	0.000	0.000
	AVERAGE	0.268	0.196	0.072	0.834	0.662	0.821	0.635
	HIGH	101.522	234.937	35.794	10.168	41.637	9.977	40.087
Pasco	LOW	0.000	0.000	0.000	0.000	0.000	0.000	0.000
	AVERAGE	1.429	1.085	2.727	0.413	0.697	0.406	0.688
	HIGH	220.687	83.490	150.347	11.216	16.919	11.112	16.841
Pinellas	LOW	0.000	0.000	0.000	0.000	0.000	0.000	0.000
	AVERAGE	1.559	1.434	2.411	1.223	2.050	1.223	2.011
	HIGH	197.620	142.321	83.526	98.152	52.792	99.027	52.499
Polk	LOW	0.000	0.000	0.000	0.000	0.001	0.000	0.001
	AVERAGE	1.578	0.750	0.795	0.270	0.246	0.263	0.235
	HIGH	150.785	109.726	135.459	4.840	10.032	4.764	9.670
Putnam	LOW	0.000	0.000	0.000	0.000	0.000	0.000	0.000
	AVERAGE	0.731	0.425	0.474	0.319	0.061	0.312	0.058
	HIGH	46.161	15.201	84.546	7.216	0.736	7.057	0.702

County	Loss Costs	Frame Owners	Masonry Owners	Manufactured Homes	Frame Renters	Masonry Renters	Frame Condo Unit	Masonry Condo Unit
Santa Rosa	LOW	0.000	0.000	0.000	0.000	0.001	0.000	0.001
	AVERAGE	1.307	5.002	1.414	1.455	2.226	1.419	2.154
	HIGH	107.548	96.452	106.372	25.369	53.828	24.890	52.266
Sarasota	LOW	0.000	0.000	0.000	0.000	0.000	0.000	0.000
	AVERAGE	1.871	0.750	4.668	0.329	0.580	0.328	0.572
	HIGH	105.726	42.163	46.476	6.651	13.759	6.659	13.199
Seminole	LOW	0.000	0.000	0.000	0.001	0.001	0.001	0.001
	AVERAGE	0.523	0.388	0.099	0.345	0.438	0.334	0.420
	HIGH	61.874	91.294	8.167	5.360	8.594	5.208	8.253
St. Johns	LOW	0.000	0.000	0.000	0.000	0.000	0.000	0.000
	AVERAGE	0.432	0.432	0.327	0.285	0.157	0.283	0.155
	HIGH	332.290	95.287	35.212	26.034	49.635	26.568	49.482
St. Lucie	LOW	0.000	0.000	0.000	0.170	0.001	0.163	0.001
	AVERAGE	0.279	0.315	1.564	1.301	1.052	1.256	1.033
	HIGH	37.490	58.118	65.262	3.260	14.756	3.151	14.478
Sumter	LOW	0.000	0.000	0.000	0.028	0.001	0.027	0.001
	AVERAGE	0.390	0.324	0.275	0.116	0.275	0.112	0.262
	HIGH	28.157	18.773	23.208	0.341	3.077	0.331	2.952
Suwannee	LOW	0.000	0.000	0.000	0.004	0.049	0.004	0.046
	AVERAGE	2.980	1.438	2.016	0.592	12.436	0.573	12.029
	HIGH	139.374	57.733	129.414	2.783	47.934	2.688	46.478
Taylor	LOW	0.000	0.000	0.000	0.002	0.004	0.002	0.003
	AVERAGE	5.430	1.698	4.989	2.116	0.034	2.118	0.033
	HIGH	223.054	59.377	183.810	20.933	0.068	20.888	0.067
Union	LOW	0.002	0.002	0.000	0.014	0.005	0.013	0.004
	AVERAGE	1.349	0.344	0.401	0.177	0.107	0.171	0.102
	HIGH	53.103	4.163	32.046	0.611	0.210	0.590	0.200

County	Loss Costs	Frame Owners	Masonry Owners	Manufactured Homes	Frame Renters	Masonry Renters	Frame Condo Unit	Masonry Condo Unit
Volusia	LOW	0.000	0.000	0.000	0.000	0.000	0.000	0.000
	AVERAGE	0.589	0.327	0.420	0.254	0.100	0.250	0.097
	HIGH	85.745	59.748	66.808	24.341	27.619	23.998	26.799
Wakulla	LOW	0.000	0.000	0.000	0.002	0.226	0.002	0.226
	AVERAGE	4.317	10.627	5.773	1.255	0.802	1.260	0.801
	HIGH	213.146	91.554	168.068	7.364	3.361	7.407	3.358
Walton	LOW	0.000	0.000	0.000	0.000	0.000	0.000	0.000
	AVERAGE	0.913	0.591	4.084	0.164	0.043	0.162	0.041
	HIGH	80.664	17.166	65.164	7.884	2.278	7.769	2.181
Washington	LOW	0.000	0.001	0.000	0.325	NA	0.321	NA
	AVERAGE	1.962	0.823	1.952	1.076	NA	1.051	NA
	HIGH	64.823	33.075	72.096	1.827	NA	1.781	NA
Statewide	LOW	0.000	0.000	0.000	0.000	0.000	0.000	0.000
	AVERAGE	2.529	1.408	4.655	2.789	0.617	2.786	0.603
	HIGH	374.082	234.937	373.535	109.475	86.055	109.587	83.916

Table 52:Standard Flood loss costs per $1,000 of exposure for specified deductibles

County	Loss Costs	Frame Owners	Masonry Owners	Manufactured Homes	Frame Renters	Masonry Renters	Frame Condo Unit	Masonry Condo Unit
Alachua	LOW	0.000	0.000	0.000	0.001	0.001	0.001	0.001
	AVERAGE	1.053	0.696	1.101	0.216	0.961	0.218	0.946
	HIGH	83.207	57.801	100.814	6.526	26.930	6.548	26.318
Baker	LOW	0.001	0.001	0.000	0.071	NA	0.071	NA
	AVERAGE	1.266	0.385	2.472	0.259	NA	0.261	NA
	HIGH	64.401	13.704	123.021	0.448	NA	0.451	NA
Bay	LOW	0.000	0.000	0.000	0.000	0.000	0.000	0.000
	AVERAGE	0.385	0.368	0.634	0.173	0.997	0.177	1.015
	HIGH	70.848	48.978	88.409	18.509	7.227	18.695	7.353

County	Loss Costs	Frame Owners	Masonry Owners	Manufactured Homes	Frame Renters	Masonry Renters	Frame Condo Unit	Masonry Condo Unit
Bradford	LOW	0.001	0.001	0.000	0.001	0.004	0.001	0.004
	AVERAGE	2.284	0.590	0.467	0.035	0.543	0.036	0.542
	HIGH	90.270	17.658	129.490	0.177	1.567	0.178	1.563
Brevard	LOW	0.000	0.000	0.000	0.000	0.000	0.000	0.000
	AVERAGE	0.378	0.395	0.107	0.704	0.599	0.711	0.600
	HIGH	80.642	64.237	70.579	43.071	28.103	42.921	27.561
Broward	LOW	0.000	0.000	0.000	0.000	0.000	0.000	0.000
	AVERAGE	0.485	0.318	0.158	0.276	0.303	0.287	0.305
	HIGH	27.288	120.589	3.003	5.449	33.157	5.642	32.940
Calhoun	LOW	0.000	0.001	0.000	NA	NA	NA	NA
	AVERAGE	1.710	2.010	4.617	NA	NA	NA	NA
	HIGH	97.881	125.337	190.954	NA	NA	NA	NA
Charlotte	LOW	0.000	0.000	0.000	0.000	0.000	0.000	0.000
	AVERAGE	3.331	3.255	7.572	1.831	1.377	1.866	1.402
	HIGH	54.976	131.769	111.429	9.418	10.446	9.563	10.580
Citrus	LOW	0.001	0.000	0.000	0.026	0.000	0.026	0.000
	AVERAGE	4.848	5.137	7.305	2.993	3.883	3.083	3.943
	HIGH	85.427	99.856	144.505	14.616	42.889	15.180	43.519
Clay	LOW	0.000	0.000	0.000	0.000	0.000	0.000	0.000
	AVERAGE	0.937	0.311	0.992	0.083	0.099	0.083	0.099
	HIGH	142.718	73.045	144.453	4.210	1.485	4.266	1.480
Collier	LOW	0.000	0.000	0.000	0.000	0.040	0.000	0.042
	AVERAGE	6.827	0.243	28.165	5.508	1.267	5.612	1.285
	HIGH	324.514	5.150	145.432	103.697	50.437	106.017	51.178
Columbia	LOW	0.000	0.001	0.000	NA	NA	NA	NA
	AVERAGE	2.369	1.544	2.647	NA	NA	NA	NA
	HIGH	111.838	101.635	109.890	NA	NA	NA	NA

County	Loss Costs	Frame Owners	Masonry Owners	Manufactured Homes	Frame Renters	Masonry Renters	Frame Condo Unit	Masonry Condo Unit
De Soto	LOW	0.000	0.000	0.000	0.002	0.000	0.002	0.000
	AVERAGE	1.180	1.336	0.513	0.135	0.080	0.137	0.081
	HIGH	40.025	49.383	21.977	0.534	9.347	0.547	9.460
Dixie	LOW	0.000	0.000	0.000	0.002	0.028	0.002	0.028
	AVERAGE	8.794	2.028	9.518	0.739	0.028	0.762	0.028
	HIGH	358.500	68.546	137.941	5.792	0.028	5.938	0.028
Duval	LOW	0.000	0.000	0.000	0.000	0.000	0.000	0.000
	AVERAGE	0.369	0.304	0.334	0.275	0.292	0.279	0.292
	HIGH	66.266	53.217	26.293	15.902	14.275	16.046	14.464
Escambia	LOW	0.030	0.000	0.000	0.000	0.000	0.000	0.000
	AVERAGE	1.235	0.941	0.799	0.591	0.813	0.608	0.797
	HIGH	101.209	92.639	63.179	35.321	41.517	35.512	40.477
Flagler	LOW	0.000	0.000	0.000	0.000	0.000	0.000	0.000
	AVERAGE	0.259	0.164	0.096	0.321	0.113	0.331	0.114
	HIGH	14.082	9.599	3.461	8.657	4.470	9.003	4.563
Franklin	LOW	0.000	0.000	0.000	0.000	0.001	0.000	0.001
	AVERAGE	1.223	1.084	0.823	0.272	0.459	0.281	0.469
	HIGH	200.762	46.770	28.462	2.670	0.576	2.727	0.588
Gadsden	LOW	0.001	0.001	0.000	NA	NA	NA	NA
	AVERAGE	1.655	0.736	1.392	NA	NA	NA	NA
	HIGH	99.709	14.750	100.678	NA	NA	NA	NA
Gilchrist	LOW	0.000	0.000	0.000	0.010	0.003	0.010	0.003
	AVERAGE	2.357	0.672	1.997	0.422	0.003	0.427	0.003
	HIGH	86.432	19.967	139.232	1.215	0.003	1.227	0.003
Glades	LOW	0.001	0.001	0.000	0.002	0.107	0.002	0.106
	AVERAGE	0.237	0.072	0.049	0.085	0.129	0.085	0.128
	HIGH	7.265	1.583	9.617	0.505	0.151	0.509	0.150
Gulf	LOW	0.000	0.000	0.000	0.000	0.002	0.000	0.002

County	Loss Costs	Frame Owners	Masonry Owners	Manufactured Homes	Frame Renters	Masonry Renters	Frame Condo Unit	Masonry Condo Unit
	AVERAGE	1.245	0.729	2.575	0.619	0.372	0.634	0.377
	HIGH	188.269	93.306	204.690	20.366	2.484	21.048	2.500
Hamilton	LOW	0.000	0.002	0.000	NA	0.002	NA	0.002
	AVERAGE	3.225	0.230	1.827	NA	0.108	NA	0.108
	HIGH	53.352	0.607	94.158	NA	0.863	NA	0.866
Hardee	LOW	0.000	0.000	0.000	NA	NA	NA	NA
	AVERAGE	1.253	0.489	0.166	NA	NA	NA	NA
	HIGH	77.225	28.926	18.874	NA	NA	NA	NA
Hendry	LOW	0.001	0.001	0.000	0.001	0.001	0.001	0.001
	AVERAGE	0.234	0.196	0.012	0.082	0.198	0.083	0.197
	HIGH	11.755	100.209	5.343	0.991	5.148	1.000	5.094
Hernando	LOW	0.000	0.000	0.000	0.000	0.000	0.000	0.000
	AVERAGE	3.621	1.226	4.318	0.386	0.356	0.390	0.356
	HIGH	88.167	77.466	103.373	13.106	7.386	13.396	7.492
Highlands	LOW	0.001	0.001	0.000	0.001	0.001	0.001	0.001
	AVERAGE	2.627	1.031	0.267	2.880	3.025	2.915	2.975
	HIGH	97.198	89.237	21.507	29.147	23.930	29.226	23.419
Hillsborough	LOW	0.000	0.000	0.000	0.000	0.000	0.000	0.000
	AVERAGE	1.024	0.742	1.421	0.446	0.627	0.453	0.631
	HIGH	121.583	178.206	100.520	9.363	20.150	9.448	19.718
Holmes	LOW	0.000	0.000	0.000	NA	NA	NA	NA
	AVERAGE	1.331	1.637	1.020	NA	NA	NA	NA
	HIGH	80.929	45.760	92.838	NA	NA	NA	NA
Indian River	LOW	0.000	0.000	0.000	0.000	0.000	0.000	0.000
	AVERAGE	0.210	0.154	0.208	0.084	0.093	0.085	0.094
	HIGH	156.870	36.921	57.938	4.470	4.861	4.588	4.844
Jackson	LOW	0.000	0.001	0.000	0.030	0.005	0.030	0.005
	AVERAGE	1.496	0.812	1.006	0.211	0.220	0.213	0.220
	HIGH	49.371	35.121	102.790	0.445	0.523	0.449	0.522

County	Loss Costs	Frame Owners	Masonry Owners	Manufactured Homes	Frame Renters	Masonry Renters	Frame Condo Unit	Masonry Condo Unit
Jefferson	LOW	0.000	0.001	0.000	0.012	0.076	0.012	0.076
	AVERAGE	6.577	4.411	4.353	0.328	0.197	0.331	0.196
	HIGH	84.881	48.435	105.070	0.836	0.313	0.844	0.312
Lafayette	LOW	0.001	0.001	0.000	NA	NA	NA	NA
	AVERAGE	2.817	0.822	2.218	NA	NA	NA	NA
	HIGH	125.670	39.314	91.540	NA	NA	NA	NA
Lake	LOW	0.000	0.000	0.000	0.001	0.002	0.001	0.002
	AVERAGE	2.067	0.822	1.258	0.682	1.095	0.692	1.107
	HIGH	141.059	37.767	144.195	40.938	2.540	40.871	2.564
Lee	LOW	0.000	0.000	0.000	0.000	0.000	0.000	0.000
	AVERAGE	5.174	8.209	15.481	3.805	3.906	3.911	3.981
	HIGH	336.776	146.232	318.874	103.038	58.652	105.227	59.358
Leon	LOW	0.000	0.000	0.000	0.000	0.003	0.000	0.003
	AVERAGE	1.322	0.057	1.875	0.625	0.866	0.635	0.855
	HIGH	115.145	0.511	150.097	46.954	9.995	46.936	9.840
Levy	LOW	0.001	0.000	0.000	0.002	0.000	0.002	0.000
	AVERAGE	1.214	3.281	2.641	3.829	2.649	3.885	2.710
	HIGH	15.822	207.188	363.631	13.228	41.237	13.429	42.196
Liberty	LOW	0.001	0.002	0.000	NA	NA	NA	NA
	AVERAGE	2.200	0.859	2.679	NA	NA	NA	NA
	HIGH	67.776	12.394	116.002	NA	NA	NA	NA
Madison	LOW	0.002	0.001	0.000	0.002	0.572	0.002	0.570
	AVERAGE	1.239	0.813	1.297	0.367	0.572	0.371	0.570
	HIGH	32.678	14.168	99.215	2.257	0.572	2.268	0.570
Manatee	LOW	0.000	0.000	0.000	0.000	0.000	0.000	0.000
	AVERAGE	1.011	0.542	1.916	0.390	0.400	0.400	0.405
	HIGH	40.389	28.570	44.601	14.244	10.065	14.523	10.187
Marion	LOW	0.000	0.000	0.000	0.001	0.001	0.001	0.001

County	Loss Costs	Frame Owners	Masonry Owners	Manufactured Homes	Frame Renters	Masonry Renters	Frame Condo Unit	Masonry Condo Unit
	AVERAGE	1.602	1.119	1.501	0.913	0.623	0.924	0.617
	HIGH	140.301	101.531	112.575	44.503	13.236	44.619	13.195
Martin	LOW	0.000	0.000	0.000	0.000	0.000	0.000	0.000
	AVERAGE	0.694	0.282	1.003	0.405	0.138	0.410	0.139
	HIGH	78.829	60.169	49.946	14.614	10.786	14.764	11.018
Miami-Dade	LOW	0.000	0.000	0.000	0.000	0.000	0.000	0.000
	AVERAGE	0.646	0.860	0.901	0.035	0.412	0.036	0.416
	HIGH	8.551	58.745	77.514	5.777	59.059	5.921	59.196
Monroe	LOW	0.000	0.000	0.000	0.000	0.000	0.000	0.000
	AVERAGE	1.643	2.233	14.489	0.676	0.400	0.694	0.408
	HIGH	109.978	108.123	131.423	14.376	12.908	14.579	13.106
Nassau	LOW	0.000	0.000	0.000	0.000	0.000	0.000	0.000
	AVERAGE	0.290	0.254	0.309	0.241	0.061	0.247	0.062
	HIGH	36.358	8.747	20.330	2.652	1.644	2.694	1.656
Okaloosa	LOW	0.000	0.000	0.000	0.000	0.000	0.000	0.000
	AVERAGE	6.942	7.429	1.150	5.015	7.498	5.110	7.613
	HIGH	124.880	113.898	91.486	71.700	77.326	72.784	78.382
Okeechobee	LOW	0.000	0.001	0.000	0.001	0.001	0.001	0.001
	AVERAGE	0.208	0.110	0.099	0.169	0.092	0.171	0.092
	HIGH	7.962	3.093	119.095	1.944	3.134	1.969	3.137
Orange	LOW	0.000	0.000	0.000	0.001	0.000	0.001	0.000
	AVERAGE	1.870	0.859	0.543	0.415	0.759	0.420	0.749
	HIGH	155.438	154.707	43.270	55.067	81.590	55.149	80.427
Osceola	LOW	0.000	0.000	0.000	0.001	0.001	0.001	0.001
	AVERAGE	0.666	0.438	0.130	0.251	0.314	0.254	0.313
	HIGH	95.138	77.752	18.077	7.050	5.127	7.131	5.106
Palm Beach	LOW	0.000	0.000	0.000	0.000	0.000	0.000	0.000

County	Loss Costs	Frame Owners	Masonry Owners	Manufactured Homes	Frame Renters	Masonry Renters	Frame Condo Unit	Masonry Condo Unit
	AVERAGE	0.235	0.167	0.065	0.775	0.611	0.792	0.608
	HIGH	93.639	223.743	31.839	9.428	39.165	9.593	38.234
Pasco	LOW	0.000	0.000	0.000	0.000	0.000	0.000	0.000
	AVERAGE	1.330	1.009	2.514	0.383	0.657	0.390	0.665
	HIGH	210.949	78.382	141.168	10.149	16.072	10.610	16.326
Pinellas	LOW	0.000	0.000	0.000	0.000	0.000	0.000	0.000
	AVERAGE	1.445	1.322	2.199	1.150	1.917	1.182	1.933
	HIGH	187.808	133.564	78.671	92.756	49.834	96.122	50.873
Polk	LOW	0.000	0.000	0.000	0.000	0.001	0.000	0.001
	AVERAGE	1.446	0.657	0.709	0.250	0.226	0.253	0.225
	HIGH	140.354	104.330	126.069	4.513	9.236	4.593	9.058
Putnam	LOW	0.000	0.000	0.000	0.000	0.000	0.000	0.000
	AVERAGE	0.655	0.362	0.430	0.293	0.056	0.300	0.056
	HIGH	43.549	13.536	78.246	6.651	0.675	6.783	0.674
Santa Rosa	LOW	0.000	0.000	0.000	0.000	0.001	0.000	0.001
	AVERAGE	1.207	4.700	1.320	1.354	2.132	1.371	2.096
	HIGH	101.986	93.253	101.618	24.124	51.810	24.151	50.870
Sarasota	LOW	0.000	0.000	0.000	0.000	0.000	0.000	0.000
	AVERAGE	1.742	0.694	4.134	0.307	0.542	0.315	0.549
	HIGH	99.273	39.279	42.823	6.262	12.817	6.409	12.547
Seminole	LOW	0.000	0.000	0.000	0.001	0.001	0.001	0.001
	AVERAGE	0.469	0.336	0.089	0.318	0.403	0.321	0.399
	HIGH	59.095	87.547	7.289	4.937	7.914	5.011	7.774
St. Johns	LOW	0.000	0.000	0.000	0.000	0.000	0.000	0.000
	AVERAGE	0.397	0.395	0.297	0.266	0.146	0.273	0.148
	HIGH	318.284	89.229	32.201	24.050	44.870	25.626	47.220
St. Lucie	LOW	0.000	0.000	0.000	0.151	0.001	0.154	0.001

County	Loss Costs	Frame Owners	Masonry Owners	Manufactured Homes	Frame Renters	Masonry Renters	Frame Condo Unit	Masonry Condo Unit
	AVERAGE	0.249	0.281	1.380	1.192	0.981	1.205	0.990
	HIGH	35.222	54.731	59.790	3.000	13.758	3.029	13.885
Sumter	LOW	0.000	0.000	0.000	0.026	0.001	0.026	0.001
	AVERAGE	0.349	0.276	0.245	0.107	0.252	0.108	0.251
	HIGH	26.247	17.024	20.456	0.314	2.827	0.318	2.785
Suwannee	LOW	0.000	0.000	0.000	0.004	0.045	0.004	0.045
	AVERAGE	2.786	1.289	1.904	0.545	11.927	0.551	11.720
	HIGH	134.055	55.158	125.356	2.550	46.217	2.579	45.407
Taylor	LOW	0.000	0.000	0.000	0.002	0.003	0.002	0.003
	AVERAGE	5.132	1.573	4.776	1.998	0.032	2.046	0.032
	HIGH	213.195	55.951	177.926	19.819	0.064	20.289	0.065
Union	LOW	0.002	0.002	0.000	0.013	0.004	0.013	0.004
	AVERAGE	1.215	0.285	0.371	0.162	0.099	0.164	0.098
	HIGH	50.079	3.436	29.787	0.558	0.193	0.566	0.192
Volusia	LOW	0.000	0.000	0.000	0.000	0.000	0.000	0.000
	AVERAGE	0.537	0.286	0.373	0.235	0.092	0.240	0.092
	HIGH	81.356	55.463	62.413	22.995	25.796	23.062	25.422
Wakulla	LOW	0.000	0.000	0.000	0.002	0.214	0.002	0.219
	AVERAGE	4.090	10.097	5.506	1.171	0.748	1.213	0.771
	HIGH	203.301	87.260	162.406	6.903	3.129	7.141	3.233
Walton	LOW	0.000	0.000	0.000	0.000	0.000	0.000	0.000
	AVERAGE	0.843	0.523	3.868	0.152	0.040	0.156	0.040
	HIGH	77.129	15.934	62.224	7.225	2.093	7.459	2.091
Washington	LOW	0.000	0.001	0.000	0.303	NA	0.311	NA
	AVERAGE	1.817	0.724	1.836	0.985	NA	1.009	NA
	HIGH	61.591	30.955	69.098	1.667	NA	1.707	NA
Statewide	LOW	0.000	0.000	0.000	0.000	0.000	0.000	0.000
	AVERAGE	2.357	1.295	4.239	2.619	0.574	2.677	0.578

County	Loss Costs	Frame Owners	Masonry Owners	Manufactured Homes	Frame Renters	Masonry Renters	Frame Condo Unit	Masonry Condo Unit
	HIGH	358.500	223.743	363.631	103.697	81.590	106.017	80.427

Table 53: Standard Flood Time Element loss costs per $1,000 of exposure for 0% deductibles

County	Loss Costs	Frame Owners	Masonry Owners	Manufactured Homes	Frame Renters	Masonry Renters	Frame Condo Unit	Masonry Condo Unit
Alachua	LOW	0.001	0.000	0.000	0.001	0.000	0.001	0.000
	AVERAGE	0.651	0.529	0.566	0.099	0.391	0.099	0.391
	HIGH	50.942	35.249	43.437	2.933	10.150	2.933	10.150
Baker	LOW	0.001	0.001	0.000	0.032	NA	0.032	NA
	AVERAGE	0.767	0.319	1.130	0.117	NA	0.117	NA
	HIGH	34.747	9.471	50.098	0.202	NA	0.202	NA
Bay	LOW	0.000	0.000	0.000	0.000	0.000	0.000	0.000
	AVERAGE	0.241	0.212	0.293	0.172	0.444	0.172	0.444
	HIGH	39.166	30.027	35.527	8.527	3.230	8.527	3.230
Bradford	LOW	0.001	0.001	0.000	0.001	0.002	0.001	0.002
	AVERAGE	1.332	0.462	0.317	0.015	0.226	0.015	0.226
	HIGH	49.510	13.492	51.610	0.073	0.641	0.073	0.641
Brevard	LOW	0.000	0.000	0.000	0.000	0.000	0.000	0.000
	AVERAGE	0.233	0.237	0.085	0.324	0.287	0.324	0.287
	HIGH	49.147	41.771	27.488	18.936	10.888	18.936	10.888
Broward	LOW	0.000	0.000	0.000	0.000	0.000	0.000	0.000
	AVERAGE	0.276	0.213	0.105	0.148	0.137	0.148	0.137
	HIGH	13.848	57.230	1.834	2.764	13.755	2.764	13.755
Calhoun	LOW	0.001	0.001	0.000	NA	NA	NA	NA
	AVERAGE	1.070	1.499	1.900	NA	NA	NA	NA
	HIGH	55.216	74.783	75.490	NA	NA	NA	NA
Charlotte	LOW	0.000	0.000	0.000	0.000	0.000	0.000	0.000
	AVERAGE	1.950	1.793	3.114	1.160	0.737	1.160	0.737
	HIGH	29.480	67.832	44.843	5.324	5.497	5.324	5.497

County	Loss Costs	Frame Owners	Masonry Owners	Manufactured Homes	Frame Renters	Masonry Renters	Frame Condo Unit	Masonry Condo Unit
Citrus	LOW	0.001	0.000	0.000	0.013	0.000	0.013	0.000
	AVERAGE	2.802	3.018	2.978	1.739	1.928	1.739	1.928
	HIGH	48.534	52.161	65.730	7.103	20.016	7.103	20.016
Clay	LOW	0.000	0.000	0.000	0.000	0.000	0.000	0.000
	AVERAGE	0.611	0.238	0.492	0.042	0.043	0.042	0.043
	HIGH	93.033	44.350	65.060	1.825	0.586	1.825	0.586
Collier	LOW	0.000	0.000	0.000	0.000	0.020	0.000	0.020
	AVERAGE	3.648	0.125	11.297	2.856	0.586	2.856	0.586
	HIGH	176.177	2.866	56.200	55.682	24.364	55.682	24.364
Columbia	LOW	0.001	0.001	0.000	NA	NA	NA	NA
	AVERAGE	1.463	1.070	1.234	NA	NA	NA	NA
	HIGH	67.400	58.922	48.026	NA	NA	NA	NA
De Soto	LOW	0.000	0.000	0.000	0.001	0.000	0.001	0.000
	AVERAGE	0.754	0.792	0.256	0.075	0.042	0.075	0.042
	HIGH	22.322	27.841	9.538	0.296	5.181	0.296	5.181
Dixie	LOW	0.000	0.000	0.000	0.001	0.012	0.001	0.012
	AVERAGE	5.064	1.149	3.639	0.996	0.012	0.996	0.012
	HIGH	186.818	34.166	51.269	6.114	0.012	6.114	0.012
Duval	LOW	0.000	0.000	0.000	0.000	0.000	0.000	0.000
	AVERAGE	0.236	0.208	0.176	0.159	0.138	0.159	0.138
	HIGH	38.555	32.998	11.504	7.755	8.532	7.755	8.532
Escambia	LOW	0.021	0.000	0.000	0.000	0.000	0.000	0.000
	AVERAGE	0.754	0.672	0.396	0.314	0.310	0.314	0.310
	HIGH	64.389	58.031	25.159	21.561	14.984	21.561	14.984
Flagler	LOW	0.000	0.000	0.000	0.000	0.000	0.000	0.000
	AVERAGE	0.156	0.107	0.061	0.182	0.051	0.182	0.051
	HIGH	8.160	6.240	1.630	4.600	2.007	4.600	2.007
Franklin	LOW	0.000	0.000	0.000	0.000	0.000	0.000	0.000
	AVERAGE	0.801	0.571	0.318	0.364	0.195	0.364	0.195
	HIGH	102.095	23.685	10.030	3.729	0.244	3.729	0.244

County	Loss Costs	Frame Owners	Masonry Owners	Manufactured Homes	Frame Renters	Masonry Renters	Frame Condo Unit	Masonry Condo Unit
Gadsden	LOW	0.001	0.001	0.000	NA	NA	NA	NA
	AVERAGE	1.003	0.565	0.688	NA	NA	NA	NA
	HIGH	62.932	9.509	42.425	NA	NA	NA	NA
Gilchrist	LOW	0.000	0.000	0.000	0.005	0.002	0.005	0.002
	AVERAGE	1.487	0.517	0.903	0.183	0.002	0.183	0.002
	HIGH	44.578	15.394	59.782	0.527	0.002	0.527	0.002
Glades	LOW	0.001	0.001	0.000	0.001	0.043	0.001	0.043
	AVERAGE	0.165	0.062	0.059	0.040	0.057	0.040	0.057
	HIGH	4.544	1.295	4.967	0.217	0.071	0.217	0.071
Gulf	LOW	0.000	0.000	0.000	0.000	0.001	0.000	0.001
	AVERAGE	0.735	0.435	1.083	0.321	0.168	0.321	0.168
	HIGH	118.229	55.390	83.275	9.941	1.093	9.941	1.093
Hamilton	LOW	0.000	0.002	0.000	NA	0.001	NA	0.001
	AVERAGE	1.872	0.189	0.839	NA	0.059	NA	0.059
	HIGH	29.880	0.496	35.938	NA	0.371	NA	0.371
Hardee	LOW	0.001	0.001	0.000	NA	NA	NA	NA
	AVERAGE	0.775	0.375	0.160	NA	NA	NA	NA
	HIGH	42.209	18.581	8.081	NA	NA	NA	NA
Hendry	LOW	0.001	0.001	0.000	0.001	0.001	0.001	0.001
	AVERAGE	0.157	0.153	0.039	0.039	0.087	0.039	0.087
	HIGH	6.527	63.480	2.768	0.418	1.966	0.418	1.966
Hernando	LOW	0.000	0.000	0.000	0.000	0.000	0.000	0.000
	AVERAGE	2.270	0.751	1.820	0.251	0.153	0.251	0.153
	HIGH	47.154	39.250	46.819	6.976	3.400	6.976	3.400
Highlands	LOW	0.001	0.001	0.000	0.001	0.001	0.001	0.001
	AVERAGE	1.621	0.788	0.201	1.266	1.183	1.266	1.183
	HIGH	64.173	57.042	9.982	13.066	9.139	13.066	9.139
Hillsborough	LOW	0.000	0.000	0.000	0.000	0.000	0.000	0.000
	AVERAGE	0.608	0.454	0.629	0.253	0.296	0.253	0.296

County	Loss Costs	Frame Owners	Masonry Owners	Manufactured Homes	Frame Renters	Masonry Renters	Frame Condo Unit	Masonry Condo Unit
	HIGH	70.903	106.149	41.718	9.875	7.650	9.875	7.650
Holmes	LOW	0.001	0.002	0.000	NA	NA	NA	NA
	AVERAGE	0.822	1.144	0.507	NA	NA	NA	NA
	HIGH	42.355	28.454	37.909	NA	NA	NA	NA
Indian River	LOW	0.000	0.000	0.000	0.000	0.000	0.000	0.000
	AVERAGE	0.136	0.110	0.137	0.042	0.049	0.042	0.049
	HIGH	76.858	17.412	25.855	2.035	1.996	2.035	1.996
Jackson	LOW	0.001	0.001	0.000	0.018	0.003	0.018	0.003
	AVERAGE	0.898	0.610	0.513	0.123	0.092	0.123	0.092
	HIGH	26.967	22.460	44.168	0.204	0.205	0.204	0.205
Jefferson	LOW	0.001	0.001	0.000	0.007	0.046	0.007	0.046
	AVERAGE	4.121	2.424	1.797	0.147	0.099	0.147	0.099
	HIGH	46.904	25.112	40.431	0.368	0.137	0.368	0.137
Lafayette	LOW	0.001	0.001	0.000	NA	NA	NA	NA
	AVERAGE	1.788	0.652	0.968	NA	NA	NA	NA
	HIGH	74.536	24.075	37.692	NA	NA	NA	NA
Lake	LOW	0.000	0.000	0.000	0.001	0.001	0.001	0.001
	AVERAGE	1.272	0.575	0.632	0.306	0.544	0.306	0.544
	HIGH	93.216	24.420	65.827	17.920	1.092	17.920	1.092
Lee	LOW	0.000	0.000	0.000	0.000	0.000	0.000	0.000
	AVERAGE	2.994	4.293	6.243	2.157	1.966	2.157	1.966
	HIGH	186.551	78.133	125.564	59.302	30.613	59.302	30.613
Leon	LOW	0.000	0.001	0.000	0.001	0.001	0.001	0.001
	AVERAGE	0.803	0.046	0.841	0.304	0.357	0.304	0.357
	HIGH	70.360	0.422	61.868	24.490	4.111	24.490	4.111
Levy	LOW	0.001	0.000	0.000	0.001	0.001	0.001	0.001
	AVERAGE	0.868	1.909	1.103	1.782	1.456	1.782	1.456
	HIGH	10.926	100.629	127.850	6.366	19.523	6.366	19.523
Liberty	LOW	0.001	0.002	0.000	NA	NA	NA	NA

County	Loss Costs	Frame Owners	Masonry Owners	Manufactured Homes	Frame Renters	Masonry Renters	Frame Condo Unit	Masonry Condo Unit
	AVERAGE	1.449	0.765	1.211	NA	NA	NA	NA
	HIGH	39.572	10.086	50.828	NA	NA	NA	NA
Madison	LOW	0.001	0.001	0.000	0.001	0.237	0.001	0.237
	AVERAGE	0.751	0.702	0.657	0.159	0.237	0.159	0.237
	HIGH	17.087	10.570	41.938	1.011	0.237	1.011	0.237
Manatee	LOW	0.000	0.000	0.000	0.000	0.000	0.000	0.000
	AVERAGE	0.590	0.309	0.753	0.222	0.215	0.222	0.215
	HIGH	21.994	14.321	17.291	7.424	4.533	7.424	4.533
Marion	LOW	0.000	0.000	0.000	0.001	0.001	0.001	0.001
	AVERAGE	0.959	0.803	0.747	0.435	0.266	0.435	0.266
	HIGH	91.976	63.069	45.910	22.573	5.605	22.573	5.605
Martin	LOW	0.000	0.000	0.000	0.000	0.000	0.000	0.000
	AVERAGE	0.418	0.211	0.471	0.184	0.062	0.184	0.062
	HIGH	38.099	26.596	21.030	6.835	4.604	6.835	4.604
Miami-Dade	LOW	0.000	0.000	0.000	0.000	0.000	0.000	0.000
	AVERAGE	0.347	0.482	0.444	0.036	0.188	0.036	0.188
	HIGH	4.483	35.556	32.118	2.882	34.895	2.882	34.895
Monroe	LOW	0.000	0.000	0.000	0.000	0.000	0.000	0.000
	AVERAGE	1.419	1.473	5.515	0.567	0.366	0.567	0.366
	HIGH	53.955	52.920	51.191	12.037	6.074	12.037	6.074
Nassau	LOW	0.000	0.000	0.000	0.000	0.000	0.000	0.000
	AVERAGE	0.171	0.165	0.157	0.125	0.032	0.125	0.032
	HIGH	19.162	6.098	8.336	1.243	0.724	1.243	0.724
Okaloosa	LOW	0.000	0.000	0.000	0.000	0.000	0.000	0.000
	AVERAGE	3.886	4.355	0.541	3.193	4.136	3.193	4.136
	HIGH	76.464	67.034	37.613	46.574	50.387	46.574	50.387
Okeechobee	LOW	0.000	0.001	0.000	0.001	0.001	0.001	0.001
	AVERAGE	0.148	0.096	0.081	0.079	0.040	0.079	0.040
	HIGH	5.242	2.484	49.829	0.839	1.344	0.839	1.344

County	Loss Costs	Frame Owners	Masonry Owners	Manufactured Homes	Frame Renters	Masonry Renters	Frame Condo Unit	Masonry Condo Unit
Orange	LOW	0.000	0.000	0.000	0.001	0.000	0.001	0.000
	AVERAGE	1.170	0.606	0.296	0.189	0.313	0.189	0.313
	HIGH	102.751	96.897	18.427	24.621	39.121	24.621	39.121
Osceola	LOW	0.001	0.001	0.000	0.001	0.001	0.001	0.001
	AVERAGE	0.494	0.359	0.148	0.117	0.130	0.117	0.130
	HIGH	50.773	47.007	8.036	3.069	2.181	3.069	2.181
Palm Beach	LOW	0.000	0.000	0.000	0.000	0.000	0.000	0.000
	AVERAGE	0.157	0.133	0.066	0.368	0.279	0.368	0.279
	HIGH	47.159	98.739	13.770	5.947	14.580	5.947	14.580
Pasco	LOW	0.000	0.000	0.000	0.000	0.000	0.000	0.000
	AVERAGE	0.841	0.546	1.028	0.222	0.300	0.222	0.300
	HIGH	115.192	39.238	63.662	5.753	7.368	5.753	7.368
Pinellas	LOW	0.000	0.000	0.000	0.000	0.000	0.000	0.000
	AVERAGE	0.780	0.712	0.904	0.588	0.838	0.588	0.838
	HIGH	93.419	64.407	30.811	50.427	22.248	50.427	22.248
Polk	LOW	0.001	0.000	0.000	0.001	0.001	0.001	0.001
	AVERAGE	0.870	0.489	0.374	0.115	0.100	0.115	0.100
	HIGH	92.251	66.643	53.094	2.029	3.799	2.029	3.799
Putnam	LOW	0.000	0.000	0.000	0.000	0.000	0.000	0.000
	AVERAGE	0.413	0.300	0.238	0.144	0.025	0.144	0.025
	HIGH	25.612	9.822	33.667	3.199	0.267	3.199	0.267
Santa Rosa	LOW	0.000	0.000	0.000	0.000	0.001	0.000	0.001
	AVERAGE	0.864	3.758	0.624	1.269	1.080	1.269	1.080
	HIGH	65.380	58.830	42.124	15.957	22.956	15.957	22.956
Sarasota	LOW	0.000	0.000	0.000	0.000	0.000	0.000	0.000
	AVERAGE	0.963	0.378	1.702	0.208	0.264	0.208	0.264
	HIGH	49.881	20.707	17.023	3.202	4.695	3.202	4.695
Seminole	LOW	0.000	0.000	0.000	0.001	0.001	0.001	0.001
	AVERAGE	0.315	0.270	0.106	0.145	0.166	0.145	0.166
	HIGH	32.642	55.645	3.918	2.335	3.111	2.335	3.111

County	Loss Costs	Frame Owners	Masonry Owners	Manufactured Homes	Frame Renters	Masonry Renters	Frame Condo Unit	Masonry Condo Unit
St. Johns	LOW	0.000	0.000	0.000	0.000	0.000	0.000	0.000
	AVERAGE	0.228	0.221	0.147	0.140	0.067	0.140	0.067
	HIGH	164.528	42.496	13.211	13.556	21.745	13.556	21.745
St. Lucie	LOW	0.000	0.000	0.000	0.102	0.001	0.102	0.001
	AVERAGE	0.165	0.185	0.605	0.501	0.420	0.501	0.420
	HIGH	19.234	31.429	25.256	1.225	5.947	1.225	5.947
Sumter	LOW	0.000	0.000	0.000	0.010	0.001	0.010	0.001
	AVERAGE	0.228	0.225	0.207	0.050	0.108	0.050	0.108
	HIGH	15.430	11.198	8.965	0.149	1.134	0.149	1.134
Suwannee	LOW	0.000	0.000	0.000	0.002	0.020	0.002	0.020
	AVERAGE	1.778	0.978	0.894	0.235	4.914	0.235	4.914
	HIGH	81.093	32.829	54.474	1.033	19.362	1.033	19.362
Taylor	LOW	0.000	0.000	0.000	0.001	0.002	0.001	0.002
	AVERAGE	3.182	0.959	1.895	1.821	0.014	1.821	0.014
	HIGH	111.833	32.283	68.772	10.351	0.027	10.351	0.027
Union	LOW	0.001	0.002	0.000	0.007	0.002	0.007	0.002
	AVERAGE	0.812	0.239	0.222	0.076	0.062	0.076	0.062
	HIGH	27.985	2.732	11.956	0.253	0.122	0.253	0.122
Volusia	LOW	0.000	0.000	0.000	0.000	0.000	0.000	0.000
	AVERAGE	0.327	0.208	0.190	0.118	0.041	0.118	0.041
	HIGH	45.951	33.646	23.513	11.337	11.583	11.337	11.583
Wakulla	LOW	0.000	0.000	0.000	0.001	0.332	0.001	0.332
	AVERAGE	2.552	5.261	2.148	1.322	0.946	1.322	0.946
	HIGH	104.879	45.014	60.779	7.387	3.380	7.387	3.380
Walton	LOW	0.000	0.000	0.000	0.000	0.000	0.000	0.000
	AVERAGE	0.503	0.354	1.526	0.079	0.018	0.079	0.018
	HIGH	44.951	9.054	22.938	3.378	0.906	3.378	0.906
Washington	LOW	0.000	0.001	0.000	0.140	NA	0.140	NA
	AVERAGE	1.128	0.516	0.841	0.458	NA	0.458	NA

County	Loss Costs	Frame Owners	Masonry Owners	Manufactured Homes	Frame Renters	Masonry Renters	Frame Condo Unit	Masonry Condo Unit
	HIGH	34.239	16.032	26.715	0.776	NA	0.776	NA
Statewide	LOW	0.000	0.000	0.000	0.000	0.000	0.000	0.000
	AVERAGE	1.349	0.728	1.740	1.416	0.270	1.416	0.270
	HIGH	186.818	106.149	127.850	59.302	50.387	59.302	50.387

Table 54 Standard Flood Time Element loss costs per $1,000 of exposure for specified deductibles

County	Loss Costs	Frame Owners	Masonry Owners	Manufactured Homes	Frame Renters	Masonry Renters	Frame Condo Unit	Masonry Condo Unit
Alachua	LOW	0.001	0.000	0.000	0.001	0.000	0.001	0.000
	AVERAGE	0.651	0.529	0.566	0.099	0.391	0.099	0.391
	HIGH	50.942	35.249	43.437	2.933	10.150	2.933	10.150
Baker	LOW	0.001	0.001	0.000	0.032	NA	0.032	NA
	AVERAGE	0.767	0.319	1.130	0.117	NA	0.117	NA
	HIGH	34.747	9.471	50.098	0.202	NA	0.202	NA
Bay	LOW	0.000	0.000	0.000	0.000	0.000	0.000	0.000
	AVERAGE	0.241	0.212	0.293	0.172	0.444	0.172	0.444
	HIGH	39.166	30.027	35.527	8.527	3.230	8.527	3.230
Bradford	LOW	0.001	0.001	0.000	0.001	0.002	0.001	0.002
	AVERAGE	1.332	0.462	0.317	0.015	0.226	0.015	0.226
	HIGH	49.510	13.492	51.610	0.073	0.641	0.073	0.641
Brevard	LOW	0.000	0.000	0.000	0.000	0.000	0.000	0.000
	AVERAGE	0.233	0.237	0.085	0.324	0.287	0.324	0.287
	HIGH	49.147	41.771	27.488	18.936	10.888	18.936	10.888
Broward	LOW	0.000	0.000	0.000	0.000	0.000	0.000	0.000
	AVERAGE	0.276	0.213	0.105	0.148	0.137	0.148	0.137
	HIGH	13.848	57.230	1.834	2.764	13.755	2.764	13.755
Calhoun	LOW	0.001	0.001	0.000	NA	NA	NA	NA
	AVERAGE	1.070	1.499	1.900	NA	NA	NA	NA
	HIGH	55.216	74.783	75.490	NA	NA	NA	NA
Charlotte	LOW	0.000	0.000	0.000	0.000	0.000	0.000	0.000
	AVERAGE	1.950	1.793	3.114	1.160	0.737	1.160	0.737

County	Loss Costs	Frame Owners	Masonry Owners	Manufactured Homes	Frame Renters	Masonry Renters	Frame Condo Unit	Masonry Condo Unit
	HIGH	29.480	67.827	44.843	5.324	5.497	5.324	5.497
Citrus	LOW	0.001	0.000	0.000	0.013	0.000	0.013	0.000
	AVERAGE	2.802	3.018	2.978	1.739	1.928	1.739	1.928
	HIGH	48.534	52.161	65.730	7.103	20.016	7.103	20.016
Clay	LOW	0.000	0.000	0.000	0.000	0.000	0.000	0.000
	AVERAGE	0.611	0.238	0.492	0.042	0.043	0.042	0.043
	HIGH	93.033	44.350	65.060	1.825	0.586	1.825	0.586
Collier	LOW	0.000	0.000	0.000	0.000	0.020	0.000	0.020
	AVERAGE	3.648	0.125	11.297	2.856	0.586	2.856	0.586
	HIGH	176.177	2.866	56.200	55.682	24.364	55.682	24.364
Columbia	LOW	0.001	0.001	0.000	NA	NA	NA	NA
	AVERAGE	1.463	1.070	1.234	NA	NA	NA	NA
	HIGH	67.400	58.922	48.026	NA	NA	NA	NA
De Soto	LOW	0.000	0.000	0.000	0.001	0.000	0.001	0.000
	AVERAGE	0.754	0.792	0.256	0.075	0.042	0.075	0.042
	HIGH	22.322	27.832	9.538	0.296	5.181	0.296	5.181
Dixie	LOW	0.000	0.000	0.000	0.001	0.012	0.001	0.012
	AVERAGE	5.064	1.149	3.639	0.996	0.012	0.996	0.012
	HIGH	186.818	34.164	51.269	6.114	0.012	6.114	0.012
Duval	LOW	0.000	0.000	0.000	0.000	0.000	0.000	0.000
	AVERAGE	0.236	0.208	0.176	0.159	0.138	0.159	0.138
	HIGH	38.555	32.998	11.504	7.755	8.532	7.755	8.532
Escambia	LOW	0.021	0.000	0.000	0.000	0.000	0.000	0.000
	AVERAGE	0.754	0.672	0.396	0.314	0.310	0.314	0.310
	HIGH	64.389	58.031	25.159	21.561	14.984	21.561	14.984
Flagler	LOW	0.000	0.000	0.000	0.000	0.000	0.000	0.000
	AVERAGE	0.156	0.107	0.061	0.182	0.051	0.182	0.051
	HIGH	8.160	6.239	1.630	4.600	2.007	4.600	2.007
Franklin	LOW	0.000	0.000	0.000	0.000	0.000	0.000	0.000

County	Loss Costs	Frame Owners	Masonry Owners	Manufactured Homes	Frame Renters	Masonry Renters	Frame Condo Unit	Masonry Condo Unit
	AVERAGE	0.801	0.571	0.318	0.364	0.195	0.364	0.195
	HIGH	102.095	23.684	10.030	3.729	0.244	3.729	0.244
Gadsden	LOW	0.001	0.001	0.000	NA	NA	NA	NA
	AVERAGE	1.003	0.565	0.688	NA	NA	NA	NA
	HIGH	62.932	9.509	42.425	NA	NA	NA	NA
Gilchrist	LOW	0.000	0.000	0.000	0.005	0.002	0.005	0.002
	AVERAGE	1.487	0.517	0.903	0.183	0.002	0.183	0.002
	HIGH	44.578	15.394	59.782	0.527	0.002	0.527	0.002
Glades	LOW	0.001	0.001	0.000	0.001	0.043	0.001	0.043
	AVERAGE	0.165	0.062	0.059	0.040	0.057	0.040	0.057
	HIGH	4.544	1.295	4.967	0.217	0.071	0.217	0.071
Gulf	LOW	0.000	0.000	0.000	0.000	0.001	0.000	0.001
	AVERAGE	0.735	0.435	1.083	0.321	0.168	0.321	0.168
	HIGH	118.229	55.390	83.275	9.941	1.093	9.941	1.093
Hamilton	LOW	0.000	0.002	0.000	NA	0.001	NA	0.001
	AVERAGE	1.872	0.189	0.839	NA	0.059	NA	0.059
	HIGH	29.880	0.496	35.938	NA	0.371	NA	0.371
Hardee	LOW	0.001	0.001	0.000	NA	NA	NA	NA
	AVERAGE	0.775	0.375	0.160	NA	NA	NA	NA
	HIGH	42.209	18.581	8.081	NA	NA	NA	NA
Hendry	LOW	0.001	0.001	0.000	0.001	0.001	0.001	0.001
	AVERAGE	0.157	0.153	0.039	0.039	0.087	0.039	0.087
	HIGH	6.527	63.480	2.768	0.418	1.966	0.418	1.966
Hernando	LOW	0.000	0.000	0.000	0.000	0.000	0.000	0.000
	AVERAGE	2.270	0.751	1.820	0.251	0.153	0.251	0.153
	HIGH	47.154	39.247	46.819	6.976	3.400	6.976	3.400
Highlands	LOW	0.001	0.001	0.000	0.001	0.001	0.001	0.001
	AVERAGE	1.621	0.788	0.201	1.266	1.183	1.266	1.183
	HIGH	64.173	57.042	9.982	13.066	9.139	13.066	9.139

County	Loss Costs	Frame Owners	Masonry Owners	Manufactured Homes	Frame Renters	Masonry Renters	Frame Condo Unit	Masonry Condo Unit
Hillsborough	LOW	0.000	0.000	0.000	0.000	0.000	0.000	0.000
	AVERAGE	0.608	0.454	0.629	0.253	0.296	0.253	0.296
	HIGH	70.903	106.142	41.718	9.875	7.650	9.875	7.650
Holmes	LOW	0.001	0.002	0.000	NA	NA	NA	NA
	AVERAGE	0.822	1.144	0.507	NA	NA	NA	NA
	HIGH	42.355	28.454	37.909	NA	NA	NA	NA
Indian River	LOW	0.000	0.000	0.000	0.000	0.000	0.000	0.000
	AVERAGE	0.136	0.110	0.137	0.042	0.049	0.042	0.049
	HIGH	76.858	17.411	25.855	2.035	1.996	2.035	1.996
Jackson	LOW	0.001	0.001	0.000	0.018	0.003	0.018	0.003
	AVERAGE	0.898	0.610	0.513	0.123	0.092	0.123	0.092
	HIGH	26.967	22.460	44.168	0.204	0.205	0.204	0.205
Jefferson	LOW	0.001	0.001	0.000	0.007	0.046	0.007	0.046
	AVERAGE	4.121	2.424	1.797	0.147	0.099	0.147	0.099
	HIGH	46.904	25.108	40.431	0.368	0.137	0.368	0.137
Lafayette	LOW	0.001	0.001	0.000	NA	NA	NA	NA
	AVERAGE	1.788	0.652	0.968	NA	NA	NA	NA
	HIGH	74.536	24.075	37.692	NA	NA	NA	NA
Lake	LOW	0.000	0.000	0.000	0.001	0.001	0.001	0.001
	AVERAGE	1.272	0.575	0.632	0.306	0.544	0.306	0.544
	HIGH	93.216	24.420	65.827	17.920	1.092	17.920	1.092
Lee	LOW	0.000	0.000	0.000	0.000	0.000	0.000	0.000
	AVERAGE	2.994	4.293	6.243	2.157	1.966	2.157	1.966
	HIGH	186.551	78.113	125.564	59.302	30.613	59.302	30.613
Leon	LOW	0.000	0.001	0.000	0.001	0.001	0.001	0.001
	AVERAGE	0.803	0.046	0.841	0.304	0.357	0.304	0.357
	HIGH	70.360	0.422	61.868	24.490	4.111	24.490	4.111
Levy	LOW	0.001	0.000	0.000	0.001	0.001	0.001	0.001
	AVERAGE	0.868	1.909	1.103	1.782	1.456	1.782	1.456
	HIGH	10.926	100.620	127.850	6.366	19.523	6.366	19.523

County	Loss Costs	Frame Owners	Masonry Owners	Manufactured Homes	Frame Renters	Masonry Renters	Frame Condo Unit	Masonry Condo Unit
Liberty	LOW	0.001	0.002	0.000	NA	NA	NA	NA
	AVERAGE	1.449	0.765	1.211	NA	NA	NA	NA
	HIGH	39.572	10.086	50.828	NA	NA	NA	NA
Madison	LOW	0.001	0.001	0.000	0.001	0.237	0.001	0.237
	AVERAGE	0.751	0.702	0.657	0.159	0.237	0.159	0.237
	HIGH	17.087	10.570	41.938	1.011	0.237	1.011	0.237
Manatee	LOW	0.000	0.000	0.000	0.000	0.000	0.000	0.000
	AVERAGE	0.590	0.309	0.753	0.222	0.215	0.222	0.215
	HIGH	21.994	14.320	17.291	7.424	4.533	7.424	4.533
Marion	LOW	0.000	0.000	0.000	0.001	0.001	0.001	0.001
	AVERAGE	0.959	0.803	0.747	0.435	0.266	0.435	0.266
	HIGH	91.976	63.069	45.910	22.573	5.605	22.573	5.605
Martin	LOW	0.000	0.000	0.000	0.000	0.000	0.000	0.000
	AVERAGE	0.418	0.211	0.471	0.184	0.062	0.184	0.062
	HIGH	38.099	26.596	21.030	6.835	4.604	6.835	4.604
Miami-Dade	LOW	0.000	0.000	0.000	0.000	0.000	0.000	0.000
	AVERAGE	0.347	0.482	0.444	0.036	0.188	0.036	0.188
	HIGH	4.483	35.556	32.118	2.882	34.895	2.882	34.895
Monroe	LOW	0.000	0.000	0.000	0.000	0.000	0.000	0.000
	AVERAGE	1.419	1.473	5.515	0.567	0.366	0.567	0.366
	HIGH	53.955	52.915	51.191	12.037	6.074	12.037	6.074
Nassau	LOW	0.000	0.000	0.000	0.000	0.000	0.000	0.000
	AVERAGE	0.171	0.165	0.157	0.125	0.032	0.125	0.032
	HIGH	19.162	6.098	8.336	1.243	0.724	1.243	0.724
Okaloosa	LOW	0.000	0.000	0.000	0.000	0.000	0.000	0.000
	AVERAGE	3.886	4.355	0.541	3.193	4.136	3.193	4.136
	HIGH	76.464	67.034	37.613	46.574	50.387	46.574	50.387
Okeechobee	LOW	0.000	0.001	0.000	0.001	0.001	0.001	0.001
	AVERAGE	0.148	0.096	0.081	0.079	0.040	0.079	0.040

County	Loss Costs	Frame Owners	Masonry Owners	Manufactured Homes	Frame Renters	Masonry Renters	Frame Condo Unit	Masonry Condo Unit
	HIGH	5.242	2.484	49.829	0.839	1.344	0.839	1.344
Orange	LOW	0.000	0.000	0.000	0.001	0.000	0.001	0.000
	AVERAGE	1.170	0.606	0.296	0.189	0.313	0.189	0.313
	HIGH	102.751	96.896	18.427	24.621	39.121	24.621	39.121
Osceola	LOW	0.001	0.001	0.000	0.001	0.001	0.001	0.001
	AVERAGE	0.494	0.359	0.148	0.117	0.130	0.117	0.130
	HIGH	50.773	47.007	8.036	3.069	2.181	3.069	2.181
Palm Beach	LOW	0.000	0.000	0.000	0.000	0.000	0.000	0.000
	AVERAGE	0.157	0.133	0.066	0.368	0.279	0.368	0.279
	HIGH	47.159	98.739	13.770	5.947	14.580	5.947	14.580
Pasco	LOW	0.000	0.000	0.000	0.000	0.000	0.000	0.000
	AVERAGE	0.841	0.546	1.028	0.222	0.300	0.222	0.300
	HIGH	115.192	39.236	63.662	5.753	7.368	5.753	7.368
Pinellas	LOW	0.000	0.000	0.000	0.000	0.000	0.000	0.000
	AVERAGE	0.780	0.712	0.904	0.588	0.838	0.588	0.838
	HIGH	93.419	64.406	30.811	50.427	22.248	50.427	22.248
Polk	LOW	0.001	0.000	0.000	0.001	0.001	0.001	0.001
	AVERAGE	0.870	0.489	0.374	0.115	0.100	0.115	0.100
	HIGH	92.251	66.643	53.094	2.029	3.799	2.029	3.799
Putnam	LOW	0.000	0.000	0.000	0.000	0.000	0.000	0.000
	AVERAGE	0.413	0.300	0.238	0.144	0.025	0.144	0.025
	HIGH	25.612	9.822	33.667	3.199	0.267	3.199	0.267
Santa Rosa	LOW	0.000	0.000	0.000	0.000	0.000	0.000	0.000
	AVERAGE	0.228	0.221	0.147	0.140	0.067	0.140	0.067
	HIGH	164.528	42.495	13.211	13.556	21.745	13.556	21.745
Sarasota	LOW	0.000	0.000	0.000	0.102	0.001	0.102	0.001
	AVERAGE	0.165	0.185	0.605	0.501	0.420	0.501	0.420
	HIGH	19.234	31.429	25.256	1.225	5.947	1.225	5.947
Seminole	LOW	0.000	0.000	0.000	0.000	0.001	0.000	0.001

County	Loss Costs	Frame Owners	Masonry Owners	Manufactured Homes	Frame Renters	Masonry Renters	Frame Condo Unit	Masonry Condo Unit
	AVERAGE	0.864	3.758	0.624	1.269	1.080	1.269	1.080
	HIGH	65.380	58.830	42.124	15.957	22.956	15.957	22.956
St. Johns	LOW	0.000	0.000	0.000	0.000	0.000	0.000	0.000
	AVERAGE	0.963	0.378	1.702	0.208	0.264	0.208	0.264
	HIGH	49.881	20.701	17.023	3.202	4.695	3.202	4.695
St. Lucie	LOW	0.000	0.000	0.000	0.001	0.001	0.001	0.001
	AVERAGE	0.315	0.270	0.106	0.145	0.166	0.145	0.166
	HIGH	32.642	55.645	3.918	2.335	3.111	2.335	3.111
Sumter	LOW	0.000	0.000	0.000	0.010	0.001	0.010	0.001
	AVERAGE	0.228	0.225	0.207	0.050	0.108	0.050	0.108
	HIGH	15.430	11.198	8.965	0.149	1.134	0.149	1.134
Suwannee	LOW	0.000	0.000	0.000	0.002	0.020	0.002	0.020
	AVERAGE	1.778	0.978	0.894	0.235	4.914	0.235	4.914
	HIGH	81.093	32.829	54.474	1.033	19.362	1.033	19.362
Taylor	LOW	0.000	0.000	0.000	0.001	0.002	0.001	0.002
	AVERAGE	3.182	0.959	1.895	1.821	0.014	1.821	0.014
	HIGH	111.833	32.281	68.772	10.351	0.027	10.351	0.027
Union	LOW	0.001	0.002	0.000	0.007	0.002	0.007	0.002
	AVERAGE	0.812	0.239	0.222	0.076	0.062	0.076	0.062
	HIGH	27.985	2.732	11.956	0.253	0.122	0.253	0.122
Volusia	LOW	0.000	0.000	0.000	0.000	0.000	0.000	0.000
	AVERAGE	0.327	0.208	0.190	0.118	0.041	0.118	0.041
	HIGH	45.951	33.646	23.513	11.337	11.583	11.337	11.583
Wakulla	LOW	0.000	0.000	0.000	0.001	0.332	0.001	0.332
	AVERAGE	2.552	5.261	2.148	1.322	0.946	1.322	0.946
	HIGH	104.879	45.010	60.779	7.387	3.380	7.387	3.380
Walton	LOW	0.000	0.000	0.000	0.000	0.000	0.000	0.000
	AVERAGE	0.503	0.354	1.526	0.079	0.018	0.079	0.018
	HIGH	44.951	9.054	22.938	3.378	0.906	3.378	0.906

County	Loss Costs	Frame Owners	Masonry Owners	Manufactured Homes	Frame Renters	Masonry Renters	Frame Condo Unit	Masonry Condo Unit
Washington	LOW	0.000	0.001	0.000	0.140	NA	0.140	NA
	AVERAGE	1.128	0.516	0.841	0.458	NA	0.458	NA
	HIGH	34.239	16.031	26.715	0.776	NA	0.776	NA
Statewide	LOW	0.000	0.000	0.000	0.000	0.000	0.000	0.000
	AVERAGE	1.349	0.728	1.740	1.416	0.270	1.416	0.270
	HIGH	186.818	106.142	127.850	59.302	50.387	59.302	50.387

Figure 4

State of Florida by County

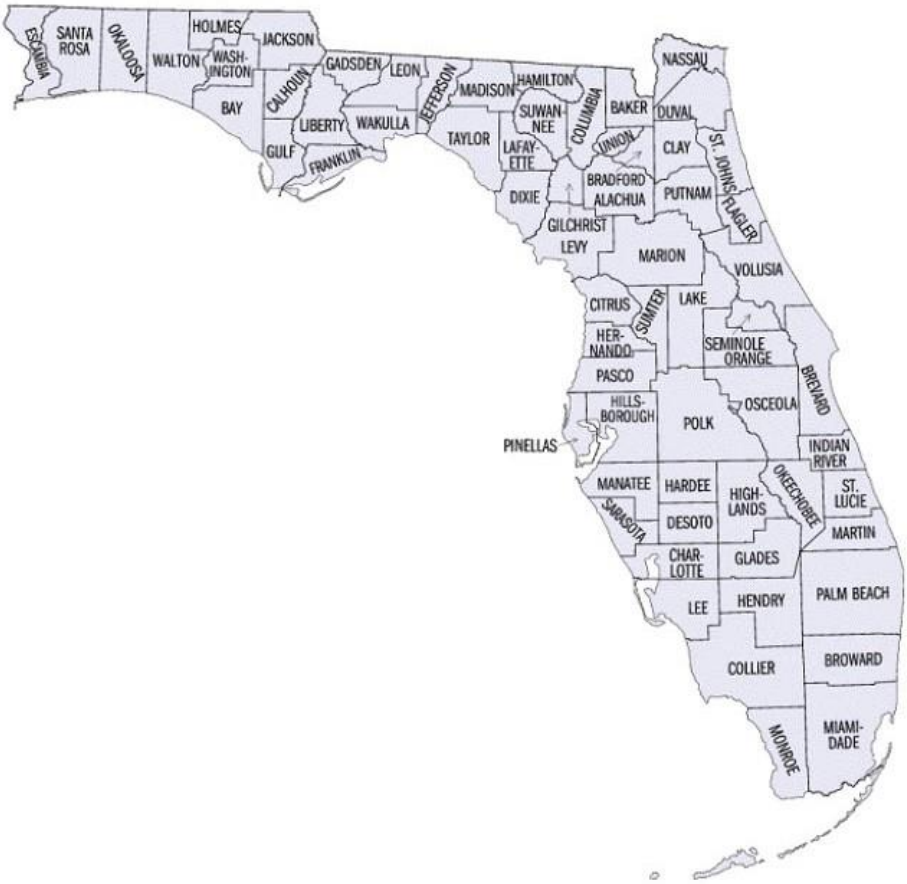

Flood Output Range Specifications

Policy Type	Assumptions
Owners	**Coverage A = Building Property** • Coverage A limit = $100,000 • Replacement cost equal to Coverage A limit • Deductible = $1,500 **Coverage B = Personal Property** • Coverage B limit = $40,000 • Actual cash value equal to Coverage B limit • Deductible = $1,000 **Time Element Coverage** • To be defined by the modeling organization
	✧ Flood loss costs per $1,000 should be related to the Coverage A limit for Coverage A, to the Coverage B limit for Coverage B, and to the Time Element limit for Time Element Coverage
Renters	**Coverage B = Personal Property** • Coverage B limit = $50,000 • No coverage for tenant improvements • Deductible = $1,000 • Actual cash value equal to Coverage B limit **Time Element Coverage** • To be defined by the modeling organization
	✧ Flood loss costs per $1,000 should be related to the Coverage B limit for Coverage B and to the Time Element limit for Time Element Coverage

Policy Type	Assumptions
Condo Unit Owners	**Coverage A = Building Property** • Coverage A limit = 10% of Coverage B limit • Replacement cost equal to Coverage A limit **Coverage B = Personal Property** • Coverage B limit = $50,000 • Actual cash value equal to Coverage B limit • Deductible = $500 **Time Element Coverage** • To be defined by the modeling organization

✧ Flood loss costs per $1,000 should be related to the Coverage A limit for Coverage A, to the Coverage B limit for Coverage B, and to the Time Element limit for Time Element Coverage

Manufactured Homes	**Coverage A = Building Property** • Coverage A limit = $50,000 • Replacement cost equal to Coverage A limit • Deductible = $500 **Coverage B = Personal Property** • Coverage B limit = $25,000 • Actual cash value equal to Coverage B limit **Time Element Coverage** • To be defined by the modeling organization

✧ Flood loss costs per $1,000 should be related to the Coverage A limit for Coverage A, to the Coverage B limit for Coverage B, and to the Time Element limit for Time Element Coverage

Form AF-5: Percentage Change in Flood Output Ranges

A. One or more automated programs or scripts should be used to generate and arrange the data in Form AF-5, Percentage Change in Flood Output Ranges.

An automated script is used to generate and arrange the data in Form AF-5.

B. Provide summaries of the percentage change in average flood loss cost output range data compiled in Form AF-4, Flood Output Ranges, relative to the equivalent data compiled from the currently accepted flood model in the format shown in the file named "2021FormAF5.xlsx."

For the change in flood output range exhibit, provide the summary by regions as defined in Figure 1 (Panhandle, North Florida, Southwest Florida, East Florida, and Southeast Florida) and Statewide (overall percentage change). The East Florida Region boundary in Orange and Polk Counties is based on the South Florida Water Management District boundary.

C. Provide this form in Excel format. The file name should include the abbreviated name of the modeling organization, the flood standards year, and the form name. Also include all tables in Form AF-5, Percentage Change in Flood Output Ranges, in a submission appendix.

Form AF-5, Percentage Change in Flood Output Ranges, is provided in Excel format in the file "IF2021FormAF5.xlsx" at the link provided to the FCHLPM and appears below in

Color-coded maps by county are provided in Figure 154 through Figure 160.

Table 55 (zero deductible), Table 57 (specified deductible), Table 56 (Time Element zero deductible), and

Region	Frame Owners	Masonry Owners	Manufactured Homes	Frame Renters	Masonry Renters	Frame Condo Unit	Masonry Condo Unit
Panhandle	-81.44%	-77.16%	-51.96%	-40.02%	-61.43%	-37.05%	-60.68%
North Florida	-87.52%	-91.89%	-45.44%	-46.46%	-56.56%	-43.72%	-54.96%
Southwest Florida	-55.49%	-77.30%	-32.74%	-29.18%	-42.63%	-27.18%	-40.81%
East Florida	-92.67%	-96.99%	-62.77%	-32.21%	-63.89%	-30.08%	-62.91%
Southeast Florida	-94.02%	-95.30%	-14.18%	-30.74%	-68.26%	-24.80%	-67.53%
Statewide	-74.06%	-89.49%	-40.25%	-30.64%	-62.34%	-28.22%	-61.31%

Table 58 (Time Element specified deductible).

D. Provide color-coded maps by county reflecting the percentage changes in the average flood loss costs with specified deductibles for frame owners, masonry owners, frame renters, masonry renters, frame condo unit owners, masonry condo unit owners, and manufactured homes from the flood output ranges from the currently accepted flood model.

Counties with a negative percentage change (reduction in flood loss costs) should be indicated with shades of blue, counties with a positive percentage change (increase in flood loss costs) should be indicated with shades of red, and counties with no percentage change should be white. The larger the percentage change in the county, the more intense the color-shade.

Color-coded maps by county are provided in Figure 154 through Figure 160.

Table 55: Percentage Change in $0 Deductible Flood Output Ranges

Region	Frame Owners	Masonry Owners	Manufactured Homes	Frame Renters	Masonry Renters	Frame Condo Unit	Masonry Condo Unit
Panhandle	-80.88%	-76.84%	-49.54%	-38.78%	-61.30%	-35.85%	-60.33%
North Florida	-86.96%	-91.54%	-41.75%	-45.21%	-56.08%	-42.82%	-54.39%
Southwest Florida	-53.88%	-76.48%	-25.34%	-27.55%	-41.56%	-25.57%	-39.64%
East Florida	-92.28%	-96.77%	-59.12%	-31.11%	-63.31%	-29.00%	-62.38%
Southeast Florida	-93.74%	-95.02%	-6.50%	-26.56%	-67.74%	-23.98%	-67.11%
Statewide	-73.15%	-89.04%	-34.52%	-28.84%	-61.75%	-26.68%	-60.74%

Table 56: Percentage Change in $0 Deductible, Time Element Flood Output Ranges

Region	Frame Owners	Masonry Owners	Manufactured Homes	Frame Renters	Masonry Renters	Frame Condo Unit	Masonry Condo Unit
Panhandle	-	-	-	-	-	-	-
North Florida	-	-	-	-	-	-	-
Southwest Florida	-	-	-	-	-	-	-
East Florida	-	-	-	-	-	-	-
Southeast Florida	-	-	-	-	-	-	-
Statewide	-	-	-	-	-	-	-

Table 57: Percentage Change in Specified Deductible Flood Output Ranges

Region	Frame Owners	Masonry Owners	Manufactured Homes	Frame Renters	Masonry Renters	Frame Condo Unit	Masonry Condo Unit
Panhandle	-81.44%	-77.16%	-51.96%	-40.02%	-61.43%	-37.05%	-60.68%
North Florida	-87.52%	-91.89%	-45.44%	-46.46%	-56.56%	-43.72%	-54.96%
Southwest Florida	-55.49%	-77.30%	-32.74%	-29.18%	-42.63%	-27.18%	-40.81%

Region	Frame Owners	Masonry Owners	Manufactured Homes	Frame Renters	Masonry Renters	Frame Condo Unit	Masonry Condo Unit
East Florida	-92.67%	-96.99%	-62.77%	-32.21%	-63.89%	-30.08%	-62.91%
Southeast Florida	-94.02%	-95.30%	-14.18%	-30.74%	-68.26%	-24.80%	-67.53%
Statewide	-74.06%	-89.49%	-40.25%	-30.64%	-62.34%	-28.22%	-61.31%

Table 58: Percentage Change in Specified Deductible, Time Element Flood Output Ranges

Region	Frame Owners	Masonry Owners	Manufactured Homes	Frame Renters	Masonry Renters	Frame Condo Unit	Masonry Condo Unit
Panhandle	-	-	-	-	-	-	-
North Florida	-	-	-	-	-	-	-
Southwest Florida	-	-	-	-	-	-	-
East Florida	-	-	-	-	-	-	-
Southeast Florida	-	-	-	-	-	-	-
Statewide	-	-	-	-	-	-	-

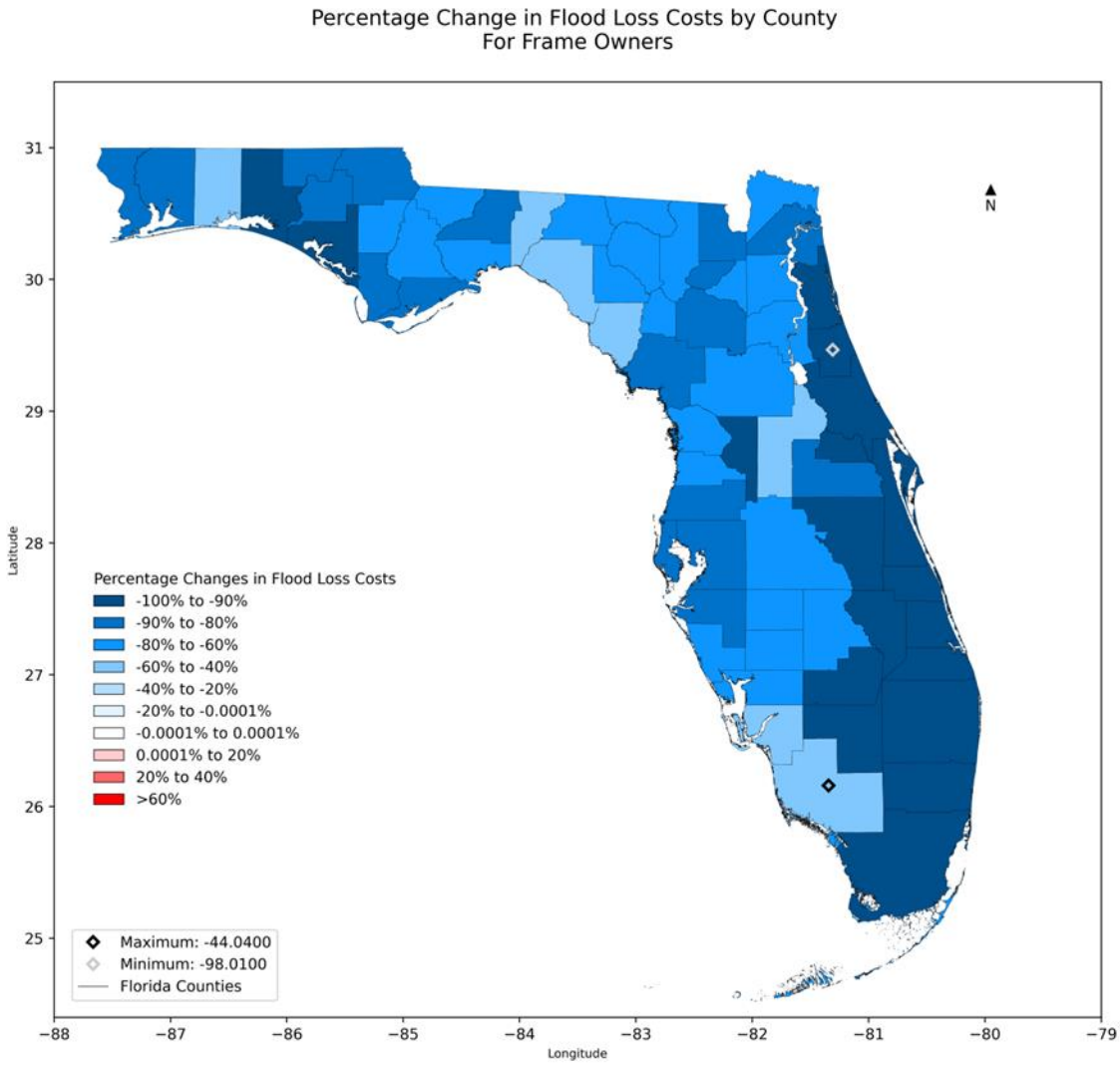

Figure 154: Percentage Change in Specified Deductible Flood Loss Costs by County for Frame Owners

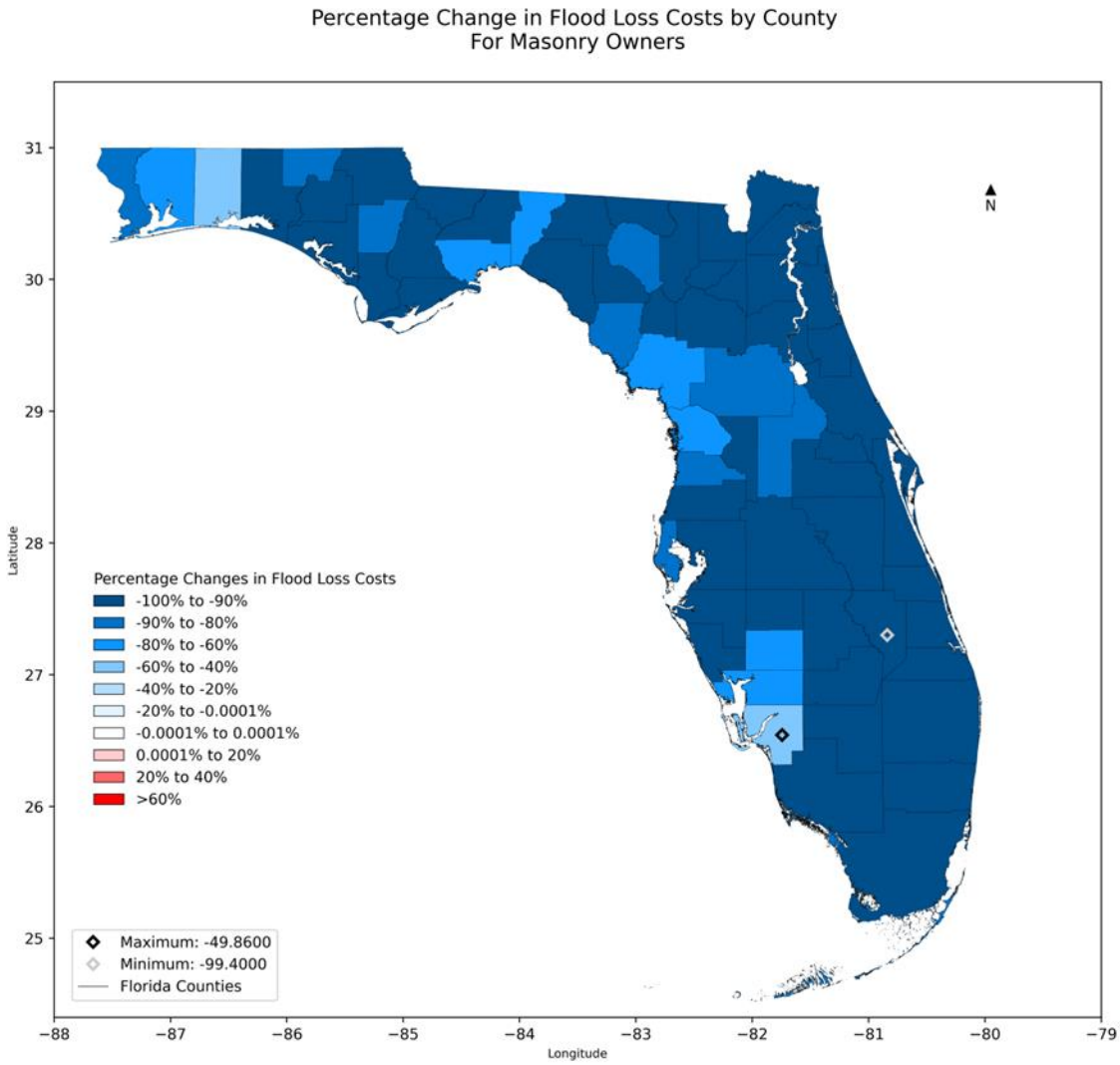

Figure 155: Percentage Change in Specified Deductible Flood Loss Costs by County for Masonry Owners

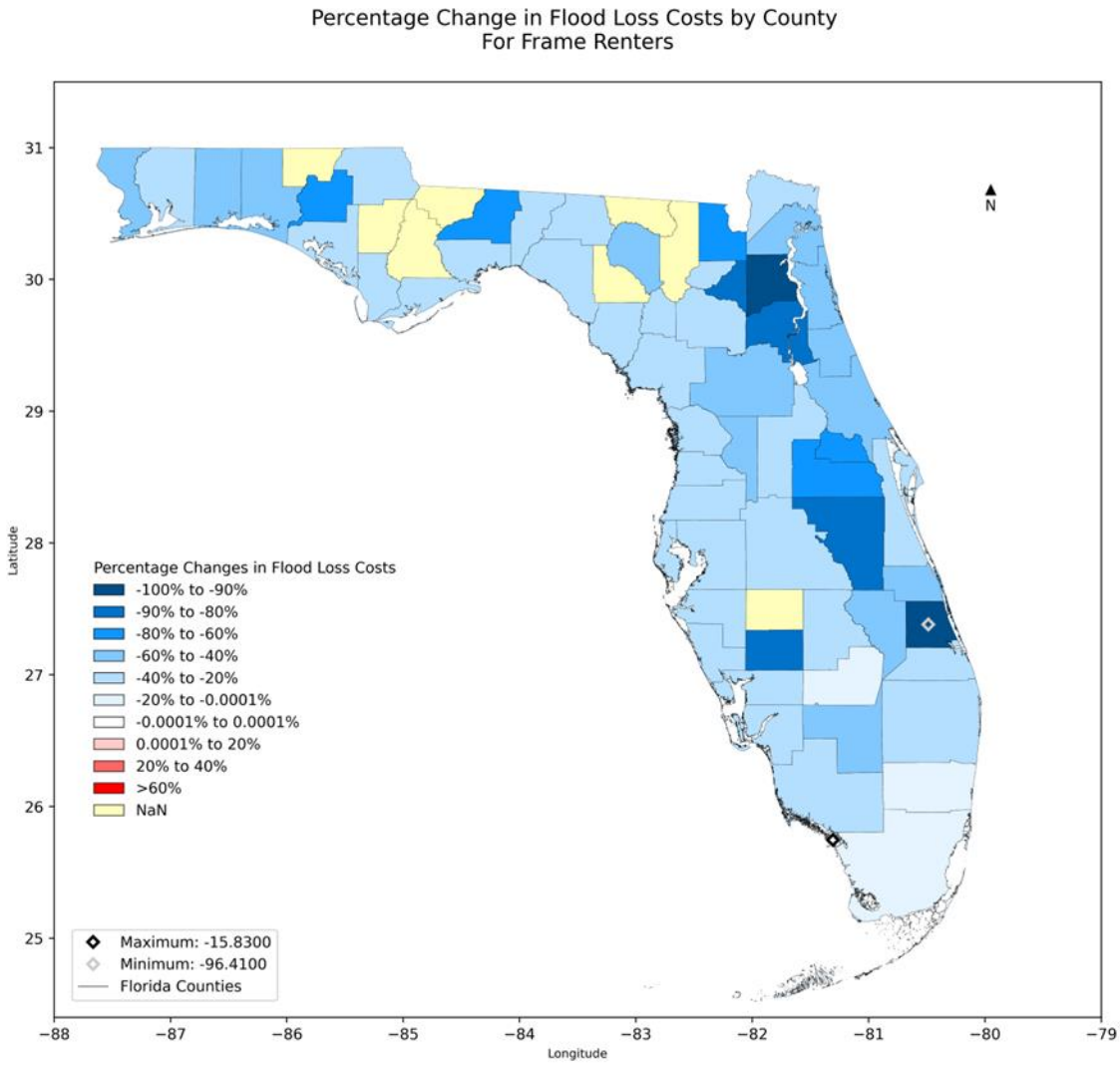

Figure 156: Percentage Change in Specified Deductible Flood Loss Costs by County for Frame Renters

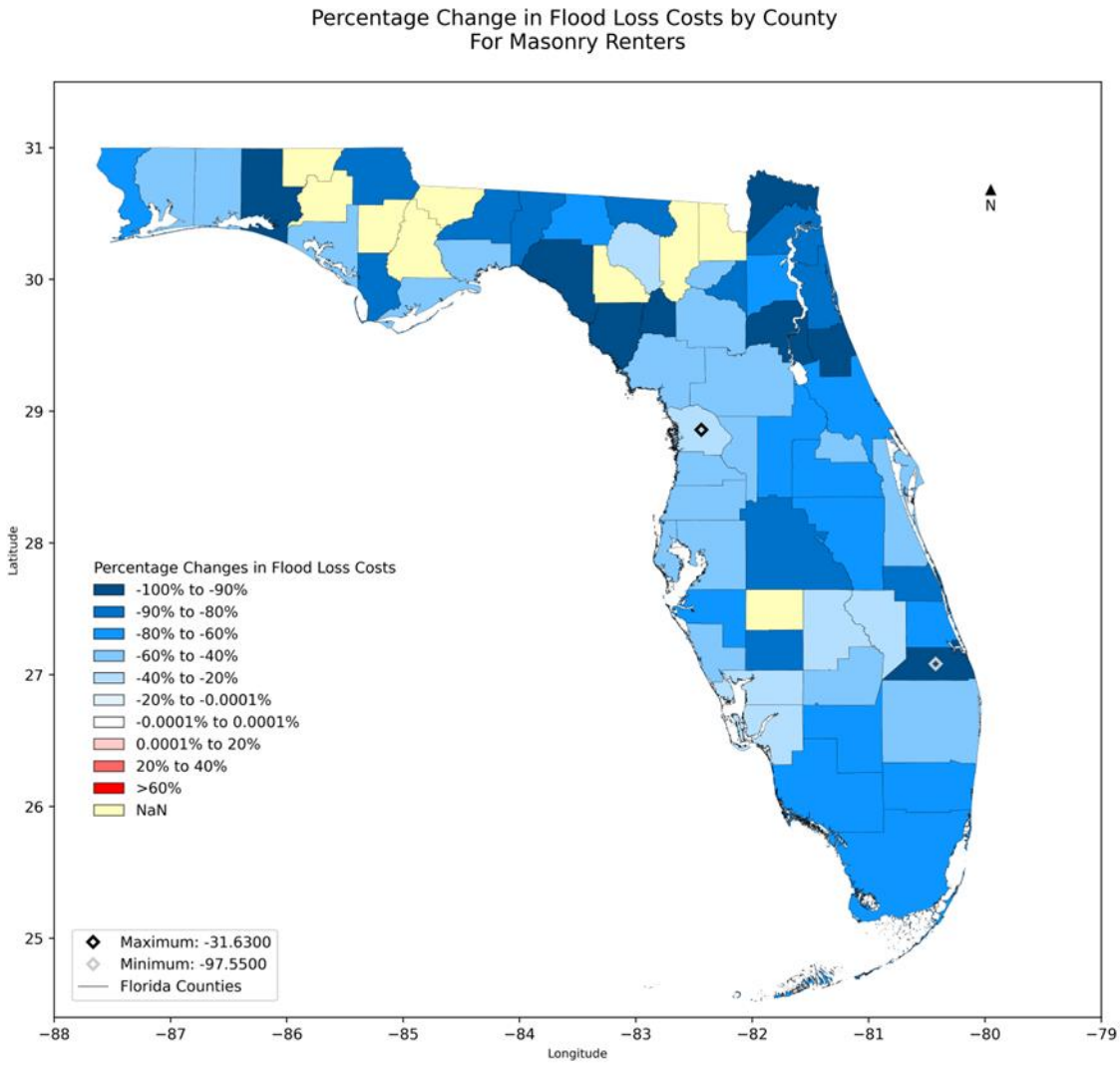

Figure 157: Percentage Change in Specified Deductible Flood Loss Costs by County for Masonry Renters

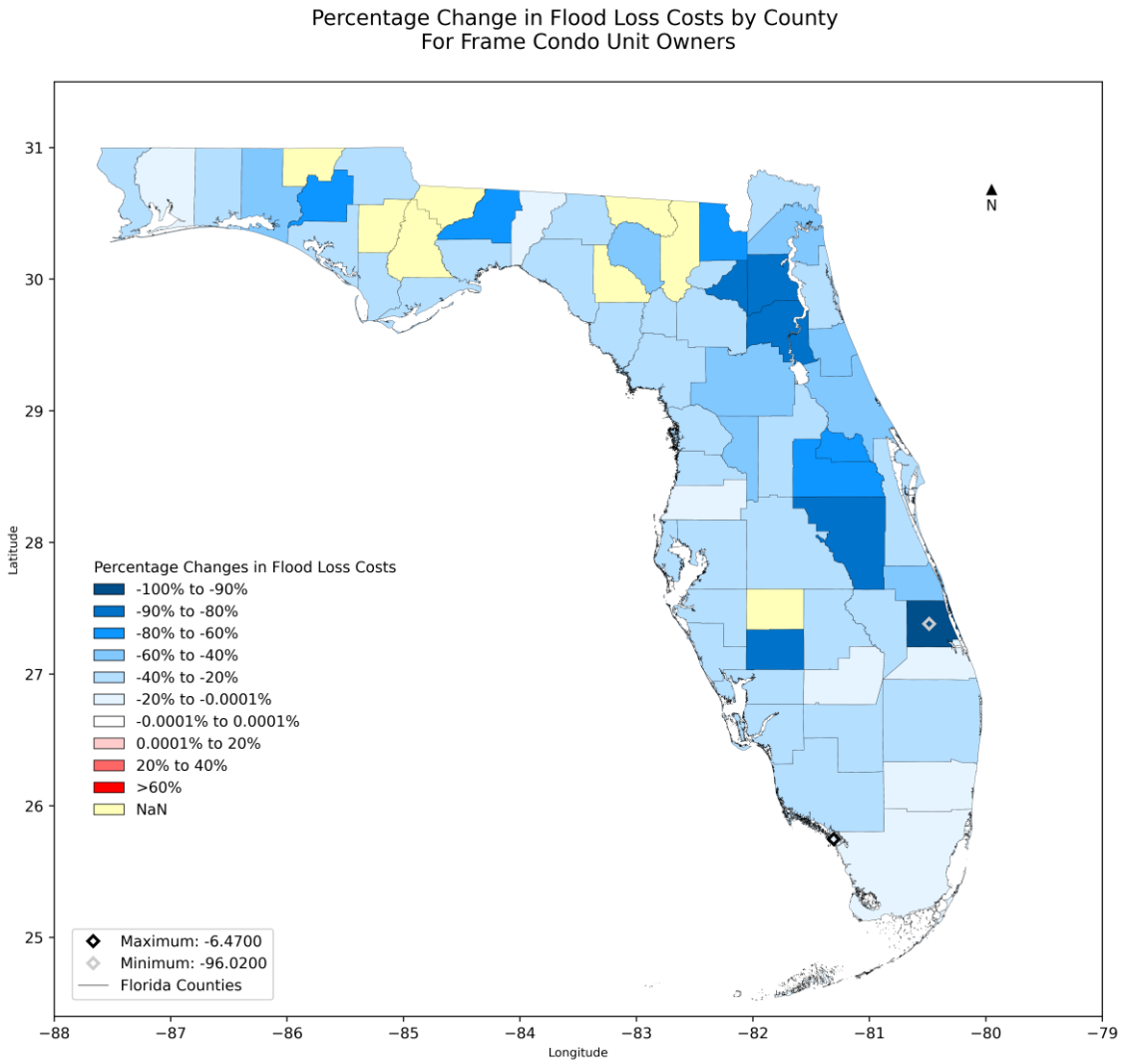

Figure 158: Percentage Change in Specified Deductible Flood Loss Costs by County for Frame Condo Unit Owners

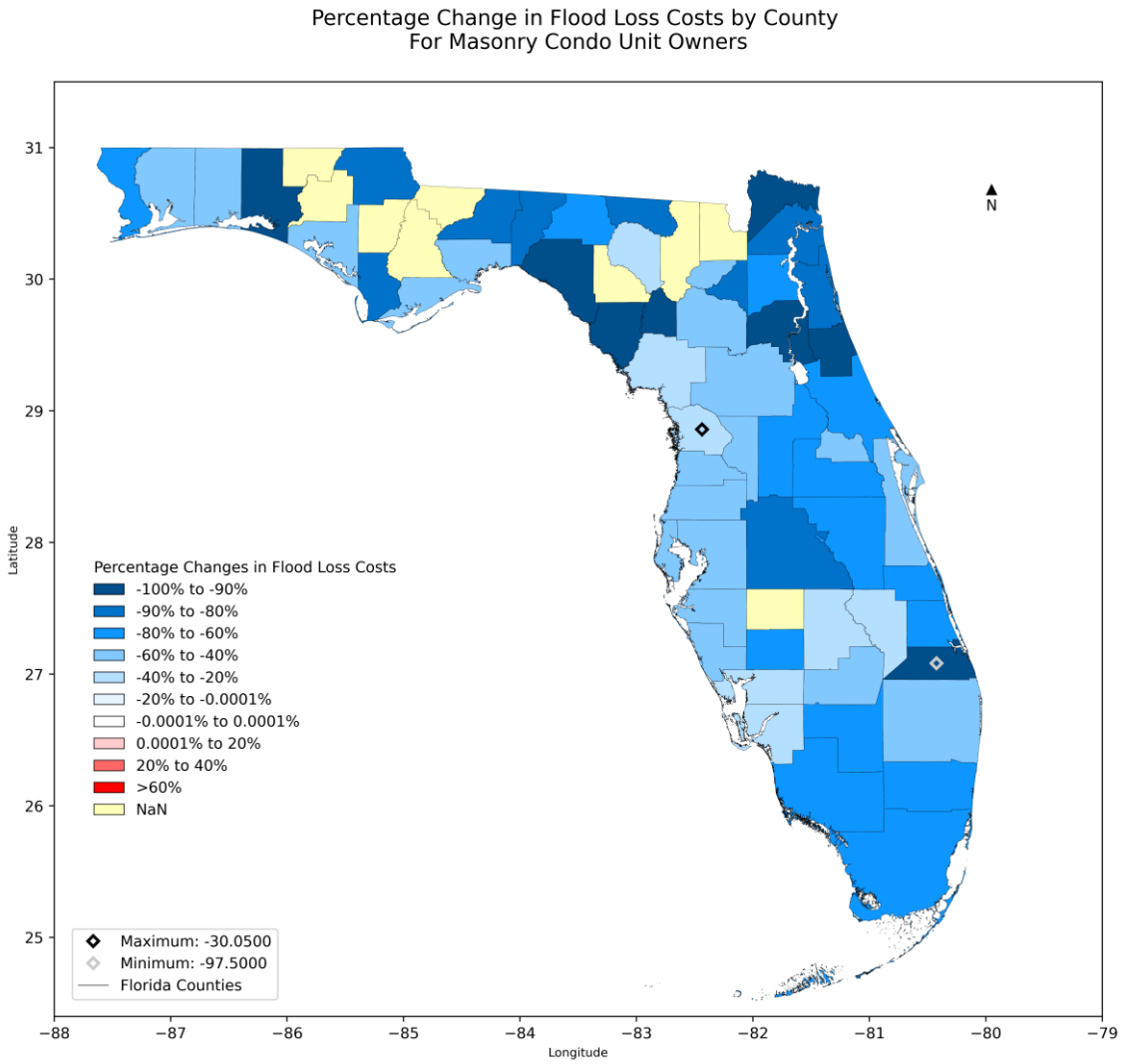

Figure 159: Percentage Change in Specified Deductible Flood Loss Costs by County for Masonry Condo Unit Owners

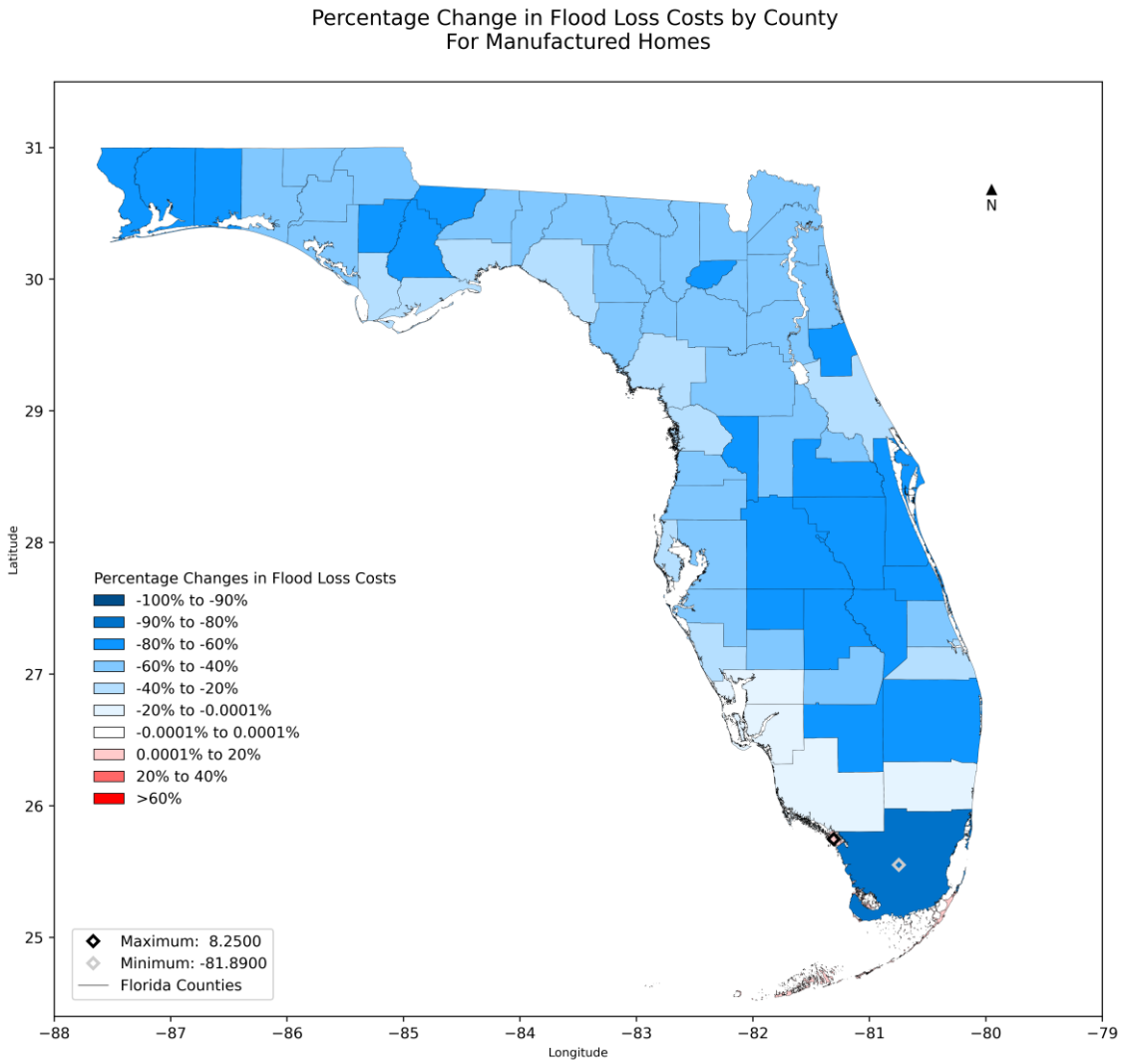

Figure 160: Percentage Change in Specified Deductible Flood Loss Costs by County for Manufactured Homes

Figure 1

State of Florida by Region

Form AF-6: Logical Relationships to Flood Risk (Trade Secret Item)

Form AF-6 is considered to be trade secret material and will be provided to the Professional Team for review during the on-site visit and to the Commission during the closed portion of the Acceptability Meeting.

Form AF-7: Percentage Change in Logical Relationships to Flood Risk

A. One or more automated programs or scripts should be used to generate the exhibits in Form AF-7, Percentage Change in Logical Relationships to Flood Risk.

B. Provide summaries of the percentage change in logical relationship to flood risk exhibits from the currently accepted flood model in the format shown in the file named "2021FormAF7.xlsx."

C. Create exposure sets for each exhibit by modeling all of the coverages from the appropriate Notional Set listed below at each of the locations in Location Grid B as described in the file "NotionalInput21_Flood.xlsx." Refer to the Notional Hurricane Policy Specifications provided in Form AF-6, Logical Relationships to Flood Risk (Trade Secret Item), for additional modeling information.

Exhibit	Notional Set
Deductible Sensitivity	Set 1
Policy Form Sensitivity	Set 2
Construction Sensitivity	Set 3
Coverage Sensitivity	Set 4
Year Built Sensitivity	Set 5
Foundation Type Sensitivity	Set 6
Number of Stories Sensitivity	Set 7
Lowest Floor Elevation of Residential Structure Sensitivity	Set 8

D. Flood models are to treat points in Location Grid B as coordinates that would result from a geocoding process. Flood models should treat points by simulating flood loss at exact location or by using the nearest modeled parcel/street/cell in the flood model. Provide the results statewide (overall percentage change) and by the regions defined in Form AF-5, Percentage Change in Flood Output Ranges.

E. Provide this form in Excel format. The file name should include the abbreviated name of the modeling organization, the flood standards year, and the form name. Also include all exhibits in Form AF-7, Percentage Change in Logical Relationships to Flood Risk, in a submission appendix.

This is the first Impact Forecasting flood model submission.

Form AF-8: Flood Probable Maximum Loss for Florida

A. *One or more automated programs or scripts should be used to generate and arrange the data in Form AF-8, Flood Probable Maximum Loss for Florida.*

Automated scripts are used to generate and arrange data in Form AF-8.

B. *Provide the expected flood loss and 10% (lower bound) and 90% (upper bound) flood loss levels for each of the Personal Residential Annual Exceedance Probabilities given in Part A, Annual Aggregate and Part B, Annual Occurrence. Describe how the uncertainty in flood vulnerability functions has been propagated to the uncertainty in portfolio loss and how it relates to the 10% and 90% flood loss levels. If the modeling methodology does not allow the flood model to produce a viable answer for certain exceedance probabilities, state so and why.*

The expected flood loss and 10% and 90% flood loss levels were computed using Impact Forecasting's personal residential exposure and the AEP and OEP results were provided in Table 59 and Table 60. Each event in the stochastic event set were simulated 10 times to capture the variation of loss due to uncertainty in the flood vulnerability functions. Those were then converted to year losses by taking either max or sum of the individual event losses for a given year. The return period for each year was calculated based on the averaged sample loss for each year. The expected flood loss and 10% and 90% flood loss levels for the desired return periods were computed from the 10 samples of certain years.

C. *If additional assumptions are necessary to complete this form, provide the rationale for the assumptions as well as a detailed description of how they are included.*

No additional assumptions were made to complete this form.

D. *Provide this form in Excel format. The file name should include the abbreviated name of the modeling organization, the flood standards year, and the form name. Also include Form AF-8, Flood Probable Maximum Loss for Florida, in a submission appendix.*

Form AF-8 is provided in Excel format in the file "IF2021FormAF8.xlsx" at the link provided to the FCHLPM and appears in Table 59 and Table 60 below.

Part A – Personal Residential Flood Probable Maximum Loss for Florida – Annual Aggregate

Table 59: Personal Residential Flood Probable Maximum Loss for Florida – Annual Aggregate

Annual Exceedance Probability	Expected Flood Loss Level	10% Loss Level	90% Loss Level
Top Event	185,743,902,149	185,577,027,910	186,013,349,416
0.001	89,502,542,800	89,400,816,955	89,628,892,282
0.002	78,906,907,251	78,795,746,037	78,993,664,207
0.004	66,523,139,201	66,356,567,406	66,616,042,319
0.01	48,436,340,018	48,300,499,395	48,520,546,889
0.02	31,725,207,355	31,663,187,848	31,821,266,625
0.05	12,409,850,818	12,324,825,979	12,557,684,280
0.10	4,523,920,264	4,492,215,697	4,564,043,660
0.20	1,463,207,788	1,446,240,319	1,477,021,491

Part B – Personal Residential Flood Probable Maximum Loss for Florida –Annual Occurrence

Table 60: Personal Residential Flood Probable Maximum Loss for Florida – Annual Occurrence

Annual Exceedance Probability	Expected Flood Loss Level	10% Loss Level	90% Loss Level
Top Event	152,296,371,062	151,912,057,576	152,529,709,233
0.001	85,120,568,380	85,010,619,247	85,271,287,642
0.002	75,691,477,297	75,567,552,908	75,800,599,906
0.004	63,762,555,412	63,550,690,584	63,868,601,297
0.01	46,074,843,504	46,004,910,813	46,143,440,575
0.02	29,621,503,697	29,580,487,743	29,731,390,484
0.05	11,283,154,666	11,208,695,912	11,336,544,286
0.10	3,944,313,165	3,894,817,740	4,013,432,180
0.20	1,179,721,927	1,151,616,209	1,207,667,675

Appendix B: Individuals Involved in the Impact Forecasting Florida Flood Model (FCHLPM) Model Acceptability Process

Dr. Nans Addor, MSci, PhD., Geography, University of Zurich, Switzerland. Principal Hydrologist, Fathom.

Nans Addor is the Principal Hydrologist for Fathom, operating within the Technical team. He undertook his PhD in Physical Geography at the University of Zurich in Switzerland and worked as a postdoctoral researcher at the National Center for Atmospheric Research (NCAR) in Boulder, USA and at the Universities of East Anglia and Exeter in the UK. His expertise is in hydrological modelling from the catchment to the continental scale, the quantification of climate change impacts on hydrological processes, and the creation and use of large datasets (such as the CAMELS dataset) to better understand and simulate hydrological diversity. Nans joined Fathom in 2022 and works on a variety of client and in house technical developments, with a particular focus on large scale hydrological modelling under current and future climate.

Nans has contributed to generation of high river flows caused by non-TC as well as historical and synthetic TC rainfall.

Sushma Bhat, B.S., Computer Technology, University of Mumbai, India

Ms. Bhat is an Associate Director and a solution architect for Impact Forecasting's software development team. Her experience includes involvement at all stages of software development life cycle for catastrophe modeling, customer deployments and operations. She has hands-on experience with C#, MS SQL Server, and user interface design.

Ms. Bhat's contribution to Impact Forecasting's Florida Flood Model includes deployment of ELEMENTS and conforming to application standards and procedures, coding guidelines, and software documentation, as well as acting at the Computer / Information Signatory.

David Byrne, PhD., Oceanography, University of Liverpool, United Kingdom.

David Byrne is a Senior Scientist in the Hurricane group at Impact Forecasting who has expertise in the application and development of numerical and statistical models in the context of storm surges, tides and climate risk. He published his PhD thesis in 2019 on the application of data assimilation techniques to operational storm surge forecasting. Since then, he has worked at the National Oceanography Center (U.K.) and Woodwell Climate Research Center (MA) developing key global and regional data products, leading research into ocean model development and collaborating with software developers on toolkits to aid in the standardization of oceanographic analyses. During this time, he has authored nine peer-reviewed publications on topics ranging from storm surge modelling to global projections of dangerous heat.

David recently joined the team at Impact Forecasting and is contributing to the research and development of their storm surge hazard model.

David Colbus, M.A., Climate and Society, Columbia University

David Colbus is an Associate Director for Impact Forecasting, operating within a Program Management team. He operates within the Program Management team, focusing on Impact Forecasting's models related to America's weather and climate, and his responsibilities include achieving strategic initiatives and satisfying regulatory requirements. Prior to joining Impact Forecasting, Mr. Colbus was responsible for client relationships and expert catastrophe risk analysis as a Catastrophe Risk Consultant at Verisk. Mr. Colbus holds a Master of Arts in Climate and Society from Columbia University.

Mr. Colbus' contributions to the IF Florida Flood Model include project management, production, and review of the submission document as the editorial signatory.

Anthony Cooper, MEng., Engineering, University of Cambridge. Hydraulic Model Developer, Fathom.

Anthony Cooper is a Hydraulic Model Developer for Fathom, operating within the Technical team. He works on all aspects of hydraulic modelling, including data sourcing and processing, hydraulic model build and simulation and model evaluation. He has undertaken hydraulic modelling for Fathom's US and Global flood models as well as working on many other client projects including for the UK government Foreign and Commonwealth Development Office and supporting major engineering consultancies. Prior to joining Fathom, Anthony worked as a Water Engineer at Arup for five years where he worked on flood risk modelling and management projects for governmental bodies and major infrastructure projects.

Anthony's contributions to the IF Florida Flood Model include work on the input data that is incorporated into the inland hydraulic models, as well as model simulation and processing.

William Dong, Ph.D., Civil Engineering, University of Nebraska - Lincoln

Dr. Dong is Associate Director and Tech Lead within Impact Forecasting's software development team. Since joining Impact Forecasting in 2017, Dr. Dong has led development of ELEMENTS, Impact Forecasting's catastrophe loss modeling platform, as well as overseen development of IF's Automated Event Response service for North Atlantic hurricane. Dr. Dong has a Ph.D. in Civil Engineering from the University of Nebraska and prior to joining Impact Forecasting was involved in software development for multiple government grant projects from Illinois Transportation Department and Environmental Protection Agency.

Dr. Dong's contribution to Impact Forecasting's Florida Flood Model includes deployment of ELEMENTS and conforming to application standards and procedures, coding guidelines, and software documentation.

Radovan Drinka, M.S., Physics, Comenius University in Bratislava, Slovakia

Radovan Drinka is a Director – Analytics and Impact Forecasting's Global Head of Tropical Cyclone Model Development. He leads development for Impact Forecasting's tropical cyclone models, including the U.S. Hurricane model and Impact Forecasting's Asia and Pacific typhoon models, and has previously worked on model development for European Windstorm, Southwest Pacific Tropical Cyclone, Vietnam Typhoon, Japan Typhoon, and bespoke vulnerability damage functions. Mr. Drinka holds a Master of Science in Physics, focusing on Meteorology and Climatology, from Comenius University in Bratislava, Slovakia

Mr. Drinka acts as the meteorology signature for Impact Forecasting's Florida Flood Model.

Xian He, Ph.D., Civil Engineering, University of Illinois at Urbana-Champaign

Dr. He, Associate Director, earned a Ph.D. in Civil Engineering with additional coursework in Mathematics and Statistics. Dr. He has published several research papers on hazard mitigation planning for interdependent infrastructure systems with a focus on hurricane hazards. Dr. He's Ph.D. research is related to developing a mathematical model that simulates the damage and recovery of interdependent infrastructure systems under hazard events and proposing risk-informed decision frameworks to support strategic pre-disaster risk mitigation and post-disaster recovery planning. She has completed extensive coursework in mathematics, probability and statistics, and risk analysis.

Dr. He's contributions to the Impact Forecasting Florida Flood Model include leading the development of the storm surge peril.

Yuliia Khmurovska, Ph.D., Civil Engineering, Czech Technical University in Prague

Dr. Khmurovska is Catastrophe model developer at Impact Forecasting. Dr. Khmurovska joined Aon in February 2023. Her contribution within Impact Forecasting includes development of in-house terrorism and flood vulnerability simulators, numerical simulations using 3D computational fluid dynamics (CFD) blast commercial software as well as advanced 3D applied element method (AEM) and finite element method (FEM) commercial software, assessment of structural and non-structural damage of buildings and content, assessment of progressive collapse possibility. Dr. Khmurovska completed her doctoral studies in civil engineering at Czech Technical University in Prague. Prior to joining Impact Forecasting she was working as assistant professor and academic researcher Czech Technical University in Prague (with a special interest in construction and maintenance of nuclear power plants) as well as structural engineer.

Alec Killoran

Alec Killoran is an Associate Director for Impact Forecasting, operating within the Program Management team as a Technical Writer. He holds a Bachelor of Arts in English from the University of California, Santa Barbara. Prior to joining Impact Forecasting, Mr. Killoran worked as a catastrophe model analyst at Risk Management Solutions and Berkshire Hathaway Specialty Insurance. His contributions to the IF Florida Flood model include documentation improvement and review.

Yujin Liang, Ph.D., P.E., Structural Engineering, University of Illinois at Chicago

Dr. Liang is a Director at Impact Forecasting and holds a Ph.D. in structural engineering from the University of Illinois at Chicago. He is a licensed Professional Engineer (Minnesota). Dr. Liang's research contributions within Impact Forecasting include developing advanced models to improve vulnerability and hazard assessments of insurance interests for various natural perils. He is experienced in the design and construction of hydroelectric dams and power plants and has published multiple research articles on the evaluation of structural damage. His work has achieved an ASCE Best Paper Award.

Dr. Liang contributes to the development of the Impact Forecasting Florida Flood Model's vulnerability functions and acts as the vulnerability signatory.

Minchong Mao, M.S., FCAS, MAAA, CCRMP, Computer Science, University of Missouri

Minchong Mao is a Senior Managing Director at Aon Reinsurance Solutions. She is a Fellow of the Casualty Actuarial Society (FCAS, 2007) and a member of American Academy of Actuaries (MAAA, 2005). At Aon, Ms. Mao advises clients in catastrophe actuarial services, such as rate making and rate filing strategy, ASOP 38 compliance, reinsurance cost allocation and profitability. Ms. Mao is responsible for Aon's homeowner ROE study and residual market study. Ms. Mao is a consulting actuary for the Impact Forecasting Florida Hurricane Model. Before joining Aon in 2018, Ms. Mao worked at State Farm Insurance Company for 18 years where she was responsible for the use of catastrophe models in pricing, underwriting, claims, enterprise risk managements, and rating agency reporting. Ms. Mao has a wealth of experience in the securitization of insurance risk and the use of catastrophe model outputs for pricing, risk selection and capital modeling.

In January 2015, Ms. Mao was appointed by Florida CFO Jeff Atwater to serve on the Florida Commission on Hurricane Loss Projection Methodology (FCHLPM) as the industry actuary. For over three years Ms. Mao represented the property insurance industry on the FCHLPM to review and accept hurricane models for use in ratemaking in the State of Florida. From 2010 to 2013, Ms. Mao was a member of an advisory group to the Insurance Bureau of Canada (IBC) and Office of the Superintendent of Financial Institutions (OSFI) to provide expert opinions on insurance and economic impact of major earthquakes in Canada. From 2011 to 2013, Ms. Mao was a member of an advisory group for IBC and OSFI to revise OSFI Guideline B-9 (Earthquake Exposure Management Sound Practice Guideline for insurance companies). Ms. Mao is a member of the CAS Climate Change Committee and member of AAA Extreme Event Risk Committee. In 2017, Ms. Mao contributed to AAA's Flood Monograph. In 2018, she was one of the main authors for AAA's catastrophe modeling monograph. Ms. Mao was one of the recipients of Casualty Actuarial Society's Above and Beyond Achievement Award in 2019 to recognize her leadership and contributions to establish the Certified Catastrophe Risk Management Professional (CCRMP) designation for CAS Institute. Ms. Mao has a bachelor's degree in Biochemical Engineering from Beijing University of Chemical Technology, a master's degree in Chemistry from Eastern Illinois University and a master's degree in Computer Science from University of Missouri - Columbia.

Ms. Mao's actuarial contributions to Impact Forecasting Florida Flood Model include advising and reviewing how insurance terms are applied in the financial model, reviewing actuarial forms to ensure results are reasonable and consistent, developing contents for the actuarial standards of the submission document and performing ASOP 38 compliance tasks.

Ricardo Wong Montoya, B.S., Civil Engineering, Pontifical Catholic University of Peru

Mr. Wong is a Catastrophe Model Developer at Impact Forecasting. Mr. Wong joined Impact Forecasting in June 2021 to support the development of the vulnerability component of flood models. He was responsible for developing the flood vulnerability component of Impact Forecasting models for Central European territories, including Austria, Poland, and Slovakia. Before joining Impact Forecasting, he worked in Peru as a Site Engineer in residential and commercial projects, developing a broad understanding of construction practices and building engineering.

Mr. Wong's contribution to the Impact Forecasting Florida Flood Model includes the development of the vulnerability component, including the engineering-based methodology for flood damage quantification.

Andres Paleo, Ph.D., Structural Engineering, University of Florida

Dr. Paleo is an Associate Director for Impact Forecasting's Research and Development team. His research and contributions within Impact Forecasting include the development of advanced vulnerability models for perils such as severe convective storms and inland and coastal floods.

Before joining Impact Forecasting in January 2022, he worked as a Senior Engineer at Karen Clark and Company, contributing to the vulnerability components of several models. In addition to developing vulnerability components for different perils, he has conducted extensive post-event reconnaissance surveys including for Hurricanes Ian (2022), Ida (2021), and Irma (2017). Dr. Paleo completed his doctoral studies in structural engineering at the University of Florida, where he was part of the Florida Public Hurricane/Flood Loss Model's engineering team and where he published multiple peer-reviewed research articles on the vulnerability of residential structures to coastal flood perils.

Dr. Paleo's contribution to the Impact Forecasting Florida Flood Model includes the development and peer review of key vulnerability components.

Purvish Patel, B.S., Mathematics/Computer Science/Business Administration, Wayne State College, Wayne, Nebraska

Mr. Patel is Director of Software Quality Assurance at Impact Forecasting. His responsibilities include designing, developing and implementing test plans, test cases, and test processes for the ELEMENTS modeling platform. Mr. Patel has over 20 years of professional experience in business process engineering and software development lifecycle, working in a complex, project-based environment.

Mr. Patel's contribution to the Impact Forecasting Florida Flood Model includes developing and executing functional and end-to-end ELEMENTS modeling workflow tests.

Ankit Prashnani, M.S., Geomatics, CEPT University

Mr. Prashnani is a senior consultant at Impact Forecasting, based in the Bangalore office. With six years of experience in catastrophe modelling, he holds a bachelor's degree in civil engineering and a master's degree in geomatics. At Impact Forecasting, his role primarily involves providing essential geospatial and programming support for flood model development. He has been an integral part of Impact Forecasting since November 2020 and has previously worked at RMS and WTW in similar capacities.

Mr. Prashnani's contribution to the Impact Forecasting Florida Flood Model includes managing geospatial data, encompassing procurement, processing, and automation, throughout all stages of model development.

Petr Puncochar, Ph.D., Hydrology and Open-Channel Hydraulics, Czech Technical University, Prague, Czechia

Dr. Puncochar is the Head of Flood Model Development for Impact Forecasting. Dr. Puncochar has worked with Aon's Impact Forecasting team since February 2010. From 2013 Dr. Puncochar managed Impact Forecasting's flood model development hub in Prague and represented it both internally and externally. In 2015, Dr. Puncochar became responsible for APAC region and was relocated to for 2-years period to Singapore, where he gained a rich and valuable insight into this region. In 2021, Dr. Puncochar received the responsibility for the US Flood models, which globalized his role.

Dr. Puncochar's contribution to the Impact Forecasting Florida Flood Model includes coordination of the model's development and the partnership between Impact Forecasting and Fathom, as well as widely participating in the overall model development.

Dr. Niall Quinn, MSci, PhD., Geographical Sciences, University of Southampton. Principal Modeller, Fathom.

NIall Quinn is a Principal Modeller for Fathom, operating within the Technical team. He undertook his PhD in Physical Geography at the University of Southampton. His research focused on nearshore coastal tide-surge-wave modelling with a view to risk calculation and forecasting. From Southampton he became a postdoctoral researcher at the University of Bristol, working under Professor Paul Bates for 5 years before joining Fathom. At Fathom Niall works on a variety of client and in house technical developments, with a particular focus on large scale stochastic and coastal modelling frameworks.

Dr. Quinn has contributed to the creation of the Fathom-IF merged US stochastic event set and resulting flood maps.

Venkatesh Ramaiah, M.S., Computer Science, Birla Institute of Technology and Science, Pilani, India

Mr. Ramaiah has 15 years of software development experience building enterprise applications using Microsoft technologies. He has supported the development of Impact Forecasting's ELEMENTS catastrophe modeling platform since joining Impact Forecasting. Mr. Ramaiah's contribution to the Impact Forecasting's Florida Flood Model involves implementing model components into the ELEMENTS modeling platform.

Dan Rees, M.A., Geographic Information Science, Clark University

Mr. Rees is the Director of US Flood Model Development for Impact Forecasting. Mr. Rees joined Impact Forecasting in 2023. Prior to joining Aon, Mr. Rees was a member of the flood modelling research group within Verisk Extreme Event Solutions (formerly known as AIR Worldwide) from 2011 to 2023. During his tenure, Mr. Rees participated in the development of inland and storm surge models for Albania, Austria, Brazil, Canada, China, The Czech Republic, Germany, India, Italy, Japan, Macedonia, Poland, Serbia, Switzerland, Thailand, The United Kingdom, and The United States. Mr. Rees joined Impact Forecasting in 2023, and is responsible for managing the strategy and development of Impact Forecasting's US flood model.

Mr. Rees had led development of Impact Forecasting's Florida Flood Model, contributing widely to the overall model development, and directing and engaging in research and development of the underlying model inputs.

Dr. Christopher Sampson, MSci, PhD., Geographical Sciences, University of Bristol. Chief Technical Officer, Fathom.

Dr Christopher Sampson co-founded Fathom in 2013 whilst undertaking his PhD in Physical Geography at the University of Bristol. His academic studies focused on developing experimental flood Catastrophe models and it was through this work that the need for better flood risk analytics at the global scale was identified, ultimately leading to the formation of Fathom. As CTO, Christopher now leads the technical development and strategy for Fathom and has guided the development of our modelling framework, becoming known as a leading expert in the field of large-scale flood models through his growing record of academic publications (>4000 citations).

Dr. Sampson has contributed to hydraulic model development over Florida and has coordinated the AON/Fathom partnership from the Fathom side.

Dr. James Savage, PhD., Geographical Sciences, University of Bristol. Principle Hydraulic Modeller, Fathom.

James Savage is a Principal Hydraulic Model Developer for Fathom, operating within the Technical team. He works on all aspects of hydraulic modelling, including data sourcing and processing, hydraulic model build and simulation and model evaluation. He has undertaken hydraulic modelling for Fathom's US, UK, Japan and Global flood modes as well as working on many other client projects including for the UK government Foreign and Commonwealth Development Office. Prior to joining Fathom, James worked as a Water Engineer at Jacobs for three years where he worked on a number of flood and water resources modelling projects. Dr. Savage holds a Doctor of Philosophy in Geographical Sciences from the University of Bristol..

Dr. Savage's contributions to the IF Florida Flood Model include work on the input data that is incorporated into the inland hydraulic models, as well as model simulation and processing.

Elham Sharifineyestani, Ph.D., Civil Engineering, Old Dominion University

Elham is a Senior Scientist at Aon Impact Forecasting, specializing in the development of the US inland flood model. She joined Aon Impact Forecasting team in August 2020. In her role, Elham has played a crucial role in the development of the Tropical Cyclone Rainfall model for the US inland flood model.

Elham holds a Ph.D. in Civil Engineering from Old Dominion University, earned in 2019, marked by extensive research into nonlinear ocean wave evolution. Her research findings have been published in prestigious scientific journals.

Elham's contributions to the Aon Impact Forecasting Florida Flood Model encompass the development, calibration, and validation of the Tropical Cyclone Rainfall model, as well as the validation of the Inland Flood model. Additionally, she has adeptly developed geospatial Python code to automate various processes for the Florida Commission on Hurricane Loss Projection Methodology.

Radek Solnicky, M.S., Mathematical Statistics, Charles University, Prague, Czechia

Mr. Solnicky, Senior Scientist, earned a M.S. in Probability, Mathematical Statistics and Econometrics from Charles University. Mr. Solnicky's work within Impact Forecasting includes the development of advanced event set generation methodologies for flood models, spatial and extreme value analyses of hydrological data, and implementation of uncertainty linked to exposure and vulnerability data into the model. He also supervises statistical aspects of catastrophe model testing and implementation into ELEMENTS, the firm's catastrophe modelling software platform.

Mr. Solnicky's contribution to the Impact Forecasting Florida Flood Model includes the peer review of key statistical work as well as ensuring compliance with the statistical standards as the statistical signatory.

Vipin Unnikrishnan, Ph.D., Structural Engineering, Louisiana State University, Baton Rouge

Dr. Unnikrishnan is a Principal Research Consultant at Impact Forecasting. His research and contributions within Impact Forecasting include development of advanced vulnerability models for perils such as wind, flood, and storm surge. Before joining Impact Forecasting, he was working as a post-doctoral fellow at the NIST Center of Excellence for Risk-Based Community Resilience Planning at Colorado State University. Dr. Unnikrishnan completed his doctoral studies in structural engineering at Louisiana State University and has published multiple research articles on the performance-based risk assessment of buildings and critical infrastructure in peer reviewed journals.

Dr. Unnikrishnan's contribution to the Impact Forecasting Florida Flood Model includes the development and peer review of key vulnerability components.

Chad Xu, M.S., Actuarial Science, Temple University

Mr. Xu is a Catastrophe Actuarial Analyst at Aon Reinsurance Solutions. Mr. Xu joined Aon in June 2021. At Aon, Mr. Xu assists Minchong Mao in catastrophe actuarial client services, Aon's homeowner ROE study, inflation study and residual market study. Mr. Xu has practical experience with multiple programming languages and automated app development. Before joining Aon, Mr. Xu published two research papers on political economic and actuarial product pricing/hedging topics. Mr. Xu earned a Bachelor of Science degree majoring Applied Mathematics in China, a Master of Science degree majoring Finance from Dayton University and a Master of Science degree majoring Actuarial Science from Temple University.

Mr. Xu's contributions to the Impact Forecasting Florida Flood Model include generation and QA of actuarial and statistical forms, as well as assisting Minchong Mao in conducting due diligence on reasonableness and consistency in actuarial results.

Shruthi Srikantegowda, Post-Graduate Diploma, Information Technology, Symbiosis University, Pune, India

Ms. Srikantegowda holds the title of Principal Consultant I and leads many quality assurance tasks to ensure appropriate implementation of Impact Forecasting models within the ELEMENTS modeling platform. Ms. Srikantegowda holds a post-graduate diploma in information technology from Symbiosis University, Pune, India, and an engineering degree in electronics and communications from the Visvesvaraya Technical University, Belgaum Karnataka, India. Ms. Srikantegowda's contributions to the Impact Forecasting Florida Flood Model includes testing and validating model data and software functionality using automation scripts, as well as documenting and maintaining traceability matrixes.

Appendix C: External Expert Review of Vulnerability Modules

ERN International

Mexico City, November 10, 2023

Dr. Xian He and Mr. Daniel Rees
Impact Forecasting
200 East Randolph St.
Chicago, IL 60601

Dr. He and Mr. Rees,

ERN has completed an external and unbiased review of the vulnerability components of the Impact Forecasting Florida Flood Model v3.0. ERN completed this review based on published scientific literature and data, the team's educational background in civil and structural engineering and professional background in structural and vulnerability engineering, the company's past experiences in post-disaster investigations, and our prior experience developing storm surge and inland flood risk models for infrastructure. It is our opinion that the vulnerability component of the Impact Forecasting Florida Flood Model v3.0 follows a scientifically and technically sound methodology that meets the vulnerability standards outlined in the Flood Standards Report of Activities as of November 1, 2021 by the Florida Commission on Hurricane Loss Projection Methodology. Details of our independent review are outlined in the attached document.

Sincerely,

Eduardo Reinoso, PhD
eduardo.reinoso@ern.com.mx
Vito Alessio Robles 179
Hda. de Gpe. Chimalistac, 01050
Álvaro Obregón, CDMX
+52 555616-8161 ext101

ERN Evaluación de Riesgos Naturales
Vito Alessio Robles 179, Hacienda de Gpe. Chimalistac, Del. Álvaro Obregón 01050, México, D.F.
Tel./FAX: +52 (55) 56 16 - 81 61, 62 y 64; www.ern.com.mx

Independent Vulnerability Review of the Impact Forecasting Florida Flood Model v3.0

Overview

The Impact Forecasting Florida Flood Model v3.0 vulnerability component methodology was reviewed alongside the vulnerability standards for the 2023 submission to the Florida Commission on Hurricane Loss Projection Methodology.

During the peer-review process of the Impact Forecasting Florida Flood Model v3.0, Impact Forecasting provided comprehensive documentation on the vulnerability component methodology and damage functions exhibits, with focus on the most representative risks in Florida. Based on the shared information, the methodological aspects and the specific behavior of the damage functions were discussed through several meetings and professional correspondence between ERN and Impact Forecasting.

Vulnerability Component Methodology

The Impact Forecasting Florida Flood Model v3.0 follows an engineering-based approach to develop a robust suite of vulnerability curves that vary by sub-peril, region, occupancy class, construction class, number of stories, year built, foundation type, and first floor height.

Impact Forecasting uses a proprietary component-based flood damage Monte Carlo simulator that applies engineering principles to estimate the load and capacity of various components of a building. The simulator provides estimates of direct building components damage, as well as damage to contents and restoration time for various levels of hazard intensity (still water depth). This engineering-based approach is combined with empirical data obtained from post-disaster surveys as well as published studies to obtain base vulnerability curves.

From an engineering perspective, the following points from the methodology were discussed as part of the review:

- Hydrodynamic and hydrostatic forces for inland and coastal flood hazards
- Water intrusion modelling
- Failure mechanisms
- Structural capacity of components
- Water-contact capacity of components

Damage Functions Exhibits

The following aspects were reviewed from the multiple damage function exhibits provided by Impact Forecasting:

- Damage function relativities by sub-peril (inland flood, storm surge)
- Damage function relativities and function behavior by coverage (building, contents, time element)
- Damage function relativities by building characteristics (construction class, number of stories, year built, foundation type, and first floor height)

ERN concluded that relativities between vulnerability curves when compared by individual characteristics appear logical.

ERN Evaluación de Riesgos Naturales
Vito Alessio Robles 179, Hacienda de Gpe. Chimalistac, Del. Álvaro Obregón 01050, México, D.F.
Tel./FAX: +52 (55) 56 16 - 81 61, 62 y 64; www.ern.com.mx

Based on the evolution of damage observed in the vulnerability curves and the information provided as part of the methodology, the following aspects were also considered as part of the review:

- The representation of a building envelope's physical behavior under flood action for different construction classes
- Cost catalogs (for building components and contents) and their influence on the behavior of the damage functions
- Content catalogue representativity for various construction classes
- The mechanical behavior of critical components that can lead to the total collapse of a structure and its representation in the damage functions.

Finally, direct comparisons of the Impact Forecasting model outputs against damage estimations reported by the U.S. Army Corps of Engineers and curves developed by HAZUS were analyzed to further validate Impact Forecasting's methodology and vulnerability curves.

Final Remarks

In our opinion, the vulnerability component of the Impact Forecasting Florida Flood Model v3.0 follows a sound methodology that incorporates engineering principles, on-site damage surveys, structural engineering expertise, claims datasets, and publicly available damage functions. This methodology delivers a well-designed and validated suite of vulnerability functions.

ERN Evaluación de Riesgos Naturales
Vito Alessio Robles 179, Hacienda de Gpe. Chimalistac, Del. Álvaro Obregón 01050, México, D.F.
Tel./FAX: +52 (55) 56 16 - 81 61, 62 y 64; www.ern.com.mx

Appendix D: External Expert Review of Meteorology and Vulnerability Modules

Empower Results®

Katie Carter, CCRMP | Managing Director, Aon | katie.carter@aon.com

January 22, 2024

Dr. Xian He, Associate Director and Head of U.S. Storm Surge Model Development and Mr. Dan Rees, Director and Head of U.S. Flood Model Development
Impact Forecasting
200 East Randolph St.
Chicago, IL 60601

Dr. Xian and Mr. Rees,

I have completed an external and unbiased review of the hazard and vulnerability components of the Impact Forecasting Florida Flood Model (FCHLPM) Version 3.0. I have completed this review using published scientific literature and data, my educational background in climatology and geography, my professional background in model evaluation, my own personal experiences in post-disaster investigations, and National Flood Insurance Program (NFIP) claims data. It is my opinion that the meteorology and vulnerability components of the Impact Forecasting Florida Flood Model (FCHLPM) Version 3.0 meet the meteorology and vulnerability standards outlined in the Flood Standards Report of Activities as of November 1, 2021, by the Florida Commission on Hurricane Loss Projection Methodology and that state and county-level modeled loss relationships are reasonable. Details of my independent review are outlined in the attached document.

Sincerely,

Holly M. Widen

Holly M. Widen, Ph.D.
Director, Aon

8200 Tower | 5600 West 83rd Street | Suite 1100 | Minneapolis, MN 55437
t +1.952.886.8263 | m +813-546-8716 | aon.com

Empower Results®

Katie Carter, CCRMP | Managing Director, Aon | katie.carter@aon.com

Independent Hazard, Vulnerability, and Loss Review of the Impact Forecasting Florida Flood Model (FCHLPM) Version 3.0

Holly M. Widen, Ph.D.

Hazard Review

Overview

The Impact Forecasting Florida Flood Model (FCHLPM) Version 3.0 methodology documentation was reviewed alongside the meteorology standards for the 2024 submission to the Florida Commission on Hurricane Loss Projection Methodology.

The Impact Forecasting Florida Flood Model (FCHLPM) Version 3.0 leverages Fathom's U.S. flood model and the National Weather Service's Sea, Lake, and Overland Surges from Hurricanes (SLOSH) model to generate more than 178K stochastic events that are the basis of a fully probabilistic flood model. Historical data sources, such as HURDAT2, NOAA Atlas 14, USGS gauge and elevation data, and USACE National Levee Database, are reputable sources for stochastic flood model development and are used in the event generation process.

Fathom's non-tropical cyclone events are used in the Impact Forecasting Florida Flood Model (FCHLPM) Version 3.0 directly and are derived using well-established statistical methods for generating flood event extents and depths that encompass both fluvial and pluvial flooding. For fluvial flood modeling, a regional flood frequency analysis is utilized to relate gauged and ungauged catchments to enable simulations of extreme river discharge using historical USGS gauge data across the entire model domain. Fathom uses a conditional multivariate model for this simulation that characterizes the dependence between gauges and employs the Laplace distribution to better represent the relationship between the extreme discharge observations. The pluvial model component uses rainfall scenarios derived from the widely used NOAA Intensity-Duration-Frequency (IDF) relationships to obtain extreme rainfall estimations, which are then utilized to simulate rainfall-runoff while accounting for infiltration and urban drainage. The simulated rainfall-runoff and river discharge are translated into flood extents and depths leveraging the well-known 2-D shallow water equations and grouped into events utilizing a spatial clustering algorithm while considering contiguous USGS watershed boundaries and a 7-day temporal window (based on published research on flood wave travel times).

Katie Carter, CCRMP | Managing Director, Aon | katie.carter@aon.com

For tropical cyclone events, stochastic tropical cyclone track information (e.g., track position, central pressure, radius of maximum wind speed, timestamps, etc.) from the Impact Forecasting Florida Hurricane Model Version 2 are used in the 2021 vintage of the SLOSH model to generate storm surges and in the peer-reviewed Tropical Cyclone Rainfall (TCR) model developed by Lu et al. (2018)[1] and Feldmann et al. (2019)[2] to simulate precipitation over the lifecycle of the event. The SLOSH model is a simplified numerical model that utilizes regional meshes and simplified shallow water equations to force coastal flooding on land and is used by the National Weather Service, U.S. Army Corps of Engineers, and FEMA. The storm surges are modeled along the Gulf and Atlantic coasts considering impacts due to bathymetry/topography, land use land cover, tidal impacts, and coastal levees. The TCR model calculates rain rates and accumulated rainfall on a 0.1°×0.1° grid across the continental U.S. using the track information along with environmental parameters from NOAA reanalysis data. Kerry Emanuel, a well-regarded climate scientist and professor of meteorology for over 40 years at MIT, was one of the developers of the TCR model which continues to be leveraged in the hurricane research community. The maximum 24-hour accumulated rainfall generated from the TCR model for each event was used as input for Fathom's hydrological/hydraulic model to obtain fluvial and pluvial flood extents and depths as described above.

It is my opinion that the development of the hazard module in the Impact Forecasting Florida Flood Model (FCHLPM) Version 3.0 uses up-to-date data and scientifically sound approaches to generate a stochastic flood event set that is calibrated and validated against peer-reviewed and reputable publicly available historical data sources (e.g., FEMA flood zone extents, USGS gauge data and high water marks, NOAA rainfall, etc.). The event set is robust and provides a comprehensive view of historical experience as well as reasonable uncertainty to account for plausible events not recorded in the historical data.

[1]Lu, P., N. Lin, K. Emanuel, D. Chavas, and J. Smith, 2018: Assessing hurricane rainfall mechanisms using a physics-based model: Hurricanes Isabel (2003) and Irene (2011). J. Atmos. Sci., 75, 2337–2358, https://doi.org/10.1175/JAS-D-17-0264.1.

[2]Feldmann, M., K. Emanuel, L. Zhu, and U. Lohmann, 2019: Estimation of Atlantic tropical cyclone rainfall frequency in the United States. J. Appl. Meteor. Climatol., 58, 1853–1866, https://doi.org/10.1175/JAMC-D-19-0011.1.

Vulnerability Review

Overview

The Impact Forecasting Florida Flood Model (FCHLPM) Version 3.0 methodology documentation was reviewed alongside the vulnerability standards for the 2024 submission to the Florida Commission on Hurricane Loss Projection Methodology.

The Impact Forecasting Flood Model (FCHLPM) Version 3.0 combines an engineering-based and empirical-based approach to develop a robust suite of vulnerability curves that vary by occupancy class, construction class, number of stories, year built, foundation type, first floor height, and several

Katie Carter, CCRMP | Managing Director, Aon | katie.carter@aon.com

additional "secondary risk characteristics" related to key building features and mitigation efforts that are important for assessing flood risk.

Impact Forecasting uses a proprietary building component-based damage simulator that applies engineering principles and reliability methods to estimate the load and capacity characteristics of various building components susceptible to flood damage. The simulator is based on a Monte Carlo framework which performs statistical sampling for various flood loading conditions (water depth, flow velocity and wave height) and resistance values on different structural components in order to estimate damage outcomes for each component. The component-based results are aggregated into overall building outcomes and combined with a restoration cost model to determine repair cost and time estimates. This engineering-based approach is used along with empirical data from post-disaster surveys and published studies (e.g., USACE depth-damage curves) to derive base damage functions by coverage (i.e., building, contents, and time element) that also consider the impact of building code requirements and regional vulnerability with respect to FEMA flood zone classifications.

Secondary risk characteristics are also supported in the model to further differentiate risks based on building enclosure type and mitigation efforts covering flood-resistant design, construction, and retrofit techniques, such as floodproofing and flood openings. These characteristics are important to accurately reflect estimated damage in a flood model as they impact a building's resilience against flooding.

Impact Forecasting provided results from relativity testing they conducted to validate the damage functions during the independent review. This testing leveraged select locations from their Florida Residential Industry Exposure Database (IED) with different sets of building characteristic combinations to examine the relative change in modeled loss that occurs by varying only one characteristic at a time. The relationships between supported occupancy classes, construction classes, story bands, year built bands, foundation types, and first floor height bands as well as the directional impact of the supported secondary risk characteristics appear logical based on expert judgement and comparison with available USACE damage functions. Impact Forecasting also used detailed policy-level NFIP claims data for personal residential exposure from the OpenFEMA dataset totaling approximately $9.6B across more than 103K policies countrywide to validate the damage functions.

It is my opinion that the vulnerability module in the Impact Forecasting Florida Flood Model (FCHLPM) Version 3.0 utilizes a comprehensive approach to deriving a robust suite of damage functions. The approach encompasses engineering-based simulations at a component-level along with real-world experience from post-disaster surveys and published studies and is further calibrated with extensive claims data.

Loss Review

Overview

Empower Results®

Katie Carter, CCRMP | Managing Director, Aon | katie.carter@aon.com

Impact Forecasting provided state and county-level modeled losses by coverage, event type (tropical cyclone and non-tropical cyclone), and sub-peril (inland flood and storm surge flooding) for the independent review using their Florida Residential Industry Exposure Database (IED).

County-level average annual losses (AALs) were examined to evaluate the spatial distribution of loss across the state and compare against aggregated NFIP claims from 1970 to 2022. The spatial loss pattern generally aligns between the two showing consistency in regional flood risk. Sub-peril county loss costs and state-level AAL contributions by event type were also examined and appear reasonable. For example, Gulf coast counties tend to have higher storm surge loss costs given the increased risk due to more gradually sloping bathymetry than the steeper sloping Atlantic coast. Storm surge also typically has a greater contribution to the statewide AAL than inland flood for tropical cyclone-driven flood events as storm surge is more often the dominant damage-causing peril. In addition, state-level PMLs by coverage and sub-peril were examined and follow expected behavior. Relationships between sub-peril coverage loss contributions appear logical, with building coverages having greater loss contributions for storm surge than inland flood as the former typically causes more structural damage.

Impact Forecasting also shared modeled and trended NFIP loss results for select historical events during the independent review. The modeled insured event losses are comparable to the trended NFIP losses. Estimated historical event return periods based on the modeled stochastic exceedance probability curves also appear reasonable.

Appendix E: Flood Model Input Form

Location Information

Table 61: Impact Forecasting Florida Flood Model (FCHLPM) input fields for location information

Field Name	Description
PropertyID	Identifies a specific site/location and should be unique
BuildingID	Identifies a specific building within a site
BuildingName	This field is for user reference and not used in modeling
BuildingNumber	For U.S. locations, BuildingNumber is prepended to the StreetName when passed to the geocoding engine
StreetName	The street on which the property is located
City	The name of the city (used only for street-level geocoding of U.S. locations)
PostalCode	ZIP Code or postal code of the location
District	The name of the district (not used for U.S. locations)
StateAbbreviation	2-character state abbreviation
State	The name of the U.S. state (used only for street-level geocoding of U.S. locations)
TerritoryCode	The country in which the property is located. Use ISO 2-character country IDs or 3-digit ISO country number
NumOfStories	The number of stories in the building.
YearBuilt	Year of construction
OccupiedFloors	Field not currently used
BuildingType	The construction class of the building
OccupancyType	The occupancy class of the building
BuildingScheme	The classification scheme for BuildingType.
OccupancyScheme	The classification scheme for OccupancyType.
PropertyName	The name of the property, for user reference
PropertyNum	The number of the property, for user reference
GarageDoor	Type of garage door

Field Name	Description
FloorSize	Square footage area of building
RoofCover	Type of roof covering
RoofType	Roof type (geometry)
RoofConnections	Type of roof connection
RoofAge	Age of the roof
WindowProtection	Type of window protection
RoofSheathing	Type of roof sheathing
CoverageType1	Building coverage
CoverageSumInsured1	Replacement value of Building coverage
CoverageLimit1	The limit value assigned to the Building
CoverageDeductible1	The deductible value assigned to the Building
CoverageFraction1	This is a fraction that is applied to the Building loss after all insurance terms and before it is aggregated to the account level, currently not used
AggregationKey1	An integer to group similar user-defined coverages together at the Property Coverage level on the Building coverage
CoverageType2	Contents coverage
CoverageSumInsured2	Replacement value of Contents coverage
CoverageLimit2	The limit value assigned to the Contents
CoverageDeductible2	The deductible value assigned to the Contents
CoverageFraction2	This is a fraction that is applied to the Contents loss after all insurance terms and before it is aggregated to the account level, currently not used
AggregationKey2	An integer to group similar user defined coverages together at the Property Coverage level on the Contents coverage
CoverageType3	Time Element coverage
CoverageSumInsured3	The value of Time Element coverage.
CoverageLimit3	The limit for Time Element coverage
CoverageDeductible3	The deductible for Time Element coverage. This can be Additional Living Expenses (Residential) or Business Interruption (Commercial)
CoverageFraction3	This is a fraction that is applied to the Time Element loss after all insurance terms and before it is aggregated to the account level, currently not used
AggregationKey3	An integer to group similar user defined coverages together at the Property Coverage level on the Time Element coverage
CoverageType4	User-specified coverage type

Field Name	Description
CoverageSumInsured4	Replacement value of coverage type selected
CoverageLimit4	The limit value assigned to the coverage type selected
CoverageDeductible4	The deductible value assigned to the coverage type selected
CoverageFraction4	This is a fraction that is applied to the coverage loss after all insurance terms and before it is aggregated to the account level, currently not used
AggregationKey4	An integer to group similar user defined coverages together at the coverage type selected
LocationNum	This field is for user reference
LocationName	This field is for user reference
LocationLimit	This is the limit at the site/location level. Usually expressed as an amount but can also be expressed as a fraction of the underlying TIV
LocationDeductible	This is an all other perils (AOP) (occurrence-based) deductible value at the site/location level. Usually expressed as an amount but can also be expressed as a fraction of the underlying TIV or loss
LocationAnnualDeductible	This is an annual deductible value at the site/location level. Usually expressed as an amount but can also be expressed as a fraction of the underlying TIV or loss
LocationDeductibleFractionBasis	1 – Deductible applies to total underlying value 2 – Deductible applies to structure coverage only
LocationDeductibleType	1 – Additional 2 – Net (default chosen by ELEMENTS) 3 – Loss based deductible
CombinedLimit	Combined limit at the site/location level. Applies before other site/location level limits
CombinedDeductible	Combined deductible at the site/location level. Applies before other site/location level deductibles
SiteFraction	Site level loss fraction paid by the insurer
AccountID	Unique identifier for the account
Latitude	The latitude of the location in decimal degrees
Longitude	The longitude of the location in decimal degrees
Matchcode	Indicates what the given latitude/longitude represents (exact coordinates of location, centroid of ZIP Code, etc.)
CrestaZone	Used in some models for geocoding
GridCellID	An internal geocode used for R&D and in a few of the non-U.S. models where geocoding is difficult. It is a geolocation value defined by the hazard modelers
Municipality	Used in some non-U.S. models for Geocoding

Field Name	Description
County	Used in some non-U.S. models for Geocoding
Group1	User-defined name of group
Group2	User-defined name of group
Group3	User-defined name of group
Group4	User-defined name of group
Group5	User-defined name of group
RoofTypeScheme	Field not currently used
FloorArea	This is the floor area used by the parameter adjustment feature
BasementScheme	The classification scheme for basement characteristics
BasementClass	Used with basement scheme to describe the basement characteristics
CustomElevation	User-defined elevation of the location, expressed in feet (not used for modeling, only reporting)
FirstFloorAdjustment	Height of the building above ground specified in meters
FoundationClass	The foundation type of the building
FoundationScheme	The classification scheme for foundation type

Policy Information

Table 62: Impact Forecasting Florida Flood Model (FCHLPM) input fields for policy information

Field Name	Description
AccountID	Unique identifier for the account
PolicyID	Unique identification number for the policy
PolicyNum	This field is for user reference
PolicyNote1	This field is for user reference
PolicyNote2	This field is for user reference
Attachment	The value of the lower bound of the layer. For step policies, this is the lesser boundary of the step. It is expressed in monetary amounts rather than fractions
Layer	The thickness of the layer. This can be expressed either in monetary amounts or as a fraction of the underlying TIV
Deductible	The deductible for standard policies. If expressed as a fraction, it will be the fraction of the TIV

Field Name	Description
MinimumDeductible	Minimum deductible amount paid by insured
MaximumDeductible	Maximum deductible amount paid by insured
DeductibleFractionBasis	1 – Deductible applies to total underlying value 2 – Deductible applies to structure coverage only
BlanketLimit	This is the maximum payout on the policy layer. If expressed as a fraction, it will be the fraction of the layer or fraction of the TIV if no layer is defined
DeductibleTypeCode	1 – Additional 2 – Net 11 – Step entered based on B losses 12 – Step entered based on B+C losses 13 – Step entered based on either B or C losses 14 – Step entered based on B and/or C losses (not supported) 15 – Step entered based on C losses
LocationDeductibleMax	1 – No 2 – Yes
PolicyType	1 – Standard policy 3 – California Earthquake Authority (CEA) 4 – PDTE (Physical Damage & Time Element) 11 – Fixed payment step policy 12 – Loss value step policy
LineOfBusiness	An identifier for the line of business
PolicyFraction	This fraction is used where the cedant is only participating in a part of the defined layer structure. It is applied after the policy deductible but before policy layer, blanket limit and policy attachment
PolicyCoverageLimit	This is the maximum payout on the policy coverage
PolicyCoverageDeductible	The deductible that applies to the policy coverage
PolicyCoverageFraction	Fraction that applies to policy coverage
PolicyCoverageCoverage	0 – Structure 1 – Appurtenant structure 2 – Contents 3 – Not currently used 4 – Time Element 5 – Not currently used 6 – Injury 7 – Death 8 – Death & Injury
PolicyCoverageType	1 – Additional 2 – Net

Field Name	Description
CedantName	Name of the cedant
SubPolicyType1	0 – Sublimit 1 – Policy restriction (currently not supported)
SubPolicyDeductible1	The value of the lower bound of the sub-limit.
SubPolicyDeductibleType1	0,1 – Additional 2 – Net 3 – Minimum 4 – Maximum
SubPolicyLimit1	This is the maximum payout on the sub-limit
SubPolicyGroupName1	Name of the sub-policy group
SubPolicyType2	0 – Sublimit 1 – Policy restriction (currently not supported)
SubPolicyDeductible2	The value of the lower bound of the sub-limit
SubPolicyDeductibleType2	0,1 – Additional 2 – Net 3 – Minimum 4 – Maximum
SubPolicyLimit2	This is the maximum payout on the sub-limit
SubPolicyGroupName2	Name of the sub-policy group
SubPolicyType3	0 – Sublimit 1 – Policy restriction (currently not supported)
SubPolicyDeductible3	The value of the lower bound of the sub-limit
SubPolicyDeductibleType3	0,1 – Additional 2 – Net 3 – Minimum 4 – Maximum
SubPolicyLimit3	This is the maximum payout on the sub-limit
SubPolicyGroupName3	Name of the sub-policy group
SubPolicyType4	0 – Sublimit 1 – Policy restriction (currently not supported)
SubPolicyDeductible4	The value of the lower bound of the sub-limit
SubPolicyDeductibleType4	0,1 – Additional 2 – Net 3 – Minimum 4 – Maximum
SubPolicyLimit4	This is the maximum payout on the sub-limit

Field Name	Description
SubPolicyGroupName4	Name of the sub-policy group
SubPolicyType5	0 – Sublimit 1 – Policy restriction (currently not supported)
SubPolicyDeductible5	The value of the lower bound of the sub-limit
SubPolicyDeductibleType5	0,1 – Additional 2 – Net 3 – Minimum 4 – Maximum
SubPolicyLimit5	This is the maximum payout on the sub-limit
SubPolicyGroupName5	Name of the sub-policy group
Payment	The payment for a fixed payment step policy

Treaty Information

Table 63: Impact Forecasting Florida Flood Model (FCHLPM) Model input fields for treaty information

Field Name	Description
TreatyID	This is the unique identifier for each treaty
TreatyRiskID	This is the unique identifier for each treaty record
TreatyName	This field is used to enter the treaty name
TreatyDescription	This field is used to enter the treaty description
TreatyType	1 – Facultative 2 – Working Excess 3 – Surplus Share 4 – Quota Share
TreatyLevel	Indicates level at which the treaty is applied: 2 – Site 3 – Account 4 – Policy
ConnectionID	The SiteID, AccountID, PolicyID or LOBID that the treaty applies to (depends on TreatyLevel)
LOB	Field used to enter LOB that the treaty applies to, multiple LOBs can be separated by a “;”
Attachment	The lower bound of loss above which the treaty is active
OccurenceLimit	This is occurrence limit of the treaty

Field Name	Description
TotalLimit	This is the maximum payout on the reinsurance layer
PercentPlaced	Indicates percentage of recovery from the treaty
Inuring Order	This is the inuring priority of the reinsurance

Please note that quota share and working excess treaties only apply if selected in the analysis setting window in the UI.

Secondary Modifier Information

Table 64: Impact Forecasting Florida Flood Model (FCHLPM) input fields for secondary modifier information

Field Name	Description
Property ID	Unique identifier ID
SecondaryModifierGroup	Secondary modifier group ID for the group names
Value	Secondary modifier value IDs for the respective secondary modifier group.

Sample Input Data File and Import Options Screenshots

PropertyID	BuildingID	BuildingName	BuildingNumber	StreetName	City	PostalCode	district	StateAbbreviation	state	TerritoryCode	NumOfStories	yearbuilt	occupiedFloors	BuildingType	OccupancyType	BuildingScheme	OccupancyScheme	User1	User2	User3	User4	User5
1	1									US	3	1989	0	5050	1055	IFE	IFE	1				
2	2									US	3	1989	0	5050	1055	IFE	IFE	2				
3	3									US	3	1989	0	5050	1055	IFE	IFE	3				
4	4									US	3	1989	0	5050	1055	IFE	IFE	4				
5	5									US	3	1989	0	5050	1055	IFE	IFE	5				

PropertyName	PropertyNum	YearRetrofit	GarageDoor	FloorSize	RoofCover	RoofType	RoofConnections	RoofAge	WindowProtection	RoofSheathing	coverageType1	CoverageSumInsured1	coveragelimit1	CoverageDeductible1	coveragefraction1
	1	0	0	0	0	0	0	0	0	0	0	5000	5000	0	1
	2	0	0	0	0	0	0	0	0	0	0	5000	5000	0	1
	3	0	0	0	0	0	0	0	0	0	0	5000	5000	0	1
	4	0	0	0	0	0	0	0	0	0	0	5000	5000	0	1
	5	0	0	0	0	0	0	0	0	0	0	5000	5000	0	1

aggregationkey1	coverageType2	CoverageSumInsured2	coveragelimit2	CoverageDeductible2	coveragefraction2	aggregationkey2	coverageType3	CoverageSumInsured3	coveragelimit3	CoverageDeductible3	coveragefraction3	aggregationkey3
1	2	50000	50000	0	1	1	4	0	0	0	1	1
1	2	50000	50000	0	1	1	4	0	0	0	1	1
1	2	50000	50000	0	1	1	4	0	0	0	1	1
1	2	50000	50000	0	1	1	4	0	0	0	1	1
1	2	50000	50000	0	1	1	4	0	0	0	1	1

coverageType4	CoverageSumInsured4	coveragelimit4	CoverageDeductible4	coveragefraction4	aggregationkey4	LocationNum	LocationName	User11	User21	User31	LocationLimit	LocationDeductible	LocationDeductibleFractionBasis	LocationDeductibleType
0	0	0	0	0	0	0	0	0	0	0	0	0	1	0
0	0	0	0	0	0	0	0	0	0	0	0	0	1	1000
0	0	0	0	0	0	0	0	0	0	0	0	0	1	1500
0	0	0	0	0	0	0	0	0	0	0	0	0	1	1000
0	0	0	0	0	0	0	0	0	0	0	0	0	1	2500

CombinedLimit	CombinedDeductible	SiteFraction	AccountID	Latitude	Longitude	MatchCode	DamageFunctionStub	CrestaZone	CrestaZoneVersion	GridCellID	Municipality	County	CustomDFStubPrimary	CustomDFStubSecondary
0	0	1	1	29.720063	-82.086798	1	0			0			0	0
0	0	1	2	29.720063	-82.086798	1	0			0			0	0
0	0	1	3	29.720063	-82.086798	1	0			0			0	0
0	0	1	4	29.720063	-82.086798	1	0			0			0	0
0	0	1	5	29.720063	-82.086798	1	0			0			0	0
0	0	1	6	29.720063	-82.086798	1	0			0			0	0

Group1	Group2	Group3	Group4	Group5	RoofTypeScheme	CoverageTIVStub1	CoverageTIVStub2	CoverageTIVStub3	CoverageTIVStub4	CoverageMajorInjuryValue1	CoverageMinorInjuryValue1	CoverageDeathValue1	CoverageMajorInjuryValue2	CoverageMinorInjuryValue2
						0	0	0	0	0	0	0	0	0
						0	0	0	0	0	0	0	0	0
						0	0	0	0	0	0	0	0	0
						0	0	0	0	0	0	0	0	0
						0	0	0	0	0	0	0	0	0

CoverageDeathValue2	CoverageMajorInjuryValue3	CoverageMinorInjuryValue3	CoverageDeathValue3	CoverageMajorInjuryValue4	CoverageMinorInjuryValue4	CoverageDeathValue4	FloorArea	BasementScheme	BasementClass	CustomElevation	FirstFloorAdjustment
0	0	0	0	0	0	0	0	IFE	UNK		
0	0	0	0	0	0	0	0	IFE	UNK		
0	0	0	0	0	0	0	0	IFE	UNK		
0	0	0	0	0	0	0	0	IFE	UNK		
0	0	0	0	0	0	0	0	IFE	UNK		

LocationAnnualDeductible	FoundationScheme	FoundationClass
	IFE	Unknown
	IFE	Unknown
	IFE	Unknown
	IFE	Unknown
	IFE	Unknown

Figure 161: Screenshot of sample hurricane model input file (parts 1 through 9).

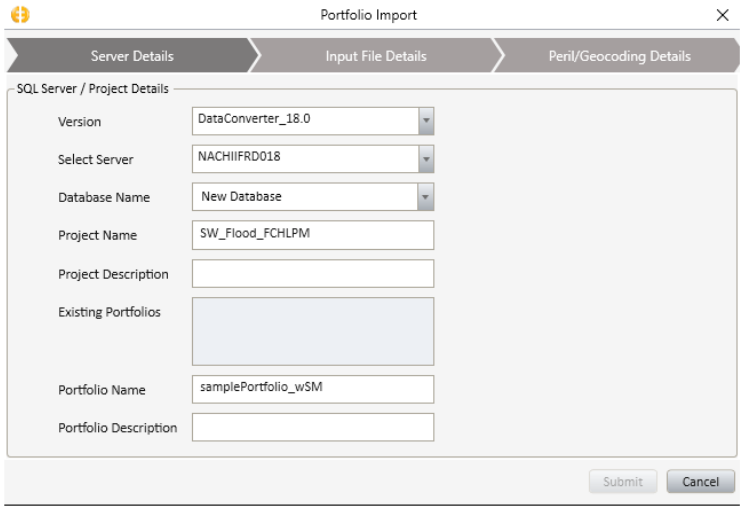

Figure 162: Screenshots of ELEMENTS input file import options (Server Details, part 1 of 3).

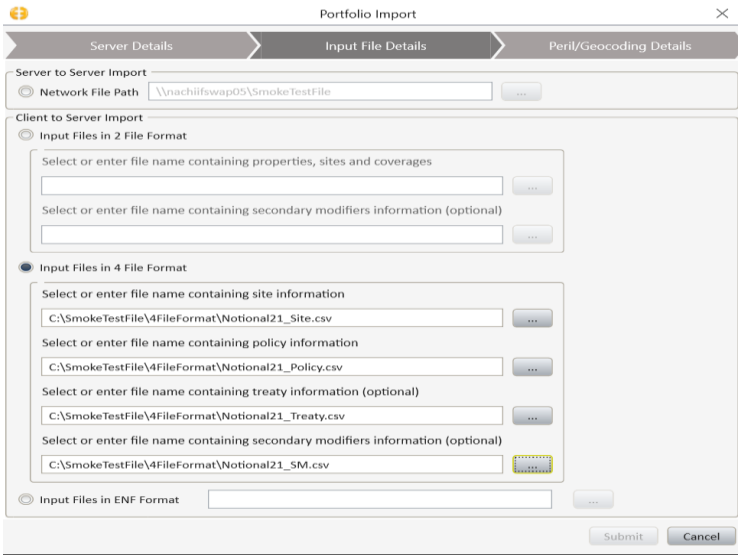

Figure 163: Screenshots of ELEMENTS input file import options (Input File Details, part 2 of 3).

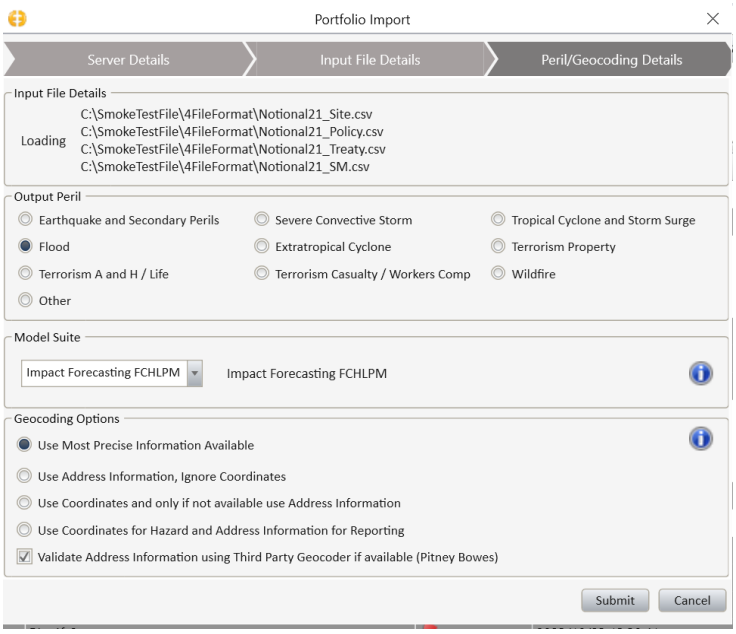

Figure 164: Screenshots of ELEMENTS input file import options (Peril / Geocoding Details, part 3 of 3).

Appendix F: Flood Model Output Form

Analysis Settings

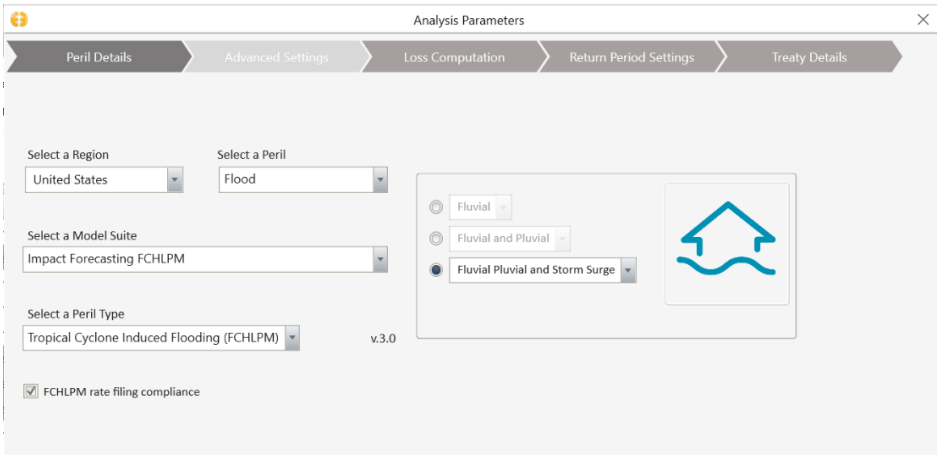

Figure 165: Screenshot of flood model analysis settings required for Tropical Cyclone Induced Flooding (FCHLPM) (part 1 of 2).

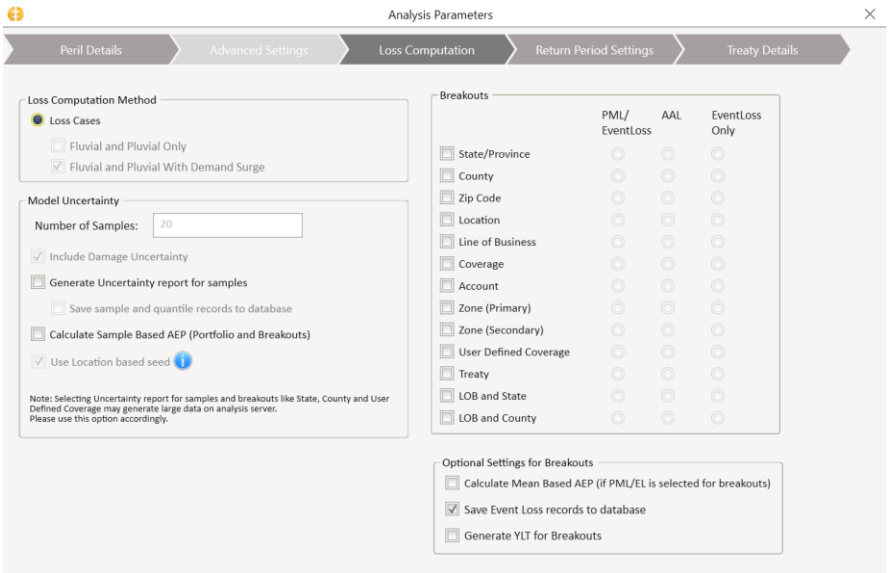

Figure 166: Screenshot of flood model analysis settings required for Tropical Cyclone Induced Flooding (FCHLPM) (part 2 of 2).

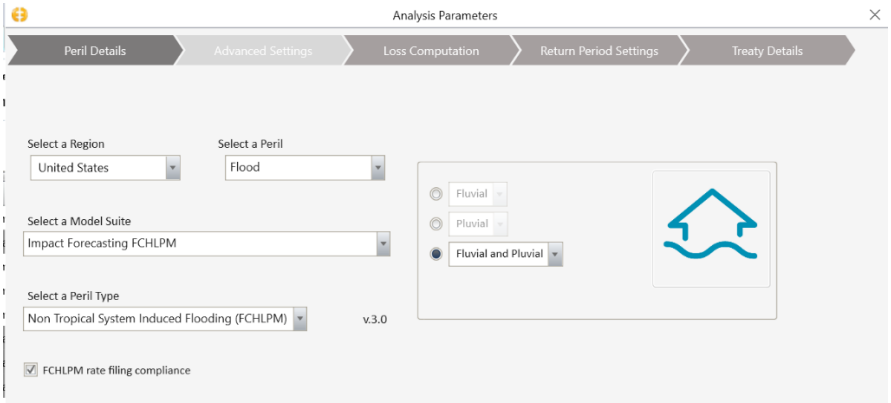

Figure 167: Screenshot of flood model analysis settings required for Non-Tropical Cyclone Induced Flooding (FCHLPM) (part 1 of 2).

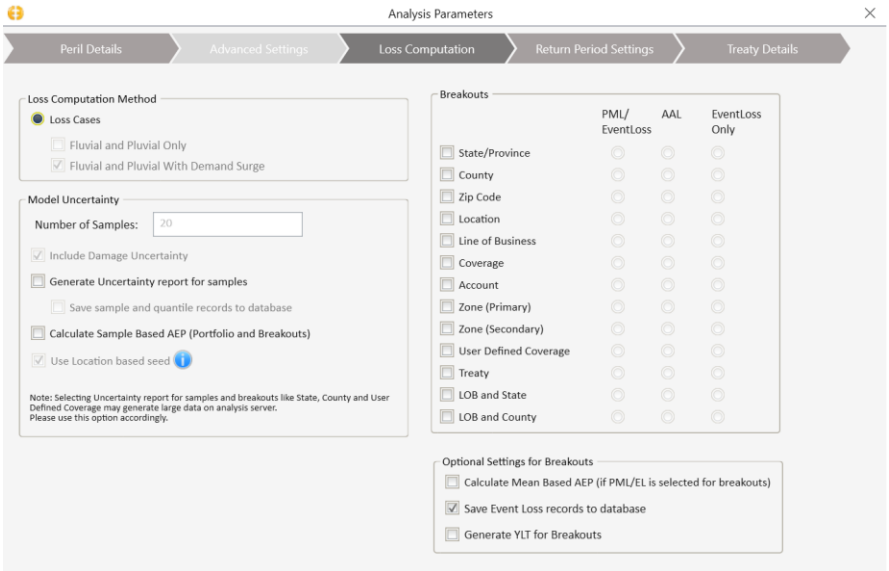

Figure 168: Screenshot of flood model analysis settings required for Non-Tropical Cyclone Induced Flooding (FCHLPM) (part 2 of 2).

Output Report

Tropical Cyclone Induced Flooding (FCHLPM) - v.3.0

Guidance on using outputs from ELEMENTS 18.0

If the sample based EP curve (default) and the mean based EP curves differ significantly it may be due to aggregation, please follow the rules below. For more details please see ELEMENTS Quick Guide

Input data	EP curve for PML reporting		DFA, roll-ups and other Event Loss based analysis			
	Default (sample based, full line)	Mean (mean per event, dashed line)	QLT (quantile loss table)	Samples per event	Mean loss per event with stdev	Mean loss per event without stdev
Individual – one row contains TIV for one location or coverage	USE	DO NOT USE	USE (default)	USE	USABLE	DO NOT USE
Aggregated – one row contains TIV for multiple locations	DO NOT USE	USABLE *	DO NOT USE	DO NOT USE	DO NOT USE	USABLE *

* WARNING : ELEMENTS assumes 100% correlation of losses among locations aggregated to one large TIV, we advise to disaggregate the data to individual locations for example using Impact Workbench

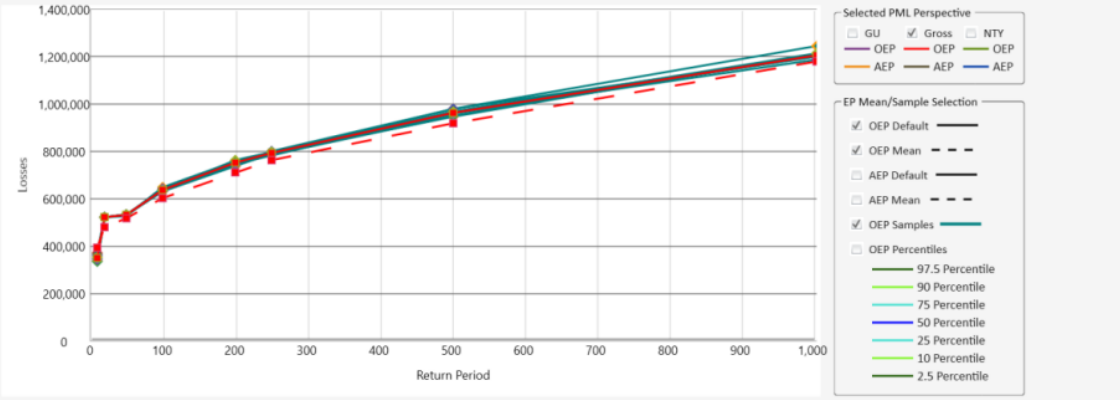

Figure 169: Screenshot of flood model output report (part 1 of 2).

* Table values in Actuals

OEP Default

Return Period	Ground Up	Gross	Net of Treaty
10,000	57,925,591	51,112,913	51,112,913
5,000	53,103,873	46,595,126	46,595,126
2,000	45,579,724	40,458,657	40,458,657
1,000	40,711,928	36,359,465	36,359,465
500	35,839,528	32,250,272	32,250,272
250	31,036,646	28,235,094	28,235,094
200	29,483,621	26,977,630	26,977,630
100	24,479,857	22,694,084	22,694,084
50	18,641,127	17,533,240	17,533,240
20	10,871,536	10,345,266	10,345,266
10	6,928,972	6,766,892	6,766,892
AAL	2,242,304	2,146,543	2,146,543
STDDEV	5,376,397	5,036,258	5,036,258

OEP Mean

Return Period	Ground Up - Mean	Gross - Mean	Net of Treaty - Mean
10,000	57,493,709	50,119,494	50,119,494
5,000	52,791,967	45,821,687	45,821,687
2,000	44,718,350	39,512,972	39,512,972
1,000	40,233,502	36,032,932	36,032,932
500	34,861,535	31,642,313	31,642,313
250	30,627,231	27,827,369	27,827,369
200	29,219,763	26,542,368	26,542,368
100	24,326,985	22,457,729	22,457,729
50	18,498,556	17,374,079	17,374,079
20	10,746,239	10,256,002	10,256,002
10	6,222,054	6,023,543	6,023,543
AAL	2,242,304	2,146,543	2,146,543
STDDEV	5,301,070	4,962,733	4,962,733

Figure 170: Screenshot of flood model output report (occurrence exceedance probability, left, and aggregate exceedance probability, right) (part 2 of 2)

Project Name: _FloridaFlood_Demo
Portfolio Name: FloridaFlood_Example
User ID: ifadmin
Date of Run: 9/16/2024 2:21:08 PM
Region: United States
Peril: Flood
Model Suite: Impact Forecasting FCHLPM
Model Name: Florida Flood (FCHLPM)
Model Version: v.3.0
ELEMENTS Version: 18.0.0.0
Damage Option: Fluvial Pluvial and Storm Surge
Loss Cases: Fluvial Pluvial And Storm Surge With Demand Surge
Include Damage Uncertainty: Yes
Custom Damage Samples Used: No
Custom Damage Function Used: No
Parameter Adjustment Used: No
Special Note: Selected analysis settings are suitable for Florida rate filing. Compiled - (Report 3 of 3).
Analyses 4|3

Figure 171: Screenshot of flood model output report from FCHLPM Florida Flood TC/Non-TC Loss Compiler tool

Appendix G: Glossary of Acronyms

Abbreviation	Description
1D	A 1-dimensional schematisation of solution of partitial differential equation used in hydrodynamic flood model
2D	A 2-dimensional schematisation of solution of partitial differential equation used in hydrodynamic flood model
AAL	Average annual loss
ADCIRC	System of computer programs for solving time dependent, free surface circulation and transport problems in two and three dimensions
AEP	Aggregate exceedance probability
API	Application programming interface
ARe	Associate in Reinsurance
ARM	Associate in Risk Management
ASCE	American Society of Civil Engineers
BA	Bachelor of Arts
BE	Bachelor of Engineering
BPMN	Business Process Model and Notation
BFE	Base Flood Elevation
BS	Bachelor of Science
CAT	Catastrophe, abbreviated
CCRMP	Certified Catastrophe Risk Management Professional
CDF	Cumulative distribution function
CIRES	Cooperative Institute for Research in Environmental Sciences
CONUS	Contiguous United States
Cp	Central pressure
CPU	Central processing unit
CRS	Community Rating System
CSI	Critical Success Index
CSPA	Certified Specialist in Predictive Analytics

Abbreviation	Description
DB	Database
DBAN	Darik's Boot and Nuke
DEM	A Digital Elevation Model captures a surface—including natural and human-made structure such as vegetation and buildings. They illustrate reflective surfaces of all features elevated above the 'bare earth'. In short, DEMs represent the Earth's surface and all objects on it.
DRGs	National Geographic Digital Raster Graphics
DS	Demand Surge
DTM	Topographic model of the bare Earth that can be manipulated by computer programs.The data files contain the elevation data of the terrain in a digital format which relates to a rectangular grid. Vegetation, buildings and other cultural features are removed digitally - leaving just the underlying terrain.
EGM08	Earth Gravitational Model EGM2008 has been publicly released by the National Geospatial-Intelligence Agency (NGA) EGM Development Team
ELT	Event Loss Table
ENF	ELEMENTS Normalized Format
ERA 5	Climate reanalysis dataset, covering the period 1950 to present. ERA5 is being developed through the Copernicus Climate Change Service
ERN	Evaluación de Riesgos Naturales
ERT	Emergency Response Time
FABDEM	Forest And Buildings removed Copernicus DEM
FBC	Florida Building Code
FCAS	Fellow of the Casualty Actuarial Society
FCHLPM	Florida Commission on Hurricane Loss Projection Methodology
FEMA	Federal Emergency Management Agency
FFH	First Floor Height
FFP	Far field pressure
FFT	Fast Fourier Transform

Abbreviation	Description
FFTW	Fastest Fourier Transform in the West
FHCF	Florida Hurricane Catastrophe Fund
FHCF	Florida Hurricane Catastrophe Fund
FIRM	Flood Insurance Rate Maps, Official map of a community on which FEMA has delineated the Special Flood Hazard Areas (SFHAs), the Base Flood Elevations (BFEs) and the risk premium zones applicable to the community.
FUSE	Framework for Understanding Structural Errors: A modular framework to diagnose differences between hydrological models
GB	Gigabyte
GEV	
GFK	Growth from Knowledge – A Data and Intelligence Company
GRWL	Global River Widths from Landsat
HadISST	Hadley Centre Sea Ice and Sea Surface Temperature Dataset
HCI	Human-Computer Interaction
HUC	Hydrologic unit codes. Are developed using a progressive two-digit system where each successively smaller areal unit is identified by adding two digits to the identifying code the smaller unit is nested within. WBD contains eight levels of progressive hydrologic units identified by unique 2- to 16-digit codes
HUD	U.S. Department of Housing and Urban Development
HURDAT	HURricane DATabase
HWM	High Water Marks
IBTrACs	The International Best Track Archive for Climate Stewardship
ICCOH	Interagency Coordinating Committee on Hurricanes
ICEYE	ICEYE Ltd. (natively ICEYE Oy) is a Finnish microsatellite manufacturer. www.iceye.com
IDF	Intensity Duration Frequency
IDS	Intrusion detection systems (IDS)
IED	Industry Exposure Database
IF	Impact Forecasting

Abbreviation	Description
IPS	Intrusion prevention systems (IPS)
IRF-UH	Impulse Response Function – Unit Hydrograph (IRF-UH) routing procedure transfering rainfall into runoff in hydrological models
ISCM	International Society of Catastrophe Managers
ISO	International Organization for Standardization
IT	Information Technology
KGE	Kling–Gupta efficiency
km	Kilometers
KS	Kolmogorov-Smirnov Test Statistic
L&O	Law and Ordinance
LiDAR	Light Detection and Ranging is a remote sensing method used to examine the surface of the Earth
LISFLOOD-FP	LISFLOOD-FP is a two-dimensional hydrodynamic model specifically designed to simulate floodplain inundation in a computationally efficient manner over complex topography.
LLC	Limited liability company
LULC	Land Use and Land Cover - usually GIS dataset that holds information about the land use and land cover
m	Meters
m/s	Meters per second
MA	Master of arts
MAAA	Member of the American Academy of Actuaries
MAF	Mean annual flow
MBA	Master of Business Administration
MDR	Mean damage ratio
MERIT DTM	Multi-Error-Removed Improved-Terrain DEM
MERIT HYDRO	MERIT Hydro is a global hydrography datasets, developed based on the MERIT DEM and multiple inland water maps
MH	Mobile Home
mizuRoute	A tool that post-processes runoff outputs from any distributed hydrologic model or land surface model to produce spatially distributed streamflow at various spatial scales from

Abbreviation	Description
	headwater basins to continental-wide river systems
mph	Miles per hour
MRLC	Multi-Resolution Land Characteristics Consortium
MS	Master of Science
MSWEP	Multi-Source Weighted-Ensemble Precipitation; a sub-daily precipitation dataset with full global coverage at 0.1° resolution, spanning the period 1979 to present
MSWX	Multi-Source Weather is an operational, high-resolution (3-hourly 0.1°), bias-corrected meteorological product with global coverage from 1979 to 7 months from now
NAD83	The North American Datum of 1983
NAVD88	The North American Vertical Datum of 1988 is the vertical control datum established in 1991 by the minimum-constraint adjustment of the Canadian-Mexican-United States leveling observations.
NCAR	National Center for Atmospheric Research
NCEP	National Centers for Environmental Prediction
NED	National Elevation Dataset
NFIP	National Flood Insurance Program
NGDC	National Geophysical Data Center of NOAA
NHC	National Hurricane Center
NHD	The National Hydrography Dataset represents the water drainage network of the United States with features such as rivers, streams, canals, lakes, ponds, coastline, dams, and streamgages.
NLCD	National Land Cover Database that definitives land cover database for the United States
NLD	National Levee Database
NOAA	National Oceanic and Atmospheric Administration
non-TC	Non-Tropical System Induced Flooding
NOS	National Ocean Service
NWIS	Nationa Water Information System
NWS	National Weather Service

Abbreviation	Description
OEP	Occurrence exceedance probability
PE	Professional Engineer
PFDS	Precipitation Frequency Data Server
PhD	Doctor of Philosophy
PML	Probable maximum loss level
POI	Points of Interest
PRMS	The Precipitation-Runoff Modeling System (PRMS) is a deterministic, distributed-parameter, physical process based modeling system developed to evaluate the response of various combinations of climate and land use on streamflow and general watershed hydrology.
Q	Discharge, Q is generally accepted quantity
QA	Quality Assurance
R&D	Research and Development
RAM	Random access memory
RDP	Remote Desktop Access
RFFA	Regional Flood Frequency Analyses
Rmax	Radius of maximum winds
RMW	Radius of Maximum Wind Speed
RP	Return Period, also known as a recurrence interval or repeat interval, is an average time or an estimated average time between events such as earthquakes, floods,[1] landslides,[2] or river discharge flows to occur
RRT	Requires Restoration Time
SACRAMENTO	Continuous rainfall-runoff model used to generate daily stream flow from daily rainfall and potential evapotranspiration data
SFHA	Special Flood Hazard Area
SFTP	Secure File Transfer Protocol
SLOSH	The Sea, Lake and Overland Surges from Hurricanes (SLOSH) model is a computerized numerical model developed by the National Weather Service (NWS) to estimate storm surge heights resulting from historical, hypothetical, or predicted hurricanes by taking into account the atmospheric pressure, size, forward speed, and track data.

Abbreviation	Description
SMO	SQL Server Management Object
SoP	Standard of Protection: The likelihood that a certain level of flooding will occur is described as 'flood risk' or the 'chance' that a location will flood in any one year.
sq mi	Square miles
SQL	Structured Query Language
SRC	Standardized Regression Coefficients
SRTM	Shuttle Radar Topography Mission
SSBN	The former organizational name of the entity now known as Fathom.
SSD	Solid state drive
SSURGO	The Soil Survey Geographic Database
SURGEDAT	SURGEDAT is the world's storm surge data center that has archived the location and height of more than 700 tropical surge events around the world since 1880 and has identified more than 8,000 unique high water marks from tropical surges along the U.S. Gulf and Atlantic Coasts.
TC	Tropical System Induced Flooding)
TCR	Tropical Cyclone Rainfall
TFS	Microsoft Team Foundation Server
TOPMODEL	Physically based, distributed watershed model that simulates hydrologic fluxes of water through a watershed
TS	Tropical Storm
TUR	Take Up Rate
UAM	User Access Management
UFT	Unified Function Test
UML	Unified Modeling Language
USACE	U.S. Army Corps of Engineers
USGS	United States Geological Survey
UX	User Experience
VDATUM	VDatum stands for Vertical Datum Transformation under development by NOAA's National Ocean Service. its primary purpose is to convert elevation data from various sources into a common reference system.

Abbreviation	Description
VIC	The VIC model is a macroscale hydrologic model used to solve full water and energy balances. In addition to hydrologic processes, VIC models land-surface interactions and flow routing
Vmax	Maximum sustained wind speed
VPN	Virtual private network
VT	Translational velocity (forward speed)
WBD	Watershed Boundary Dataset is a comprehensive aggregated collection of hydrologic unit data consistent with the national criteria for delineation and resolution
WGS84	Current version of the World Geodetic System (WGS) is a standard used in cartography, geodesy, and satellite navigation including GPS.
WL	Water-level
WPF	Windows Presentation Foundation
YLT	Year Loss Table
ZIP Code	Zone Improvement Plan – the postal code used by the United States Postal Service

Contact us

David Colbus
Associate Director
Aon | Impact Forecasting
+1.978.305.1995
david.colbus@aon.com

About Aon:

Aon plc (NYSE: AON) exists to shape decisions for the better — to protect and enrich the lives of people around the world. Our colleagues provide our clients in over 120 countries with advice and solutions that give them the clarity and confidence to make better decisions to protect and grow their business. Follow Aon on Twitter and LinkedIn.
Stay up-to-date by visiting the Aon Newsroom and sign up for News Alerts here.

Aon
200 E. Randolph St.
Aon Center, floors 3-15
Chicago, Illinois 60601
+1 (312) 381-1000
https://www.aon.com/reinsurance/impact-forecasting/

Published by Aon's Reinsurance Solutions business, part of Aon UK Limited.
Registered office: The Aon Centre, The Leadenhall Building,
122 Leadenhall Street, London, EC3V 4AN.
©Copyright Aon UK Limited 2024. All rights reserved.
No part of this publication may be reproduced, stored in a retrieval system, or transmitted in any way or by any means, including photocopying or recording, without the written permission of the copyright holder, application for which should be addressed to the copyright holder.
Aon UK Limited is a wholly owned subsidiary of Aon plc.
Aon UK Limited is authorised and regulated by the Financial Conduct Authority.